



한국해양대학교  
KOREA MARITIME & OCEAN UNIVERSITY



Global R&E Program for Interdisciplinary  
Technologies of Ocean Renewable Energy



# ICACE PROCEEDINGS OF THE 4TH INTERNATIONAL CONFERENCE ON 2023 ADVANCED CONVERGENCE ENGINEERING

August 14<sup>th</sup> - 16<sup>th</sup>, 2023 Ho Chi Minh City University of Technology, VNUHCM  
Ho Chi Minh City, Vietnam



## CONTENTS

<b>WELCOME MESSAGE .....</b>	<b>vii</b>
<b>COMMITTEES.....</b>	<b>viii</b>
<b>CONFERENCE SCHEDULE.....</b>	<b>x</b>
<b>KEYNOTE LECTURE .....</b>	<b>xii</b>
<b>SESSION SCHEDULE.....</b>	<b>xiv</b>
<b>Monday, August 14<sup>th</sup>, 2023</b>	
Registration (3:00 PM – 4:00 PM, B4 Hall Lobby).....	xiv
<b>Tuesday, August 15<sup>th</sup>, 2023</b>	
Keynote Session (8:50 AM – 9:50 AM, B4 Hall) .....	xiv
Poster Session (10:00 AM – 12:00 PM, B4 Hall Lobby).....	xiv
Morning Session I (10:00 AM – 12:00 PM, B4 Hall) .....	xvi
Morning Session II (10:00 AM – 12:00 PM, Room 305B4) .....	xvii
Afternoon Session III (1:30 PM – 3:30 PM, B4 Hall).....	xviii
Afternoon Session IV (3:40 PM – 5:40 PM, B4 Hall).....	xix
Afternoon Session V (1:30 PM – 3:30 PM, Room 305B4) .....	xix
Afternoon Session VI (3:40 PM – 5:40 PM, Room 305B4) .....	xx
<b>Wednesday, August 16<sup>th</sup>, 2023</b>	
Field Trip (8:00 AM – 4:00 PM) .....	xx
<b>ABSTRACTS.....</b>	<b>1</b>
P-6 Applying Production Planning and Scheduling for Sport Production: A Case Study of Vifa Sport.....	2
<i>Tinh T Tieu, Duong Vo Nhi Anh, Do Vinh Truc</i>	
P-8 Implementation of Lean Six Sigma for Production Process Optimization: A Case Study in ScanCom 6	
<i>Tran Anh Quan, Duong Vo Nhi Anh</i>	
P-10 Application of TSGA, a Hybrid Mega Heuristic Model, to Solve Flow Shop Scheduling Problems with Changeover Times in Operations. A Case Study.....	12
<i>Nguyen Nhu Phong, Nguyen Thi Thuy Nhi</i>	
P-11 Application of Tabu Search to Solve Parallel Machine Scheduling Problems with Capacity Constraints. A Case Study .....	19
<i>Nguyen Nhu Phong, Nguyen Nhat Ha</i>	

P-13 Application of GATS, a Hybrid Mega Heuristic Model, to Solve Flexible Flow Shop Scheduling Problems with Setup and Batch Production. A Case Study .....	25
<i>Nguyen Nhu Phong, Nguyen Le Thu Trang</i>	
P-14 Application of Genetic Algorithm to Solve Vehicle Routing Problems in Distribution Planning Systems. A Case Study .....	32
<i>Nguyen Nhu Phong, Do Thi Thao</i>	
P-15 Utilizing Project Management Principles in the Implementation of the KETO BISTRO Business Plan at a Seaport Location .....	39
<i>Le Duc Dao, Hoang Tuan Anh, Tran Hoai Phuc, Vu Minh Phuong, Nguyen Vu Bich Ngoc, Thai Thi Minh Tram</i>	
P-17 Maritime Logistics Model Optimization - A Case Study on Minimizing Distribution Cost on Port-to-Port System .....	45
<i>Le Duc Dao, Le Nguyen Khoi, Huynh Nhat Huy, Dao Quang Chinh, Ngo Xuan Minh</i>	
P-19 A Hybrid Improved Case-Based Reasoning Approach and Metaheuristics for Cost Estimation .....	51
<i>Pham Ngoc Xuan Mai, Phan Nguyen Ky Phuc</i>	
P-21 Deep Learning for Quality Inspection of Manufacturing Product.....	58
<i>Doan Huu Chanh, Phan Nguyen Ky Phuc, Luu Trong Hieu</i>	
P-26 Designing Management Information System for Container Truck Transport.....	65
<i>Le Cao Ngoc Anh, Dinh Ba Hung Anh</i>	
P-28 Applying the AHP Process to Select Policy Implications to Improve Employee Performance: A Case Study of Joint Stock Commercial Banks in Ho Chi Minh City .....	71
<i>Vo Thi Hoang Quanh, Dinh Ba Hung Anh</i>	
P-33 Development of Automated Welding Machine for Industrial Applications .....	78
<i>Pham Son Minh, Tran Anh Son, Jong Il Yoon, Nguyen Van Minh, Do Ngoc Hao,</i>	
<i>Huynh Van Nhat, Pham Minh Khoi</i>	
P-38 Control to Manipulate the Target Task for Industrial Manipulator.....	82
<i>Minh Tuan Nguyen</i>	
P-40 A Two-Phase Optimization Algorithm for Solving the Heterogeneous Capacitated Vehicle Routing Problem: A Case Study on the Delivery Problem in Viet Nam.....	88
<i>Mai-Ha Phan, Thanh-Hoa Nguyen</i>	
P-43 Supplier Management Information System and Support Tools for Supplier Selection: A Case Study in Garment Industry, Viet Nam.....	96
<i>Mai-Ha Phan, Thanh-Huyen Thi Ho, Gia-Nhi Thi Nguyen</i>	
P-44 Ultrafast Laser Selective Welding of Sapphire and Invar Alloy .....	102
<i>J. Yang, Q. Jiang, M. Yang, Y.X. Zhao, R. Pan</i>	

P-45 Preparation and Research of MXene-Graphite Oxide Thin Films Based on Humidity Driving....	103
<i>Jianguang Zhai, Minghui Zou</i>	
P-49 Long-Term Effects of Sustained Loading and Outdoor Conditioning on Bond between Glass Fiber Reinforced Polymer (GFRP) and Concrete Using Epoxy.....	104
<i>Jaeha Lee, Meeju Lee, Charles E. Bakis</i>	
P-59 Applying Grey Wolf Optimization to Stochastic Inventory with Multi-Objective.....	105
<i>Nguyen Duy Tan, Hwan-Seong Kim, Sam-Sang You</i>	
P-60 Control Theory Application in Supply Chain Management by Considering Stochastic Disruptions	107
<i>Ho Van Roi, Hwan-Seong Kim, Sam-Sang You</i>	
P-61 Data-Driven Approach for State Space Reconstruction of Container Throughput: A Case Study of Korean Port.....	109
<i>Truong Ngoc Cuong, Hwan-Seong Kim, Sam-Sang You</i>	
P-63 A Study of Changing Velocity on Maritime Vessel's Pitch-Roll Motion.....	112
<i>Tatsuhiko Terada, Hwan-Seong Kim, Sam-Sang You, Hitoi Tamaru</i>	
P-64 Optimal Solution for Quay Crane Scheduling Problem Using Hybrid Metaheuristic Approach...	114
<i>Long Le Ngoc Bao, Ji-Hoon Park, Byung-Kwon Jeong, Hwan-Seong Kim, Sam-Sang You</i>	
P-65 Optimization of Stochastic Inventory Model Using Hamilton-Jacobi-Bellman Equation.....	116
<i>Bui Minh Hau, Hwan-Seong Kim, Sam-Sang You</i>	
P-66 Reach Stacker Assistance by Object Detection and Distance Estimation in Container Terminal .	118
<i>Ngô Quang Vinh, Ji-Hoon Park, Byung-Kwon Jeong, Hyeon-Soo Shin, Hwan-Seong Kim</i>	
P-67 Shipping Network Selection Based on Advanced Prospect Theory - A Case Study of Vietnam Seaport	120
<i>Pham Thi Yen, Hwan-Seong Kim, Truong Ngoc Cuong, Phung Hung Nguyen</i>	
S1-3 Designing Shape for Two Elongated Undulating Fin Underwater Vehicle Using Computational Fluid Dynamics .....	122
<i>Quoc Tuan Vu, Van Binh Duong Nguyen, Quoc Minh Lam, Laprelle Boucher Ernest, Huy Hung Nguyen, Van Tu Duong, Tan Tien Nguyen</i>	
S1-32 Classification of Fatigued Electromyography Signals Using Support Vector Machine in Combination with Root Mean Square and Mean Absolute Value Features .....	129
<i>Nghi Tran Huu, Gia Thien Luu, Bao Minh Pham, Philippe Ravier, Olivier Buttelli</i>	
S1-36 Adjusting Technical Parameters to Improve the Quality of 3D Printed Products Using ABS Material	134
<i>Huu Nghi Huynh, Dinh Tam Ngo, Tung Lam Khoa, Trong Hieu Bui</i>	

S1-39 Design of Nested-Stator Coaxial BLDC Motor for Underwater Vehicle.....	142
<i>Lam Cuong Quoc Thai, Van Tu Duong, Huy Hung Nguyen, Jotje Rantung, Xuan Tan Pham, Tan Tien Nguyen</i>	
S1-52 Study on Energy Conversion Efficiency of Wave Actuating Ship.....	147
<i>Phan Huy Nam Anh, Hyeung-Sik Choi</i>	
S1-1 Design of Two-Shaft Crusher in Domestic Waste Treatment System .....	148
<i>Phung Tran Hanh, Thanh-Long Le, Thi-Hong-Nhi Vuong, Nguyen Quang Minh, Nguyen Thanh Hai, Tran Dang Long, Tran Quang Lam, Tran Thien Hau, Tran Trong Hy</i>	
S1-53 Structural Characteristic Evaluation of Self-Elevating Crane System .....	153
<i>Hoseung Jeong, Manjung Yoon, Jongrae Cho</i>	
S2-12 Harvesting Magnetic Field Energy from Power Lines and Using It as a Power Source for Low-power Wireless Sensor Systems .....	155
<i>Kyung-Rak Sohn, Hyun-Sik Kim</i>	
S2-20 A Cost-Effective Workflow Scheduling Considering Deadline Constraint in a Cloud .....	157
<i>Nguyen Bui Thanh Truc, Phan Nguyen Ky Phuc</i>	
S2-22 Application of Developed Dual Nozzle System that is able to Multi-Layer Printing in FDM Method .....	163
<i>Yaegun Kwon, Hyeonjong Kim, Junghyuk Ko</i>	
S2-34 Smart Farm with Hydroponic Cultivation Method Using Renewable Energy .....	165
<i>HoYeong Kim, Dohyung Kim, Inwoo Kim, Junghyuk Ko</i>	
S2-35 Analysis of Implantable Catheters for Draining Malignant Ascites.....	167
<i>Inwoo Kim, Hyeonjong Kim, Il-Hwan Kim, Junghyuk Ko</i>	
S2-50 Use of Drone-Based Thermal Images for 3D Thermal Point Cloud and Target Surface Temperature Estimation .....	169
<i>Hyeonjeong Jo, Junhoo Lee, Jaehong Oh</i>	
S2-58 The Application of Blockchain in Logistics: Enhancing Transparency and Efficiency.....	170
<i>Linh Do, Thai Le, Duy Thanh Tran</i>	
S3-2 Research Impact of Solar Panel Cleaning Robot on Photovoltaic Panel's Deflection .....	172
<i>Trung Dat Phan, Minh Duc Nguyen, Maxence Auffray, Nhut Thang Le, Cong Toai Truong, Dae Hwan Kim, Van Tu Duong, Huy Hung Nguyen, Tan Tien Nguyen</i>	
S3-4 Hyperbolic Tangent Reaching Law-Based Sliding Mode Controller for Position Control of Rajiform Biomimetic Underwater Robot .....	180
<i>Van Hien Nguyen, Phuc Long Duong, Vu Nguyen Phung, Vuong Quang Huy Trinh, Van Tu Duong, Huy Hung Nguyen, Tan Tien Nguyen</i>	

S3-5 Nonlinear Regression of Thrust Force Produced by Rajiform Undulating Fin.....	186
<i>Van Hien Nguyen, Phuc Long Duong, Vu Nguyen Phung, Vuong Quang Huy Trinh, Van Tu Duong, Huy Hung Nguyen, Tan Tien Nguyen</i>	
S3-24 5-Axis Robotic Arm Gripper Following a Human Arm.....	192
<i>Geunho Do, HoYeong Kim, Jaewon Choi, Taegang Kim, Seokhyun Jeon, Seongmin Lee, Hyeonjong Kim, Junghyuk Ko</i>	
S3-37 A Novel Development of the Decentralized Scheme to Avoid Collision for the Large-Scale System .....	193
<i>The Cuong Le, Minh Tuan Nguyen</i>	
S3-46 Prediction of Aerodynamic Coefficient Using Deep Learning .....	199
<i>Bo Ra Kim, Seung Hun Lee, Seung Hyun Jang, Min Yoon</i>	
S4-7 Multi-Scale Approach for Low Concentration CO <sub>2</sub> Selective Adsorption.....	201
<i>Tuan Huy Lo, Il Seouk Park</i>	
S4-30 The Intelligent Waste Management System Using IoT for Smart Cities .....	202
<i>Thai Le, Linh Do, Duy Thanh Tran</i>	
S4-47 A Study of the Synthesis of Zeolite Using Residual By-Products of Indirect Carbonation .....	204
<i>Seonmi Shin, Myoung-Jin Kim</i>	
S4-48 An Experimental Study on the Fracture Energy of Seawater Mortar Reinforced with Recycled PET Fibers .....	205
<i>Meeju Lee, Kyeongjin Kim, Jeongho Kim, Seungbok Lee, Jaeha Lee</i>	
S4-54 Direct Carbonation for Zero By-Product in Mineral Carbonation Process Using Oyster Shells and Seawater.....	206
<i>Eunbit Koh, Myoung-Jin Kim</i>	
S4-55 Carbon Dioxide Conversion to Bioplastic (Poly 3-Hydroxybutyrate) through Microbial Electrosynthesis System.....	207
<i>Giang T. H. Le, Dipak A. Jadhav, Jung-Min Lee, Miri Jae, Ju-Hyeong Kim, Kyu-Jung Chae</i>	
S4-56 Improvement of Hydrogen Production through Methanogen Suppression in Microbial Electrolysis Cells for Swine Manure Treatment.....	208
<i>Trang T. Q. Le, Dipak A. Jadhav, Mohammed Hussien, Jung-Min Lee, Sumin Jo, Miri Jae, Kyung-Jung Chae</i>	
S5-18 Capacitated Drone Routing Problem with Time Windows and Scheduled Lines: Mathematical Formulation.....	209
<i>Dang Le To Uyen, Phan Nguyen Ky Phuc, Pham Ngoc Xuan Mai</i>	
S5-23 Predictive Maintenance for Machine Breakdown - An Application in Manufacturing .....	215
<i>Nguyen Thi Thanh Xuan, Tran Duc Vi</i>	

S5-25 Overview in IT-based Power Plants and Electric Users.....	221
<i>Thi-Ngot Pham, Jun-Ho Huh</i>	
S5-31 Multi-Criteria Decision-Making with Preference Scale.....	222
<i>Sanghyuk Lee, Youpeng Yang, Kyeong Soo Kim, Fei Ma</i>	
S5-51 Deep Learning Model Combined with CNN and LSTM used for Fault Diagnosis of Sensors in the Monitoring of Anaerobic Digestion.....	228
<i>Hyein Jung, YoungChae Song, Junghui Woo, Keugtae Kim, Seong-Wook Oa</i>	
S5-57 Building a New Machine Learning Model to Detect the Insurance Fraud.....	229
<i>Ai Vu, Anh Tran, Duy Thanh Tran</i>	
S5-68 Experiment and Numerical Simulation of Microchannel Pulsating Heat Pipes.....	231
<i>Hye-Seong Hwang, Duy-Tan Vo, Kwang-Hyun Bang</i>	
S6-9 Application of GATS, a Hybrid Mega Heuristic Model, to Solve Flow Shop Scheduling Problems with Changeover Times in Operations. A Case Study.....	232
<i>Nguyen Nhu Phong, Nguyen Thi Kim Ngan</i>	
S6-16 Addressing the Housing Shortage for Harbor Workers during High-Risk Respiratory Seasons: A Step-by-Step Logistics Design Process for Providing Safe Accommodation.....	240
<i>Le Duc Dao, Huynh Nguyen Khang Thinh, Trinh Minh Khoa, Lam Hien Dang Khoa, Truong Quoc Khoi, Phan Van Bach</i>	
S6-27 Rearrangement of Finished Product Warehouse of Tran Hiep Thanh Textile Joint Stock Company.....	246
<i>Nguyen Viet Hai Duy, Dinh Ba Hung Anh</i>	
S6-29 Multi-Objective Model in Aggregate Production Planning: A Case Study of ScanCom Vietnam Plant.....	252
<i>Nguyen Truong Xuan Thinh, Duong Vo Nhi Anh, Do Vinh Truc</i>	
S6-41 Application of Multi-Criteria Classification and Inventory Management Model for Spare Parts: A Vietnamese Case Study.....	258
<i>Tai Duc Nguyen, Mai-Ha Phan</i>	
S6-42 Building Model Supporting Maintenance Schedule at a Technology Solution Company.....	264
<i>Tuan-Phat Ngo, Mai-Ha Phan</i>	
S6-62 Dynamical Analysis and Optimal Management of Chaotic Multi-Echelon Supply Chain System with Temporary Disruptions.....	274
<i>Seung-Pil Lee, Hwan-Seong Kim, Dae-Hyeun Kim, Sam-Sang You</i>	

## **WELCOME MESSAGE**

### **The 4<sup>th</sup> International Conference on Advanced Convergence Engineering (ICACE 2023)**

August 14-16, 2023, Ho Chi Minh City University of Technology, Ho Chi Minh City, Viet Nam

On behalf of the ICACE 2023 organizing committee, I am honored and delighted to welcome you to the 4<sup>th</sup> International Conference on Advanced Convergence Engineering (ICACE) held from August 14-16, 2023, at Ho Chi Minh City University of Technology, Ho Chi Minh City, Viet Nam. I believe we have chosen a venue that guarantees a successful technical conference amid the culture and scenery of Vietnam.

There will be exciting material for all areas of the maritime field from academics through industries. We have planned ICACE 2023 in a way that would actually help the maritime industry in this particularly difficult time. My hope is, therefore, that many would participate in this conference to actively debate the future of the marine engineering industry.

The maritime industry is expected to recover from long-term financial difficulties. Although the basic current condition of low oil price and low growth is not likely to be resolved soon, based on analyses, it is predicted the economy will be able to fully recover by 2023. It is the time to prepare for the future through efforts for the development of new technologies. At the same time, I believe that international human exchanges should be actively pursued and enhanced.

Herein, I believe that ICACE 2023 will serve as an excellent venue for such discussions. We will do our utmost efforts to make this event successful. We cordially invite you to take part in this exciting opportunity for maritime industries and affairs.



***Prof. Nguyen Tan Tien***

***Chairman of ICACE 2023***

***Director of DCSELab, Ho Chi Minh City University of Technology, VNUHCM, Viet Nam***



## COMMITTEES

### Committee Members

#### Conference Chair

- **Nguyen Tan Tien**, DCSELab, Viet Nam

#### Conference Co-Chair

- **Hwan-Seong Kim**, KMOU, Korea
- **You-Taek Kim**, KOSME, Korea
- **Chao-Min Zhang**, SUES, China

#### The International Advisory Committees

- **Bui Trong Hieu**, HCMUT, Viet Nam
- **Nguyen Duy Anh**, HCMUT, Viet Nam
- **Do Ngoc Hien**, HCMUT, Viet Nam
- **Kweonha Park**, KMOU, Korea
- **Kyu-Jung Chae**, KMOU, Korea
- **Dongwoo Sohn**, KMOU, Korea
- **Chong-Gui Li**, SUES, China
- **Jian Zhao**, SUES, China
- **Bui Duc Hong Phuc**, USA
- **Daisuke Watanabe**, Japan

### Organizing Committee

#### General Secretary

- **Thanh-Long Le**, HCMUT, Viet Nam
- **Thi-Hong-Nhi Vuong**, HCMUT, Viet Nam
- **Jaeha Lee**, KMOU, Korea
- **Junghyuk Ko**, KMOU, Korea
- **Jian-Guang Zhai**, SUES, China

### The Technical and Organizing Committee

- **Nguyen Huy Hung**, Saigon University, Viet Nam
- **Nguyen Truong Long**, HCMUT, Viet Nam
- **Nguyen Quoc Chi**, HCMUT, Viet Nam
- **Thanh-Long Le**, HCMUT, Viet Nam
- **Luu Thanh Tung**, HCMUT, Viet Nam

- **Duong Van Tu**, HCMUT, Viet Nam
- **Thi-Hong-Nhi Vuong**, HCMUT, Viet Nam
- **Jae-Hong Oh**, KMOU, Korea
- **Do-Sik Shim**, KMOU, Korea
- **Keun-Jae Yoo**, KMOU, Korea
- **Jun-Ho Huh**, KMOU, Korea
- **Min Yoon**, KMOU, Korea
- **Jin Yang**, SUES, China
- **Dong-Hong Wang**, SUES, China
- **Tian-Li Zhang**, SUES, China

### **Organized By**

National Key Laboratory of Digital Control and System Engineering (DCSELab), Viet Nam

National Korea Maritime & Ocean University, Korea

Shanghai University of Engineering Science, China

Global R&E Program for Interdisciplinary Technologies of Ocean Renewable Energy (KMOU BK21-Four group)

### **Sponsored By**

Viet Nam National University, Ho Chi Minh City

Ho Chi Minh City University of Technology (HCMUT), Viet Nam

Department of Science and Technology, Ho Chi Minh City

## CONFERENCE SCHEDULE

**Monday, August 14<sup>th</sup>, 2023**

<b>3:00 PM – 4:00 PM</b> <b>B4 HALL – LOBBY</b> <b>Registration</b>
<b>4:00 PM – 6:00 PM</b> <b>Committee Board Meeting – DCSELab</b>

**Tuesday, August 15<sup>th</sup>, 2023**

<b>8:00 AM – 8:30 AM</b> <b>B4 HALL – LOBBY</b> <b>Registration</b>
<b>8:30 AM – 8:50 AM</b> <b>OPENING CEREMONY – B4 HALL</b> <b>Welcome Address</b>
<b>8:50 AM – 9:50 AM</b> <b>KEYNOTE SESSION – B4 HALL</b> <b>Keynote Lectures</b> <b>SESSION CHAIRS:</b> Prof. Nguyen Tan Tien, DCSELab, HCMUT, Viet Nam Prof. HwanSeong Kim, Korea Maritime and Ocean University, Korea
<b>9:50 AM – 10:00 AM</b> <b>Tea Break</b>

<b>10:00 AM – 12:00 PM</b> <b>POSTER SESSION – B4 HALL LOBBY</b> <b>Poster Presentation</b> <b>SESSION CHAIR:</b> Dr. Thi-Hong-Nhi Vuong, Ho Chi Minh City University of Technology, VNUHCM, Viet Nam
<b>12:00 PM – 1:30 PM</b> <b>Lunch</b>

<b>10:00 AM – 12:00 PM</b> <b>MORNING SESSION I – B4 HALL</b> <b>Mechanical Engineering and Materials</b> <b>SESSION CHAIRS:</b> Prof. Hyeung-Sik Choi, Korea Maritime and Ocean University, Korea Dr. Le Thanh Long, Ho Chi Minh City University of Technology, VNUHCM, Viet Nam
<b>12:00 PM – 1:30 PM</b> <b>Lunch</b>

**10:00 AM – 12:00 PM**

**MORNING SESSION II – ROOM 305B4**

**Electrics, Electronics, Electronic Materials, Data Information**

**SESSION CHAIRS:**

Prof. Junghyuk Ko, Korea Maritime and Ocean University, Korea

Dr. Duong Van Tu, Ho Chi Minh City University of Technology, VNUHCM, Viet Nam

**12:00 PM – 1:30 PM Lunch**

**1:30 PM – 3:30 PM**

**AFTERNOON SESSION III – B4 HALL**

**Mechatronics, Control and Automation Engineering**

**SESSION CHAIRS:**

Prof. Jun-Ho Huh, Korea Maritime and Ocean University, Korea

Prof. Nguyen Quoc Chi, Ho Chi Minh City University of Technology, VNUHCM, Viet Nam

**3:30 PM – 3:40 PM Tea Break**

**3:40 PM – 5:40 PM**

**AFTERNOON SESSION IV – B4 HALL**

**Civil and Environmental Engineering**

**SESSION CHAIRS:**

Prof. Jaeha Lee, Korea Maritime and Ocean University, Korea

Prof. Vo Le Phu, Ho Chi Minh City University of Technology, VNUHCM, Viet Nam

**6:00 PM – 8:00 PM Gala Dinner**

**1:30 PM – 3:30 PM**

**AFTERNOON SESSION V – ROOM 305B4**

**Radio Communication and Computer Engineering**

**SESSION CHAIRS:**

Prof. YoungChae Song, Korea Maritime and Ocean University, Korea

Dr. Nguyen Huy Hung, Saigon University, Viet Nam

**3:30 PM – 3:40 PM Tea Break**

**3:40 PM – 5:40 PM**

**AFTERNOON SESSION VI – ROOM 305B4**

**Logistics**

**SESSION CHAIRS:**

Prof. HwanSeong Kim, Korea Maritime and Ocean University, Korea

Prof. Luu Thanh Tung, Ho Chi Minh City University of Technology, VNUHCM, Viet Nam

**6:00 PM – 8:00 PM Gala Dinner**

**Wednesday, August 16<sup>th</sup>, 2023**

**8:00 AM – 4:00 PM**

**FIELD TRIP – HO CHI MINH CITY**

## KEYNOTE LECTURE

8:50 AM – 9:20 AM - Tuesday, August 15<sup>th</sup>, 2023 – B4 Hall

Sang Bong Kim, *Pukyong National University, Korea*

### [K-1] Mobile Manipulator Control Based on Nonlinear Control Theories

Sang Bong Kim

*Pukyong National University, Korea*

#### Abstract

This keynote presents a nonlinear feedback control framework and controller design concept for mobile robots with manipulators. The approach uses a constructive Lyapunov function and the well-known backstepping concept which allows the formulation of a control law with asymptotic stability of the equilibrium point of the system and a computable stability region. The dynamic equations are simplified through normalization and partial feedback linearization. The latter allows linearizing only the actuated coordinate. The description of the control law is complemented by the stability analysis of the closed-loop dynamics of the system. An end-effector mounted at the end of a manipulator of the mobile manipulator system is controlled to track a desired trajectory with constant desired velocity. A distributed control method is applied to control the mobile manipulator system that includes two subsystems such as a mobile platform and a manipulator. Two controllers are designed to control two subsystems, respectively. A kinematic controller for the end-effector of the manipulator is designed to track a reference point by referring to the tracking error vector between a point of the end-effector and a reference point. The controller of the dynamic model is designed for the mobile platform to move so that the manipulator tracks the desired posture without its singularity based on a tracking error vector between a target point and a real point of the end-effector. The control laws are obtained based on the backstepping technique and make the tracking error vectors go to zero asymptotically. The system stability is proved using the Lyapunov stability theory. Several paper results are introduced to illustrate the usefulness of the proposed control scheme based on the nonlinear theoretical concept.

**Keywords:** *Nonlinear, Mobile robot, Dynamic, Manipulator*

## KEYNOTE LECTURE

9:20 AM – 9:50 AM - Tuesday, August 15<sup>th</sup>, 2023 – B4 Hall

Nguyen Duy Anh, *Ho Chi Minh City University of Technology, VNUHCM, Viet Nam*

### [K-2] Planning Optimal Trajectory for Automatic Container Crane Utilizing Genetic Algorithm

Thanh-Nhat Luong<sup>1,3</sup>, Duy-Anh Nguyen<sup>1,3</sup>, Hoang-Lien-Son Chau<sup>1,3</sup>, Tat-Hien Le<sup>2,3</sup>, Duy-Anh Nguyen<sup>1,3,\*</sup>

<sup>1</sup> Faculty of Mechanical Engineering, Ho Chi Minh City University of Technology (HCMUT), Ho Chi Minh City, Viet Nam, 700000

<sup>2</sup> Faculty of Transportation Engineering, Ho Chi Minh City University of Technology (HCMUT), Ho Chi Minh City, Viet Nam, 700000

<sup>3</sup> Viet Nam National University Ho Chi Minh City, Ho Chi Minh City, Viet Nam, 700000

\*Corresponding author: duyanhnguyen@hcmut.edu.vn

#### Abstract

In recent years, there has been a notable escalation in the scale of container transportation and the dimensions of vessels, necessitating the advancement of automatic container cranes. One critical aspect of unmanned crane control is the determination of the optimal route, which plays a crucial role in minimizing the cycle time through the efficient coordination of horizontal and vertical movements during container loading and unloading operations. This research comprehensively investigates various route planning challenges across diverse domains. Subsequently, a mathematical model is presented, derived from an in-depth analysis of the loading/unloading process. Specifically, an optimal route methodology based on the genetic algorithm is proposed, designed to meet various criteria such as route length, smoothness, and safety distance. Finally, computational experiments are conducted to corroborate the algorithm's effectiveness and to explore innovative avenues for enhancing the overall efficiency of container loading and unloading processes.

**Keywords:** Automatic container crane, Optimal route planning, Genetic algorithm

**SESSION SCHEDULE****Monday, August 14<sup>th</sup>, 2023****Registration – B4 Hall Lobby - 3:00 PM – 4:00 PM****Tuesday, August 15<sup>th</sup>, 2023****Keynote Session – B4 Hall – 8:50 AM - 9:50 AM****SESSION CHAIRS:**

Prof. Nguyen Tan Tien, DCSELab, HCMUT, Viet Nam

Prof. HwanSeong Kim, Korea Maritime and Ocean University, Korea

ID	Paper Title	Authors	Time
K-1	Mobile Manipulator Control Based on Nonlinear Control Theories	Sang Bong Kim	8:50 - 9:20
K-2	Planning Optimal Trajectory for Automatic Container Crane Utilizing Genetic Algorithm	Thanh-Nhat Luong, Duy-Anh Nguyen, Hoang-Lien-Son Chau, Tat-Hien Le, Duy-Anh Nguyen	9:20 - 9:50

**Poster Session – B4 Hall Lobby – 10:00 AM - 12:00 PM****SESSION CHAIR:**

Dr. Thi-Hong-Nhi Vuong, Ho Chi Minh City University of Technology, VNUHCM, Viet Nam

ID	Paper Title	Authors	Time
P-6	Applying Production Planning and Scheduling for Sport Production: A Case Study of Vifa Sport	Tinh Tri Tieu Duong Vo Nhi Anh Do Vinh Truc	
P-8	Implementation of Lean Six Sigma for Production Process Optimization: A Case Study in ScanCom	Tran Anh Quan Duong Vo Nhi Anh	
P-10	Application of TSGA, a Hybrid Mega Heuristic Model, to Solve Flow Shop Scheduling Problems with Changeover Times in Operations. A Case Study	Nguyen Nhu Phong Nguyen Thi Thuy Nhi	
P-11	Application of Tabu Search to Solve Parallel Machine Scheduling Problems with Capacity Constraints. A Case Study	Nguyen Nhu Phong Nguyen Nhat Ha	
P-13	Application of GATS, a Hybrid Mega Heuristic Model, to Solve Flexible Flow Shop Scheduling Problems with Setup and Batch Production. A Case Study	Nguyen Nhu Phong Nguyen Le Thu Trang	
P-14	Application of Genetic Algorithm to Solve Vehicle Routing Problems in Distribution Planning Systems. A Case Study	Nguyen Nhu Phong Do Thi Thao	
P-15	Utilizing Project Management Principles in the Implementation of the KETO BISTRO Business Plan at a Seaport Location	Le Duc Dao Hoang Tuan Anh Tran Hoai Phuc Vu Minh Phuong Nguyen Vu Bich Ngoc Thai Thi Minh Tram	

<b>P-17</b>	Maritime Logistics Model Optimization - A Case Study on Minimizing Distribution Cost on Port-to-Port System	Le Duc Dao Le Nguyen Khoi Huynh Nhat Huy Dao Quang Chinh Ngo Xuan Minh	
<b>P-19</b>	A Hybrid Improved Case-Based Reasoning Approach and Metaheuristics for Cost Estimation	Pham Ngoc Xuan Mai Phan Nguyen Ky Phuc	
<b>P-21</b>	Deep Learning for Quality Inspection of Manufacturing Product	Doan Huu Chanh Phan Nguyen Ky Phuc Luu Trong Hieu	
<b>P-26</b>	Designing Management Information System for Container Truck Transport	Le Cao Ngoc Anh Dinh Ba Hung Anh	
<b>P-28</b>	Applying the AHP Process to Select Policy Implications to Improve Employee Performance: A Case Study of Joint Stock Commercial Banks in Ho Chi Minh City	Vo Thi Hoang Quanh Dinh Ba Hung Anh	
<b>P-33</b>	Development of Automated Welding Machine for Industrial Applications	Pham Son Minh Tran Anh Son Jong Il Yoon Nguyen Van Minh Do Ngoc Hao Huynh Van Nhat Pham Minh Khoi	
<b>P-38</b>	Control to Manipulate the Target Task for Industrial Manipulator	Minh Tuan Nguyen	
<b>P-40</b>	A Two-Phase Optimization Algorithm for Solving the Heterogeneous Capacitated Vehicle Routing Problem: A Case Study on the Delivery Problem in Viet Nam	Mai-Ha Phan Thanh-Hoa Nguyen	
<b>P-43</b>	Supplier Management Information System and Support Tools for Supplier Selection: A Case Study in Garment Industry, Viet Nam	Mai-Ha Phan Thanh-Huyen Thi Ho Gia-Nhi Thi Nguyen	
<b>P-44</b>	Ultrafast Laser Selective Welding of Sapphire and Invar Alloy	J. Yang Q. Jiang M. Yang Y.X. Zhao, R. Pan	
<b>P-45</b>	Preparation and Research of MXene-Graphite Oxide Thin Films Based on Humidity Driving	Jianguang Zhai Minghui Zou	
<b>P-49</b>	Long-Term Effects of Sustained Loading and Outdoor Conditioning on Bond between Glass Fiber Reinforced Polymer (GFRP) and Concrete Using Epoxy	Jaeha Lee Meeju Lee Charles E. Bakis	
<b>P-59</b>	Applying Grey Wolf Optimization to Stochastic Inventory with Multi-Objective	Nguyen Duy Tan Hwan-Seong Kim Sam-Sang You	
<b>P-60</b>	Control Theory Application in Supply Chain Management by Considering Stochastic Disruptions	Ho Van Roi Hwan-Seong Kim Sam-Sang You	
<b>P-61</b>	Data-Driven Approach for State Space Reconstruction of Container Throughput: A Case Study of Korean Port	Truong Ngoc Cuong Hwan-Seong Kim Sam-Sang You	
<b>P-63</b>	A Study of Changing Velocity on Maritime Vessel's Pitch-Roll Motion	Tatsuhiko Terada Hwan-Seong Kim	



		Sam-Sang You Hitoi Tamaru	
<b>P-64</b>	Optimal Solution for Quay Crane Scheduling Problem Using Hybrid Metaheuristic Approach	Long Le Ngoc Bao Ji-Hoon Park Byung-Kwon Jeong Hwan-Seong Kim Sam-Sang You	
<b>P-65</b>	Optimization of Stochastic Inventory Model using Hamilton-Jacobi-Bellman Equation	Bui Minh Hau Hwan-Seong Kim Sam-Sang You	
<b>P-66</b>	Reach Stacker Assistance by Object Detection and Distance Estimation in Container Terminal	Ngo Quang Vinh Ji-Hoon Park Byung-Kwon Jeong Hyeon-Soo Shin Hwan-Seong Kim	
<b>P-67</b>	Shipping Network Selection Based on Advanced Prospect Theory - A Case Study of Vietnam Seaport	Pham Thi Yen Hwan-Seong Kim Truong Ngoc Cuong Phung Hung Nguyen	

**Morning Session I – B4 Hall – 10:00 AM - 12:00 PM****Mechanical Engineering and Materials****SESSION CHAIRS:**

Prof. Hyeung-Sik Choi, Korea Maritime and Ocean University, Korea

Dr. Le Thanh Long, Ho Chi Minh City University of Technology, VNUHCM, Viet Nam

<b>ID</b>	<b>Paper Title</b>	<b>Authors</b>	<b>Time</b>
<b>S1-3</b>	Designing Shape for Two Elongated Undulating Fin Underwater Vehicle Using Computational Fluid Dynamics	Quoc Tuan Vu Van Binh Duong Nguyen Quoc Minh Lam Laprelle Boucher Ernest Huy Hung Nguyen Duong Van Tu Nguyen Tan Tien	10:00 – 10:15
<b>S1-32</b>	Classification of Fatigued Electromyography Signals using Support Vector Machine in Combination with Root Mean Square and Mean Absolute Value Features	Nghi Tran Huu Gia Thien Luu Bao Minh Pham Philippe Ravier Olivier Buttelli	10:15 – 10:30
<b>S1-36</b>	Adjusting Technical Parameters to Improve the Quality of 3D Printed Products Using ABS Material	Huu Nghi Huynh Dinh Tam Ngo Tung Lam Khoa Trong Hieu Bui	10:30 – 10:45
<b>S1-39</b>	Design of Nested-Stator Coaxial BLDC Motor for Underwater Vehicle	Lam Cuong Quoc Thai Van Tu Duong Huy Hung Nguyen Jotje Rantung Xuan Tan Pham	10:45 – 11:00

<b>S1-52</b>	Study on Energy Conversion Efficiency of Wave Actuating Ship	Phan Huy Nam Anh Hyeung-Sik Choi	11:00 – 11:15
<b>S1-1</b>	Design of Two-Shaft Crusher in Domestic Waste Treatment System	Phung Tran Hanh Thanh-Long Le Thi-Hong-Nhi Vuong Nguyen Quang Minh Nguyen Thanh Hai Tran Dang Long Tran Quang Lam Tran Thien Hau Tran Trong Hy	11:15 – 11:30
<b>S1-53</b>	Structural Characteristic Evaluation of Self-Elevating Crane System	Hoseung Jeong Manjung Yoon Jongrae Cho	11:30 – 11:45

**Morning Session II – Room 305B4 – 10:00 AM - 12:00 PM****Electrics, Electronics, Electronic Materials, Data Information****SESSION CHAIRS:**

Prof. Junghyuk Ko, Korea Maritime and Ocean University, Korea

Dr. Duong Van Tu, Ho Chi Minh City University of Technology, VNUHCM, Viet Nam

<b>ID</b>	<b>Paper Title</b>	<b>Authors</b>	<b>Time</b>
<b>S2-12</b>	Harvesting Magnetic Field Energy from Power Lines and Using It as a Power Source for Low-power Wireless Sensor Systems	Kyung-Rak Sohn Hyun-Sik Kim	10:00 – 10:15
<b>S2-20</b>	A Cost-Effective Workflow Scheduling Considering Deadline Constraint in a Cloud	Nguyen Bui Thanh Truc Phan Nguyen Ky Phuc	10:15 – 10:30
<b>S2-22</b>	Application of Developed Dual Nozzle System that is able to Multi-Layer Printing in FDM Method	Yaegun Kwon Hyeonjong Kim Junghyuk Ko	10:30 – 10:45
<b>S2-34</b>	Smart Farm with Hydroponic Cultivation Method Using Renewable Energy	HoYeong.Kim Dohyung Kim Inwoo Kim Junghyuk Ko	10:45 – 11:00
<b>S2-35</b>	Analysis of Implantable Catheters for Draining Malignant Ascites	Inwoo Kim Hyeonjong Kim Il-Hwan Kim Junghyuk Ko	11:00 – 11:15
<b>S2-50</b>	Use of Drone-Based Thermal Images for 3D Thermal Point Cloud and Target Surface Temperature Estimation	Hyeonjeong Jo Junhoo Lee Jaehong Oh	11:15 – 11:30
<b>S2-58</b>	The Application of Blockchain in Logistics: Enhancing Transparency and Efficiency	Linh Do Thai Le Duy Thanh Tran	11:30 – 11:45

**Afternoon Session III – B4 Hall – 1:30 PM - 3:30 PM****Mechatronics, Control and Automation Engineering****SESSION CHAIRS:**

Prof. Jun-Ho Huh, Korea Maritime and Ocean University, Korea

Prof. Nguyen Quoc Chi, Ho Chi Minh City University of Technology, VNUHCM, Viet Nam

<b>ID</b>	<b>Paper Title</b>	<b>Authors</b>	<b>Time</b>
<b>S3-2</b>	Research Impact of Solar Panel Cleaning Robot on Photovoltaic Panel's Deflection	Trung Dat Phan Minh Duc Nguyen Maxence Auffray Nhut Thang Le Cong Toai Truong Dae Hwan Kim Van Tu Duong Huy Hung Nguyen Tan Tien Nguyen	1:30 – 1:45
<b>S3-4</b>	Hyperbolic Tangent Reaching Law-Based Sliding Mode Controller for Position Control of Rajiform Biomimetic Underwater Robot	Van Hien Nguyen Phuc Long Duong Vu Nguyen Phung Vuong Quang Huy Trinh Van Tu Duong Huy Hung Nguyen Tan Tien Nguyen	1:45 – 2:00
<b>S3-5</b>	Nonlinear Regression of Thrust Force Produced by Rajiform Undulating Fin	Van Hien Nguyen Phuc Long Duong Vu Nguyen Phung Vuong Quang Huy Trinh Van Tu Duong Huy Hung Nguyen Tan Tien Nguyen	2:00 – 2:15
<b>S3-24</b>	5-Axis Robotic Arm Gripper Following a Human Arm	Geunho Do HoYeong Kim Jaewon Choi Taegang Kim Seokhyun Jeon Seongmin Lee Hyeonjong Kim Junghyuk Ko	2:15 – 2:30
<b>S3-37</b>	A Novel Development of the Decentralized Scheme to Avoid Collision for the Large-Scale System	The Cuong Le Minh Tuan Nguyen	2:30 – 2:45
<b>S3-46</b>	Prediction of Aerodynamic Coefficient Using Deep Learning	Bo Ra Kim Seung Hun Lee Seung Hyun Jang Min Yoon	2:45 – 3:00

**Afternoon Session IV – B4 Hall – 3:40 PM - 5:40 PM****Civil and Environmental Engineering****SESSION CHAIRS:**

Prof. Jaeha Lee, Korea Maritime and Ocean University, Korea

Prof. Vo Le Phu, Ho Chi Minh City University of Technology, VNUHCM, Viet Nam

<b>ID</b>	<b>Paper Title</b>	<b>Authors</b>	<b>Time</b>
<b>S4-7</b>	Multi-Scale Approach for Low Concentration CO <sub>2</sub> Selective Adsorption	Tuan Huy Lo Il Seouk Park	3:40 – 3:55
<b>S4-30</b>	The Intelligent Waste Management System Using IoT for Smart Cities	Thai Le Linh Do Duy Thanh Tran	3:55 – 4:10
<b>S4-47</b>	A Study of the Synthesis of Zeolite Using Residual By-Products of Indirect Carbonation	Seonmi Shin Myoung-Jin Kim	4:10 – 4:25
<b>S4-48</b>	An Experimental Study on The Fracture Energy of Seawater Mortar Reinforced with Recycled PET Fibers	Meeju Lee Kyeongjin Kim Jeongho Kim Seungbok Lee Jaeha Lee	4:25 – 4:40
<b>S4-54</b>	Direct Carbonation for Zero By-Product in Mineral Carbonation Process Using Oyster Shells and Seawater	Eunbit Koh Myoung-Jin Kim	4:40 – 4:55
<b>S4-55</b>	Carbon Dioxide Conversion to Bioplastic (Poly 3-Hydroxybutyrate) through Microbial Electrosynthesis System	Giang T. H. Le Dipak A. Jadhav Jung-Min Lee Miri Jae Ju-Hyeong Kim Kyu-Jung Chae	4:55 – 5:10
<b>S4-56</b>	Improvement of Hydrogen Production through Methanogen Suppression in Microbial Electrolysis Cells for Swine Manure Treatment	Trang T. Q. Le Dipak A. Jadhav Mohammed Hussien Jung-Min Lee Sumin Jo Miri Jae Kyu-Jung Chae	5:10 – 5:25

**Afternoon Session V – Room 305B4 – 1:30 PM - 3:30 PM****Radio Communication and Computer Engineering****SESSION CHAIRS:**

Prof. YoungChae Song, Korea Maritime and Ocean University, Korea

Dr. Nguyen Huy Hung, Saigon University, Viet Nam

<b>ID</b>	<b>Paper Title</b>	<b>Authors</b>	<b>Time</b>
<b>S5-18</b>	Capacitated Drone Routing Problem with Time Windows and Scheduled Lines: Mathematical Formulation	Dang Le To Uyen Phan Nguyen Ky Phuc Pham Ngoc Xuan Mai	1:30 – 1:45
<b>S5-23</b>	Predictive Maintenance for Machine Breakdown - An Application in Manufacturing	Nguyen Thi Thanh Xuan Tran Duc Vi	1:45 – 2:00

<b>S5-25</b>	Overview in IT-based Power Plants and Electric Users	Thi-Ngot Pham Jun-Ho Huh	2:00 – 2:15
<b>S5-31</b>	Multi-Criteria Decision-Making with Preference Scale	Sanghyuk Lee Youpeng Yang Fei Ma Kyeong Soo Kim	2:15 – 2:30
<b>S5-51</b>	Deep Learning Model Combined with CNN and LSTM Used for Fault Diagnosis of Sensors in the Monitoring of Anaerobic Digestion	Hyein Jung YoungChae Song Junhui Woo Keugtae Kim Seong-Wook Oa	2:30 – 2:45
<b>S5-57</b>	Building a New Machine Learning Model to Detect the Insurance Fraud	Ai Vu Anh Tran Duy Thanh Tran	2:45 – 3:00
<b>S5-68</b>	Experiment and Numerical Simulation of Microchannel Pulsating Heat Pipes	Hye-Seong Hwang Duy-Tan Vo Kwang-Hyun Bang	3:00 – 3:15

**Afternoon Session VI – Room 305B4 – 3:40 PM - 5:40 PM****Logistics****SESSION CHAIRS:**

Prof. HwanSeong Kim, Korea Maritime and Ocean University, Korea

Prof. Luu Thanh Tung, Ho Chi Minh City University of Technology, VNUHCM, Viet Nam

<b>ID</b>	<b>Paper Title</b>	<b>Authors</b>	<b>Time</b>
<b>S6-9</b>	Application of GATS, a Hybrid Mega Heuristic Model, to Solve Flow Shop Scheduling Problems with Changeover Times in Operations. A Case Study	Nguyen Nhu Phong Nguyen Thi Kim Ngan	3:40 – 3:55
<b>S6-16</b>	Addressing the Housing Shortage for Harbor Workers during High-Risk Respiratory Seasons: A Step-by-Step Logistics Design Process for Providing Safe Accommodation	Le Duc Dao Huynh Nguyen Khang Thinh Trinh Minh Khoa Lam Hien Dang Khoa Truong Quoc Khoi Phan Van Bach	3:55 – 4:10
<b>S6-27</b>	Rearrangement of Finished Product Warehouse of Tran Hiep Thanh Textile Joint Stock Company	Nguyen Viet Hai Duy Dinh Ba Hung Anh	4:10 – 4:25
<b>S6-29</b>	Multi-Objective Model in Aggregate Production Planning: A Case Study of ScanCom Vietnam Plant	Nguyen Truong Xuan Thinh Duong Vo Nhi Anh Do Vinh Truc	4:25 – 4:40
<b>S6-41</b>	Application of Multi-Criteria Classification and Inventory Management Model for Spare Parts: A Vietnamese Case Study	Tai Duc Nguyen Mai-Ha Phan	4:40 – 4:55
<b>S6-42</b>	Building Model Supporting Maintenance Schedule at a Technology Solution Company	Tuan-Phat Ngo Mai-Ha Phan	4:55 – 5:10
<b>S6-62</b>	Dynamical Analysis and Optimal Management of Chaotic Multi-Echelon Supply Chain System with Temporary Disruptions	Seung-Pil Lee Hwan-Seong Kim Dae-Hyeun Kim Sam-Sang You	5:10 – 5:25

**Wednesday, August 16<sup>th</sup>, 2023****Field Trip – Ho Chi Minh City**

# **ABSTRACTS**

## [P-6] Applying Production Planning and Scheduling for Sport Production: A Case Study of Vifa Sport

Tinh T Tieu\*, Duong Vo Nhi Anh, Do Vinh Truc

*International University, Ho Chi Minh City, Viet Nam, 70000*

\*Corresponding author: tietritinh2001@gmail.com

### Abstract

Currently on the market, sports products are sold a lot, along with the constant change in customer demand. Demand increases usually lead to providing the good not on time due to shortage of materials, workers, machinery, and importantly, lack of reasonable planning to meet market and customer demand. Vifa Sport Company is a typical case, and a company that is quite strong in terms of manufacturing sports equipment with many different products. Company needs to improve on the planning of production, demand planning, inventory, product distribution. During the research process, I found that through the development stages, the company has come up with many policies to optimize production planning and schedule but still not really clear. I will propose a plan to have the best strategy of planning and scheduling for production so that the company can overcome the problems

**Keywords:** *Vifa sport, sport industry, production planning and scheduling*

## 1. INTRODUCTION

### 1.1. The importance of production planning and schedule for the study

Production planning and scheduling creates a complete plan based on customer needs and other factors, thereby reducing lead time, cost and increasing company budget.

A good production planning and schedule brings many benefits:

- It gives you an inventory of your entire stock, so you always know what you have and where you need to replenish items.
- It helps HR know in advance how many staff you'll need at any given time.
- It'll help you navigate risks and prevent issues from bringing production to a standstill.
- It helps you avoid stockouts because you know how much raw material you have, how long production will take, and how much you'll need.

### 1.2. Objectives

Provide methods to support the production process, production execution and decision making in order to create the right amount of product to meet the needs of the customer without exceeding the specified inventory level and in a specific time. Vifa sport specializes in outdoor sports products so I will target those product items.

- Find solutions to optimize cost, stock and avoid bottle neck to improve the financial level of the company.
- Take full advantage of the advantage that the company has and plan carefully on people and machines to avoid wasting more time and money.

## 2. METHODOLOGY

### 2.1. Research process

Specify problem: After I got the topic and selected the company as the target, I studied their problems in the production and schedule process including the positives and difficulties they are facing. From there, define the project's objectives that can help overcome the difficulty and set up a math model to get the appropriate solution.

Build mathematical model: After setting up the resolution from the objectives, gather information from sources, journal related to the topic. Mathematical models must come from verified sources. These model will be verified and validated to ensure they are suitable for the project.

Collect data: After having a complete mathematical model, it is now necessary to collect the data to input into the model. Data can be done from looking up the company's documentation, but this way is quite difficult and passive. The fastest and most accurate way is to survey the company and ask the department in charge; here is the

production department. Then I will analyze the data and input it into the model before running it with the support software.

Run model and show output result: The data will be run in the Cplex software and the results will be extracted. The results will be compared with the original data as well as validated to see the appropriateness.

Implementation: After being authenticated, the data model will be judged and applied if conditions are met.

## 2.2. Cplex

The problem will be worked on Cplex. Cplex is very useful in business because it contributes to solving problems and providing logical solutions in decision. It uses a technology to optimize users decisions making which can help optimize business decision, and develop the model with fast, high accuracy. With these functions, it can build and solve complex models that can help solve planning and scheduling problem.

## 2.3. Stochastic programming

It is a framework used to optimize problems involving uncertainty with the goal is to find a solution which is feasible for all such data and optimal in some sense. Stochastic mathematical models have always been proposed to solve problems proportionally in order to provide useful information to a decision-maker.

# 3. MATHEMATICAL MODEL

## 3.1. Materials

**Objective 1:** Minimise the expected costs of inventory and lost sales over the different scenarios where the lost-sales penalty cost  $\gamma^k$  adjusts the conservativeness of the solution:

### Data set:

K:	Set of products $\{1, \dots, K\}$	(products)
A:	Set of raw materials $\{1, \dots, A\}$	(unit of materials)
T:	Set of time periods $\{1, \dots, T\}$	(hours)
W:	Set of production sites $\{1, \dots, W\}$ .	(sites /factories)
N:	Set of scenario $\{1, \dots, N\}$	
L:	Production line $\{1, \dots, L\}$	

### Parameters:

$\mu_{k,w}$ :	Inventory holding cost of product k at site w	(VND)
$v_a$ :	Inventory holding cost of raw material a	(VND)
$f_{k,t}$ :	Demand forecast for product k in period t	(units)
$\beta_{k,a}$ :	Consumption of raw material a per unit of product k l	(units)
$\kappa_l$ :	Capacity of line l	

### Decision variable:

$i_{k,w,t,n}$ :	Inventory of product k on hand at site w at the end of period t in scenario n.	(units)
$Y_{a,t,n}$ :	Inventory of raw material a at the end of period t in scenario n.	(units)
$\gamma^k$ :	Lost-sale penalty cost of product k.	(VND)
$b_{k,t,n}$ :	Lost sales of product k at the end of period t in scenario n.	(units)
$q_{k,l,t}$ :	Production volume of product k on line l in period t.	(units)
$s_{k,w,t,n}$ :	Sales of product k assigned to site w in period t in scenario n.	(units)
$z_{a,t}$ :	Order of raw material a for period t.	(units)

Minimise the expected costs of finished-goods inventory, raw-material inventory and lost sales

$$\sum_{t=1}^T \left( \frac{1}{N} \sum_{k=1}^K \sum_{w=1}^W \mu_{k,w} \sum_{n=1}^N i_{k,w,t,n} + \sum_{a=1}^A v_a * y_{a,t} + \frac{1}{N} \sum_{k=1}^K \gamma^k \sum_{n=1}^N * b_{k,t,n} \right)$$

Subject to:

Describe the inventory balance of finished goods at each production site.

$$i_{k,w,t,n} = i_{k,w,t-1,n} + \sum_{l \in LW} q_{k,l,t} - s_{k,w,t,n} \quad \forall k, w, t, n. \quad (1)$$



Track the demand satisfaction from the sites.

$$f_{k,t,n} = b_{k,t,n} + \sum_{w=1}^W s_{k,w,t,n} \quad \forall k, t, n. \quad (2)$$

Specify that production on a line which is restricted to its feasible portfolio.

$$\sum_{k=1}^K q_{k,l,t} \leq \kappa_l \quad \forall l, t \quad (3)$$

Describe the raw material balance.

$$y_{a,t,n} = y_{a,t-1,n} + z_{a,t} - \sum_{k=1}^K \sum_{l=1}^L \beta_{k,a} * q_{k,l,t} \quad \forall a, n, t \quad (4)$$

### 3.2. Employee resources

Minimize **the total cost of** the process, considering the costs associated with the workers assigned to production, fired workers, hired workers, in addition to inventory costs, backlogs and production.

N: Number of scenarios for capacity production

M: Number of scenarios for demand

T: Time horizon

( $\Omega$ ): Set of random events

i: Possible scenarios for capacity production

j: Possible scenarios for demand

#### Parameter:

$C_p$ : Salary of the production workers per month. (VND)

$C_f$ : Cost of firing a worker. (VND)

$C_r$ : Cost of hiring a worker. (VND)

$C_i$ : Inventory cost per product (VND)

$C_s$ : Backlog cost per product (VND)

$C_x$ : Unit cost of producing a product (VND)

$k_t^i$ : monthly production capacity per worker

#### Decision variable:

$W_{t(H)}^{ij}$ : Number of workers per month (workers)

$P_{t(H)}^{ij}$ : Number of workers assigned to production per month. (workers)

$R_{t(H)}^{ij}$ : Number of hired workers per month (workers)

$F_{t(H)}^{ij}$ : Number of fired workers per month (workers)

$X_{t(H)}^{ij}$ : Number of products to be produced per month (units)

$I_{t(H)}^{ij}$ : Number of products in the inventory per month (units)

$S_{t(H)}^{ij}$ : Backlog per month (units)

#### Objective 2:

Minimize the total cost of the process, considering the costs associated with the workers assigned to production, fired workers, hired workers, in addition to inventory costs, backlogs and production

$$\begin{aligned} & \sum_{j=1}^M \sum_{i=1}^N p^{ijt} \sum_{t=1}^T P_{t(h-1)}^{ij}(\Omega) C_p + \sum_{j=1}^M \sum_{i=1}^N p^{ijt} \sum_{t=1}^T F_{t(h-1)}^{ij}(\Omega) C_f + \sum_{j=1}^M \sum_{i=1}^N p^{ijt} \sum_{t=1}^T R_{t(h-1)}^{ij}(\Omega) C_r + \sum_{j=1}^M \sum_{i=1}^N p^{ijt} \sum_{t=1}^T I_{t(h)}^{ij}(\Omega) C_i \\ & + \sum_{j=1}^M \sum_{i=1}^N p^{ijt} \sum_{t=1}^T X_{t(h)}^{ij}(\Omega) C_x + \sum_{j=1}^M \sum_{i=1}^N p^{ijt} \sum_{t=1}^T S_{t(h)}^{ij}(\Omega) C_s \end{aligned}$$

Subject to:

- Define how many workers will be assigned to production and the number of workers that will be laid off in period  $t$ :

$$W_{t(h)}^{ij} = P_{t(h)}^{ij} + F_{t(h)}^{ij} \quad (1)$$

$$\forall t=2 \dots T, h=1 \dots H$$

- Size of the workforce in the company, total number of workers in period  $t$

$$W_{t(h)}^{ij}(\Omega) = P_{t(h)}^{ij}(\Omega) + F_{t(h)}^{ij}(\Omega) + R_{t(h)}^{ij}(\Omega) \quad (2)$$

$$\forall t=2 \dots T, h=1 \dots H$$

- Production capacity; it ensures that the workers assigned to production can manufacture the units required in period  $t$ .

$$W_{t(h)}^{ij}(\Omega) = W_{t(h-1)}^{ij}(\Omega) + R_{t-1(h-1)}^{ij}(\Omega) - F_{t-1(h-1)}^{ij}(\Omega) \quad (3)$$

$$\forall t=2 \dots T, h=1 \dots H$$

- Balance of demand and inventory in the company

$$X_{t(h)}^{ij}(\Omega) + I_{t(h-1)}^{ij}(\Omega) = D_t^j + S_{t-1(h-1)}^{ij}(\Omega) + I_{t(h)}^{ij}(\Omega) - S_{t(h)}^{ij}(\Omega) \quad (4)$$

$$\forall t=2 \dots T, h=1 \dots H$$

- Ensures that the workers assigned to production can manufacture the units required in period  $t$ .

$$X_{t(h)}^{ij}(\Omega) \leq k_t^{ij} P_{t(h)}^{ij}(\Omega) \quad (5)$$

$$\forall t=2 \dots T, h=1 \dots H$$

- Ensures that the workers assigned to production can manufacture the units required in period  $t$ .

$$D_t^j - S_{t(h)}^i(\Omega) \geq 90 * D_t^j \quad (6)$$

$$\forall t=2 \dots T, h=1 \dots H$$

#### 4. CONCLUSION

Following the momentum, sports services and products are becoming more and more popular in the world. With the increasing demand for sports products and services, the production stage must also be carefully and accurately planned since production planning has a big and important role in satisfying necessary standard. This research work analyzes the production and scheduling plan for Vifa sport, a sport equipment manufacture company by applying Stochastic Programming. The aim of this study is to maximize the profit for the company and propose a reasonable method for production planning and scheduling for a system of many products of the company

#### Acknowledgements

I would like to express my gratitude to my advisor, Professor Duong Vo Nhi Anh for his enthusiastic help during the process of making this paper. He has provided me with a lot of useful practical knowledge as well as appropriate advice to get the best results for me. He was always ready to help me even though he was very busy with his teaching schedule, and thanks to that, the proposal phase of my thesis was completed in the best way. He also supported me with whole-hearted effort for my process too.

#### References

- [1] Alexandre Forel, Martin Grunow (2022). Stochastic programming in master production scheduling: overcoming barriers to industry application
- [2] Jose Emmanuel Gomez-Rocha, Eva Selene Hernandez-Gres, Hector Rivera-Gome (2021). Production planning of a furniture manufacturing company with random demand and production capacity using stochastic programming

## [P-8] Implementation of Lean Six Sigma for Production Process Optimization: A Case Study in ScanCom

Tran Anh Quan\*, Duong Vo Nhi Anh

*Department of Logistics and Supply Chain Management, International University – Viet Nam National University Ho Chi Minh City, Viet Nam*

\*Corresponding author: ielsiu19247@student.hcmiu.edu.vn

### Abstract

**Purpose** – The purpose of this paper is to share the experience and knowledge of optimizing production process by implementing Lean Six Sigma (LSS) in academic manner. Authors are specialist in Logistics and Supply Chain Management with high skills and experience in conducting over 50 paper and conference to the topics of Lean Six Sigma.

**Design/methodology/approach** – The approach is to evaluate the efficiency of the production line through methods such as: OEE to evaluate the overall efficiency of the machine, Value Stream Mapping and Yamazumi to analyze the cycle time of the production line, and pareto charts along with many other root cause analysis methods to analyze defects.

**Findings** – The author initially presents the production process and efficiency of a specified production process ScanCom production line. Then, the author identifies the root cause of inefficiency in the process and suggest solutions.

**Practical Implications** – This paper is conducted to somehow eliminate or reduce the inefficiency in the production process of ScanCom. From a pure practical standpoint, the paper gives the method and calculation of LSS in detail and effectively as a powerful business strategy and problem-solving methodology for all industrial sectors

**Originality/value** – In author best knowledge, there are many journal articles which cover the optimization by using LSS; this paper contributes to the field with carefully analyzed report and insight of the production line. The document of the recent and future in implementing LSS in optimizing production line may use this paper as a strong reference.

**Keywords:** *Lean six sigma, OEE, Yamazumi, Pareto chart, Value stream mapping, Wood product*

## 1. INTRODUCTION

The wood and furniture industry faced significant challenges during and after the Covid-19 pandemic, causing negative fluctuations in exports and a decline in consumer spending. Vietnam's wood exports to the US accounted for 54.4% of the global market in 2022, with 60% going to the US. However, high inflation in the US has impacted the wood business, with many American importers scaling back their purchases. The US market is experiencing record growth in 2021, but exporting furniture to the US remains challenging due to high production costs and inflation. The real estate market is quiet, and businesses exporting exterior and furniture products struggle with a lack of orders and a shortage of new clients. ScanCom, a leading company in the wood chair sector, must focus on product prices, quality standards, and effective after-sales policies to stay competitive. To achieve the above goals, the optimization of the production system is important. Fortunately, Lean Six Sigma is an effective optimization method.

### 1.1. Lean Six Sigma (LSS)

LSS model as proposed by (Crawford, 2004) has presented how Six Sigma can first be applied to improve the processes effectiveness followed by lean to improve the system efficiency. The concept of Lean Six Sigma is a combination of both the Lean and Six Sigma. Lean Six Sigma is a methodology and company strategy that aims to increase process efficiency, client satisfaction, and results. LSS is an effective process management strategy with the goal of reducing variations and eliminating flaws in product production and service processes, which results in excellent business processes. While Six Sigma assists in the identification of process variation and the elimination of quality defects, Lean focuses on speed, efficiency, sources of waste, and improvement methods to

eliminate them (Gibbons et al., 2012). The combination of these two methodologies, known as "Lean Six Sigma", has been used by some organizations even though these methodologies are typically separate. (Antony, 2003; Pojasek, 2003)

LSS is a combination of Lean manufacturing and Six Sigma methodology that brings a multitude of tools to analyze and measure a production line. The main methods used in this paper include: DMAIC, Value Stream Mapping, Yamazumi Chart, Pareto Chart and analysis, Fishbone Diagram.

## 2. METHODOLOGY

First, the need to optimize ScanCom's production line needs to be demonstrated through OEE, Availability, Performance, Quality parameters. After assessing OEE parameters, the condition and suboptimal points in the operation of the production line will be analyzed according to the Six Big Losses of the OEE method.

Second, after analyzing and getting the results of the factors: Availability, Performance, Quality, we analyze the affected factors or in other words that do not meet the standards of the world OEE standard. With performance and quality ratios failing, the next steps will use appropriate methods to analyze the root cause of each of those factors.

Third, analyze performance through value stream mapping analysis and create Yamazumi tables to evaluate the efficiency of each stage that draws the stage or stages that are bottlenecks of the line. From here, use python software to program a program to search for cycle time of suboptimal stages with the goals: increase line output, reduce Tak time, increase balance ratio. Then apply KPI measures and arrange operators to monitor and adjust stage parameters.

Fourth, analyze defect rates by listing and analyzing defects by defect process, and reduced yields of quality inefficiency of Six Big Losses. After having a list of errors, we use the Pareto chart to extract errors that occur repeatedly, seriously affecting the quality of the component or the finished product. Next, use the 5 Why questions method to analyze the root cause of the error.

Fifth, after putting in place specific measures for each issue, make a plan for periodic assessment and monitoring methods to ensure that the measures are applied stably and long-term.

## 3. MEASUREMENT AND ANALYSIS

### 3.1. Output performance

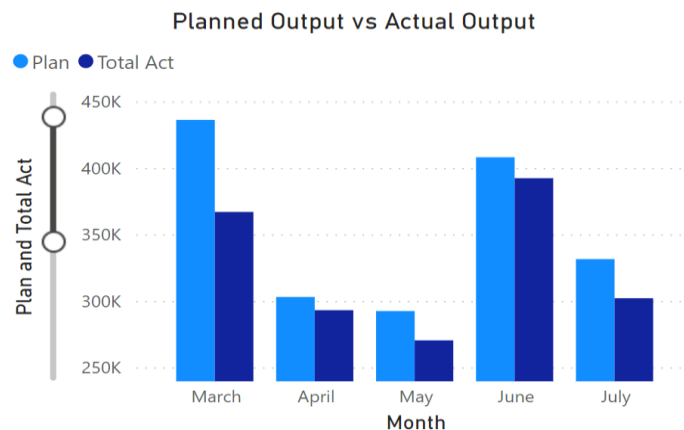


**Figure 1.** Planned output vs Actual output of ScanCom production line of a specific component

Lost Output and Total Act

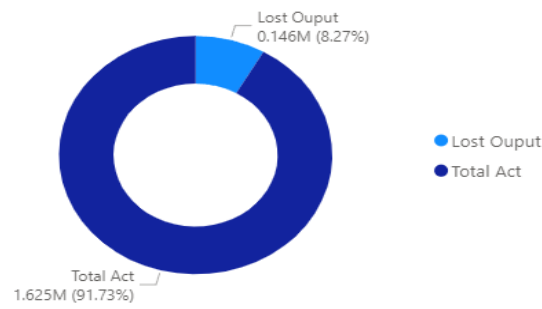


Figure 2. Lost output due to inefficiency vs total actual good output

The lost output takes up to 8.27% of total output lead to the loss of 146 thousand products in 5 months (March – July).

### 3.2. Pareto chart to analyze top inefficiency

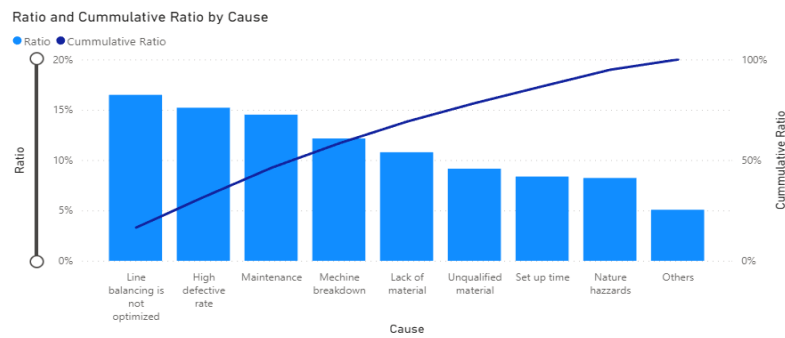


Figure 3. Pareto chart of inefficiency factor in production line

The Production line is not balanced and high defect rate is the main cause for low performance and quality factor in OEE.

### 3.3. OEE value and factors

Table 1. Availability factor

AVAILABILITY RATE BEFORE PROJECT

Month	Downtime (Hour)	Planed Production (Hour)	Run time (Hour)	Avaibility ratio
May	562.3852778	4680	4117.614722	87.98%
Jun	821.9019444	4680	3858.098056	82.44%
July	670.5019444	4680	4009.498056	85.67%
				85%

Table 2. Performance factor

PERFORMANCE BEFORE PROJECT

Month	Output	Operating time	Idea cycle time	Performance Ratio
May	335477	9828000	23	78.51%
Jun	340329	9828000	23	79.65%
July	507155	14742000	23	79.12%
				79.09%

**Table 3.** Product quality factor

PRODUCT QUALITY BEFORE PROJECT

Month	Component Passed	Component Fail	Total	Quality ratio
Apr	209649	60707	270356	78%
May	304865	87473	392338	78%
Jun	232156	69872	302028	77%
				77%

**Table 4.** OEE ratio of the production line

OEE FACTOR BEFORE PROJECT

Month	Quality ratio	Performance Ratio	Availaility ratio	OEE Factor
May	77.55%	79%	87.98%	54%
Jun	77.70%	80%	82.44%	51%
July	76.87%	79%	85.67%	52%
				52%

The 52% of OEE indicate there are inefficiencies in production, namely the Quality and Performance ratio is below OEE global standards, which is 85%.

**3.4. Yamazumi**

**3.4.1. Yamazumi chart**

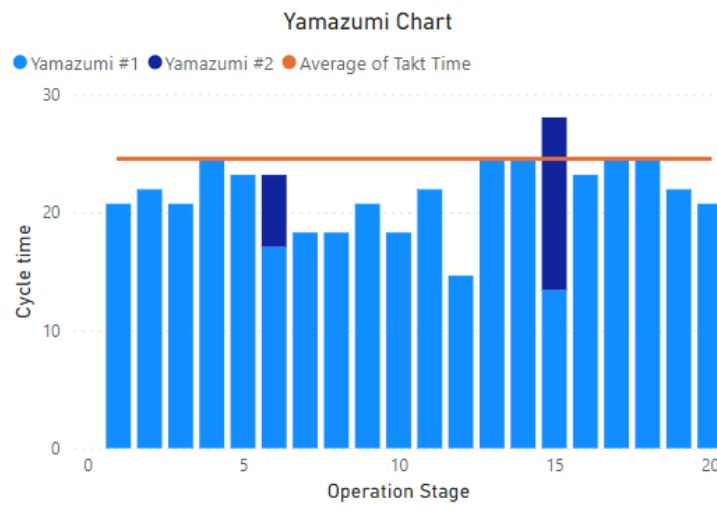


**Figure 4.** Yamazumi chart for production line

Stage 15 exceeds the Takt time while stage 12 is very low compared to other operation stage.

**3.4.2. Error margin of Yamazumi by stage**

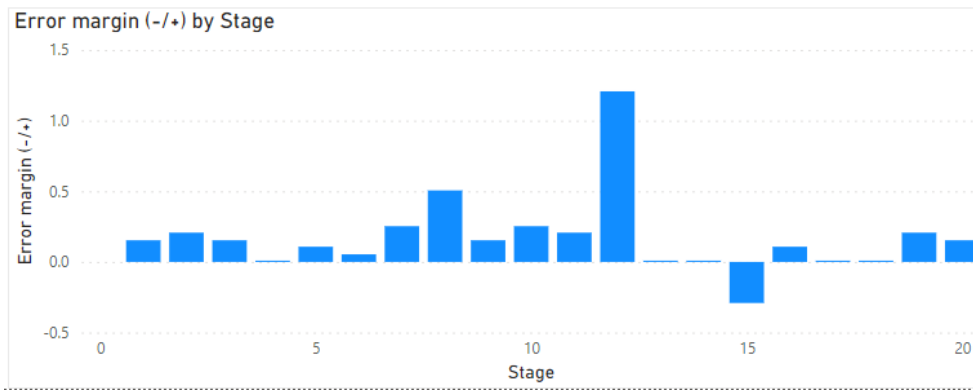


Figure 5. Yamazumi error margin of the production line

The error margin justifies the problem of stage 15 and 12. Stage 15 has negative margin which means it has more time to process than needed. Stage 12 on the other hand has the highest margin which indicates it lack of processing time. Thus, adjustment should take in place to balance these two work station.

3.5. DPMO

Table 5. DPMO value of production line

Process	Opportunity for Error	Total production (pcs)	Total Sample (pcs)	Total defect (pcs)	DPU %	DPMO
AE	63	642,852	15,510	1,446	9.32%	1479.844033
CB	125	272,335	6,150	184	2.99%	239.3495935
WG	79	14,414	14,414	1,626	11.28%	1427.936623
Aging	9					
ES	66	15,451	1,385	131	9.46%	1433.103599
PA	60	17,547	3,511	314	8.94%	1490.553499
Total	402	962,599	40,970	3,701	9.03%	<b>224.7124155</b>

DPMO calculated from sample data indicates the Six Sigma level of the production line is at level 4; there is still inefficiency in the quality, which has to reach to level 5 or above. This shows the quality of product is still at a average level. To be able to increase the product value, root cause has to be addressed and eliminated.

3.6. Value Stream Mapping

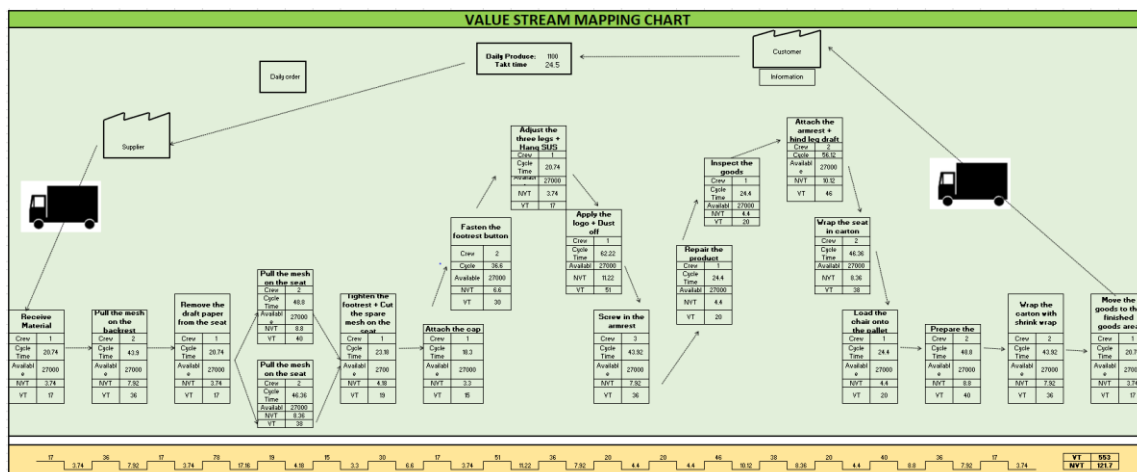


Figure 6. Value Stream Mapping chart for the whole production

4. CONCLUSION

The paper gives analysis and solution to optimize the ScanCom production line by implementing LSS with many of its tools. The result showed the OEE raised significantly and production capacity has increased 50 products, from 1100 products per shift to 1150 per shift.

### References

- [1] Crawford, R. (2004). Ammunition enterprise excellence ready for tomorrow, USA Armor School Research Library.
- [2] Gibbons, P. M., Kennedy, C., Burgess, S., & Godfrey, P. (2012). The development of a value improvement model for repetitive processes (VIM) combining Lean, Six Sigma and systems thinking. *International Journal of Lean Six Sigma*, 3(4), 315-338.
- [3] Pojasek, R. B. (2003). Lean, Six Sigma, and the systems approach: Management initiatives for process improvement. *Environmental Quality Management*, 13(2), 85–92. doi:10.1002/tqem.10113
- [4] Antony, J., Escamilla, J. L., & Caine, P. (2003). Lean sigma. *Manufacturing Engineer*, 82(2), 40-43. doi:10.1049/me:20030203



**[P-10] Application of TSGA, a Hybrid Mega Heuristic Model, to Solve Flow Shop Scheduling Problems with Changeover Times in Operations. A Case Study**Nguyen Nhu Phong<sup>1,\*</sup>, Nguyen Thi Thuy Nhi<sup>1</sup><sup>1</sup> *HCMC University of Technology, Viet Nam*

\*Corresponding author: nnphong@hcmut.edu.vn

**Abstract**

Flow Shop Scheduling (FSS) Problems are NP-hard combinatorial optimization problems. It is quite difficult to achieve an optimal solution for real size problems with mathematical modelling approach because of its NP-hard structure. Mega-heuristics algorithms, like Tabu Search (TS) and Genetic Algorithm (GA), play a major role in searching for near-optimal solutions for NP-hard optimization problems. This paper develops the TSGA model by combining TS and GA for solving FSS problems. In the model, TS is used as the platform for local search, and GA is used to support TS in global search. The performance of the model is compared with traditional heuristic, being used. The result indicates that the model is a good approach for FSS problems.

**Keywords:** *Flow shop scheduling problems, Changeover times, Tabu search, Genetic algorithm*

**1. INTRODUCTION**

Scheduling is the allocation of resources to perform a collection of tasks over a period of time. Scheduling problems determine the order or sequence for processing a set of jobs through several machines in an optimal manner. FSS problems consider  $m$  different machines and  $n$  jobs; each job consists of  $m$  operations and each operation requires a different machine and all the jobs are processed in the same processing order. For FSS problems, Widmer and Hertz presented a heuristic called SPIRIT, composed of two phases: first, get an initial solution to FSS problems by using an analogy with the travelling salesman problem, then improve the initial solution by using TS.

The problem to be solved is a FSS problem with assumption that the orders are ready at the start of the scheduling process. The objective of the problem is to minimize the total weighted tardiness of orders. The constraints are on the sequence of orders, on the sequence of operations in the orders, and on machine changeover time. The model of the problem is built based on the above assumptions, objectives and constraints. The TSGA is built based on the combination of TS and GA with the foundation of TS. Based on the model of the problem, the TSGA will find a good solution for the problem; this solution will be compared with the solution of the currently used heuristic model to evaluate the effectiveness of the algorithm.

**2. LITERATURE REVIEW****2.1. Tabu search**

Tabu search (TS), suggested by Glover and Laguna in 1997, is one of the most popular meta-heuristics to find solutions of various combinatorial optimization problems. In order to apply TS to a problem, generally the solution space of the problem is represented by a population of codes. An evaluation value is associated with each code. The evaluation function is a measure of the extent to which the objective of the problem is achieved. The Fbest value is the best evaluation value, found during the search. TS guides a local search procedure to explore the solution space beyond local optimality. TS allows intelligent problem-solving by the incorporation of adaptive memory and responsive exploration. Key elements of the search path are selectively remembered and strategic choices are made to guide the search out of local optima and into diverse regions.

However, considering every possible move from the current solution may be extremely time-consuming and computationally expensive. In order to avoid cycling and becoming trapped in local optima, certain moves that lead to previously explored regions are forbidden. Attributes of recently visited solutions are set to be tabu for a certain number of iterations, and these moves are stored in the Tabu List. Elements of Tabu List define all tabu moves that cannot be applied to the current solution. The size of Tabu List is bounded by a parameter. The tabu status of a move may be cancelled making it an allowable move if an aspiration criterion is satisfied. A tabu move can be always allowed to be chosen if it creates a solution better than the incumbent best solution.

A typical TS implementation starts from an initial solution and moves from the current solution to the best one among its neighborhoods at each iteration, even if this new solution is worse than the one available, until a pre-specified termination rule becomes true.

## 2.2. Genetic algorithm

Genetic algorithm (GA), first introduced by Holland in 1975, is an artificial intelligence search method that uses the process of evolution and natural selection of individuals called chromosomes. In order to apply GA to a problem, generally the solution space of the problem is represented by a population of chromosomes where each chromosome is a possible solution to the problem. A method of coding is the selection of a string format for the chromosomes. A fitness value is associated with each chromosome. The fitness function is a measure of the extent to which the objective of the problem is achieved. A certain number of chromosomes are chosen to form the initial generation. The chromosomes of the next generation are generated by applying genetic operators, including selection, crossover, mutation and replacement, to the chromosomes of the existing generation.

Starting from an initial population, the algorithm produces a new population of individuals, which are presumably more fit than their ancestors. The process is repeated until a pre-specified termination rule becomes true. At each generation, every new chromosome corresponds to a solution.

## 3. THE FLOW SHOP SCHEDULING PROBLEM

The problem to be solved is a FSS problem with 10 orders,  $O_i$ ,  $i=1 \div 10$ , scheduling on 4 machines, M1, M2, M3, M4. Each order has 3 parts, P1, P2, P3, processed in 8 operations,  $O_j$ ,  $j=1 \div 8$ , distributed on the 4 machines.

	M1	M2	M3	M4
P1	O1	O4	-	O8
P2	O2	O5	O7	
P3	O3	O6	-	

The weight  $W_i$ ,  $i=1 \div 10$ , and the due date  $D_i$ ,  $i=1 \div 10$ , of order  $i$  are estimated in Table 1. The processing time  $P_{ij}$  of order  $i$ ,  $i=1 \div 10$ , on operation  $j$ ,  $j=1 \div 8$ , are estimated in Table 2.

**Table 1.** The weight  $W_i$ ,  $i=1 \div 10$ , and the due date  $D_i$ ,  $i=1 \div 10$ , of order  $i$

$i$	1	2	3	4	5	6	7	8	9	10
$W_i$	3.70	3.40	3.30	4.65	3.90	2.35	2.70	4.55	4.65	4.30
$D_i$ (h)	24	36	40	60	68	80	88	88	96	96

**Table 2.** The processing time  $P_{ij}$  of order  $i$ ,  $i=1 \div 10$ , on operation  $j$

$j$	$P_{1j}$	$P_{2j}$	$P_{3j}$	$P_{4j}$	$P_{5j}$	$P_{6j}$	$P_{7j}$	$P_{8j}$	$P_{9j}$	$P_{10j}$
1	2.34	6.17	6.20	7.09	2.47	9.56	3.44	14.74	5.26	1.39
2	2.25	0.94	7.05	3.22	1.07	5.26	1.81	7.49	5.26	0.66
3	0.00	3.99	4.34	4.38	2.60	9.52	0.00	16.75	14.74	0.44
4	2.63	1.33	1.08	9.00	2.60	12.56	1.32	17.54	16.52	1.29
5	1.06	1.00	6.58	9.00	4.21	12.64	0.65	17.54	16.52	1.29
6	0.00	8.33	6.58	3.60	3.95	12.64	0.00	13.33	15.79	0.40
7	2.67	3.29	1.13	2.21	0.68	4.00	1.11	5.26	1.60	0.44
8	4.08	3.31	3.42	12.00	3.95	6.12	2.21	8.22	5.26	1.32

The changeover times on operation  $j$ ,  $j=4 \div 8$  are equal to 0,  $S_j = 0$ ,  $j=4 \div 8$ . The changeover times on operation  $j$ ,  $j=1 \div 3$  are the same and depend on the current order  $i=1 \div 10$ , and the next order,  $i'=1 \div 10$ , shown as follows.

**Table 3.** Change over time (h)  $S_j$ ,  $j=1 \div 3$

	1	2	3	4	5	6	7	8	9	10
1	0.0	0.5	2.0	0.0	0.0	2.0	2.0	2.0	2.0	2.0
2	0.5	0.0	0.0	0.0	2.0	2.0	2.0	2.0	2.0	2.0
3	2.0	0.0	0.0	2.0	0.5	2.0	0.5	0.5	2.0	0.5
4	0.0	0.0	2.0	0.0	0.0	0.0	2.0	2.0	2.0	2.0
5	0.0	2.0	0.5	0.0	0.0	2.0	0.5	2.0	0.5	0.5

6	2.0	2.0	2.0	0.0	2.0	0.0	0.5	2.0	0.0	0.0
7	2.0	2.0	0.5	2.0	0.5	0.5	0.0	0.5	2.0	0.0
8	2.0	2.0	0.5	2.0	2.0	2.0	0.5	0.0	0.0	0.0
9	2.0	2.0	2.0	2.0	0.5	0.0	2.0	0.0	0.0	2.0
10	2.0	2.0	0.5	2.0	0.5	0.0	0.0	0.0	2.0	0.0

The model is set up with variables  $TS_{ij}$  being the start time,  $TE_{ij}$  being the completion time of order  $i$  at operation  $j$ ,  $T_i$  being the tardiness time of order  $i$ . The constraints on the sequence of operation on each order are as follows.

$$TS_{i4} \geq TE_{i1}, TS_{i5} \geq TE_{i2}, TS_{i6} \geq TE_{i3}, TS_{i7} \geq TE_{i5}, TS_{i8} \geq \max(TE_{i4}, TE_{i6}, TE_{i7}).$$

The start time of order  $i$  at operation  $j$ ,  $TS_{ij}$  depends on the end time of the previous order  $i'$ ,  $TE_{ij}$  and the changeover time between the orders on operation  $j$ .

$$TS_{ij} = TC_{ij} + S_j$$

The end time of order  $i$  on operation  $j$ ,  $TE_{ij}$  is determined by the start time and processing time of the order.

$$TC_{ij} = TS_{ij} + P_{ij}$$

The tardiness time of order  $i$ ,  $T_i$  is determined by the end time in the last operation and due time of the order.

$$T_i = \text{Max}(0, TE_{i8} - D_i)$$

The objective function that minimizes the total tardiness is defined as follows.

$$T_{\text{best}} = \text{Min } T, T = \sum(W_i * T_i, i = 1 \div 11)$$

The company is currently using the EDD dispatching method. The sequence of dispatching  $S$ , the value of the objective function are as follows:

$$S = (1, 2, 3, 4, 5, 6, 7, 8, 9, 10); T = 215.95 \text{ (h)}$$

#### 4. THE TSGA MODEL FOR THE FLOW SHOP SCHEDULING PROBLEM

The above FSS problem is a NP hard problem with the size of the solution space of  $10!$  or 3,628,800. The TSGA model is used to solve the problem. In the model, TS is used to perform a local search, and GA is used to support TS in global search on the solution space. The TSGA procedure is as follows:

Step 1: Initialize the TSGA model.

Step 2: Generate the initial solution  $S_0$ . Set  $k=0$ .

Step 3: Generate the neighbourhood population  $P_N^{(k)}$ .

Step 4: Generate elite population  $P_E^{(k)}$ .

Step 5: Generate the genetic population  $P_G^{(k)}$ .

Step 6: Find the next solution  $S_{k+1}$ . Set  $k = k+1$ ,

Step 7: Check the termination rule. If No, return to step 3. If Yes, finish the loop.

Step 8: Run the algorithm a number of times to choose the best scheduling result.

##### 4.1. Step 1: Initialize the TSGA model.

This step setups factors of TSGA models, including the method of coding, the TS parameters, the GA parameters, and the termination rule.

The method of coding: The orders are numbered from 1 to 10. Each code is a string of 10 numbers. Each number is corresponding to an order. The sequence of numbers  $G_i$ ,  $i=1 \div 10$ , represents the sequence of order scheduled:

$$C = (G1, G2, G3, G4, G5, G6, G7, G8, G9, G10)$$

The **TS parameters** include the evaluation function, the current best value, the parameters of the TS operators, and the Tabu List. The evaluation function is the objective function  $T$ , used to evaluate scheduling codes. The current best value  $T_{\text{best}}$  is the best objective value, updated after each iteration. The TS operators include the neighbourhood and the search operator. The neighbourhood operator uses the method of permutation of adjacent numbers in the string to find the neighbourhood. The search operator finds the best solution in the neighbourhood solution region to prepare for the next iteration, if any. This solution must not be on the tabu list. Tabu List will contain the solutions found in the previous loops, and is updated after each iteration.

The **GA parameters** include the fitness function, and the parameters of GA operators. The fitness function  $F$  is defined as  $F_i = T_{\text{max}} - T_i$ . Where  $F_i$ ,  $T_i$  are the fitness and objective values of chromosome  $i$ ,  $T_{\text{max}}$  is the maximum objective value in the population. The crossover method is POX (Precedence Operation Crossover), the mutation method is SWAP. The crossover probability  $P_c$ , the mutation probability  $P_m$  are chosen as follows:

$$P_c = 0.8; P_m = 0.2.$$

**The termination rule:** The best objective value  $T_{best}$  does not improve after 10 consecutive iterations.

#### 4.2. Step 2: Generate the initial population $P^{(0)}$ , set $k = 0$ .

A good initial solution will be a good starting point for the search. The initial solution is often chosen by heuristic methods. With the objective of minimizing lateness, the initial solution selected from the EDD method is represented as the following string:

$$S_0 = (1, 2, 3, 4, 5, 6, 7, 8, 9, 10); \text{Tabu list} = \{S_0\}; T_{best} = 215.95.$$

#### 4.3. Step 3: Generate the neighbourhood population $P_N^{(k)}$ .

This step uses the neighbourhood operator to generate the neighbourhood population  $P_N^{(k)}$  from the current string. The neighbourhood population  $P_N^{(0)}$  generated from the initial string is as follows.

**Table 4.** The neighbourhood population  $P_N(0) = \{N1, N2, N3, N4, N5, N6, N7, N8, N9\}$

$P^{(0)}$	G1	G2	G3	G4	G5	G6	G7	G8	G9	G10	$T_i$
N1	2	1	3	4	5	6	7	8	9	10	224.60
N2	1	3	2	4	5	6	7	8	9	10	203.75
N3	1	2	4	3	5	6	7	8	9	10	242.49
N4	1	2	3	5	4	6	7	8	9	10	175.90
N5	1	2	3	4	6	5	7	8	9	10	241.39
N6	1	2	3	4	5	7	6	8	9	10	221.26
N7	1	2	3	4	5	6	8	7	9	10	224.11
N8	1	2	3	4	5	6	7	9	8	10	239.71
N9	1	2	3	4	5	6	7	8	10	9	175.65

#### 4.4. Step 4: Generate elite population $P_E^{(k)}$ .

This step uses the selection operator to generate  $P_E^{(k)}$  from  $P_N^{(k)}$ . Each chromosome in  $P_N^{(k)}$  has a corresponding fitness value  $F_i$ , and is selected for inclusion in  $P_E^{(k)}$  with selection probability  $P_i$  as follows:

$$P_i = F_i / \sum_{i=1}^{10} F_i$$

With population  $P_N^{(0)}$  the values of  $F_i$  and  $P_i$  are calculated as shown in the following table.

**Table 5.** The values of  $F_i$  and  $P_i$  of strings in  $P_N(0)$

$P_N^{(0)}$	G1	G2	G3	G4	G5	G6	G7	G8	G9	G10	$F_i$	$P_i$
N1	2	1	3	4	5	6	7	8	9	10	17.89	0.08
N2	1	3	2	4	5	6	7	8	9	10	38.74	0.17
N3	1	2	4	3	5	6	7	8	9	10	0.00	0.00
N4	1	2	3	5	4	6	7	8	9	10	66.59	0.29
N5	1	2	3	4	6	5	7	8	9	10	1.10	0.00
N6	1	2	3	4	5	7	6	8	9	10	21.23	0.09
N7	1	2	3	4	5	6	8	7	9	10	18.38	0.08
N8	1	2	3	4	5	6	7	9	8	10	2.78	0.01
N9	1	2	3	4	5	6	7	8	10	9	66.84	0.29

Based on  $P_i$ , 10 random numbers are generated, the strings, selected into  $PE(0)$  are as follows:

$$P_E^{(0)} = \{N1, N2, N3, N4, N5, N1, N7, N4, N4\}$$

#### 4.5. Step 5: Generate the genetic population $P_G^{(k)}$ .

This step uses the crossover and mutation operators to generate genetic population  $P_G^{(k)}$  from the elite population  $P_E^{(k)}$ . The genetic population  $P_G^{(k)}$  includes the new strings generated from the crossover and mutation operators. The strings of  $P_E^{(0)}$  are selected to be included in the crossover list  $P_c$  with the crossover probability of 0.8. After generating random numbers, the set  $P_c$  is determined as follows:

$$P_c = \{N1, N3, N4, N5\}$$

Each pair of strings in  $P_c$  is selected to cross over by the POX method, resulting in 12 new strings in population  $P^C$  as shown in the following table.

**Table 6.** The population  $P^C$ 

$P^C$	G1	G2	G3	G4	G5	G6	G7	G8	G9	G10	T <sub>i</sub>
C1	1	2	3	4	5	6	7	8	9	10	215.95
C2	1	4	3	2	5	6	7	8	10	9	254.34
C3	1	4	3	2	5	7	6	8	9	10	294.78
C4	1	4	3	2	5	6	7	8	10	9	294.78
C5	1	2	3	4	5	6	7	8	9	10	215.95
C6	1	4	3	2	5	6	7	8	10	9	254.34
C7	1	4	3	2	5	7	6	8	9	10	294.78
C8	1	2	3	4	5	6	7	8	9	10	215.95
C9	1	4	3	2	5	6	7	8	10	9	254.34
C10	1	4	3	2	5	7	6	8	9	10	294.78
C11	1	4	3	2	5	6	7	8	10	9	254.34
C12	1	2	3	4	5	6	7	8	9	10	215.95

The strings of  $P_E^{(0)}$  are also selected to be included in the mutation list  $P_m$  with the mutation probability of 0.2. After generating random numbers, the set  $P_m$  is determined as follows:

$$P_m = \{N5\}$$

Each chromosome in  $P_m$  is selected to mutate by the SWAP method, resulting in new chromosomes in population  $P^M$  as shown in the following table.

**Table 7.** The population  $P^M$ 

$P^M$	G1	G2	G3	G4	G5	G6	G7	G8	G9	G10	T <sub>i</sub>
M1	1	10	3	4	6	5	7	8	9	2	185.62

After crossover and mutation, 13 new chromosomes are created in  $P_G(0)$ :

$$P_G(0) = \{C1, C2, C3, C4, C5, C6, C7, C8, C9, C10, C11, C12, M1\}$$

#### 4.6. Step 6: Find the next solution $S_{k+1}$ .

This step uses the search operator to find the best solution in the solution regions defined by  $P_N(k)$  and  $P_G(k)$ . The search operator relies on the objective function and the Tabu List to find the best solution that is not in the Tabu List. This solution will be selected for the next iteration, if any. This step also updates the Tabu List and the current best Tbest if the objective value of the solution is better than the current Tbest.

At iteration 1, based on  $P_N^{(k)}$ ,  $P_G^{(k)}$  and current tabu list the next solution is:

$$N9 = (1, 2, 3, 4, 5, 6, 7, 8, 10, 9); TL = \{S_0, N9\}; Tbest = 175.65.$$

#### 4.7. Step 7: Check the termination rule.

After iteration 1, N1 is the best string with the best objective value of 175.65, appearing only once. The termination rule is not satisfied, so iteration 2 is executed. The result after 16 iterations is as follows.

**Table 8.** The result after 16 iterations

Iteration	G1	G2	G3	G4	G5	G6	G7	G8	G9	G10	Tbest
0	1	2	3	4	5	6	7	8	9	10	215.95
1	1	2	3	4	5	6	7	8	10	9	175.65
2	1	2	3	5	4	6	7	8	10	9	135.60
3	1	2	3	5	4	6	7	8	10	9	135.60
4	1	2	3	5	4	6	7	8	10	9	135.60
5	1	2	3	5	4	6	7	8	10	9	135.60
6	1	2	3	4	5	10	8	7	9	6	129.87
...	1	2	3	4	5	10	8	7	9	6	129.87
16	1	2	3	4	5	10	8	7	9	6	129.87

The best objective value Tbest remains the same from the 6th iteration to the 16th iteration, the termination rule is satisfied, the algorithm ends. The scheduling result in this run is as follows:

$$S = (1, 2, 3, 4, 5, 10, 8, 7, 9, 6), T_{best} = 129.87 \text{ (h)}$$

#### 4.8. Step 8: Run the algorithm a number of times to choose the best scheduling result.

The algorithm is run 5 times with the results as shown in the following table.

**Table 9.** The results after 5 runs

Run	G1	G2	G3	G4	G5	G6	G7	G8	G9	G10	L	NoI
1	1	2	3	4	5	10	8	7	9	6	129.87	16
2	1	3	2	4	5	7	8	9	10	6	124,67	18
3	1	3	2	4	5	7	8	9	10	6	124,67	14
4	1	3	2	4	5	10	8	7	9	6	123.07	16
5	1	3	2	4	5	10	8	7	9	6	123.07	14

The best scheduling result is found on the 5th run, with a number of iterations NoI of 14. The sequence of dispatching S, the value of the objective function are as follows:

$$S = (1, 3, 2, 4, 5, 7, 8, 9, 10, 6); L = 123.07$$

The objective value according to TSGA model (123.07 h) is better than the objective value according to the EDD heuristic currently used (215.95 h).

## 5. CONCLUSION

The TSGA model has been constructed and used to solve the Flow Shop Scheduling Problem with 10 jobs on 4 machines. In the model, TS is used as the platform to perform a local search of the solution space, and GA is used to perform a global search to support TS. The results show that the TSGA model gives better objective value of tardiness time than the heuristic EDD method, being used. However, the factors of the model, including the method of finding the neighbourhood strings, the crossover probability  $P_c$ , the mutation probability  $P_m$ , the method and parameter of the termination rule, are only selected empirically, so the results are not very good. The future research is to use experimental design DOE to determine the model parameters to get better suboptimal results.

## References

- [1] Etiler, B Toklu, M Atak, Jwilson. A genetic algorithm for flow shop scheduling problems, Journal of the Operational Research Society (2004) 55, 830–835.
- [2] Moch Saiful Umam, Mustafid Mustafid, Suryono Suryono. A hybrid genetic algorithm and tabu search for minimizing makespan in flow shop scheduling problem. Computer and Information Sciences 34 (2022) 7459–7467.
- [3] Hakimi, Oyewola, Yahaya, Bolarin. Comparative Analysis of Genetic Crossover Operators in Knapsack Problem, J. Appl. Sci. Environ. Manage. Sept. 2016, 20(3), 593-596.
- [4] Justin Schrack, Roy Ortega, Kevin Dabu, Daniel Truong, Michal Aibin, Ania Aibin. Combining Tabu Search and Genetic Algorithm to Determine Optimal Nurse Schedules, 2021.

- [5] Farhad Kolahan, Ahmad Tavakoli, Behrang Tajdin, Modjtaba Hosayni. Analysis of neighborhood generation and move selection strategies on the performance of Tabu Search, Proceedings of the 6th WSEAS International Conference on Applied Computer Science, Tenerife, Canary Islands, Spain, December 16-18, 2006.
- [6] Yunus Demira, Selçuk Kürşat İşleyen. An effective genetic algorithm for flexible job-shop scheduling with overlapping in operations, International Journal of Production Research, 2014.
- [7] Kevin Boston, Pete Bettinger. Combining Tabu Search and Genetic Algorithm Heuristic Techniques to Solve Spatial Harvest Scheduling Problems, Forest Science 48(1), 2002.
- [8] Jatinder N. D. Gupta. Designing a tabu search algorithm for the two-stage flow shop problem with secondary criterion, Production Planning & Control: The Management of Operations, 10(3), 251-265.
- [9] Ahmad Hassanat, Khalid Almohammadi, Esra'a Alkafaween, Eman Abunawas, Awni Hammouri, V. B. Surya Prasath. Choosing Mutation and Crossover Ratios for Genetic Algorithms-A Review with a New Dynamic Approach, Information 2019, 10, 390.
- [10] Burduk A., Musiał K., Kočańska J., Górnicka D., Stetsenko A., 2019. Tabu Search and genetic algorithm for production process scheduling problem, LogForum 15(2), 181-189.

## [P-11] Application of Tabu Search to Solve Parallel Machine Scheduling Problems with Capacity Constraints. A Case Study

Nguyen Nhu Phong\*, Nguyen Nhat Ha

*HCMC University of Technology, Viet Nam*

\*Corresponding author: nnphong@hcmut.edu.vn

### Abstract

Parallel Machines Scheduling (PMS) problems are combinatorial optimization problems. It is quite difficult to achieve an optimal solution for real size problems with mathematical modeling approaches because of its NP-hard structure. Meta-heuristics algorithms, like Tabu Search (TS), play a major role in searching for near-optimal solutions for NP-hard optimization problems. This paper develops a TS model for solving PMS problems. The performance of the model is compared with the traditional heuristic, being used. The result indicates that the model is a good approach for PMS problems.

**Keywords:** *Parallel machines scheduling, Tardiness, Setup times, Capacity constraints, Tabu search*

### 1. INTRODUCTION

Scheduling is the allocation of resources to perform a collection of tasks over a period of time. Scheduling problems determine the order or sequence for processing a set of jobs through several machines in an optimal manner.

Parallel Machine Scheduling (PMS) problems consider dispatching  $n$  jobs on  $m$  parallel machines. A job can be performed on any of the machines. Machines can be homogeneous or heterogeneous. Machines are homogenous when they have the same processing time for each job. Machines are heterogeneous when the times to process the same job on different machines are different.

The problem to be solved is a PMS problem with assumption that all orders and all machines are ready at the start of the scheduling process. The objective of the problem is to minimize the total weighted tardiness of orders. The constraints are on the capabilities and setup times of the machines, on the order execution sequence on each machine, and on the order processing times.

The model of the problem is built based on the above assumptions, objective and constraints. The TS algorithm is built. Based on the model of the problem, the TS algorithm will find a good solution for the problem; this solution will be compared with the solution of the currently used heuristic model to evaluate the effectiveness of the TS algorithm.

### 2. LITERATURE REVIEW

#### 2.1. Parallel machine scheduling

Production mode using parallel machines for processing in practice has actually been widely applied on various kinds of industries. The scheduling problems of parallel machines are always of special interest.

Objectives of parallel machines scheduling are to increase throughput, reduce production cycle time and tardiness, and enhance machine utilisation.

Theoretically, scheduling problem of parallel machines can be found into two steps. Firstly, it must determine whichever task is to be processed at which machine, and processing order of task is allocated to each machine afterward (Pinedo, 2002).

When parallel machines are processing different types of orders, there will also be problems of set-up times. Considering set-up times in the study is necessary when parallel machines handle different types of jobs. The primary goal is to enhance validity of applying parallel machines in manufacturing.

When the number of machines increases, even optimised mathematical programming is hard to demonstrate its effect. As such, many intelligent search methods have, in sequence, been put forth, and gradually become the resolution methods for streamlined scheduling problem. Among these, GAs, Simulated Annealing (SA) and Tabu Search (TS) are considered as those most often used.



## 2.2. Tabu search

Tabu search (TS), suggested by Glover and Laguna in 1997, is one of the most popular meta-heuristics to find solutions of various combinatorial optimization problems.

In order to apply TS to a problem, generally the solution space of the problem is represented by a population of codes. Each code is a possible solution to the problem. Codes are represented by strings. A method of coding is the selection of a string format for the codes.

An evaluation value is associated with each code. The evaluation function is a measure of the extent to which the objective of the problem is achieved. The evaluation function is derived from the objective function of the problem. The Fbest value is the best evaluation value, found during the search.

TS guides a local search procedure to explore the solution space beyond local optimality. TS allows intelligent problem solving by the incorporation of adaptive memory and responsive exploration. Key elements of the search path are selectively remembered and strategic choices are made to guide the search out of local optima and into diverse regions.

However, considering every possible move from the current solution may be extremely time consuming and computationally expensive. In order to avoid cycling and becoming trapped in local optima, certain moves that lead to previously explored regions are forbidden. Attributes of recently visited solutions are set to be tabu for a certain number of iterations, and these moves are stored in the Tabu List. Elements of tabu list define all tabu moves that cannot be applied to the current solution. The size of Tabu List is bounded by a parameter.

The tabu status of a move may be cancelled making it an allowable move if an aspiration criterion is satisfied. A tabu move can be always allowed to be chosen if it creates a solution better than the incumbent best solution.

A typical TS implementation starts from an initial solution and moves from the current solution to the best one among its neighbourhoods at each iteration, even if this new solution is worse than the one available, until a pre-specified termination rule becomes true.

## 3. THE PARALLEL MACHINE SCHEDULING PROBLEM

The problem to be solved is a PMS problem with 11 orders,  $O_i$ ,  $i = 1 \div 11$ , scheduling on 3 parallel machines,  $M_j$ ,  $j = 1 \div 3$ .

The scheduling problem is done in two steps. Step 1 allocates orders to machines. Step 2 determines the order sequence on each machine. The order allocation step determines which orders are processed on each machine; this step is subject to machine capacity constraints.

In this case, orders 4 and 6 can only be processed on M3, the remaining orders can be processed on all 3 machines. The weight  $W_i$ , the due date  $D_i$ , the processing time  $P_{ij}$ ,  $i = 1 \div 11$ , of order  $i$  are estimated in the following table.

**Table 1.** Order attributes

<b>i</b>	1	2	3	4	5	6	7	8	9	10	11
<b>W<sub>i</sub></b>	3	3	1	1	3	1	3	2	1	3	3
<b>D<sub>i</sub>(h)</b>	24	24	24	24	24	48	48	48	48	48	48
<b>P<sub>i</sub>(h)</b>	11.67	12.6	21.39	12.77	11.61	14.14	21.7	12.4	12.5	9.19	8.17

The changeover times from orders  $i'$  to order  $i$ ,  $S_{i'i}$  are the same for all machines:

$$S_{i'i} = [ 0.5h, \text{ if } (i', i) \in \{(1,2), (2,1), (2,11), (11,2), (4,6), (6,4), (7,8), (8,7)\}; 0h \text{ if } (i', i) \in \{(1,11), (11,1)\}, 2.5h \text{ otherwise}$$

After performing the step of allocating orders to machines. The start time of order  $i$  at machine  $j$ ,  $TS_{ij}$  depends on the end time of the previous order  $i'$ ,  $TE_{i'j}$  and the changeover time between the orders.

$$TS_{ij} = TE_{i'j} + S_{i'i}$$

The end time of order  $i$  on machine  $j$ ,  $TE_{ij}$  is determined by the start time and processing time of the order.

$$TE_{ij} = TS_{ij} + P_i$$

The tardiness time of order  $i$ ,  $T_i$  is determined by the end time and due time of the order.

$$T_i = \text{Max} (0, TE_{ij} - D_i)$$

The objective function that minimizes the total weighted tardiness is defined as follows.

$$T_{\text{best}} = \text{Min } T, T = \sum w_i * T_i, i = 1 \div 11)$$

The company is currently using the EDD dispatching method. The sequence of dispatching  $S$  on machine M1, M2, M3, the value of the objective function, and the Gantt Chart are as follows:

$$S = (1-5-7-8, 2-3-10-11-9, 4-6); T = 105.13 \text{ (h)}$$



Figure 1. The Gantt Chart by EDD

#### 4. THE TS MODEL FOR THE PMS PROBLEM

The above PMS problem is a non-linear problem and is solved by a TS model. The TS procedure is as follows:

- Step 1: Initialize the TS model.
- Step 2: Generate the initial solution  $S_0$ . Set  $k = 0$ .
- Step 3: Generate the neighbourhood population  $P_N^{(k)}$ .
- Step 4: Find the next solution  $S_{k+1}$ . Set  $k = k+1$ ,
- Step 5. Check the termination rule. If No, return to step 3. If Yes, finish the loop.

##### Step 1: Initialize the TS model.

This step setups factors of TS models, including the method of coding, the TS parameters, and the termination rule.

**The method of coding:** The orders are numbered from 1 to 11. Each code is a string of 3 sub-strings, corresponding to 3 machines,  $M_j$ ,  $j=1\div 3$ . Each sub-string corresponds to orders allocated for a machine. For example, the string by EDD is as follows:

$$S = (1-5-7-8, 2-3-10-11-9, 4-6)$$

**The TS parameters** include the evaluation function, the current best value, and the parameters of the TS operators, including the neighbourhood and search operators, and the Tabu list.

The evaluation function is the objective function  $T$ , used to evaluate scheduling strings. The current best value  $T_{best}$  is the best objective value, updated after each iteration. The neighbourhood operator uses the method of permutation of adjacent numbers in the string to find the neighbourhood.

The neighbourhood operator creates the neighbourhood region of a solution using two methods, SWAP and INSERT. The SWAP method swaps between any 2 orders in the same machine. The INSERT method inserts an order in any position on the remaining machines.

The search operator finds the best solution in the neighbourhood solution region to prepare for the next iteration, if any. This solution must not be on the Tabu list. Tabu list contains all moves in the previous loops, and is updated after each iteration. Tabu list size is chosen 9.

In an iteration, if INSERT is used, Tabu list will store a code segment of the string moving to the best string. This segment consists of 2 orders, the insert order and its side order. If using SWAP, Tabu list will store 2 code segments of the 2 permutation strings. Each of these segments consists of 2 orders, the swap order and its side order. If the insert or swap order is at the beginning of the string, its side order is behind it. If not, the side order is in front of it.

**The termination rule:** The best objective value  $T_{best}$  does not improve after 40 consecutive iterations.

##### Step 2: Generate the initial solution $S_0$ , set $k=0$ .

A good initial solution will be a good starting point for the search. The initial solution is often chosen by heuristic methods, SPT, LPT, EDD. The strings and corresponding objective values of the methods are as follows:

- SPT:  $S = (11-5-8-2-7, 10-1-9-3, 4-6)$ ;  $T = 202.51$  (h)
- LPT:  $S = (7-9-1-5, 2-3-8-10-11, 6-4)$ ;  $T = 362.9$  (h)

– EDD:  $S = (1-5-7-8, 2-3-10-11-9, 4-6)$ ,  $T = 105.13$  (h)

With the objective of minimizing total weighted tardiness, the initial solution is generated from the EDD method:

$$S_0 = (1-5-7-8, 2-3-10-11-9, 4-6); \text{Tabu list} = \emptyset; \text{Tbest} = 105.13.$$

From the initial solution  $S_0$ , iteration 1 is executed with step 3, 4, 5.

### Iteration 1

#### Step 3: Generate the neighbourhood population $P_N^{(0)}$ .

This step uses the neighbourhood operator to generate the neighbourhood population  $P_N^{(0)}$  from the current string  $S_0$ .

From string  $S_0$ , use SWAP and INSERT methods to find neighbouring strings. For example, swapping orders 1 and 5 in the machine 1 will get the string  $S_1$  as follows.

$$S_0 = (1-5-7-8, 2-3-10-11-9, 4-6) \rightarrow S_1 = (5-1-7-8, 2-3-10-11-9, 4-6)$$

Inserting order 2 in machine 2 before order 4 in machine 3 will get the string  $S_2$  as follows.

$$S_0 = (1-5-7-8, 2-3-10-11-9, 4-6) \rightarrow S_{02} = (5-1-7-8, 3-10-11-9, 2-4-6)$$

The 2 methods SWAP and INSERT will generate 113 strings in the neighbourhood population  $P_N^{(0)}$  from the current string  $S_0$ .

#### Step 4: Find the next solution $S_1$ .

This step uses the search operator to find the best solution in the solution regions defined by  $P_N^{(0)}$ . The search operator relies on the objective function and the Tabu list to find the best solution that is not in the Tabu list. This solution will be selected for the next iteration, if any. This step also updates the Tabu list and the current best Tbest if the objective value of the solution is better than the current Tbest.

The best string in the neighbouring population  $P_N^{(0)}$  without violating Tabu list is as follows.

$$S_0 = (1-5-7-8, 2-3-10-11-9, 4-6) \rightarrow S_1 = (1-5-7-8, 3-10-11-9, 2-4-6)$$

In this iteration, the objective value of  $S_1$  is 51.39 (h), which is less than the current best of 105.13 (h). The current best Tbest is updated to the value of 51.39 (h). The Tabu list, TL is also updated as follows.

$$\text{Tbest} = 51.39 \text{ (h)}; \text{TL} = \{2-3\}$$

#### Step 5: Check the termination rule.

After iteration 1,  $S_1$  is the best string with the best objective value of 51.39, appearing only once. The termination rule is not satisfied, so iteration 2 is executed.

### Iteration 2

#### Step 3: Generate the neighbourhood population $P_N^{(1)}$ .

This step uses the neighbourhood operator to generate the neighbourhood population  $P_N^{(1)}$  from the current string  $S_1$ . As in iteration 1, the 2 methods SWAP and INSERT will generate 113 strings in the neighbourhood population  $P_N^{(1)}$  from the current string  $S_1$ .

#### Step 4: Find the next solution $S_2$ .

This step uses the search operator to find the best solution in the solution regions defined by  $P_N^{(1)}$ . The best string  $S_2$  in the neighbouring population  $P_N^{(1)}$  is generated from the current string  $S_1$  by inserting order 8 in machine 1 to the position in front of order 6 in machine 3.

$$S_1 = (1-5-7-8, 3-10-11-9, 2-4-6) \rightarrow S_2 = (1-5-7, 3-10-11-9, 2-4-8-6)$$

The string  $S_2$  does not violate Tabu list and has the objective value of 33.30 (h), which is less than the current best of 51.39 (h). The current best Tbest is updated to the value of 33.30 (h). The Tabu list, TL is also updated as follows.

$$\text{Tbest} = 33.30 \text{ (h)}; \text{TL} = \{7-8, 2-3\}$$

**Step 5: Check the termination rule.**

After iteration 2,  $S_2$  is the best string with the best objective value of 33.30, appearing only once. The termination rule is not satisfied, so iteration 3 is executed.

**Iteration 3**

**Step 3: Generate the neighbourhood population  $P_N^{(2)}$ .**

This step uses the neighbourhood operator to generate the neighbourhood population  $P_N^{(2)}$  from the current string  $S_2$ . As in previous iterations, the 2 methods SWAP and INSERT will generate 111 strings in the neighbourhood population  $P_N^{(2)}$  from the current string  $S_2$ .

**Step 4: Find the next solution  $S_3$ .**

This step uses the search operator to find the best solution in the solution regions defined by  $P_N^{(2)}$ . The best string  $S_3$  in the neighbouring population  $P_N^{(2)}$  is generated from the current string  $S_2$  by swapping orders 1 and 5 in machine 1.

$$S_2 = (1-5-7, 3-10-11-9, 2-4-8-6) \rightarrow S_3 = (5-1-7, 3-10-11-9, 2-4-8-6)$$

The string  $S_3$  does not violate tabu list and has the objective value of 33.30 (h), which is the same as the current best of 33.30 (h). The current best  $T_{best}$  remain unchanged (h). The tabu list, TL is also updated as follows.

$$T_{best} = 33.30 \text{ (h)}; TL = \{1-5, 7-8, 2-3\}$$

**Step 5: Check the termination rule.**

After iteration 3,  $S_3$  is the best string with the best objective value of 33.30, appearing only twice. The termination rule is not satisfied, so iteration 4 is executed.

The results after 86 iterations are shown in the following table.

**Table 2.** The results after 86 iterations

Iteration	0	1	2	3	4	5	6	7	8	9	...
<b>T</b>	51.38	33.3	33.3	33.3	33.3	39.53	45.65	30.96	38.13	38.13	...
<b>Tbest</b>	51.38	33.29	33.29	33.3	33.3	33.3	33.3	30.96	30.96	30.96	...
Iteration	...	46	47	48	49	50	51	52	53	...	86
<b>T</b>	...	36.58	28.43	31.44	36.91	40.79	43.05	43.05	44.72	...	33
<b>Tbest</b>	...	28.43	28.43	28.43	28.43	28.43	28.43	28.43	28.43	...	28.43

The best objective value remains the same from the 46th iteration to the 86th iteration, the termination rule is satisfied, the algorithm ends. The scheduling result is as follows:

$$S = (3-7-9, 5-1-11-8, 2-4-10-6), T = 28.43 \text{ (h)}$$

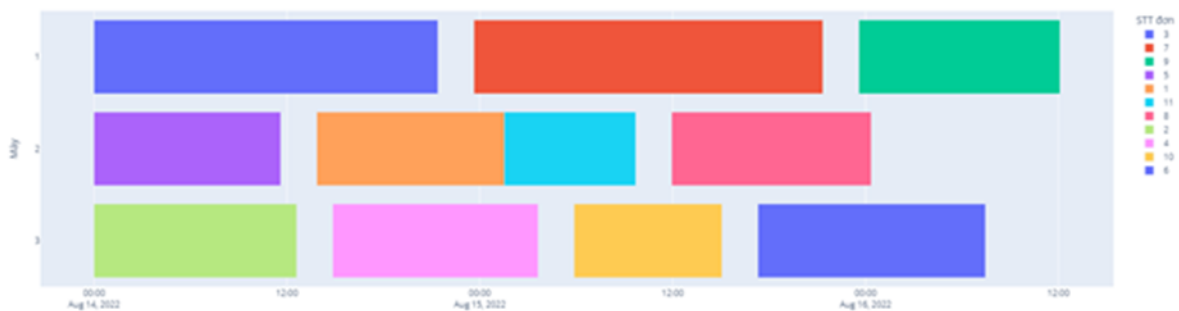


**Figure 2.** The Gant chart by TS algorithm

The objective value according to the TS scheduling model, that is 28.43 (h), is better than the objective value according to the current EDD scheduling model that is 28.43 (h).

## 5. CONCLUSION

The TS model is used to solve the Parallel Machines Scheduling Problem with 11 jobs on 3 parallel machines. The results show that the TS model gives better objective value of tardiness time than the heuristic EDD method, being used. However, the factors of the model, including the method of finding the neighbourhood strings, the method and the parameter of the termination rule, are only selected empirically, so the results are not very good. Future research is to use experimental design DOE to determine the model parameters to get better suboptimal results.

## References

- [1] Jae-Ho Lee & Jae-Min Yu & Dong-Ho Lee, “A tabu search algorithm for unrelated parallel machine scheduling with sequence- and machine-dependent setups: minimizing total tardiness”. *International Journal of Advanced Manufacturing Technology*, 69 (2013), pp. 2081-2089.
- [2] Johnny C. Ho, Yih-Long Chang, “Minimizing the number of tardy jobs for m parallel machines”. *European Journal of Operational Research*, 84 (1993), pp. 343-355
- [3] Magdy Helal, Ghaith Rabadi, and Ameer Al-Salem, “A Tabu Search Algorithm to Minimize the Makespan for the Unrelated Parallel Machines Scheduling Problem with Setup Times”. *International Journal of Operations Research*, Vol. 3, No. 3 (2006), pp. 182-192
- [4] Umit Bilge, Furkan Kirac, Mukde Kurtulan, Pelin Pekgun, “A tabu search algorithm for parallel machine total tardiness problem”. *Computers & Operations Research*, 31 (2002), pp. 397-414

**[P-13] Application of GATS, a Hybrid Mega Heuristic Model, to Solve Flexible Flow Shop Scheduling Problems with Setup and Batch Production. A Case Study**

Nguyen Nhu Phong\*, Nguyen Le Thu Trang

*HCMC University of Technology, Viet Nam*

\*Corresponding author: nnphong@hcmut.edu.vn

**Abstract**

Flexible Flow Shop Scheduling (FFSS) problems are NP-hard combinatorial optimization problems. It is quite difficult to achieve an optimal solution for real size problems with mathematical modelling approaches because of its NP-hard structure. Mega-heuristics algorithms, like Genetic Algorithm (GA) and Tabu Search (TS) play a major role in searching for near-optimal solutions for NP-hard optimization problems. This paper develops a GATS model by combining GA and TS for solving FFSS problems. In the model, GA is used as the platform for global search, and TS is used to support GA in local search. The performance of the model is compared with traditional heuristics, being used. The result indicates that the model is a good approach for FFSS problems.

**Keywords:** *Flexible flow shop scheduling, Mathematical modelling, Parallel machines, Setup time, Batch production, Hybrid mega heuristic, Genetic algorithm, Tabu search*

**1. INTRODUCTION**

Scheduling problems determine the order or sequence for processing a set of jobs through several machines in an optimal manner. Flow Shop Scheduling (FSS) problems consider  $m$  different machines and  $n$  jobs, each job consists of  $m$  operations and each operation requires a different machine and all the jobs are processed in the same processing order. Parallel Machine Scheduling (PMS) problems consider dispatching  $n$  jobs on  $m$  parallel machines. A job can be performed on any of the machines. FFSS problems are problems that combine FFS problems and PMS problems. FFSS problems consider dispatching  $n$  jobs across  $w$  stations, each station has several parallel machines. Each job is executed sequentially through the stations in the same sequence and only 1 machine at each station is selected for execution.

The problem to be solved is a FFSS problem with assumption that the orders are ready at the start of the scheduling process. The objective of the problem is to minimize the total tardiness of orders. The constraints are on the sequence of orders, on the sequence of operations in each order, on allocation of orders on parallel machines in each station, on machine changeover time, and on batches produced in each machine. The model is built based on the above assumption, objective and constraints. The GATS is built based on the combination of GA and TS with the foundation of GA. Based on the model of the problem, the GATS will find a good solution for the problem, this solution will be compared with the solution of the currently used heuristic model to evaluate the effectiveness of the algorithm.

**2. LITERATURE REVIEW****2.1. Flexible Flow Shop Scheduling**

For FSS problems, Chen et al. applied GA to FSS problems with make-span as the criterion. Murata et al. applied a GA to FSS problems by using two-point crossover and the shift change mutation. The convergence speed of simple GAs is relatively slow (Gen and Cheng 2000). PMS problems can be solved into two steps. Firstly, it must determine whichever task is to be processed at which machine, and processing order of task is allocated to each machine afterward (Pinedo, 2002). Many intelligent search methods have been used. Among these, GAs, Simulated Annealing (SA) and Tabu Search (TB) are considered as those most often used.

One promising approach for improving the convergence speed to the global optimum is the use of local search in GAs (Krasnogor and Smith, 2000). Because of the complementary properties of GAs and conventional heuristics, the hybrid approach often outperforms either method operating alone (Gao, Gen, and Sun, 2006).

## 2.2. Genetic algorithm

Genetic algorithm (GA), first introduced by Holland in 1975, is an artificial intelligence search method that uses the process of evolution and natural selection of individuals called chromosomes. In order to apply GA to a problem, generally the solution space of the problem is represented by a population of chromosomes. A method of coding is the selection of a string format for the chromosomes. A fitness value is associated with each chromosome. The fitness function is a measure of the extent to which the objective of the problem is achieved. A certain number of chromosomes are chosen to form the initial generation. The chromosomes of the next generation are generated by applying genetic operators, including selection, crossover, mutation and replacement, to the chromosomes of the existing generation. Starting from an initial population, the algorithm produces a new population of individuals, which are presumably more fit than their ancestors. The process is repeated until a pre-specified termination rule becomes true. At each generation, every new chromosome corresponds to a solution.

## 2.3. Tabu search

Tabu search (TS), suggested by Glover and Laguna in 1997, is one of the most popular meta-heuristics to find solutions of various combinatorial optimization problems. In order to apply TS to a problem, generally the solution space of the problem is represented by a population of codes. A method of coding is the selection of a string format for the codes. An evaluation value is associated with each code. The evaluation function is a measure of the extent to which the objective of the problem is achieved. The Fbest value is the best evaluation value, found during the search. TS guides a local search procedure to explore the solution space beyond local optimality. In order to avoid cycling and becoming trapped in local optima, certain moves that lead to previously explored regions are forbidden. Attributes of recently visited solutions are set to be tabu for a certain number of iterations, and these moves are stored in the Tabu list. A typical TS implementation starts from an initial solution and moves from the current solution to the best one among its neighbourhoods at each iteration, even if this new solution is worse than the one available, until a pre-specified termination rule becomes true.

## 3. THE FLEXIBLE FLOW SHOP SCHEDULING PROBLEM

The problem to be solved is a FFSS problem with 9 orders  $O_i$ ,  $i=1\div 9$ , scheduling on 4 stations,  $S_j$ ,  $j=1\div 4$ . Each order consists of many products, manufactured in batches at each machine in the stations. Each station has 3 homogeneous machines. The due time  $D_i$ , the processing time  $P_{ij}$ , and the batch time  $B_{ij}$  for order  $i$ ,  $i=1\div 9$ , on station  $j$ ,  $j=1\div 4$  are estimated in the following table.

**Table 1.** Input data for model

<b>i</b>	<b>D<sub>j</sub></b> <b>(h)</b>	<b>P<sub>i1</sub></b> <b>(h)</b>	<b>P<sub>i2</sub></b> <b>(h)</b>	<b>P<sub>i3</sub></b> <b>(h)</b>	<b>P<sub>i4</sub></b> <b>(h)</b>	<b>B<sub>i1</sub></b> <b>(h)</b>	<b>B<sub>i2</sub></b> <b>(h)</b>	<b>B<sub>i3</sub></b> <b>(h)</b>	<b>B<sub>i4</sub></b> <b>(h)</b>
1	21	20.04	12.14	0	13.74	1.33	4.83	0	2.5
2	12	6.83	10.62	7.63	1.33	0.92	1.75	1.57	0.67
3	15	0	4.58	1.65	7.04	0	1.17	1.31	0.09
4	11	23.05	7.42	0	0	0.28	0.12	0	0
5	21	0	5.39	9.18	0	0	0.31	0.68	0
6	25	0	2.67	8	0	0	1	3	0
7	18	9	13	14.67	3.67	1.35	1.95	2.2	0.55
8	20	0	3.12	3.63	0	0	1.81	2.1	0
9	18	0	1.17	1.53	0	0	2.33	3.06	0

The setup times of machine in station  $j$  are estimated in the following table.

**Table 2.** Setup times of machine station

<b>j</b>	1	2	3	4
<b>S<sub>j</sub> (h)</b>	0.15	0.2	0.15	0.1

The model is set up with variables  $TS_{ijk}$  being the time to start order  $O_i$ ,  $i=1\div 9$  on station  $S_j$ ,  $j=1\div 4$ , machine  $k$ ,  $k=1\div 3$ ;  $X_{ijk}$  being the binary variable, that order  $O_i$ ,  $i=1\div 9$  will process on station  $S_j$ ,  $j=1\div 4$ , machine  $k$ ,  $k=1\div 3$

or not;  $TE_{ij}$  being the time to end order  $O_i$ ,  $i=1\div 9$  on station  $S_j$ ,  $j=1\div 4$ , machine  $k$ ,  $k=1\div 3$ ;  $T_i$  being the tardiness time of job  $i$ . The model of the problem is as follows.

$$T_{\min} = \text{Min } T, T = \sum(T_i, i=1\div 9)$$

St.

- $TE_{ijk} = TS_{ijk} + (S_j + P_{ij}) * X_{ijk}$ ,  $i=1\div 9$ ,  $j=1\div 4$ ,  $k=1\div 3$
- $T_i = \max(TE_{i4k} - D_i, 0)$ ,  $i=1\div 9$ ,  $k=1\div 3$
- $\sum_k X_{ijk} = 1$ ,  $\sum_i X_{ijk} = 1$ ,  $i=1\div 9$ ,  $j=1\div 4$ ,  $k=1\div 3$
- $TS_{ijk} \geq \text{Max}(TS_{i(j-1)k} + B_{i(j-1)}, TE_{(i-1)jk})$ ,  $i=1\div 9$ ,  $j=1\div 4$ ,  $k=1\div 3$
- $TS_{ij1} = \max(0, \min(TE_{(i-1),j1}))$ ,  $i=1\div 9$ ,  $j=1\div 4$
- $TS_{ijk} = \max(\min(TE_{(i-1)jk}), TS_{ij(k-1)} + B_{ij})$ ,  $i=1\div 9$ ,  $j=1\div 4$ ,  $k=2\div 3$
- $TS_{ijk}, TE_{ijk} \geq 0$ ;  $X_{ijk} = \{0,1\}$ ,  $i=1\div 9$ ,  $j=1\div 4$ ,  $k=1\div 3$

The company is currently using the LPT dispatching method. The the objective value  $T$  is 46.93 (h).

#### 4. THE GATS MODEL FOR THE FLOW SHOP SCHEDULING PROBLEM

The above FFSS problem is a non-linear problem with the size of the solution space of  $4^*9!$  or 1,451,520. The GATS model is used to solve the problem. In the model, GA is used to perform a global search of the solution space, and TS is used to perform a local search to refine the solution found by GA. The GATS procedure is as follows:

- Step 1: Initialize the GATS model.
- Step 2: Generate the initial population  $P^{(0)}$ . Set  $k=0$ .
- Step 3: Generate elite population  $P_E^{(k)}$ .
- Step 4: Generate the genetic population  $P_G^{(k)}$ .
- Step 5: Generate the neighbourhood population  $P_N^{(k)}$ .
- Step 6: Generate the next population  $P^{(k+1)}$ . Set  $k=k+1$ .
- Step 7: Check the termination rule. If No, return to step 3. If Yes, finish the loop.
- Step 8: Run the algorithm a number of times to choose the best scheduling result.

##### Step 1: Initialize the GATS model.

This step setups factors of GATS models, including the method of coding, the GA parameters, the TS parameters, and the termination rule.

**The method of coding:** Each chromosome  $C$  is a string of 4 sub-chromosomes,  $S_j$ ,  $j=1\div 4$ , corresponding to 4 stations. The orders are numbered from 1 to 9. Each sub-chromosome is a string of 9 genes,  $G_i$ ,  $i=1\div 9$ , corresponding to 9 orders. The sequence of genes in a sub-chromosome represents the sequence of order scheduled in the corresponding station.

$$C = [S_1, S_2, S_3, S_4]; S_j = (G_{j1}, G_{j2}, G_{j3}, G_{j4}, G_{j5}, G_{j6}, G_{j7}, G_{j8}, G_{j9}), j=1\div 4$$

**The GA parameters** include fitness function, the population size, and the parameters of GA operators, including selection, crossover, mutation, and replacement operators. The fitness function  $F$  is defined as  $F_i = T_{\max} - T_i$ . Where  $F_i$ ,  $T_i$  are the fitness and objective values of chromosome  $i$ ,  $T_{\max}$  is the maximum objective value in the population. The crossover method is POX (Precedence Operation Crossover), the mutation method is REM (Reciprocal Exchange Mutation), the replacement method is acceptance threshold. The population size  $P$ , the crossover probability  $P_c$ , the mutation probability  $P_m$ , and threshold  $K$  are chosen as follows:

$$P = 9, P_c = 0.8; P_m = 0.2, K = 2.$$

**The TS parameters** include the neighbourhood operator, and the Tabu list. The neighbourhood operator uses SWAP method to find the neighbourhood chromosomes of a chromosomes. Tabu list contains the chromosomes found in the previous iterations. At the end of each iteration, chromosomes moving into the next population must not be in Tabu list.

**The termination rule:** The best objective value of the population  $T_{\min}$  does not improve or decrease after 10 consecutive iterations.

##### Step 2: Generate the initial population $P^{(0)}$ , set $k=0$ .

The initial population consists of 9 chromosomes. There are 4 chromosomes generated from 4 heuristic rules, EDD, ERD, SPT and LPT. The remaining chromosomes  $R_1, \dots, R_5$  are randomly generated. The chromosomes



in the initial population, arranged in descending order of their objective values with their corresponding objective and fitness values are shown in the following table.

**Table 3.** The initial population  $P^{(0)} = \{EDD, ERD, R2, SPT, R1, R4, R3, R5, LPT\}$

$P^{(0)}$	S1	S2	S3	S4	$T_i$ (h)	$F_i$ (h)	$P_i$
EDD	423798156	423798156	423798156	423798156	9.41	37.52	0.215
ERD	123456789	123456789	123456789	123456789	13.68	33.25	0.191
R2	741295863	172635498	876425913	238915674	15.21	31.72	0.182
SPT	356892714	968354217	149382657	456892731	16.34	30.59	0.176
R1	247195683	512637894	856724913	436215879	30.32	16.61	0.095
R4	546298173	342156879	874256913	236194567	33.87	13.06	0.075
R3	146295873	372651489	372456918	136254897	39.32	7.61	0.044
R5	826495173	649153872	124736985	631294758	43.15	3.78	0.022
LPT	417235689	712453869	756283914	137245689	46.93	0	0

This step also initializes the Tabu list TL, containing the chromosomes in  $P^{(0)}$ .

$$TL = \{EDD, ERD, R2, SPT, R1, R4, R3, R5, LPT\}$$

**Step 3: Generate elite population  $P_E^{(k)}$ .**

This step uses the selection operator to generate  $P_E^{(k)}$  from  $P^{(k)}$ . Each chromosome in the current population has a corresponding fitness value  $F_i$ , and is selected for inclusion in  $P_E^{(k)}$  with selection probability  $P_i$  determined as follows:

$$P_i = F_i / \sum_{i=1}^9(F_i)$$

The selection probabilities  $P_i$  are calculated as shown in the table above. Random numbers are generated 9 times, based on  $P_i$ , the chromosomes in  $P^{(0)}$ , selected into the population  $P_E^{(0)}$  are as follows:

$$P_E^{(0)} = \{R2, ERD, SPT, R3, R3, SPT, ERD, R4, EDD\}$$

**Step 4: Generate the genetic population  $P_G^{(k)}$ .**

This step uses the crossover and mutation operators to generate genetic population  $P_G^{(k)}$  from the elite population  $P_E^{(k)}$ . The genetic population  $P_G^{(k)}$  includes the new chromosome generated from the crossover and mutation operators. The chromosomes of  $P_E^{(0)}$  are selected to be included in the crossover list  $P_c$  with the crossover probability of 0.8. After generating 9 random numbers, the set  $P_c$  is determined as follows:

$$P_c = \{EDD, ERD, SPT, R3\}.$$

Each pair of chromosomes in  $P_c$  is selected to cross over by the POX method, resulting in 2 new chromosomes in population  $P^C$ . R2 and ERD are crossed over to each other, and generate 2 childs, C1 and C2. SPT and R4 are crossed over to each other, and generate 2 childs C3 and C4. The chromosomes in  $P^C$  with their objective values are shown in the following table.

**Table 4.** The crossover population  $P^C = \{C1, C2, C3, C4\}$

$P^C$	S1	S2	S3	S4	T
C1	421356789	421356789	421356789	421356789	28.16
C2	327498156	327498156	327498156	327498156	32.05
C3	426958713	367254819	137245698	326548971	12.84
C4	136589274	983651427	493826517	146589273	21.29

The chromosomes of  $P_E^{(0)}$  are also selected to be included in the mutation list  $P_m$  with the mutation probability of 0.2. After generating 9 random numbers, the set  $P_m$  is determined as follows:

$$P_m = \{R2, SPT\}.$$

Each chromosome in  $\mathbf{P}_m$  is selected to mutate by the REM method, resulting in 1 new chromosome in population  $\mathbf{P}^M$ . R3 is mutated and generate M1. SPT is mutated and generate M2. The chromosomes in  $\mathbf{P}^M$  with their objective values are shown in the following table.

**Table 5.** The mutation population  $\mathbf{P}^M = \{M1, M2\}$

$\mathbf{P}^M$	S1	S2	S3	S4	T
M1	741259863	172635498	876425913	238915674	17.15
M2	356892714	968453217	149382657	456892731	27.03

After crossover and mutation, 6 new chromosomes are created in the population  $\mathbf{P}_G^{(0)}$ .

$$\mathbf{P}_G^{(0)} = \{C1, C2, C3, C4, M1, M2\}$$

**Step 5: Generate the neighbourhood population  $\mathbf{P}_N^{(k)}$**

The populations  $\mathbf{P}^{(k)}$  &  $\mathbf{P}_G^{(k)}$  form the union population  $\mathbf{P}_U^{(k)} = \mathbf{P}^{(k)} \cup \mathbf{P}_G^{(k)}$ . This step uses the neighbourhood operator to generate the  $\mathbf{P}_N^{(k)}$  from  $\mathbf{P}_U^{(k)}$ . For the first iteration,  $\mathbf{P}_U^{(0)}$  includes 15 chromosomes, of which 9 are in  $\mathbf{P}^{(0)}$  and 6 are in  $\mathbf{P}_G^{(0)}$ .

$$\mathbf{P}_U^{(0)} = \mathbf{P}^{(0)} \cup \mathbf{P}_G^{(0)} = \{EDD, ERD, R2, SPT, R1, R4, R3, R5, LPT, C1, C2, C3, C4, M1, M2\}$$

The neighbourhood operator swaps adjacent sub-chromosomes in each chromosome to generate neighbourhood chromosomes. Each chromosome in  $\mathbf{P}_U^{(0)}$  will have 3 neighbourhood chromosomes. The best chromosome will be selected to move into  $\mathbf{P}_N^{(0)}$  to go forward. Population  $\mathbf{P}_N^{(0)}$  includes the best neighbourhood chromosomes as shown in the following table

**Table 6.** The neighbourhood population  $\mathbf{P}_N^{(0)}$

$\mathbf{P}_N^{(0)}$	S1	S2	S3	S4	T	Tabu
N1	423798156	423798156	423798156	423798156	9.41	Yes
N2	123456789	123456789	123456789	123456789	13.68	Yes
N3	172635498	741295863	876425913	238915674	14.11	No
N4	968354217	356892714	149382657	456892731	15.02	No
N5	546298173	342156879	236194587	874256913	25.94	No
N6	247195683	512637894	436215879	856724913	26.71	No
N7	146295873	372456918	372651489	136254897	38.79	No
N8	826495173	124736985	649153872	631294758	39.17	No
N9	712453869	417235689	756283914	137245689	42.13	No
N10	421356789	421356789	421356789	421356789	28.16	No
N11	327498156	327498156	327498156	327498156	32.05	No
N12	367254819	426958713	137245698	326548971	11.25	No
N13	136589274	493826517	983651427	146589273	75.00	No
N14	172635498	741259863	876425913	238915674	33.91	No
N15	356892714	968453217	456892731	149382657	18.55	No

In  $\mathbf{P}_N^{(0)}$  there are 2 chromosomes, N1 and N2 in the Tabu list, the rest are not.

**Step 6: Generate the next population  $\mathbf{P}^{(k+1)}$ .**

This step uses the replacement operator to generate  $\mathbf{P}^{(k+1)}$  from  $\mathbf{P}^{(k)}$  &  $\mathbf{P}_N^{(k)}$ . The chromosomes from  $\mathbf{P}_N^{(k)}$  will be added to  $\mathbf{P}^{(k)}$  to make  $\mathbf{P}^{(k+1)}$ , if they are not in the current Tabu list and their objective values exceed an acceptable threshold, defined by the objective value of the threshold chromosome. The threshold chromosome is a chromosome in  $\mathbf{P}^{(k)}$  with position n defined by population size P and threshold parameter K as follows.

$$n = P/K$$

With population size of 9 and threshold parameter of 2 as chosen, the threshold chromosome is the 4th chromosome of  $\mathbf{P}^{(k)}$  in the top-down ranking. In order to keep the next population size constant, chromosomes in  $\mathbf{P}^{(k)}$  with lowest values are removed from the next population. This step also updates the Tabu list by adding the chromosomes, moved into  $\mathbf{P}^{(k+1)}$ . In this iteration, the threshold chromosome is SPT, with the threshold value of 16.34. Chromosomes N3, N4, and N12 move into, R3, R5, LPT move out of the population. The chromosomes in  $\mathbf{P}^{(2)}$  are shown in the following table.

**Table 7.** The next population  $P^{(2)} = \{ EDD, N12, ERD, N3, N4, R2, SPT, R1, R4 \}$ 

$P^{(2)}$	S1	S2	S3	S4	T
EDD	423798156	423798156	423798156	423798156	9.41
N12	367254819	426958713	137245698	326548971	11.25
ERD	123456789	123456789	123456789	123456789	13.68
N3	172635498	741295863	876425913	238915674	14.11
N4	968354217	356892714	149382657	456892731	15.02
R2	741295863	172635498	876425913	238915674	15.21
SPT	356892714	968354217	149382657	456892731	16.34
R1	247195683	512637894	856724913	436215879	30.32
R4	546298173	342156879	874256913	236194567	33.87

The Tabu list is updated after iteration 1 as follows.

$$TL = \{ EDD, ERD, R2, SPT, R1, R4, R3, R5, LPT, N3, N4, N12 \}$$

**Step 7: Check the termination rule.**

After iteration 1, EDD is again the best chromosome with the best objective value of 9.41, appearing twice. The termination rule is not satisfied, so iteration 2 is executed. The result after 14 iterations is as follows.

**Table 8.** The result after 14 iterations

Iteration	1	2	3	4	5	6	7	8	9	10	11	12	13	14
T	9	8	8	6	6	5	5	5	5	3	3	2	2	2
(h)	.41	.89	.89	.11	.11	.55	.55	.12	.12	.82	.82	.37	.37	.37

From the 12<sup>nd</sup> iteration to the 21<sup>st</sup> iteration, the best objective value remains the same, the termination rule is satisfied, the algorithm ends. The scheduling result in this run is as follows:

$$C = (413296857, 413297856, 142379856, 472319856), T = 2.37 \text{ (h)}$$

**Step 8: Run the algorithm a number of times to choose the best scheduling result.**

The algorithm is run 10 times with the results as shown in the following table.

**Table 9.** The results after 10 runs

Run	1	2	3	4	5	6	7	8	9	10
T (h)	2.37	5.98	4.86	3.71	3.63	5.01	4.12	2.88	3.96	3.82

The best scheduling result is found on the 1<sup>st</sup> run. The scheduling sequence, the objective value are as follows:

$$C = (423981756, 498132756, 982713546, 439782156), T = 2.37 \text{ (h)}$$

The objective value according to GATS model (2.37 h) is less than the objective value according to the LPT model currently used (46.93 h).

## 5. CONCLUSION

The GATS model has been used to solve the Flexible Flow Shop Scheduling Problem with 9 orders on 4 stations with 3 homogeneous parallel machines. In the model, GA is used as the platform to perform a global search of the solution space, and TS is used to perform a local search to refine the solution found by GA. The results show that the GATS model gives better objective value of tardiness time than the heuristic LPT method, being used. However, the factors of the model, including the population size, the crossover probability  $P_c$ , the mutation probability  $P_m$ , the method of finding the neighbourhood chromosomes, the method and parameter of the termination rule, are only selected empirically, so the results are not very good. The future research is to use experimental design DOE to determine the model parameters to get suboptimal results.

## References

- [1] O Etiler1, B Toklu, M Atak, Jwilson, "A genetic algorithm for flow shop scheduling problems", Journal of the Operational Research Society (2004) 55, pp. 830–835.

- [2] Yunus Demira, Selçuk Kürşat İşleyen, “An effective genetic algorithm for flexible job-shop scheduling with overlapping in operations”, *International Journal of Production Research*, 2014.
- [3] Jae-Ho Lee & Jae-Min Yu & Dong-Ho Lee, “A tabu search algorithm for unrelated parallel machine scheduling with sequence- and machine-dependent setups: minimizing total tardiness”. *International Journal of Advanced Manufacturing Technology*, 69 (2013), pp. 2081-2089.
- [4] Umit Bilge, Furkan Kirac, Mukde Kurtulan, Pelin Pekgun, “A tabu search algorithm for parallel machine total tardiness problem”. *Computers & Operations Research* 31 (2002), pp. 397– 414
- [5] Ahmad Hassanat, Khalid Almohammadi, Esra’a Alkafaween, Eman Abunawas, Awni Hammouri, V. B. Surya Prasath, “Choosing Mutation and Crossover Ratios for Genetic Algorithms - A Review with a New Dynamic Approach”, *Information* 2019, 10, p. 390.
- [6] Jatinder N. D. Gupta, “Designing a tabu search algorithm for the two-stage flow shop problem with secondary criterion”, *Production Planning & Control: The Management of Operations*, 10:3, pp. 251-265.
- [7] Justin Schrack, Roy Ortega, Kevin Dabu, Daniel Truong, Michal Aibin, Ania Aibin, “Combining Tabu Search and Genetic Algorithm to Determine Optimal Nurse Schedules”, 2021.
- [8] Kevin Boston, Pete Bettinger, “Combining Tabu Search and Genetic Algorithm Heuristic Techniques to Solve Spatial Harvest Scheduling Problems”, *Forest Science* 48(1) 2002.
- [9] Moch Saiful Umam, Mustafid Mustafid, Suryono Suryono, “A hybrid genetic algorithm and tabu search for minimizing makespan in flow shop scheduling problem”, *Computer and Information Sciences* 34 (2022), pp. 7459–7467.

**[P-14] Application of Genetic Algorithm to Solve Vehicle Routing Problems in Distribution Planning Systems. A Case Study**

Nguyen Nhu Phong\*, Do Thi Thao

*HCMC University of Technology, Viet Nam*

\*Corresponding author: nnphong@hcmut.edu.vn

**Abstract**

Most of 3PL companies that provide transportation services are handling thousands of orders per day. Vehicle Routing Problems, VRPs, help plan the distribution of goods with the optimum fleet of vehicles and delivery routes, and play an important role in helping businesses reduce transportation costs while ensuring service level. VRPs are NP-hard combinatorial optimization problems. It is quite difficult to achieve an optimal solution for real size problems with mathematical modelling approach because of its NP-hard structure. Genetic Algorithm (GA) plays a major role in searching for near-optimal solutions for NP-hard optimization problems. This paper develops the GA model for VRPs. The result show that the delivery cost is reduced by 17.88 %, while the service level increase from 88.7% to 100%. It indicates that the model can be good techniques for VR problems.

**Keywords:** *Distribution planning, Mathematical modelling, Vehicle routing problems, Genetic algorithm*

**1. INTRODUCTION**

In today's fiercely competitive business environment, companies need to optimize their supply chains. Logistics is one of the key areas in supply chain management. Vehicle Routing Problem (VRP) is a core problem in Logistics that refers to a class of combinatorial optimization in which customers are served by several vehicles. VRP is a problem in which there is a set of vehicles and a set of customers; each customer requires a certain number of goods. This problem is a type of distribution problem that determines the transportation facilities and their delivery routes with specific objective and constraints. The problem to be solved is a VRP with assumption that the trucks start at the real warehouse and end at the virtual warehouse, the travel time between the points is fixed, the unloading time at the points is fixed, the speed of the trucks is the same and fixed, and the factors of failure, accident, weather are not taken into account. The objective of the problem is to minimize the transportation cost. The constraints are on the level of customer service, on the capacity of the transportation facilities. The model of the problem is built based on the above assumptions, objective and constraints. A GA algorithm is built. Based on the model of the problem, the GA algorithm will find a good solution for the problem, this solution will be compared with the solution of the currently used heuristic model to evaluate the effectiveness of the GA algorithm.

**2. LITERATURE REVIEW****2.1. Vehicle Routing Problems**

There are many classes of VRP problems, such as Multi Depot VRP, Capacitated VRP, Distance Constrained VRP, VRP with Time Windows, VRP with Pickup and Delivery, VRP with multiple trips, Periodic VRP, Multi Objective VRP, Open VRP. In Open VRP (OVRP), routes finish after servicing the last client. The OVRP, which was first proposed by Sariklis (1997), is relevant for companies without a vehicle fleet of its own that decide to hire or rent vehicles to make their deliveries (Tarantilis, Ioannou, Kiranoudis, & Prastacos, 2005). OVRPs are of type NP-hard combinatorial optimization problems. Many heuristics have been used to solve OVRPs. Tabu search algorithms proposed by Fu et al. (2005) and Brandão (2004). Genetic Algorithm proposed by Dutta, Barma, Kar, and De (2019).

**2.2. Genetic algorithm**

Genetic algorithm (GA), first introduced by Holland in 1975, is an artificial intelligence search method that uses the process of evolution and natural selection of individuals called chromosomes. In order to apply GA to a problem, generally the solution space of the problem is represented by a population of chromosomes where each chromosome is a possible solution to the problem. A method of coding is the selection of a string format for the

chromosomes. A fitness value is associated with each chromosome. The fitness function is a measure of the extent to which the objective of the problem is achieved. A certain number of chromosomes are chosen to form the initial generation. The chromosomes of the next generation are generated by applying genetic operators, including selection, crossover, mutation and replacement, to the chromosomes of the existing generation.

Starting from an initial population, the algorithm produces a new population of individuals, which are presumably more fit than their ancestors. The process is repeated until a pre-specified termination rule becomes true. At each generation, every new chromosome corresponds to a solution.

### 3. THE VEHICLE ROUTING PROBLEM

The problem to be solved is an OVRP, where vehicles after delivery to customers do not need to return to the starting point. The distribution system consists of a warehouse, and a fleet of vehicles  $V_v$ ,  $v=1 \div V$ . Each vehicle  $V_v$  has max load  $Q_v$ , limited delivery time  $T_v$ , and operating cost  $f_v$ . The system distributes for  $N$  customers, each customer is 1 point on the distribution network. The distribution network consists of  $N+1$  nodes, with node 0 being the warehouse, node  $i$ ,  $i=1 \div N$  corresponding to the  $i$ th customer. Customers at node  $i$  have demand  $d_i$ , unloading time  $S_i$ ,  $i=1 \div N$ . On a distributed network, the travel time from node  $i$  to node  $j$  is  $T_{ij}$ ,  $i=0 \div N-1$ ,  $j=1 \div N$ .

The objective of the problem is to minimize the total delivery cost. The constraints of the problem include: Each route starts at the warehouse and ends at a customer point. The number of vehicles starting at the real warehouse and ending at the virtual warehouse is equal and does not exceed the limited number of vehicles. The number of cars arriving and leaving at each node is equal. Each customer is only served once by one vehicle. The total delivery time does not exceed the time limit. The total demand of the customers in each route does not exceed the vehicle tonnage.

The model is set up with the decision variable  $y_{ij}^v$ ,  $i=0 \div N-1$ ,  $j=1 \div N$ ,  $v=1 \div V$ . If vehicle  $v$  moves from node  $i$  to node  $j$  then  $y_{ij}^v$  is 1, otherwise  $y_{ij}^v$  is 0. The model is as follows:

$$\text{Min } Z, Z = \sum_{v=1}^V \sum_{j=1}^N f_v y_{0j}^v$$

St.

$$\sum_{v=1}^V \sum_{j=1}^N y_{0j}^v = \sum_{v=1}^V \sum_{i=1}^N y_{i0}^v \leq V$$

$$\sum_{v=1}^V \sum_{i=0}^N y_{ij}^v = 1, j \in N \setminus \{0\}, i \neq j$$

$$\sum_{i=0}^N y_{ie}^v = \sum_{j=0}^N y_{ej}^v, v \in V, e \in N \setminus \{0\}, e \neq i, e \neq j$$

$$\sum_{i=0}^N \sum_{j=1}^N (d_j y_{ij}^v) \leq Q_v, v \in V, i \neq j$$

$$\sum_{i=0}^N \sum_{j=0}^N [(t_{ij} + s_j) y_{ij}^v] \leq T, v \in V, i \neq j$$

$$y_{ij}^v \in \{0, 1\}, v \in V, j \in N, i \in N, i \neq j$$

### 4. THE GA MODEL FOR THE PILOT VRP

The pilot problem is a VRP problem with 6 trucks and 8 customers ( $V=6$ ,  $N=8$ ). The parameters of fleet, customers, travel time between nodes are as in Tables 1, 2 and 3. The pilot problem model is set up according to the above parameters. The GA model is used to solve the problem by the following procedure:

Step 1: Initialize the GA model.

Step 2: Generate the initial population  $\mathbf{P}^{(0)}$ . Set  $k=0$ .

Step 3: Generate elite population  $\mathbf{P}_E^{(k)}$ .

Step 4: Generate the genetic population  $\mathbf{P}_G^{(k)}$ .

Step 5: Generate the next population  $\mathbf{P}^{(k+1)}$ . Set  $k=k+1$ .

Step 6: Check the termination rule. If No, return to step 3. If Yes, finish the loop.

**Table 1.** Loads, Time Limits, and Fleet Costs

v	1	2	3	4	5	6
<b>Q<sub>v</sub> (kgs)</b>	300	300	300	400	400	500
<b>f<sub>v</sub> (M)</b>	3	3	3	4	4	5
<b>T<sub>v</sub> (h)</b>	8	8	8	8	8	8

**Table 2.** Demand, unloading time at delivery points

i	1	2	3	4	5	6	7	8
<b>d<sub>i</sub> (kgs)</b>	50	300	200	150	100	150	50	100
<b>S<sub>i</sub>(h)</b>	0.25	0.25	0.25	0.25	0.25	0.25	0.25	0.25

**Table 3.** Travel Time T<sub>ij</sub> (h) between nodes

i\j	0	1	2	3	4	5	6	7	8
<b>0</b>	-	0.068	0.137	0.133	0.143	0.345	0.203	0.261	0.202
<b>1</b>		-	0.08	0.065	0.076	0.345	0.228	0.265	0.236
<b>2</b>			-	0.062	0.049	0.301	0.221	0.231	0.238
<b>3</b>				-	0.019	0.362	0.27	0.289	0.283
<b>4</b>					-	0.349	0.265	0.279	0.28
<b>5</b>						-	0.165	0.084	0.189
<b>6</b>							-	0.088	0.03
<b>7</b>								-	0.117
<b>8</b>									-

**Step 1: Initialize the GA model.**

This step setups factors of GA models, including the method of coding, the population size, the fitness function, the parameters of GA operators, and the termination rule.

**The method of coding:** Each chromosome C is a string of 2 sub-chromosomes, S1 is corresponding to customer sequence, and S2 is corresponding to vehicle sequence:  $C = [S1, S2]$

Customers are numbered from 1 to 8. Each sub-chromosome S1 is a string of 8 genes,  $G_{ci}$ ,  $j=1\div 8$ , corresponding to 8 customers. The sequence of genes in a sub-chromosome represents the sequence of customers being served:  $S1 = (G_{c1}, G_{c2}, G_{c3}, G_{c4}, G_{c5}, G_{c6}, G_{c7}, G_{c8})$ . Vehicles are numbered from 1 to 6. Each sub-chromosome S2 is a string of 6 genes,  $G_{vi}$ ,  $j=1\div 6$ , corresponding to 6 vehicles. The sequence of genes in a sub-chromosome represents the sequence of vehicles being used:  $S2 = (G_{v1}, G_{v2}, G_{v3}, G_{v4}, G_{v5}, G_{v6})$

**The population size** P is chosen to be 4:  $P=4$ .

**The fitness function** F is defined as  $F_i = Z_{max} - Z_i$ . Where  $F_i$ ,  $Z_i$  are the fitness and objective values of chromosome i,  $Z_{max}$  is the maximum objective value in the population.

**The GA operators** include selection, crossover, mutation, replacement operators. The selection method is based on selection probabilities, determined by fitness values. The crossover method is *OX (Order Crossover)*, the mutation method is *SWAP*, the replacement method is acceptance threshold. The the crossover probability  $P_c$ , the mutation probability  $P_m$ , and threshold K are chosen as follows:  $P_c = 0.8$ ;  $P_m = 0.2$ ,  $K=2$ .

**The termination rule:** The best objective value of the population  $Z_{min}$  does not decrease after 15 consecutive iteration.

**Step 2: Generate the initial population P<sup>(0)</sup>, set k=0.**

The initial population consists of 4 chromosomes. Each initial individual is created including customer sequence and vehicle sequence, by randomizing the customer delivery points and available vehicles. The initial population  $P^{(0)}$  is shown in Table 4:  $P^{(0)} = \{C1, C2, C3, C4\}$

**Table 4.** The initial population  $P^{(0)}$ 

$P^{(0)}$	S1	S2	Routes	v	Z	F
C1	[1, 3, 2, 4, 7, 5, 6, 8]	[2, 3, 4, 5, 1, 6]	[1,3]; [2]; [4,7,5]; [6,8]	2, 3, 4, 5	14	1
C2	[1, 4, 3, 8, 2, 6, 7, 5]	[3, 1, 2, 4, 5, 6]	[1,4]; [3,8]; [2]; [6,7,5]	3, 1, 2, 4	13	2
C3	[6, 4, 1, 7, 8, 3, 5, 2]	[1, 3, 4, 5, 6, 2]	[6,4]; [1,7,8]; [3,5]; [2]	1, 3, 4, 5	14	1
C4	[8, 5, 1, 7, 6, 2, 3, 4]	[1, 2, 4, 6, 3, 5]	[8,5,1,7]; [6]; [2]; [3,4]	1, 2, 4, 6	15	0

From customer sequence  $S_1$ , vehicle sequence  $S_2$ , based on the constraints, the vehicles used and their corresponding routes are determined as above table. From that, the objective values  $Z$  and fitness values  $F$  of each chromosome can be determined. In the initial population  $P^{(0)}$ , the best chromosomes are C2, with the best objective value  $Z$  of 13 (M).

### Step 3: Generate elite population $P_E^{(k)}$ .

This step uses the selection operator to generate elite population  $P_E^{(k)}$  from  $P^{(k)}$ . Each chromosome in the current population has a corresponding fitness value  $F_i$ , and is selected for inclusion in the elite population  $P_E^{(k)}$  with selection probability  $P_i$  determined as follows:  $P_i = F_i / \sum_{i=1}^4(F_i)$ . With population  $P^{(0)}$ , the values of  $F_i$ ,  $P_i$ , and the *CPF* (*Cumulative Probability Function*) are calculated as shown in Table 5. Random numbers  $R_i$  are generated 4 times. Based on CPF, the chromosomes, selected into the population  $P_E^{(0)}$  are as table 6.

**Table 5.** Values of  $F_i$ ,  $P_i$ , and the CPF

$P^{(0)}$	S1	S2	Z	F	P	CPF
C1	[1, 3, 2, 4, 7, 5, 6, 8]	[2, 3, 4, 5, 1, 6]	14	1	0.25	0.25
C2	[1, 4, 3, 8, 2, 6, 7, 5]	[3, 1, 2, 4, 5, 6]	13	2	0.5	0.75
C3	[6, 4, 1, 7, 8, 3, 5, 2]	[1, 3, 4, 5, 6, 2]	14	1	0.25	1
C4	[8, 5, 1, 7, 6, 2, 3, 4]	[1, 2, 4, 6, 3, 5]	15	0	0	1

**Table 6.** The elite population  $P_E^{(0)} = \{C2, C1, C3, C3\}$ 

$R_i$	0.569	0.194	0.828	0.913
$P_E^{(0)}$	C2	C1	C3	C3

### Step 4: Generate the genetic population $P_G^{(k)}$ .

This step uses the crossover and mutation operators to generate genetic population  $P_G^{(k)}$  from the elite population  $P_E^{(k)}$ . The genetic population  $P_G^{(k)}$  includes the new chromosome generated from the crossover and mutation operators.

The chromosomes of  $P_E^{(0)}$  are selected to be included in the crossover list  $P_c$  with the crossover probability of 0.8. After generating 4 random numbers  $R_i$ , the set  $P_c$  is determined as Table 7. Each pair of chromosomes in  $P_c$  is selected to cross over by the OX method, on both sub-chromosomes, resulting in 2 new chromosomes in population  $P^C$ . C2 and C3 are crossed over to each other, and generate 2 childs, C5 and C6. The population  $P^C$  are shown in Table 8.

**Table 7.** The crossover list  $P_c = \{C2, C3\}$ 

$P_E^{(0)}$	C2	C1	C3	C3
$R_i$	0.47	0.91	0.11	0.88
$P_c$	C2	-	C3	-

**Table 8.** The crossover population  $P^C = \{C5, C6\}$ 

$P^C$	S1	S2
C5	[6, 4, 3, 8, 1, 7, 5, 2]	[3, 1, 2, 4, 5, 6]
C6	[1, 4, 2, 8, 3, 5, 6, 7]	[1, 3, 4, 5, 2, 6]

The chromosomes of  $P_E^{(0)}$  are also selected to be included in the mutation list  $P_m$  with the mutation probability of 0.2. After generating 4 random numbers  $R_i$ , the set  $P_m$  is determined as Table 9. Each chromosome in  $P_m$  is



selected to mutate by the SWAP method, on both sub-chromosomes, resulting in 1 new chromosome in population  $\mathbf{P}^M$ . C1 is mutated and generate C7. The population  $\mathbf{P}^M$  is shown in Table 10.

**Table 9.** The mutation list  $\mathbf{P}_m = \{C1\}$

$\mathbf{P}_E^{(0)}$	C2	C1	C3	C3
$\mathbf{R}_i$	0.49	0.12	0.23	0.86
$\mathbf{P}_m$	-	C1	-	-

**Table 10.** The mutation population  $\mathbf{P}^M = \{C7\}$

$\mathbf{P}^M$	S1	S2
C7	[6, 8, 2, 4, 7, 5, 1, 3]	[4, 5, 2, 3, 1, 6]

After crossover and mutation, 3 new chromosomes are created in the population  $\mathbf{P}_G^{(0)}$ . Chromosomes in  $\mathbf{P}_G^{(0)}$  with their genes and objective values are shown in Table 11.

**Table 11.** The genetic population  $\mathbf{P}_G^{(0)} = \{C5, C6, C7\}$

$\mathbf{P}_G^{(0)}$	S1	S2	Z
C5	[7, 4, 3, 8, 2, 6, 1, 5]	[3, 1, 6, 4, 5, 2]	13
C6	[2, 8, 7, 1, 4, 3, 6, 5]	[3, 4, 5, 1, 2, 6]	14
C7	[6, 8, 2, 4, 7, 5, 1, 3]	[4, 5, 2, 3, 1, 6]	14

#### Step 5: Generate the next population $\mathbf{P}^{(k+1)}$ .

This step uses the replacement operator to generate the next population  $\mathbf{P}^{(k+1)}$  from the populations  $\mathbf{P}^{(k)}$  &  $\mathbf{P}_G^{(k)}$ . The chromosomes from  $\mathbf{P}_G^{(k)}$  will be added to the current population  $\mathbf{P}^{(k)}$  to make the next population  $\mathbf{P}^{(k+1)}$ , if their objective values are better than the acceptable threshold, defined by the objective value of the threshold chromosome. The threshold chromosome is a chromosome in  $\mathbf{P}^{(k)}$  with position  $n$  defined by population size  $P$  and threshold parameter  $K$ :  $n = P/k$ . With population size of 4, and the replacement parameter  $K$  of 2, the acceptable threshold is selected as the value of the 2<sup>nd</sup> chromosome of  $\mathbf{P}^{(k)}$  in the top-down ranking. On the other side, in order to keep the next population size constant, some chromosomes in  $\mathbf{P}^{(k)}$  with the lowest fitness values are removed. In  $\mathbf{P}^{(0)}$ , C1 is the 2<sup>nd</sup> chromosome in the top-down list, the acceptable threshold is 14. Look at the objective values of the chromosomes in population  $\mathbf{P}_G^{(0)}$ , C5, C6, C7 move into  $\mathbf{P}^{(1)}$  and C1, C3, C4 have to move out to keep  $\mathbf{P}^{(1)}$  population size constant. The following table shows the chromosomes in the next population  $\mathbf{P}^{(1)}$ . In  $\mathbf{P}^{(1)}$ , the best chromosomes are C2 and C3, with the best objective value is 13.

**Table 12.** The next population  $\mathbf{P}^{(1)} = \{C2, C5, C6, C7\}$

$\mathbf{P}^{(1)}$	S1	S2	Z	F
C2	[1, 4, 3, 8, 2, 6, 7, 5]	[3, 1, 2, 4, 5, 6]	13	2
C5	[7, 4, 3, 8, 2, 6, 1, 5]	[3, 1, 6, 4, 5, 2]	13	2
C6	[2, 8, 7, 1, 4, 3, 6, 5]	[3, 4, 5, 1, 2, 6]	14	1
C7	[6, 8, 2, 4, 7, 5, 1, 3]	[4, 5, 2, 3, 1, 6]	14	1

#### Step 6: Check the termination rule.

After iteration 1, the best objective value is 13, appearing only twice. The termination rule is not satisfied, so iteration 2 is executed.

## 5. THE GA MODEL WITH EXPERIMENTS FOR THE PILOT VRP

Experiments are performed on the above GA model with a population size  $P$  of 20, the two input factors are the probability of crossover  $P_c$  and the probability of mutation  $P_m$ . The probability  $P_c$  has 3 levels 0.8, 0.9, and 1. The probability  $P_m$  has 3 levels 0.3, 0.5, 0.7. The run-charts of the objective values  $Z$  in 9 combinations of  $(P_c,$

$P_m$ ) are shown in the following figure. The 9 combinations ( $P_c, P_m$ ) give the same objective value, but combination (0.8, 0.5) has the smallest number of iterations. This combination is used to solve real problems.

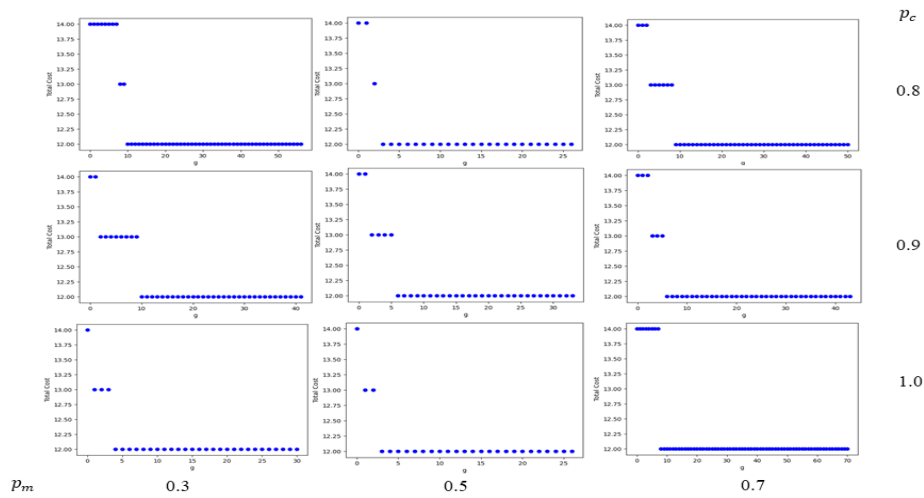


**Figure 1.** The objective values  $Z$  in 9 combinations of ( $P_c, P_m$ )

### 6. THE GA MODEL FOR THE REAL VRP

The real problem is a VRP problem with 12 trucks and 97 customers ( $V = 12, N = 97$ ). The parameters of fleet, customers, travel time between nodes are as in the following tables. The model is set up according to the above parameters. The GA model is used to solve the problem with the parameter:  $P = 20, P_c = 0.8, P_m = 0.5$ .

**Table 13.** Loads, Time Limits, and Fleet Costs

$v$	1÷6	7÷9	10	11÷12
$Q_v$ (kg)	1000	1400	1900	2000
$f_v$ (M)	1.150	1.600	1.800	2.000
$T_v$ (h)	8	8	8	8

**Table 14.** Demand, unloading time at delivery points

$i$	1	2	3	4	...	97
$d_i$ (kgs)	14.5	17	9	14.5	...	1000
$S_i$ (h)	0.25	0.25	0.25	0.25	...	0.25

**Table 15.** Travel time  $T_{ij}$  (h) between nodes

	0	1	2	3	4	...	97
0	-	0.313	0.214	0.124	0.521	...	0.365
1		-	0.651	0.145	0.689	...	0.287
2			-	0.09	0.871	...	0.697
3				-	0.416	...	1.010
4					-	...	0.723
...						-	...
97							-

The result has a total cost of 7.1 (M) with the vehicles used and the corresponding route as shown in Table 16. The comparison between the current method and the GA model is shown in Table 17. Compared to the current model, the GA model has a cost reduction of 7.55 to 7.1 (17.88%), the number of late delivery points reduced from 11 to 0, service level increased from 88.7% to 100%.

**Table 16.** The vehicles used and corresponding route by GA

v	Route
2	[0, 12, 77, 82, 64, 50, 60, 42, 69, 93, 28, 87, 30, 11, 21, 32, 96, 25, 56, 91, 53, 5, 23]
5	[0, 6, 75, 66, 57, 9, 72, 73, 22, 16, 41, 89, 81, 13, 19, 36, 20, 79, 92, 74, 24, 43, 2, 90]
7	[0, 97, 26, 44, 95, 48, 15, 4]
8	[0, 71, 94, 45, 18, 51, 14, 3, 59, 84, 70, 65, 88, 52, 8, 38, 61, 63, 86, 58, 10, 54, 62]
9	[0, 7, 31, 47, 1, 29, 80, 40, 76, 67, 39, 49, 37, 35, 68, 46, 83, 17, 78, 34, 55, 27, 33, 85]

**Table 17.** Total cost between current method and the GA model

Model	Total cost (M)	Number of late delivery nodes	Service level (%)
Current model	7.55	11	88.7
GA	7.1	0	100

## 7. CONCLUSION

The GA model has been used to solve the VRP in a distribution system with 1 warehouse, 12 trucks, and 97 customers. The results show that the GA model gives lower cost and higher service level than the heuristic method, being used. However, the parameters of the model are only selected empirically, so the results are not very good. The future research is to use experimental design DOE to determine the model parameters to get suboptimal results.

## References

- [1] He-Yau Kan and Amy H. I. Lee (2018), *An Enhanced Approach for the Multiple Vehicle Routing Problem with Heterogeneous Vehicles and a Soft Time Window*. *Symmetry* 2018, 10, p. 650.
- [2] Shuguang Liu, Weilai Huang and Huiming Ma (2008), *An effective genetic algorithm for the fleet size and mix vehicle routing problems*. *Transportation Research Part E* 45 (2008), pp. 434–445.
- [3] Danlian Li, Qian Cao, Min Zuo, Fei Xu (2020), *Optimization of Green Fresh Food Logistics with Heterogeneous Fleet Vehicle Route Problem by Improved Genetic Algorithm*. *Sustainability*
- [4] Efrain Ruiz, Valeria Soto-Mendoza, Alvaro Ernesto Ruiz Barbosa, Ricardo Reyes (2019), *Solving the open vehicle routing problem with capacity and distance constraints with a biased random key genetic algorithm*. *Computers & Industrial Engineering*, pp. 207-219.
- [5] Ahmad Hassanat, Khalid Almohammadi, Esra'a Alkafaween, Eman Abunawas, Awni Hammouri, V. B. Surya Prasath (2019), *Choosing Mutation and Crossover Ratios for Genetic Algorithms—A Review with a New Dynamic Approach*. *Information* 2019.
- [6] D Sariklis, S Powell (2000), *A heuristic method for the open vehicle routing problem*. *Journal of the Operational Research Society*.
- [7] Reza Alizadeh Foroutan, Javad Rezaeian, Iraj Mahdavi (2020), *Green vehicle routing and scheduling problem with heterogeneous fleet including reverse logistics in the form of collecting returned goods*. *Applied Soft Computing*.
- [8] Vickie Dawn Wester (1993), *A Genetic Algorithm for the Vehicle Routing Problem*. University of Tennessee, Knoxville.

## [P-15] Utilizing Project Management Principles in the Implementation of the KETO BISTRO Business Plan at a Seaport Location

Le Duc Dao\*, Hoang Tuan Anh, Tran Hoai Phuc, Vu Minh Phuong,

Nguyen Vu Bich Ngoc, Thai Thi Minh Tram

*Faculty of Mechanical Engineering, Ho Chi Minh City University of Technology (HCMUT), 268 Ly Thuong Kiet Street, District 10, Ho Chi Minh City, Viet Nam*

*Viet Nam National University Ho Chi Minh City, Linh Trung Ward, Thu Duc City, Ho Chi Minh City, Viet Nam*

\*Corresponding author: lddao@hcmut.edu.vn

### Abstract

Ports are essential elements of a vibrant and dynamic society since they play a critical role in supporting both economic and cultural progress. This study emphasizes the significance of culinary image in enhancing tourist satisfaction and fostering repeat visits, with particular relevance to the tourism industry in Viet Nam. Leveraging technologies such as Microsoft Project (MsP) and project management principles, this research aims to create a comprehensive project plan for the establishment of a healthful Vietnamese restaurant that offers a multitude of advantages. The Analytic Hierarchy Process (AHP) technique and consideration matrix are employed to investigate the selection of an optimal location, replacing outdated labor-intensive and complex approaches. The findings of this study provide valuable insights for tourism marketers and restaurant owners, shedding light on the pivotal role of culinary experiences in driving sustainable tourism and fostering economic growth.

**Keywords:** *Culinary tourism, Tourism industry, Project management*

### 1. INTRODUCTION

Ports serve as crucial catalysts for both economic growth and cultural development. Economically, ports act as vital gateways for international trade, connecting regions and countries, facilitating the movement of goods, and driving economic activities [1]. They generate employment opportunities, attract foreign investments, and stimulate local businesses, contributing to job creation and income generation. They serve as entry points for tourists, exposing them to different cultures, traditions, and experiences. Hence, ports are key drivers of cultural growth as they bring together people from diverse backgrounds, facilitating cultural exchange, and promoting multiculturalism. Overall, ports play a pivotal role in fostering both economic and cultural growth, making them crucial components of a thriving and dynamic society.

Vietnamese traditional cuisines have played an important role in the country's economic development. Referring to [2], the paper examines the satisfaction and intentions of foreign tourists in Ho Chi Minh City, Vietnam by focusing on their satisfaction with local food. The study suggests five aspects of food presentation, including flavor, price, serving method, and vendor/restaurant staff. The study intends to offer insights for tourist marketers by examining the connection between these features and meal pleasure as well as the relationship between food satisfaction and behavioral intentions. The information was gathered by conducting a face-to-face poll with 210 foreign tourists in well-known areas of the city. The findings show that each of the five aspects of food image positively influences satisfaction, with taste being the most important one. This study has important ramifications for tourism marketers, highlighting the role that culinary image plays in raising visitor happiness, and promoting return trips.

However, besides the urge of developing culture to the world, the growth of healthy diet, recent research has explored the relationship between perceived and actual changes in healthy food intake, shedding light on the effectiveness of public health campaigns promoting healthier eating habits. The paper carried out the research where participants were then classified into different groups based on their perceived changes in eating patterns over a six-month period. The results revealed that participants who reported making a healthy shift in their eating behavior demonstrated an actual improvement in their dietary patterns, including a reduction in the consumption of less healthy food categories. These positive changes were associated with a decrease in body mass index (BMI)

and potentially reduced risks of non-communicable diseases. These findings highlight the importance of both perceived and actual changes in promoting healthier food choices and support the effectiveness of public health campaigns that encourage individuals to adopt healthier eating habits [3].

Investing in a Vietnamese healthy restaurant at the seaport offers numerous benefits, including promoting Vietnamese cuisine, catering to the demand for nutritious food, contributing to public health, boosting the local economy, and enhancing the tourism experience. By developing a project plan that emphasizes menu development, sustainable sourcing, and collaboration with local stakeholders, the restaurant can become a successful platform for showcasing Vietnamese culinary traditions while encouraging a healthy lifestyle.

However, to successfully undertake this new project, it is crucial to incorporate Project Management principles and utilize tools such as Microsoft Project (MsP). Project Management involves using knowledge, skills, and techniques to meet specific goals in a temporary project, which is designed to produce a special product, service, or result. This process includes planning, organizing, inspiring, and controlling resources to achieve the objectives. It is a strategic ability that helps organizations to achieve their goals and better compete in their markets. Project Management became a professional practice in the mid-20th century and is essential for successful project outcomes. The paper has concluded that the traditional method of building construction is time-consuming, complex, and prone to errors. The planning process lacks proper subdivision of tasks, leading to overallocation of resources and improper allocation of resources for specific activities. To overcome these challenges, MsP is a modern tool for project management that optimally and effectively organizes project activities to complete the project within the planned duration and budget [4].

## 2. METHOD

The paper offered a broad planning framework for a Vietnamese healthy restaurant that a project manager or investor might take into consideration. Feasibility Analysis and Minimizing Project Cost are two crucial elements of the framework. There are unique characteristics and processes for each phase, which will be covered in more detail.

### 2.1. Feasibility analysis

In project management, feasibility analysis is the process of determining if a proposed project is worth pursuing by examining its technical, economic, and operational characteristics. Consequently, the study performs studies on these factors for the two key phases of setting up a restaurant, namely the selection of Location and Suppliers. The Analytic Hierarchy Process (AHP) approach and consideration matrix are used to examine the Location selection in order to identify the best site for a business. A separate strategy is used for the final aspect, which is the selection of Suppliers. The paper can identify the greatest supplier by carrying out the following three steps: (1) Create an evaluation scoring scale based on the set criteria; (2) Summarize the supplier's characteristics based on the evaluation scoring scale criteria; (3) Create an evaluation table using the Weighted-Score Models method and select the supplier with the highest score.

### 2.2. Minimizing project cost

The process of identifying and putting methods in place to lower a project's overall cost while still meeting its goals is commonly known as minimizing project cost. With a view to achieving this objective, the paper proposes the application of the tools from MsP for project planning. Additionally, the utilization of the AON (Activity On Node) network and Critical path method (CPM) for scheduling the project also reveals a great decline in the total expense of the project.

## 3. RESULTS AND DISCUSSION

### 3.1. Feasibility analysis

#### 3.1.1. Location feasibility study

With the goal of selecting a healthy restaurant and being able to promote the image of Vietnamese cuisine to international customers, the paper would first evaluate some common features and factors of a site. The paper takes into account three features: (1) Located near a crowded area with foreign tourists, (2) Placed on the facade,

and (3) Placed in a secure area where customers can move easily. Simultaneously, the factors of competitive advantage, possibility, and prospect are also taken into consideration. The completion of the Consideration matrix of site selection provides insight on how the features influence the factors. For instance, a site that is located near an area crowded with foreign tourists, or placed on the facade would have a higher advantage over competitors and a greater likelihood of development. However, the possibility of this site being chosen would be dramatically reduced due to the high expense for rent. On the other hand, a site that is placed in a secure area would have higher possibility thanks to the ease of traveling that is provided to the customer. Yet, this site tends to not attract as many customers, which would result in the little prospect of premises. From the guidelines, the study mentions three locations that are suitable for the site selection process: the area near the international seaport, the area near the airport, and the area near the tourist destination.

The AHP method is used with five main criteria: Accessibility, Location price, Competitors, and the Number of foreigners nearby. The Fundamental Scale is a scale of importance levels with corresponding scores for each level, ranging from considerably less important (1/9) to extremely important (9). The scores between criteria are then calculated in the study. The consistency ratio, as its name implies, indicates the relative importance of each pair of factors in a decision-making process. These criteria include accessibility, location prices, competitors, and the number of foreigners nearby. Scores are produced for each pair of these criteria. Accessibility, Location Price, Competitors, and the number of foreigners close by are all compared pairwise. Seaport, Tourist destination, and Airport are the three criteria used to evaluate each of the components, with their respective consistency ratios serving as the main determining factors. The findings indicate that a potential area is near the seaport. With the above results, the area near Phu My seaport will be the expected area to choose because it is the southern region's first deep-water seaport and primarily welcomes foreign delegations [5] with monthly rental rates ranging from 5,000,000 VND to 10,000,000 VND for areas ranging from 100 m<sup>2</sup> [6].

### *3.1.2. Supplier feasibility study*

Supplier feasibility study presents a scoring scale for evaluating suppliers of food ingredients based on criteria such as transportation cost, quality, flexibility, and variability. Each criterion is assigned within the range 1 to 9, indicating different levels of performance or characteristics of the suppliers in terms of their offerings, support, and capabilities. The suppliers are then evaluated and scored based on the criteria given. The process follows the aforementioned three steps are to select suitable suppliers. Three suppliers are being considered for Food Ingredient suppliers: **Thucphamso1 Dong Nai** [7], **Thanh Nam Food Company** [8], and **Hiep Phat Food Company** [9]. **Thucphamso1 Dong Nai** is a superior supplier in terms of flexibility, quality, and transportation costs. It is consequently selected as the potential supplier. With a physical site in Phu My Ward, Phu My Town, Ba Ria-Vung Tau Province, Supplier Thucphamso1 Dong Nai is a business that specializes in delivering clean food countrywide for more than 05 Big Companies including Co.opmart, Metro, Vissan, and others.

## **3.2. Minimizing project cost**

### *3.2.1. Project planning*

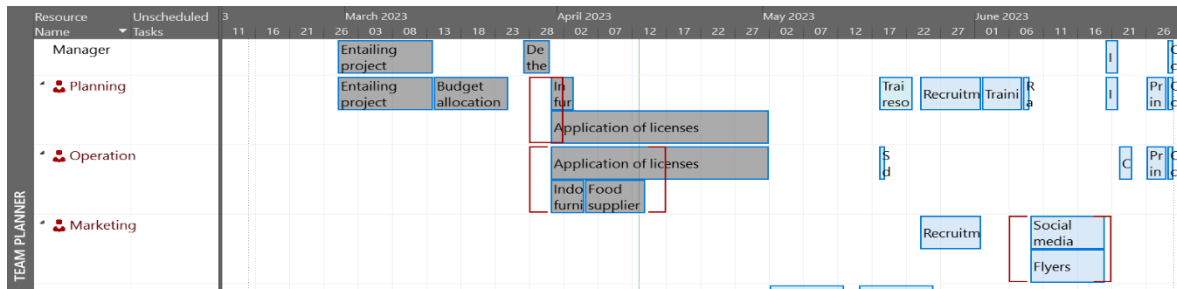
Project personnel includes two levels including managers and project staff. Project staff consisting of the marketing, planning, and operation teams will take on many tasks due to the nature and scale of the project and make the work progress reports to the managers. Following the definition of the organization chart, the job description is created, which is the expected number of employees, the corresponding salary, the main tasks and an overview of the project tasks, shown in Table 1, Table 2, and Figure 1.

**Table 1.** Primary tasks of the project

WBS order	Task name	Number of subtasks
1	Project planning and analysis	4
2	Construction	4
3	Installations	7
4	Resources	1
5	Human resources	3
6	Marketing and advertising	1
7	Finalizing the project	4

**Table 2.** Personnel details

Team	Role	Salary/Month	Quantity	Job description	Number of responsible tasks
	Manager	0 VND	1	Review, discuss with project staff and make decisions on proposals, monitor and accelerate the progress of works.	4
Marketing	Project staff	7,000,000 VND	1	Make a marketing plan for the bistro including identifying the audience, finding marketing channels and forms	3
Planning			2	Define project charter and scope, allocate budgets, and train chefs and cashiers	12
Operation			2	Responsible for preparing ingredients and eating utensils	7



\*Note: Red color represents overallocated personnel

Figure 1. Example of initial task allocation and timeline

3.2.2. Project scheduling

The workload moderation is then conducted using the Earliest Start Time rule (works start at the earliest possible time): The AON network describing the project’s tasks including the following components: work order, work completion time, earliest start time (ES), earliest finish time (EF), latest start time (LS), latest end time (LF).

Based on the CPM, the paper distinguishes the main work on the **critical path** from the normal work of the project. The critical path is the path that runs from the beginning to the finish of the project; changing any link on the critical path will have a direct impact on the project’s completion. The CPM method is integrated in MsP to determine the critical path in the most convenient way with as much workload as in the project. The seven tasks that make up the critical path for a project are Project planning and analysis, Construction, Installations, Resources, Human resources, Marketing and advertising, and Finalizing the project.

Subsequent to the analysis of the project’s initial workload distribution, it was discovered that there was an inadequacy problem: some jobs in departments such as Planning, Operations, and Marketing, had overallocated problems **as shown in Figure 1**. Following a review, there are two solutions to this problem: hire more workers or extend the project time. After comparing their change percentages on MsP, the option to lengthen the project time is the best fit because its change percentage is substantially smaller, only 7.45%, than the other.

Table 3. Summary of solutions

	Original plan	Hire more staffs	Lengthen the time
Number of staffs	5	7	5
Cost	84 350 000 VND	130 200 000 VND	84 350 000 VND
Working day	94	94	101
End date	07/07/2023	07/07/2023	18/07/2023
Change percentage	-	54.36%	7.45%

4. CONCLUSION

In conclusion, the location feasibility study for the healthy restaurant project has identified three suitable locations: the area near the international seaport, the area near the airport, and the area near the tourist destination. Using the Analytic Hierarchy Process (AHP) method, the area near the seaport received the highest score, making it the preferred choice due to its proximity to the Phu My seaport and monthly rental rates ranging from 5,000,000 VND to 10,000,000 VND for areas ranging from 100 m2.

Moving on to the supplier feasibility study, Thucphamso1 Dong Nai was selected as the preferred food ingredient supplier based on its track record of providing clean food to major companies and its physical location in Phu My Ward, Ba Ria-Vung Tau Province.



To minimize project costs, a project planning phase was conducted, defining the project personnel structure and roles. Work breakdown structures were created using the MsP tool, and project scheduling was performed using the Earliest Start Time rule and Critical Path Method (CPM). It was determined that extending the project time was the optimal solution for workload moderation, as it resulted in a lower change percentage compared to hiring additional workers.

Overall, with a thorough location feasibility study, supplier analysis, and careful project planning, the healthy restaurant project aims to establish a strategic and cost-effective operation in the chosen location, ensuring successful implementation and minimizing project costs.

### References

- [1] T. N.-M. Nong, “Performance efficiency assessment of Vietnamese ports: An application of Delphi with Kamet principles and DEA model,” *The Asian Journal of Shipping and Logistics*, vol. 39, no. 1, pp. 1–12, Nov. 2022, doi: 10.1016/j.ajsl.2022.10.002.
- [2] H. H. Nguyen, L. C. Dang, and T. D. Ngo, “The Effect of Local Foods on Tourists’ Recommendations and Revisit Intentions: The Case in Ho Chi Minh City, Vietnam,” *The Journal of Asian Finance, Economics and Business*, vol. 6, no. 3, pp. 215–223, Aug. 2019, doi: 10.13106/jafeb.2019.vol6.no3.215.
- [3] H. Szymczak *et al.*, “‘I’m eating healthy now’: The relationship between perceived behavior change and diet,” *Food Quality and Preference*, vol. 89, p. 104142, Apr. 2021, doi: 10.1016/j.foodqual.2020.104142.
- [4] P. M. Wale, N. D. Jain, N. R. Godhani, S. R. Beniwal, and A. H. Mir, “Planning and Scheduling of Project using Microsoft Project (Case Study of a building in India),” *Journal of Mechanical and Civil Engineering*, vol. 12, no. 3, pp. 57–63, Jul. 2015, doi: 10.9790/1684-12335763.
- [5] “Phu My - the perfect advantage to become the leading ‘Port City’ in Southeast Asia.,” *LEC Group Corporation*.
- [6] SoSanhNha, “Cho Thuê Nhà Nguyên Căn Tiện Buôn Bán, Tổng Diện Tích 85M2,” ©2022 *sosanh nha.com*.
- [7] “Công Ty TNHH Thực Phẩm Số Một Đồng Nai.”
- [8] “Thực Phẩm Thành Nam - Công Ty TNHH MTV Nông Lâm Sản Thành Nam.”
- [9] “Công Ty TNHH Thực Phẩm Hiệp Phát - Hiep Phat Food Company.”

## [P-17] Maritime Logistics Model Optimization - A Case Study on Minimizing Distribution Cost on Port-to-Port System

Le Duc Dao\*, Le Nguyen Khoi, Huynh Nhat Huy, Dao Quang Chinh, Ngo Xuan Minh

*Faculty of Mechanical Engineering, Ho Chi Minh City University of Technology (HCMUT), 268 Ly Thuong Kiet Street, District 10, Ho Chi Minh City, Viet Nam*

*Viet Nam National University Ho Chi Minh City, Linh Trung Ward, Thu Duc City, Ho Chi Minh City, Viet Nam*

\*Corresponding author: lddao@hcmut.edu.vn

### Abstract

The development of sea-freight logistics systems allows efficient and effective response to customers, thus assisting the maritime industry in developing sustainably. Logistics function is concerned with controlling and delivering the flow of products such as raw material, work in progress and finished goods where they are needed at the right time and right quantity. In logistics characteristics, total landed cost is considered as one of the key factors affecting the success of maritime business. This article aims to develop a logistics mathematical model for maritime logistics distribution system which is used for applying to XYZ corporation - a 3PL company to minimize the transportation cost consisting of fixed cost for operating vessels and distribution cost which is depended on shipped cubic metre of products. Results of the model deliver the flow matrix from start port to end port aligned with quantity and vessel types, consequently supporting decision makers for obtaining their appropriate business strategy.

**Keywords:** *Logistics system, Maritime industry, Transportation cost, 3PL company*

### 1. INTRODUCTION

Since the past two decades, logistics has played a crucial role in many aspects of the supply chain, which the very significant growth mainly comes from the increase of the purchase behavior of the end ports. When consumers are now more likely to buy products on the websites, not only because of the convenience, but the fairly lower price is also an aspect of online orders improvement. With that increase in demand, the logistics terms had changed and adapted quickly to respond to the end ports in the fastest process, procedures, and transparency with the lowest cost of transportation. From that, one of the aspects of the logistics, which is sea freight transportation, has experienced several trends and challenges.

When dealing with the significant increase of global trade, which is leading to the higher frequency of sea transportation as this is the type of transportation that could access almost every continental of the world with the large quantity of products in one vesselment, while bringing back the cost effectiveness along with lower impact on the environment. For that reason, sea freight transportation is such a problem for the business. They are now seeking the most cost-effective shipping type for their transportation needs, which types of vessels they should use, how large would it be, how much vessel to be used, and other constraints that they must deal with to minimize the cost of transportation. Besides, the business must clearly understand the impact of vessel selection on capacity, cost, and flexibility, and their implications for operations and end port satisfaction, along with the guarantee of delivery timelines and product quality, or have the appropriate strategy to deal with any risk that could happen when making a decision on shipping selection.

The theoretical approach in our paper is to propose an optimization mathematical model. Melkote *et al.* [1] introduces a mathematical model that aims to optimize the location of facilities and the design of transportation networks in a way that minimizes the total costs. Teixeira *et al.* [2] highlight the importance of location decisions for different types of public facilities by proposing a mathematical model to emphasize the significant impact these locations can have on accessibility, access, and quality of services provided to the people. Moreover, plenty of factors that affect the choosing decision are also considered. Bařligil *et al.* [3] recognize that efficient distribution network design is crucial for 3PLs to meet customer demands while minimizing costs, with the consideration of various factors such as transportation costs, warehouse locations, inventory management, and customer service levels. On the other hand, when dealing with sea transportation problems, several factors that

are related to overseas shipping must be considered. Nguyen Khoi Tran *et al.* [4] developed a comprehensive approach that takes into account multiple cost factors and environmental impact, such as cost for operating the fleet. Jane *et al.* [5] found out that maritime transport costs involve various factors, including shipping fees, port charges, and so on. These costs can significantly impact the competitiveness of products in international markets. Sun *et al.* [6] develop a mathematical model that considers factors such as ship characteristics, transportation costs to demonstrate the linkages between ship choices and transportation cost to port. Alev *et al.* [7] emphasize the importance of selecting the appropriate sea vessel type for an efficiency marine transportation. Duan *et al.* [8] focus on the optimization of vessel routing to minimize the transportation cost.

From the mentioned situation, the team found that it is necessary to create a more comprehensive view for business when making decisions on choosing the type of vesselment. The method is to create a mathematical model for sea freight transportation, with the objective of minimizing the variable cost and fixed cost when using vessels to deliver the products between two hubs overseas. Which means that the model results will be minimizing the cost of choosing the appropriate type of vessel (small, medium or large) to deliver the product when maximizing all the demand served at the same time. The concrete model of optimization will be discussed in the below sections. In section 2, we discuss the optimized model when applying the framework of the basic model to overseas freight forwarding. In section 3, we illustrate the case study of the model, and section 4 is the results obtained with the model.

## 2. MATHEMATICAL MODEL

### Notation:

$i$ : the index of the start port ( $i = 1, 2, \dots, I$ )

$j$ : the index of the end port ( $j = 1, 2, \dots, J$ )

$w$ : the index of the size of vessel (*Small, Medium, Large*)

### Parameters:

$Cw_{i,j}$ : the cost of each weight of unit from port  $i$  to end port  $j$  (\$)

$Op_{i,w}$ : Operation cost of each vesselment from port  $i$  with weight  $w$  (\$)

$Op_{i,w}$ : Operation cost of each vesselment from port  $i$  with weight  $w$  (\$)

$MaxW_{i,w}$ : The maximum CBM that vessels with size  $w$  can deliver

$AW_i$ : The required CBM transportation of beginning port  $i$

$Own_{i,w}$ : The number of vessels in port  $i$  with weight  $w$

### Decision variables:

$W_{i,j}$ : Weight of unit from port  $i$  to end port  $j$

$X_{i,w}$ : The number of vessels from port  $i$  with weight  $w$  (vessels)

### Full Formulation:

$$\text{Minimize: } \sum_{i \in I} \sum_{j \in J} Cw_{i,j} w_{i,j} + \sum_{i \in I} \sum_{w \in W} Op_{i,w} X_{i,w}$$

Subject to

$$(1) \sum_{i \in I} w_{i,j} \leq Cap_j; \forall j \in J$$

$$(2) \sum_{w \in W} X_{i,w} MaxW_{i,w} \geq \sum_{i \in I} W_{i,j}; \forall j \in J$$

$$(3) \sum_{j \in J} w_{i,j} = AW_i; \forall i \in I$$

$$(4) X_{i,w} \leq Own_{i,w}; \forall i \in I, \forall w \in W$$

$$(5) W_{i,j} \in integer; \forall i \in I, \forall j \in J$$

$$(6) X_{i,w} \in integer; \forall i \in I, \forall w \in W$$

Constraints (1) illustrate the weight  $w$  transported from  $i$  to  $j$  is less than the total weight the vessel can carry.

Constraints (2) sets the maximum weight of the total number of vessels  $X_{i,w}$  is greater than the sum of the weight  $w$  transferred from  $i$  to  $j$ .

Constraints (3) means the total weight  $w$  transported from  $i$  to  $j$  can be served the demand weight of good of end ports.

Constraints (4) tells that the number of transport vessels is less than the number of vessels currently owned. Constraints (5) (6) define decision variables.

### 3. CASE STUDY: PORT-TO-PORT TRANSPORTATION

In these days of ocean freight industry, transportation cost significantly impacts the profitability and efficiency of businesses engaged in international trade. Selecting the appropriate type of vessel for ocean freight plays a crucial role in optimizing transportation costs. The case study focuses on analyzing major factors involved in selecting the appropriate kind of vessel for transportation and identifying the most cost-effective option for a hypothetical company. We now consider an explanatory case study of a multinational company for further constructing the mathematical model to practical issues. In particular, we investigate the XYZ Corporation, involved in the import and export of consumer goods. XYZ Corporation operates globally, shipping goods from different ports located in Asia to various destinations worldwide. Currently, XYZ Corporation utilizes a standard container vessel for its freight transport. However, rising transportation costs have prompted the company to explore alternatives to optimize costs without compromising delivery timelines and product quality.

#### 3.1. Data collection

The necessary input data for mathematical analysis has been mentioned in the mathematical model as required parameters. The purpose of the data collection process is to gather the transportation data, including vessel's volumes, destinations and costs associated with the existing container vessel. By utilizing 5-10 min interviews with prepared questionnaires related to extract necessary information as well as referencing past operational data to ensure highly realistic data input. Table 1 shows the available cubic metre that a port  $i$  want to deliver to port  $j$ . Table 2 illustrates the maximum cubic metre can be received in a port  $j$ . For instance, Port 1 can receive lower than 10000 CBM and if the received amount exceeds  $Cap_j$ , the rest of them will be sent to other available ports.  $Cw_{ij}$  (Table 3) matrix shows the transportation cost per CBM from destination  $i$  to  $j$ . In this situation, each CBM will cost 3 dollars per unit if the route from beginning port 1 to ending port 1 is chosen and cost 1 dollar per unit when the product is moved from beginning port 2 to ending port 1 instead of starting from beginning port 1. The operation cost for 3 different sizes of vessel: Small, Medium and Large in different ports is shown in Table 4 and the currently available vessels in 5 ports are presented in Table 5. The data for maximum carrying cubic meter for 3 types of shipping in different ports is shown in Table 4. In the next section, the objective function and constraint for the mathematical model are built from the collected data for achieving the optimal solution for the case study.

**Table 1.** The required CBM transportation of beginning port  $i$

Port index	$AW_i$
1	10000
2	3000
3	7000
4	8000

**Table 2.** Maximum capacity at port  $i$ 

Port $i$	$Cap_j$
1	10000
2	5000
3	5000
4	6000
5	4000

**Table 3.** Cost per CBM from port  $i$  to  $j$ 

$Cw_{ij}$		TO Ending port $j$				
		1	2	3	4	5
FROM Beginning port $i$	1	3	2	3	4	1
	2	1	4	5	3	2
	3	8	3	9	4	6
	4	7	1	2	1	8
	5					

**Table 4.** Operation cost for 3 sizes of vessels  $w$  in port  $i$ 

$Op_{i,w}$	Small	Medium	Large
1	300	500	750
2	200	600	700
3	350	550	600
4	400	500	550

**Table 5.** Current number of vessels size  $w$  in port  $i$ 

$Own_{i,w}$	Small	Medium	Large
1	2	3	2
2	2	0	1
3	1	1	2
4	2	2	1

**Table 6.** Maximum capacity of vessels type  $w$  in port  $i$ 

$\text{Max}W_{i,w}$	Small	Medium	Large
<b>1</b>	1500	2000	2500
<b>2</b>	1200	2300	3000
<b>3</b>	1400	2100	2700
<b>4</b>	1400	2000	2900

### 3.2. Optimal result for case study

In terms of finding the optimal result for case study, the objective function is identified and constructed based on two major components: coefficient (including  $Cw_{i,j}$  matrix and  $Op_{i,w}$ ) and decision variable (including  $w_{i,j}$  and  $X_{i,w}$ ). For solving technique, the “Simplex Linear Programming” is considered to be the appropriate solver to process the linear model [9]. Based on the mathematical model section, we merge objective function, decision variables and constraints to “Excel solver” and addresses the program with “Simplex LP” method to obtain the optimal results. Consequently, Table 7 illustrates the result for the integer variable, which is the optimal CBM from port  $i$  to port  $j$  that XYZ should be allocated to achieve the minimum transportation cost times CBM. The required number of vessels in each port  $i$  should use for transportation is shown in Table 8. To conclude, the achievable result of objective function represents the total transportation cost for allocating CBM and number of vessels is shown in Table 9 which means the business only spent \$66,950.00 for transportation for the results.

**Table 7.** Optimal result for  $W_{i,j}$ 

$W_{i,j}$		TO Ending Port $j$				
		<b>1</b>	<b>2</b>	<b>3</b>	<b>4</b>	<b>5</b>
<b>FROM Beginning port <math>i</math></b>	<b>1</b>	6000	0	0	0	4000
	<b>2</b>	3000	0	0	0	0
	<b>3</b>	0	5000	0	2000	0
	<b>4</b>	0	0	4000	4000	0

**Table 8.** Optimal result of  $X_{i,w}$ 

$X_{i,w}$	Small	Medium	Large
<b>1</b>	1	3	1
<b>2</b>	0	0	1
<b>3</b>	0	1	2
<b>4</b>	1	2	1

**Table 9.** Optimal total cost in port *i*

Port <i>i</i>	Transportation cost	Operating cost
1	22000	2550
2	3000	700
3	23000	1750
4	12000	1950
<b>Total optimal cost (\$)</b>	<b>66,950</b>	

#### 4. CONCLUSION AND FUTURE RESEARCH

This case study aims to assist XYZ Corporation in optimizing transportation costs for freight transport systems. By evaluating key points and considering the company's specific requirements, the mathematical model supports XYZ Corporation in making strategic decisions that aligns with its business goals and ensures efficient and cost-effective transportation operations. The total transportation cost is 66,950\$ aligned with optimal decision variables shown in section 4.2. Specifically, XYZ corporation, according to the model results, can evaluate the vessel selection based on capacity, cost, and flexibility, thus identifying the most cost-effective type of vessel for their transportation needs. They also can reduce potential cost by switching to recommended vessel types and balance between delivery time and transportation cost. Future research can extend in several directions. First of all, stochastic demand will be the challenging problem that should be addressed in the future. The combination of traveling methods - intermodal transportation or multi-modal transportation such as sea and road freight will be promising issues for further investigation. The model can be applied to the other fields related to logistics networks.

#### References

- [1] Melkote, S. and Daskin, M.S. (2001) 'An integrated model of facility location and Transportation Network Design', *Transportation Research Part A: Policy and Practice*, 35(6), pp. 515–538.
- [2] Teixeira, J.C. and Antunes, A.P. (2008) 'A hierarchical location model for public facility planning', *European Journal of Operational Research*, 185(1), pp. 92–104.
- [3] Başlıgil, H. et al. (2011) 'A distribution network optimization problem for third party logistics service providers', *Expert Systems with Applications*, 38(10), pp. 12730–12738.
- [4] Tran, N.K., Haasis, H.-D. and Buer, T. (2017) 'Container shipping route design incorporating the costs of shipping, inland/feeder transport, inventory and CO2 Emission', *Maritime Economics & Logistics*, 19(4), pp. 667–694.
- [5] Korinek, J. and Sourdin, P. (2010) 'Clarifying trade costs: Maritime transport and its effect on agricultural trade', *Applied Economic Perspectives and Policy*, 32(3), pp. 417–435.
- [6] Sun, Y. et al. (2023) 'Study of channel upgrades and ship choices of river-shipping of Port Access-Transportation', *Transportation Research Part D: Transport and Environment*, 119, p. 103733.
- [7] Taskin Gumus, A. and Yilmaz, G. (2010) 'Sea vessel type selection via an integrated VAHP–ANP methodology for high-speed public transportation in Bosphorus', *Expert Systems with Applications*, 37(6), pp. 4182–4189.
- [8] Duan, G. et al. (2021) 'A hybrid algorithm on the vessel routing optimization for Marine Debris Collection', *Expert Systems with Applications*, 182, p. 115198.
- [9] Berry, N. (2021) 'Linear programming problems in solving maximum difficulties by simplex method', *RESEARCH REVIEW International Journal of Multidisciplinary*, 6(6). doi:10.31305/rrijm.2021.v06.i06.016.

**[P-19] A Hybrid Improved Case-Based Reasoning Approach and Metaheuristics for Cost Estimation**

Pham Ngoc Xuan Mai, Phan Nguyen Ky Phuc\*

*International University, Ho Chi Minh City, Viet Nam, 700000*

\*Corresponding author: pnkphuc@hcmiu.edu.vn

**Abstract**

This study developed a cost predicting model based on a combination of Case-Based Reasoning (CBR) and Genetic algorithm (GA) to optimize the impact of attributes that forecast the installation cost for a new production line. This model will retrieve the old data to calculate the similarity against the problem to be solved, from which the prediction cost will be given. The goal of the model is to minimize forecast errors while finding the weights of the corresponding attributes. Besides GA, Particle swarm optimization (PSO) is considered in determining the impact of features to improve error rates. The results from GA and PSO will be compared to find the metaheuristics method that is accordant to the properties of the data set. Some analysis is also carried out to evaluate the sensitivity of specific attributes and parameter to the installation cost.

**Keywords:** *Installation cost, Genetic algorithm, Particle swarm optimization, Forecast*

**1. INTRODUCTION**

In recent years, cost prediction or cost estimation has become one of the vital stages when enterprises or companies (e.g., constructors, manufacturers, etc.) start investing in a new project. Through this stage, the cost estimation information provides their project managers and financial managers with an approximate and reasonable budget, contributing to the project's success. In particular, the project members first define all project scopes related to how large the project is, which purposes the project is used for, which kind of techniques the project is used, etc. Based on that information, companies can therefore evaluate the feasibility of the project compared to their financial status based on the cost prediction approaches. In addition, the accuracy of the cost estimation must be strictly measured, which has a considerable effect on the project's success. Providing a cost estimation with high accuracy can benefit the projects such as more accurate profit margin, easily to manage resources, and control the risk.

For many years, cost prediction was a vital requirement in the project life cycle. Researchers in this field proposed many approaches for solving cost prediction problems, in which the Case-Based Reasoning (CBR) model is one of the efficient methods introduced by [1]. The Case-Based Reasoning (CBR) model includes four phases (i.e., Retrieve, Reuse, Revise, Retain), which aim to preview the previous data to measure the weights of the new project cost attributes. However, using only CBR cannot define the weights accurately; the Analytic Hierarchy Process (AHP) systematically captures domain knowledge from experts helping the result be more accurate within 17.5% of the error rate [2]. [3] realized that the lack of previous CBR papers focused on adopting the CBR model. Hence, the author decided to investigate the case adoption in the CBR model using 164 Korean public apartment projects with a 6.05% error ratio.

Furthermore, [3] research concluded that qualitative aspects are practical on the estimation model and are also efficient for verifying and analyzing the bias resulting from different sources of data based. For their later research, the authors have then improved the CBR approach [4] by concentrating on the "Revise" phase, which improves the accuracy of the CBR process. The author used the Multiple regression analysis (MRA) process in this phase to improve the outcomes of the CBR model. The performance of its application on 99 multi-family housing projects enhanced the accuracy by 4.39%. In addition to the two improved CBR models above, [5] combined the CBR model with a Genetic algorithm (GA) to estimate the cost in the early construction state by conducting the optimal weights of attributes. The initial weights were resolved many times following the GA process: creating population, cross-over, and mutation to optimize the cost estimation model. This development actually brings the successful cost prediction with 5.60% for the error rate of the GA-CBR system, and it inspires many later papers proposing GA to improve the accuracy.



Another technique was proposed by [6] to forecast the construction cost by combining the fuzzy logic into Artificial Neuron Network (ANN) but it has not been widely used in this field because it cannot adopt the dynamic in market price. Then, inspired by their paper, an improved back propagation (BP) neural network was developed by combining the current version with the Genetic Algorithm (GA) approach [7]. Then, the 1.89% error of this model will be tested by using training data. During this time, another research has been researched by [8], which has used MRA to determine the cost of new cases for residential buildings in Jakarta. The results from the MRA formulation provide cost estimations with the model's accuracy range of 5.40%.

[9] investigated the Case-Based Reasoning (CBR) process with a Genetic algorithm (GA) to optimize the weights of impact attributes. The developed CBR model can consistently reduce errors and be effective in the early stages of financial planning. According to the authors, the developed CBR model can offer decision-makers reliable cost information for evaluating and comparing multiple choices to find the best solution while keeping costs low. In addition, the application of a Multi-Layer Feed-forward (MLF) neural network model was presented to estimate the cost of construction projects in India (i.e., construct 78 buildings).

Besides that, meta-heuristics was also applied in this line of research [10] implemented a population-based approach (i.e., Particle swarm optimization (PSO)) to estimate the new construction cost and duration time from 60 historical constructed projects. The main procedure of this model is creating the swarm initialization by randomly giving a location for each particle. Then, it evaluates the objective function of the proposed model for each particle and compares the objective function value of each particle with *pbest*. The value of its target function is determined to be *gbest*, and its location is *gbest* from particles with the best objective function value. Even though only eight attributes are considered, including the number of bricks, the quantity of concrete, type of grounding, number of elevators, floor area, ground area, floors number, and security system, PSO still can provide the result with high accuracy, Coefficient of Variation (10.87% and 4.94%).

The main contributions of this research are summarized as follows: (1) build a cost estimation model based on the Case-Based Reasoning (CBR) method, adopted by larger attributes and current production lines. (2) propose Genetic algorithm (GA) and Particle Swarm Optimization (PSO) approaches to optimize the impact of characteristics and release the accurate construction cost for a new production line.

## 2. METHODOLOGY

A considered installation project includes the several main properties (known as attributes), which effects on the installation cost of production lines. Therefore, those attributes are utilized in the proposed prediction model (i.e., Case-Based Reasoning approach (CBR)) to evaluate the similarity of installation projects, based on the similar scores of attributes. Then, the similarity of projects (i.e., similar indexes) can be determined based on similar scores and weighted values. In addition, the proposed CBR model needs to provide the optimal set of weighted values, which represents how much each attribute affects to the predicting values of the model. We propose an efficient Genetic algorithm (GA) to improve the results to find the optimal set of weighted values while minimizing the errors of forecast and actual installation costs. The detailed process (i.e., CBR model and embedding GA) is illustrated in Figure 1.

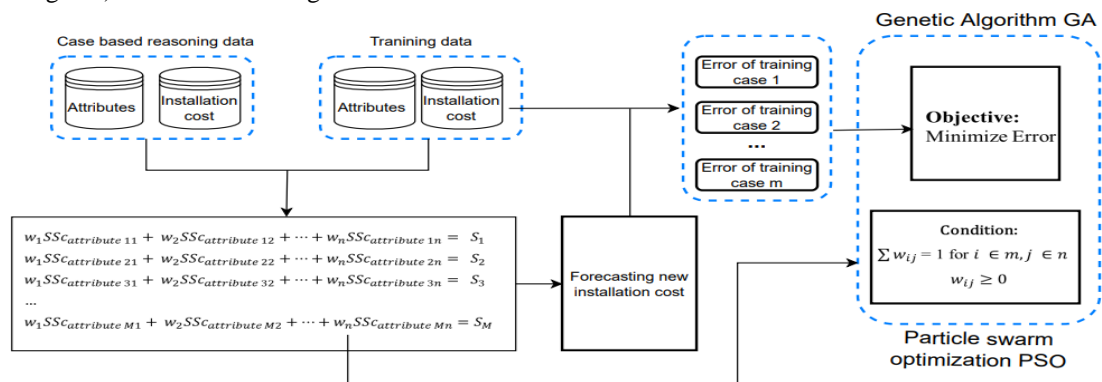


Figure 1. Optimization model of weighted value of attributes

## 2.1. Case-Based Reasoning Model

• **Step 1: Evaluate similar scores.** Installation costs for a new production line will be estimated by finding the most similar cases in Case-Based Reasoning data (CBR data) corresponding to the new cases. Regarding the training model, we utilized two sets, including (1) Case-Based Reasoning (CBR) data and (2) Retrieved data (Train data) to find the similarity of production lines. The similarity of attributes between CBR data and Train data is calculated as follows.

$$SSc_{Attribute} = 100 \left( 1 - \frac{AV_{Train} - AV_{CBR}}{Max[AV_{Train} - AV_{CBR}]} \right)$$

where  $SSc_{Attribute}$  denotes similar scores of attributes between CBR data and Train data and  $AV_{Train}$  and  $AV_{CBR}$  represent attribute values of Train and CBR, respectively.

• **Step 2: Estimate the error installation cost.** After having similar scores for production lines, a certain number of similar cases will be selected to predict the installation cost and the standard deviation of the new cases. In this research, the number of most similar cases initially equals 3, which can be tuned to improve the minimum error in. In particular, there are three components:

- (1) *Calculating the similarity index of the case.* A similar score has been determined in the above step, but it only compares the attributes' values between CBR data and Train data. Because attributes have different effects on installation costs, calculating a similar score is not enough to express the similarity of cases, so the weights of attributes are included as the magnitude of each attribute's influence on cost.

$$\sum_j^n w_{ij} SSc_{ij} = S_i, \quad \forall i \in M$$

where  $n$  denotes the number of attributes,  $M$  denotes the number of production in CBR data,  $S_i$  denotes the similar index of the installation cost, and  $w_{ij}$  denotes the optimal weighted value of the attribute.

- (2) *Granting the most similarity cases.* Cases with high similar indexes will be retrieved for the forecasting phase. First, three highest similar cases will be retrieved, and it can be changed. These similar cases will be normalized before forecasting. The similar score of the selected cases is evaluated as follows.

$$N\_S_i = \frac{S_i}{\sum S_i}$$

- (3) *Estimating the error installation cost.* Based on similar scores and costs of the three cases with the highest similar scores. The costs of training data are determined as follows.

$$EC_i = N\_S_i \times C_{CBR_i}$$

where  $C_{CBR_i}$  denotes the installation costs of case-based reasoning data.

The errors will be calculated to consider forecast's accuracy. This is also the objective of this study: “*Minimize the errors of forecasting*”. And the optimal weights which is “*variables*”, will be used to forecast the installation cost for the new production line.

$$Err = EC_i - C_{Train_i}$$

where  $C_{Train_i}$  is the installation costs of train data.

## 2.2. Genetic Algorithm

GA is one of the popular algorithms for solving optimization problems. In this subsection, the main concepts of GA are discussed as follows:

• **Creating an initial population of attribute weights.** A “population” is a set of “individuals” representing attribute weights to identify the forecast cost or the error. A population is randomly generated in this problem with 30 individuals, which can be changed to improve the solution. An individual is represented by an array with size of  $p$ , denoted by  $ind = [score_1, \dots, score_p]$ . Let  $p$  denote the number of attributes. Each element follows the uniform distribution  $U \sim (0,1)$ . In addition, since the sum of weights must equal to 1, attribute weights ( $weight_i$ ) is normalized as follows.

$$weight_i = \frac{score_i}{\sum_{j=1..p} score_j}$$

• **Evaluating the fitness function.** With a given set of attribute weights (i.e., an individual), the CBR model is re-called for predicting the forecast installation cost and its standard errors, which is the fitness value of GA. Based on the fitness value, GA can find better set of attribute weights.

• **Operators (i.e., cross-over and mutation).**

**Crossover.** Two individuals are selected known as two parents to produce two offspring. In this algorithm, each pair of two consecutive individuals will be selected until all individuals in population are implemented in crossover. In particular, each parent is divided into two parts by a point  $n$ , then two parts of two parents will have crossed each other to obtain two offspring solutions, as illustrated in Figure 2. Let  $n$  be the random number in the range of number of attributes.

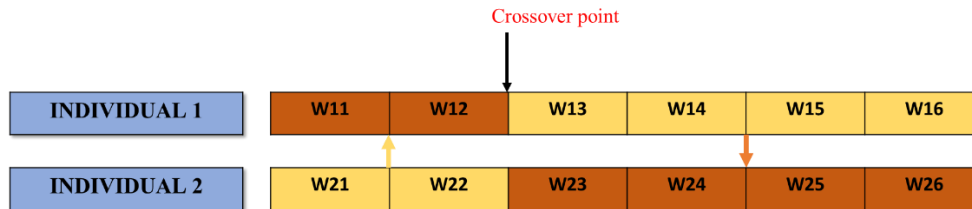


**Figure 2.** An illustration of the crossover operator

After operating the crossover to obtain two new offspring solutions, those solutions will be also normalized for satisfying the sum of weights must equal to 1 (similar to the above-mentioned method). Then, the fitness values of two new offspring solutions will be evaluated and stored to the population for the next iteration. Moreover, if any solution obtained after operating the cross over provides better errors than the current best. Also, it will be assigned to the global best solution if the better solution is found.

**Mutation.** Each individual in the current population will be considered to mutate with the probability of 0.4, called the threshold of mutation. Regarding the operation, a randomly point in the individual is selected, whose values will be changed by randomizing a new weight value following  $U \sim (0,1)$ , as illustrated in Figure 3. The solution will be normalized again.

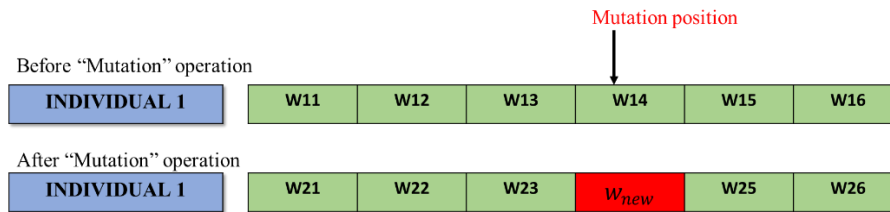


**Figure 3.** An illustration of the mutation operator

Similar to "Crossover", the new weighted values will be used to calculate the new errors. And the optimal set of weighted values is defined at this stage. Then this optimal set will be used to forecast the installation cost for the new production line.

### 2.3. Particle Swarm Optimization

PSO is a research metaheuristic based on the movement of the boid flocking process. The algorithm is represented by positions (they are sets of  $weight_i$  in this paper) and velocity randomly chosen in the search space (which is the changes of weights). Let  $w_i$  be inertia weighted  $w$  (i.e., the proportion of the previous velocity),  $c_1^i$  (resp.  $c_2^i$ ) denote correction factors (i.e., the proportion of personal best (resp. global best) retained),  $v_p^i$  represent the velocity of particles, and  $r_1$  and  $r_2$  be random number follows uniform distribution  $U \sim (0,1)$ . At each iteration  $i$ , the set of parameters ( $c_1^i, c_2^i, w_i$ ) will be update by the equations below:  $w_i = w_{max} - (w_{max} - w_{min}) \frac{i}{num\_iter}$ ,  $c_1^i = c_{1max} - (c_{1max} - c_{1min}) \frac{i}{num\_iter}$ , and  $c_2^i = c_{1max} - (c_{1max} - c_{1min}) \frac{i}{num\_iter}$ .

The terms "cognitive coefficient" and "social coefficient" refer to the parameters  $c_1^i$  and  $c_2^i$ , respectively. They decide how much weights should be placed on both recognizing the search result of the swarm and fine-tuning

the search result of the particle itself. These factors can be thought of as influencing the trade-off between exploration and exploitation. Then, the values of velocity  $v_p^i$  will be updated as the rule below:

$$v_p^{i+1} = w_i v_p^i + c_1^i r_1 (current_{best\_solution} - pop_p) + c_2^i r_2 (global\_best\_solution - pop_p)$$

- The new position particles (set of weights) are updated:  $pop_p^{i+1} = pop_p + v_p^{i+1}$
- Normalizing the set of weights:  $pop_p^{i+1} = \frac{pop_p^{i+1}}{\sum pop_p^{i+1}}$ .

### 3. CASE STUDY

Our research considers a case study, which aims to develop a prediction model for the installation cost of production lines. The data records the actual costs that factories have to pay to install the production line: TRB Xlife. There are eight main attributes as follows. The number of most similar cases are three production lines.

- **Installation year:** Time is an essential factor that significantly affects the installation cost. At different times, the price of the same machine will be different due to increased raw material costs, war, and shortage of materials. Therefore, in this study, installation time is an indispensable factor in reducing the deviation of results. The closer the time is, the less the price difference will be.

- **Country:** Machines are mostly imported from Europe, the place where the production line is installed will affect import costs, transportation costs, and exchange rate differences. Additionally, in the actual case, the price of equipment in different countries will be different because each factory will get a different discount.

- **The main manufacturing procedures:** The installation of a new production line, and its process cannot be ignored. Here, the production process of TBR Xlife is shown as follows: From Heat treatment to Grinding, then Top Coating according to customer requirements, and finally, Honing and Assembly. The primary process considers three attributes: Heat Treatment Furnace, Grinding & Honing, Top Coating and Assembling.

- **Digital technology level:** Digital investment is an indispensable thing to make production management easier and more efficient. However, the investment cost of digital systems is very large, so the decision of digital technology will significantly affect the cost of installing production lines. According to current data, there are 3 types of digital technology level namely: medium, high, advanced.

- **Maintenance level:** It is also important factor affecting the cost of installing a new production line The maintenance system has to suit the factory layout and the level of the system includes: medium, high, advance.

**To implement the case study.** GA and PSO approaches are implemented with 20 individuals and 100 iterations. Five training cases are used to calculate the minimum standard deviation error. The model's results using GA and PSO are shown in Table 1. It can be seen that with 3 most similar cases, the model can give standard deviation of error is VND 309,489,390.5 corresponding with the set of weighted values [0.130, 0.006, 0.399, 0.209, 0.235, 0.001, 0.020, 0.001]. Based on the results of PSO, the standard deviation of error from PSO is 323,968,826.4VND corresponding with the set of weighted values [0.42943, 0.02204, 0.29240621, 0.11430, 0.06247, 0.00180, 0.06705, 0.01049] as shown Figure 4.

**Table 1.** Results of forecasted cost for training and test cases by GA and PSO (Unit: 1000VND)

Train	Genetic Algorithm				Particle Swarm Optimization			
	Forecast	Actual	Forecast	Actual	Forecast	Actual	Forecast	Actual
1	11,704,93 7	10,888,22 4	11,547,76 7	10,888,22 4	11,754,93 7	10,888,22 4	11,147,76 7	10,888,22 4
2	11,201,46 9	11,171,11 2	10,891,92 7	11,171,11 2	11,179,11 2	11,171,11 2	11,091,92 7	11,171,11 2
3	11,192,39 6	11,361,11 2	11,897,46 6	11,361,11 2	11,176,47 0	11,361,11 2	11,797,46 6	11,361,11 2
4	11,355,01 4	10,798,22 4	10,166,54 4	10,798,22 4	11,417,97 4	10,798,22 4	10,166,54 4	10,798,22 4
5	11,151,26 1	11,356,11 2	11,058,07 6	11,356,11 2	11,169,90 3	11,356,11 2	11,658,07 6	11,356,11 2
STD Error	309,489		507,627		323,969		482,493	

After getting the results from GA and PSO, it can be seen that although both give good results, the error is nearly 3%. However, the standard deviation of GA is better than that of PSO. This proves that GA is more suitable for current data than PSO.

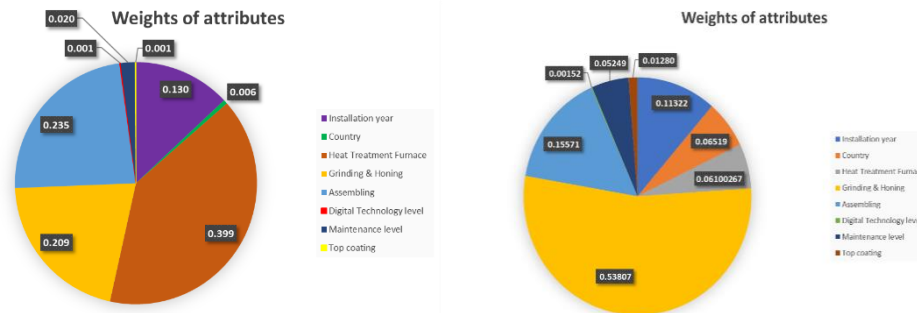


Figure 4. The set of weights solved by GA and PSO

In addition, there are some highlights for attributes as follows.

- Effect of “Country”. It is not a major factor in building the production line; it is possible to remove “Country” from the list of attributes to reduce research errors.
- Effect of “Top coating”. Like “Country” attribute, top coating is one of the attributes with the smallest weights. It was also selected to remove for sensitivity analysis. However, the new production line requires a top coating process, so it is not feasible to consider removing this attribute.

#### 4. CONCLUSION

This research proposes a model to predict installation costs for production lines based on similar cases in the past. This problem arises from companies spending much time forecasting new project costs, but the accuracy is not high. Meanwhile, they have a database of systems such as SAP, ERP, COUPA, etc., but have not been able to exploit them fully. In addition, the implicit factors affecting production costs are also not carefully considered. We build a cost estimation model based on a hybrid of the Case-Based Reasoning (CBR) method and a Genetic algorithm (GA) to optimize the impact of characteristics and release the accurate construction cost for a new production line. Besides GA, other metaheuristics, namely Particle Swarm Optimization (PSO), are considered to optimize the impact of characteristics to improve the error rates.

Selecting attributes related to the production line is vital as it will affect the forecast for new production lines. There are 8 attributes consisting of "Installation year", "Country", "Number of Heat Treatment Furnace", "Number of Grinding & Honing machine", "Number of Assembling machines", "Digital Technology level", "Maintenance level", "Top coating". After running the model with GA and PSO, the results show that PSO gave a standard deviation that is 36% lower than the company's current standard deviation, while GA gives a possible result of 39%. Hence, GA is more suitable for this data set.

#### References

- [1] I. Watson, “An introduction to case-based reasoning,” in UK Workshop on Case-Based Reasoning, 1995, pp. 1–16.
- [2] S.-H. An, G.-H. Kim, and K.-I. Kang, “A case-based reasoning cost estimating model using experience by analytic hierarchy process,” *Build. Environ.*, vol. 42, no. 7, 2007, pp. 2573–2579.
- [3] S.-H. Ji, M. Park, and H.-S. Lee, “Cost estimation model for building projects using case-based reasoning,” *Can. J. Civ. Eng.*, vol. 38, no. 5, 2011, pp. 570–581.
- [4] R. Jin, K. Cho, C. Hyun, and M. Son, “MRA-based revised CBR model for cost prediction in the early stage of construction projects,” *Expert Syst. Appl.*, vol. 39, no. 5, 2012, pp. 5214–5222.
- [5] S. Kim and J. H. Shim, “Combining case-based reasoning with genetic algorithm optimization for preliminary cost estimation in construction industry,” *Can. J. Civ. Eng.*, vol. 41, no. 1, 2014, pp. 65–73.
- [6] X. Wang, “Application of fuzzy math in cost estimation of construction project,” *J. Discret. Math. Sci. Cryptogr.*, vol. 20, no. 4, 2017, pp. 805–816.

- [7] Z. Du and B. Li, “Construction project cost estimation based on improved BP Neural Network,” in 2017 International Conference on Smart Grid and Electrical Automation (ICSGEA), 2017, pp. 223–226.
- [8] M. Amin, “Development of cost estimation model for residential building,” *Int J Civ Struct Eng Res*, vol. 5, no. 1, 2017, pp. 1–4.
- [9] W.-G. Hyung, S. Kim, and J.-K. Jo, “Improved similarity measure in case-based reasoning: A case study of construction cost estimation,” *Eng. Constr. Archit. Manag.*, 2019.
- [10] T. Z. Khalaf, H. Çağlar, A. Çağlar, and A. N. Hanoon, “Particle swarm optimization based approach for estimation of costs and duration of construction projects,” *Civ. Eng. J.*, vol. 6, no. 2, 2020, pp. 384–401.

**[P-21] Deep Learning for Quality Inspection of Manufacturing Product**Doan Huu Chanh<sup>1</sup>, Phan Nguyen Ky Phuc<sup>2,\*</sup>, Luu Trong Hieu<sup>3</sup><sup>1,2</sup> *International University, Ho Chi Minh City, Viet Nam, 700000*<sup>3</sup> *College of Engineering, Can Tho University, Can Tho City, Viet Nam, 900000*

\*Corresponding author: pnkphuc@hcmiu.edu.vn

**Abstract**

Product inspection is essential for ensuring the quality and dependability of manufactured goods. Traditional manual examination procedures are time-consuming, subjective, and error prone. As manufacturing complexity and production volumes increase, there is a rising need for automated inspection systems with accurate defect detection and classification. This research presents a deep learning-based quality inspection approach for submersible pump impellers. Three convolutional neural network (CNN) architectures, VGG16, ResNet50, and a custom model, are employed. A graphical user interface (GUI) is developed for real-time inspection. The approach achieves up to 99.8% accuracy in identifying defects, including surface scratches, corrosion, and geometric irregularities. It improves the quality assurance process by reducing manual inspection efforts. The GUI improves usability and decision-making. This study contributes to industrial quality control by introducing a novel deep learning application. Future research could explore advanced techniques like anomaly detection to further enhance system performance and versatility.

**Keywords:** *Deep learning, CNN, ResNet50, VGG16, Custom model, Defect detection, GUI, Quality inspection, Submersible pump impellers*

**1. INTRODUCTION**

Automation stands out as a vital contributor in ensuring reliable high-quality products in the field of product quality inspection. Manual inspection methods are time-consuming and error-prone, emphasizing the importance of automated and intelligent inspection systems. Convolutional neural networks (CNNs), for example, have shown potential in enhancing manufacturing and inspection processes. This study focuses on automating the inspection of submersible pump impellers, which are prone to various casting defects. By employing CNN architectures like VGG16 [1], ResNet50 [2], and a custom model, the aim is to enhance the accuracy and efficiency of defect detection and classification. Additionally, a graphical user interface (GUI) is developed to improve usability and real-time decision-making capabilities. This research addresses the limitations of manual inspection, offering a deep learning-based approach for quality inspection. The integration of CNN models and GUI technology contributes to more efficient and accurate defect identification, paving the way for smarter production and inspection systems in the era of Industry 4.0 and manufacturing digitization.

**2. LITERATURE REVIEW**

Deep learning systems have outperformed traditional machine learning approaches in image processing, computer vision, and pattern identification. Several research have been conducted to investigate the efficacy of CNNs and their various topologies in various application domains. Using huge ImageNet datasets, Krishna et al. (2020) [3] evaluated CNN architectures such as LeNet, AlexNet, and GoogleNet. They discovered that the amount of data available could influence the number of epochs necessary for training as well as the accuracy obtained. Kim et al. (2021) [4] concentrated on deep transfer learning methods for product inspection procedures. They stressed the automation potential of CNNs while emphasizing the significance of dataset preparation and effective model tuning. Guan et al. (2020) [5] addressed steel surface defect identification using an enhanced deep learning network model. They proposed a technique that combined feature visualization and quality rating to improve defect detection accuracy, thereby improving quality control in the steel industry. Sustika et al. (2018) [6] investigated various CNN architectures for evaluating strawberry quality. Their findings emphasized deep learning's potential for automating fruit quality verification processes. Ha et al. [7] proposed a CNN-based injection molding defect detection strategy. They achieved real-time defect assessment and improved the effectiveness of the injection molding process by integrating edge computing and industrial IoT technologies.

### 3. IMAGES DATASET

The dataset used in this study is comprised of 7348 images with 300x300 pixel dimensions that were obtained from the "Real-life Industrial Dataset of Casting Product" on Kaggle [8]. 6633 of these images were used for training and validation, with 3758 representing defective and 2875 representing non-defective pump impellers. An 80/20 split was used to divide the training and validation data. The test folder contains 453 images of faulty pump impellers and 262 images of non-faulty pump impellers.

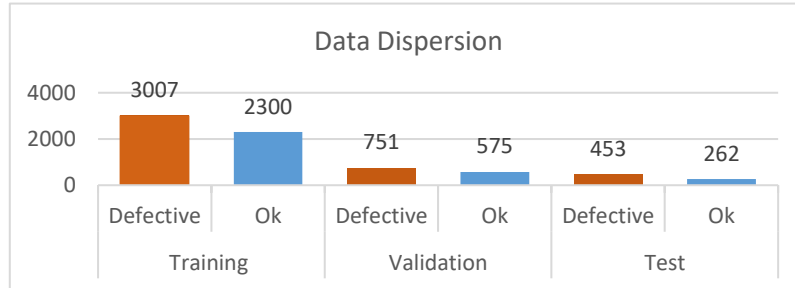


Figure 1. Data Dispersion

Augmentation techniques have been applied to all the images in the dataset to enhance the diversity and variability of the data. The images are labeled with tags indicating whether they are classified as "ok" (normal) or "def" (defect/anomaly).

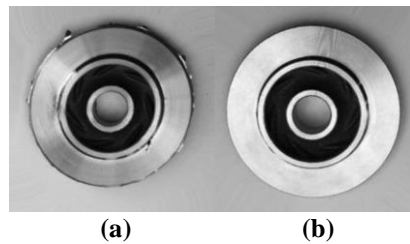


Figure 2. Random images of pump impellers from dataset, (a) defective, (b) normal

### 4. METHODOLOGY

The proposed methodology for this study entails using CNN architecture to train the dataset and PyQt5 to create a graphical user interface (GUI) for image classification. CNN architectures such as VGG16, ResNet50, and a custom model will be used to train the dataset in this study. The dataset, which consists of images of submersible pump impellers, will be fed into CNN models for training. During the training process, the CNN models will learn to identify and classify various defects in pump impellers with high accuracy. In addition, we used PyQt5 to create a graphical user interface (GUI). The GUI functions as an interactive image classification tool, allowing users to input images of pump impellers and receive real-time outcomes for classification.

#### 4.1. Convolutional neural networks architecture

CNN architecture typically comprises two main components: feature extraction and classification. The feature extraction phase involves a series of convolution layers, max-pooling, and activation functions. The classifier stage typically involves fully connected layers.

Two-dimensional (2D) convolution is a key operation in image processing and computer vision. It involves sliding a 2D kernel over an image, computing dot products, and generating a feature map that captures important patterns or features in the input image. The operation can be represented mathematically as follows:

$$(f * g)[x, y] = \sum_{i, j=-\infty}^{\infty} f[i, j] \cdot g[x - i, y - j] \quad (1)$$

Where  $f$  is input image and  $g$  is the kernel,  $x$  and  $y$  are the indices or coordinates of the output function resulting from the convolution. They determine the specific location in the output where the convolution operation is applied. The dot product operation is performed between the values in the kernel and the corresponding values in the image that are located within the window defined by the kernel.



In this research, the dataset will be trained using various CNN architectures, including VGG16, ResNet50, and a customized model.

VGG16 is a CNN architecture built by the Visual Geometry Group. The feature extraction layer in VGG16 is composed of the first 13 layers which are convolutional and pooling layers. It begins with a convolutional layer with 64 filters and progresses to a max pooling layer. The following blocks feature an increasing number of filters (128, 256, and 512) in pairs of convolutional layers, each followed by a max pooling layer. The final max pooling layer's generated feature maps are subsequently used for classification. The final max pooling layer's resulting feature maps are then passed on to the classification layer for prediction.

Following that, ResNet50 is a well-known CNN architecture in computer vision. For feature extraction, it employs a convolutional layer with max pooling. The architecture incorporates residual blocks with many convolutional layers, allowing residual mappings to be learned. By allowing information to pass between layers, residual connections preserve crucial properties. Fully connected layers are utilized for feature-based classification. ResNet50 is well-known for its performance in image classification, object detection, and picture segmentation.

Finally, for comparison with popular models, we created a unique CNN architecture. It consists of many convolutional layers activated by ReLU, followed by max pooling for dimension reduction. The first layer employs 32 3x3 filters with ReLU activation. In 2x2 windows, output is routed through max pooling. This method is repeated two more times. The final maximum pooling output is flattened and sent to a dense layer with sigmoid activation to reduce dimensionality. For probability distribution over classes, the last dense layer employs Softmax activation.

#### 4.1.1. Activation function

Activation functions are crucial in CNNs because they introduce non-linearity and allow the network to learn complicated patterns and relationships in input. To introduce non-linear modifications to the output of CNNs, activation functions are often used after each convolutional layer.

- The Rectified Linear Unit (ReLU) [9] is a popular activation function used in neural networks, including CNNs. The ReLU activation function is defined mathematically as:

$$f(x) = \max(0, x) \quad (2)$$

In this equation,  $x$  is the input to the activation function, and the output  $f(x)$  is the maximum of  $x$  and 0. In other words, the ReLU function sets all negative values in the input to 0, while leaving all positive values unchanged.

- The Sigmoid [10] activation function is a popular non-linear function used in CNNs. It is especially useful for binary classification tasks, where the output should be between 0 and 1, expressing the probability of a specific class. The equation defines the sigmoid function:

$$\sigma(x) = \frac{1}{1 + e^{-x}} = \frac{e^x}{e^x + 1} \quad (3)$$

In this equation,  $\sigma(x)$  indicates the sigmoid function's output for a given input  $x$ . The sigmoid function features a distinctive S-shaped curve, with large positive values approaching 1 and large negative values approaching 0.

- The Softmax [11] activation function is frequently utilized in the output layer of Convolutional Neural Networks (CNNs) for multi-class classification applications. It converts the final layer outputs into a probability distribution over numerous classes, allowing the network to make predictions for each class. The Softmax function is defined by the equation:

$$\sigma(z_i) = \frac{e^{z_i}}{\sum_{j=1}^K e^{z_j}} \quad (4)$$

In this equation,  $\sigma(z_i)$  represents the output probability of the  $i^{th}$  class,  $e^{z_i}$  is the exponential function applied to the  $i^{th}$  class output, and  $\sum_{j=1}^K e^{z_j}$  represents the sum of exponential functions applied to all class outputs. The Softmax function assures that the output probabilities sum to one, making it suited for multi-class classification tasks. It assigns higher probabilities to classes with larger output values and lower probabilities to classes with smaller output values.

#### 4.2. Training parameters

The training parameters used in this work include the selection of loss functions, optimization techniques, the number of epochs, and batch size.

Two distinct functions are used to compute the loss function. The first is Sparse Categorical Cross Entropy, which is appropriate for multi-class classification jobs where the target variable is integer-encoded. This was used in the custom model, and the math is stated in equation (5). The second is binary cross entropy, which is often used for binary classification tasks and is employed in VGG16 and Resnet50. The binary cross entropy loss function is mathematically represented by equation (6).

$$L = - \sum_{i=1}^N t_i * \log(p_i) \quad (5)$$

Where L represents the loss value, N is the number of classes,  $t_i$  is the true label and  $p_i$  is the predicted probability distribution over  $i^{th}$  the classes.

$$L = - \frac{1}{N} \sum_{i=1}^N y_i * \log(\hat{y}_i) + (1 - y_i) * \log(1 - \hat{y}_i) \quad (6)$$

Where L represents the loss value, N is the of samples in the batch,  $y_i$  is the target label for the  $i^{th}$  sample and  $\hat{y}_i$  is the predicted probability by the model for the  $i^{th}$  sample belong to the positive class.

Stochastic Gradient Descent (SGD) and Adam optimization methods are used to update network parameters during training. SGD changes parameters based on gradients determined on a subset of training data, whereas Adam combines adaptive learning rates and momentum. Training uses a batch size of 32 to maximize computational efficiency. Each architecture is trained for ten epochs, allowing the network to learn and modify weights and biases over time. An epoch is one trip through the complete training dataset. This method optimizes the loss function, changes parameters, and increases convergence speed.

#### 4.3. Developing the graphical user interface

The graphical user interface (GUI) was created with PyQt5, a Python package for constructing interactive and user-friendly programs. The GUI allows the user to upload photos and select the desired architecture for inspection. When the application is launched, the user is presented with an intuitive interface in which they can browse and upload images from their local system. The selected photos are then inspected using the architecture of choice (e.g., VGG16, ResNet50, or the custom model).

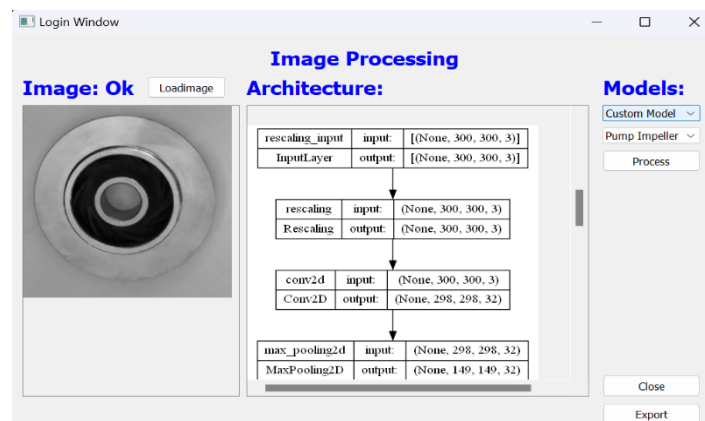


Figure 3. Graphical user interface for image classification

After the inspection is over, the GUI gives the user the option to export the results to an Excel file. This functionality is implemented using a dedicated button that, when pressed, initiates the export process. The produced Excel file comprises the recognized conditions of the tested products, making it easy for further analysis and record-keeping.

A	B	C	D	E	F	G
Product Type	ID	Time	Date	Condition	Model	
Pump Impeller	973	16:45	31-05-202	Ok	Model VGG	
Pump Impeller	27	16:45	31-05-202	Def	Model VGG	
Pump Impeller	50	16:45	31-05-202	Def	Custom Model	
Pump Impeller	95	16:45	31-05-202	Def	Model VGG	
Pump Impeller	71	16:46	31-05-202	Ok	Custom Model	
Pump Impeller	118	16:46	31-05-202	Ok	Custom Model	
Pump Impeller	118	16:46	31-05-202	Ok	Model VGG	
Pump Impeller	126	16:46	31-05-202	Def	Model VGG	

**Figure 4.** The results are exported to Excel

The PyQt5-based GUI provides a smooth and interactive experience, allowing users to quickly submit photos, choose the architecture, and export inspection results. It improves usability and allows for more effective data handling and analysis for quality control.

## 5. RESULTS

### 5.1. Training results

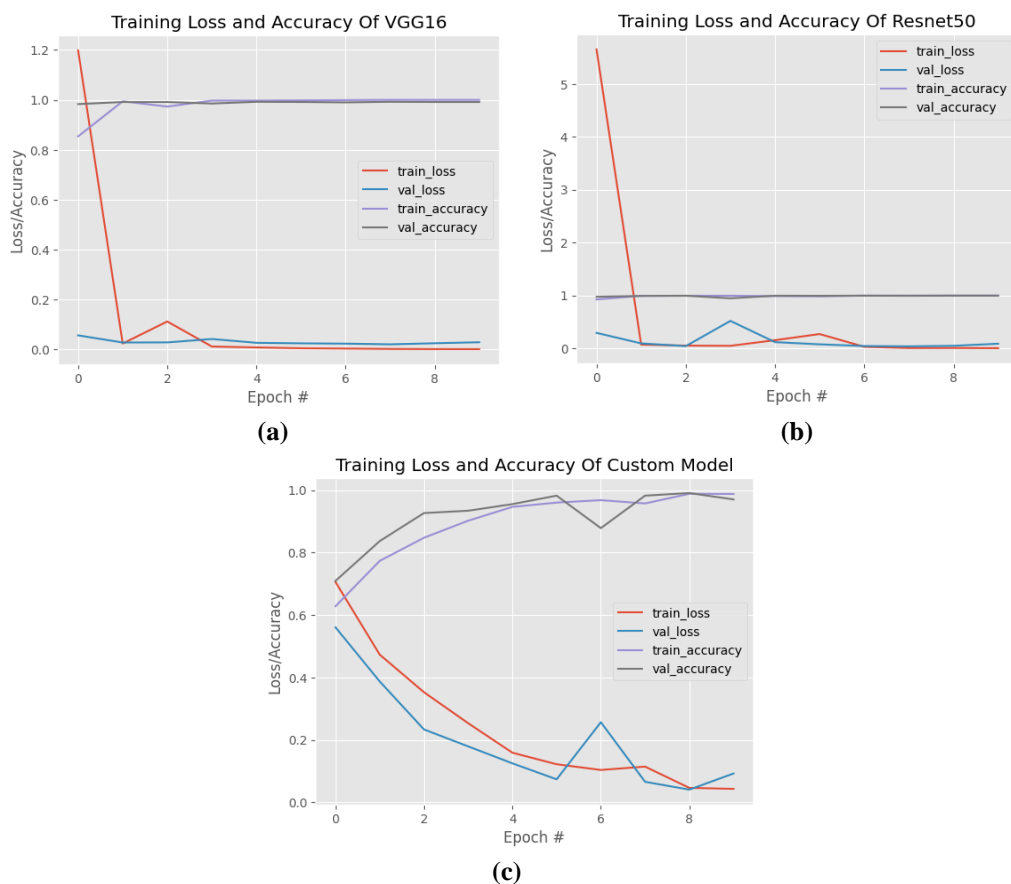


**Figure 5.** Training loss and accuracy of architectures, (a) VGG16, (b) Resnet50, (c) Custom Model

The results of the training process revealed the performance of VGG16, ResNet50, and the custom model in classifying the images.

VGG16 performed efficiently, with a training accuracy of 100% and a validation accuracy of 99.24% after 10 epochs. Within two epochs, it had swiftly converged to a high accuracy level of around 99%. After 10 epochs, ResNet50 achieved a training accuracy of 99.92% and a validation accuracy of 99.47%, demonstrating quick convergence with 99% accuracy obtained after only 1 epoch. The custom model obtained 98.79% training accuracy and 99.10% validation accuracy. After 9 epochs, it gradually improved its accuracy to roughly 98%. These results demonstrate the accuracy with which VGG16, ResNet50, and the custom model classified the training and validation data.

VGG16, ResNet50, and the custom model all displayed good accuracy in picture classification. VGG16 and ResNet50 attained impressive levels of accuracy fast, whereas the custom model improved consistently across the training epochs. These findings highlight the designs' applicability and usefulness for picture categorization in the dataset used in this study.

## 5.2. Testing results

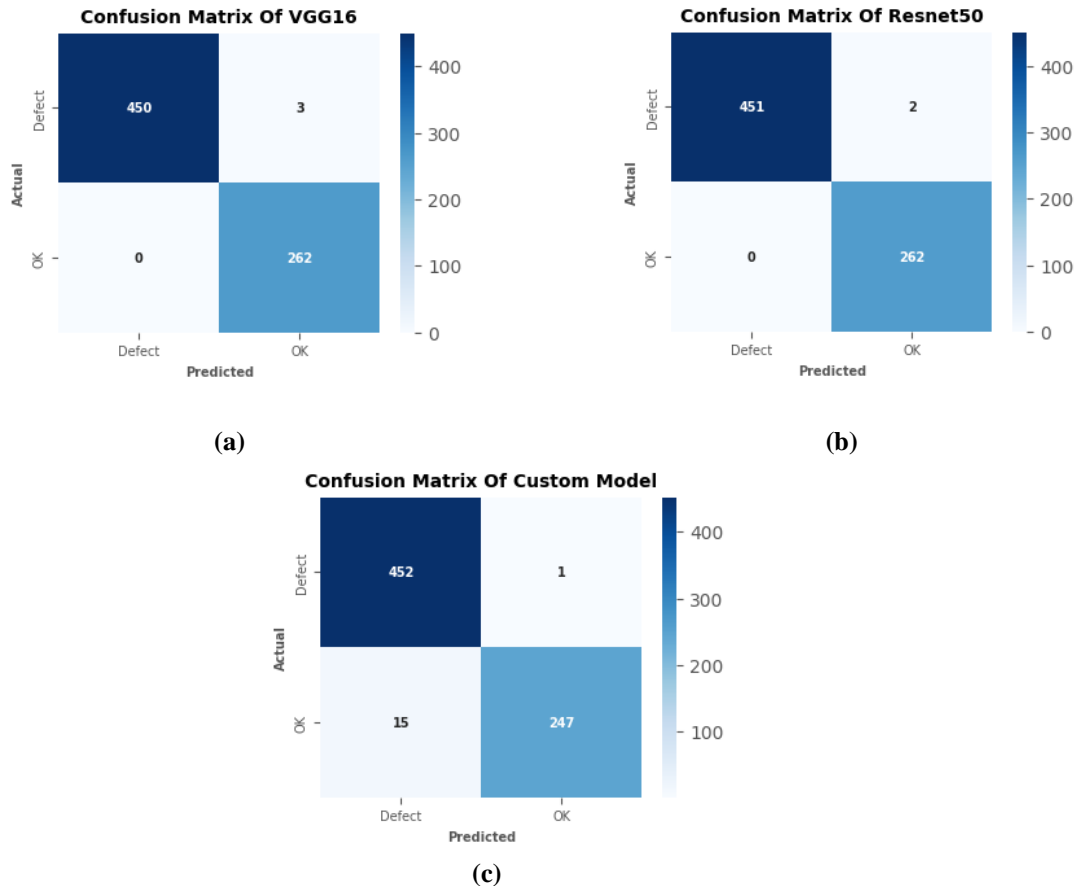


**Figure 6.** Confusion Matrix in prediction of testing data, (a) VGG16, (b) Resnet50, (c) Custom Model

The VGG16 model attained an amazing accuracy of 99.6% while analyzing the testing photos. It successfully predicted 450 of 453 faulty photos and properly identified all non-defective images. Similarly, the ResNet50 model was 99.7% accurate. It successfully predicted 451 of 453 faulty photos and all non-defective images. The custom model has a 97.8% accuracy, accurately categorizing 452 of 453 photos in the defective class and 247 of 263 images in the non-defective class.

These results demonstrate the effectiveness of all three models in accurately predicting the class labels of the testing images. The VGG16 and ResNet50 models achieved exceptionally high accuracies, while the custom model performed slightly lower but still achieved a commendable accuracy rate.

## 6. CONCLUSION

The study used VGG16, ResNet50, and the custom model to accurately categorize photos of casting products, specifically pump impellers. The models performed admirably, obtaining high accuracies on both training and testing datasets. Furthermore, PyQt5 was used to create a user-friendly graphical user interface (GUI) that allows users to input photos, pick different architectures, and export the categorization results to an Excel file. However, for future research, it is suggested that various datasets be used to train the models. This will aid in evaluating the models' performance on a variety of manufacturing products and determining their generalization capabilities. Furthermore, increasing the GUI functions, such as adding real-time image capturing and offering visualization tools for improved model interpretation, would improve the user experience even further. This study highlights

the successful implementation of CNN architectures in industrial quality control and exhibits the possibilities of using GUI technology for efficient and user-friendly picture categorization systems.

### References

- [1] Simonyan, K., & Zisserman, A. (2014). Very deep convolutional networks for large-scale image recognition. arXiv preprint arXiv:1409.1556.
- [2] He, K., Zhang, X., Ren, S., & Sun, J. (2016). Deep residual learning for image recognition. In Proceedings of the IEEE conference on computer vision and pattern recognition (pp. 770-778).
- [3] Krishna, S. T., & Kalluri, H. K. (2019). Deep learning and transfer learning approaches for image classification. *International Journal of Recent Technology and Engineering (IJRTE)*, 7(5S4), pp. 427-432.
- [4] Kim, T. H., Kim, H. R., & Cho, Y. J. (2021). Product inspection methodology via deep learning: an overview. *Sensors*, 21(15), p. 5039.
- [5] Guan, S., Lei, M., & Lu, H. (2020). A steel surface defect recognition algorithm based on improved deep learning network model using feature visualization and quality evaluation. *IEEE Access*, 8, 49885-49895.
- [6] Sustika, R., Subekti, A., Pardede, H. F., Suryawati, E., Mahendra, O., & Yuwana, S. (2018). Evaluation of deep convolutional neural network architectures for strawberry quality inspection. *Int. J. Eng. Technol*, 7(4), pp. 75-80.
- [7] Ha, H., & Jeong, J. (2021). CNN-based defect inspection for injection molding using edge computing and industrial IoT systems. *Applied Sciences*, 11(14), p. 6378.
- [8] Public Datasets, Casting Product Image Data for Quality Inspection, [Online].
- [9] Nair, V., & Hinton, G. E. (2010). Rectified linear units improve restricted boltzmann machines. In Proceedings of the 27th international conference on machine learning (ICML-10) (pp. 807-814).
- [10] Rumelhart, D. E., Hinton, G. E., & Williams, R. J. (1986). Learning representations by back-propagating errors. *nature*, 323(6088), pp. 533-536.
- [11] Bridle, J. S. (1990). Probabilistic interpretation of feedforward classification network outputs, with relationships to statistical pattern recognition. In *Neurocomputing: Algorithms, architectures and applications* (pp. 227-236). Springer Berlin Heidelberg.

## [P-26] Designing Management Information System for Container Truck Transport

Le Cao Ngoc Anh, Dinh Ba Hung Anh\*

*Department of Industrial System Eng., Faculty of Mechanical Engineering, Ho Chi Minh City University of Technology (HCMUT), 268 Ly Thuong Kiet Street, District 10, Ho Chi Minh City, Viet Nam*

\*Corresponding author: anhdbh@hcmut.edu.vn

### Abstract

In order to best meet the increasing demand and improve competitive advantage, transport companies are increasingly investing in improving and applying technology to optimize management and operation processes. This study deals with improving service quality for Quoc Thinh Transport Co., Ltd. using a transportation management information system. The information system is designed with the goal of helping the coordination and monitoring of container trailers during transportation be effective, information being updated quickly, ensuring coordination between departments, at the same time supporting data storage and easy report retrieval. Research uses supporting tools, data collection and analysis and software such as Diagram, Figma, ...

**Keywords:** *Management information system, Container transport, Database*

### 1. INTRODUCTION

In recent years, the increasing trade of goods between countries has led to a significant increase in the demand for freight transport, especially containers for import and export. According to statistics, every year about 200 million containers are transported and the number is increasing every day. This shows that shipping by container is essential for economic development in the country. Currently, Vietnam has initially completed the development of international trade, and domestic transportation services have also increased. This makes conventional forms of transport unable to carry out the task of transporting goods. Therefore, when the container transport service was born, it helped businesses to thoroughly solve this problem (Kenneth et al. [5]). Cost optimization, bulk cargo capacity, environmental benefits and convenience in delivering goods from the port to the place of production are advantages that help transport Containers become the preferred choice of many shippers when there is a need to transport goods for import and export (Dipo et al. [2]; Kristijan et al. [6]).

Quoc Thinh Transport Co., Ltd is a company that provides container truck rental services. Currently, the tools used by the company in the process of coordination, monitoring and communication between departments are not linked with each other; many manual operations and stored data are still discrete. Order information is manually entered and vehicle dispatch planning is done using Excel software, based on staff experience. This leads to loss of time and ineffective coordination because employees have to measure the quantity so that it is reasonable; if it is not reasonable, it may have to be adjusted many times. The plan is scheduled by day, each day is an Excel file, and the plan of the days in a month is stored in multiple sheets in one file. As the company grows, the amount of goods transported increases, and the amount of data also increases. If the planner's computer crashes, it can lead to data loss. Therefore, it is essential to improve this situation as soon as possible.

And the first step should be to find out what caused this condition. The reasons why planning takes a long time are the five main groups of causes related to methods, data, tools, people and the environment. The above problems require an information system to be able to store information for the quick and efficient planning and coordination of container trucks; as well as helping the staff in the dispatching department and the sales department to quickly communicate with each other, and notify the driver when problems arise for timely handling. Finally, it helps managers and operators to access information when needed.

An Information System (IS) is a system consisting of many interrelated elements. They are used to jointly collect, process and store and distribute data and information to achieve a certain goal. According to the provisions of Clause 3, Article 3 of the Law on Cyberinformation Security 2015, Information system is a collection of hardware, software and databases established for the purpose of creating, providing, transmitting, collecting, processing, storing and exchanging information on the network (Blancas et al. [1]). To design and develop an information system, it is necessary to perform the following 4 steps: Needs survey – System analysis – System

design – System installation and maintenance. Figure 1 below shows an overview of this process. The main task in the survey phase is to find out and collect the necessary information to prepare for the settlement of the requirements. The analysis phase then determines the system's information and functionality through the BFD diagram. From the BFD diagram will continue to build the DFD data stream. The design phase is divided into two steps, the overall design and the detailed design. At this stage, the system database will be designed through ERD diagram and then converted into RDM diagram. Finally, build a test and maintenance system.

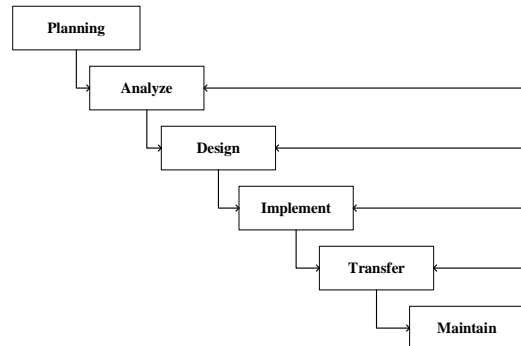


Figure 1. The process of building and developing a management information system

## 2. CONDUCTING RESEARCH

### 2.1. System analysis

**Business Function Flow Diagram:** The information system consists of 8 main functional groups: Setting up a resource database, Order management, Trip coordination, Trip monitoring, Financial management, Vehicle management, Driver mobile app, and Dashboard reports. In addition to the 8 main groups of functions presented, the system also has an indirect function of logging in, which is a function to ensure the security of the information system (Dwi et al. [4]).

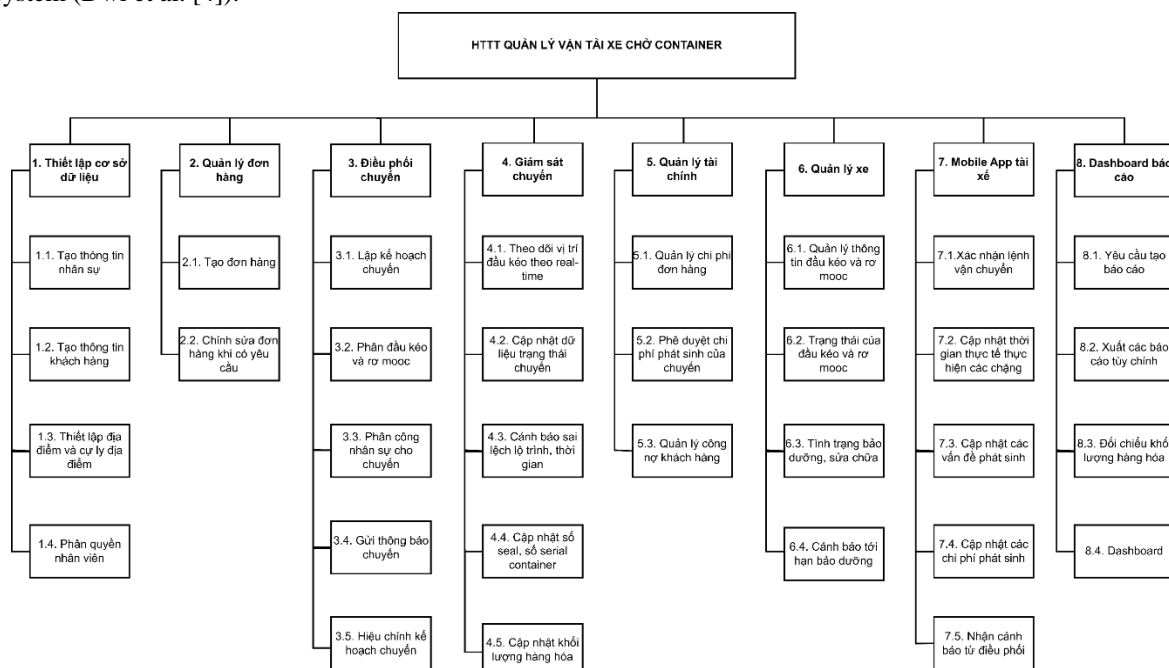


Figure 2. Business Function Flow Diagram

### Data Flow Diagram

**Context Diagram:** Context diagrams give the most general view of the environment in which the system operates; include external entities or in other words the place that provides data and or receives results from the system and the data flows in and out of the system (Dwaraganath [3]). In the container truck transport management information system, there are 6 external entities including: Customer, Container truck location tracking system,

Repair and maintenance department, Weighing station department, Customs clearance department and Board of Directors.

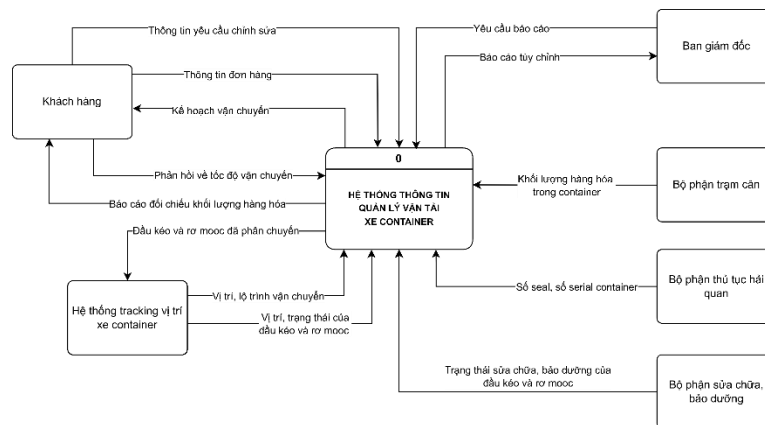


Figure 3. Context Diagram

In which, the Customer provides information about the order, along with feedback for order management and coordination, and receives planning information and volume comparison results for payment purposes. The container truck location tracking system provides and receives information for coordination and monitoring. Updates from the Repair and maintenance department and the Customs clearance department also serve for coordination and monitoring purposes. The weighing station department will weigh the volume of goods in the container and send it to the general department for the general department to compare the volume with the customer for payment purposes. Finally, there is the board of directors, who need reports to know how to monitor the status and performance of the system.

*DFD diagram at level 0:* Level 0 DFD diagrams are decomposed from context diagrams and ensure that input and output data flows are preserved. Each process in the DFD corresponds to a function in the BFD diagram. From the order information received from the customer along with the established resource database to create the order. Once the order is created, it will move to the dispatching process. The dispatching process takes data from the container truck location tracking system and established resource database for planning and staffing. The completed trip plan will be sent to the customer, and the delivery order will be sent to the driver's mobile app and the supervision command will be sent to the supervisor and start monitoring.

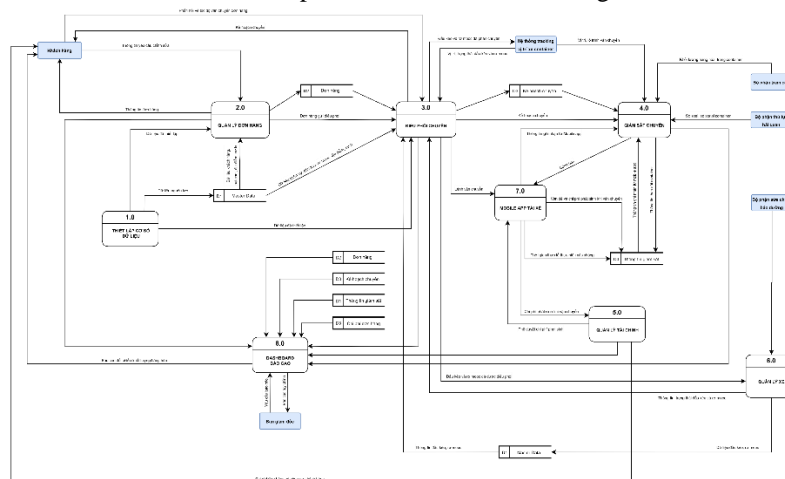


Figure 4. DFD diagram at level 0

The data recorded from the monitoring staff and the driver's mobile app will serve the trip monitoring process; the real-time tracking of the container truck's location during the transportation process is supported by the container truck location tracking system. In addition, the information provided from the customs clearance department also serves this process. In addition, the vehicle management department will indicate whether the vehicle is in a state of repair or maintenance and whether the vehicle can receive the trip at the time it needs to be



coordinated and pass this information to dispatcher to help dispatcher easily track the status and assign vehicles for the trip.

From the order information and the number of containers included in the created order, the accounting department will calculate the cost for the order, and consider and approve the costs incurred in the transportation process from the driver. Then sum up all the success costs owed to the customer. Finally, notify the debtor and monitor the payment progress of the customer's debt. In addition, the weighing station department will send information about the volume of goods to the general department for the purpose of comparison and payment with customers.

After each process, data is recorded into the corresponding data warehouse for storage and retrieval purposes. Finally, the reporting process connects and pulls information from the order management processes, flight coordination and supervision, financial management and the results of the reporting process will be made available to the client and to management.

**Business Function Flow Diagram**

Use case - Actor model represents the interaction between the user and the system.

For a Use case that is used by many Actors, there should be a Representative Actor covering the rest of the Actors to perform. Whichever function the representative actor performs, the included Actors will also inherit those functions. For example, for the login use case, all Actors perform this function, so take the Actor named Transport Operations Department to represent (Lan Jin and Xiujuan Liang [7]).

In the model, there is a transport tracking system, a weighing station department, a repair and maintenance department and a customs clearance department that is not the main actor directly interacting with the system but is necessary to support the performance of functions. Other capabilities should also be represented in the model. For example, to plan a trip for a container truck that needs to know the current status and location of the vehicle, the transportation tracking system will assist the dispatcher to know this information.

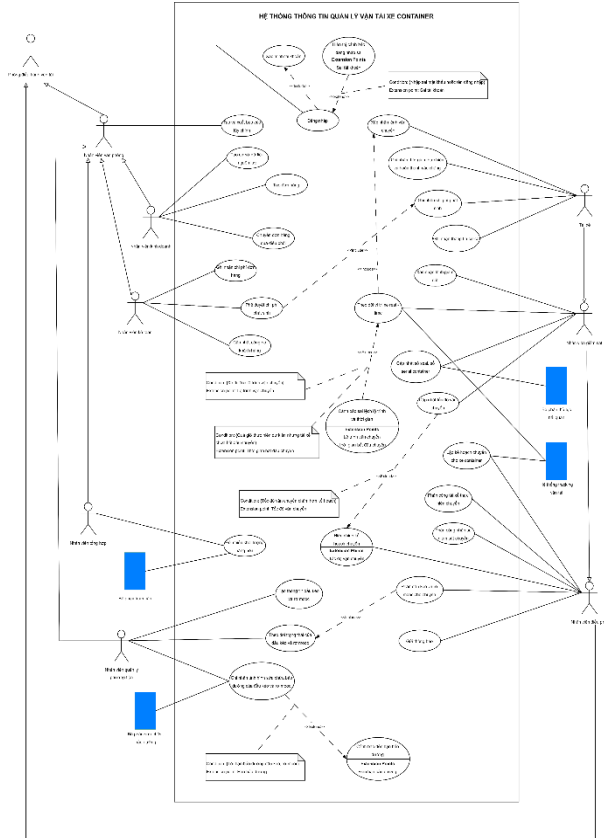


**Figure 5.** Use case - Actor diagram

**2.2. System design**

*Entity-Relationship Diagram:* An ERD diagram shows the relationship of entity sets stored in a database, providing a visual view of how entities are related to each other. In the diagram, each entity is listed with its corresponding attributes and marked with an identifying attribute. The ERD diagram is shown in Figure 6.

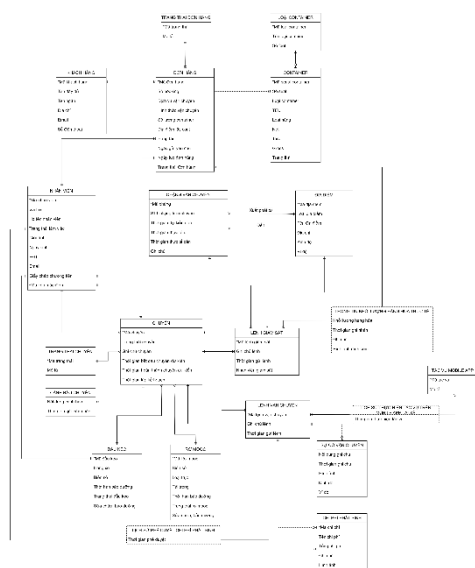


**Figure 6.** ERD Diagram

*Design a database from an Entity-Relationship diagram:* Based on the conversion principles presented in the Theoretical basis, convert the ERD diagram into an RDM diagram. Each relation is organized in a two-way table

with attributes and keys. Attributes underlined and bold are primary keys; attributes in italics are foreign keys referencing another data table. Figure 7 shows the RDM diagram of the system.

*Design the theme:* After modeling the system in terms of data and processes, proceed to design the interface to have a more intuitive view of the information system.

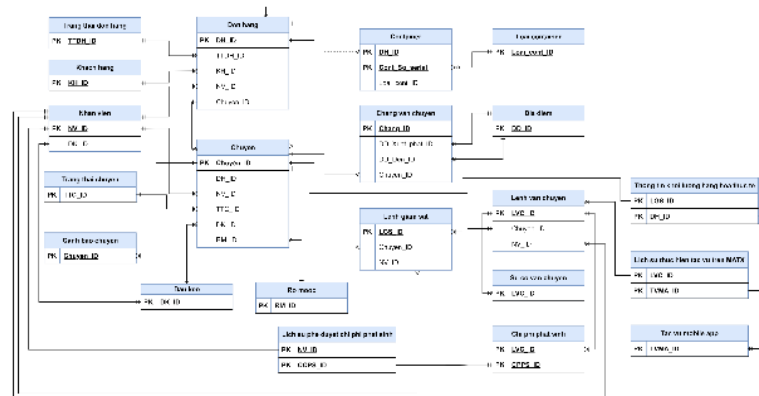


**Figure 7. RDM Diagram**

### 3. RESULT AND DISCUSSION

The information system is designed according to the standard information system design process that ensures documentation to make programming and installation easy and has the following advantages: Make the process of order creation, coordination and monitoring faster and more efficient; especially in terms of monitoring, tracking the real-time vehicle route during transportation, along with arising problems, which are continuously updated. The combination of web app and mobile app to exchange and connect information helps reduce paperwork as well as information is updated accurately and quickly from the field to the operating office. Nice interface and easy to use. There is support for creating reports and visual displays on the dashboard, helping users save time.

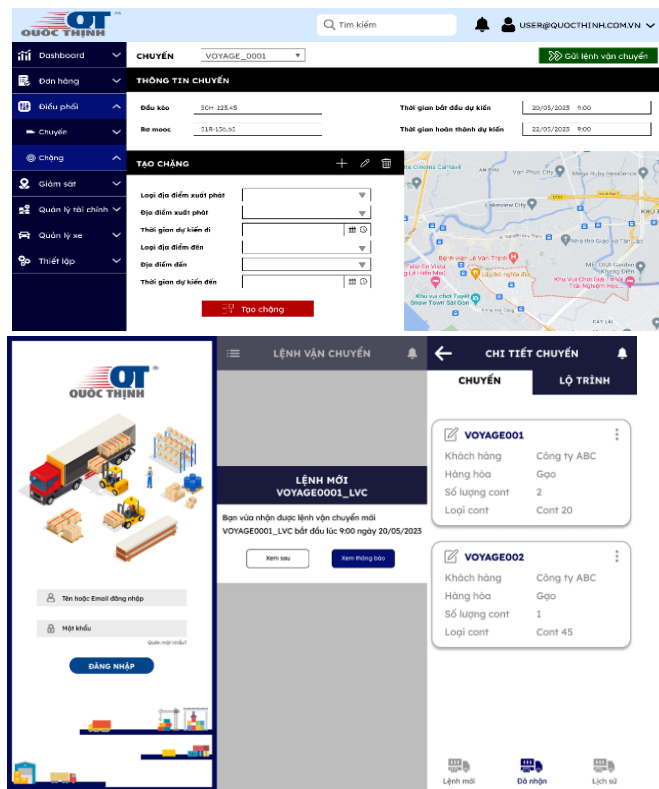


**Figure 8. Web dispatching screen and Driver's mobile app screen**

### Acknowledgement

We acknowledge Ho Chi Minh City University of Technology (HCMUT), VNUHCM for supporting this study.

### References

- [1] Blancas, Luis C., M. Baher El-Hifnaw, 2014. *Facilitating Trade Through Competitive, Low-Carbon Transport: The Case for Vietnam's Inland and Coastal Waterways*. Washington, D.C.
- [2] Dipo Theophilus Akomolafe, Naomi Timothy, Francis Ofere, 2014. *Using database management system to develop and implement an automated motor vehicle management system*. European Scientific Journal, ISSN: 1857 – 7881.
- [3] Dwaraganath Prabakaran, 2020. *Solving the barge routing and scheduling problem with a hybrid metaheuristic*. Master Thesis, University of Twente, Enschede, the Netherlands.
- [4] Dwi Ardiada, Merta Suryani, Ni Wayan Sri Aryani, 2017. *Design of Vehicle Asset Management Information System (Case Study: STMIK STIKOM Bali)*. International Journal of Engineering and Emerging Technology, ISSN: 2579 – 5988.
- [5] Kenneth C. Laudon, Jane P. Laudon, 2011. *Management Information Systems: Managing the Digital Firm*. 12<sup>th</sup> edition, Prentice Hall, United States of America.
- [6] Kristijan Rogic, Branisla V Sutic, Go Ran Kolaric, 2008. *Methodology Of Introducing Fleet Management System*. Promet- Traffic&Transportation, Vol. 20, 2008, No.2, 105-111.
- [7] Lan Jin, Xiujuan Liang, 2012. *Vehicle management information system based on UML*. 2012 Second International Conference on Business Computing and Global Informatization, DOI: 10.1109/BCGIN.2012.211.

## **[P-28] Applying the AHP Process to Select Policy Implications to Improve Employee Performance: A Case Study of Joint Stock Commercial Banks in Ho Chi Minh City**

Vo Thi Hoang Quanh\*, Dinh Ba Hung Anh

*Department of Industrial System Eng., Faculty of Mechanical Engineering, Ho Chi Minh City University of Technology (HCMUT), 268 Ly Thuong Kiet Street, District 10, Ho Chi Minh City, Viet Nam*

\*Corresponding author: vthquanh@gmail.com

### **Abstract**

The research objective of this paper is to propose managerial implications to improve the performance of joint stock commercial banks employees in HCMC. With due consideration to different criteria, in order to make the best choice, multi-criteria decision-making (MCDM) techniques can be used. This article has tried to present a favorable model for managerial implications selection by using a suitable modeling, analytic hierarchy process (AHP) which has been used.

**Keywords:** *Organizational culture, Knowledge sharing, Bank employee performance, AHP multi-objective optimization, Joint stock commercial bank*

### **1. INTRODUCTION**

For the field of joint stock commercial banking, previous studies on organizational culture, knowledge sharing and job performance have not been considered holistically and are incomplete in terms of science and theory (Masa'deh et al. [11], Nguyen Phan Nhu Ngoc [15], Nguyen Phuc Quy Thanh [16]). That is the reason why the author conducted the study to better analyze the relationship between organizational culture, knowledge sharing and the impact of knowledge sharing on the performance of bank employees. The paper presents the policy-based as a result of the SEM analysis, policies being applied at joint stock commercial banks in Ho Chi Minh City as well as the policy experience of the world, as input to the AHP process. The focus of the paper is the analysis of policies (input) by the AHP optimization process to understand in order to select the policy to prioritize for implementation.

### **2. THEORETICAL BASIS**

The theoretical basis of the article is related to the following topics: organizational culture, knowledge sharing and job performance. Organizational culture has the role of linking members into a community of sympathy, mutual benefit and common destiny; create stability by setting standards to guide members to follow the common purpose of the organization voluntarily and voluntarily. Selected and created cultural factors act as a mechanism for affirming organizational goals, guiding and shaping mutual behaviors among members of the organization, between individuals and organizations, and between members and leaders. This concept is drawn from statements from (Laura [9], Kucharska and Wildowicz [7]). Similarly, the concept of knowledge sharing used in this article "is the process of giving knowledge to colleagues and at the same time acquiring knowledge that is lacking or needs to be supplemented for the employee's working process". Knowledge sharing is a parallel process where each individual contributes and receives knowledge in relation to his or her colleagues and to the organization. Adel Hasan and Al Ali [1], Tsui et al. [18] have stated the same concept in their research. Finally, the concept of job performance includes three components: Working attitude (Dinh Ba Hung Anh and To Ngoc Hoang Kim [3]), Capacity development (Galbraith [5]; Kuruppuge and Gregar [8]) and Goal Accomplishment (Laura [9]).

For the field of joint stock commercial banking, previous studies on organizational culture, knowledge sharing and job performance have not been considered holistically and are incomplete in terms of science and theory (Masa'deh et al. [11], Nguyen Phan Nhu Ngoc [15], Nguyen Phuc Quy Thanh [16]). That is the reason why the author conducted the study to better analyze the relationship between organizational culture, knowledge sharing and the impact of knowledge sharing on the performance of bank employees. The paper presents the policy-based as a result of the SEM analysis, policies being applied at joint stock commercial banks in Ho Chi Minh City as well as the policy experience of the world, as input to the AHP process. The focus of the paper is the analysis of

policies (input) by the AHP optimization process to understand in order to select the policy to prioritize for implementation.

### 3. LITERATURE REVIEW METHODOLOGY

Many authors have used the AHP process in their research, showing that AHP effectively supports tasks such as objective scoring, policy selection. AHP analysis combined with SWOT to adjust as well as integrate experience into policymaking is shown in the study of Nguyen Ngoc Duy Phuong and Pham Thai Son [14]. Besides, in his research, Tran Vinh [17] also used this process to support the analysis of the results formed from the EFA exploratory factor analysis technique. The main method used in this paper is the AHP multi-objective optimization process with the weights of the criteria determined using the expert method. The alternative (policy) score is given in the form of a pairwise comparison matrix by experts based on the actual operation of a joint stock commercial bank in Ho Chi Minh City. The details of the research procedure with a focus on the AHP process are presented in Figure 1 as follows.

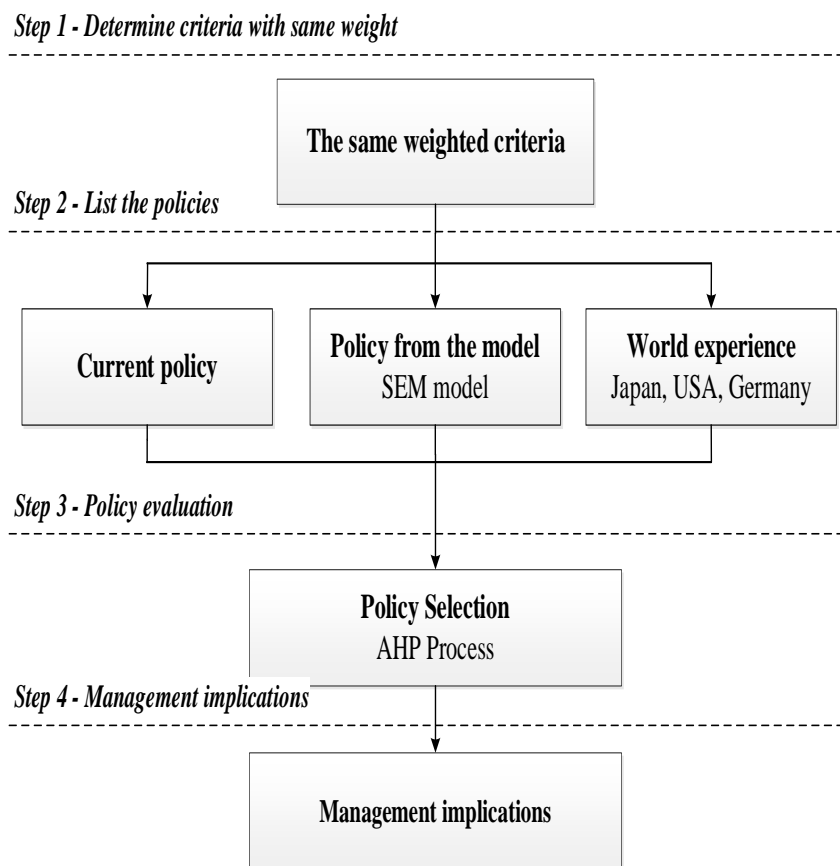


**Figure 1.** The AHP process supports policy formulation to promote knowledge sharing

## 4. POLICY LISTING

### 4.1. Results from SEM analysis and current policy

#### 4.1.1. Organizational structure

The standardized regression coefficient of the organizational structure factor is at the highest level (0.538), demonstrating the importance of this factor to work performance. Improving the organizational structure so that it is lean and efficient, with the connection between departments and employees, contributing to increasing operational efficiency, and making knowledge sharing easier. Policy implications include: (1) Arrangement of management departments and divisions; (2) Flexible organizational structure; (3) Appropriate organizational structure for knowledge transfer. Policies related to organizational structure are denoted CS3.

#### **4.1.2. Knowledge dedication**

Knowledge dedication (KD) is correlated with knowledge sharing at  $\beta = 0.295$ . In which, knowledge dedication affects the work performance of bank employees at 0.37. Dedicating knowledge is one of the biggest challenges for managers because employees often do not want to participate in this sharing. Dedication not only takes time but can also become a threat to their position in the organization. Policies related to knowledge dedication are denoted CS4.

#### **4.1.3. Output orientation**

Based on the author's previous research [6], output orientation correlates with organizational culture at an impact level of 0.1. Raising wages for employees will help employees try to complete work on time, increasing work productivity. In addition, employees working at the bank should be trained in professional skills in customer consulting and handling work in accordance with the bank's procedures; ensure that they are highly knowledgeable about the other duties of the bank. For policy analysis to prioritize deployment by AHP multi-objective optimization process, this study assigns output orientation by identifier CS1.

#### **4.1.4. Leadership**

Leadership (LS) correlates with organizational culture at an impact level of 0.174. Some of the proposed policy implications include: (1) Create opportunities for staff to learn and improve professional knowledge; (2) Help employees develop skills and ability to solve problems; (3) Capable leadership, vision and executive ability; (4) Leaders always help, answer questions and motivate employees; (5) Guide employees to find solutions to their own problems; (6) Treat fairly and always acknowledge employees' contributions. Policies related to leadership are denoted CS2.

### **4.2. Policy experience in some countries**

#### **4.2.1. Experience in performance management from the US - Germany**

Konrad and Deckop (2001) applied measures to evaluate and comment on emulation. To evaluate performance, the US government used the balanced scorecard method with four criteria: (1) Customer orientation; (2) Financial orientation; (3) Orienting the internal operation process; (4) Orientation for improvement and development. The US policies focused on implementation including: Work and relationships, Optimal performance, Training.

German knowledge-sharing governance, presented by Laura Martina Zurheiden (2017), encompasses the following policies: (1) Focus on goals and value face-to-face communication; (2) Working hours are for work only. To serve the content of policy analysis as well as understand the priority in implementation, the study of the symbol of policy experience from the US - Germany is CS5.

#### **4.2.2. Japanese experience**

According to Japan's Abenomics economic policy, the following policies apply: (1) Lifetime employment; (2) Employee participation in the decision-making process; (3) Quality inspection team; (4) Team work. In order to serve the content of policy selection to prioritize implementation, Japan's policy experience is denoted CS6.

## **5. POLICY SELECTION (AHP PROCESS)**

Conduct a multi-objective optimization process to better understand the impact of policies and to identify which policies should be prioritized for implementation. Start by implementing the task of determining the weights. Weights represent the importance of a criterion; the sum of the weights is usually adjusted to 1. The use of the Inconsistency index to validate the reasonableness of the weights. If the value of the Inconsistency index is greater than the significance level  $\alpha$  (usually chosen as 0.05), the conclusion is that the weight is not reasonable (unreliable). Score the evaluation criteria as follows:

**Table 1.** Pairwise comparison score matrix for evaluation criteria

Criteria	Teamworking	Engagement	Belief	Communicate with colleagues	Leadership concern	Commend and reward
Teamworking	1	3	4	2	3	3
Engagement	1/3	1	2	2	1	2
Belief	1/4	½	1	1/4	1/3	1
Communicate with colleagues	1/2	1/2	4	1	1	1
Leadership concern	1/3	1	3	1	1	1
Commend and reward	1/3	1/2	1	1	1	1
Total	3	7	15	7	7	9

The weighted results of the evaluation criteria for the option are extracted and presented in Table 2.

**Table 2.** Weight results of each option evaluation criteria

Teamworking	0.353
Engagement	0.174
Belief	0.070
Communicate with colleagues	0.151
Leadership concern	0.144
Commend and reward	0.108

Based on the Inconsistency index to evaluate the normalization score: If the Inconsistency index value < the significance level  $\alpha$  (selected by 0.05) will stop the process, otherwise go back to Step 1; continue to process the results using Expert Choice software, the results of the weights and the Inconsistency index are presented in Figure 2.

**Figure 2.** Weight and Inconsistency results for the set of criteria

The Inconsistency index of the set of criteria reached  $0.04 \leq$  significance level  $\alpha = 0.05$ , so the values of these weights are reliable. The conclusion uses the criteria together with the weight values shown in Table 2 as criteria for evaluating the plan.

## 6. POLICY LISTING

The author conducts a policy review based on the AHP multi-objective optimization process to better understand the implied policies and select them to prioritize in implementation. From the policies listed above, the writer includes the AHP process for analysis. There are six policies that are considered inputs to the AHP process with symbols CS1 to CS6 shown in Table 3.

**Table 3.** Input policy of the ERP process

	CS1	CS2	CS3	CS4	CS5	CS6
Explanation	Output Orientation	Leadership	Organizational structure	Dedication of knowledge	American - German experience	Japanese experience

Score the alternatives (policies) according to each criterion for enough process input data to conduct the AHP multi-objective optimal analysis process. The next section presents the scores of the options (policies) according to the evaluation criteria listed in Table 2.

To analyze the policy, the thesis follows a 2-step process:

Sub-step 1: Scoring, use Expert Choice software to export the score results.

Sub-step 2: Sensitivity analysis, similar to using Expert Choice to output sensitivity results, should choose the policy with the highest score and sensitivity.

The results of the priority order of policies calculated by Expert Choice software are shown in Figure 3.

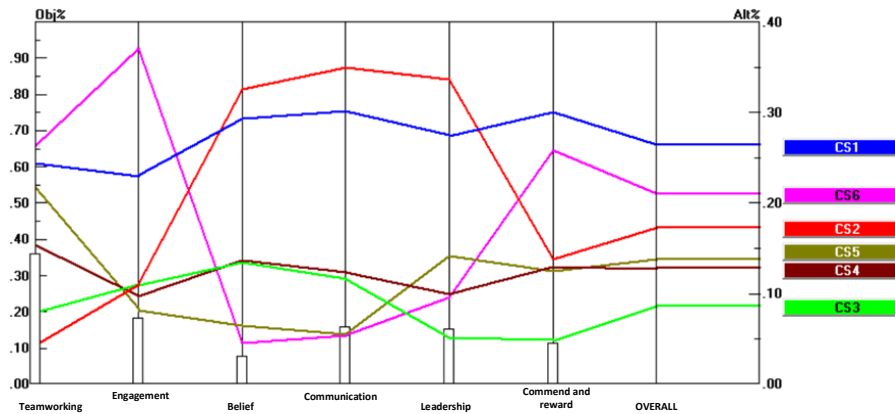


Figure 3. Score chart of policies

From Figure 3, we see that policies 1 (output orientation) and policy 6 (Japanese experience) have the highest scores, meaning that these two policies should be prioritized for implementation. The results of the policy sensitivity analysis according to the group work criteria (weight equal to 0.353). Similar analysis for the output orientation criteria, openness and openness, the writer finds that policy 6 (CS6, policy experience from Japan) is most sensitive to the evaluation criteria.

In conclusion, based on the results of sensitivity analysis, we find that policy 6 should be preferred over 1 even though policy 1 currently has a higher score.

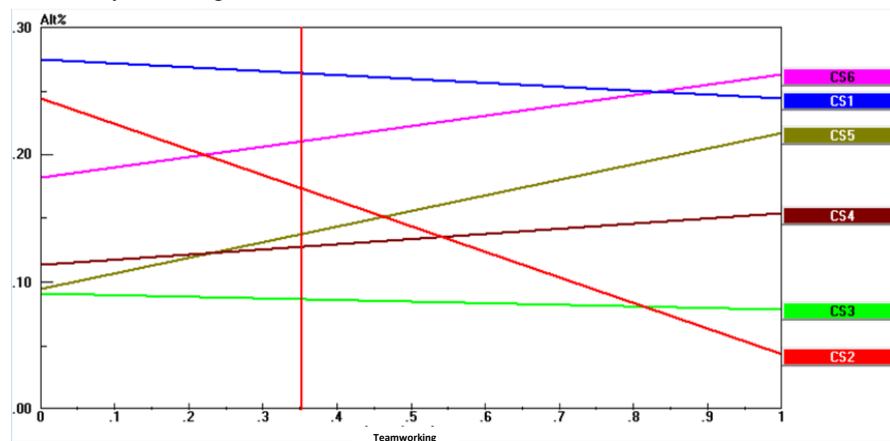
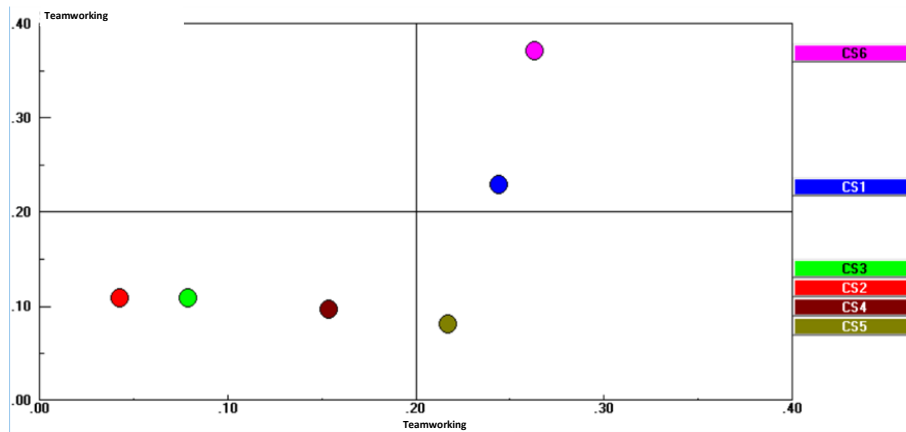


Figure 4. Sensitivity analysis results (teamwork criteria, Expert choice)

In addition, in the space of two important criteria related to knowledge sharing behavior is teamwork and engagement. Policies 1 and 6 have higher scores and separate distribution than the rest of the policies. Based on the results in this policy distribution chart, the author prioritizes to choose two policies CS1 and CS6.





**Figure 5.** Policy distribution results (Teamwork and Engagement Criteria)

Combination of option score (Figure 3) with sensitivity (Figure 4) and policy distribution (Figure 5), in conclusion, it is necessary to prioritize the selection of policies 1 and 6 to develop macro policies to promote knowledge sharing in order to improve job performance.

The results from the SEM model concluded that organizational structure has the strongest interaction with organizational culture (normalized impact level: 0.538). Next, organizational culture affects bank employee performance at 0.14 (normalized). Similarly, interactive knowledge dedication to knowledge sharing is at 0.295; and knowledge dedication affects job performance at 0.37. In contrast, the results of the proposed AHP process should prioritize the implementation of two output orientation policy groups (under the organizational culture group) and policy experience from Japan (not shown in the SEM model). Thus, the results of the AHP process have supported implementers to choose policies to prioritize in implementation. In addition, this AHP process also supports the integration of experience (qualitative) into the policy implementation process.

## 7. CONCLUSION

The paper presents the application of the AHP multi-objective optimization process to the analysis and selection process in the implementation of policies. In addition to identifying policies that need to be prioritized for implementation, the AHP process also supports the integration of solutions derived from quantitative methods with solutions generated from practical (qualitative) experience. The job performance of employees at joint stock commercial banks in Ho Chi Minh City will be significantly improved if the analysis and solutions outlined in the study of this paper are applied.

## Acknowledgments

We acknowledge Ho Chi Minh City University of Technology (HCMUT), VNUHCM for supporting this study.

## References

- [1] Adel Hasan, Al Ali (2013). "The Effect of Knowledge Sharing Practices on Organization Performance". The British University in Dubai.
- [2] Babin, B. J., & Boles, J. S. (1998). "Employee Behavior in a Service Environment: A Model and Test of Potential Differences between Men and Women". *Journal of Marketing*, 62(2), pp. 77–91.
- [3] Dinh Ba Hung Anh, To Ngoc Hoang Kim (2018). "Scientific Research in Socio-Economics & Dissertation Writing Guide". Economic Publishing House. HCM City.
- [4] Eldridge, A. Crombie (2013). "A Sociology of Organisations". Taylor and Francis Group.
- [5] Galbraith, J.R. (2021). "Matrix organization designs: How to combine functional and project forms". *Business Horizons*, 14, pp. 29–40.
- [6] Hair, J. F., Black, W. C., Babin, B. J., & Anderson, R. E. (2016). "Multivariate Data Analysis". (7th Edition). Pearson.

- [7] Kucharska, W. & Wildowicz-Giegiel, A. (2017). “Company Culture, Knowledge Sharing and Organizational Performance: The Employee’s Perspective”. In Proceedings of the 18th European Conference on Knowledge Management, Vol.1, pp. 524-531.
- [8] Kuruppuge, R. H. & Gregar, A. (2017). “Knowledge sharing and job performance: the intervening role of technological competency in knowledge-based industries”. International Journal Of Economics And Statistics, Vol. 5.
- [9] Laura (2017). “Knowledge Sharing in a German Municipality”. Thesis at Faculty of Social Sciences, Radboud University.
- [10] Le Thi Hoa Binh (2017). “Building a business strategy for the retail franchise of petrol and oil at Petrolimex Saigon in the period of 2018 – 2023”. Thesis of Business Administration, Hong Bang International University.
- [11] Masa'deh, R., Obeidat, B.Y. and Tarhini, A. (2016). “A Jordanian empirical study of the associations among transformational leadership, transactional leadership, knowledge sharing, job performance, and firm performance: A structural equation modelling approach”. Journal of Management Development, Vol. 35 No. 5, pp. 681-705.
- [12] Mueller, J. (2013). “A specific knowledge culture: Cultural antecedents for knowledge sharing between project teams”. European Management Journal, 32(2), pp. 190-202.
- [13] Nguyen Huu Nghi and Mai Truong An (2018). “Relationship between knowledge sharing, job satisfaction and work performance: The case of tourism startups in Ho Chi Minh City”. Journal of Science Open University Ho Chi Minh City, 59(2), pp. 76-87.
- [14] Nguyen Ngoc Duy Phuong and Pham Thai Son (2018). “Factors affecting knowledge sharing of bank employees - Research at Joint Stock Commercial Bank for Industry and Trade of Vietnam, Lam Dong province”. Industry and Trade Journal.
- [15] Nguyen Phan Nhu Ngoc (2018). “Factors affecting knowledge sharing of employees in the information technology industry”. Faculty of Economics, Ho Chi Minh City University of Technology and Education.
- [16] Nguyen Phuc Quy Thanh (2019). “Analysis of operational efficiency at Vietnamese commercial banks”. Industry and Trade Magazine.
- [17] Tran Vinh (2016). “Developing solutions for the FMCG industry on the basis of exploiting the influence of cultural factors”. Asia Pacific Magazine, Issue 480.
- [18] Tsui et al. (2006). “Organizational Culture in China: An Analysis of Culture Dimensions and Culture Types”. Management and Organization Review 2(3), pp. 345 – 376, November 2006.

**[P-33] Development of Automated Welding Machine for Industrial Applications**

Pham Son Minh<sup>1,\*</sup>, Tran Anh Son<sup>2</sup>, Jong Il Yoon<sup>3</sup>, Nguyen Van Minh<sup>1</sup>, Do Ngoc Hao<sup>1</sup>,  
Huynh Van Nhat<sup>1</sup>, Pham Minh Khoi<sup>1</sup>

<sup>1</sup> HCMC University of Technology and Education, Ho Chi Minh City 71307, Viet Nam

<sup>2</sup> Ho Chi Minh City University of Technology (HCMUT), 268 Ly Thuong Kiet Street, District 10, Ho Chi Minh City 72506, Viet Nam

<sup>3</sup> Korea Construction Equipment Technology Institute (KOCETI), 36, Sandan-ro, Gunsan-si, Jeollabuk-do 54004, Republic of Korea

\*Corresponding author: minhps@hcmute.edu.vn

**Abstract**

This research paper focuses on the design, analysis, and testing of a semi-automatic pipe welding machine. The objective was to propose efficient designs and evaluate their performance for welding different pipe joints, specifically lap joints and 90° angle joints. The machine's components were carefully calculated to ensure optimal functionality. The experimental phase involved testing the fabricated machine on various welding tasks. The results indicated that the welding joints achieved consistent and aesthetically pleasing quality, meeting the rigorous standards required for industrial applications. The developed semi-automatic pipe welding machine offers several advantages, including improved efficiency, enhanced weld quality, and reduced manual labor. It presents a viable solution for streamlining pipe welding processes in diverse industrial sectors. This study contributes to the advancement of welding technology by introducing an innovative machine design and validating its performance through practical experiments. The findings support the potential for widespread adoption of the semi-automatic pipe welding machine, fostering productivity and quality in industrial welding operations of injection molding processes, contributing to overall productivity and quality improvements in the plastic industry.

**Keywords:** *Erosion Machine, Ejection pin, Injection molds, Cycle*

**1. INTRODUCTION**

The majority of manufacturing processes in automotive, bicycle, and motorcycle factories in Vietnam involve manual labor and traditional assembly methods. This leads to limitations in productivity and quality, despite the high demand for efficient production processes. Welding technology, one of the key technologies in heavy industries, has rapidly advanced in recent years and is essential for various sectors such as shipbuilding, automotive, machinery assembly, petroleum, and construction. Prominent automobile manufacturers including Ford, GM, Mercedes, Toyota, Hyundai, Honda, and Nissan utilize automated production and assembly lines, with 40% of these lines consisting of welding processes.

Prof. Dr. Doan Quang Vinh, Vice Director of Da Nang University, and his team conducted research on "Robot Applications in Automotive Welding Production Lines" in Vietnam, which is one of the few countries globally engaged in automated welding research. The research topic has been successfully implemented at Truong Hai Auto Joint Stock Company. Additionally, researchers at Ho Chi Minh City University of Technology have designed, fabricated, and successfully deployed an automated pipe welding system with support from the Department of Science and Technology. The system has dimensions of 2,500 x 650 x 1,300 mm, and its welding torch can move in the x, y, and rotational directions within a range of -450 to 450 mm. The welding system accommodates pipe diameters ranging from 20 to 200 mm, and the flexible control panel can be folded for safety and protection. The developed welding system has been effectively utilized at Plant A41 (Ministry of Defense), exhibiting stable weld quality and showing high commercial potential.

In heavy industries such as oil and gas, thermal power, and shipbuilding, welded connections between tube structures have gained significant popularity. Current welding procedures for tube connections adhere to American standards such as AWS, ASTM, API, or ASME. These procedures typically involve welding component assembly, alignment or fitting, weld layering, and subsequent inspection for weld quality. Quality requirements in the welding process are rigorously assessed based on parameters such as strength, leak tightness, and heat-affected zones. However, deformation of welded components after the welding process has not been thoroughly considered, especially for highly precise connections.

Existing welding training programs primarily focus on basic welding movements, such as straight lines and circles, without addressing more complex trajectories such as ellipses or waves. Square tube welding with wave-like orbital welding has received limited discussion, mainly relying on technology adoption and importing welding equipment, often utilizing highly advanced robotic arms that come with high commercial costs and maintenance requirements.

As Vietnam undergoes industrialization, the manufacturing sector is experiencing rapid growth, marked by the increasing adoption of modern machinery and automated production lines. The existence of precision machinery and equipment is crucial for the success of mechanical enterprises. Welding, as a time-consuming, energy-intensive, and costly process in mechanical device fabrication, significantly affects the durability and structural integrity of welded joints. However, reliance on manual labor is unsustainable as the number of skilled workers decreases. To address these challenges, this research proposes a solution and design for a semi-automatic pipe welding machine suitable for industrial applications. The machine operates on a standard 220V power supply and can adjust welding speed using a frequency converter. However, it can only handle one welding batch every ten seconds to prevent overheating. With both manual and automatic control modes, the operation is user-friendly, eliminating the need for specialized safety equipment and simplifying maintenance tasks.

## 2. DESIGN OPTIONS FOR PIPE WELDING EQUIPMENT

The semi-automatic welding equipment will be designed to weld the joint between two perpendicular square pipes, as shown in the diagram below.



**Figure 1.** T-shaped Pipe Joint

The weld joint is a closed 3D curve. Therefore, when designing the automated welding machine, attention must be given to its rotational and translational capabilities.

The proposed design options and their advantages and disadvantages are as follows:

**Option 1:** The two pipes are clamped perpendicular to each other on the machine table, with the center of the table acting as a rotating axis driven directly by a motor. The welding torch is then clamped and brought into contact with the two threaded rods, as shown above, with each rod being driven by a separate motor. The purpose of the threaded rods is to create vertical motion along the Y-axis of the welding torch, combined with rotational motion around the axis of the two pipes, forming a wave-like welding trajectory.

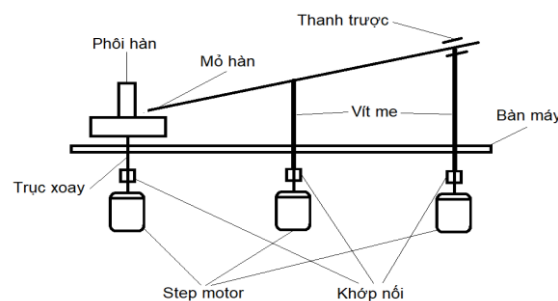


**Figure 2.** Option 1

This option has the following advantages and disadvantages:

Advantages:

- No interference with the welding wire since the welding torch remains stationary.
- Relatively simple structure.

Disadvantages:

- Lack of automated control, resulting in uncertainty regarding the welding trajectory.
- The rotating table and clamping mechanism pose significant safety risks, as the welding torch rotates, potentially causing collisions.

**Option 2:** Compared to Option 1, Option 2 incorporates the following adjustments:

- The welding torch rotates while the clamping mechanism remains stationary.
- Application of an automatic control system to generate the wave-like motion of the welding torch.
- The main axis rotation is driven by an AC motor with an internal gear reducer, reducing the motor speed to meet the welding speed requirements.
- The main motor and rotating axis are placed above.

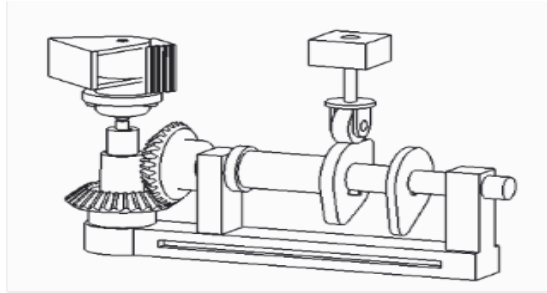


**Figure 3.** Option 2

With these improvements, Option 2 has the following advantages and disadvantages:

Advantages:

- Resolves space constraints and facilitates easier arrangement below the machine.

Disadvantages:

- Requires additional motor clamping components.
- Increased safety risks when the entire clamping mechanism is in motion.
- Reliance on external assistance for the fully automated control system, limiting the scope for learning.
- Introduces unnecessary complexity when using the automatic control system.
- Interference from welding-generated magnetic fields makes the use of an automatic control system unfeasible, as it could cause disturbances and damage expensive control components, leading to maintenance and replacement costs.

Therefore, Option 1 is selected as the preferred design solution.

### 3. RESULT AND DISCUSSION

#### 3.1. Calculation of screw and nut assembly

The selection of the screw and nut assembly depends on several factors, as follows:

Load to be transmitted.

Installation position (quick feed or slow feed).

Layout diagram (ball screw or roller screw).

Rigidity of the system.

Surface hardness (ability to run smoothly).

Manufacturing accuracy.

For the screw and nut assembly, we will choose a 1:1 transmission ratio and a ball screw.

Geometry parameters of the screw and nut assembly:

Maximum travel distance,  $L = 400$  mm.

Lead,  $m = 1$ .

Screw diameter,  $\varnothing d = 12$  mm.

#### 3.2. Calculation of motor selection

Calculation of the system power: Overall efficiency:  $\eta = \eta_{ol} \times \eta_{tv} \times \eta_{kn}$

We have:  $\eta_{ol} = 0.99$ : Efficiency of one pair of rolling elements.  $\eta_{tv} = 0.9$ : Efficiency of one screw.  $\eta_{kn} = 0.98$ : Efficiency of shaft coupling. Therefore,  $\eta = 0.99 \times 0.98 \times 0.9 = 0.87318$ .

Motor selection: To rotate the welding workpiece (consisting of two 304 stainless steel pipes with a length of 150 mm, maximum diameter of 42 mm, perpendicular arrangement, and thickness of 1.5 mm), we need to calculate:

Density of 304 stainless steel:  $d = 7.93 \text{ g/cm}^3$

Weight of the steel disc:  $D = d \times V = 7.93 \times 2[15 \times (2.12\pi - 1.952\pi)] = 454.04 \text{ g}$

Moment of inertia of the steel disc:  $I = (1/2) \times m \times R^2 = (1/2) \times 454.04 \times R^2 = 17026.5 \text{ g.mm}^2$

Force required to rotate the workpiece:  $F = (I \times g) / (1000 \times R) = (17026.5 \times 9.81) / (1000 \times 75) = 2.227 \text{ N}$

Torque:  $T = F \times R \rightarrow T = 2.227 \times 75 = 167.025 \text{ N.mm}$

1 revolution  $\rightarrow$  32 seconds, so the number of revolutions per minute:  $n = 1.875$  (revolutions/minute)  $T = P \times n / (9.55 \times 10^6) = (167.025 \times 1.875) / (9.55 \times 10^6) = 3.279 \times 10^{-5} \text{ kW}$  Required power for the motor:  $P_{ct} = P / \eta = (3.279 \times 10^{-5}) / 0.87318 = 3.756 \times 10^{-5} \text{ kW}$

We need to select a motor that meets the condition:  $P_{\text{motor}} > P_{ct}$ .

There are many motors that meet this condition. Based on the given parameters and considering economic factors, we choose a DK52-4 type motor.

The pipe welding equipment is processed and assembled as shown in the figure below.



Figure 4. Welding machine

The control unit of the device is compactly housed in a control box, with the wiring connected internally to the vertical bar. The actuating mechanism and transmission are designed to be robust, as shown in the figure. The welding torch is fixed at an inclined angle, and the suspension wire is positioned above to avoid interference during machine operation.

#### 4. CONCLUSION

In this research, various designs of semi-automatic pipe welding machines were proposed and analyzed. The detailed components of the machine were calculated prior to the fabrication of the automated pipe welding equipment. The constructed device was then tested with common pipe welding joints such as lap joints and 90° angle joints. Overall, the welding joints achieved satisfactory results, displaying uniformity and aesthetic appeal. They met the requirements for industrial products.

#### Acknowledgments

This research was funded by the HCMC University of Technology and Education (HCMUTE) under grant of 2023, number **T2023-114**. The authors would like to thank the HCMC University of Technology and Education (HCMUTE), and the Ho Chi Minh City University of Technology (HCMUT) for the support of time and facilities for this study.

#### References

- [1] Trần Quốc Hùng, *GT Dung sai - Kỹ thuật đo*, Nhà xuất bản ĐHQG TPHCM, 2012.
- [2] TS.Phạm Sơn Minh, ThS.Trần Minh Thế Uyên, *GT Thiết kế và Chế tạo khuôn phun ép nhựa*, Nhà xuất bản ĐHQG TPHCM, 2014.
- [3] Robert A. Malloy, *Plastic Part Design for Injection Molding: An Introduction*, 2010.
- [4] D.V. Rosato, M. Rosato, and D. Rosato, *Injection Molding Handbook*, 2000.
- [5] David O. Kazmer, *Injection Mold Design Engineering*, Hanser Publishers, Munich, 2016.

**[P-38] Control to Manipulate the Target Task for Industrial Manipulator**

Minh Tuan Nguyen

*Faculty of Mechanical Engineering, Ho Chi Minh City University of Technology (HCMUT), 268 Ly Thuong Kiet, District 10, HCMC, Viet Nam**Viet Nam National University Ho Chi Minh City (VNUHCM), Linh Trung Ward, Thu Duc City, HCMC, Viet Nam*

Corresponding author: thinhpfiev2003@yahoo.com

**Abstract**

The research presents the method of designing and controlling the industrial robot via virtual reality techniques so that human can witness diverse behaviors of the robot in many environments. Robot motions can be checked through the simulation program and robot program can be generated for the real task execution. The algorithm which controls the industrial robot to serve interactions with human is also analyzed. The robot is used in the research is restored and upgraded from the damaged SCORBOT-ERVII robot which was not equipped with electrical cabinet. After upgrading the mechanical part and electrical circuits, the virtual set which includes a headset and 2 hand controllers are combined to the controller of the robot so that the robot can be controlled via this device. The shared control approach and artificial potential field is exploited in control algorithm of this robot so that it has ability to avoid obstacles according to the repulsive force and attractive force. After all, the experimental results are presented to the real model of robot.

**Keywords:** Robot control, Manipulator, Cyber-Physical system, Complex system

**1. INTRODUCTION**

A robotic arm or robot manipulator is a programmable machine which can replace human tasks in many aspects. The robot arm comprises links which are connected by joints. There are six different main types of joint: revolute, prismatic, cylindrical, screw, spherical, and planar. As highlight for this point [1-3], revolute joint and prismatic joint are the most common kinds of joint in robot arm structure: the revolute joint allows rotation between two links while prismatic joint allows a translation between two links. The links of the manipulator can be considered to form a kinematic chain. The number of joints in a robot will probably determine the degree of freedom (DOF) for this device. Mostly, high DOFs can make the robot have more reachable area in movements. The final tool which is placed in the final point of the chain of the manipulator is called end-effectors [4, 5]. This element which depends on different applications can be a gripper, a magnet plate, a drilling tool and the like. Apart from mechanical components, actuators are devices which drive joints to change their configurations. The actuators can be of electric, hydraulic, or pneumatic type. Computers are commonly valued in control unit.

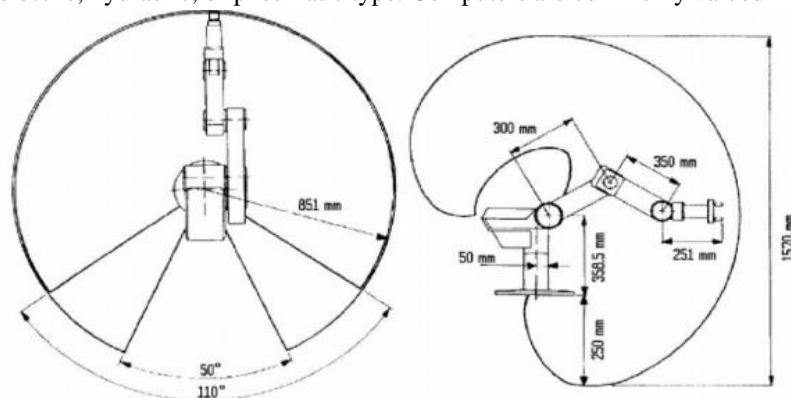


**Figure 1.** Scrobot-ER-VII robotic diagram. Top view (left). Side view (right).

In this research, Scrobot-ER [6] is used, the robot for which the spike-based controller has been developed is a six-axis arm robot with 12V DC motors for performing axis movement and double optical encoders to register the said movements. A descriptive image of the robot can be seen in Figure 1. The controller developed effectively controls these six 12V DC motors through the use of a set of six H-bridges that are driven through an external

12V-25A power supply, as shown in Figure 2. This external supply is not affected whatsoever by the controller's programming, other than by the PFM signal that the controller generates to command different movements to each motor.

## 2. PRELIMINARIES

### 2.1. VR (Virtual Reality) technology

Extended reality (XR) is the combination of real and virtual environments, and this is the place where the interaction between human and virtual object can appear via computer technology. In short, Extended Reality is a compilation of Augmented Reality (AR), Virtual Reality (VR) & Mixed Reality (MR):

Virtual reality (VR) is the use of computer technology to create an artificial environment in which the user can experience a three-dimensional domain. It tricks the user's senses into thinking they are in a different environment by wearing a headset. Moreover, virtual objects in that technique can be interacted by the user via haptic controllers. However, all virtual subjects in this technology are formed in virtual environment so that human cannot witness any real objects except using the external camera window inside that place. The process of VR experience can be described as:

- The VR headset will probably replace the real world by 3D environment due to the screen in front of the eyes of the users.

- The VR lens or autofocus lens which are placed between each eye and the screen. The lens can be adjusted owing to the positions of each eye.

- The visuals are displayed on the screen to eyes via graphic processing unit which can be known as computers or mobile devices. With the computer, visuals are mostly transferred to VR headsets by link cable. However, the internet can be considered as tools to handle these issues. Mobile device is another case: The phone is mounted directly on the headset such that the lenses of the headset simply lie over the mobile device's display to magnify the images to finally create the visuals.

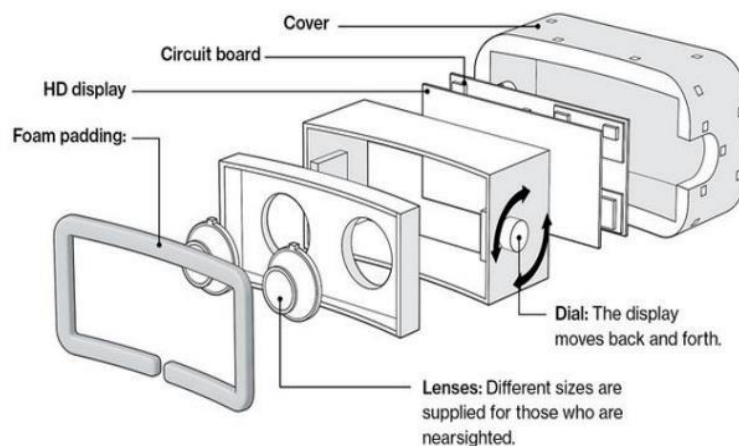


**Figure 2.** Illustration of the internal structure-for the Oculus headset.

### 2.2. Unity

Unity is a game engine for both 2D and 3D games that has been around since 2005. It was created by Unity Technologies in order to give more developers access to game production tools, which was an innovative effort at the time.

Unity includes a robust scripting API that gives easy access to the most frequently used features. This includes both general game features and particular API calls that provide access to specific engine features and quirks. Besides, the main programming language for this cross-platform software is C#. Many C# scripts can run at the same time in 1 project. This means that in a specific project, many different objects can have their own scripts. However, there are some restrictions of packages or library in C# of Unity environments.



### 2.3. Camera setup

There are various types of sensors which can obtain locations of obstacles on the working area of robot arm. To simplify the process, Kinect V1 camera is utilized to detect the coordinates of obstacles. Kinect camera is connected to a computer, and image data is transferred to here for processing.

The general parameters of Kinect camera V1 are:

- RGB camera resolution: 640x480, 30fps.
- Infrared camera resolution: 640x480, 30fps.
- Working range: 0.8m-4m in default mode;
- 0.4m-0.35m in near mode.

Both 2D and depth images captured by Kinect cameras have a resolution of 640x480 pixels, and each pixel in 2D photos corresponds to a depth camera point. When the pixel coordinates of a point in an RGB image are obtained, the x, y, and z values of that point may be recovered in the camera coordinates, because Kinect's true coordinate system is defined to coincide with the color camera's coordinate system.

## 3. SYSTEM DESIGN

### 3.1. Implementation of robot model

Unity3D does support to create 3D model in the project. However, the complicated appearance of models will probably be tough in design with unprofessional tools of Unity3D owing to the fact that the Unity3D is more compatible for design games.

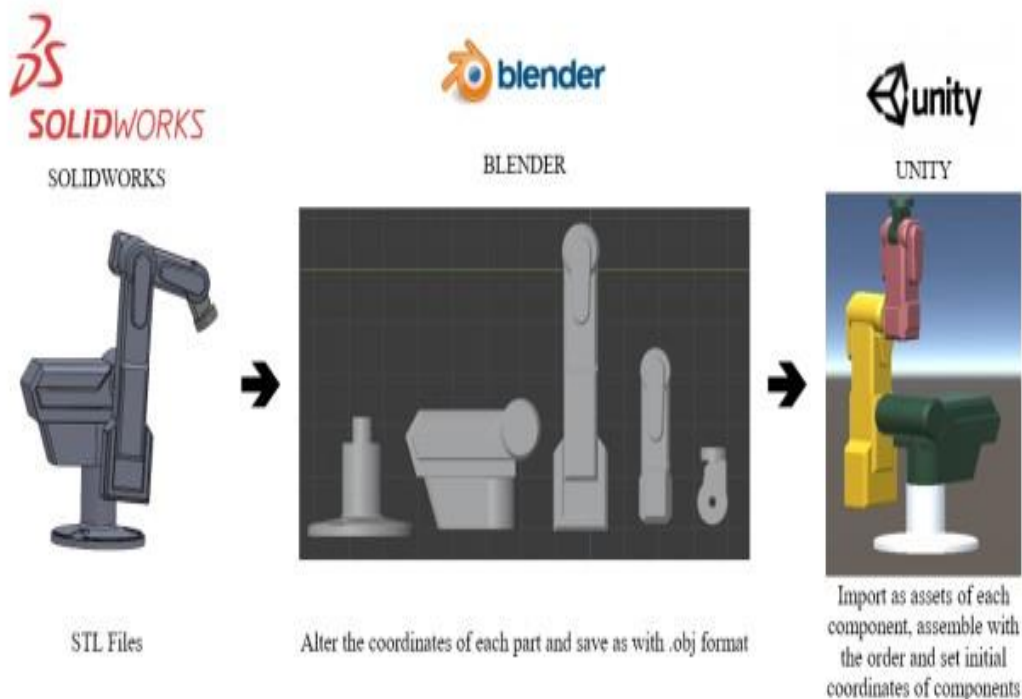


**Figure 3.** Overall scheme for the proposed system.

Therefore, it is the most common to design a mechanical model in other professional software such as: AutoCAD, SolidWorks, Fusion and the like. Nevertheless, there is no way to import directly 3D files to Unity3D because it only supports specific files. By this, this thesis goes for modifying the format of files to compatible formats of Unity. By this it means that the original files would go to a middleware to alter the format without changing the data of original files. In this case, Blender is used to handle the problem. The process can be described as Figure 3.

### 3.2. Process of programming

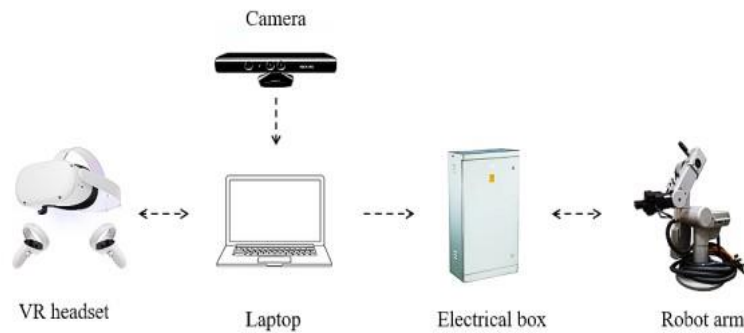


**Figure 4.** Demonstration of data transmission in the proposed system.

The working in virtual environment includes 1 working table (500mm in length, 300 in width before scale) and a leader cube. The user will lead the cube to desired positions, and the robot arm will follow the path of the cube. In this case, the coordinate of the cube needs to be transformed to be coordinate of the robot because the robot is controlled due to inverse kinematic method. As Fig. 5, it is prominent to pay attention to the coordinate of Unity system: Unity uses a left-handed, Y-Up coordinate system.

Due to the different model of robot, the DH table is based on SCORBOT-ER-IX model, although the general placement of coordinates is same as SCORBOT-ER-VII. The components are set with order parents so that rotation angles of each link will create rotation movement for each part. Because of the automatic placements of coordinates, each part needs to be put into a virtual coordinate which is coincident with rotation axis. This means that it will lead whole part to rotate as demands.

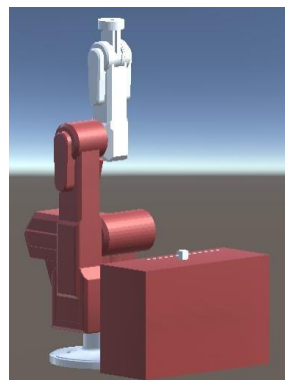


**Figure 5.** The virtual model of the proposed robot.

### 3.3. Camera calibration

It is necessary to obtain data of the obstacle from the OpenCV apart from Kinect library. OpenCV (Open-Source Computer Vision Library) is a library of programming functions mainly aimed at real-time computer vision. The main programming language in this thesis is C#. In order to transfer the data to Unity, Socket communication based on local host is used.

### 3.4. Data transmission

The sampling time based on computer is the time to produce the new control data for robot after collecting data from VR and process them according to algorithm without caring the camera factor. This time can be estimated less than 3ms. Therefore, the condition to select the sampling time is:  $T_{samp} > T_{samp} \cdot T_{computer}$  for computer program is 500ms.

Nevertheless, after setting the pose of the real robot, the time which let robot follow the next movements cannot be determined. This means that drivers will generate new control signals to motors if the last movements

are accomplished. In contrast, drivers will probably show bug, so they cannot be controlled anymore. Due to these elements, the time to receive new signals of drivers is randomly chosen: 3 second with a condition: the displacement of the end-effector is short in each sampling time.

This means that the MCU will receive the signal in every 1 second while the VR and camera program are always implemented in every 500ms.

### 3.5. Design the proposed control scheme

There are 2 main components in the artificial potential field: repulsion potential energy and attractive potential energy. In general, due to this algorithm the robot moves in the direction towards where the total potential energy is lowered, attracting to the target while avoiding the obstacles.

\* Repulsion potential energy: The obstacle will trigger a repulsive force on the robot arm from the obstacle on a specific distance. This means that the force orientation will probably be opposite to the direction of vector from robot arm to obstacle as Fig. 6. Due to this, the robot can avoid from obstacles. In this thesis, these kinds of force will be applied on each joint in order to avoid obstacles for the whole manipulator. The repulsion potential energy of each joint is calculated as:

$$U_{ir} = \begin{cases} \frac{1}{2} Kr \left( \frac{1}{d_i} - \frac{1}{d_{safe}} \right)^2, & d_i \leq d_{safe} \\ 0, & d_i > d_{safe} \end{cases} \quad (1)$$

With:

i: the order of each joint. i=3 for this thesis

Kr: repulsion gain

d<sub>i</sub>: distance between joint to obstacles.

d<sub>safe</sub>: safe distance which allow robot work in normal mode

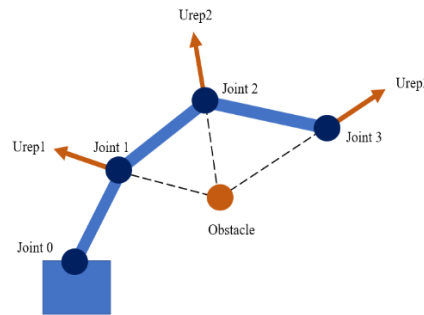


**Figure 6.** The modeling of repulsion forces in the proposed robot.

However, there would be many obstacles in the reality. Therefore, the total repulsion potential of manipulator can be described as:

$$U_{rep} = \sum_{i=1}^n \sum_{j=1}^m U_{ir} \quad (2)$$

With:

m: the number of obstacles having influence on a manipulator.

Attractive potential energy: The target will generate gravity to the end-effector of the robot. This means that the end-effector of the robot would try to reach the target. The attractive potential of the manipulator can be described as:

$$U_{att} = \frac{1}{2} Ka (\|X_{goal} - X_l\|)^2 \quad (3)$$

With:

Ka: attractive gain

X<sub>goal</sub>: coordinate of the target;

X<sub>l</sub>: coordinate of the end-effector.

#### 4. RESULTS OF INVESTIGATION

In this section, the real-world validations of the proposed method are performed to evaluate the feasibility and effectiveness. The system consists of robotic platform, electric cabinet, motion controller, virtual glass and teach pendant. The overall set-up is depicted as Fig. 7a while an operator mainly manipulated with the proposed system. During the robot manipulation, data is collected from various sensors as Fig. 7b and it is transmitted to host computer.

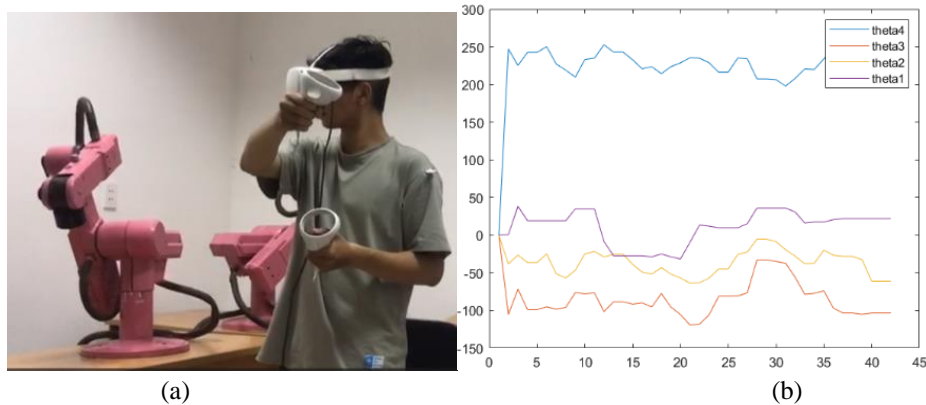


**Figure 7.** Experimental results in this study, (a) practical interaction and (b) data collection

In our tests, this system could work well in many practical situations. Also, it provides a flexible motion when human moves or vibrate. Since the human motion is continuous and complicated, data collection needs to be filtered in order to achieve the precise estimation. Furthermore, this data set could be utilized to predict any action of human or support the human-robot interaction if needed.

#### 5. CONCLUSION

In this study, a method to control the robotic platform via the virtual environment was proposed. The motivations of the proposed system are (1) to establish the hardware connection that allows smooth transmission and continuous data, (2) to realize the concept of cyber-physical system in the scope of robot manipulation, and (3) to enhance the human-robot interaction. In this design, several components are to describe and install in the specific requirements. The proposed method suggested a mechanism to exchange the data flow as well as overall scheme to manipulate. To demonstrate the effectiveness and feasibility of this approach, the real-world example to drive the robotic system was implemented. In future, the modern hardware platform should be deployed to reach the high performance. In addition, the improved scheme, i.e., machine learning or human-in-loop, could be considered enhancing the behavior of this system.

#### References

- [1] Billard, A., & Kragic, D. (2019). Trends and challenges in robot manipulation. *Science*, 364(6446), eaat8414.
- [2] Mason, M. T. (2018). Toward robotic manipulation. *Annual Review of Control, Robotics, and Autonomous Systems*, 1, pp. 1-28.
- [3] Zhang, D., & Han, X. (2020). Kinematic reliability analysis of robotic manipulator. *Journal of Mechanical Design*, 142(4).
- [4] Shome, R., Tang, W. N., Song, C., Mitash, C., Kourtev, H., Yu, J., ... & Bekris, K. E. (2019, May). Towards robust product packing with a minimalistic end-effector. In *2019 International Conference on Robotics and Automation (ICRA)* (pp. 9007-9013). IEEE.
- [5] Ma, Z., Poo, A. N., Ang Jr, M. H., Hong, G. S., & See, H. H. (2018). Design and control of an end-effector for industrial finishing applications. *Robotics and Computer-Integrated Manufacturing*, 53, pp. 240-253.
- [6] Kumar, R. R., & Chand, P. (2015, February). Inverse kinematics solution for trajectory tracking using artificial neural networks for SCORBOT ER-4u. In *2015 6th International Conference on Automation, Robotics and Applications (ICARA)* (pp. 364-369). IEEE.

## [P-40] A Two-Phase Optimization Algorithm for Solving the Heterogeneous Capacitated Vehicle Routing Problem: A Case Study on the Delivery Problem in Viet Nam

Mai-Ha Phan\*, Thanh-Hoa Nguyen

*Department of Industrial Systems Engineering, Faculty of Mechanical Engineering  
University of Technology (HCMUT), 268 Ly Thuong Kiet Street, District 10, Ho Chi Minh City, Viet Nam  
Viet Nam National University Ho Chi Minh City, Linh Trung Ward, Ho Chi Minh City, Viet Nam*

\*Corresponding author: ptmaiha@hcmut.edu.vn

### Abstract

Most small and medium-sized logistics companies in Viet Nam are planning daily deliveries manually and purely by experience. This is one of the reasons causing the high total transportation costs problem. Reducing transportation costs has long been a goal that many businesses aim to increase their competitiveness in the logistics field. One of the ways to minimize the transportation cost is by optimizing the routing of its vehicles. Therefore, the main objective of this research is to find a set of optimal routes that minimize the total driving distance for all vehicles to serve customers. The proposed algorithm is a variant of the Fisher and Jaikumar Algorithm (FJA), which consists of two phases: a clustering phase and a route generation phase. After determining the numbers and types of vehicles used, this research conducts the first phase - clustering with two steps: (1) defining the seed node and (2) allocating the customers into each cluster by using the Generalized Assignment Problem model (GAP model). Next, in the second phase – route generation, this research uses Branch and Bound (B&B) algorithm to find optimum routes for each cluster. Computational results from its application to a real-world case in a logistic company in Vietnam are presented. This paper compares the results of the FJA algorithm with the exact method (CPLEX software) for small-scale problem instances to verify the effectiveness of the algorithm. Finally, the obtained vehicle routes are compared against the existing daily delivery routes showing that the number of vehicles used for delivery and the distance traveled is reduced. As a result, the daily cost of transportation, including petrol costs and fixed costs per vehicle is significantly decreased, specifically by 12,5% of the actual.

**Keywords:** *Capacitated vehicle routing problem, Optimization, Heterogeneous fleet, Fisher and jaikumar algorithm, Experimental design, Cluster-first-route-second*

### 1. INTRODUCTION

Logistics services are growing strongly, in Vietnam currently accounting for about 20.9% of the country's GDP. In particular, Vietnam's road transport currently accounts for about 77% of the country's total freight transport (Source: World Bank Blogs). This leads to increasing competitiveness in terms of price and service quality - two important factors for customers. Manually planning deliveries can increase costs and delay deliveries. Therefore, optimizing delivery routes is the way many transport businesses aim to reduce costs and increase logistics efficiency.

The logistics company where the author conducted the study was established a long time ago. However, the planning of daily deliveries of this company till now is done manually and purely by experience. As a result, it takes a lot of fuel costs because the distance traveled is not optimal. With the desire to reduce the total transportation costs and increase profits, the company needs to replace the find of delivery routes with experience as before thanks to the optimization method. This research will support that by leveraging optimal information technology and algorithms to improve route planning models to reduce transportation costs, thereby improving competitiveness, building the reputation of the company.

### 2. LITERATURE REVIEW

The well-known Vehicle Routing Problem (VRP) was firstly introduced by Dantzig and Ramser in 1959 [2]. They tackled the optimum routing of a fleet of gasoline delivery trucks between a bulk terminal and a large number of service stations supplied by the terminal. They tried to find a way to assign stations to trucks in such a manner that the station demands are satisfied and the total mileage covered by the fleet is minimized. The Capacitated VRP (CVRP) is its most common form with an additional constraint of fixed vehicle carrying capacity. In general,

CVRP considers equal capacities for all the vehicles; although vehicles with different capacities can be used. Laporte [3] gave good overviews on solution methodologies for VRP. Those are exact algorithms, classical heuristics, and metaheuristics. Since no exact method can be guaranteed to find optimal tours within reasonable computing time when the number of nodes is large, the heuristics/metaheuristics method has often been used in solving large problems of VRPs in the literature.

The Fisher and Jaikumar (FJA) algorithm [4] is also a well-known 2-phase algorithm for CVRPs. The general procedure of the FJA is comprised of four calculation steps [4] which are (1) assign seed points for each route, (2) evaluate insertion cost for each customer, (3) assign customers to routes and (4) sequence customers within route. Undoubtedly, this algorithm has a major disadvantage: the efficiency of this algorithm is very sensitive to the location of the seed customers. To find a seed node effectively, there are many ways be proposed such as which creates clusters with a geometric method partitioning the customer plane into equal angular cones [5], each cluster contains equal number of nodes [6]. Moreover, there is a new clustering-based model for which all customers are viewed as candidate seed nodes then solve MILP model [1]. This approach solved the MCVRP problem with a heterogeneous fleet for fuel delivery efficiently and has not been applied to the heterogeneous CVRP. Therefore, in this research, this variant of FJA algorithm was selected for solving case study at a logistics company in Vietnam.

### 3. MATHEMATICAL MODEL AND PROPOSED METHODOLOGY

The heterogeneous CVRP is modelled as a Mixed Integer Programming model (MIP) in the same way as the CVRP model, where the constraints are adjusted so that different types of vehicles are allowed.

#### 3.1. Mathematical model of the heterogeneous capacitated vehicle routing problem

The main assumptions of the model are as follows: (1) it is assumed that there is no time restriction, (2) traffic disruptions and weather factor are ignored, and (3) the distance between the first leg and the return leg is the same. The mathematical model of heterogeneous CVRP is demonstrated as follows:

**Notations:**

$N$  = Set of nodes  $\{0, 1, 2, \dots, n\}$  where node 0 represents the depot and a set  $N'$  of  $n$  customers.

$K$  = Set of vehicles  $\{1, 2, \dots, k\}$

$Q_k$  = Capacity of  $k^{\text{th}}$  vehicle

$dt_{ij}$  = Actual distance from node  $i$  to node  $j$

$d_j$  = Demand of customer  $j$

**Decision variable:**

$X_{ij}^k = 1$  if vehicle  $k$  travels directly from node  $i$  to node  $j$ ;  $X_{ij}^k = 0$  otherwise.

**Objective function:**

*Minimize*

$$Z = \sum_{k=1}^K \sum_{i=0}^N \sum_{j=1}^N dt_{ij} X_{ij}^k \quad (1)$$

*Subject to*

$$\sum_{i=0}^N \sum_{k=1}^K X_{ij}^k = 1 \quad j \in N \setminus \{0\} \quad (2)$$

$$\sum_{i=0}^N X_{ij}^k = \sum_{i=1}^N X_{ji}^k \quad j \in N \setminus \{0\}, \forall k \in K \quad (3)$$

$$\sum_{j=1}^N \sum_{i=0}^N (X_{ij}^k d_j) \leq Q_k \quad \forall k \in K \quad (4)$$

$$\sum_{i=1}^N \sum_{j=1}^N X_{ij}^k \leq 10 \quad \forall k \in K \quad (5)$$

$$\sum_{j=1}^N X_{0j}^k = 1 \quad \forall k \in K \quad (6)$$

$$\sum_{i=1}^N X_{i0}^k = 1 \quad \forall k \in K \quad (7)$$

$$X_{ij}^k \in \{0, 1\} \quad (8)$$

The objective function (1) is for minimizing the total driving distance of the transport routes. Each customer  $j$  can only be visited once defined by constraint (2). Constraint (3) is a flow constraint, meaning that if a vehicle

enters customer  $j$ , it must leave it. Constraint (4) is the capacity constraint for each vehicle, which guarantees that the demand picked up by a vehicle does not exceed the vehicle's capacity. Constraint (5) states that at most 10 customers should be visited by any vehicle. Constraint (6) and constraint (7) ensure that each vehicle assigned to any route should leave and arrive at depot once. Constraint (8) says that  $X_{ij}^k$  is a binary variable.

### 3.2. A variant of FJA for solving the heterogeneous CVRP

To be able to solve medium-sized instances of the designated heterogeneous CVRP, we use a variant of FJA - first proposed by Chowmali and Sukto (2020) for solving the MCVRP for fuel delivery. Due to the variety of the candidate vehicle, determining the numbers and types of vehicles used must be evaluated first in order to minimize the fixed cost of vehicles. Details of the steps of FJA for this research are illustrated in Fig. 1.

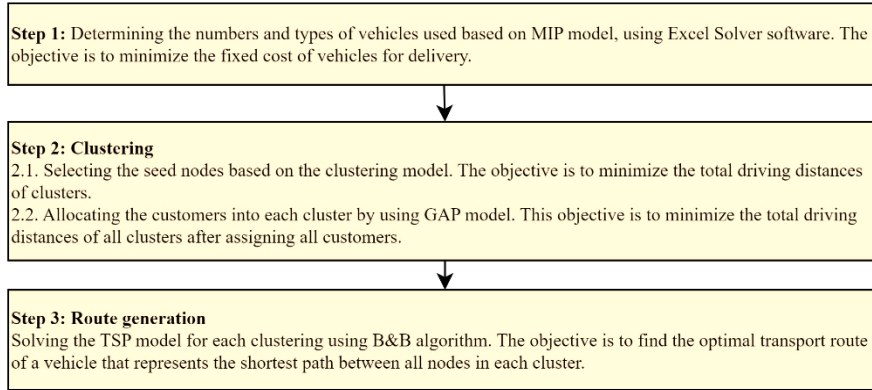


**Figure 1.** Details of the steps of solution methodology

In this section, the mathematical model of each step will be shown.

Firstly, details of the model of step 1 are as follows:

**Notations:**

$N$  = Set of customers  $\{1, 2, \dots, n\}$

$K$  = Set of vehicles  $\{1, 2, \dots, k\}$

$Q_k$  = Capacity of  $k^{\text{th}}$  vehicle

$dt_{ij}$  = Actual distance from node  $i$  to node  $j$

$d_j$  = Demand of customer  $j$

$X_{min}$  = Lower limit of the total number of vehicles used =  $n / 10$

**Decision variable:**

$X_k = 1$  if the vehicle  $k$  is used for delivery;

$X_k = 0$  otherwise.

**Objective function:**

Minimize

$$Z = \sum_{k=1}^K vc_k X_k \quad (9)$$

Subject to

$$\sum_{k=1}^K X_k \geq X_{min} \quad (10)$$

$$\sum_{k=1}^K X_k Q_k \geq \sum_{j=1}^N d_j \quad (11)$$

$$X_k \in \{0, 1\} \quad (12)$$

The objective function given by Eq. (9) represents the total fixed cost of the selected vehicles to be minimized. Constraint (10) ensures that the total number of vehicles used is greater than or equal to the minimum number of vehicles. Constraint (11) states that the total capacity of the vehicles used must meet the needs of all customers. Constraint (12) says that  $X_k$  is a binary variable.

Because the capacity of all vehicles is various, selecting the number and type of vehicles is very important. It will significantly affect the final result. Using vehicles with heterogeneous capacity will occur situations where

fixed costs are high whereas petrol costs are low because the vehicles must travel longer distance to guarantee capacity constraint. Therefore, to avoid these situations, this research conducts trial and error method with 3 cases and compares the final results with each other. Specifically, the cases are respectively:

+ Case 1: Get the results of the MIP model of step 1.

+ Case 2: Keep the total number of vehicles selected and replace the vehicle having the smallest capacity of list with the vehicle having the next larger capacity.

+ Case 3: Increase the total number of vehicles selected by 1 and replace the vehicle having the highest capacity of the results of model with two vehicles having suitable smaller capacity.

After determining the numbers and types of vehicles used, this research conducts the **step 2** – clustering, including two mathematical model. The first model is used to select the seed nodes is described as follows:

**Notations:**

$N$  = Set of customers  $\{1, 2, \dots, n\}$

$K$  = Set of vehicles  $\{1, 2, \dots, k\}$  where  $K$  is determined in step 1 and  $K$  is also the number of clusters.

$Q_k$  = Capacity of  $k^{\text{th}}$  vehicle

$dt_{ij}$  = Actual distance from node  $i$  to node  $j$

$d_j$  = Demand of customer  $j$

**Decision variable:**

$X_{ij} = 1$  if the customer  $j$  is serviced by seed node  $i$ ;  $X_{ij} = 0$  otherwise.

$Y_{ik} = 1$  if the vehicle  $k$  is selected by seed node  $i$ ;  $Y_{ik} = 0$  otherwise.

**Objective function:**

Minimize

$$Z = \sum_{i=1}^N \sum_{j=1}^N dt_{ij} X_{ij} \quad (13)$$

Subject to

$$\sum_{i=1}^N X_{ij} = 1 \quad \forall j \in N \quad (14)$$

$$\sum_{i=1}^N Y_{ik} \leq 1 \quad \forall k \in K \quad (15)$$

$$\sum_{i=1}^N \sum_{k=1}^K Y_{ik} = K \quad (16)$$

$$\sum_{j=1}^N (X_{ij} d_j) \leq \sum_{k=1}^K (Y_{ik} Q_k) \quad \forall i \in N \quad (17)$$

$$\sum_{j=1}^N X_{ij} \leq 10 \quad \forall i \in N \quad (18)$$

$$X_{ij}, Y_{ik} \in \{0, 1\} \quad (19)$$

The objective function given by Eq. (13) represents the total the total driving distance, to be minimized. Each customer  $j$  can only be clustered into only a seed node  $i$  defined by constraint (14). Constraint (15) states that each seed node  $i$  can select the number and type of vehicles that does not exceed one. Constraint (16) guarantees that the number of clusters must not exceed a predetermined number of vehicles. Constraint (17) is the capacity constraint for each vehicle, meaning that the total demand for each cluster having seed node  $i$  does not exceed the capacity of vehicle  $k$  serving that cluster. Constraint (18) states that each cluster has at most 10 customers. Constraint (19) means that variables  $X$  and  $Y$  are binary constraints.

Next, the second model in step 2 is used to allocate the customers into each cluster. The assignment of customers to vehicles is done in such a way that vehicle capacity is not violated and the traveled distance is as less as possible, specifically according to the increasing order of insertion cost. In this article, the insertion cost of customer  $j$  ( $dt_{jk}$ ) is equal to the distance if customer  $j$  is visited on the way while visiting seed node ( $D_j$ ) minus the distance of visiting seed node and returning to depot ( $D_S$ ), be described by Eq. (20) below:

$$dt_{jk} = D_j - D_S = (D_{0s} + D_{Sj} + D_{j0}) - (D_{0s} + D_{S0}) = D_{Sj} + D_{j0} - D_{0s} \quad (20)$$

Details of the model for assigning customers to vehicles is shown as follows:

**Notations:**

$N$  = Set of customers  $\{1, 2, \dots, n\}$

$K$  = Set of vehicles  $\{1, 2, \dots, k\}$  where  $K$  is determined in step 1 and  $K$  is also the number of clusters.

$Q_k$  = Capacity of  $k^{\text{th}}$  vehicle

$dt_{jk}$  = The insertion cost of customer  $j$  into cluster  $k$ .



$d_j$  = Demand of customer  $j$

**Decision variable:**

$X_{jk} = 1$  if the customer  $j$  is assigned into cluster  $k$ ;  $X_{jk} = 0$  otherwise.

**Objective function:**

Minimize

$$Z = \sum_{k=1}^K \sum_{j=1}^N dt_{jk} X_{jk} \quad (21)$$

Subject to

$$\sum_{j=1}^N X_{jk} = 1 \quad \forall k \in K \quad (22)$$

$$\sum_{j=1}^N X_{jk} \leq 10 \quad \forall k \in K \quad (23)$$

$$\sum_{j=1}^N (X_{jk} d_j) \leq Q_k \quad \forall k \in K \quad (24)$$

$$\sum_{j=1}^N (X_{jk} d_j) \geq 75\% * Q_k \quad \forall k \in K \quad (25)$$

$$X_{jk} \in \{0, 1\} \quad (26)$$

The objective function given by Eq. (21) is to minimize the total driving distance of all clusters. Each customer  $j$  can be assigned into only a cluster  $k$  defined by constraint (22). Constraint (23) states that each cluster has at most 10 customers. Constraint (24) is the capacity constraint, which guarantees that the demand of all customer  $j$  in each cluster  $k$  does not exceed the vehicle's capacity serving that cluster. Constraint (25) ensures that the efficiency of vehicle  $k$  is at least 75%. Constraint (26) says that  $X_{jk}$  is a binary variable.

After completing step 2, this research turns to the final step – route generation to get the heterogeneous CVRP solution with the clustered customer. The aim of it is to determine the optimal route for serving these customers. In this step, each cluster is an individual traveling salesman problem (TSP). Because each cluster has at most 10 customers, the exact algorithm such as Branch & Bound, column generation can give optimize solution in a short time. Therefore, this paper used the B&B algorithm to solve TSP problem using Python.

## 4. COMPUTATIONAL RESULTS

### 4.1. Algorithm testing

To evaluate the performance of the proposed FJA algorithm, this research compares the results of the FJA algorithm with the exact method (CPLEX software) for small-scale problem instances. This paper considered instances having the number of customers and total demand being different to evaluate two factors: solution result and computational time. Table 1 below shows that the comparison results:

**Table 1.** Comparison results of the FJA algorithm with the exact method

No. of customer	Demand (ton)	Capacity (ton)	Exact method (km)	FJA (km)	Error (%)	Time of exact method	Time of FJA
9	4.97185	2 – 3.4	1315.508	1315.508	0	55s	8s
11	11.9781	5 – 8	1426.686	1426.686	0	2276s	10s
11	14.980	2 – 5 – 8	2094.109	2094.109	0	9s	3s
11	14.980	3.4 – 5 – 8	1741.737	1741.737	0	1877s	12s
11	14.980	2 – 2 – 5 – 6.2	2510.382	2510.382	0	9s	3s
12	14.980	3.4 – 5 – 8	<b>1746.188</b>	<b>1746.207</b>	0.001%	27236s	10s

The result in Table 1 shows that if using the vehicle with the same capacity, the results of both algorithms have no difference in 5 instances first. In instance 6, the result of the exact method is better than FJA results but the computation time of exact method is 2700 times more than FJA and exceed maximum time that company require (3600 seconds). Besides, the error is only equal to 0.001% so using the proposed FJA algorithm is suitable for solving the heterogenous CVRP problem of the case study in this research.

### 4.2. Numerical example in a real case

After conducting the algorithm testing, this paper used the proposed FJA algorithm to solve cast study at a logistics company located in District 12, HCM City, Vietnam. This company will deliver goods for customers

located in 4 provinces: Dak Nong, Dak Lak, Gia Lai, Kon Tum. To implement the FJA algorithm, the locations and demands information of customers are first defined. The number of available vehicles is also determined. The actual distance between coordinates  $(x_i, y_i)$  and  $(x_j, y_j)$  is calculated based on Bings Map API by using Python. Applications of FJA to solve case 18/10/2022 with 14.98 ton, this research has taken results as Table 2:

**Table 2.** The result of routing delivery in case 18/10/2022

Case 1 (15 ton)	Vehicle 1 (2 ton): 0 1 6 16 3 4 0 Vehicle 2 (5 ton): 0 2 15 14 13 10 12 0 Vehicle 3 (8 ton): 0 8 7 17 5 9 11 18 0	666.47 km 864.22 km 787.69 km	Total distance: 2318.384km
Case 2 (16.4 ton)	Vehicle 1 (3.4 ton): 0 7 13 10 5 9 12 11 14 0 Vehicle 2 (5 ton): 0 2 16 15 8 17 6 0 Vehicle 3 (8 ton): 0 1 3 4 18 0	858.242 km 678.511 km 433.097 km	Total distance: 1969.85km
Case 3 (15.2 ton)	Vehicle 1 (2 ton): 0 7 5 10 9 12 11 0 Vehicle 2 (2 ton): 0 1 6 16 3 4 0 Vehicle 3 (5 ton): 0 2 13 17 8 14 15 0 Vehicle 4 (6.2 ton): 0 18 0	856.898 km 666.473 km 698.68 km 422.222 km	Total distance: 2644.273km

The results from Table 2 show that the numbers and types of vehicles selected from the MIP model in step 1 are not the best solution in the final step. Therefore, conducting a trial-and-error method is necessary.

#### 4.3. Results and discussion

Application of the proposed FJA algorithm to solve the delivery problem at the company from 03/10/2022 to 19/10/2022, the results are average total driving distances per day decreased by **773km** and average total transportation costs reduced by **12.5%** compared to the actual result. Currently, the number of customers per day ranges from 12 to 30 and the total demand of all customers per day ranges from 10 to 35 tons, which is not large-scale instances, and the FJA algorithm can find an optimal solution quickly in the limited computation time. In case this company wants to scale up, in what instances can the FJA algorithm get the optimal solution? This research conducted a test with the following set of numbers: customers range from 30 to 80 and demand ranges from 40 to 70 tons. The results are shown in Table 3 below:

**Table 3.** The result of larger-scale instances

Instance	Demand	Capacity	Diff	Total distance	Time (s)
40	51029	61200	10171	6344	666
40	61842	68000	6158	6743	1267
50	54950	61200	6250	6512	640
50	66839	68000	1161	6819	1369
60	40324	48600	8276	No solution in limited time	
70	48644	48600	63	No solution in limited time	

It can be seen that the FJA algorithm can only show instances that have at most 50 customers with the maximum computation times. To solve larger-scale instances, we should consider metaheuristics algorithms.

## 5. CONCLUSION AND FUTURE WORK

In conclusion, this research proposed a variant of the Fisher and Jaikumar Algorithm (FJA) to solve the heterogeneous CVRP. We tested the proposed algorithm on small-scale instances to see the performance of the algorithm compared to the exact solution. The results indicated that there are several instances showing FJA is not the optimal solution but the error is very small (only 0.001%) and the computation time of FJA is very quick. The application of FJA helped the company in the case study reduce transportation costs by 12.5% compared to the actual result. However, in terms of computational time, FJA needs a longer time to achieve the optimal solution in large-scale instances. Therefore, in the future, researchers may focus on developing more effective algorithms for solving heterogeneous CVRP instances based on this proposed.

### **Acknowledgments**

We acknowledge Ho Chi Minh City University of Technology (HCMUT), VNUHCM for supporting this study.

### **References**

- [1] Wasana Chowmalia and Seekharin Suktoa, “A novel two-phase approach for solving the multi-compartment vehicle routing problem with a heterogeneous fleet of vehicles: a case study on fuel delivery”, *Decision Science Letters* (2020).
- [2] Dantzig G B and Ramser J H, “The Truck Dispatching Problem”, *Management Science* 6(1) (1959), pp. 80-91.
- [3] Laporte G, “What you should know about the vehicle routing problem”, *Naval Research Logistics* 54 (2007), pp. 811-819.
- [4] M. Islam, S. Ghosh, M. Rahman, “Solving Capacitated Vehicle Routing Problem by Using Heuristic Approaches: A Case Study”, *Journal of Modern Science and Technology* (3) (2015), pp.135-146.
- [5] M. L. Fisher and R. Jaikumar, “A Generalized Assignment Heuristic for Vehicle Routing”. *Networks*, Vol. 11 (1981), pp. 109-124.
- [6] Tanzima Sultana and M. A. H. Akhand, M. M. Hafizur Rahman, “A variant fisher and Jaikumr algorithm to solve capacitated vehicle routing problem”, 8th International Conference on Information Technology (2017)

## [P-43] Supplier Management Information System and Support Tools for Supplier Selection: A Case Study in Garment Industry, Viet Nam

Mai-Ha Phan\*, Thanh-Huyen Thi Ho, and Gia-Nhi Thi Nguyen

*Department of Industrial Systems Engineering, Faculty of Mechanical Engineering  
University of Technology (HCMUT), 268 Ly Thuong Kiet Street, District 10, Ho Chi Minh City, Viet Nam  
Viet Nam National University Ho Chi Minh City, Linh Trung Ward, Ho Chi Minh City, Viet Nam*

\*Corresponding author: ptmaiha@hcmut.edu.vn

### Abstract

Procurement is an important function for every business. Input materials account for 50% to 60% of production cost. It is easy to see that sourcing is a high-value-added function in procurement. In addition, as technology develops, suppliers are also expanded, so procurement requires an efficient supplier selection process and proper supplier management. Although raw materials in the garment industry in Vietnam are largely dependent on imports, many companies lack formal supplier selection processes appropriate to the specific context and the industry is at an early stage. Moreover, technology 4.0 is gradually developing, it is necessary that information technology supports the supplier selection process to ensure objectivity and accuracy.

The study has two main objectives: i) Building a tool to support supplier selection; ii) Designing a supplier management information system. The results of the study are: i) A tool to support supplier selection based on the VBA (Visual Basic for Applications) programming language by combining two methods AHP (Analytic Hierarchy Process) and TOPSIS (Technique for order of preference by similarity to an ideal solution), whereby suppliers are selected based on sustainability criteria; ii) A supplier management information system including 5 main functions: material demand management, supplier selection, order monitoring, order evaluation, and reporting. The system is modeled by using DFD (Data Flow Diagram), use case diagram, ERD (Entity-Relationship Diagram), and interface design.

**Keywords:** *Supplier, Selection, Information system, Sustainability, Apparel industry*

### 1. INTRODUCTION

In Vietnam's garment industry, the cost of sewing materials accounts for 85% of the product's cost [11]. Currently, garment companies in Vietnam have to import most of their raw materials (about 70% - 80%) from China, Taiwan, and Korea [10]. Although most of the materials are imported, many Vietnamese garment companies lack formal supplier selection criteria and processes [6].

In addition, the transformation of digital technology requires Vietnamese garment enterprises to change direction but the level of readiness is not high (2.85/5), and the fact that the garment industry is in the early stages of digitization [10]. If companies want to succeed in digitizing their supply chain, they need to expand their horizons beyond the sourcing departments.

Therefore, the study built a tool to support the selection of suppliers by the Vietnamese garment industry context and design a supplier management information system following the trend of digital transformation for the garment industry. The relationship between buyers and vendors determines the actual value-added component of procurement activities.

### 2. LITERATURE REVIEW

Supplier management is an important function in supply chain optimization [5]. In some sectors, 80% or more of product sales go directly to suppliers [5]. The significant shift in the value stream underscores the importance of supplier management. A long and close relationship between buyers and suppliers is an important factor in the success of the supply chain [9].

Evaluating and selecting the right suppliers in the supply chain with a focus on sustainability is extremely important as the success of a business depends on the role of suppliers [4].

AHP is a popular method to determine weights - one of the classic problems in multi-criteria decision analysis [8]. AHP is characterized by the decomposition of a complex problem into a multilevel hierarchy structure: final objectives, criteria, sub-criteria, and alternatives [8].

The TOPSIS method is a multi-criteria decision-making technique proposed by Hwang and Yoon in 1981. The best alternative is the closest one to the positive ideal solution and the furthest from the negative ideal solution [3]. Chen (2011) proposed a structured methodology for supplier evaluation and selection in Taiwan garment companies. Marzouk and Sabbah [7] applied AHP and TOPSIS in selectin supplier. These techniques are useful for supplier selection process.

Management Information System (MIS) generally involves the process of collecting, processing, storing, retrieving, and communicating relevant information for the purpose of efficient management operations and for business planning in the organization [1].

### 3. METHODOLOGY

The study implemented parallel steps to accomplish two main objectives: i) building a tool to support supplier selection; ii) designing a supplier management information system design. Objective i) is presented in section 3.1 and objective ii) is presented in section 3.2.

#### 3.1. Tool to assist in supplier selection

To accomplish this goal, *first*, the authors defined criteria for supplier evaluation by studying the academic literature and interviewing experts working in the garment industry.

*Second*, the authors designed a supplier selection and evaluation model by combining two methods: AHP and TOPSIS.

*Third*, VBA programming language was applied to build the support tools.

#### 3.2. Designing a supplier management information system

To accomplish this goal, *first*, the authors analyzed the needs of the stakeholders who are the users of the system, those who provide information to the system, and those who receive results from the system.

*Second*, from the needs analysis results, the authors conducted a system analysis including business function flow diagram analysis (BFD), data flow diagram (DFD), and Usecase-Actor model.

*Third*, after analyzing the system, the authors' group conducted system design including analysis of the entity-relationship diagram (ERD), database design from the entity-relationship diagram, and the user interface.

### 4. RESULTS AND DISCUSSION

The results of the article research are shown in sections 4.1 and 4.2. Section 4.1 is the result of building a tool to support supplier selection, and section 4.2 is the result of designing a supplier management information system.

#### 4.1. Result of building a tool to support supplier selection

The evaluation criteria were designed according to three aspects of sustainability, including economic, social, and environmental. By studying academic documents and interviewing experts working in the garment industry, the authors proposed 15 evaluation criteria presented in Table 1.

**Table 1.** Criteria for selecting the proposed supplier

Criteria group	Criteria
Economics (A)	Supplier Profile (A1)
	Production Capacity (A2)
	Total cost (A3)
	Leadtime (A4)
	Product quality (A5)
	Flexibility (A6)
	Technology (A7)
	Continuous Improvement (A8)

	Payment Terms (A9)
	Service, after-sales (A10)
<b>Social (B)</b>	Occupational Safety (B1)
	Organizational Structure (B2)
	Working time (B3)
<b>Environment (C)</b>	Environmentally friendly packaging (C1)
	Hazardous waste treatment process (C2)

The study combines two methods (AHP and TOPSIS) into the supplier selection model. In which, AHP is used to determine the weights for the criteria, and TOPSIS is used to rank the priority order of suppliers. Figure 1 illustrates the supplier selection model proposed by the authors.

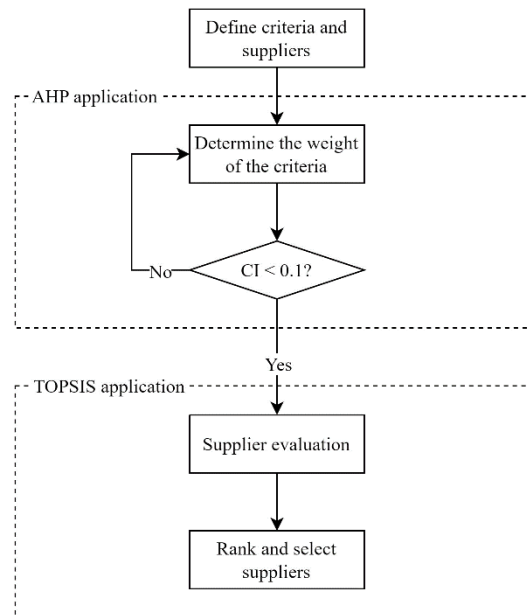
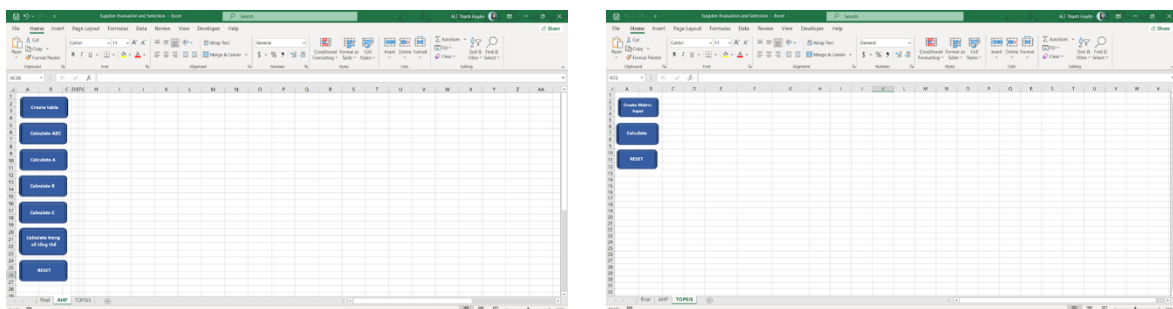


**Figure 1.** Supplier selection model

The authors applied the VBA programming language to build a tool to support supplier selection based on the proposed model and 15 criteria were designed. Figure 2a and Figure 2b are the main interface of the tool.



*a. AHP interface*

*b. TOPSIS interface*

**Figure 2.** The main interface of the tool to support supplier selection

#### 4.2. Design results of supplier management information system

From the results of the stakeholder needs analysis, the major functional groups and their sub-functions are identified and presented in Figure 3.

The context diagram presents an overview of the system scope, that is, the operating environment of the system. It is a diagram that identifies external objects, specifically the place that provides input data or receives

output from the system. The main functional groups are represented by the Vendor Management Information System located at the center of the diagram. The context diagram is presented in Figure 4.

Level-0 DFD of the supplier management information system is decomposed from the context diagram, including the main modules based on the BFD diagram, representing the data flow between the major functions of the system and presented in Figure 5.

Usecase – actor illustrates the context of the interaction between the actor and the system. The system consists of 2 actors and 19 use cases. The use-case diagram is presented in Figure 6.

The authors determined that 17 entities will be built based on the analysis of the data flow diagram and the entity relationship diagram presented in Figure 7a and Figure 7b.

Finally, the interface was designed based on the properties of the database shown in Figure 8.

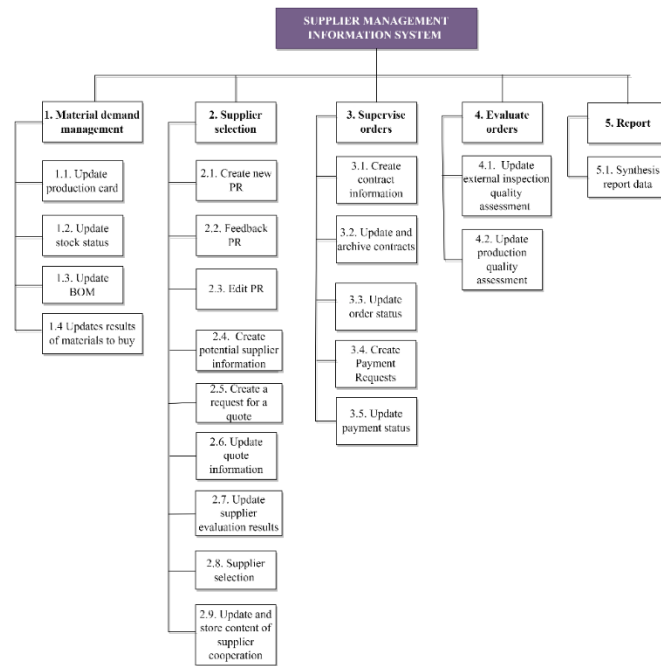


Figure 3. Business Function Flow Diagram BFD

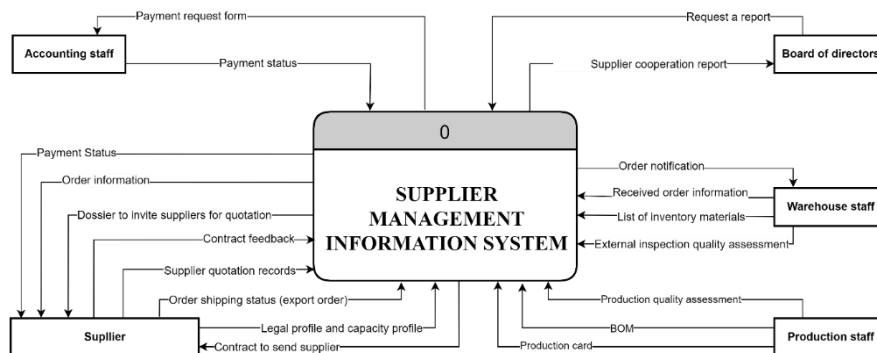


Figure 4. Context Diagram

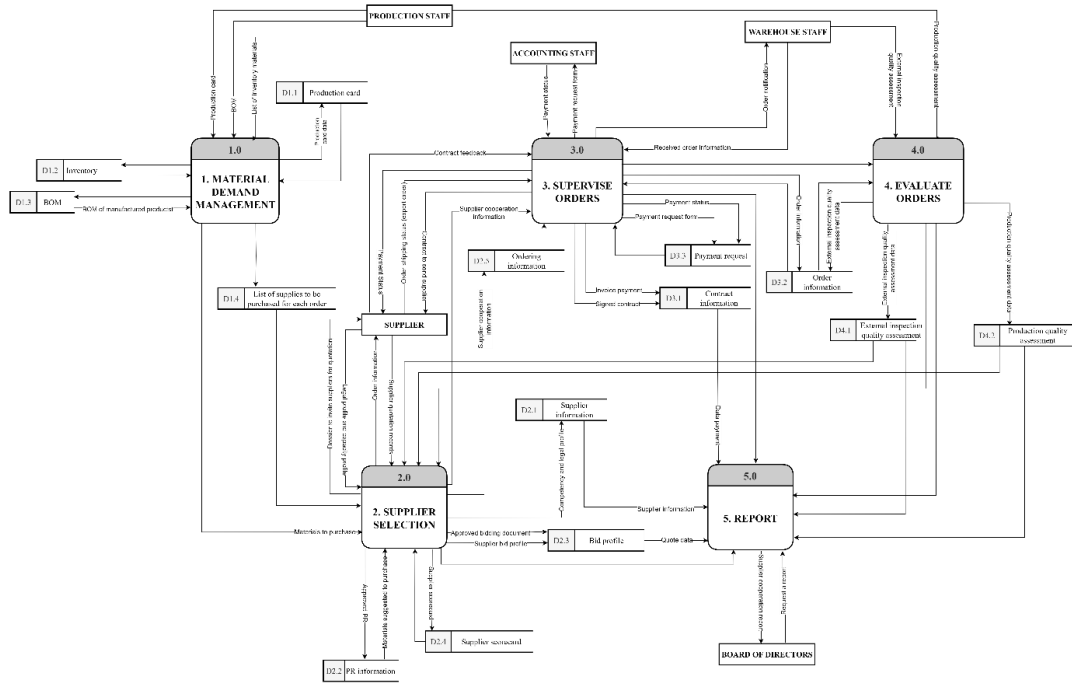


Figure 5. Level-0 DFD

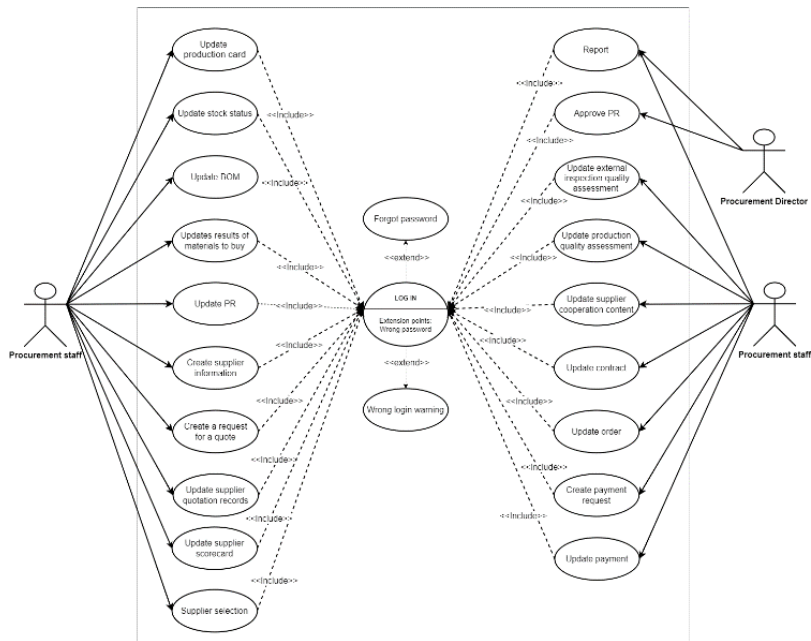


Figure 6. Use case diagram



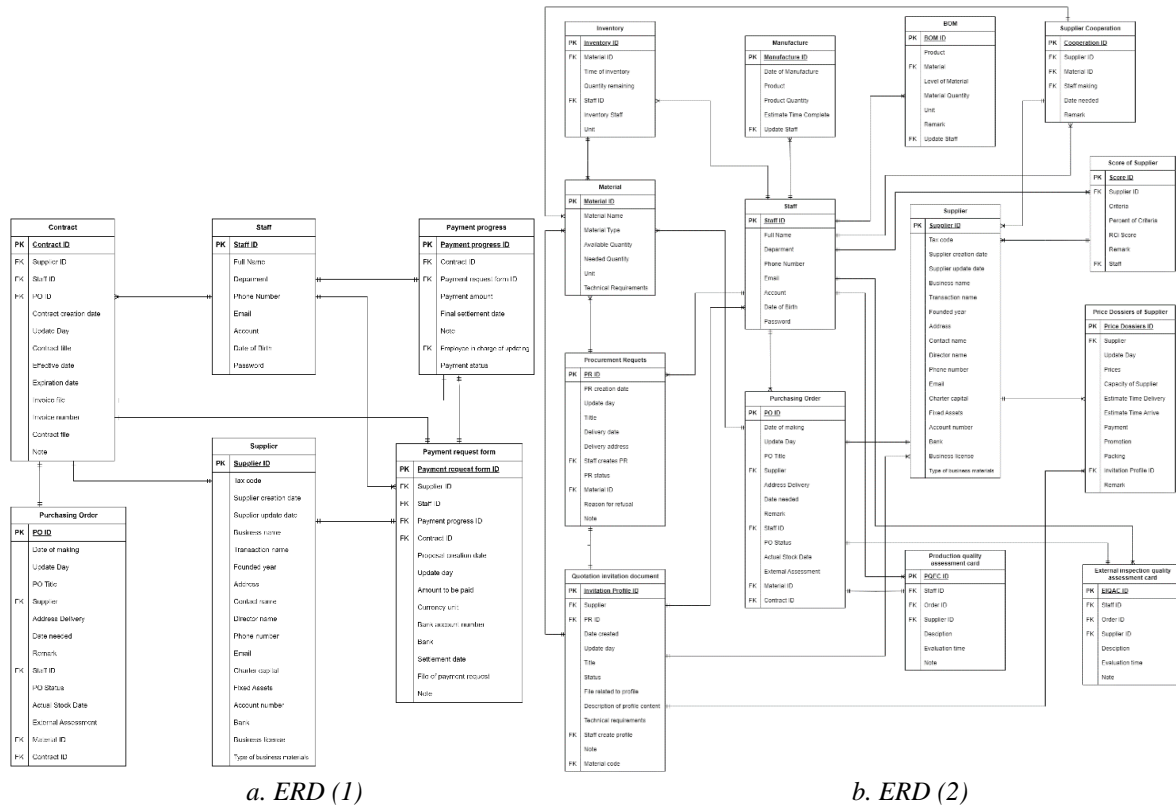


Figure 7. ER Diagram



Figure 8. System's main interface

## 5. CONCLUSION

The global textile and garment industry is witnessing a clear change toward a more sustainable supply chain and becoming a new trend that directly affects the competitiveness of the global textile and garment industry, including Vietnam.

The authors have designed a set of supplier evaluation criteria based on sustainability and proposed a model to evaluate and rank suppliers by combining two methods, AHP and TOPSIS, which are relatively simple and easy to understand. From there, a support tool was built using the VBA programming language. In addition, the authors have designed a supplier management information system sequentially, including analyzing needs and providing 5 main functions of the system, using function and data modeling tools. The design phase has designed the database; the interface is suitable for the user's needs.

In the future, the authors will try to integrate the supplier selection support tool into the supplier management information system. Furthermore, the author team will continuously edit the evaluation criteria to suit the actual context.

### Acknowledgments

We acknowledge Ho Chi Minh City University of Technology (HCMUT), VNUHCM for supporting this study.

### References

- [1] Al-mamary YH, Shamsuddin A, and Aziati N, “*The Impact of Management Information Systems Adoption in Managerial Decision Making: A Review*,” Management Information Systems,” Manag. Inf. Syst., Vol. 8, No. 4, pp. 010–017, 2013.
- [2] Chen, Y. J. (2011). Structured methodology for supplier selection and evaluation in a supply chain. Information Sciences, 181(9), pp. 1651-1670.
- [3] Joshi, R., Banwet, DK and Shankar, R. (2011). *A Delphi-AHP-TOPSIS based benchmarking framework for performance improvement of a cold chain*. Expert Systems with Applications, Vol. 38, No. 8, pp. 10170–10182.
- [4] Hsu, CW, Kuo, TC, Chen, SH, & Hu, AH (2013). *Using DEMATEL to develop a carbon management model of supplier selection in green supply chain management*. Journal of cleaner production, 56, pp. 164-172.
- [5] Krause, DR, Pagell, M., & Curkovic, S. (2001). *Toward a measure of competitive priorities for purchasing* . Journal of operations management, 19(4), pp. 497-512.
- [6] Mai, NTN, & Phong, HT (2020). *Supplier selection criteria in Vietnam: A case study in textile and apparel industry*. Journal of Asian Business and Economic Studies, 26(S02), 71-100.
- [7] Marzouk, M., & Sabbah, M. (2021). *AHP-TOPSIS social sustainability approach for selecting supplier in construction supply chain*. Cleaner environmental systems, 2, 100034.
- [8] Saaty, TL (2008). *Decision making with the analytical hierarchy process*, International Journal of Services Sciences, Vol. 1, No. 1, pp.83–98.
- [9] Saen, RF (2007). *Suppliers selection in the presence of both cardinal and ordered data*. European Journal of Operational Research, 183(2), pp. 741-747.
- [10] Virac. (2016). *Report on Vietnam textile and apparel industry Q3/2016 (Report on Vietnam textile and apparel Q3/2016)*. Hanoi: Vietnam Industry Research and Consultancy.
- [11] Ho Thi Minh Huong (2018). *Manufacture of industrial garments*. Ho Chi Minh City National University Publishing House.
- [12] Vietnam Textile and Garment Group, Hanoi University of Textile Industry, Textile Research Institute and Institute of Economics & Management (Hanoi University of Technology). 2019. *Studying and assessing the impact of the 4th Industrial Revolution on the Vietnamese textile industry in order to propose strategic orientations, policies and development solutions in the period of 2019 - 2030*.

**[P-44] Ultrafast Laser Selective Welding of Sapphire and Invar Alloy**

J. Yang<sup>1</sup>, Q. Jiang<sup>1</sup>, M. Yang<sup>1</sup>, Y.X. Zhao<sup>1</sup>, R. Pan<sup>2,\*</sup>

<sup>1</sup> School of Materials Engineering, Shanghai University of Engineering Science, Shanghai 201620, China

<sup>2</sup> Faculty of Materials and Manufacturing, Beijing University of Technology, Beijing 100124, China

\*Corresponding author: Jyang@sues.edu.cn

**Abstract**

The dissimilar joint of sapphire/Invar alloy was prepared using femtosecond laser selective welding technology, and the effects of laser power on the sealing performance, microstructure, and shear strength of the joint were investigated. The interface welding defects, elemental distribution, and fracture behavior of the joint were characterized using scanning electron microscopy (SEM), energy dispersive spectroscopy (EDS), and laser scanning confocal microscope (LSCM). The results showed that under ultrafast laser irradiation, sapphire and Invar alloy underwent melting, mixing, and diffusion processes through nonlinear absorption and linear absorption, respectively. This resulted in the formation of interlocking interfaces with intermingled features, indicating the presence of both metallurgical bonding and mechanical interlocking. The shear strength of the joint increased initially and then decreased with increasing laser power, reaching a maximum shear strength of 182 MPa. Fracture analysis revealed the presence of island-like and granular alloy residues on the sapphire side, while various morphologies of micro/nano-strips and void structures were observed on the alloy side, further indicating the promotion of metallurgical reactions at the interface by the ultrafast laser.

**Keywords:** Ultrafast laser selective welding, Sapphire and Invar alloy

**References**

- [1] Junwen Li, Heping Li, Zhuang Wang, et al. Dynamics of soliton explosions in a polarization-multiplexed ultrafast fiber laser. *Results in Physics*, 2023, vol. 49, Article number 106503.
- [2] Joong-Han Shin, Hyeong-Chang Noh, Go-Dong Park. Effect of spiral welding path and laser power on weld in laser welding of aluminum tab for lithium-ion battery. *The International Journal of Advanced Manufacturing Technology*, 2023, vol. 126, pp. 1317–1327.

## [P-45] Preparation and Research of MXene-Graphite Oxide Thin Films Based on Humidity Driving

Jianguang Zhai\*, Minghui Zou

*School of Materials Engineering, Shanghai University of Engineering Science, Shanghai China,*

\*Corresponding author: zhai\_jianguang@sues.edu.cn

### Abstract

Pure MXene exhibits severe interlayer stacking and is prone to oxidation in water/oxygen environments. It has been found that when MXene is doped with other materials, some composite materials with better performance can be obtained. Therefore, MXene can be intercalated, modified, doped, or composite with other materials to prevent its stacking, inhibit its oxidation, and improve its stability.

In this work, graphite oxide was introduced into MXene to prepare MXene-Graphite oxide films. Through the interdependence between graphite oxide and MXene, the humidity driving properties of composite films were studied, and the mechanical properties and stability of the films were explored. The driving properties of MXene-Graphite oxide films under different humidity conditions were studied by comparing the indoor relative humidity and film bending angle, and the related driving mechanism was discussed based on the characterization of composite films. The results show that the bending rate of MXene-Graphite oxide film in high humidity environment is 29°/s, the maximum bending angle is 116° and it has highly reversible characteristics. The mechanical properties of MXene-Graphite oxide films were studied based on the atomic force microscope nanoindentation. The Young's modulus ( $E_r$ ) and hardness ( $H$ ) of the films were calculated to be 8.38 GPa and 0.48 GPa respectively through the force displacement curve.

**Keywords:** *Graphene oxide, MXene, Humidity drive, Drive*

### References

- [1] Wang L, Zhang Y, Zhang J, et al. Preparation of an Au nanoparticle-graphene oxide quantum dot hybrid and its use in surface-enhanced Raman scattering. *New Carbon Mater.*, 2019, vol. 34, no. 6, pp. 606-610
- [2] Chen Z, Zhang Y, Yang Y, et al. Hierarchical nitrogen-doped holey graphene as sensitive electrochemical sensor for methyl parathion detection. *Sensors and Actuators B: Chemical*, 2021, 336:129721.

**[P-49] Long-Term Effects of Sustained Loading and Outdoor Conditioning on Bond between Glass Fiber Reinforced Polymer (GFRP) and Concrete using Epoxy**

Jaeha Lee<sup>1,2,\*</sup>, Meeju Lee<sup>2,3</sup>, Charles E. Bakis<sup>4</sup>

<sup>1</sup>*Department of Civil Engineering, Korea Maritime & Ocean University, Busan, 49112, Republic of Korea*

<sup>2</sup>*Interdisciplinary Major of Ocean Renewable Energy Engineering, Korea Maritime & Ocean University  
Busan, 49112, Republic of Korea*

<sup>3</sup>*Department of Civil and Environmental Engineering, Korea Maritime & Ocean University, Busan, 49112,  
Republic of Korea*

<sup>4</sup>*Department of Engineering Science and Mechanics, 212 Earth-Engineering Sciences Building, Pennsylvania  
State University, University Park, PA, 16802, USA*

\*Corresponding author: jeaha@kmou.ac.kr

### **Abstract**

This study investigates the behavior of small-scale plain concrete beams with notches, strengthened using GFRP sheets using epoxy, under sustained loading for 6 and 13 years in indoor and outdoor environments. Flexural testing was conducted to assess changes in debond onset strain and fracture energy of the GFRP sheets attached to the surface of the concrete. Indoor conditioning revealed a decrease in debond onset strain, while outdoor conditioning resulted in significant reductions in debond onset strain. The interfacial fracture energy ( $G_F$ ) between GFRP and concrete was also evaluated. The experiments demonstrated higher  $G_F$  values as the debonded zone moved away from the notch, particularly in beams exposed to outdoor conditions. Both indoor and outdoor environments showed reductions in  $G_F$ . Notably, direct sunlight exposure did not induce additional degradation in  $G_F$  compared to indirect exposure.

**Keywords:** *Fracture energy, Environmental degradation, Debonding, GFRP-Concrete interface*

### **Acknowledgments**

This work was supported by the National Research Foundation of Korea (NRF) grant funded by the Korea government (MSIT) (No. 2021R1I1A3044831)

### **References**

- [1] Lee, J., Kim, J., Bakis, C. E., & Boothby, T. E. (2021). Durability assessment of FRP-concrete bond after sustained load for up to thirteen years. *Composites Part B: Engineering*, 224, 109180.
- [2] Zhou, Y. W., Wu, Y. F., & Yun, Y. (2010). Analytical modeling of the bond-slip relationship at FRP-concrete interfaces for adhesively-bonded joints. *Composites Part B: Engineering*, 41(6), 423-433.

**[P-59] Applying Grey Wolf Optimization to Stochastic Inventory with Multi-Objective**Nguyen Duy Tan<sup>1</sup>, Hwan-Seong Kim<sup>2,\*</sup>, Sam-Sang You<sup>3</sup><sup>1,2</sup> Department of Logistics, Korea Maritime and Ocean University, Busan, Republic of Korea<sup>3</sup> Division of Mechanical Engineering, Korea Maritime and Ocean University, Busan, Republic of Korea

\*Corresponding author: kimhs@kmou.ac.kr

**Abstract**

This study considers multi-period inventory systems for optimizing profit and storage space under stochastic demand. A nonlinear programming model based on random demand is proposed to simulate the inventory operation. The effective inventory management system is realized using a multi-objective grey wolf optimization (MOGWO) method, reducing storage space while maximizing profit. Numerical outcomes are used to confirm the efficacy of the optimal solutions. The numerical analysis and tests for multi-objective inventory optimization are performed in the four practical scenarios. The inventory model's sensitivity analysis is performed to verify the optimal solutions further. Especially the proposed approach allows businesses to optimize profits while regulating the storage space required to operate in inventory management. The supply chain performance can be significantly enhanced using novel inventory management strategies and inventory management practices.

**Keywords:** Multi-item multi-period inventory, Stochastic demand, Grey wolf optimizer (GWO), Multi-objective optimization

**1. INTRODUCTION**

Over the past several decades, several inventory models have been an attractive topic of conversation in operations research, highlighting the distinctions between historical academic research and real-world implementations. While academic research focuses on employing mathematical control techniques for a few unique inventory models, industrial situations attempt to address practical issues by examining the maximal revenues or the minor expenses rather than balancing several objectives. Most inventory management issues are focused on a single goal, mainly using the classic inventory model, which defines an item as manufactured or acquired by management. However, those assumptions might not hold for a real test of business resilience and risk management in logistics and supply chain management.

**2. METHODOLOGY**

A company might randomly handle several items to meet customer needs over time within a finite planning horizon covering several periods. The planning horizon begins with a period and stops at a specific time. The shortage might impact the inventory carrying policy as the lost sale, and the storage space cost is formulated from the batch sizes of each item and the required space storage per unit item. The total available budget is limited and not changing. There exist limitations on ordering or production that regulate the order quantities of all items during different periods to their upper limits. Holding costs, backorder costs, and lost sales are associated with the inventory management policy. In addition, new production policies (such as installing a new manufacturing line, expanding a warehouse, or constructing a new storage area) will require optimum total storage space and profit.

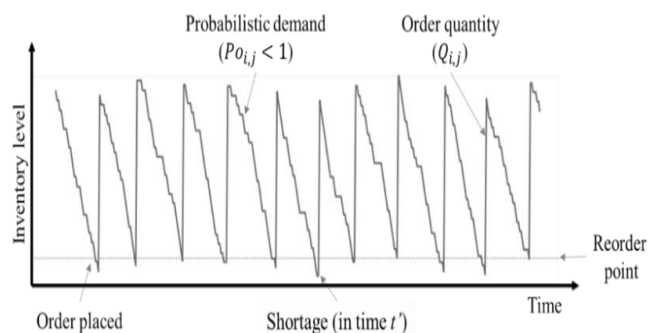


**Figure 1.** Inventory level of an item with multiple periods (discrete demand)

### 3. MULTI-OBJECTIVE OPTIMIZATION USING THE GWO ALGORITHM

The grey wolf algorithm mimicking wolves' social structures and hunting behavior in multi-objective search spaces is a novel swarm intelligence and metaheuristic algorithm [1]. First, it is essential to note that grey wolves hunt in groups and have a hierarchy within their herds. Wolves will take on quests of the corresponding difficulty with higher ranks, and levels will also be adjusted to match related requirements as they decrease. They have a strict social dominance hierarchy, as depicted in Fig. 2.

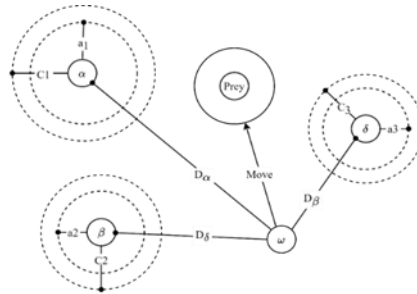


Figure 2. Implementation of positions updating in grey wolf optimizer

### 4. NUMERICAL SIMULATION

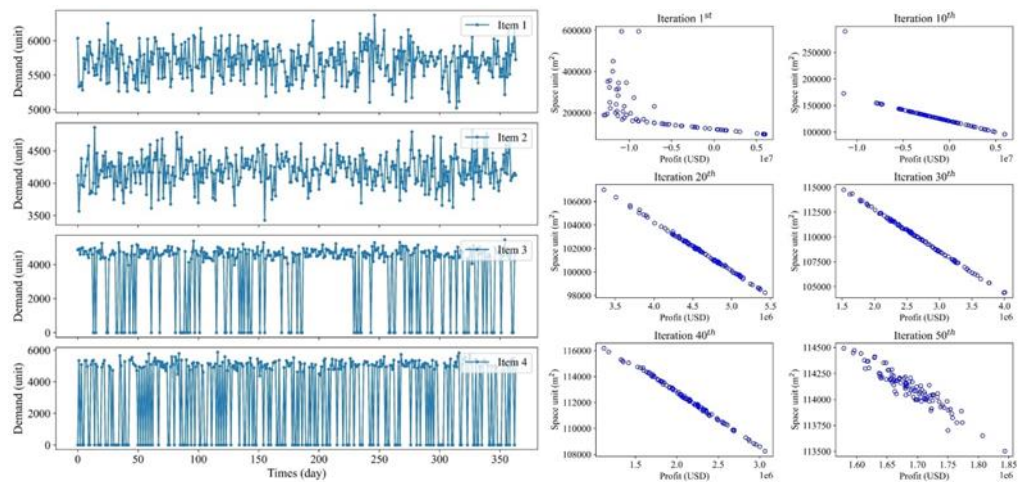


Figure 3. Random demand for four items in 365 days and Convergence analysis for the optimal solutions in the search space

The convergence processes of four items are all guaranteed. In the first iterations of each item, all the particles are placed randomly in different positions of the solution spaces, which could not reveal optimal points for objective functions. Finally, all the particles are guided toward the best-known positions in the search space that could satisfy the requirements of objective, targeted goals.

### 5. CONCLUSION AND FUTURE WORKS

This article presents an efficient inventory management model employing a multi-objective optimization framework under stochastic demand. The beginning inventory level in the prior period is different for each item, and the lead time in each unit varies. The multiple goals are to maximize profit and minimize the required storage space. The study aims to determine each product's optimal order quantity and reorder point to optimize the objective functions with the constraints. The developed model is an integer nonlinear programming model mixed with binary variables, and the optimization algorithms have been realized to solve the inventory management problem.

### References

- [1] Mirjalili, S., Mirjalili, S. M., & Lewis, A. (2014). Grey wolf optimizer. *Advances in engineering software*, 69, 46-61.

## [P-60] Control Theory Application in Supply Chain Management by Considering Stochastic Disruptions

Ho Van Roi<sup>1</sup>, Hwan-Seong Kim<sup>2,\*</sup>, Sam-Sang You<sup>3</sup>

<sup>1,2</sup> Department of Logistics, Korea Maritime and Ocean University, Busan, Republic of Korea, 49112

<sup>3</sup> Division of Mechanical Engineering, Korea Maritime and Ocean University, Busan, Republic of Korea, 49112

\*Corresponding author: kimhs@kmou.ac.kr

### Abstract

This paper proposes an active decision-making strategy in supply chain management. A four-echelon supply chain model, including the manufacturer, distributor, retailer, and customer, is considered with the addition of a recycling channel. The stochastic customer demand is mentioned in this study, which affects chains in the system. The problem is solved by using active decision-making, which is designed based on the combination of adaptive super-twisting sliding mode control (ASTSMC) and metaheuristics optimization algorithm. The particle swarm optimization algorithm (PSO) chooses and updates the parameters of STSMC. The novel decision-making strategy can offer new insights into effectively managing digital supply chain networks against market volatility.

**Keywords:** Stochastic environment, Supply chain management, Super twisting sliding mode control, Adaptive particle swarm optimization.

### 1. INTRODUCTION

Efficient supply chain management is crucial to business success and customer satisfaction. Customer demand is changing rapidly and typically unknown, so it must be correctly predicted to improve supply chain efficiency. Currently, most works deal with managing supply chains using continuous-time models, and just a few papers analyze the systems with discrete-time models. The discrete-time models fit more naturally to describe supply chain activities. The objective of control theory is to ensure that a supply chain network operates in perfect harmony at its optimal performance and efficiency by continuously monitoring and adjusting its parameters. In the context of decision-making strategy, control theory is used to regulate inventory levels, production rates, and transportation schedules in order to optimize the supply chain network for resilience, efficiency, and agility. Recently, many studies have applied the control theory to manage the supply chain system: linear control theory [1], nonlinear control theory [2,3], adaptive control [4], and intelligent controller. From that, this study focuses on applying control theory to supply chain management with using STSMC and APSO.

### 2. METHODOLOGY

The concept of the proposed model is described in Figure 1. For the control synthesis, the sliding surface is proposed based on the Proportional-Integral-Differential (PID) concept  $s_i = \lambda_{pi}e_i + \lambda_{ii} \sum_{j=1}^i e_j + \lambda_{Di} \Delta e_i$ , where  $\lambda_{pi}$ ,  $\lambda_{ii}$  and  $\lambda_{Di}$  are the positive PID coefficients, respectively;  $e_i$  is the error as  $e_i = x_d - x_i$ . The control law  $u_i = [u_{z_i}; u_{w_i}; u_{p_i}]^T$  is realized as  $u_i = k_{1i} \sqrt{|s_i|} \text{sgn}(s_i) + k_{2i} \sum_{j=1}^i e_j$ . For testing closed-loop stability, the Lyapunov function is defined in discrete time as follows,  $V_i = \frac{1}{2} s_i^T P s_i$ . The sliding surface can be described as  $s_{i+1} = \varphi s_i$ , the assumption is set as  $|\varphi| < 1$ . For the parameter vector  $\kappa = [\lambda_p, \lambda_i, \lambda_D, k_1, k_2]^T$ , the optimal parameters are determined using PSO algorithm. The position and update speed are expressed as  $v_i^{k+1} = \omega_i v_i^k + c_1 \text{rand}_i(p_{best} - \kappa_i^k) + c_2 \text{rand}_i(g_{best} - \kappa_i^k)$ , and  $\kappa_i^{k+1} = \kappa_i^k + v_i^{k+1}$ , respectively.



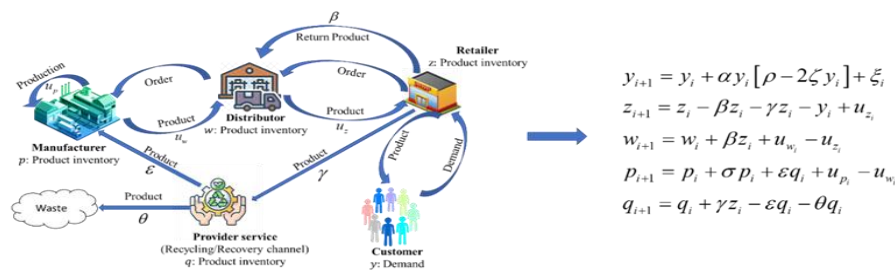


**Figure 1.** Generic diagram of the proposed supply chain model and mathematical model

### 3. EXPERIMENT SIMULATION

The numerical simulation is conducted to compare the performance of the control algorithms, including PID, super-twisting sliding mode controller (STSMC), and the proposed method (APSO-STSMC). The results are shown in Figure 2 and Table 1.

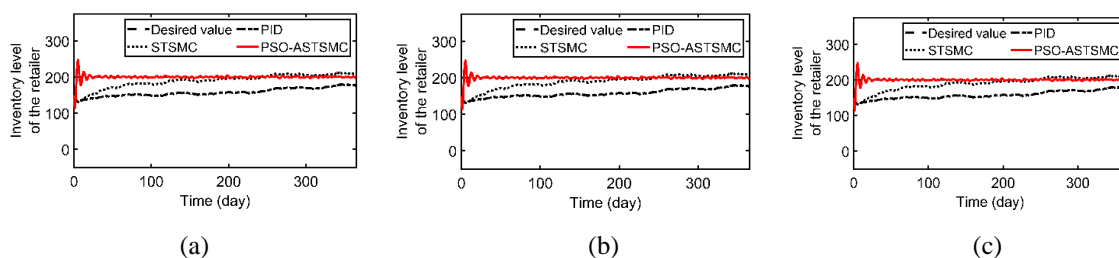


**Figure 2.** The transient responses of the supply chain system: (a) customer demand, (b) retailer, (c) distributor, (d) manufacturer, (e) recovery center, and (f) tracking error (PSO-ASTSMC)

**Table 1.** Simulation result (Unit: second)

	PSO-ASTSMC	STSMC	PID		PSO-ASTSMC	STSMC	PID
Retailer	978	5563	15496	Manufacturer	4397	4098	8353
Distributor	1433	7866	8795	Total error	6808	17527	32644

### 4. DISCUSSION AND CONCLUSION

In the IAE criterion, the proposed algorithm reduces the errors by 61.16% compared to STSMC, and 79.14% compared to PID in this numerical scenario. The hybrid PSO-ASTSMC algorithm offers a robust and flexible method for addressing uncertainties and optimizing system performance in the supply chain context. Further research could be conducted to explore the applicability of the proposed approach to other supply chain systems under more realistic market scenarios.

### References

- [1] Aslani Khiavi S, Khaloozadeh H, Soltanian F. Regulating Bullwhip Effect in Supply Chain with Hybrid Recycling Channels using Linear Quadratic Gaussian Controller TT. IUST 2021, 32, pp. 13–27. <https://doi.org/10.22068/ijiepr.32.1.13>.
- [2] Cuong TN, Kim H-S, Nguyen DA, You S-S. Nonlinear analysis and active management of production-distribution in nonlinear supply chain model using sliding mode control theory. Appl Math Model 2021, vol. 97, no. 4, pp. 418–437. <https://doi.org/https://doi.org/10.1016/j.apm.2021.04.007>.
- [3] Aslani Khiavi S, Khaloozadeh H, Soltanian F. Nonlinear modeling and performance analysis of a closed-loop supply chain in the presence of stochastic noise. Math Comput Model Dyn Syst 2019, vol. 25, no. 5, pp. 499–521. <https://doi.org/10.1080/13873954.2019.1663876>.
- [4] Xu X, Lee S-D, Kim H-S, You S-S. Management and optimisation of chaotic supply chain system using adaptive sliding mode control algorithm. Int J Prod Res 2021, vol. 59, no. 9, pp. 2571–2587. <https://doi.org/10.1080/00207543.2020.1735662>.

**[P-61] Data-Driven Approach for State Space Reconstruction of Container Throughput: A Case Study of Korean Port**Truong Ngoc Cuong<sup>1</sup>, Hwan-Seong Kim<sup>2,\*</sup>, Sam-Sang You<sup>3</sup><sup>1,2</sup> *Department of Logistics, Korea Maritime and Ocean University, Busan, Republic of Korea, 49112*<sup>3</sup> *Division of Mechanical Engineering, Korea Maritime and Ocean University, Busan, Republic of Korea, 49112*

\*Corresponding author: kimhs@kmou.ac.kr

**Abstract**

Understanding the dynamic behavior of the port system is crucial for port planning and development, but doing so is challenging due to risk and disruption. This paper presented a novel approach to reconstructing, analyzing, and forecasting the complex underlying mechanism of the disrupted port throughput using data processing and adaptive curve fitting techniques. DWT is employed to decompose the original data into a finite set of frequency components, so that the various hidden features of cargo throughput can be extracted via different modes, such as the trend, residual, and seasonal components. Thereafter, each component, obtained from the DWT spectra, is reconstructed via adaptive curve fitting techniques. Additionally, hypothesis testing, model evaluation, and statistical significance tests are employed to comprehensively evaluate the introduced forecasting models. Based on the experimental results and related analysis, it can be found that the proposed hybrid method is superior to the three comparison models in terms of prediction accuracy, thus, advocating for the accuracy and robustness of the proposed hybrid strategy as well as the suitability in perturbed container throughput forecasting. The presented state space reconstruction method can also be utilized for providing managerial insights and solutions on efficient port operations and development. These findings can help decision-makers understand disruption mechanisms in port systems, thus enabling them to successfully achieve their business goals.

**Keywords:** *Container throughput, State space reconstruction, Wavelet decomposition, Adaptation mechanism*

**1. INTRODUCTION**

Container throughput is crucial for a port since it serves as the most fundamental production indicator for gauging the port's development and as a crucial benchmark for organizing production, creating development plans, and building projects. Understanding the underlying mechanism of port throughput is a key component of port business and development strategies, along with a scientific port layout and infrastructure investment [1]. However, due to endogenous disturbances, it has become an important and challenging issue to examine the dynamic behavior and explain the evolving patterns of port throughput systems. Determining dynamical characteristics in a system using time series data may be accomplished in several ways. In this study, the data processing method and the adaptive curve fitting algorithm are used to reconstruct the state space of the container throughput system [2]. Particularly, wavelet decomposition methods are used first to divide complex time series data into smaller parts. Curve fitting is then applied to find a mathematical function in an analytic form that best fits each smaller data set. The mathematical model of the state space of the container throughput system is then produced by combining the state spaces of these components.

**2. PHASE SPACE RECONSTRUCTION OF PORT THROUGHPUT SYSTEM****2.1. State space reconstruction by hybrid curve filtering and wavelet method**

To enhance the degree of the accuracy of state space reconstruction, a novel hybrid methodology is proposed based on the wavelet decomposition and adaptive curve fitting technique. The proposed approach can improve the existing reconstruction method to cope with highly complex and chaotic trends. Figure 1 shows the overall process of the proposed methodology.

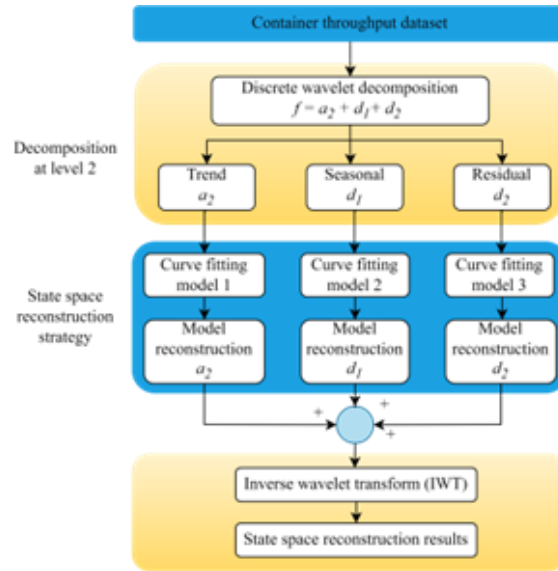


**Figure 1.** State space reconstruction by combining wavelet decomposition and curve fitting techniques

## 2.2. Case study of Busan Port

In most cases, a DWT is offered to enhance computing; in this study, the wavelet filter bank employed is the Haar wavelet. It divides the input data  $f$  into three distinct levels ( $a_2, d_1, d_2$ ).  $a$  and  $d$  stand for approximation and detail, respectively ( $f = a_2 + d_2 + d_1$ ). The results of wavelet transform 1D level 2 for Busan is shown in Figure 2.

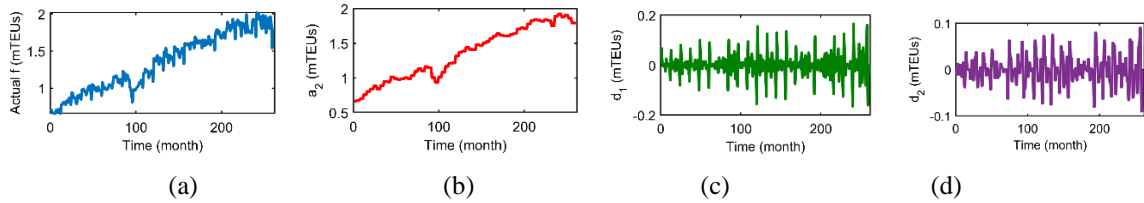


**Figure 2.** Wavelet decomposition for Busan port

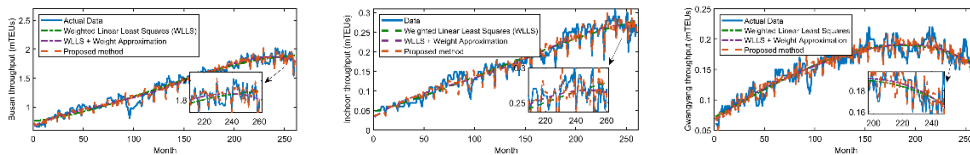


**Figure 3.** State space reconstruction by proposed techniques for Korean ports

Mathematical equation (1) represents the reconstruction form of container data of Korean ports

$$\begin{cases} \dot{x}_1 = a_1x_1^3 + b_1x_1^2 + c_1x_1 + d_1 + \alpha_1x_2x_3 \\ \dot{x}_2 = a_2x_2^3 + b_2x_2^2 + c_2x_2 + d_2 + \alpha_2x_1x_3 \\ \dot{x}_3 = a_3x_3^3 + b_3x_3^2 + c_3x_3 + d_3 + \alpha_3x_1x_2 \end{cases} \quad (1)$$

Where  $x_i, (i=1,2,3)$  represent for throughput of Busan, Incheon and Gwangyang port, respectively

## 3. CONCLUSION

In this paper, optimal decision-making approaches are proposed for reconstructing and managing the dynamic behavior of seaports in the marine logistics system. The hybrid data processing technique, including wavelet decomposition and adaptive curve fitting, is employed for reconstructing the complex underlying mechanism of port throughput under disruption. The case studies are presented to manage maritime supply chain risks for Korean

ports. The evaluation results indicated that the proposed method outperforms all other benchmarks that are widely employed in the data science community.

### References

- [1] Sanguri, K., Shankar, S., Punia, S., & Patra, S. (2022). Hierarchical container throughput forecasting: The value of coherent forecasts in the management of ports operations. *Computers & Industrial Engineering*, 173, 108651.
- [2] Notteboom, T., Pallis, T., & Rodrigue, J. P. (2021). Disruptions and resilience in global container shipping and ports: the COVID-19 pandemic versus the 2008–2009 financial crisis. *Maritime Economics & Logistics*, vol. 23, no. 22, pp. 179-210.

**[P-63] A Study of Changing Velocity on Maritime Vessel's Pitch-Roll Motion**Tatsuhiko Terada<sup>1</sup>, Hwan-Seong Kim<sup>2,\*</sup>, Sam-Sang You<sup>3</sup>, Hitoi Tamaru<sup>4</sup><sup>1,2</sup> Department of Logistics, Korea Maritime and Ocean University, 727 Taejong-ro, Yeongdo-gu, Busan, 49112, South Korea<sup>3</sup> Division of Mechanical Engineering, Korea Maritime and Ocean University, 727 Taejong-ro, Yeongdo-gu, Busan, 49112, South Korea<sup>4</sup> Department of Maritime Systems Engineering, Tokyo University of Marine Science and Technology, 2-1-6 Etchujima, Koto-Ku, Tokyo, 135-8533, Japan

\*Corresponding author: kimhs@kmou.ac.kr

**Abstract**

This study investigates maritime vessels' roll and pitch motions when they operate at different speeds. Simulated equations are used to model the ship's motion behavior and wave-encounter frequency. After adjusting parameters, the analysis reveals significant variations regarding velocity, the start time of velocity change, and acceleration. These results indicate the need to consider velocity and acceleration when constructing vessel control algorithms for better decision-making and increased safety.

**Keywords:** Pitch-roll motion, Maritime vessels, Forward-speed effects

**1. INTRODUCTION**

Analyzing a maritime vessel's pitch and roll motion requires understanding the relationship between forward velocity, acceleration, initial value, etc. Studies (Laarhoven, 2009; Deleanu et al., 2020) have examined roll motion with changing velocity. However, they do not consider pitch-roll coupling or multiple scenarios, like departing, approaching ports, and adjusting arrival times. This study analyzes the pitch and roll response to varying velocities to understand vessel behavior and ensure stability and safety.

**2. METHODOLOGY**

This study utilizes two equations to simulate ship pitch-roll motion (Pan et al., 1996; Lee et al., 2021):

$$\begin{aligned}\ddot{\theta} &= -\omega_{n1}^2\theta + \varepsilon(-2\xi_1\dot{\theta} - \sigma_1\theta^2 - \sigma_1\varphi^2) + f_1\cos(\omega_e t), \\ \ddot{\varphi} &= -\omega_{n2}^2\varphi + \varepsilon(-2\xi_2\dot{\varphi} - \xi_3|\dot{\varphi}| - \sigma_3\varphi\theta) + f_2\cos(\omega_e t)\end{aligned}\quad (1)$$

where  $\theta$  and  $\varphi$  (rad) are pitch and roll of the vessel, respectively;  $\omega_{n1}$ ,  $\omega_{n2}$  (rad/s<sup>-1</sup>) are natural angular frequencies;  $\xi_1, \xi_2$  (s<sup>-1</sup>) and  $\xi_3$  (rad<sup>-1</sup>) are damping coefficients;  $\sigma_1, \sigma_2, \sigma_3$  (rad/s<sup>-2</sup>) are nonlinear restoring coefficients;  $f_1, f_2$  (rad/s<sup>-2</sup>) are the amplitudes of wave excitation;  $\varepsilon$  is small dimensionless oscillation parameter. Encounter frequency can be given by (Fossen, 2011):

$$\omega_e = \omega_0 + \frac{\omega_0^2}{g} U(t) \cos\beta \quad (2)$$

where  $g$  (m/s<sup>-2</sup>) is acceleration of gravity;  $U$  (m/s) is forward velocity;  $\omega_0$  is wave frequency;  $\beta$  is the angle between the heading and the direction of the wave.

**3. RESULT**

Simulation followed these parameters. The speed started to change after at specific time.  $U_{max} = 15$ (m/s) with an acceleration range is [0.001,0.06]. The initial speed range is [1,11] and time span is 2000s. The values of main parameters are selected as follows (Lee et.al., 2021):

$$\omega_{n2} = 0.84, \omega_{n1} = 2\omega_{n1}, \xi_1 = 0.1, \xi_2 = 0.2, \xi_3 = 0.1, \varepsilon = 0.01, \sigma_1 = 1, \sigma_2 = 1, \sigma_3 = 2.$$

Initial conditions:  $\theta = 0.01, \varphi = 0.01, \beta = 0$ .

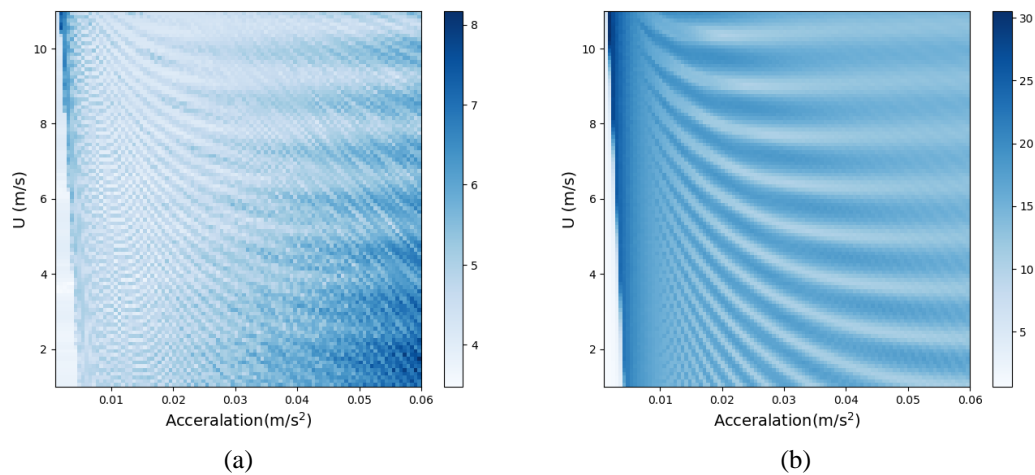


**Figure 1.** Maximum angle value: U changes after 200s (a) pitch; (b) roll

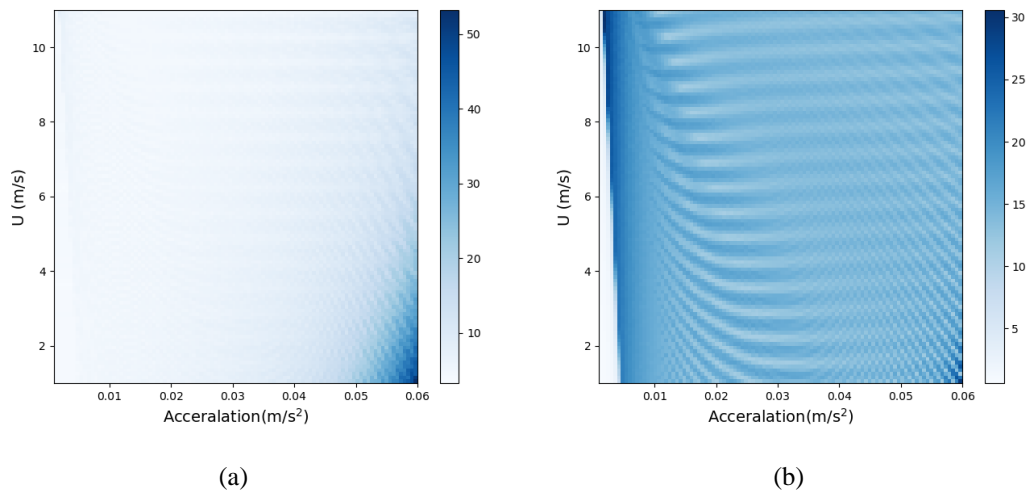


**Figure 2.** Maximum angle value: U changes after 400s (a) pitch; (b) roll

Roll motion exhibits similar behavior between Figures 1 and 2. However, pitch motion is noticeably different. Figure 2. shows following the change time grows, pitch amplitudes will rise significantly, especially with greater acceleration and lower initial speed.

#### 4. CONCLUSION

In this study highlights the importance of understanding how changes in velocity and acceleration can affect the pitch and roll behavior of a maritime vessel. The results indicate that acceleration plays a crucial role in vessel motion. Further research could create a reinforcement learning model to optimize the pitch-roll motion based on this study's simulation data, considering the velocity control start and end times.

#### Acknowledgments

This research was supported by the Northeast-Asia Shipping and Port Logistics Research Center from KMOU, Korea.

#### References

- [1] Deleanu Dumitru, and Constantin Dumitrache. "Controlling the Parametric Roll of a Container Ship Model by Changing the Forward Velocity." IOP Conference Series: Materials Science and Engineering 916 (2020), 012024.
- [2] Fossen, T. I, Handbook of Marine Craft Hydrodynamics and Motion Control, John Wiley & Sons Ltd (2011), pp. 192-211.
- [3] Lee S.D., You S.S., Xu X and Cuong T.N. "Active control synthesis of nonlinear pitch-roll motions for marine vessels", Ocean Engineering 221 (2021), 108537

## [P-64] Optimal Solution for Quay Crane Scheduling Problem Using Hybrid Metaheuristic Approach

Long Le Ngoc Bao<sup>1</sup>, Ji-Hoon Park<sup>2</sup>, Byung-Kwon Jeong<sup>3</sup>, Hwan-Seong Kim<sup>1,\*</sup>, Sam-Sang You<sup>4</sup>

<sup>1</sup>Department of Logistics, Korea Maritime and Ocean University, Busan, Republic of Korea, 49112

<sup>2</sup>Department of Smart Port Logistics, Korea Maritime & Ocean University, Busan, Korea, 49112

<sup>3</sup>Department of Shipping and Port Logistics, Korea Maritime & Ocean University, Busan, Korea, 49112

<sup>4</sup>Division of Mechanical Engineering, Korea Maritime and Ocean University, Busan, Republic of Korea

\*Corresponding author: kimhs@kmou.ac.kr

### Abstract

Quay crane scheduling problem (QCSP) is one of the most important optimization problems for container terminal operation at the quayside and has been immensely studied in the literature. Many metaheuristic approaches have been proposed in the past, which mainly aim to figure out the best schedule to handle all containers at the assigned vessel, given a list of available quay cranes (QCs). In this study, a novel combination between Greedy Randomized Adaptive Search Procedure (GRASP) and Ant Colony Optimization (ACO) – two well-known metaheuristics, is introduced to solve the QCSP. GRASP generates a probabilistic mechanism for the QCs to select the next task for each moment. At the same time, ACO enhances this selection by a nature-inspired mechanism mimicking the biological attraction of ants. The performance of the proposed approach is demonstrated via simulations for two key scenarios: single QC and multiple QCs working simultaneously. The final output of the algorithm yields the best sequence of tasks to be handled by each QC, which would be considerably useful in practice as it helps significantly reduce operational costs.

**Keywords:** Quay crane scheduling problem, Metaheuristics, Combinatorial optimization, Greedy randomized adaptive search procedure, Ant colony optimization

### 1. INTRODUCTION

Following the surprising growth of maritime trade in the last two decades, container terminals must improve their capacity and efficiency to earn competitive advantages against others by applying new technologies and optimization methods. Numerous studies on container terminal operations have been conducted and gained immense attraction from academics and industrial organizations. The Quay crane (QC) is the main equipment of the quayside area that is responsible for loading and discharging containers on vessels, whose performance contributes a great proportion to the overall efficiency at the quayside. Optimization for QC, such as QCSP, is a crucial topic in operational management. According to the survey of Kizilay and Elliyi (2020), the objective of the optimal schedule will vary, in which minimization of the task completion time was considered the critical factor in terms of port competitiveness (Steenken et al., 2004) and has dominated among other objectives in the literature.

### 2. MATHEMATICAL FORMULATION

The optimization problem for QCSP can be formulated as follows:

$$\min W \quad (1)$$

$$\text{Subject to:} \quad 0 \leq E_q \leq W, \quad \forall q \in Q \quad (2)$$

$$\sum_{j \in \Omega} X_{0j}^q = 1, \quad \sum_{j \in \Omega} X_{iF}^q = 1, \quad \forall q \in Q \quad (3)$$

$$\sum_{q \in Q} \sum_{j \in \Omega} X_{ij}^q = 1, \quad \forall i \in \Omega \quad (4)$$

$$\sum_{i \in \Omega} X_{ij}^q - \sum_{i \in \Omega} X_{ji}^q = 0, \quad \forall j \in \Omega, q \in Q \quad (5)$$

$$C_i + p_j - C_j \leq M(1 - Z_{ij}), \quad C_j + p_j - C_i \leq MZ_{ij}, \quad \forall (i, j) \in \Phi \quad (6)$$

$$r_q + t_{0j}^q + p_j - C_j \leq M(1 - X_{0j}^q), \quad C_j - E_q \leq M(1 - X_{jF}^q), \quad \forall q \in Q, j \in \Omega \quad (7)$$

Eqs. (1) and (2) define the make span  $W$  of the operation as the latest completion time  $E_q$  of all QCs. Eq. (3) describes that every QC  $q$  has an initial state 0 and a final state F (0 and F are two dummy indices in the task list), respectively. Eqs. (4) and (5) indicate the balance flow of the QCs in which each task can only be performed

by one QC. Eq (6) implies the relationship between the pair task  $(i, j)$  in precedence set  $\Phi$  that cannot be handled simultaneously. Finally, Eq. (7) explicitly defines the relations between ready time  $r_q$ , moving time  $t_{0j}^q$ , processing time  $p_j$ , task completion time  $C_j$  and crane completion time  $E_q$  of every task  $j$  and crane  $q$ .

### 3. METHODOLOGY

#### 3.1. Greedy Randomized Adaptive Search Procedure (GRASP)

GRASP is specialized to solve the combinatorial optimization, by including many iterations of search based on traditional greedy algorithm and a randomized selection to bypass the local optimum points. By considering every required task as a step in the sequence of action, for every iteration, GRASP tries to search for the optimal next task based on current status and repeats step-by-step until all given tasks are assigned.

#### 3.2. Ant Colony Optimization (ACO)

ACO is a swarm-based intelligent metaheuristic approach that specialized for solving sequential problems such as path-finding issues, which is inspired by biological attraction of ant's pheromone. It is considered that each step solved in the sequence leaves a trace that could enhance the selection of that step in later stages.

### 4. NUMERICAL RESULTS

Two scenarios are considered: single QC and two QCs at the same time. For the multiple-QC case, it is noted that the safety margin between two nearby QCs must be maintained during the whole operation. Also, two QCs cannot interfere each other since they are mounted on a same track. These constraints must be added in the model for the practicability.

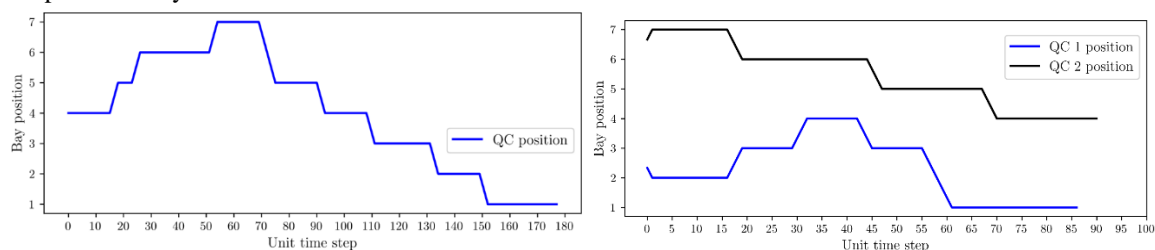


Figure 1. Performance of the proposed approach in two scenarios

### 5. CONCLUSION

This study proposes a novel approach to solve the QCSP by combining two well-known metaheuristics (GRASP and ACO). The simulation results highlight the remarkable performance of the algorithm that could be applied for both single and multiple QCs, while still preserve the physical and logical constraints of the problem. This will aid to the decision-making process of the quayside operation and have great managerial implications.

### References

- [1] D. Kizilay and D.T. Eliyi, "A comprehensive review of quay crane scheduling, yard operations and integrations thereof in container terminals", *Flexible Services and Manufacturing Journal*, 33(1), 2021, pp. 1-42.
- [2] D. Steenken, S. Voß and R. Stahlbock, "Container terminal operation and operations research – a classification and literature review", *OR Spectrum*, 26(1), 2004, pp. 3-49.
- [3] R.I. Peterkofsky and C.F. Daganzo, "A brand and bound solution method for the crane scheduling problem", *Transportation Research Part B: Methodological*, 24(3), 1990, pp. 159-172.
- [4] M. Dorigo, M. Birattari and T. Stutzle, "Ant colony optimization", *IEEE Computational Intelligence Magazine*, 1(4), 2006, pp. 28-39.



## [P-65] Optimization of Stochastic Inventory Model Using Hamilton-Jacobi-Bellman Equation

Bui Minh Hau<sup>1</sup>, Hwan-Seong Kim<sup>2,\*</sup>, Sam-Sang You<sup>3</sup>

<sup>1,2</sup>*Department of Logistics, Korea Maritime and Ocean University, Busan, Republic of Korea*

<sup>3</sup>*Division of Mechanical Engineering, Korea Maritime and Ocean University, Busan, Republic of Korea*

\*Corresponding author: kimhs@kmou.ac.kr

### Abstract

Inventory control is essential for a manufacturer to achieve the desired profit in successful supply chain management. The manufacturer's profit comes from importing raw materials, processing, producing, storing, and supplying items. Finding the initial value of the production rate can make the inventory level and production rate ensure their desired value and get the target profit within a specified time. This paper employs the economic order quantity (EOQ) framework to evaluate costs in the inventory model. For optimizing the manufacturer's profit with stochastic factor, Hamilton–Jacobi–Bellman (HJB) equation is presented to find the production rate to make the inventory model to ensure their intended goals.

**Keywords:** *Inventory model, Deteriorating items, Stochastic optimal control, HJB equation*

### 1. INTRODUCTION

Production-inventory management helps adjust production strategies based on changing customer demands and imported raw materials. Manufacturers set targets for production rate and inventory level to ensure adequate supply and smooth business operations. This paper aims to determine the initial production rate that achieves desired inventory and production values, leading to target profits. The deteriorating inventory model is a significant concern for manufacturers. Inventory management involves costs like replenishment and maintenance. The economic order quantity (EOQ) is a widely appreciated approach for evaluating total costs in efficient inventory management. The optimization problem is analytically solved by the HJB equation, demonstrated by numerical simulation.

This paper is organized as follows. Section 2 provides a problem description with the notations and the inventory model. Section 3 presents the methodology and the optimal solution. Section 4 provides the numerical experiment to demonstrate the feasibility and efficacy of the proposed method. Finally, the conclusions are presented in Section 5.

### 2. NOTATIONS AND PROBLEM DEFINITION

This paper will deal with a deteriorating inventory model with a stochastic factor in inventory level. In this study, it is assumed that the inventory is deteriorating at the beginning of the cycle with keeping customer demand constant. The objective is to find an optimal production-production rate to maximize company profit.

**Table 1.** Notation

Variable	Definition	Variable	Definition
$D(t)$	Customer's demand rate	$o$	Ordering cost for 1 item
$u(t)$	Production rate	$h$	Holding cost for 1 item
$I(t)$	Inventory level	$s$	Shortage cost for 1 item
$u_d$	The desired production rate	$p$	Price unit
$I_d$	The desired inventory level	$O$	Ordering cost
$\theta$	Deteriorating rate	$H$	Holding cost
$dz(t)$	Stochastic variable	$TP$	Total profit
$\sigma$	Diffusion coefficient	$B$	Desired profit rate

The stochastic inventory model can be described as follows,

$$dI(t) = [u(t) - D(t) - \theta I_1(t)] dt + \sigma dz(t) \quad (1)$$

$$O = \int_0^T o(u - u_d)^2 dt \quad (2)$$

$$H = h \int_0^T (I - I_d)^2 dt \quad (3)$$

$$TP = \text{Desired profit} - \int_0^T (O + H) dt \quad (4)$$

The objective functions for inventory levels are described as follows,

$$J = \max \left\{ \int_0^T [-o(u - u_d)^2 - h(I - I_d)^2] dt + BpI \right\} \quad (5)$$

### 3. METHODOLOGY

Besides the HJB equation, other methods, such as particle swarm optimization (PSO) or grey wolf optimization (GWO), are often used to optimize the inventory models. Both methods above will search for the optimal value in a given domain. This topic uses the HJB equation because the results from this method will give the formula for calculating the value of the optimal variable, which can easily be re-calculated when the model's parameters are changed. Let  $V(I, t)$  denote the expected value of the objective function  $J$  such that it satisfies the HJB equation [1] described by,

$$0 = \max_{u(t)} \left\{ [-o(u - u_d)^2 - h(I - I_d)^2] + V_t + V_I [u - D - \theta I] + \frac{1}{2} \sigma^2 V_{II} \right\} \quad (6)$$

$$\text{Where, } V_t = \frac{\partial V}{\partial t}, V_I = \frac{\partial V}{\partial I}, V_{II} = \frac{\partial^2 V}{\partial I^2}$$

Solving the equation (6), we have the optimal production rate,

$$u = \frac{V_I + 2ou_d}{2o} \quad (6)$$

### 4. NUMERICAL EXPERIMENT

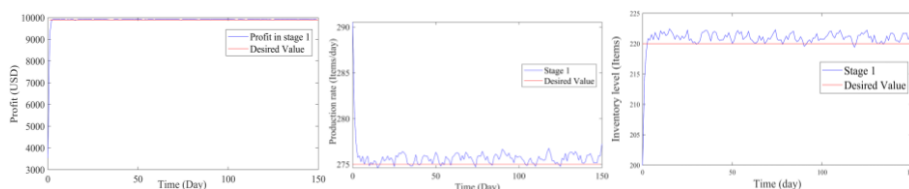


Figure 1. Optimal result using HJB equation

Using the optimal production rate equation (7), we determined the starting value of the production rate. Production rate values and inventory levels always follow the manufacturer's desired values. The producer can thus obtain the desired total profit as the objective function (5).

### 5. CONCLUSION

During production, a manufacturer may experience a decrease in inventory due to quality deterioration. At the same time, balancing production costs and storage costs is necessary. Selecting the starting value of the production rate can help the manufacturer maintain the required inventory and achieve the desired profit.

### References

- [1] Sethi S.P. & Thompson G.L. (2000). Optimal control theory: Applications to management science and economics, 2<sup>nd</sup> ed. Springer New York.

## [P-66] Reach Stacker Assistance by Object Detection and Distance Estimation in Container Terminal

Ngo Quang Vinh<sup>1</sup>, Ji-Hoon Park<sup>2</sup>, Byung-Kwon Jeong<sup>3</sup>, Hyeon-Soo Shin<sup>1</sup>, Hwan-Seong Kim<sup>1,\*</sup>

<sup>1</sup> Department of Logistics, Korea Maritime and Ocean University, Busan, Republic of Korea, 49112

<sup>2</sup> Department of Smart Port Logistics, Korea Maritime & Ocean University, Busan, Korea, 49112

<sup>3</sup> Department of Shipping and Port Logistics, Korea Maritime & Ocean University, Busan, Korea, 49112

\*Corresponding author: kimhs@kmou.ac.kr

### Abstract

Object detection and distance estimation technology is essential in-vehicle assistance in civil cases. To exploit the advantage of this technology, terminal port environments are applied to ensure safety and provide operational assistance. By harnessing the power of advanced computer vision techniques, this research utilizes Single Shot MultiBox Detector (SSD) model to identify handled containers from the reach stacker view in terminal space and estimate the object's distances accurately by using the Pinhole camera rule. It enables real-time monitoring and alerts, allowing terminal operators to proactively address collision risks or hazardous conditions. This technology assists in preventing accidents and improving overall safety measures. Additionally, to enhance the robustness of the proposed method, various terminal port scenarios with multi-environmental conditions are collected to build up the dataset more abundantly. The application of object detection and distance estimation in terminal environments not only elevates safety levels but also enhances operational efficiency, creating a smart port with the support of advanced technology.

**Keywords:** Container terminal, Reach stacker assistance, Computer vision, Object detection, Distance estimation

## 1. INTRODUCTION

With an average annual growth rate of around 8% from 1996 until now, the global maritime containerization market expected that container terminal operations will experience a surge in demand in the near future [1]. Consequently, there is a growing focus among leading researchers worldwide on developing Autonomous Container Trucks (ACTs) and smart ports. The primary objective behind this attention is to enhance productivity, achieve cost-effective management, lean operations, and minimize idle time. These efforts are driven by the aim of optimizing container handling processes and meeting the increasing demands of the industry. One of the most important criteria in terminal ports is safety container handling. Implementing the advanced technologies of the 4.0 revolution (Blockchain, Big Data, Artificial Intelligence, Internet of Things, etc.) provides a significant improvement in container port operations. In this paper, a neural network model is employed to assist the Reach Stacker handling operation in the terminal port.

## 2. METHODOLOGY

Container handling is a fundamental and recurrent operation in terminal ports, necessitating utmost attention to safety. The proposed method integrates the SSD model and Pinhole camera rule to address this paper. By combining these techniques, the method effectively improves the overall safety level of reach stackers involved in container handling activities within port operations, ensuring the secure and efficient handling of containers.

### 2.1. Object detection in terminal port with SSD model

The SSD model is a state-of-the-art deep learning algorithm designed to accurately detect objects in images or video frames in real-time [2]. In the context of terminal ports, the SSD model can be utilized to detect and localize various objects of interest, such as containers, cranes, vehicles, and personnel. Furthermore, the SSD model's real-time detection capabilities enable quick response and decision-making, facilitating timely intervention in case of any safety concerns.

The algorithm applies a convolutional approach that evaluates a small set (e.g., 4) of default boxes with varying aspect ratios at each location in different feature maps, utilizing multiple scales for enhanced accuracy (e.g., 8 x 8 in Figure 1(b) and 4 x 4 in Figure 1(c)). The SSD model predicts shape offsets and confidences for each default box for all object categories.

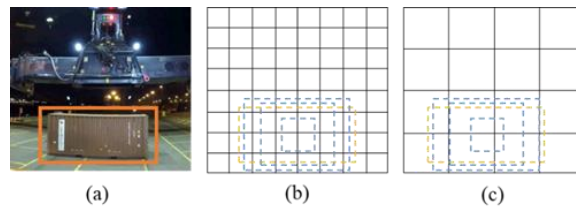


**Figure 1.** The Single Shot MultiBox Detector Framework:  
(a) Ground truth boxes for object; (b) 8 x 8 feature map; (c) 4 x 4 feature map

The proposed methodology aims to identify and extract crucial information, specifically the container and its corresponding container code, from the perspective of reach stackers.



**Figure 2.** The results of object detection in container terminal ports

## 2.2. Distance estimation with Pinhole camera rule

Various techniques can be employed to estimate the distance, known as depth. One common approach is to use reference objects of dimensions within the scene, namely the Pinhole camera rule. By comparing the size of these reference objects in the image to their known dimensions, it is possible to calculate the distance to other objects in the scene based on their relative size.



**Figure 3.** The results of the distance estimation method

## 3. CONCLUSION

In conclusion, applying the SSD model combined with the Pinhole camera rule in terminal port operations, particularly from the reach stackers' perspective, holds significant potential for improving the safety of container handling. By utilizing the SSD model, the system can effectively detect containers and container codes, providing real-time awareness of their presence and location. This enables operators to have better visibility and reduce the risk of accidents for mishandling during container operations. In terms of future research, a container code recognition method will be employed to build an automated system for real-time tracking containers during transshipment.

## Acknowledgments

This research was supported by the 4th Educational Training Program of Shipping, Port and Logistics from the Ministry of Oceans and Fisheries, Korea.

## References

- [1] Review of Maritime Report 2022. Available online: [https://unctad.org/system/files/official-document/rmt2022\\_en.pdf](https://unctad.org/system/files/official-document/rmt2022_en.pdf) (accessed on May 24th, 2023).
- [2] W. Liu, D. Anguelov, D. Erhan, C. Szegedy, S.E. Reed, C. Fu, and A.C. Berg, "SSD: Single Shot MultiBox Detector." European Conference on Computer Vision (2015).

**[P-67] Shipping Network Selection Based on Advanced Prospect Theory - A Case Study of Vietnam Seaport**Pham Thi Yen<sup>1</sup>, Hwan-Seong Kim<sup>1,\*</sup>, Truong Ngoc Cuong<sup>1</sup>, Phung Hung Nguyen<sup>2</sup><sup>1</sup>Department of Logistics, Korea Maritime and Ocean University, Busan, Republic of Korea, 49112<sup>2</sup>Maritime Academy, Ho Chi Minh City Univ. of Transport, Binh Thanh District, 70000, Viet Nam

\*Corresponding author: kimhs@kmou.ac.kr

**Abstract**

This paper aims to propose an optimal method to evaluate and cumulate the daily net profit for liner shipping services to support the shipping lines in making optimal decisions under risk in the choice of the optimal route with the highest average daily profit for container liner shipping under the uncertain combination factors: freight rate, shipment demand, and fuel oil price. A cumulative prospect theory (CPT) approach considers the decision-makers' attitude under uncertainty applicable for any number of consequences to calculate the daily net profit model for container vessels. The results are compared to benchmark methods such as the expected utility theory. In addition, the adaptive parameters proposed can enhance a model's performance when the data distribution varies either chronologically or in different scenarios. An application is Hai An container shipping lines in 2022 as a case study in Vietnam is presented in this paper. The obtained results indicate that Hai Phong (HP)-Tan Cang Cai Mep (TCIT) - Ho Chi Minh (HCM) – Hai Phong is the most effective route with the finest economics. However, in reality, Hai Phong – Ho Chi Minh – Hai Phong is the first preference option.

**Keywords:** Adaptive cumulative prospect theory, Cumulative prospect theory, Daily profit model, Decision-making, Expected utility theory, Shipping network

**1. INTRODUCTION**

Route selection models play a crucial role for decision-makers in determining the most effective strategies to improve efficiency. There are a few methods that can be used to support decision-making; however, they are too complex, difficult for many decision-makers, and often lack a reflection of the complexity of human psychology in decision-making under risk and uncertainty. Therefore, this paper suggests an average daily profit model with uncertain combination factors influencing shipping route choice behavior by applying adaptive cumulative prospect theory (CPT) [1]. The rest of this work is structured as follows. Section 2 proposes system modeling and methodology for evaluating daily business effectiveness in container operation. The third section contains an empirical study of Vietnam. Finally, in section 4, the conclusions are presented.

**2. METHODOLOGY**

Assume that the variable elements that influence to the results of daily average profit are divided into probabilistic ranges including shipment demand, freight rate, and fuel oil price. A daily profit model from cumulating the prospect approach of daily profit equals the resulting daily revenue minus daily cost.

$$pr^d = \frac{r^t - c^t}{t^{t^{cv}}} \quad (1)$$

Where:  $c^t$  presents the total cost of the round voyage;  $r^t$  shows total revenue of the round voyage;  $pr^d$  presents daily profit of the round voyage and  $t^{t^{cv}}$  total time spent for the round voyage (day). The cumulative prospect value (CPV) is calculated by accumulating losses and gains. Assume the pair  $(pr_i^d; p_i)$  where  $i = (-m, \dots, n)$  is the corresponding risk. The positive part CPV, denoted by  $CPV(pr^{d+})$  and the negative part of  $CPV(pr^d)$ , denoted  $CPV(pr^{d-})$ . Hence, cumulative decision weight is defined as follows:

$$CPV(pr^d) = CPV(pr^{d+}) + CPV(pr^{d-}) = \sum_{i=-m}^0 v(pr_i^d) \pi^-(p_i) + \sum_{i=0}^n v(pr_i^d) \pi^+(p_i) \quad (2)$$

$$\pi^-(p_i) = w\left(\sum_{k=-m}^i p_k\right) - w\left(\sum_{k=-m}^{i-1} p_k\right) = w^-(p_{-m} + \dots + p_i) - w^-(p_{-m} + \dots + p_{i-1}) \text{ if } -m \leq i \leq 0 \quad (3)$$

$$\pi^+(p_i) = w\left(\sum_{k=1}^n p_k\right) - w\left(\sum_{k=1+i}^n p_k\right) = w^+(p_i + \dots + p_n) - w^+(p_{i+1} + \dots + p_n) \text{ if } 0 \leq i \leq n \quad (4)$$

The value function of an alternative is:  $v(pr_i^d) = \begin{cases} (pr_i^d)^\alpha & \text{if } (pr_i^d) \geq 0 \\ -2.25(pr_i^d)^\beta & \text{if } (pr_i^d) < 0 \end{cases}$

The median exponent of the value function was  $\alpha = \beta = 0.88 < 1$  in accordance with diminishing sensitivity; it is convexity in losses and concave in gains. The loss aversion coefficient  $\lambda = 2.25 > 1$  means that individual perceives loss 2.5 times more than gain. In order to improve the performance of a model in situations where the distribution of the data changes over time or across different contexts, a parametric parameter was proposed. Therefore, the adaptiveness of weighting function is proposed by the designer as below:

$$\hat{w}^+(p_i) = \frac{p_i^{0.61+\sigma_1}}{[p_i^{0.61+\sigma_1} + (1+p_i)^{0.61+\sigma_1}]^{1/(0.61+\sigma_1)}} \quad (5)$$

$$\hat{w}^-(p_i) = \frac{p_i^{0.69+\sigma_2}}{[p_i^{0.69+\sigma_2} + (1+p_i)^{0.69+\sigma_2}]^{1/(0.69+\sigma_2)}} \quad (6)$$

People are overweight on low probabilities and underweight on moderate and high probabilities. Where  $\hat{w}^+(p_i)$  and  $\hat{w}^-(p_i)$  are adaptive parameters, which are automatically updated by using gains and loss function.  $\sigma_1 = \mu_1 p(f_i^{sd}) p_i^{FO}$ ,  $\sigma_2 = \mu_2 p(f_i^{sd}) p_i^{FO}$ ; and  $\mu_1, \mu_2$  are the positive parametric adaptation coefficients in gains, and losses respectively that are used to update parameter for  $\gamma$  and  $\delta$ .

### 3. A CASE STUDY IN VIETNAM

Data for three main routes are gathered, three main routes including Hai Phong to Ho Chi Minh and vice versus is called alternative 1; alternative 2 is the journey Hai Phong – TCIT – Ho Chi Minh – Hai Phong (directly) and the journey Hai Phong – Ho Chi Minh – TCIT – Ho Chi Minh – Hai Phong (transshipment between Ho Chi Minh and TCIT) is considered the alternative 3. The round voyages of the vessel named HAI AN TIME are deployed in 1 year from 2021. This paper refers to calculation steps was introduced by Aytek Güngör and Barış Barlas (2021) [2]. The obtained results from the two methods are illustrated as below:

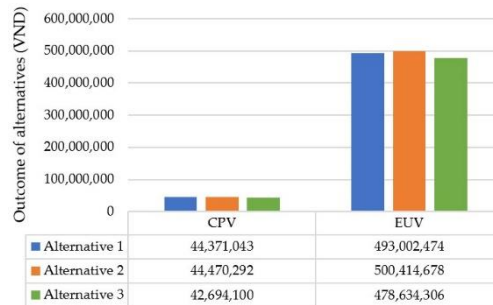


Figure 1. CPV and EUV of alternatives

### 4. CONCLUSION

This paper proposes a quantitative method that has used econometric cognitive parameters to calculate the round voyage efficiency on shipping network decisions. This paper has demonstrated and compared values from two backbone methods for decision analysis are EUT and CPT. This work will be useful and easier for strategy makers of liner shipping companies to consider decision-making under uncertain environmental. This fact can be explained that the decision-makers prefer certainty tend to be averse to risks in gains, and are willing to sacrifice potentially high profit for a greater level of assurance.

### References

- [1] Tversky, A., & Kahneman, D. (1992). Advances in prospect theory: Cumulative representation of uncertainty. *Journal of Risk and uncertainty*, 5, pp. 297-323.
- [2] Gungor, A., & Barlas, B. (2022). Decision-making under Risk: A Ship Sale and Purchase Problem by Utilizing Cumulative Prospect Theory. *Journal of ETA Maritime Science*, 10(1), pp. 16-28.

## [S1-3] Designing Shape for Two Elongated Undulating Fin Underwater Vehicle Using Computational Fluid Dynamics

Quoc Tuan Vu<sup>1,2</sup>, Van Binh Duong Nguyen<sup>1,2</sup>, Quoc Minh Lam<sup>1,2</sup>, Laprelle Boucher Ernest<sup>4</sup>,  
Huy Hung Nguyen<sup>3</sup>, Van Tu Duong<sup>1,2</sup>, Tan Tien Nguyen<sup>1,2,\*</sup>

<sup>1</sup>National Key Laboratory of Digital Control and System Engineering (DCSELab), Ho Chi Minh City University of Technology (HCMUT), 268 Ly Thuong Kiet Street, District 10, Ho Chi Minh City, Viet Nam.

<sup>2</sup>Viet Nam National University Ho Chi Minh City, Linh Trung Ward, Thu Duc City, Ho Chi Minh City, Viet Nam.

<sup>3</sup>Faculty of Electronics and Telecommunication, Sai Gon University, Viet Nam.

<sup>4</sup>Institut Supérieur des Matériaux et Mécanique Avancée du Mans, France.

\*Corresponding author: nttien@hcmut.edu.vn.

### Abstract

It would appear that capturing the impact of fluid for the purpose of designing bio-inspired underwater vehicles is not only a crucial process to stabilize energy, but it is also endurance enhancement. To what extent, shape optimization and drag coefficient are two concerned critical factors in the fields of fluid mechanics and aerodynamics to reduce drag force or improve lift force. In this day and age, with the goal to determine the optimal shape that can provide the benefit in terms of drag coefficient reduction, numerous methods are used. In comparison with conventional calculation with experiments, computational fluid dynamics have unceasingly ameliorated to aid engineers to achieve a suitable shape with quick-time saving as well as precise estimations. In this paper, shape optimization for an amphibious bionic fish robot using elongated undulating fins, that is, based on determining the benefit drag coefficient will be depicted beneath elucidations and simulations.

**Keywords:** *Bio-inspired underwater vehicles, Computational fluid dynamics, Drag coefficient, shape optimization, Elongated undulating fins*

## 1. INTRODUCTION

The enhancement of autonomous underwater vehicles (AUVs) has been concerned and revolutionized with distinguishing purposes namely coastal structure inspection, ocean exploration, object underwater detection, and military defense [1]. These days, it is an unceasing progress in technology as well as science, bio-inspired robot has a tendency to achieve far more replacement compared to classical propulsion systems. Due to fins and torso for movement providing flexible maneuverability and good posture correction, bio-inspired robot fish has become much more special. These capabilities inspire innovative designs that improve the way artificial systems work and interact with aquatic environments. Underwater ecology is also a vital enthusiasm in biomimetic fish robot research, in specific, marine life is being degraded by the use of high-bandwidth noise-producing propellers.

Devising a biological fish robot is to serve humans. Wave-like propulsion is well-known by virtue of high efficiency and stable maneuvers as performed by stingrays, knife fish, and cuttlefish. Researchers the whole world over realized the realization of this requires studies in many aspects: mechanical design, materials of biomimetic propulsion, actuator design, sensor system, and electronic system to measure as well as control robot movement with high performance.

Albeit et al., there have been studies on the hydrodynamics of biologically-inspired UAVs with fish-like underwater vehicles that have undulating fins, nonetheless, there are quite a few foci on the hydrodynamic analysis of UAVs with two symmetrical elongated long fins. To ensure a well-designed robot, it is essential to analyze how the drag coefficient can lead to optimizing the design [2].

In this paper, the 3D Computational Fluid Dynamics simulation was carried out to evaluate the drag coefficient of the hull shape of two symmetrical bilateral continuous undulating fins with distinct designs. The beneath-mentioned results will be depicted by valid numerical simulation.

## 2. DEFINITIONS OF FLOW PAST IMMersed BODY

### 2.1. Forces generated on a body

As can be seen that whenever a body is placed in a flow, the body is subject to a force from the surrounding fluid. The force in the direction of flow exerted by the fluid on the solid is called drag. By Newton's third law of motion, an equal and opposite net force is exerted by the body on the fluid. For instance, when a flat surface is

placed parallel to a moving stream of fluid, it is only subject to a force in the downstream direction. An airplane wing in a moving stream of fluid, nevertheless, is subject to the force  $R$ , which can be resolved into two components: a lift force  $L$  (perpendicular to the direction of the velocity) and a drag force  $D$  (parallel to the direction of the velocity) [3].

The lift and drag forces originate from the distribution of pressure and frictional stress on the surface: pressure force  $D_p$  perpendicular to the surface and friction force  $D_f$  tangential to the surface. Let the pressure of fluid acting on a given minute area  $dA$  on the body surface be  $p$ , and the friction force per unit area be  $\tau$ . The drag  $D_p$  and  $D_f$  are the integrations over the whole body surface of the component in the direction of the flow velocity  $U$  of force  $p dA$  and force  $\tau dA$ . The drag  $D_p$  and  $D_f$  equations are described as follows:

$$\begin{cases} D_p = \int_A p \cos \theta dA \\ D_f = \int_A \tau \sin \theta dA \end{cases} \quad (1)$$

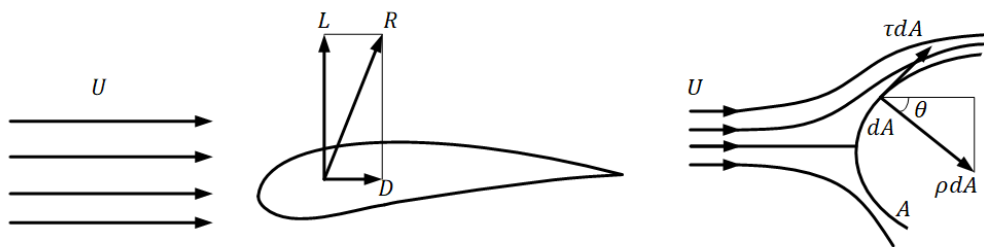


Figure 1. Force acting on the robot's body

The total drag  $D$  on a body is the sum of the pressure force and friction force. However, the body has a complex shape, so the calculation based on the above formula is difficult. Consequently, it is proven by experiments and empirical data to conclude a new formula for drag force, which is shown as follows:

$$D = \frac{1}{2} C_d A \rho U^2 \quad (2)$$

where  $\rho$  is the density of fluids;  $U$  is the speed of the object relative to the fluid;  $A$  is the characteristic area, with distinct interpretations that encompass the frontal area, corresponding to the perpendicular cross-sectional area; the platform area, associated with the surface area visible from a top-down perspective and the wetted area, which denotes the portion of the surface that comes into direct contact with the fluid;  $C_d$  is the non-dimensional number called the drag coefficient.

## 2.2. Drag coefficient

For different objects such as spheres, cylinders, and other shapes, the drag coefficient depends on several factors, including size, shape, the surface of the object, or the thickness of the fluid. Smooth objects tend to have a lower drag coefficient than rough, complex objects.

The drag coefficient also depends on the Reynolds number of the fluid flowing around the object. The Reynolds number is a physical parameter used to determine the motion of the fluid, including its viscosity, density, velocity, and the size of the object. As the Reynolds number increases, the fluid motion becomes unsteady, producing vortices and other fluid dynamic phenomena that can increase the drag coefficient. In some cases, increasing the Reynolds number may reduce the drag coefficient because the fluid becomes less viscous and less prone to vortex formation. Thus, the drag coefficient for complex objects is often based on experimental data tables and charts that relate the coefficient to the Reynolds number [4].

## 3. CALCULATION AND SIMULATION

### 3.1. Principle diagram of simulation

The simulation implementation process includes steps: geometry creation, geometry environment, geometry processing, meshing method, parameter settings, solutions settings, simulation implementation, convergence check, data analysis, optimization evaluation check, and result processing. In ANSYS, the simulation requires



four parts, namely: Geometry, Mesh, Solution, and Results. In the geometry step, the geometry can be created with CAD commercial software such as SolidWorks, NX, Inventor, and Catia to create 3D models. After that, ANSYS software performs simulation. In the Meshing part, ANSYS then reads the file and generates the initial 2D mesh in Fluent in order to carry out a primary simulation. The more complex the object it is, the more complicated the meshing it made. The solving part requires knowledge of computer parameters such as Sockets, Cores, and Logical processors to properly handle the calculation. Capturing computer parameters, particularly those of workstations, can be beneficial in reducing time and maintaining consistent quality for large and intricate models. The main outcome of the solution part involves adjusting the mesh refinement level and conducting another interaction, which can be advantageous in obtaining an accurate drag value. This value holds significant importance in ensuring the reliability of optimization. The principle diagram of the simulation for the drag coefficient can be depicted by the flow chart in Fig. 2.

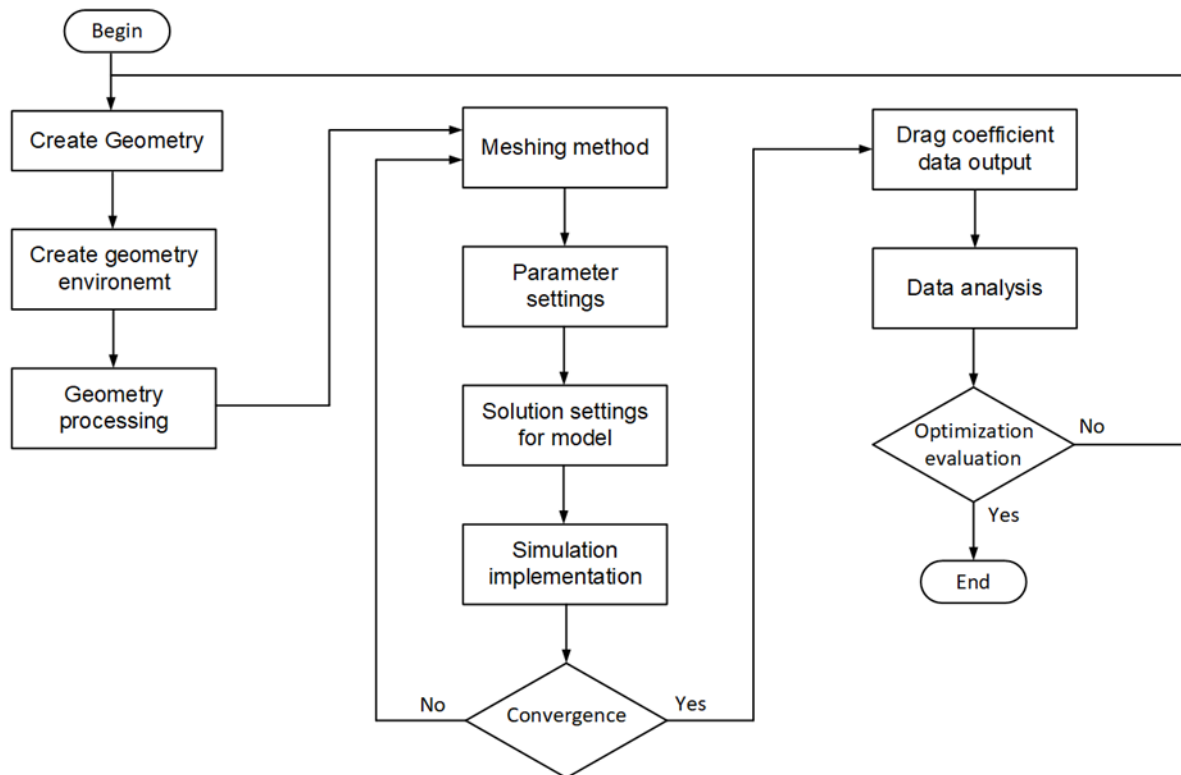


**Figure 2.** Flow chart of the optimization procedure

The results section serves to demonstrate the correlation between discovered elements throughout a given timeframe. Parameters such as velocity, pressure, resistance, and kinematic viscosity can be included in this section. The information can be saved in the form of photos or videos.

### 3.2. Design model

#### 3.2.1. Design based on numerical basis

The deformation of the shell layer only affects the drag coefficient of the shell layer concerning the fluid. According to D.F Myring [5], the optimal shell profile including the nose and tail will be determined by the formulas:

$$r_N = \frac{1}{2} dA \left\{ 1 - \left( \frac{x-a}{a} \right)^2 \right\}^{\frac{1}{n}} \quad (3)$$

$$r_r = \frac{1}{2} d - \left\{ \frac{3d}{2c^2} - \frac{\tan\theta}{c} \right\} c^2 + \left\{ \frac{d}{c^3} - \frac{\tan\theta}{c^2} \right\} c^3 \quad (4)$$

With  $n$  as the degree of the nose contour, the parameters are also given in Fig. 3. In which  $a, b, c, d$  are the size parameters depending on the desired design (the design goal is as small as possible), it is necessary to determine  $n$  and  $\theta$ . In a research paper on the optimal profile of the shell [6], João et al. gave an optimal design for a torpedo with  $n = 2, \theta = 20^\circ$ . The drag coefficient is determined by the following formula:

$$C_d = 0.12 + 0.000096((3.2 + 1.22n)^2 + (10.5 - 0.54\theta)^2) = 0.133 \quad (5)$$

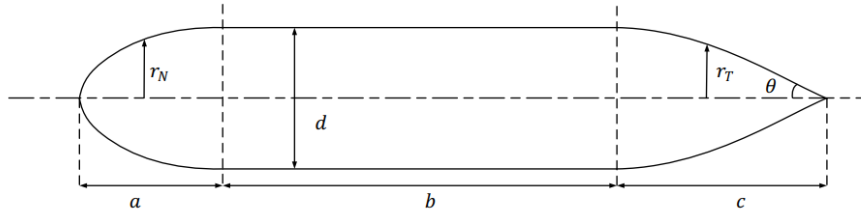


**Figure 3.** Shell profile parameters

Shell profile parameters shown as shown in Fig. 3. Based on the relates the coefficient to the Reynolds number, this paper demonstrates that the drag coefficient for a spherical object (disk) usually reaches a value of about 1.2. For a 2:1 ellipsoid, the drag coefficient is 0.5 to 0.1, while for an airship hull with high velocity, the drag coefficient is more or less 0.1. The best shape should be elliptic. To be able to find the drag coefficient for the robot, the Reynolds number is calculated:

$$R_e = \frac{\rho UL}{\mu} = \frac{UL}{\frac{\mu}{\rho}} = \frac{UL}{\nu} = \frac{0.5 \times 0.2}{10^{-6}} = 10^5 \quad (6)$$

With  $\rho$  is the density of fluid;  $\nu$  is the viscous coefficient of fluid, with water,  $\nu = 10^{-6} \text{ m}^2/\text{s}$ .  $U$  is the speed of the object relative to the fluid,  $U = 0.5 \text{ m/s}$ .  $L$  is characteristic length determined by  $L = V/A$  where  $V$  is the volume and  $A$  is the section of individuals. For spherical shape,  $L = D$ .

With the Reynolds number  $10^5$ , the drag coefficient for ellipsoid objects is just about 0.1 [4]. Thus, it is better to design with a drag coefficient lower than 0.133.

#### *Designing environment for simulation*

In these three designs, there is respectively a spherical deformation, the first improved deformation, and the second improved deformation. These dimensions are  $1\text{ m} \times \phi 0.3 \text{ m}$ ,  $1\text{ m} \times 0.3\text{ m} \times 0.2 \text{ m}$  and  $1\text{ m} \times 0.35\text{ m} \times 0.1 \text{ m}$  as shown in Fig. 4.



**Figure 4.** Shell profile design

To simulate the object in a liquid environment, create a fluid environment for the object. The dimensions of the surrounding are  $1200\text{ mm} \times 1800\text{ mm} \times 1000\text{ mm}$  as shown in Fig. 5.

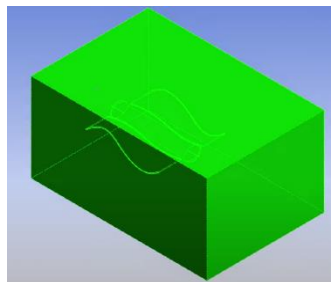


**Figure 5.** Shell profile design

In ANSYS software, the created fluid medium is supported to select the region of fluid motion. The flow will select to move from the inlet (blue) to the outlet (red) as shown in Fig. 6.

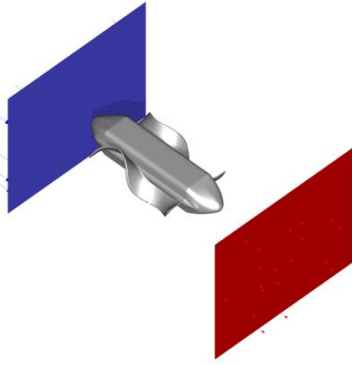


**Figure 6.** Flow direction in fluid environment

### 3.3. Meshing method

Meshing methods consist of three sub-methods: Finite Difference Method (FDM), Finite Volume Method (FVM), and Finite Element Method (FEM). With FDM, the method is based on solving differential equations by approximating derivatives with a finite difference. However, in CFD, the FDM is limited by its dependence on structured grids, making it hard to use such a method for problems involving complex-shaped boundaries. With FVM, this is a method that evolved from the conservation laws of physics. The basic idea is to subdivide the whole domain into small control volumes. In FVM, the unstructured grid can be utilized, which makes the method very attractive for flows that interact with complex geometries. With FEM, this is a method of discretizing the definite domain of the problem, by dividing it into many subdomains (elements). These elements are linked together at common nodes. In the range of each selected element, a certain function is determined through the unknown values at the nodes of the element called an approximation function satisfying the equilibrium condition of the element. Specifically, this method is powerfully and widely used.

When simulating the flow around a body of revolution, a 3D simulation method utilizing a structured mesh is commonly employed. In other to improve computational efficiency, the simulation focused on the flow past a stationary body instead of moving bodies in a still-water scenario [7]. For the given model, the physics preference is CFD, the solver preference is fluent, element size of the environment is 0.1. The boundary of the model has a sizing is 0.01. The smaller the sizing element is, the more accurate the results will be. Even if the correction for the element size is either excessively small or large, it may lead to negative-cell error in the solution part, i.e., causing a waste of simulation time and generating inaccurate outcomes. Hence, the process of selecting the appropriate meshing necessitates the expertise and computational skills of the engineer before initiating the simulation. Mesh calculation is shown in Fig. 7.

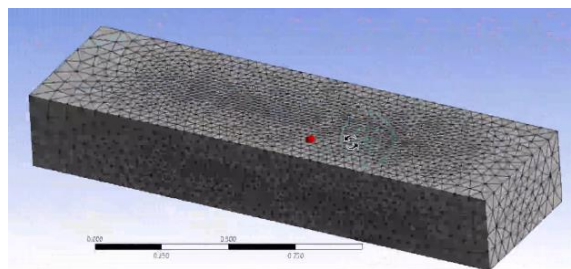


**Figure 7.** Mesh calculation

## 4. SIMULATION RESULTS

The simulation is conducted over a period of 5 seconds, with each shell shape simulated sequentially to obtain the drag coefficient. The shaped body has a gradual enlargement in its diameter, which causes a favorable pressure gradient over the front part. As a result, the friction drag is significantly reduced. Additionally, the smoother the nose is, the lower the drag force is as shown in Fig. 8 and Fig. 9.

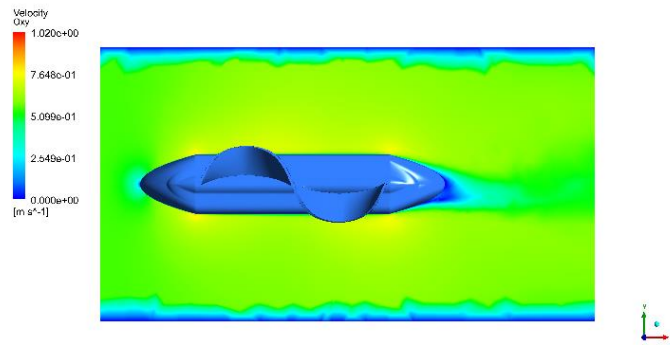


**Figure 8.** Simulation of first improved deformation

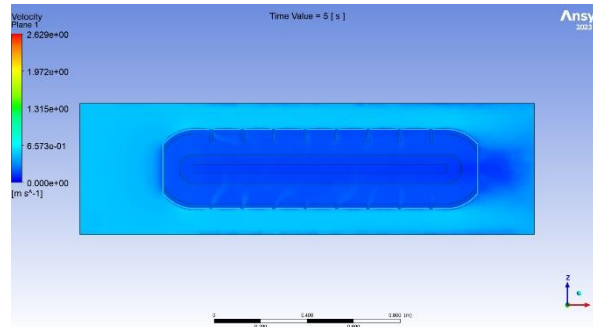


**Figure 9.** Simulation of second improved deformation

The obtained results show that all drag coefficients satisfy the criterion set, which is less than 0.133. The above model was executed multiple times by adjusting the  $\theta$ , front surface deformation, and back surface deformation to achieve lower drag results as shown in Fig. 10.

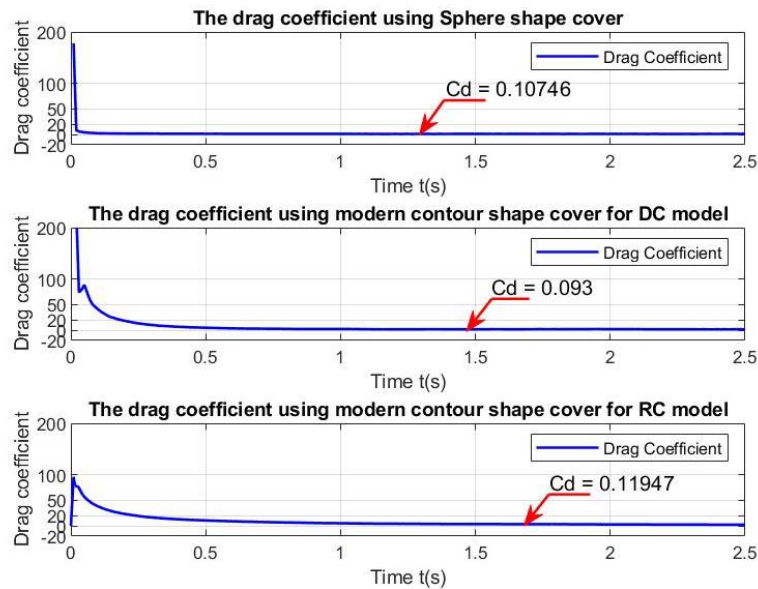


**Figure 10.** Results of drag coefficient for each shape

### Acknowledgements

This research is funded by Viet Nam National University Ho Chi Minh City (VNUHCM) under grant number TX2023-20b-01. We acknowledge the support of time and facilities from National Key Laboratory of Digital Control and System Engineering (DCSELab), Ho Chi Minh City University of Technology (HCMUT), VNUHCM for this study.

### References

- [1] Y. Yang, Y. Xiao, and T. Li, “A Survey of Autonomous Underwater Vehicle Formation: Performance, Formation Control, and Communication Capability,” *IEEE Commun. Surv. Tutorials*, vol. 23, no. 2, pp. 815–841, 2021, doi: 10.1109/COMST.2021.3059998.
- [2] K. H. Low, “Maneuvering of biomimetic fish by integrating a buoyancy body with modular undulating fins,” *Int. J. Humanoid Robot.*, vol. 4, no. 4, pp. 671–695, 2007, doi: 10.1142/S0219843607001217.
- [3] Y. Nakayama, “Introduction to Fluid Mechanics”, Tokai University, Japan, 1999.
- [4] Frank M. White, “Fluid Mechanics”, University of Rhode Island, New York, USA, 2009.
- [5] D. F. Myring, “Theoretical Study of Body Drag in Subcritical Axisymmetric Flow,” vol. 27, no. 3, pp. 186–194, 1976, doi: 10.1017/s000192590000768x.
- [6] J. Victor Nunes de Sousa, A. Roberto Lins de Macêdo, W. Ferreira de Amorim Junior, and A. Gilson Barbosa de Lima, “Numerical Analysis of Turbulent Fluid Flow and Drag Coefficient for Optimizing the AUV Hull Design,” *Open J. Fluid Dyn.*, vol. 04, no. 03, pp. 263–277, 2014, doi: 10.4236/ojfd.2014.43020.
- [7] T. Gao, Y. Wang, Y. Pang, and J. Cao, “Hull shape optimization for autonomous underwater vehicles using CFD,” *Eng. Appl. Comput. Fluid Mech.*, vol. 10, no. 1, pp. 599–607, 2016, doi: 10.1080/19942060.2016.1224735.

**[S1-32] Classification of Fatigued Electromyography Signals using Support Vector Machine in Combination with Root Mean Square and Mean Absolute Value Features**

Nghi Tran Huu<sup>1</sup>, Gia Thien Luu<sup>2,\*</sup>, Bao Minh Pham<sup>1</sup>, Philippe Ravier<sup>3</sup>, Olivier Buttelli<sup>3</sup>

<sup>1</sup> Department of Biomedical Engineering, Faculty of Applied Science, Ho Chi Minh City University of Technology (HCMUT), Ho Chi Minh City, 700000, Viet Nam

<sup>2</sup> Biomedical Department, HUTECH Institute of Engineering, HUTECH University, Ho Chi Minh, Viet Nam

<sup>3</sup> University of Orleans, France PRISME Laboratoire, 12 rue de Blois, BP 6744, 45067 Orléans, France

\*Corresponding author: lg.thien@hutech.edu.vn

**Abstract**

Muscle fatigue is a prevalent issue in daily life, particularly for individuals whose occupations involve continuous use of the upper and lower extremities or torso. It can cause discomfort and pain, as well as decreased work performance and quality of life. This study aims to classify muscle fatigue utilizing the Root Mean Square (RMS) and Mean Absolute Value (MAV) features based on EMG signal. The dataset comprises 64-channel electromyographic recordings from 10 subjects. Muscle fatigue was labeled using the MVC criterion, with a threshold value greater than 60% MVC. The wavelet algorithm denoises the signal before feeding it to the Support Vector Machine classifier. The results show that the machine learning classifier is effective and feasible, with an accuracy of 82.81%. These findings have practical applications, such as rehabilitation for people with mobility impairments or muscle disorders, as well as improving the efficiency and quality of life for workers whose jobs require continuous use of the upper and lower extremities or torso.

**Keywords:** Muscle fatigue, Root Mean Square, Mean Absolute Value, EMG signal, MVC, Support vector machine

**1. INTRODUCTION**

Muscle fatigue is a complicated phenomenon with several origins, processes, and manifestations. Changes in the effectiveness of the neurological system and a cascade of metabolic, structural, and energetic alterations brought on by a lack of oxygen and nutritive substances in the blood contribute to its onset [1]. It is generally recognized that muscle depletion occurs in healthy individuals when the muscle is required to generate a force greater than 60 percent of its MVC. This means that if a person is performing a task that requires repetitive use of a muscle, such as raising weights or maintaining a posture, the muscle will begin to fatigue when required to generate a force greater than 60 percent of its maximum capacity [2].

The electromyogram (EMG) is a bioelectrical measurement used to record the electrical activity of muscles during contraction and rest. Muscle contractions result in the generation and transmission of electrical signals along nerve fibers. Researchers measured the amount that individual electrodes contributed to the EMG signal in order to use it as a tool for determining when muscles had become fatigued. When a muscle is fatigued, its fibers become less excitable and create fewer electrodes. A notable drop in the EMG signal will be observed as a consequence of this [3]. Muscle fiber conduction velocity and myoelectric signal spectral parameters (mean and median frequency) show a linear or curvilinear decrease in time, depending on the level of voluntary or electrically elicited contraction [4]. Muscle fatigue may be detected using measurements of force [5] and muscular torsion [6] in addition to the EMG. Compared to these techniques, EMG signaling provides a number of benefits for identifying when muscles are exhausted. It is superior since it provides information in real time on muscle activity and fatigue during exercise, which is useful for creating individualized workout plans. sEMG (surface electromyogram) is also a method for quantifying the electrical activity of muscles that differs slightly from EMG. Regarding EMG, a needle electrode is directly implanted into a muscle to record the electrical activity produced by muscle fibers. This method provides a precise measurement of muscle activity, but it is invasive and must be performed by a trained professional. sEMG, on the other hand, entails positioning surface electrodes on the skin above the muscle in order to detect the electrical signals generated by the muscle fibers below. This technique is non-invasive and can be executed with minimal instruction. sEMG measurements, however, are less precise than EMG measurements. Both EMG and sEMG have their own benefits and drawbacks, and the choice of technique depends on the application and level of detail required. EMG is typically employed in clinical contexts to diagnose

and monitor neuromuscular disorders, whereas sEMG is typically employed in sports science and rehabilitation to evaluate muscle function and performance [7]. Moreover, sEMG was deemed more suitable than ultrasound for detecting alterations in the muscle activation of a fatigued muscle during submaximal isometric contractions [8]. This indicates that sEMG is the measurement most suited for the identification and forecasting of muscle fatigue; hence, the emphasis of this research will be on sEMG signal analysis.

The literature contains a wide variety of classifiers, including but not limited to: Simple Logistic Regression (SLR), Artificial Neural Networks (ANN), Linear Discriminant Analysis (LDA), Naive Bayes (NB), K-nearest neighbor (KNN), Nonlinear Logistic Regression (NLR), Multi-Layer Perceptron (MLP), and Support Vector Machines (SVM). However, classification of EMG with SVM has shown increased performance in terms of accuracy in some circumstances [9] [10]. Support Vector Machine (SVM) is a well-known machine learning algorithm employed in the prediction of muscle fatigue. SVM operates by locating a hyperplane that best separates the data into distinct classes, with the goal of classifying new data points with the utmost possible precision. SVM can be trained on a dataset of muscle activity data, such as electromyography (EMG) signals, and used to predict the level of fatigue in a muscle based on new input data in the context of muscle fatigue prediction. It has been demonstrated that SVM can accurately predict muscle fatigue in multiple muscle groups, including the forearm, biceps, and triceps. An advantage of SVM is that it can accurately manage high-dimensional data, such as EMG signals. SVM is also less susceptible to overfitting than other machine learning algorithms, which can be advantageous when working with limited datasets. Nevertheless, SVM has some limitations. It can be computationally intensive and may necessitate fine-tuning of multiple hyperparameters for optimal performance. The kernel-based SVM has a strong theoretical basis and is becoming popular for classification and regression machine learning problems. The kernel used in this technique must be strategically selected because it results in a trade-off between classifier performance and computational complexity [11]. SVM has the potential to be implemented in clinical and athletic contexts to enhance physical performance and prevent injury [12]. In this paper, the SVM algorithm is implemented to classify muscle fatigue based on MAV and RMS features. Those features have gained popularity in this discipline, as demonstrated by a previous study [9] [13] [14].

## 2. MATERIALS

10 healthy subjects, 3 women and 7 men (mean age 24, standard deviation 1.5 years) were studied. The maximal voluntary contraction of a single subject will be defined as the average of three maximum force measurements separated by five minutes. After the MVC has been determined, measurements can be conducted at various force levels, expressed as a percentage of MVC. If feasible, the subject should maintain the force for at least 10 seconds. The steps are as follows: So that the subject could learn to maintain a particular force level, we began with a test at 10% of MVC. Then, random order experiments should be conducted at 20%, 40%, 60%, and 90% of MVC. Next, an exhaustion test is conducted at 70% of MVC. Finally, we concluded with a 10% MVC final exam. There is a 5-minute break between each examination. In the following sections, 10% MVC, 20% MVC, 40% MVC, 60% MVC, and 90% MVC are implicitly understood. If nothing else is described, the condition preceding muscle fatigue will be indicated. Clearly characterized as 70% MVC during muscle fatigue and 10% MVC after muscle fatigue.

At a sampling frequency of 2KHz, the sensor matrix captures the EMG signal from the right biceps. To minimize noise, the sEMG signals from all electrodes obtained from the MVC levels were filtered (20Hz - 400Hz).

## 3. METHOD

### 3.1. Preprocessing

#### 3.1.1. Wavelet denoising

Wavelet transform is one of the compelling approaches that may be used to minimize noise. The fundamental concept underlying wavelet transforms is the decomposition of a signal or image into a set of wavelets, which are small, localized waves that can represent complex patterns and structures. By analyzing the wavelet coefficients at various scales, it is possible to identify and eliminate noise while preserving the signal's or image's essential characteristics. As a result, the data can be analyzed with greater precision, as distinct features can be isolated and treated independently. “wdenoise” built-in function of MATLAB to implement Wavelet signal denoising.

The used syntax is XDEN = wdenoise(\_\_\_,Name,Value). The “Coiflet” family of wavelets has been shown to perform very well in signal recovery, typically Coiflet 3 [15] [9]. In addition, the decomposition level parameter is set to 4 to obtain useful EMG information. In addition, the parameters of denoising method and threshold rule need to be further studied for appropriate evaluation.

### 3.1.2. Frequency filter

Band-pass filter is used to extract useful frequency components within the range of 10Hz to 500Hz. Then, high-pass and low-pass filter should be considered to apply again to improve frequency filtering efficiency. A digital notch filter would be effective at suppressing electrical noise at 50Hz or 60Hz, depending on the geographical location. In this paper, the data set has previously been filtered by hardware, so this step is not repeated. Nevertheless, for the EMG signal processing we propose, filters are required for classifying the underlying muscle fatigue signal.

## 3.2. Feature extraction

### 3.2.1. Mean absolute value (MAV)

The EMG signal represents the electrical activity produced by contracting and relaxing muscle fibers. The MAV characteristic is computed by calculating the absolute value of each EMG signal sample and then averaging these absolute values over a predetermined time window. This yields a single value that represents the average amount of electrical activity in the muscle during the specified interval of time.

$$\text{MAV}(x) = \frac{1}{T} \int_t^{t+T} |x(t)| dt$$

Where  $|x(t)|$  represents the absolute value of the signal  $x(t)$  at time  $t$ .

### 3.2.2. Root mean square (RMS)

Similar to MAV, the EMG signal is first rectified to derive each sample's absolute value. The RMS characteristic is then computed by taking the square root of the mean of the squared values of the rectified signal over a given time interval. This results in a singular value that represents the aggregate magnitude of the EMG signal during the specified time interval.

$$\text{RMS}(x) = \sqrt{\frac{1}{T} \int_t^{t+T} (x_t)^2 dt}$$

Where  $T$  is the time interval of the signal and  $\int_t^{t+T} (x_t)^2 dt$  represents the integral of the square of the signal over that time interval.

### 3.3. SVM classifier

In this paper, the SVM algorithm was used to classify muscle fatigue signals. For cross validation, the input data of the SVM model was split into 80% train and 20% test. Then the SVM classifier is subsequently constructed using a Kernel Gaussian. It was also found that Linear kernel and Gaussian kernel were equally good to identify intra-individual fatigue features [16].

## 4. RESULT AND DISCUSSION

The SVM model achieved a macro F1 score of 0.80679, indicating remarkable performance in classifying the muscle fatigue based on EMG signal features. The proposed signal processing framework was illustrated in the Figure 1 below.



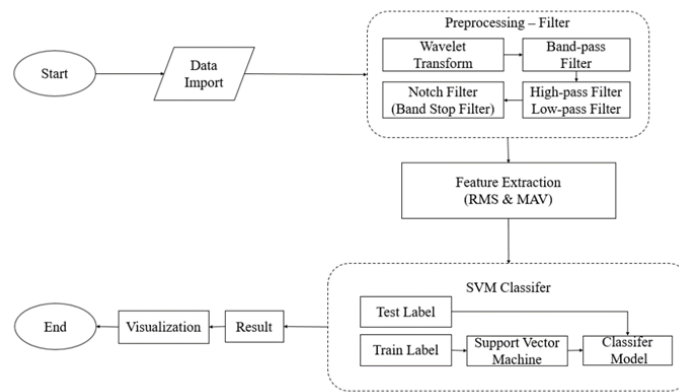


**Figure 1.** The proposed framework

Additionally, ROC analysis, shown in Figure 2, was also quite good, with an area under the curve (AUC) of 0.90264.

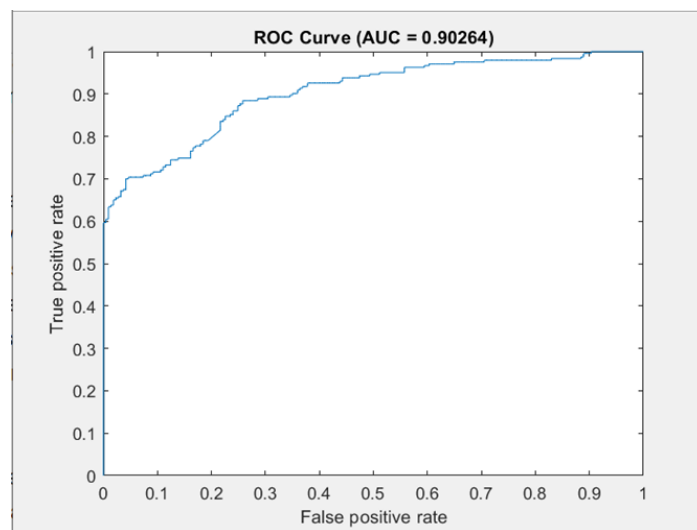


**Figure 2.** Model performance by the ROC curve

It should be noted that the input signal contained many erroneous data points, represented by the zero-value in the data table, due to the acquisition phase mistaken. To overcome this issue and retain useful signal, we applied several preprocessing techniques above.

Further analysis of the confusion matrix revealed that the model achieved high precision and recall for both fatigued and non-fatigued classes, with only a small number of misclassifications. These results have shown a robust and reliable SVM model for classifying muscle fatigue based on EMG signal features, even when the input signal contains many erroneous data points. Overall, this study demonstrated the robustness of using SVM classification models for muscle fatigue classification based on RMS and MAV features. Future research should explore the kernel selection, the use of variant classifiers, and feature selection techniques to further improve the performance of the model.

		Predicted	
		Positive (1)	Negative(0)
Actual	n = 460		
	Positive (1)	190	27
Negative(0)	64	179	

**Figure 3.** Confusion matrix

## References

- [1] S. Boyas and A. Guével, “Neuromuscular fatigue in healthy muscle: Underlying factors and adaptation mechanisms,” *Annals of Physical and Rehabilitation Medicine*, vol. 54, no. 2, pp. 88–108, Mar. 2011, doi: 10.1016/j.rehab.2011.01.001.
- [2] L. Thien, P. Ravier, and O. Buttelli, “Validation of the Time Delay Estimators Applied to the Surface Electromyography Signals during Isometric Isotonic and Isometric Anisotonic Contraction,” Oct. 2015. doi: 10.1109/ATC.2015.7388307.
- [3] R. Martinek *et al.*, “Advanced Bioelectrical Signal Processing Methods: Past, Present, and Future Approach—Part III: Other Biosignals,” *Sensors*, vol. 21, no. 18, Art. no. 18, Jan. 2021, doi: 10.3390/s21186064.
- [4] R. Merletti, L. R. Lo Conte, and C. Orizio, “Indices of muscle fatigue,” *Journal of Electromyography and Kinesiology*, vol. 1, no. 1, pp. 20–33, Jan. 1991, doi: 10.1016/1050-6411(91)90023-X.
- [5] R. M. Enoka and J. Duchateau, “Muscle fatigue: what, why and how it influences muscle function,” *J Physiol*, vol. 586, no. Pt 1, pp. 11–23, Jan. 2008, doi: 10.1113/jphysiol.2007.139477.
- [6] “A mechanomyographic frequency-based fatigue threshold test - PubMed.” <https://pubmed.ncbi.nlm.nih.gov/19945484/> (accessed Jun. 26, 2023).
- [7] M. A. Cavalcanti Garcia and T. M. M. Vieira, “Surface electromyography: Why, when and how to use it,” *Rev Andal Med Deporte*, vol. 4, no. 1, pp. 17–28, Jan. 2011.
- [8] M. R. Al-Mulla, F. Sepulveda, and M. Colley, “A Review of Non-Invasive Techniques to Detect and Predict Localised Muscle Fatigue,” *Sensors (Basel)*, vol. 11, no. 4, pp. 3545–3594, Mar. 2011, doi: 10.3390/s110403545.
- [9] D. C. Toledo-Pérez, J. Rodríguez-Reséndiz, R. A. Gómez-Loenzo, and J. C. Jauregui-Correa, “Support Vector Machine-Based EMG Signal Classification Techniques: A Review,” *Applied Sciences*, vol. 9, no. 20, Art. no. 20, Jan. 2019, doi: 10.3390/app9204402.
- [10] N. S. Ahmad Sharawardi, Y.-H. Choo, S.-H. Chong, A. K. Muda, and O. S. Goh, “Single channel sEMG muscle fatigue prediction: An implementation using least square support vector machine,” in *2014 4th World Congress on Information and Communication Technologies (WICT 2014)*, Oct. 2014, pp. 320–325. doi: 10.1109/WICT.2014.7077287.
- [11] “Performance evaluation of various classifiers for predicting knee angle from electromyography signals - Dhindsa - 2019 - Expert Systems - Wiley Online Library.” <https://onlinelibrary.wiley.com/doi/abs/10.1111/exsy.12381> (accessed Jun. 26, 2023).
- [12] Y. Paul, V. Goyal, and R. Jaswal, “Comparative analysis between SVM & KNN classifier for EMG signal classification on elementary time domain features,” Sep. 2017, pp. 169–175. doi: 10.1109/ISPCC.2017.8269670.
- [13] Y. Bouteraa, I. B. Abdallah, and K. Boukthir, “A New Wrist–Forearm Rehabilitation Protocol Integrating Human Biomechanics and SVM-Based Machine Learning for Muscle Fatigue Estimation,” *Bioengineering*, vol. 10, no. 2, Art. no. 2, Feb. 2023, doi: 10.3390/bioengineering10020219.
- [14] P. A. Karthick, D. M. Ghosh, and S. Ramakrishnan, “Surface electromyography based muscle fatigue detection using high-resolution time-frequency methods and machine learning algorithms,” *Computer Methods and Programs in Biomedicine*, vol. 154, pp. 45–56, Feb. 2018, doi: 10.1016/j.cmpb.2017.10.024.
- [15] J. Too, A. R. Abdullah, N. Mohd Saad, N. Ali, and H. Musa, “A Detail Study of Wavelet Families for EMG Pattern Recognition,” *International Journal of Electrical and Computer Engineering*, vol. 8, pp. 4221–4229, Dec. 2018, doi: 10.11591/ijece.v8i6.pp.4221-4229.
- [16] J. Zhang, T. E. Lockhart, and R. Soangra, “Classifying Lower Extremity Muscle Fatigue during Walking using Machine Learning and Inertial Sensors,” *Ann Biomed Eng*, vol. 42, no. 3, pp. 600–612, Mar. 2014, doi: 10.1007/s10439-013-0917-0.

## [S1-36] Adjusting Technical Parameters to Improve the Quality of 3D Printed Products Using ABS Material

Huu Nghi Huynh<sup>1,\*</sup>, Dinh Tam Ngo<sup>1</sup>, Tung Lam Khoa<sup>1</sup>, Trong Hieu Bui<sup>2</sup>

<sup>1</sup> Division of Manufacturing Engineering, Faculty of Mechanical Engineering, Ho Chi Minh City University of Technology (HCMUT), 268 Ly Thuong Kiet Street, District 10, Ho Chi Minh City, Viet Nam

<sup>2</sup> Division of Machine Design, Faculty of Mechanical Engineering, Ho Chi Minh City University of Technology (HCMUT), 268 Ly Thuong Kiet Street, District 10, Ho Chi Minh City, Viet Nam

\*Corresponding author: hhnghi@hcmut.edu.vn

### Abstract

Additive Manufacturing technology, also known as 3D printing technology, has been widely applied in prototyping, products serving in life as well as the manufacturing process especially in important fields such as processing industry, manufacturing, automobile, national security,... However, many open source 3D printing devices are currently not capable of manufacturing products of all kinds. Plastic materials are often used in industry such as PC (Polycarbonate), HIPS (High Impact Polystyrene), PEEK (Polyether Ether Ketone), ABS (Acrylonitrile Butadiene Styrene),... have high shrinkage leading to warping, deformation of layers. The purpose of the article is to study and adjust technological parameters, focusing on the temperature parameters of the product chamber to make 3D printed products using ABS materials. Experimental results on many different samples show that product quality has been significantly improved with the parameters found.

**Keywords:** 3D printers, Open source, ABS, Parameter process, Temperature chamber

### 1. INTRODUCTION

3D printing is an advanced manufacturing method that involves adding and bonding materials layer by layer. Industrial and open-source 3D printing devices are commercially available from well-known corporations such as 3D Systems, Stratasys, and Z Corporation. In Viet Nam, 3D printing technology is increasingly popular and widely applied. In addition to research on the fabrication of 3D printing devices to meet domestic needs, there are numerous studies aiming to improve the quality of the printed products. One research direction focuses on expanding the range of materials used in industrial applications, allowing the production of products using various materials. However, currently, most domestic 3D printers are unable to fabricate products using materials like PC (Polycarbonate), HIPS (High Impact Polystyrene), PEEK (Polyether Ether Ketone), and ABS (Acrylonitrile Butadiene Styrene) due to their high shrinkage. Therefore, the research group has designed and developed an open-source 3D printer capable of providing a controlled chamber temperature to reduce residual stress between layers (caused by temperature differences) and minimize shrinkage during the fabrication process. Additionally, the study investigates the optimization of process parameters to enhance the quality of 3D printed products using ABS material. The technology parameters utilized in the research include: stepper motor increment, extrusion multiplier, extrusion width, extra inflation distance, density infill, and temperature chamber. Experimental results demonstrate significant improvements in overall shape and geometric accuracy of the printed products.

The equipment used in the experiment is an open source FDM 3D printer with a product size of 200 × 200 × 200 mm, consisting of two extruders, one for creating the product and the other for creating support structures. The device is equipped with a convection chamber heated by resistors placed on both sides of the enclosed walls, unaffected by external temperatures. The fan speed is set to ensure even temperature distribution within the product fabrication area. ABS (Acrylonitrile Butadiene Styrene) is one of the first materials used in the 3D printing industry, composed of polymers Acrylonitrile, Butadiene, and Styrene. ABS plastic exhibits both flexibility and excellent impact resistance. It enables the production of high-strength and wear-resistant products, and its melting temperature transitions into a molten glass state at 105<sup>o</sup>C. These advantages make ABS suitable for manufacturing mechanical products and replacing some metal parts in industrial production. The quality of 3D printed products, specifically those made of ABS, and generally, other materials, depends significantly on various technological parameters. Some important technological parameters include:

*Extrusion multiplier*: also known as the flow rate factor, allows the adjustment of the material flow rate through the extruder. This parameter is applicable when excessive or insufficient material extrusion occurs on the detail surface.

*Step of the motor*: used to regulate the motions along the X, Y, and Z axes and push the filament into the extruder.

*Extrusion width*: the width of the extruded filament, which remains stable on the machine bed or the previous layer. Extrusion width and layer height are two important parameters that determine the shape and size of the extruded lines in product fabrication.



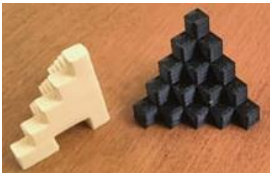
*Extra inflation distance*: supports the creation of short material bridges between separate parts of a product. Additionally, it facilitates the printing of products with gradually widening and narrowing bases. Current experiments have shown that the device can create bridges with a maximum size of 30 mm and horizontal overhangs with a maximum size of 2 mm.


*Density infill*: the amount of material filled inside the product, ranging from 0 to 100%. Higher infill density results in increased weight and improved mechanical properties of the product. Density infill also affects manufacturing time and material consumption.

*Print speed*: one of the key parameters influencing the quality of the product. Excessively slow print speed can cause distortion in the printed model due to the nozzle staying on the plastic layer for too long. Conversely, it can lead to blurred surfaces and deformation caused by insufficient cooling time, inadequate material supply, and weak adhesion between layers. For ABS material, the optimal print speed falls within the range of 40 to 60 mm/s. For highly complex surfaces, the print speed should be set at 40 mm/s, while for products with less complexity in the shaping process and requiring longer manufacturing time, the print speed can be set at 60 mm/s. Furthermore, for ABS material, the initial layer should be printed at 50% of the normal print speed to enhance material adhesion to the print bed.

## 2. EXPERIMENTATION

**Table 1.** List of sample models

No	Sample model	Shape	Purpose	Context
1	The XYZ model, measuring $25 \times 25 \times 25$ mm, designed and proposed by iDig3Dprinting.		The accuracy of machine dimensions, head extrusion temperature, extrusion level, and vibration level.	Adjustment of the step values for the drive motors was performed.
2	The $30 \times 30 \times 30$ mm wire frame cubic model was designed by Orionwnix.		The shrinkage factor, ability to manufacture bridge-shaped products, dimensional accuracy, and interlayer shifting phenomena were assessed.	Adjustment of Extrusion multiplier to regulate the amount of plastic passing through the extrusion head.
3	The staircase-like cubic pattern composed of cubic units measuring $5 \times 5 \times 5$ mm, designed by Mcroucher.		The surface quality in terms of layer height, dimensional accuracy, fan cooling performance, and material extrusion motor operation were examined to assess their quality.	Adjustment of Extrusion width

4	The clamp sample designed by Alejandra Cervantes Tetrika.		Test tightness tolerance of the components assembly. Influence of the chamber temperature on product quality was compared and analyzed.	Adjustment on chamber temperature
---	---	---	---	-----------------------------------






The experimental process was sequentially conducted using standard samples to determine optimal parameters. In this process, the XYZ cubic model was employed to evaluate dimensional accuracy, extrusion head temperature, extrusion level, and machine vibration. The wire frame cubic model was utilized to test shrinkage, the ability to manufacture bridge-shaped products, dimensional accuracy, and interlayer shifting phenomena. The staircase model was used to examine surface quality in terms of layer height, dimensional accuracy, fan cooling performance, and material extrusion motor operation. The clamp model was employed to assess the assembly tightness of the components assembly. A comparison of the chamber temperature's impact on the clamp product's quality was conducted by printing on two machines with identical parameters, differing only in the presence or absence of a heating chamber. The products were then re-manufactured using the optimized parameters for further testing and evaluation. The list of test samples and the testing sequence are presented in Table 1. The parameter values were determined based on the manufacturer's recommendations, equipment operation experience, and the calibration process to establish the optimal parameter values by the research team.

### 3. RESULT AND DISCUSSION








#### 3.1. Results

The results of parameter adjustment and the achieved products are presented from Table 2 to Table 5.




**Table 2.** Parameter adjustment results and products of the XYZ model

No	Number of motor steps	Sample dimensions	Product
1	X axis: 80 steps/mm Y axis: 80 steps/mm Z axis: 400 steps/mm E 192 steps/mm	X axis: 25.2 mm Y axis: 25.18 mm Z axis: 25.3 mm	
2	X axis: 80 steps/mm Y axis: 80 steps/mm Z axis: 400 steps/mm E 192 steps/mm	X axis: 25.22 mm Y axis: 25.2 mm Z axis: 25.28mm	
3	X axis: 80 steps/mm Y axis: 80 steps/mm Z axis: 400 steps/mm E 192 steps/mm	X axis: 25.22 mm Y axis: 25.22 mm Z axis: 25.32 mm	
4	X axis: 80 steps/mm Y axis: 80 steps/mm Z axis: 400 steps/mm E 192 steps/mm	X axis: 25.18mm Y axis: 25.18mm Z axis: 25.28mm	
5	X axis: 80 steps/mm Y axis: 80 steps/mm Z axis: 400 steps/mm E 192 steps/mm	X axis: 25.2mm Y axis: 25.2mm Z axis: 25.3mm	



**Table 3.** Parameter adjustment results and products of the wire frame cubic model

No	Parameter	Value	Other settings	Result
1	Extrusion multiplier	1.0	Support structures were implemented to mitigate the impact of the extra inflation distance parameter on product quality.	
2	Extrusion multiplier	0.8	Support structures were created to prevent the influence of the extra inflation distance parameter on product quality.	
3	Extrusion multiplier	0.7	Support structures were generated to mitigate the impact of the extra inflation distance parameter on the quality of the product.	
4	Extrusion multiplier	0.7	No support structures were created to evaluate the impact of the extra inflation distance parameter on product quality.	 Front  Side
5	Extrusion multiplier	0.7	No support structures were created to evaluate the impact of the extra inflation distance parameter on product quality.	 Front  Side

**Table 4.** Results of parameter calibration and product of the step pyramid model

No	Parameter	Value	Other settings	Result
1	Extrusion width	$0.3 \times d'$ (mm) ( $d' = 0.4$ mm)	The extrusion angle is set to $45^0$ to maximize the number of printed lines on a surface.	
2	Extrusion width	$0.35 \times d'$ (mm)	The extrusion angle is set to $45^0$	
3	Extrusion width	$0.4 \times d'$ (mm)	The extrusion angle is set to $45^0$	

**Table 5.** Results of parameter calibration and product assembly for the clamp assembly model

No	Parameter	Value	Other settings	Result
1	The chamber temperature for product formation is applied.	$70^0C$	Density Infill: 35% <u>Velocity</u> Extruder: 60 mm/s Support: No	
2	There is no chamber temperature for product formation, and the heated bed temperature is set to $34^0C$ .	No	Density Infill: 35% <u>Velocity</u> Extruder: 60 mm/s Support: No	

### 3.2. Discussion

#### For XYZ sample:

The average dimension values along the X, Y, and Z axes are determined as follows:

$$\bar{x} = \frac{\sum_{i=1}^{n=5} x_i}{n} = 25,204mm$$

$$\bar{y} = \frac{\sum_{i=1}^{n=5} y_i}{n} = 25,196mm$$

$$\bar{z} = \frac{\sum_{i=1}^{n=5} z_i}{n} = 25,296mm$$

Whereas the ratio "a" for each axis is:

$$a_x = \frac{25}{25,204} = 0,9919$$

$$a_y = \frac{25}{25,196} = 0,9923$$

$$a_z = \frac{25}{25,296} = 0,9883$$

$$a_e = 0,7$$

Therefore, the new adjusted step parameter values are as follows:

$$X = 80.0,9919 = 79,352 \text{ steps/mm}$$

$$Y = 80.0,9923 = 79,384 \text{ steps/mm}$$

$$Z = 400.0,9883 = 395,32 \text{ steps/mm}$$

$$E = 192.0,7 = 134,4 \text{ steps/mm}$$

**For the wire frame cubic model, the adjusted step parameter values are as follows:**

Sample 1: The observation results indicate that the detailed surfaces are deformed, and the layers are stacked on top of each other due to the lack of bonding between layers. The extruded material on each layer takes the form of droplets instead of fibers, indicating an excessive amount of extruded resin. This leads to dimensional discrepancies in all three X, Y, and Z directions. The size of the product measures  $32.6 \times 32.4 \times 35$  mm compared to the designed value of  $30 \times 30 \times 30$  mm.

Sample 2: The primary size discrepancies occur in the initial and final layers. The phenomenon of extruded material taking the form of particles only occurs in the first layer and at positions adjacent to the support layer. The dimensional discrepancies decrease, and the measured result is  $30.6 \times 30.6 \times 30.2$  mm compared to the designed value of  $30 \times 30 \times 30$  mm.

Sample 3: The primary size discrepancies occur in the initial and final printed layers. The phenomenon of extruded material taking the form of particles only occurs at positions adjacent to the support layer. The dimensional discrepancies continue to improve, and the measured result is  $30.2 \times 30.2 \times 30.2$  mm compared to the designed value of  $30 \times 30 \times 30$  mm.

Sample 4: The primary size discrepancies occur in the initial and final printed layers. The phenomenon of extruded material taking the form of particles no longer exists. With an extra inflation distance parameter set to 20 mm, the horizontal crossbars of the front and back material spheres of the product exhibit greater sagging compared to the two side crossbars, as they are not in contact with the hot air flow in the chamber. The two side crossbars cool down to 70°C faster, resulting in lower sagging. The measurement results show that the maximum width of the front and back crossbars is 5.68 mm and 5.2 mm, respectively, while the width of the two side crossbars is 4.6 mm. The size in the X and Y directions measures  $30.2 \times 30.2$  mm compared to the designed value of  $30 \times 30$  mm. The size in the Z direction measures 30.2 mm compared to the designed value of 30 mm. When the extrusion multiplier value is set lower than 0.7 on the sample with the phenomenon of porosity and missing material, the amount of material extruded through the nozzle is optimized for the testing machine.

Sample 5: The primary size discrepancies occur in the initial and final printed layers. The phenomenon of extruded material taking the form of particles no longer exists. With an extra inflation distance parameter set to 20 mm, the horizontal crossbars of the front and back material spheres of the product exhibit greater sagging compared to the two side crossbars, as they are not in contact with the hot air flow in the chamber. The two side crossbars cool down to 70°C faster, resulting in lower sagging. The measurement results show that the maximum width of the front and back crossbars is 5.68 mm and 5.2 mm, respectively, while the width of the two side crossbars is 4.6 mm. The size in the X and Y directions measures  $30.06 \times 30.06$  mm compared to the designed value of  $30 \times 30$  mm. The size in the Z direction measures 30.04 mm compared to the designed value of 30 mm. When the extrusion multiplier value is set lower than 0.7 on the sample with the phenomenon of porosity and missing material, the amount of material extruded through the nozzle is optimized for the testing machine.

**For the staircase model, the adjusted step parameter values are as follows:**

The surface areas of the measured block are  $25 \text{ mm}^2$  at different heights, which helps evaluate the surface filling capability of the product. For surfaces in close proximity to the machine bed, the plastic fibers bond well with each other, showing minimal variation. On the other hand, for surfaces located at the top, there is poor bonding between the plastic fibers, and the extrusion width value only affects the number of extrusion lines on each surface. Having too many extrusion lines on the same surface results in overlapping lines, leading to a



decrease in surface quality. Conversely, having too few extrusion lines can result in gaps, sinking, or unevenness on the surface. The diagonal dimension of the square surface is 5mm:  $5\sqrt{2}mm$

In sample 1, the calculated dimensions are as follows:  $0.3 \times 0.4 = 0.12$  mm

$$\text{The filling ratio is as follows: } \frac{5\sqrt{2} - \left\{ \left( \frac{5\sqrt{2}}{0,12} - \left[ \frac{5\sqrt{2}}{0,12} \right] \right) \cdot 0,4 \right\}}{5\sqrt{2}} \% = 94,7\%$$

In sample 2, the calculated dimensions are as follows:  $0.35 \times 0.4 = 0.14$  mm

$$\text{The filling ratio is as follows: } \frac{5\sqrt{2} - \left\{ \left( \frac{5\sqrt{2}}{0,14} - \left[ \frac{5\sqrt{2}}{0,14} \right] \right) \cdot 0,4 \right\}}{5\sqrt{2}} \% = 97,13\%$$

In sample 3, the calculated dimensions are as follows:  $0.4 \times 0.4 = 0.16$  mm

$$\text{The filling ratio is as follows: } \frac{5\sqrt{2} - \left\{ \left( \frac{5\sqrt{2}}{0,16} - \left[ \frac{5\sqrt{2}}{0,16} \right] \right) \cdot 0,4 \right\}}{5\sqrt{2}} \% = 99,19\%$$

Therefore, the optimal value for the Extrusion width parameter is  $0.4 \times d'$  mm, with a filling ratio of 99.19%.

#### For the clamp assembly component.

When manufacturing the product *with a temperature chamber*, the following observations were made: there was no shrinkage or delamination phenomenon; the surface of the details exhibited good glossiness and smoothness; the threaded portions were well-defined and sharp; the components did not exhibit warping and fit together well during assembly.

When manufacturing the sample *without a temperature chamber*, the following observations were made: delamination occurred in the early layers (approximately 3-4 layers away from the build plate), despite the use of a heated bed. Shrinkage also occurred at various heights of the product, resulting in misalignment of the components during assembly. The dimensional accuracy of the component axis deviated significantly, with a measured value of 9.5 mm compared to the intended design value of 10 mm. These findings indicate that when manufacturing the product using ABS plastic material, a temperature chamber with a value of 70°C or higher is necessary.

Using the optimized parameter values obtained, the cang-shaped product shown in Figure 1 was manufactured to evaluate the specified criteria. The results showed that the product no longer exhibited warping, delamination, and the dimensional error significantly decreased within an acceptable range for products manufactured using FDM technology. Specifically:

- The outer diameters of the cylindrical blocks ( $D_1$ ,  $D_2$ ) were measured as 24.42 mm, 24.43 mm, and 47.18 mm, 47.2 mm, respectively.

- The inner diameters of the holes ( $d_1$ ,  $d_2$ ) were measured as 14.4 mm, 14.38 mm, and 31.6 mm, 31.58 mm, respectively.

- The parallelism of the top and bottom surfaces was within 0.15 mm. This error was mainly due to the surface quality of the top and bottom layers. Additionally, some level of warping still existed in the product. However, the deviation values remained within an acceptable range.

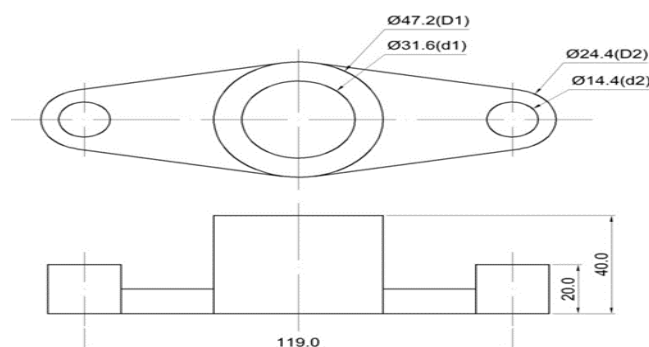


Figure 1. Clamp component

#### 4. CONCLUSION

The article presents the results of optimizing the technological parameters for an open-source FDM 3D printer using ABS material. The findings demonstrate that the quality of FDM products depends on several technological parameters, which can be effectively controlled and adjusted to improve the overall results. During the manufacturing process with ABS material, there is a phenomenon of shrinkage caused by temperature differences between layers and between the newly formed layer and the layer being formed. This phenomenon can be effectively addressed by providing and maintaining a region with a constant temperature value around the product formation area. The parameter optimization process shows a significant improvement in the quality of 3D printed products using ABS material in terms of dimensional accuracy and layer adhesion. To enable the practical application of 3D printed products using ABS material in the industrial field, further investigation is needed to determine and evaluate the influence of technological parameters, particularly the chamber temperature, on quality indicators such as surface roughness, dimensional accuracy, and mechanical properties.

#### Acknowledgements

We would like to thank Ho Chi Minh City University of Technology (HCMUT), VNUHCM for the support of time and facilities for this study.

#### References

- [1] C. C. Negrete, "Optimization of FDM parameters for improving part quality, productivity and sustainability of the process using Taguchi methodology and desirability approach", *The International Journal of Advanced Manufacturing Technology*, vol. 108, (2020), pp. 2131-2147.
- [2] H. Li, T. Wang, J. Sun, and Z. Yu, "The effect of process parameters in Fused Deposition Modelling on bonding degree and mechanical properties", *Rapid Prototyping Journal*, vol. 24, (2018), pp. 80-92.
- [3] K. C. Chyuan et al., "Minimizing warpage of ABS prototypes built with low-cost Fused Deposition Modeling machine using developed closed-chamber and optimal process parameters" *The International Journal of Advanced Manufacturing Technology*, vol. 101, (2019), pp. 593-602.
- [4] C. Casavola et al., "The effect of chamber temperature on residual stresses of FDM Parts", *Residual Stress, Thermomechanics & Infrared Imaging, Hybrid Techniques and Inverse Problems*, vol. 7, (2018), pp. 87-92.
- [5] T. M. Wang, X. J. Tong, and J. Ye, "A model research for prototype warp deformation in the FDM process", *The International Journal of Advanced Manufacturing Technology*, vol. 33, (2007), pp. 1087-1096.
- [6] Y. Liu, B. He, and P. Chen, "Structural design and numerical simulation of FDM molding chamber based on thermal-fluid-structure coupling", *Journal of Physics: Conference Series*, vol. 1600, (2020).
- [7] P. Martin et al., "Polypropylene filled with glass spheres in extrusion-based Additive Manufacturing effect of filler size and printing chamber temperature", *Macromolecular Materials and Engineering*, (2016).
- [8] W. Wu et al., "Manufacture and thermal deformation analysis of semicrystalline polymer polyether ether ketone by 3D printing", *Materials Research Innovations*, vol. 18(S5), (2014), pp. 12-16.
- [9] R. Wichniarek et al., "ABS filament moisture compensation possibilities in the FDM process", *CIRP Journal of Manufacturing Science and Technology*, vol. 35, (2021), pp 550-559.
- [10] V. A. Balogun, N. D. Kirkwood, and P. T. Mativenga, "Direct electrical energy demand in Fused Deposition Modelling", *Procedia CIRP*, vol. 15, (2014), pp. 38-43.
- [11] S. Ding et al., "Dynamic analysis of particle emissions from FDM 3D printers through a comparative study of chamber and flow tunnel measurements", *Environ Sci Technol*, vol. 54, (2020), pp. 14568-14577.
- [12] L. Baich, G. Manogharan, and H. Marie, "Study of infill print design on production cost-time of 3D printed ABS parts", *International Journal of Rapid Manufacturing*, vol. 5, (2015).
- [13] A. C. Bruijn, G. G. Gras, and M. A. Pérez, "Mechanical study on the impact of an effective solvent support-removal methodology for FDM Ultem 9085 parts", *Polymer Testing*, vol. 85, (2020).

**[S1-39] Design of Nested-Stator Coaxial BLDC Motor for Underwater Vehicle**

Lam Cuong Quoc Thai<sup>1,2</sup>, Van Tu Duong<sup>1,2</sup>, Huy Hung Nguyen<sup>3</sup>, Jotje Rantung<sup>4</sup>,  
Xuan Tan Pham<sup>5</sup>, Tan Tien Nguyen<sup>1,2,\*</sup>

<sup>1</sup> National Key Laboratory of Digital Control and System Engineering (DCSELab), Ho Chi Minh City University of Technology (HCMUT), 268 Ly Thuong Kiet Street, District 10, Ho Chi Minh City, Viet Nam

<sup>2</sup> Viet Nam National University Ho Chi Minh City, Linh Trung Ward, Thu Duc City, Ho Chi Minh City, Viet Nam

<sup>3</sup> Faculty of Electronics and Telecommunication, Sai Gon University, Viet Nam

<sup>4</sup> Department of Mechanical Engineering, Sam Ratulangi University, Indonesia

<sup>5</sup> Mechanical Engineering, École Polytechnique de Montréal, Canada

\*Corresponding author: nttien@hcmut.edu.vn

**Abstract**

A structure of a nested-stator coaxial BLDC motor, which comprises a stator positioned between the outer and inner rotor, is presented in this paper. The procedure of computational design of each rotor is provided based on the initially required specification. Subsequently, the electromagnetic simulation is implemented to verify the feasibility of design outcomes. Moreover, a coaxial BLDC motor prototype is also manufactured to validate the reliability of the proposed design through experimentally recorded motor speed and power.

**Keywords:** BLDC motor, Coaxial structure, Nested-stator, Underwater vehicle

**1. INTRODUCTION**

BLDC motors have high torque density, high performance, and efficiency, they are recommended for use in many applications, such as unmanned underwater vehicles [1], variable-speed air conditioners [2], electric superbikes [3], Plug-in Electric Vehicles (PEV) [4],... And coaxial BLDC motors which drive contra-rotating propellers have undergone extensive research because of their high-efficiency propulsion capabilities for use in underwater vehicles, in comparison to single propellers.

There are numerous coaxial motor types, which are represented in Figure 1, and a nested-stator radial-flux coaxial motor is the most popular type which has been studied recently by many researchers. In [5] and [6], the arrangement of the magnets in Halbach array structure was analyzed exactly based on the accurate solution of Laplace's and Poisson's partial differential equations by using a method of separation of variables, and proposed design principles of Dual-Rotor Hybrid PM Machine for Traction Application. In [3], and [7], these authors have indicated and analyzed the double salient dual air-gap structure – a method to improve the magnetic flux control and reduce the cogging torque and associated noise. Meanwhile, regarding dual rotor multiphase BLDC motors, [8] investigated the impact of phase numbers that the increased phase number makes the motor more fault tolerant and increases reliability in turn, decreasing phase current and torque ripples. These characteristics were specified in a five-phase dual-rotor permanent magnet synchronous motor [9], [10].

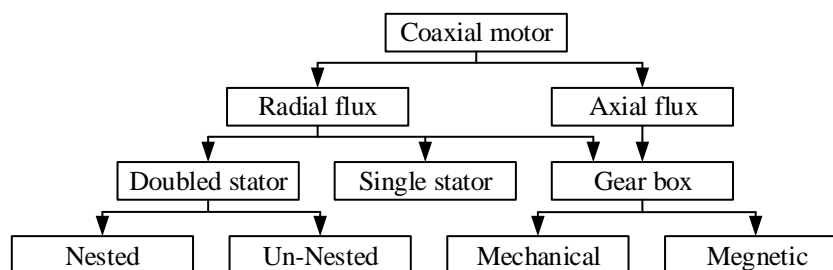


**Figure 1.** Coaxial structure classification chart

A common characteristic among all the aforementioned studies is their purely theoretical nature, lacking any experimental validation. Consequently, this paper takes into account the restrictions of designing the nested-stator radial-flux coaxial motor whose principal diagram is expressed as shown in Figure 2. In order to gain high propulsion efficiency and smooth movement in practical underwater vehicle applications, it is important to achieve a torque balance state through the reliance on a controller which serves to diminish the negative effect caused by noises. Therefore, quantitative such as torque, speed, and power of two rotors are designed to ensure as

the consistency as possible. The design procedures of the inner rotor, as well as the outer rotor, are presented in section 2. The simulation results and experimental results are carried out in section 3. In section 4, the conclusion expresses the achievements of this study.

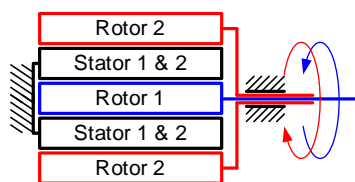


**Figure 2.** The principal diagram of nested-stator radial-flux coaxial motor

## 2. THE NESTED-STATOR COAXIAL BLDC MOTOR

### 2.1. Design

The design procedure of the outer rotor has been given in [11], so only the redesign progress of the inner rotor is presented. Each rotor is individually separated and designed as a single shaft motor, with the haft of the total power allocated for each rotor, expressed in (1).

$$p_{each\_rotor} = p_{total}/2 \quad (1)$$

**Table 1.** Specifications of each rotor

Parameters	Value
Power, w	400
Voltage, v	24
Speed, rpm	2500

According to traditional BLDC motor models, two rotors are redesigned referring to [12], [13] with the change of rotor winding parameters, which attempts to obtain the consistent specifications of both rotors as shown in Figure 2. A number of turns in a single coil are calculated:

$$N_{tc} = \frac{E_{ph} \times 1000}{2 \times n \times \phi_{tt} \times k_w \times k_s \times N_t} \quad (2)$$

where  $E_{ph}$  is the phase back EMF (V);  $n$  is the speed of the rotor (rps);  $k_w$  is the winding factor;  $k_s$  is the slope factor,  $N_t$  is the number of stator teeth.

The total air gap flux is calculated as follows:

$$\phi_{tt} = B_{av} \times \pi \times D \times L \times 0.001 \quad (3)$$

where  $B_{av}$  is the magnetic loading (T);  $D$  is the bore diameter (mm);  $L$  is the stack length (mm).

Phase back EMF is proportional to the input voltage:

$$E_{ph} = \frac{\gamma_{emf} \times V_{dc}}{2} \quad (4)$$

where  $\gamma_{emf}$ : Back EMF factor

The constants of geometrical parameters ( $D$ ,  $L$ ,  $N_t$ ,  $B_{av}$ ) have known, thus the number of turns in a single coil could be found out completely by choosing the proper factors such as winding factor, slope factor, and back EMF factor thanks to winding configuration, and results are expressed in Table 2.

**Table 2.** Redesigned Parameters of each rotor

	Inner rotor	Outer rotor
Number of magnet pair	2	20
Number of teeth	6	36
Length, mm	90	20
Number of winding	24	8

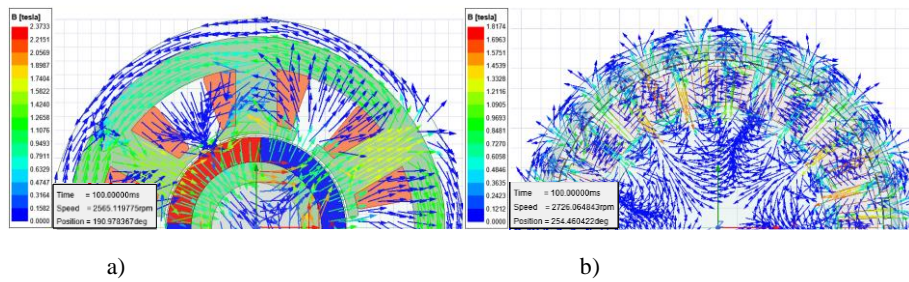


**Figure 3.** Flux density simulation results: a) Inner rotor b) Outer rotor

From the above parameters, models are built to verify the feasibility of material through electromagnetic analysis in transient simulation mode as shown in Figure 3. Observing Figure 3a), approximately 2565 (rpm) is the max speed that the inner rotor could reach. In this state, the ubiquitous value of flux density is concentrated on teeth, frame, and magnet at about 1.7 (T), this figure gains max value inside a small area of the magnet with around 2.3 (T). Regarding Figure 3b), the popular value and max value of flux density achieve nearly 1.1 (T) and 1.5 (T) respectively, at the max speed of 2726 (rpm).

The flux density obtained from simulation results is much smaller than the maximum allowable flux density of electrical steel materials, which is about 2.3 (T). Hence, all redesign parameters are feasible to manufacture both rotors.

## 2.2. Electromagnetic analysis of the nested stator

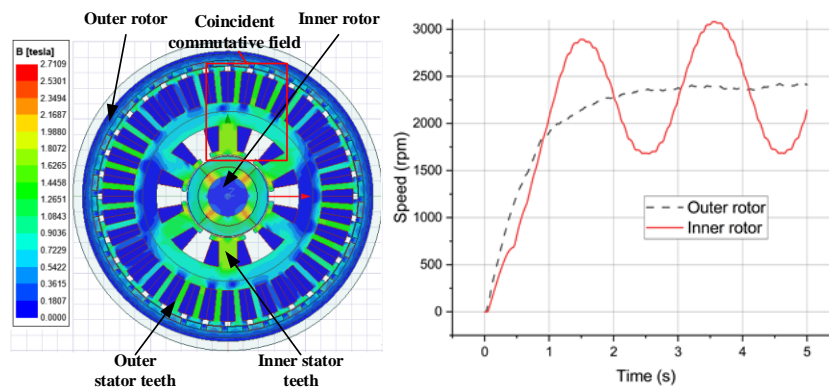


**Figure 4.** The electromagnetic interaction simulation result on the nested stator (left) and step response (right)

Two stators are connected to form a nested stator; design specifications may be affected due to the interaction of both stator fluxes. A simulation of two field rotors combination is built as shown in Figure 4 to analyze these interactions. With the outer stator combining the inner stator, the max flux density reaches a higher value of about 2.7 (T) because both stators are excited causing the fluxes of both to resonate with each other. In terms of speed, this may cause fluctuations during the operation and prevent in start-up process because the electrical cycle of the two stators is not identical. The step response of two rotors shows that the speed of the inner rotor fluctuates with a large amplitude and is difficult to stabilize in the transition period while the speed of the outer rotor is not significantly affected. The main reason is that the excitation area of the outer rotor is wider and covers almost all of the outside area of the inner one in spite of the same magnitude of flux density of the two rotors. The simulation results of the line voltage of the inner rotor as shown in Figure 5 has greater distortion than the outer one.

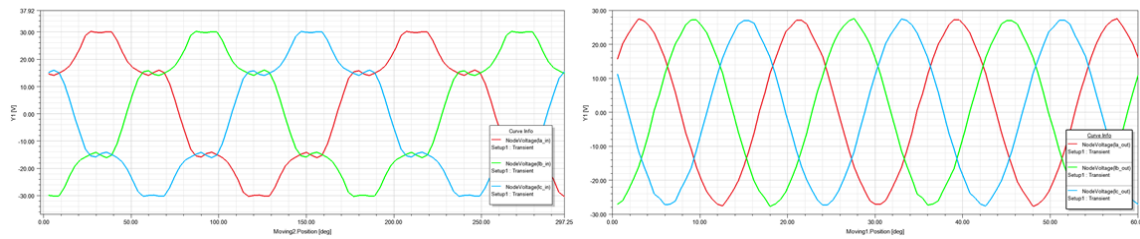


**Figure 5.** Line voltage waveform of the inner rotor (left) and the outer rotor (right)

There are some solutions to overcome these problems such as the aid of a magnetic field barrier between the two stators or separating the two stators independently; and the introduction of the manufacture of nested-stator coaxial BLDC motor in this research.

### 3. EXPERIMENT

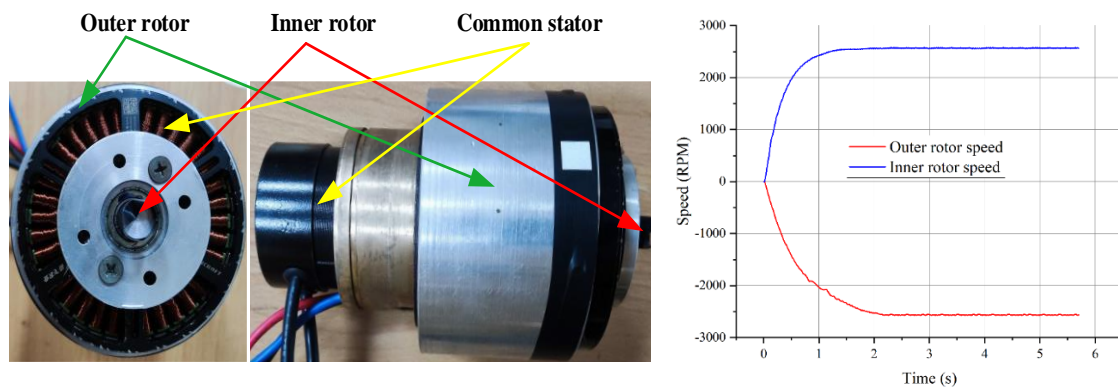


**Figure 6.** Experimental prototype (left) and step response (right) of the nested-stator coaxial BLDC motor

Figure 6 shows the step response of speed of the outer and inner rotor which rotate in opposite directions with the max speed of about 2500 (rpm). Although the max speed of the two rotors shows nearly uniform quantitative, the setting time of the inner and outer rotor is observed as 1.5 (s) and 2 (s), respectively. However, this problem can be addressed by applying a suitable control law. Hence this experimental result proves that the proposed BLDC motor might apply to underwater vehicle applications.

### 4. CONCLUSION

In this study, a design of the nested-stator coaxial BLDC motor is expressed and the results of the theoretical computation have been verified through simulation by the specialized software. The impact of flux interaction on the shared stator, specifically in terms of speed and power, is also examined. Furthermore, potential solutions to mitigate this influence are identified. Moreover, several reasons have been presented for the failure to gain design speed through the experiment with the prototype of a nested-stator coaxial BLDC motor. In the next study, an anti-torque controller is going to be studied to apply for this nested-stator coaxial BLDC motor in underwater vehicle applications.

### Acknowledgments

This research is funded by Viet Nam National University Ho Chi Minh City (VNUHCM) under grant number TX2023-20b-01. We acknowledge the support of time and facilities from National Key Laboratory of Digital Control and System Engineering (DCSELab), Ho Chi Minh City University of Technology (HCMUT), VNUHCM for this study.

## References

- [1] D. Uygun, S. Solmaz, A. Turan, and S. T. Ruzgar, “A new topology for dual rotor/stator BLDC motors applied to marine thrusters”, *Int. Conf. Power Eng. Energy Electr. Drives*, vol. 2015-Septe, no. 113, pp. 353–359, 2015, doi: 10.1109/PowerEng.2015.7266342.
- [2] Y. H. Yeh, M. F. Hsieh, and D. G. Dorrell, “Different arrangements for dual-rotor dual-output radial-flux motors”, *IEEE Trans. Ind. Appl.*, vol. 48, no. 2, pp. 612–622, 2012, doi: 10.1109/TIA.2011.2180495.
- [3] D. Golovanov, A. Galassini, L. Flanagan, D. Gerada, Z. Xu, and C. Gerada, “Dual-rotor permanent magnet motor for electric superbike”, 2019 IEEE Int. Electr. Mach. Drives Conf. IEMDC 2019, no. May, pp. 951–956, 2019, doi: 10.1109/IEMDC.2019.8785287.
- [4] A. V. Sant, V. Khadkikar, W. Xiao, and H. H. Zeineldin, “Four-Axis Vector-Controlled Dual-Rotor PMSM for Plug-in Electric Vehicles”, *IEEE Trans. Ind. Electron.*, vol. 62, no. 5, pp. 3202–3212, 2015, doi: 10.1109/TIE.2014.2387094.
- [5] D. Golovanov, and C. Gerada, “An Analytical Subdomain Model for Dual-Rotor Permanent Magnet Motor with Halbach Array”, *IEEE Trans. Magn.*, vol 55, no 12, 2019, doi: 10.1109/TMAG.2019.2941699.
- [6] Y. Li, D. Bobba, and B. Sarlioglu, “Design and optimization of a novel dual-rotor hybrid PM machine for traction application”, *IEEE Trans. Ind. Electron.*, vol. 65, no. 2, pp. 1762–1771, 2018, doi: 10.1109/TIE.2017.2739686.
- [7] C. V. Aravind, M. Norhisam, I. Aris, M. H. Marhaban, and M. Nirei, “Static characteristics of the double rotor switched reluctance motor”, *PECon 2012 – 2012 IEEE Int. Conf. Power Energy*, no December, pp. 402–407, 2012, doi: 10.1109/PECon.2012.6450246.
- [8] M. Hussain, A. Ulasyar, H. Sheh Zad, A. Khattak, S. Nisar, en K. Imran, “Design and Analysis of a Dual Rotor Multiphase Brushless DC Motor for its Application in Electric Vehicles”, *Eng. Technol. Appl. Sci. Res.*, vol. 11, no. 6, pp. 7846–7852, 2021, doi: 10.48084/etasr.4345.
- [9] J. Zhao, X. Gao, B. Li, X. Liu, and X. Guan, “Open-phase fault tolerance techniques of five-phase dual-rotor permanent magnet synchronous motor”, *Energies*, vol. 8, no. 11, pp. 12810–12838, 2015, doi: 10.3390/en81112342.
- [10] H. Chen, X. Liu, J. Zhao, and N. A. O. Demerdash, “Magnetic-Coupling Characteristics Investigation of a Dual-Rotor Fault-Tolerant PMSM”, *IEEE Trans. Energy Convers.*, vol. 33, no. 1, pp. 362–372, 2018, doi: 10.1109/TEC.2017.2747519.
- [11] L. C. Q. Thai, “Study on Designing of Coaxial BLDC Applied for Underwater Vehicle”, in *International Conference on Intelligent Unmanned Systems*, 2021, vol. 15, no. 2, pp. 1–23.
- [12] D. C. Hanselman, *Brushless Motor Design*. 1994.
- [13] D. Hanselman, *Brushless permanent magnet motor design*. 2003.

**[S1-52] Study on Energy Conversion Efficiency of Wave Actuating Ship**

Phan Huy Nam Anh\*, Hyeung-Sik Choi

*Department of Mechanical Engineering, Korea Maritime & Ocean University, Busan 49112, Korea Abstract**\*Corresponding author: phanhuynamanh97@gmail.com***Abstract**

Wave-powered vessels are a type of vehicle that has been introduced for decades. Compared with conventional vessels, it has apparent advantages, such as harnessing wave energy to propel the ship, supporting the primary propulsion device, and optimizing the ship's hull design. This study presents a new concept of the wave actuator for ship propulsion. The wave actuator efficiently converts the hydraulic force of the wave surge force to the ship into thrusting forces. In the thesis, the modeling of the wave actuator was studied. For this, the hydrodynamical modeling of the new wave actuator is presented through an analysis of the structure of the wave actuator. Also, ship motion excited by wave forces is studied. Based on the modeling of the wave actuator, analyses of the energy conversion capacity of the wave actuator were performed. To validate the good performance of the proposed wave actuator, numerous computer simulations were performed in several sea environments using MATLAB. Computational fluid dynamics (CFD) techniques are used for the hydrodynamic analysis of ships. The simulation results show that the cruise speed of the ship is exploited very efficiently by the wave energy absorption system.

**Keywords:** *The wave actuator, Regular wave, The cruise speed, Capture width ratio of wave energy converters*

**References**

- [1] Joseph A. Gause, 1348 Dundas St., Burlington, Ontario, Canada, Water-borne vessel comprising propulsion system incorporating flexible fin propulsion members, US3453981A
- [2] M. Reichela and A. Bednareka, The experimental studies on hydrofoil resistance at Ship Design and Research Centre (CTO S.A.).
- [3] Yang Song-Lin, Ma Qing-Wei, Chen Shu-Ling, Gao Lei and Wu An, Experimental Research on Resistance Performance of Gliding-Hydrofoil Craft with a T-Formed Hydrofoil and Shallow V-Shaped Bottom. The International Conference on Computational & Experimental Engineering and Sciences, 2008, 5(1), pp. 7-14.
- [4] J. E. Manley, G. Hine, Unmanned surface vessels (usvs) as tow platforms: Wave glider experience and results, Oceans 2016 Mts/Ieee Monterey (2016), pp. 1–5.
- [5] Prof. Dr.-Ing. habil. Nikolai Kornev, Rostock (2012), Ship dynamics in waves (Ship Theory II), Faculty of Mechanical Engineering and Sea Technology Chair of Modelling and Simulation.
- [6] J. M. J. Journée and W.W. Massie (2001), Offshore hydromechanics, Delft University of Technology.
- [7] Shu-Xia Bua, Min Gua, Jiang Lua, Moustafa Abdel-Maksoud, Effects of radiation and diffraction forces on the prediction of parametric roll, Ocean Engineering 175 (2019), pp. 262-272.
- [8] A. G. Abul-Azma, M. R. Gesraha, Approximation to the hydrodynamics of floating pontoons under oblique waves, Ocean Engineering, 27 (2000), pp. 365–384.
- [9] ITTC 1957 Recommended procedures and guidelines 7.5-02-02-02



**[S1-1] Design of Two-Shaft Crusher in Domestic Waste Treatment System**

Phung Tran Hanh<sup>1,5</sup>, Thanh-Long Le<sup>1,2,5,\*</sup>, Thi-Hong-Nhi Vuong<sup>3,5</sup>, Nguyen Quang Minh<sup>1,5</sup>, Nguyen Thanh Hai<sup>1,5</sup>, Tran Dang Long<sup>3,5</sup>, Tran Quang Lam<sup>3,5</sup>, Tran Thien Hau<sup>4,5</sup>, Tran Trong Hy<sup>1,5</sup>

<sup>1</sup> Faculty of Mechanical Engineering, Ho Chi Minh City University of Technology (HCMUT), 268 Ly Thuong Kiet Street, District 10, Ho Chi Minh City, Viet Nam

<sup>2</sup> National Key Laboratory of Digital Control and System Engineering (DCSELab), HCMUT, 268 Ly Thuong Kiet Street, District 10, Ho Chi Minh City, Viet Nam

<sup>3</sup> Faculty of Transportation Engineering, Ho Chi Minh City University of Technology (HCMUT), 268 Ly Thuong Kiet Street, District 10, Ho Chi Minh City, Viet Nam

<sup>4</sup> Faculty of Applied Science, Ho Chi Minh City University of Technology (HCMUT), 268 Ly Thuong Kiet Street, District 10, Ho Chi Minh City, Viet Nam

<sup>5</sup> Viet Nam National University Ho Chi Minh City, Linh Trung Ward, Thu Duc City, Ho Chi Minh City, Viet Nam

\*Corresponding author: ltlong@hcmut.edu.vn

**Abstract**

This paper presents a novel design of a two-shaft crusher aimed at improving its energy efficiency and throughput. A detailed analysis of the crusher's design and operating parameters was conducted and optimized its performance. Blade angle, thickness, and rotation speed were adjusted to determine their effects on the shredder's throughput and energy efficiency. The experimental results showed a significant improvement in the shredder's performance, particularly in energy efficiency. The study showed the details of the crusher's design parameters. The findings can contribute to the development of more efficient waste processing systems. The optimized design of the crusher can be adopted by industries that use two-shaft crushers for waste reduction.

**Keywords:** Crusher machine, Two-shaft crusher, Blades shafts, Optimized design, Crushing process

**1. INTRODUCTION**

In recent years, with the increasing demand for all aspects of human life, the issue of dealing with enormous amounts of waste has become a top priority. As a result, we need effective, safe, and environmentally friendly waste treatment measures. Currently, in Viet Nam, the issue of waste treatment and recycling is receiving more attention than ever before. In recycling areas, they have contributed to reducing costs for solid waste treatment in urban areas [1]. Modern waste treatment solutions such as waste sorting at the source, smart trash cans, and MFC (a green, clean process that generates electricity from liquid waste, especially wastewater) [2]. However, in the current situation in Viet Nam, these modern solutions have not been thoroughly researched and invested in.

The crushing process can also be applied in recycling thermoplastic and thermosetting composite materials. The product of the composite recycling process is plywood, which can be used to produce manhole covers, electrical cabinets, bricks, and a new composite recycling process in the future could convert composite materials into recycled components, oil, and original fiber [3]. The crusher has the function of classifying and crushing waste, reducing the volume of waste, and facilitating subsequent processes such as transportation and recycling. Such as being able to crush many types of waste, having a simple and sturdy structure, easy to operate and maintain, and having high productivity [4 – 7].

In this paper, we propose the design of a two-shaft crusher to increase productivity and be easy to use. The adoption of the optimized design has the potential to result in significant energy savings and cost reduction for operations.

**2. DESIGN OPTIONS****2.1. Technical requirements**

The two-shaft crusher is an important piece of equipment in the recycling and processing of scrap. To perform well the crushing and processing of scrap, the two-shaft crusher needs to meet some of the following technical requirements:

- + Simple structure, low energy consumption, suitable deceleration ratio.
- + High yield, suitable for both dry and wet grinding.
- + Easy to disassemble and maintain.
- + Maintenance, easy maintenance with low cost.
- + The output material size is guaranteed compared to the requirement.

## 2.2. Working principle

Figure 1 shows the design of a two-shaft crusher including the following parts: Motor, Belt, Cutter shaft, Lists, and Blade. Garbage is dropped through the number position. Two motors work to rotate two pulleys of the belt drive. The belt drives 5 drives two rotating shafts to cut waste to the required level. The number 2 plate works to keep the garbage from running through. Waste after being chopped will be discharged at door 4 and go down to the conveyor system at the bottom.

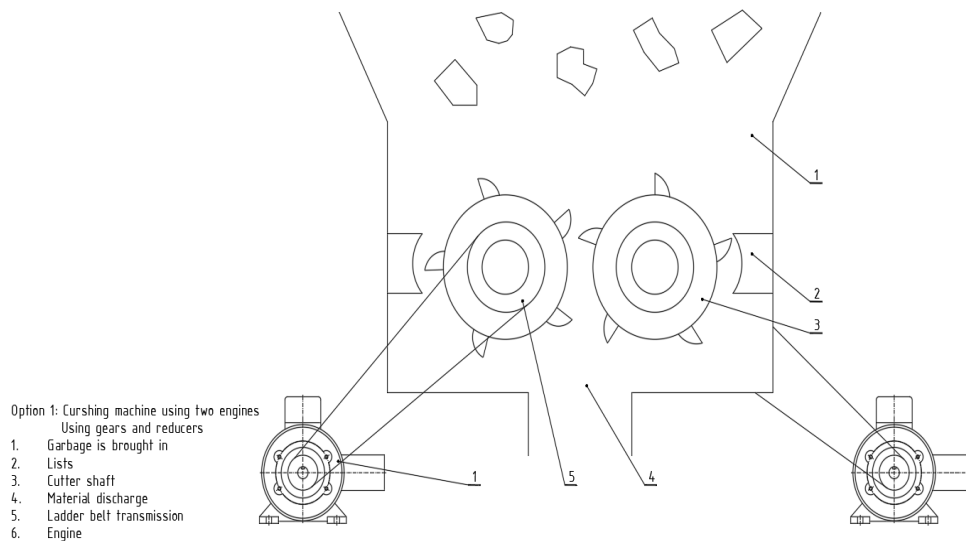


Figure 1. Crusher design plan

## 3. DESIGNING THE CRUSHERS MACHINE

### 3.1. Shaft diameter

According to theoretically calculate the minimum shaft diameter for the crusher [8], in the crushers, the actual grinding shaft diameter is usually 2.5 - 3.0 times the diameter of the shaft  $D_{\min}$ . Here we choose  $D_{\min} = 100 \text{ mm}$ . To ensure the grinding shaft has high rigidity and withstands the torque when operating:

So, we have the diameter of the shaft:

$$D = (2 \div 3) D_{\min} = 200 \div 300 \text{ mm} \quad (1)$$

Choose a shaft whose diameter is:  $D_1 = D_2 = 280 \text{ mm}$ .

For the cutter and the mill shaft to work stably without shaking, we choose the inner diameter of the knife as  $D \approx 280 \text{ mm}$ .

### 3.2. Determination of the energy requirement

According to the durable condition of the material, the force acting on the material:

$$\frac{P}{F} \geq [\tau_c] \rightarrow P \geq [\tau_c] \times F \quad (2)$$

where  $P$  is the force acting on the material ( $N$ ),  $F$  is the sectional cross-section of the material  $F = 80 \times 180 \text{ mm}^2$ , and  $[\tau_c]$  is the shear strength of the material which is said to be equivalent to aluminum:  $60 \text{ (Mpa)}$ .

So, we get  $P \geq 86400 \text{ N}$ .

### 3.3. Shaft speed

For the material not to slip back on the shaft, reducing the machine's productivity, the limited number of revolutions ( $n$ ) is calculated [9]:

$$n = 616 \times \sqrt{\frac{f}{\rho \cdot d_0 \cdot D}} \quad (\text{rpm/m}) \quad (3)$$

where,  $\rho$  is the density of the material to be crushed  $\rho = 180 \text{ kg/m}^3$ ,  $f \approx 0.15 \times D$ ,  $d_0$  is the material diameter when inserted  $d_0 = 0.25 \text{ m}$ . Get  $n = 35 \text{ rpm/m}$ .

### 3.4. Theoretical productivity of the machine

Estimated capacity ( $Q$ ) of two-shaft crusher in an hour:

$$Q = 0.235 \times \mu \times \rho \times L \times D \times d \times n = 8.36 \text{ tons/h} \quad (4)$$

where  $\mu$  is the material breaking coefficient, we choose  $\mu = 0.2$ ,  $\rho$  is the density of the material to be crushed  $\text{kg/cm}^3$ ,  $L$  is the length of the shaft, we choose  $L = 120 \text{ cm}$ ,  $d$  is the material diameter after crushing,  $d = 100 \text{ mm} = 10 \text{ cm}$ , and  $n$  is the number of revolutions of the shaft  $n = 35 \text{ rpm/m}$ .

### 3.5. Productivity of working part

The power required to overcome the material friction on the shaft, the friction on the bearing. Power ( $N$ ) is calculated by:

$$N = \frac{L \times D \times n}{35300} \left( \frac{d_0}{2} + \frac{D^2}{24000} \right) \quad (5)$$

where  $d_0$  is the material diameter before grinding  $25 \text{ cm}$ , get  $N \approx 35 \text{ kW}$ .

The power of the motor to be supplied to the two-shaft crusher [10] is:

$$P = \frac{N}{\eta} = \frac{35}{0.86} = 39.7 \text{ kW} \quad (6)$$

Choose the engine with productivity  $P = 45 \text{ kW}$  and  $n = 1470 \text{ rpm/h}$ .

### 3.6. Belt design

The number of belts ( $z$ ) used in the belt drive [11]:

$$z \geq \frac{P}{[P_0] C_\alpha C_u C_L C_Z C_v C_r} \quad (7)$$

where  $P$  is the power of the belt ( $\text{kW}$ ),  $[P_0]$  is the allowable effective power determined experimentally,  $C_\alpha, C_u, C_L, C_Z, C_v, C_r$  are the influence coefficients, we have:

$$z \geq 3.58 \text{ Choose } z = 4.$$

The length of a belt ( $L$ ) in the belt drive is:

$$L = 2a + \frac{\pi(d_1 + d_2)}{2} + \frac{(d_1 - d_2)^2}{4a} \quad (8)$$

Where  $d_1$  và  $d_2$  is the diameter of the pulley used respectively  $250 \text{ mm}$  and  $500 \text{ mm}$

$a$  is the distance between the pulleys and is  $600 \text{ mm}$ .

Therefore,  $L = 2404.14 \text{ mm}$ .

According to the standard, choose  $L = 2500 \text{ mm}$ .

### 3.7. Design of two-shaft crusher

After calculating the main parameters for the two-shaft crusher, the machine is modeled in SOLIDWORKS 2021 software. Figure 2 demonstrates the completed model of the two-shaft crusher with vertical, level, and side views.

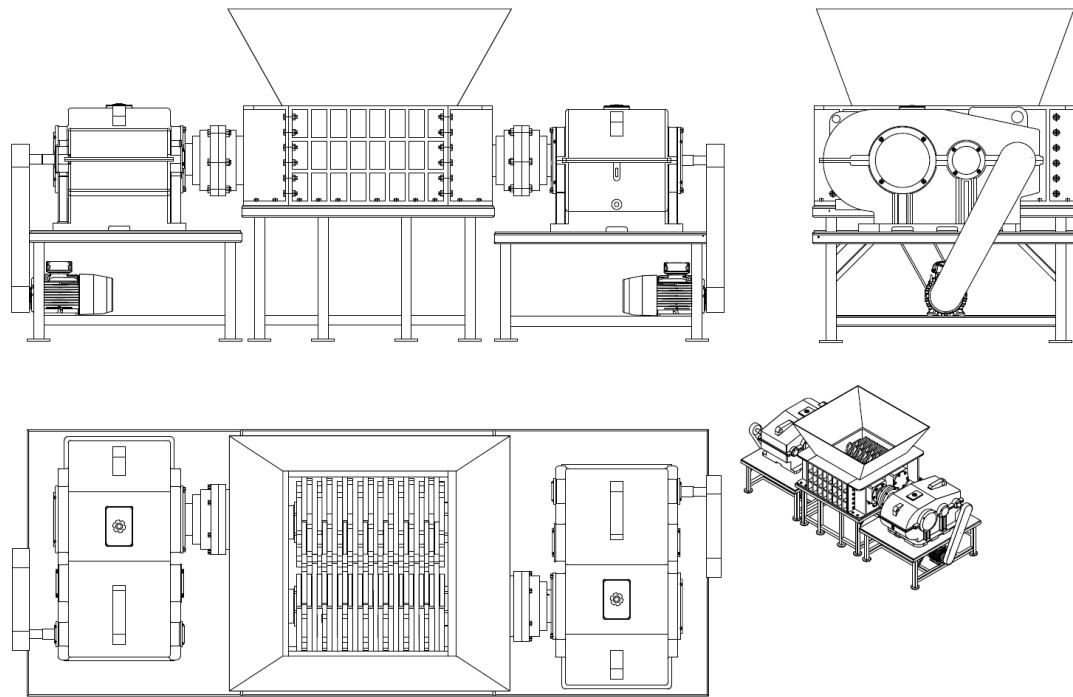


**Figure 2.** Design drawings of crushers

#### 4. CONCLUSION

In this paper, we have discussed the design of a two-shaft crusher. This crusher can be used to crush and recycle a range of materials, from plastic to metal. With its simple structure and ease of use, the two-shaft crusher can help increase productivity and reduce costs, while also contributing to reducing our impact on the environment. It is important to comply with occupational safety regulations and use protective equipment to avoid accidents. Eventually, the two-shaft crusher is an effective solution for crushing and recycling materials in manufacturing plants.

#### Acknowledgments

This research is supported by DCSELab and funded by Viet Nam National University Ho Chi Minh City (VNUHCM) under grant number TX2023-20b-01. We acknowledge the support of time and facilities from Ho Chi Minh City University of Technology (HCMUT), VNUHCM for this study.

#### References

- [1] T. N. Phuc, Y. Matsui and T. Fujiwara, Assessment of plastic waste generation and its potential recycling of household solid waste in Can Tho City, Vietnam, *Environ Monit Assess*, 175 (2011), pp. 23 – 35.
- [2] B. P. Numbi, X. Xia, Optimal energy control of a crushing process based on vertical shaft impactor, *Applied Energy*, 162 (2016), pp. 1653 – 1661.
- [3] Y. W. Li, L. L. Zhao, E. Y. Hu, K. K. Yang, J. F. He, H. S. Jiang, Q. F. Hou, Laboratory scale validation of a DEM model of a toothed double-roll crusher and numerical studies, *Power Technology*, 356 (2019), pp. 60 – 72.
- [4] D. K. T. Nhu, D. V. Tran, T. T. Phung, T. P. Tran, An overview of recycling methods from composite wastes, *Journal of Mining and Earth Sciences*, 62 (2021), pp. 69 – 79.
- [5] I. Sulaiman, E.A.P. Egbe, M. Abdullahi, Y.A. Saraki and I.A. Shehu, Design and Performance Evaluation of a Stone Crusher, *UNIOSUN Journal of Engineering and Environmental Sciences*, 3(2) (2021), pp. 70 – 77.

- [6] J. Aleluia, P. Ferrão, Characterization of urban waste management practices in developing Asian countries: A new analytical framework based on waste characteristics and urban dimension, *Waster Management*, 58 (2016), pp. 415 – 429.
- [7] J. Melicherčík, T. Kuvik, J. Krilek, I. Čabalová, Design of the Crusher for Plastic and Rubber Waste Produced in Automotive Industry, *FME Transactions*, 49 (2021), pp. 734 – 739.
- [8] R. G. Budynas, J. K. Nisbett, *Shigley's Mechanical Engineering Design*, McGraw – Hill, 9th Edition (2011).
- [9] D. G. Ullman, *The Mechanical Design Process*, McGraw – Hill, 4th Edition (2010).
- [10] R. L. Mott, *Machine Elements in Mechanical Design*, Pearson Prentice Hall, 4th Edition (2010).
- [11] J. A. Collin, H. R. Busby, G. H. Staab, *Mechanical Design of Machine Elements and Machines*, John Wiley & Sons Inc., 2nd Edition (2009).

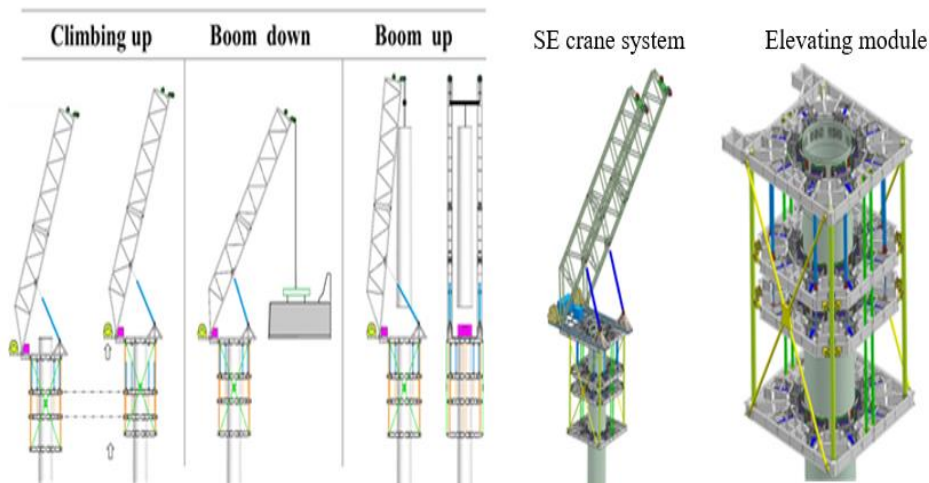
**[S1-53] Structural Characteristic Evaluation of Self-Elevating Crane System**Hoseung Jeong<sup>1</sup>, Manjung Yoon<sup>2</sup>, Jongrae Cho<sup>3,\*</sup><sup>1</sup> National Korea Maritime & Ocean University, Busan 49112, Korea<sup>2</sup> Power MnC Co., Ltd., Ulu-gun, Ulsan 44988, Korea<sup>3</sup> Division of Mechanical Engineering, National Korea Maritime & Ocean University, Busan 49112, Korea

\*Corresponding author: cjr@kmou.ac.kr

**Abstract**

Generally, large cranes are used for the installation or maintenance of onshore wind power systems. However, the limitations of available large cranes and the mobility challenges posed by mountainous terrain increase construction costs and time. In response to the global trend of increasing wind turbine size and reducing construction costs, the development of Self-Elevating crane (SE crane) systems for the installation and maintenance of wind towers is underway worldwide. This system utilizes the rigidity of the wind tower to enable self-elevation and has a maximum lifting capacity of 100 tons and a maximum working radius of 15 meters. The objective of this study is to evaluate the structural characteristics of the SE crane system and wind tower under operational conditions to ensure their safety during various operations, including elevating and lifting operations.

The safety of both the SE crane system and the wind tower must be ensured during various operations, including lifting and hoisting. It created a complete model consisting of the SE crane system attached to the elevated wind tower and observed the stress state, attachment state, and clamping load of the crane and wind tower under operating conditions. Computational structural analysis was performed on the generated model. The stress state in the SE crane system and wind tower, as well as the reaction forces on the clamping pads, were observed for elevating and lifting operation radius. As a result, we were able to determine the structural characteristics and clamping load under various operating conditions. The maximum stress and clamping load were observed during the hoisting operation at the maximum working radius. As the cylindrical shell-shaped wind tower is subjected to various clamping loads during operation, it is necessary to observe its stress and buckling characteristics. Buckling analysis was performed to evaluate the stability of the wind tower, and local buckling modes were observed at the locations where the clamping load was applied. Buckling modes and buckling critical load factors were provided.

**Figure 1.** Main operating conditions**Figure 2.** 3D CAD model of SE crane system

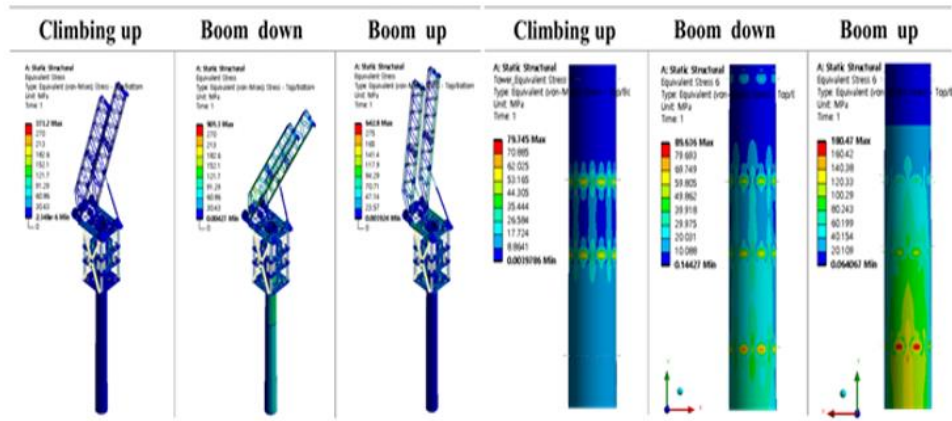


**Figure 3.** Stress distributions of SE crane      **Figure 4.** Stress distributions of wind tower

**Keywords:** Self-Elevating crane system, Wind turbine tower, Installation, Maintenance, Structural analysis, Pad reaction

### Acknowledgments

This work was supported by Korea Institute of Energy Technology Evaluation and Planning (KETEP) grant funded by the Korea government (MOTIE) (20213030020160, Development of Self-Elevating Crane System for Installation and Maintenance of Onshore Wind Turbine System).

### References

- [1] British Standard, Rules for the design of cranes, Part 1. Specification for classification, stress calculations and design criteria for structures (BS 2573: Part 1: 1983)

## [S2-12] Harvesting Magnetic Field Energy from Power Lines and Using it as a Power Source for Low-Power Wireless Sensor Systems

Kyung-Rak Sohn<sup>1,\*</sup>, Hyun-Sik Kim<sup>2</sup>

<sup>1</sup> Korea Maritime and Ocean University, Busan, Korea, 49112

<sup>2</sup> Mattron Corporation, Changwon, Korea, 51756

\*Corresponding author: krsohn@kmou.ac.kr

### Abstract

In this paper, we propose a method for harvesting the magnetic field generated by a household power line and utilizing it as a power source for a wireless sensor system. The power harvesting device is designed and simulated using COMSOL software. The device incorporates a silicon steel plate as a magnetic core and successfully harvests 400 mW of power with a primary current of 5.8 A. This harvested power is sufficient to operate an Arduino-based temperature and humidity sensing system. The proposed power harvesting method could be an effective solution for powering wireless sensor systems that monitor environmental parameters in residential or commercial settings.

**Keywords:** Magnetic energy harvesting, Soft magnetic core, Self-powered sensors, Wireless sensors

### 1. INTRODUCTION

This paper focuses on energy harvesting technology as a self-power generation method for a low-power wireless sensor system deployed in any location. Typically, these systems rely on replaceable batteries, but as the number of sensor nodes increases, regular inspection and replacement become labor-intensive tasks. Energy harvesting technologies encompass various methods such as light [1], electromagnetic radiation [2], piezoelectric vibration [3], static electricity [4], and thermoelectric energy [5]. They capture and convert wasted or discarded energy from the surrounding environment into electrical power [6]. We present a system that converts the magnetic field generated by a wire into electrical energy. The utilization of magnetic cores in the inductive coupling method allows for the generation of a relatively substantial amount of electrical energy compared to other forms of energy harvesting.

### 2. DESIGN AND EXPERIMENTAL RESULTS OF ENERGY HARVESTER

As illustrated in Figure 1, the proposed self-powered wireless sensor system comprises three main components: an energy harvester, an AC-DC converter, and a wireless sensor system. One crucial element of the energy harvester is the current transformer (CT), which extracts AC voltage from the magnetic field of the power line. The harvested AC voltage is then converted into a stable DC voltage using an AC-DC converter. This converted voltage is adjusted to fall within the allowable voltage range required by the Arduino processor circuit, guaranteeing a stable and consistent power source for the system's operation.

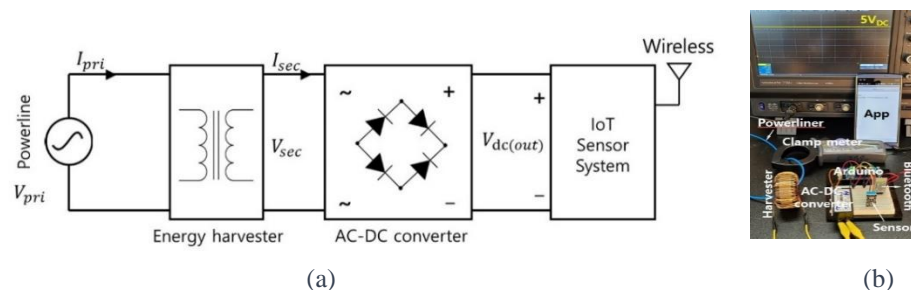


**Figure 1.** Magnetic energy harvesting system. (a) Schematic diagram, (b) experimental setup

To measure the output power, the load resistance was varied while different currents flowed through the wire. The results are shown in Figure 2. In the unsaturated region, as the load resistance increases, the power output also increases proportionally. However, in the saturation region, the power decreases with an increasing load



resistance. The maximum harvested power is achieved at the peak value between these two extremes. For instance, to harvest 500 mW of power from a primary current of 5.8 A, a load resistance of 200  $\Omega$  is sufficient.

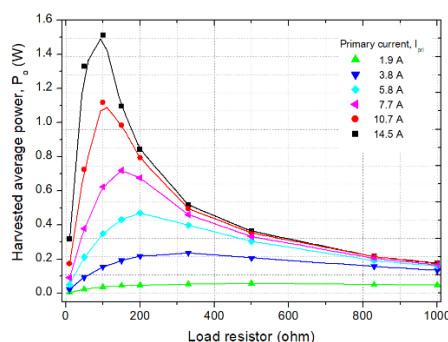


**Figure 2.** Harvested power measured as a function of primary current and load resistance

The self-powered wireless sensor system is composed of a temperature and humidity sensor (DHT-11 sensor) for data collection, and Bluetooth (HC-06) is employed for data transmission. The power consumption of the Arduino sensor system that was manufactured amounts to 330mW. Taking into account the power consumption margin, a primary current of 5.8 A and a load resistance of 330  $\Omega$  were chosen to harvest 400 mW. At these settings, the power density harvested per unit volume of the magnetic core is measured to be 25.6 mW/cm<sup>3</sup>.

### 3. CONCLUSION

This paper presents a magnetic field energy harvester that achieves a high-power density per unit volume of the core. The proposed design was evaluated through COMSOL simulations and experimental testing, demonstrating its performance. Our findings indicate that silicon steel is more suitable for magnetic energy harvesting compared to ferrite or nanocrystals due to its higher saturation magnetic flux density.

### Acknowledgments

This research was financially supported by the Ministry of SMEs and Startups (MSS), Korea, “Regional Specialized Industry Development Program (S3365146)” supervised by Korea Institute for Advancement of Technology (KIAT).

### References

- [1] X. Yue et al., “Development of an Indoor Photovoltaic Energy Harvesting Module for Autonomous Sensors in Building Air Quality Applications,” *IEEE Internet of Things Journal*, vol. 4, no. 6, pp. 2092-2103, Dec. 2017.
- [2] J. Moon, S. B. Leeb, “Analysis model for magnetic energy harvesters,” *IEEE Trans. Power Electr.*, vol. 30, no. 8, pp. 4302-4311, 2015.
- [3] H. Xiong, L. Wang, “Piezoelectric energy harvester for public roadway: On-site installation and evaluation,” *Appl. Energy*, vol. 174, 15, pp. 101-107, 2016.
- [4] Y. Zhang et al., “Micro electrostatic energy harvester with both broad bandwidth and high normalized power density,” *Appl. Energy*, vol. 212, pp. 362-371, 2018.
- [5] M. Guan, K. Wang, D. Xu, and W. Liao, “Design and experimental investigation of a low voltage thermoelectric energy harvesting system for wireless sensor nodes,” *Energy Conversion Management*, vol. 138, 15, pp. 30-37, 2017.
- [6] X. Tang et al., “Energy Harvesting Technologies for Achieving Self-Powered Wireless Sensor Networks in Machine Condition Monitoring: A Review” *Sensors* 18, no. 12: 4113.

## [S2-20] A Cost-Effective Workflow Scheduling Considering Deadline Constraint in a Cloud

Nguyen Bui Thanh Truc, Phan Nguyen Ky Phuc\*

*International University, Ho Chi Minh City, Viet Nam, 700000*

\*Corresponding author: pnkphuc@hcmiu.edu.vn

### Abstract

With the rapid advancement of cloud computing, the migration of various applications to cloud platforms has become increasingly prevalent across diverse fields. Among the challenges associated with cloud computing, workflow scheduling stands out as a critical issue that aims to ensure the efficient execution of workflows while considering important constraints such as deadlines and budget limitations. Although heuristic algorithms have been utilized to address simplified versions of the problem, they often encounter difficulties in finding feasible solutions or achieving optimization objectives. To address these challenges, this study proposes a novel approach for cost-effective workflow scheduling by employing a Mixed Integer Linear Programming (MILP) framework. The objective of the proposed scheme is to schedule workflows with the lowest possible cost while satisfying the given deadline constraint. By formulating the problem as an MILP model, the study aims to provide an optimal and efficient solution to workflow scheduling in cloud environments. The experimental results based on two common scientific workflows provide evidence of the approach's effectiveness in achieving the desired objectives, thereby highlighting its applicability and potential for enhancing workflow scheduling in cloud-based systems.

**Keywords:** *Cloud computing, Mathematical, Mixed integer linear programming, Optimization, Workflow scheduling*

### 1. INTRODUCTION

The introduction of cloud computing has emerged as a solution to address the complexities and escalating computational demand associated with large-scale scientific applications. In present times, cloud computing has become an integral part of information technology, offering virtual resources to support back-end processing across various multi-tier applications. Notably, according to IDC, the global spending on cloud computing services has surpassed \$706 billion and is projected to reach \$1.3 trillion by 2025 [1]. Gartner has estimated that the global public cloud services end-user spending will rise to \$600 billion by 2023 [2]. Moreover, a report by McKinsey & Company indicates that Fortune 500 companies can potentially leverage cloud cost-optimization levers and value-oriented business use cases, resulting in more than \$1 trillion in run-rate EBITDA by 2030. As a result, in 2022, over \$1.3 trillion in enterprise IT spending is expected to shift towards cloud computing, with this number growing to almost \$1.8 trillion by 2025, according to Gartner.

The rapid growth of cloud computing is widely recognized by both academic researchers and industry professionals, as it presents an effective solution to address the issue of limited resources and significantly reduces the costs associated with acquiring and maintaining physical resources. Additionally, cloud computing offers virtually unlimited resources at varying price points, which can be dynamically and elastically allocated to meet diverse application requirements. Consequently, a significant amount of research has been conducted in the area of optimally allocating computing resources for workflows submitted to clouds. This is due to the fact that the workflow scheduling problem is an NP-hard problem, and therefore requires tailored algorithms to minimize the total cost of VM leasing while meeting workflow deadline constraints. Previous research has primarily focused on minimizing total execution time or maximizing energy efficiency in clusters and grids. Nevertheless, tackling the complexity of workflow scheduling problems remains a significant challenge, as heuristic reasoning alone often fails to produce high-quality solutions. Even finding a feasible solution that satisfies all the problem's constraints is a formidable task. Previous research has primarily focused on simplified versions of these problems and has relied on heuristic algorithms that frequently generate solutions that violate workflow deadlines [3-7]. To confront this challenge, this study explores the utilization of mixed linear integer programming (MILP) to formulate and solve intricate workflow scheduling problems. The MILP framework has been underutilized in

previous studies within this domain. By applying MILP, workflow scheduling problems are described precisely, capturing all complex constraints, requirements, and objectives, yielding the most optimal solutions.

The highlights of the research paper are summarized as follows:

- Proposed a cost-effective workflow scheduling algorithm with deadline constraints with the objective to reduce the total cost of the scheduling process while meeting the deadline constraints.
- Numerical experiments are conducted to evaluate the effectiveness of the MILP approach.

## 2. PROBLEM DESCRIPTION

### 2.1. Application tasks

Workflows are often used to model the cloud application task of many fields such as real-time analytics or online advertising industries. These tasks are executed based on their data dependencies. These tasks have parent-child relationship. The parent task should be executed before its child task. It can be modeled as a Direct Acyclic Graph (DAG) consisting of nodes and edges. Workflows can be represented as  $W = (T, E)$ , where  $T$  is a set of tasks  $t_1, t_2, \dots, t_n$  and  $E$  is an edge  $(t_a, t_b)$ . Following diagram shows a workflow.

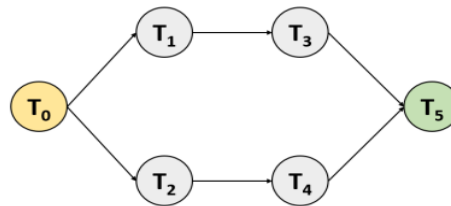


Figure 1. A simple DAG workflow

The figure above shows the dependencies among different tasks in a workflow graph  $G$ . The child tasks 1, 2 are executed after parent task 0. The child node takes input from the output of parent node. The task 0 acts as entry node and task 5 acts as an exit node. After the completion of tasks 3, 4, the task 5 is executed.

### 2.2. Cloud resources

In cloud computing, resources such as virtual machines (VMs) are provisioned to meet the computing needs of users and organizations. Cloud service providers offer VMs with varying configurations and performance capabilities. In some cases, VMs may have the same processing power and efficiency, but their cost rates can vary based on specific time intervals.

Time-based cost variations enable cloud service providers to offer flexible pricing models that align with market demand and resource availability. By adjusting the cost rates over time, users can optimize their resource utilization and costs based on their specific requirements and budgetary constraints. For example, consider a cloud provider offering VMs with identical computing power and performance capabilities. However, they implement different cost rates depending on the time of day or other predefined time intervals. This means that the cost of using the same VM can vary throughout the day. During peak usage hours when demand for cloud resources is high, the cost rate for VMs may be higher compared to off-peak hours when resource utilization is lower. This pricing model encourages users to schedule their resource-intensive tasks during non-peak hours to take advantage of lower costs.

By considering cloud resources with VMs that work with the same efficiency but have different cost rates based on time, users can strategically plan their workload scheduling to optimize cost efficiency. They can take advantage of lower cost rates during periods of lower demand while ensuring their computing requirements are met effectively.

## 3. THE PROPOSED WORKFLOW SCHEDULING

### 3.1. Assumptions

- The given resources are working in good performance, there is no VM breakdown or no interruption to the operation.
- VM can only perform one job at the time.
- The workflow can be split into jobs and these jobs can be performed by different VM.
- The completion time of the last job is the total completion time of the corresponding workflow.

### 3.2. Mathematical model

#### Sets and Indices

JM: set of tuples  $\langle j, m \rangle$  job, VM

JJ: set of tuples  $\langle j_1, j_2 \rangle$

J = {1..j} set of task

W = {1..w}: set of workflow

M = {1..m}: set of VM

T = {0..t}: set of time slot

#### Parameters

A: the starting time of workflow

D: the deadline of workflow

$p_j$ : the processing time of job j

$C_t$ : the leasing price to operate VM at time t

#### Decision variable

$B_j$ : beginning time of job j

$E_j$ : ending time of job j

$X_{\langle j, m \rangle}$ : binary variable = 1 if job j is assigned to VM m

$S_{\langle j, m \rangle}$ : the starting time of job j on VM m

$F_{\langle j, m \rangle}$ : the finishing time of job j on VM m

$R_{jm}^t$ : binary variable = 1 if job j is processing by VM m in time t

$y_m^t$ : binary variable = 1 if job is assigned to VM m at time t

$U_{jm}^t = 1$  if  $t \geq S_{\langle j, m \rangle}$ , otherwise  $U_{jm}^t = 0$

$V_{jm}^t = 1$  if  $t \leq F_{\langle j, m \rangle}$ , otherwise  $V_{jm}^t = 0$

$R_{jm}^t = 1$  if  $S_{jm} \leq t \leq F_{jm}$ , otherwise  $R_{jm}^t = 0$

#### Objective function

$$\text{Minimize } \sum_{m \in M} C_t \times y_m^t \quad (1)$$

Subject to

$$\sum_{m \in M} X_{jm} = 1, \forall j \in J \quad (2)$$

$$B_j = \sum_{m \in M} S_{jm}, \forall \langle j, m \rangle \in JM \quad (3)$$

$$E_j = \sum_{m \in M} F_{jm}, \forall \langle j, m \rangle \in JM \quad (4)$$

$$X_{jm} \geq S_{jm}, \forall \langle j, m \rangle \in JM \quad (5)$$

$$X_{jm} \geq F_{jm}, \forall \langle j, m \rangle \in JM \quad (6)$$

$$BigM \times (1 - X_{jm}) + F_{jm} \geq S_{jm} + p_j - 1, \forall \langle j, m \rangle \in JM \quad (7)$$

$$-BigM \times (1 - X_{jm}) + F_{jm} \leq S_{jm} + p_j - 1, \forall \langle j, m \rangle \in JM \quad (8)$$

$$\sum_{m \in M} S_{jm} \geq A, \forall \langle j, m \rangle \in JM \quad (9)$$

$$\sum_{m \in M} F_{jm} \leq D, \forall \langle j, m \rangle \in JM \quad (10)$$

Precedence and processing time constraints:

$$\sum_{m \in M} F_{\langle j_1, m \rangle} \leq \sum_{m \in M} S_{\langle j_2, m \rangle}, \forall \langle j_1, j_2 \rangle \in JJ \quad (11)$$

Constraint for  $U_{jm}^t$  and  $V_{jm}^t$

$$t \geq S_{jm} - 1 - BigM \times (1 - U_{jm}^t), \forall \langle j, m \rangle \in JM, t \in T \quad (12)$$

$$t \leq S_{jm} - 1 + BigM \times U_{jm}^t, \forall \langle j, m \rangle \in JM, t \in T \quad (13)$$

$$t \leq F_{jm} + 1 + BigM \times (1 - V_{jm}^t), \forall \langle j, m \rangle \in JM, t \in T \quad (14)$$

$$t \geq F_{jm} + 1 - BigM \times V_{jm}^t, \forall \langle j, m \rangle \in JM, t \in T \quad (15)$$

Constraints for  $R_{jm}^t$

$$R_{jm}^t \leq U_{jm}^t, \forall \langle j, m \rangle \in JM, t \in T \quad (16)$$

$$R_{jm}^t \leq V_{jm}^t, \forall \langle j, m \rangle \in JM, t \in T \quad (17)$$

$$R_{jm}^t \geq V_{jm}^t + U_{jm}^t - 1, \forall \langle j, m \rangle \in JM, t \in T \quad (18)$$

$$X_{jm} \geq R_{jm}^t, \forall \langle j, m \rangle \in JM \quad (19)$$

Constraints for  $y_m^t$

$$y_m^t = \sum_{\langle j, m \rangle \in JM} R_{jm}^t, \forall t \in T, \forall m \in M \quad (20)$$

$$\sum_{\langle j, m \rangle \in JM} R_{jm}^t \leq 1 \forall t \in T, \forall m \in M \quad (21)$$

$$y_m^t \leq \sum_{m \in M} R_{jm}^t, \forall t \in T, \forall \langle j, m \rangle \in JM \quad (22)$$

$$\sum_{t \in T} R_{jm}^t \leq p_j, \forall \langle j, m \rangle \in JM \quad (23)$$

**Mathematical model description**

The total production cost is minimized by objective function (1).

Constraint (2) ensures that each work station can only perform one job at time t.

Constraints (3) and (4) calculate the beginning time and ending time of job j, respectively.

According to constraints (5) and (6), if  $X_{jm} = 0$ , which means job j is not assigned in work station m, the starting time and finishing time of that job in work station m are zero.

If  $X_{jm} = 1$ , constraint (7), (8) calculates the finishing time of job j in work station m.

Constraint (9) assigns the starting time of job j is greater than or equal to the corresponding workflow, while constraint (10) ensures that job j is done before the deadline of the corresponding workflow.

Constraint (11) show that with job j1 different from job j2 is not overlap on work station m, with the finishing time of the preceding job on work station m is smaller than or equal to the beginning time of the next job on work station m.

If job j is processed by machine m at time t ( $R_{jm}^t = 1 \ \& \ X_{jm} = 1$ ), t is greater than or equal to the starting time of job j and smaller than or equal to the finishing time of job j. On the other hand, when  $R_{jm}^t = 0$ , job j is not assigned in work station m ( $X_{jm} = 0$ ), with t is smaller than the starting time of job j and greater than the finishing time of job j (constraint (12)-(19))

Constraint (20) determine whether job j is processed by work station m at time t.

Constraint (21), (22) ensures that there is only one job that can be processed by work station m at time t.

Constraint (23) ensures each job can only be processed once.

**4. EXPERIMENTS**

Verification is an essential process conducted by the modeler to ensure the proper functioning of the model. In order to verify and debug the models, the ILOG CPLEX v20.1 solver is utilized with default settings to solve the MILP model of the proposed heuristic. The experimental evaluations are performed using real-world scientific workflows, specifically CyberShake and Montage.

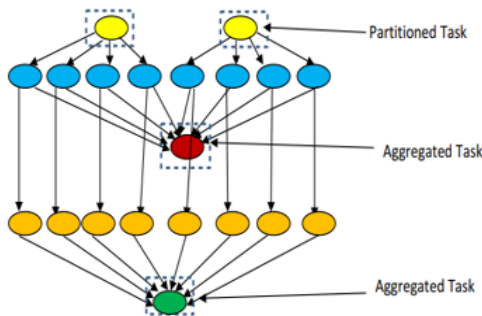


**Figure 2.** CyberShake workflow

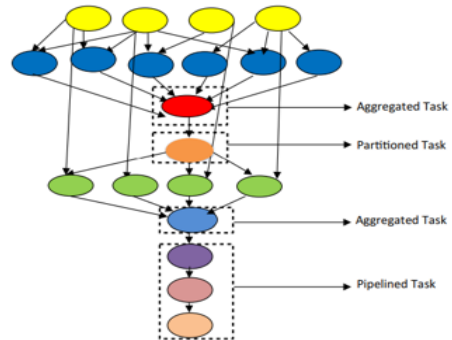


**Figure 3.** Montage workflow

**4.1. Performance by varying VMs**

In this section, the experiment is conducted to estimate performance of the proposed heuristic considering different number of VMs. The model was run with 20 tasks, under moderate deadline and the operational cost increase 1 unit after 5 timeslots

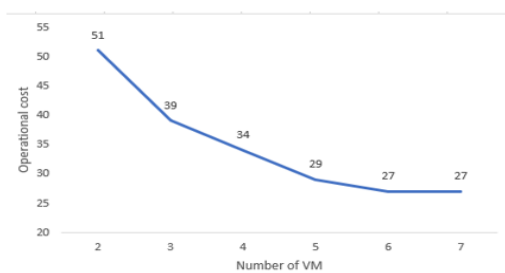


**Figure 4.** CyberShake workflow result

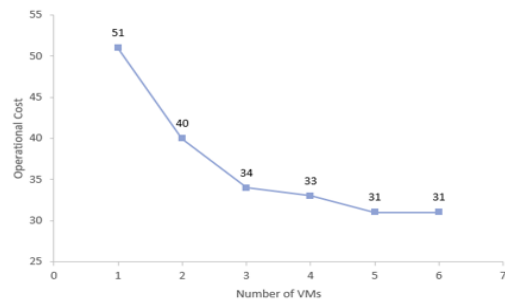


**Figure 5.** Montage workflow result

The obtained results are shown in Figs. 5 and 6. It is clearly seen that the amount of money saving increases as the VMs size increases. This happens due to the fact that when the number of VMs increases, a smaller number of tasks are allocated to each processor, and it increases the probability of finishing before deadline, hence, the operational cost for the schedule is decreased.

#### 4.2. Performance by varying deadline

If the deadline is generously relaxed, there is enough slack time to accommodate for the VM acquisition delay and the performance variation. Therefore, a comprehensive evaluation requires performance analysis on all possible deadlines: Strict, Moderate and relaxed. To this end, the deadlines were set using the rule as specified in equation (23). In this section, we have taken 20 numbers of task with 4 available VMs, the operational cost increases 1 unit after 5 timeslots.

$$\text{Deadline } D = (1 + \mu) \times \text{MET} \quad (23)$$

With MET is the minimum execution time of the workflow,  $\mu$  is the deadline factor defined as follows:

- For Strict Deadlines:  $0 \leq \mu < 1.5$
- For Moderate Deadlines:  $1.5 \leq \mu < 3$
- For Relaxed Deadlines:  $3 \leq \mu < 4.5$

For the experiments, the value of  $\mu$  is varied with a step length of 0.5.

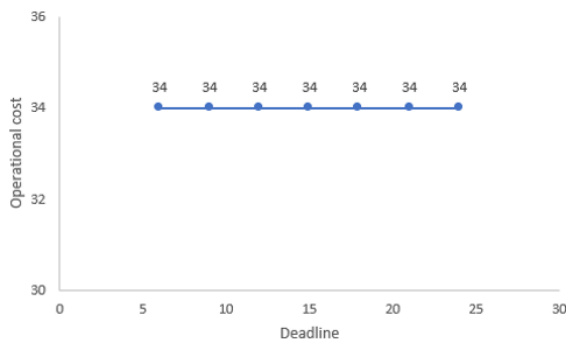


Figure 6. CyberShake workflow result

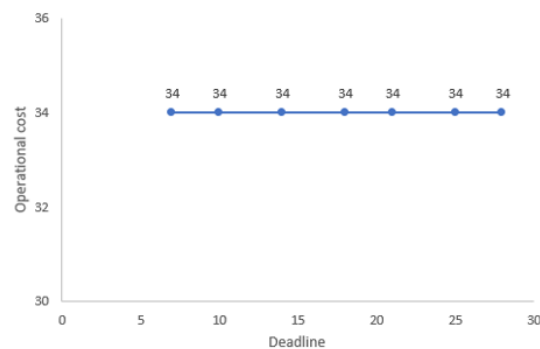


Figure 7. Montage workflow result

For all the workflows, the model successfully meets all the deadlines. In addition, the operational cost does not vary under different deadlines. This is not only because the objective is to generate a cheaper schedule but also because the operational cost varies with different timeslots, hence, the model generates the schedule that finishes as soon as possible to minimize the cost.

## 5. CONCLUSION

The objective of this paper is to investigate the feasibility of employing MILP formulations and algorithms for scheduling complex workflows in the cloud. The paper highlights the significant challenges associated with workflow scheduling problems due to their intricate constraints. Developing effective heuristic algorithms for solving such problems is a difficult task. Existing heuristic algorithms often work well for simplified versions of the problems but struggle to find feasible solutions or achieve optimization objectives.

Based on the findings of this study, it can be concluded that the MILP approach is highly suitable for problems up to a certain size. With MILP, one can precisely describe the problem and employ MILP algorithms to find both feasible and optimal solutions. In cases where MILP is capable of solving the problems, there is minimal need to seek out heuristic algorithms. Heuristic algorithms become more valuable when dealing with larger problems. Additionally, MILP-based heuristics, such as decomposition, can be employed to address large-scale problems.

The workflow scheduling problems analyzed in this study pertain to the in-advance reservation type. However, to handle workflow dynamics or manage a large number of small workflows or tasks, real-time dynamic scheduling algorithms are still necessary.

## References

- [1] "IDC Forecasts Worldwide "Whole Cloud" Spending to Reach \$1.3 Trillion by 2025". Idc.com. 2021-09-14. Archived from the original on 2022-07-29. Retrieved 2022-07-30.

- [2] "IDC Forecasts Worldwide "Whole Cloud" Spending to Reach \$1.3 Trillion by 2025". Idc.com. 2021-09-14. Archived from the original on 2022-07-29. Retrieved 2022-07-30.
- [3] L. Zeng, B. Veeravalli, and X. Li, "ScaleStar: Budget conscious scheduling precedence-constrained many-task workflow applications in cloud," in 2012 IEEE 26th International Conference on Advanced Information Networking and Applications, March 2012, pp. 534–541.
- [4] Abrishami, M. Naghibzadeh, and D. H. Epema, "Deadline constrained workflow scheduling algorithms for infrastructure as a service clouds," *Future Generation Computer Systems*, vol. 29, no. 1, pp. 158–169, 2013.
- [5] J. Sahni and D. Vidyarthi, "A cost-effective deadline constrained dynamic scheduling algorithm for scientific workflows in a cloud environment," *IEEE Transactions on Cloud Computing*, vol. 6, no. 01, pp. 2-18, 2018.
- [6] Ma, X., Xu, H., Gao, H., & Bian, M. (2021). "Real-time multiple-workflow scheduling in cloud environments". *IEEE Transactions on Network and Service Management*, vol. 18, no. 4, pp. 4002–4018. <https://doi.org/10.1109/tnsm.2021.3125395>
- [7] Abrishami, S., Naghibzadeh, M., & Epema, D. (2013). "Deadline-constrained workflow scheduling algorithms for Infrastructure as a Service Clouds". *Future Generation Computer Systems*, vol. 29, no. 1, pp. 158–169. <https://doi.org/10.1016/j.future.2012.05.004>

**[S2-22] Application of Developed Dual Nozzle System that is able to Multi-Layer Printing in FDM Method**

YaeGeun Kwon, Hyeonjong Kim, Junghyuk Ko\*

*National Korea Maritime and Ocean University, Busan, Republic of Korea*

\*Corresponding author: jko@kmou.ac.kr

**Abstract**

A 3D printer is a printer that can print three-dimensional structures using models based on computer-aided design. FDM printers are one of the most basic 3D printing methods in which thermoplastic resin (filament) is heated and extruded with an extruder among the methods of 3D printers. There are several types of FDM systems and they are single chamber single nozzle, dual chamber dual nozzle and single chamber dual nozzle. The single chamber single nozzle system is one of the most basic FDM 3D printing methods. With Single Nozzle and Single Extruder, only one material can be used for one product. A dual chamber dual nozzle system was proposed to expand the printing area. Two nozzles and two extruders correspond 1:1, so two materials can be used in a product. Each material property can therefore be used individually. However, dual-chamber dual-nozzle systems have the disadvantage of requiring additional extruder control and being more expensive than single-chamber single-nozzle systems that require only one extruder control. Finally, the single-chamber dual-nozzle system has two nozzles and one extruder. Like the dual chamber dual nozzle, this method can also use two materials in one product. However, since the two nozzles share one extruder, two different materials can be mixed. Thus, properties may not be maintained. However, it has the advantage of shorter transit time than the dual chamber dual nozzle system.

There is no problem in printing two different materials separately with the dual-nozzle 3D printing system, but it could not be used for systems that require the properties of two materials at the same time, such as bio-printers or architectural 3D printers. This is because single chamber single nozzle systems cannot use two materials. And while the dual chamber dual nozzle system can use two different materials, it requires an advanced transport control system and takes a significant amount of time to print. Also, micro-level control, which is a measure of precision machining, is impossible. Therefore, it is not suitable for applications requiring micro-scale printing using two different materials. In addition, the single chamber dual nozzle system is less expensive to transport, but the material properties are not preserved because the two materials are mixed proportionately in the single chamber. Therefore, we propose a multi-layer nozzle method that can be controlled on a micro scale and simultaneously print without mixing two materials.

The multi-layer nozzle system is a development of a dual nozzle system that can create a separate layer on a cross section without mixing the two materials. Single chamber dual nozzle system consists of two nozzles and one extruder, reducing transportation time. However, unlike the single chamber dual nozzle method, the two different materials can be used separately by separating the layers inside the nozzle, so it is easier to output products using the properties of the two different materials using the multi-layer nozzle system than the existing dual nozzle system.

The biggest feature of the multi-layer nozzle system is the composition of the separation layer cross section, and in the previous experiment, the relationship between the input material cost and the output material cost was verified with one output. In this experiment, the method for verifying the multi-layer function under various printing conditions in deposition printing is as follows. 1. The printing direction was set as an experimental condition to determine whether layers were formed according to the shape of the cross section. 2. The number of multipliers that determine the number of independent layers and the input feed rate ratio are different. Therefore, a total of 20 experimental conditions were set as variables: 2 conditions for the printing direction, 2 conditions for the multiplier, and 5 conditions for the ratio. After the experiment, the analysis process proceeded as follows. 1. Cut the printout to secure the cross section. 2. After removing fine dust from the secured cross section through post-processing, obtain an image with an optical microscope. 3. Convert the obtained image into pixel data using MATLAB software and analyze the data.

In this experiment, we investigated whether the multi-layer nozzle system functions well as a multi-layer under various conditions in deposition printing. It can be determined by differential data of pixel data because sharp changes of value occur at the boundary of the separated layers. The degree of how multi-layered the cross section



was determined by how spread out the normal distribution of the differential value of the pixel color data was. It shows if cross sections were single color, value of differential gather 0. If cross section were multi-layered, value of differential spread to high value. Based on this, cross sections made by multi-layer nozzle system has more extreme changes of value than single color cross sections so we figure out that multi-layer nozzle system can make separated layer cross sections successfully. Therefore, the multi-layer nozzle system can realize simultaneous printing of various materials, which is the advantage of dual nozzle system. In addition, we believe that it will be greatly utilized in fields such as Bio printer and Architecture 3D printer, which are research areas where two different materials are reluctant to mix.

**Keywords:** *Multi-layer, Separated layer cross section, FDM, Plural materials, Dual nozzle system, Bioprinter*

### References

- [1] Ferry P.W. Melchels, Jan Feijen, and Dirk W. Grijpma, A review on stereolithography and its applications in biomedical engineering, *Biomaterials*, vol. 31, no. 24(2010), pp. 6121-6130.
- [2] M. Too, K. Leong, C. Chua, Z. Du, S.F. Yang, C.M. Cheah, and S.L. Ho., Investigation of 3D non-random porous structures by fused deposition modelling, *Int. J. Adv. Manuf. Technol.*, vol.19, no.3(2002), pp. 217-223.
- [3] Lifton, V., Lifton, G. and Simon, S., Options for additive rapid prototyping methods (3D printing) in MEMS technology, *Rapid Prototyping Journal*, vol. 20, no. 5(2014), pp. 403-412.

**[S2-34] Smart Farm with Hydroponic Cultivation Method Using Renewable Energy**

Ho Yeong Kim, Dohyung Kim, Inwoo Kim, Junghyuk Ko\*

*National Korea Maritime and Ocean University, Busan, Republic of Korea*

\*Corresponding author: jko@kmou.ac.kr

**Abstract**

Agriculture is an important basic industry that sustains modern civilization and sustains people's lives. However, agriculture often involves hard labor. In most outdoor agricultural fields, agricultural products can be harvested only by wrestling with the soil, plowing the field, applying fertilizer, and preventing pests and rain and wind damage. Due to these factors, the number of agricultural population is decreasing. So, we developed a smart farm that can minimize labor and remotely and automatically manage the cultivation environment.

A large amount of electrical energy is required to use smart farms. However, depletion of fossil fuels, one of the largest energy sources for electric energy production, is predicted, and various environmental problems are caused by the use of fossil fuels. Renewable energy has been used to solve these problems. In addition, for more convenient system management, the hydroponic cultivation method was selected. Currently, various studies are underway on renewable energy and smart farms, and technologies are emerging. However, studies that have conducted linking the two technologies are lacking. Therefore, this study will be meaningful as a research case showing the possibility of smart farms using renewable energy.

The power generation system was installed by combining a wind generator and a photovoltaic generator with a battery on a steel frame. The cultivation system consists of a temperature controller, water level controller, humidity controller, and LED inside a plastic water tank. The temperature controller maintains a constant temperature inside the tank and is divided into a warming device and a cooling device. The thermostat receives the temperature value from the temperature sensor inside the water tank, and if the temperature is lower than the set temperature, electricity is supplied to the heating coil to heat the water. The cooling device similarly receives the temperature value from the temperature sensor, and when the temperature exceeds the set temperature, the cooling device inside the water tank operates. The water level controller is a device that keeps the total amount of nutrient solution absorbed and evaporated by plants constant. When the water level is lower than the water level set by the water level sensor inside the tank, the pump is operated in the container containing the nutrient solution and water is supplied to the tank. Humidity controller is a device for preventing the accumulation of moisture inside a closed water tank. Data is received from the humidity sensor inside the tank, and if the humidity is higher than the set value, the fan is operated to lower the humidity. The LED is a device to help plants photosynthesize, and was controlled to turn on between 12 and 4 a.m. when photosynthesis is impossible due to sunlight.

In order to verify the performance of the system, a cultivation experiment was conducted on lettuce. When the inside temperature of the water tank is below 24°C, the thermostat operates, and when it exceeds 30°C, the cooling system operates, confirming that the temperature is maintained at 24~30°C. It was confirmed that the water level controller continuously maintains the set water level (160mm). When the humidity inside the tank reached 50% or more, it was confirmed that the fan operated and the humidity did not rise any further, and that the LED also operated at the set time. As a result of the experiment on energy generation, the sum of solar power generation and wind power generation was measured as an average of 1060 Wh per day, including cloudy and sunny days.

As a result of the experiment, it was confirmed that plant cultivation is possible with the current system alone. In addition, the average daily consumption of the system is 400 Wh, and the current amount of electricity is used as a battery, and the system operates for 2.5 days when used without power generation. In addition, the problem of smart farms using existing renewable energy, which uses a lot of energy to maintain temperature, was changed to hydroponic cultivation, showing smoother temperature management.

**Keywords:** *Agriculture, Smart farm, Renewable energy, Hydroponic cultivation*

### References

- [1] Uk-hyeon Yeo, In-bok Lee, Kyeong-seok Kwon, Taehwan Ha, Se-jun Park, Rack-woo Kim, Sang-yeon Lee. Analysis of Research Trend and Core Technologies Based on ICT to Materialize Smart-farm. Protected Horticulture and Plant Factory, vol. 25, no. 1, pp. 30-41, 2016.
- [2] Sjaak Wolfert, Lan Ge, Cor Verdouw, Marc-Jeroen Bogaardt. Big Data in Smart Farming – A review, Agricultural Systems, vol. 153, pp. 69-80, 2017.
- [3] Ibrahim Dincer. Renewable energy and sustainable development: a crucial review, Renewable and Sustainable Energy Reviews, vol. 4, no. 2, pp. 157-175, 2000.

**[S2-35] Analysis of Implantable Catheters for Draining Malignant Ascites**Inwoo Kim<sup>1</sup>, Hyeonjong Kim<sup>1</sup>, Il-Hwan Kim<sup>2</sup>, Junghyuk Ko<sup>1,\*</sup><sup>1</sup> Department of Mechanical Engineering, Korea Maritime and Ocean University, Busan, Korea<sup>2</sup> Department of Oncology, Haeundae Paik Hospital, College of Medicine, Inje University, Busan, Korea

\*Corresponding author: jko@kmou.ac.kr

**Abstract**

Currently, most cancers are considered treatable diseases. This is because, unlike the poor outcomes associated with cancer treatment in the past, mortality is now gradually decreasing. However, there are still many problems in the treatment process, and it is a disease that has been sentenced to a time limit. While treatment for end-stage cancer sometimes aims for a full recovery, some patients voluntarily sign a non-resuscitation pledge, receive hospice care, and prepare for death by alleviating symptoms with the goal of improving their quality of life.

The factors that affect the quality of life of cancer patients can be divided into five factors: Mobility, Self-care, Usual activities, Pain/Discomfort, and Anxiety/Depression. At this time, malignant ascites accumulated in the abdominal cavity (AC) is one of the cancer symptoms that affects the patient's daily activities and quality of life due to Pain/Discomfort. Because this symptom interferes with the patient's behavior and daily life, the patient needs to visit the hospital frequently for drainage. The medical staff will drain ascites using ascites, which can take anywhere from 30 minutes to up to 24 hours for the procedure. It can be a catastrophic loss of time for patients who have been sentenced to a time limit and are running out of time on probation. In addition, ascites discharge can cause infection, intestinal perforation, and bleeding, which can threaten patients.

In order to overcome this loss of time and surgical complications, various methods and devices of multiple drainage have been devised. Solbach et al. have focused on catheter systems that can be implanted in the abdomen, researching time-efficient puncture catheters, which can drain ascites anytime, anywhere, when the patient has access to an appropriate drainage device. Stirnimann et al. and Fotopoulou et al. have researched a new type of multiple drainage method. It is a method of draining ascites in AC through the bladder using an 'Alfapump'. Their studies have observed positive results in puncture flow rate and frequency of procedures, but batteries must be prepared to operate these electrical devices.

In addition, we have devised another implantable puncture method in which an implantable catheter is inserted between the bladder wall and the bladder in a previous study. This catheter is designed based on a pigtail catheter and has a silicone membrane and holes. It uses the pressure difference between BC and AC to aid in drainage of ascites through the bladder cavity (BC) and urethra. In previous studies, the flow rate and water level were controlled to observe changes in the flow rate of the catheter, the activation pressure with rotation, and the change in cycle time. As a result, it was confirmed that the cycle time was affected by the flow rate, and the effect of the flow rate on the activation pressure was not identified. In contrast, no effect of cycle time on the number of revolutions of the catheter was identified, and the effect of activation pressure on the number of revolutions was identified.

Based on the results of previous experiments, we designed and built an improved version of the implantable catheter. This version of the catheter has a uniform number of revolutions of 1.5 revolutions. In addition, the size of the catheter was reduced and the holes in the silicone membrane were standardized. We conducted an experiment to see if the catheter was performing its drainage function normally while preventing reflux. Experiments were then conducted to measure the drainage performance of the catheter under pressure.

The equipment for the experiment was first equipped with two cylinders. The bottom of these two cylinders is connected so that the water level can be shared. A water level sensor was installed in one cylinder to measure the water level, and a catheter was installed in the other. Another hole was drilled at the bottom to connect a syringe pump to supply water. This syringe pump supplies water to the cylinder in which the catheter is installed, and the catheter is activated by the pressure. The syringe pump was operated by a stepper motor. In this case, the stepper motor was set up to push the syringe pump to inject 40 ml and 60 ml of water per hour through a preliminary experiment.

The experiment was carried out according to the following procedure: First, a water level sensor and a catheter were installed in each cylinder. Then fill it with water to the initial position. Second, for stepper motors, we set

two flow rates: 40 ml and 60 ml per hour. The final step is to rotate the stepper motor to observe the experimental data for 3 hours. The experimental data records the amount of change in the water level in seconds using the water level sensor and observes the amount of change. The water level in the cylinder should be increased at a constant rate by the syringe pump, but if the catheter is activated, the rate of increase will decrease or, conversely, show a tendency to decrease. By analyzing the amount of this change, the drainage performance of the catheter can be measured.

In addition, if the catheter is installed in the opposite direction, the performance of preventing reflux can be confirmed. It is possible to measure whether backflow can be completely prevented within the experimental range, or to what extent backflow can be prevented at a certain pressure.

In this study, we focused on preventing backflow, which was a problem in the previous experiment. Based on the results of the experiment, it is judged that if reflux prevention is successfully completed, it can sufficiently improve the quality of life of terminal cancer patients.

**Keywords:** *Implantable catheter, Malignant ascites, Terminal cancer, Time efficiency*

### References

- [1] Kim H, Kwon H, Park BS, Park SH, Park JH, Oh CK, et al., "Implantable ascites drainage stent designs and experiments to improve the quality of life in terminal cancer patients", *Jamet*, 45(5) (2021), pp. 269-274.
- [2] Boron WF, Boulpaep EL, "Medical Physiology E-Book", Elsevier Health Sciences (2016), p.1907.
- [3] Navarro-Rodriguez T, Hashimoto CL, Carrilho FJ, Strauss E, Laudanna AA, Moraes-Filho JPP, "Reduction of abdominal pressure in patients with ascites reduces gastroesophageal reflux", *Diseases of the Esophagus*, 16(2) (2003), pp. 77-82.
- [4] Hyeonjong Kim, Soyeong Bae, Ye-Jin Kim, So-Young Jung, Jin-Han Park, Si-Hyung Park, Il-Hwan Kim and Junghyuk Ko, "Time-efficient implantable catheters for draining malignant ascites in terminal cancer patients", *Technology and Health Care*, 31 (2023), S223–S234.
- [5] Ha Ri Kang, "Assessment of Quality of Life according to Cancer prevalence period: Based on the Korea National Health and Nutrition Examination Survey (2016~2020) ", *한양대학교 석사학위 논문*

## [S2-50] Use of Drone-Based Thermal Images for 3D Thermal Point Cloud and Target Surface Temperature Estimation

Hyeonjeong Jo<sup>1</sup>, Junhoo Lee<sup>2</sup>, Jaehong Oh<sup>3,\*</sup>

<sup>1</sup>*Interdisciplinary Major of Ocean Renewable Energy Engineering, Ph.D. student, Busan, Republic of Korea*

<sup>2</sup>*Department of Civil Engineering, Korea Maritime and Ocean University, Busan, Republic of Korea*

<sup>3</sup>*Department of Civil Engineering, Korea Maritime and Ocean University, Busan, Republic of Korea*

\*Corresponding author: jhoj@kmou.ac.kr

### Abstract

Recently, drones are widely used for generation of 3D geospatial information in the fields of mapping and construction. Mostly visible cameras are adopted for the studies but thermal cameras have high potential for 3D model with temperature information. However, unlike visible images, thermal images have low spatial resolution such that there is a limitation to high density 3D data generation. Therefore, in this study we carried out two experiments. First experiment is the dense thermal point cloud generation by integrating the visible and thermal images. A dense point cloud is generated using the high resolution visible images and the cloud is textured using the thermal infrared images. In addition, we considered occlusions in the target area for more accurate texturing. In second experiment, the conversion of thermal image DN (digital number) to the surface temperature is tested for the target surface materials including asphalt parking lot, reinforced concrete, and glass in the target building. And we checked the reliability of the estimated temperature with the field data from a thermometer. First experiment showed that the surface of the building was represented more like a real building when considering the occlusion area. In this process, when the average distance between the projection center and the 3D spatial point is used, the corners of the building showed more clearly than when the minimum and maximum values are used. Second experiment, both the value of converting the DN value into temperature and the actual surface temperature measured with thermometer obtained high values in the order of asphalt, reinforced concrete, and glass. In the case of asphalt and reinforced concrete, there was a difference of less than 2°C between the temperature converted from the DN value and the actual surface temperature measured by thermometer. But, in the case of glass, there was a big difference between the temperature converted from the DN value and the actual surface temperature measured with thermometer because of the low emissivity of glass.

**Keywords:** Point cloud, DN (Digital number), Digital twin, Thermal image processing

### Acknowledgments

An Acknowledgments section, if used, immediately precedes the References. Sponsorship and financial support acknowledgments should be included here.

### References

- [1] G. Kirchhoff, "Über das Verhältnis zwischen dem Emissionsvermögen und dem Absorptionsvermögen der Körper für Wärme und Licht", *Philosophical Magazine and Journal of Science Series 4*, 109(2) (2019), pp. 1-21.
- [2] J.H. Park, K.R. Lee, W.H. Lee and Y.K. Han, "Generation of Land Surface Temperature Orthophoto and Temperature Accuracy Analysis by Land Covers Based on Thermal Infrared Sensor Mounted on Unmanned Aerial Vehicle", *Journal of the Korean Society of Surveying*, 36(4) (2018), pp. 263-270
- [3] J.Y. Han, J.N. Guo and J.Y. Chou, "A Direct Determination of the Orientation Parameters in the Collinearity Equations", *IEEE Geoscience and Remote Sensing Letters*, 8(2) (2011), pp. 313-316.
- [4] T. Luhmann, J. Piechel and T. Roelfs, "Geometric Calibration of Thermographic Cameras", *Remote Sensing and Digital Image Processing*, (2013), pp. 27-42

## [S2-58] The Application of Blockchain in Logistics: Enhancing Transparency and Efficiency

Linh Do<sup>1</sup>, Thai Le<sup>2</sup>, Duy Thanh Tran<sup>3,4</sup>.

<sup>1,2</sup> Ho Chi Minh City University of Banking, Ho Chi Minh City, Viet Nam, 700000

<sup>3</sup> University of Economics and Law, Ho Chi Minh City, Viet Nam, 700000

<sup>4</sup> Viet Nam National University, Ho Chi Minh City, Viet Nam, 700000

\*Corresponding author: thanhtd@uel.edu.vn

### Abstract

Blockchain technology has emerged as a transformative solution with the potential to revolutionize various industries, including logistics and supply chain management. This abstract presents a comprehensive study that explores the integration of blockchain in the logistics sector and its impact on transparency, efficiency, trust, and security.

The primary objective of this research is to examine the benefits and challenges associated with implementing blockchain technology in logistics operations. By leveraging the decentralized and immutable nature of blockchain, logistics companies can transform the way they track, verify, and manage the movement of goods. This technology holds the promise of reducing fraud and counterfeiting risks, streamlining processes, and creating a more reliable and efficient supply chain ecosystem.

The proposed approach incorporates blockchain technology as a foundational layer within logistics operations. Blockchain facilitates secure and transparent data sharing among stakeholders, ensuring the integrity and authenticity of information throughout the supply chain. The integration of smart contracts enables the automation and execution of contractual agreements, enhancing compliance and reducing the need for intermediaries.

Through a comprehensive analysis of case studies and real-world applications, this research showcases the transformative potential of blockchain in logistics. It demonstrates how blockchain can enhance transparency by providing a verifiable record of all transactions and events within the supply chain. This level of transparency not only improves trust among stakeholders but also enables better traceability and accountability.

Furthermore, this study addresses the challenges associated with implementing blockchain in logistics, including scalability, interoperability, regulatory compliance, data privacy, and security. By examining these challenges, the research provides valuable insights and recommendations for overcoming barriers to successful blockchain adoption in the logistics industry.

The uniqueness and novelty of this research lie in its comprehensive analysis of the benefits and challenges of blockchain technology in logistics. By combining the strengths of blockchain with logistics operations, this study contributes to the existing body of knowledge and provides practical implications for logistics practitioners and policymakers.

The expected outcomes of this research encompass enhanced transparency, improved operational efficiency, reduced fraud risks, streamlined processes, and increased trust among stakeholders. Blockchain implementation in logistics has the potential to reshape the industry by creating a more secure, transparent, and efficient supply chain ecosystem.

In conclusion, this research highlights the transformative power of blockchain technology in the logistics sector. By leveraging blockchain's decentralized and immutable characteristics, logistics companies can enhance transparency, efficiency, trust, and security in supply chain management. The findings of this study provide valuable insights for both academia and industry, paving the way for further research, collaboration, and implementation of blockchain in the logistics landscape.

**Keywords:** *Blockchain technology, Logistics, Supply chain management, Transparency, Supply chain ecosystem, Smart contracts, Verification, Blockchain adoption, Efficiency, Counterfeit goods, Fraud mitigation*

### Acknowledgments

The authors would like to express their sincere gratitude to Dr. Thanh Tran for his invaluable contributions and support in the completion of this research paper. His insights and guidance have been instrumental in shaping the ideas presented herein.

### References

- [1] Nakamoto, S. (2008). Bitcoin: A peer-to-peer electronic cash system. Retrieved from <https://bitcoin.org/bitcoin.pdf>
- [2] Tapscott, D., & Tapscott, A. (2016). Blockchain revolution: How the technology behind Bitcoin is changing money, business, and the world. Penguin.
- [3] Yuan, Y., Wang, F. Y., & Zhao, Y. (2016). Trust model and trust evaluation for the logistics blockchain platform. *IEEE Access*, 4, 6188-6198.
- [4] Chen, J., Xu, L., Li, S., & He, W. (2020). A blockchain-based traceability system for cross-border e-commerce supply chains. *IEEE Transactions on Industrial Informatics*, 16(10), 6496-6506.
- [5] Chen, Y., & Paulraj, A. (2004). Towards a theory of supply chain management: the constructs and measurements. *Journal of Operations Management*, 22(2), 119-150.
- [6] Lai, K.H., & Cheng, T.E. (2005). A fuzzy multi-objective approach for partner selection in strategic alliances. *International Journal of Production Economics*, 96(3), 301-313.
- [7] Mentzer, J.T., DeWitt, W., Keebler, J.S., Min, S., Nix, N.W., Smith, C.D., & Zacharia, Z.G. (2001). Defining supply chain management. *Journal of Business Logistics*, 22(2), 1-25.
- [8] Simchi-Levi, D., Kaminsky, P., & Simchi-Levi, E. (2008). *Designing and managing the supply chain: concepts, strategies, and case studies*. McGraw-Hill.
- [9] Vaidya, A., & Sharma, S.K. (2016). A literature review of RFID-enabled healthcare applications and issues. *International Journal of Information Management*, 36(6), 817-830.
- [10] Yu, W., Liang, X., Gong, Y., & Xu, L.D. (2018). Internet of things for remote sensing of supply chain: A systematic literature review, framework and challenges. *Journal of Industrial Information Integration*, 9, 1-19.



**[S3-2] Research Impact of Solar Panel Cleaning Robot on Photovoltaic Panel's Deflection**

Trung Dat Phan<sup>1,2</sup>, Minh Duc Nguyen<sup>1,2</sup>, Maxence AUFFRAY<sup>4</sup>, Nhut Thang Le<sup>1,2</sup>, Cong Toai Truong<sup>1,2</sup>, Dae Hwan Kim<sup>5</sup>, Van Tu Duong<sup>1,2</sup>, Huy Hung Nguyen<sup>3</sup>, Tan Tien Nguyen<sup>1,2,\*</sup>

<sup>1</sup> National Key Laboratory of Digital Control and System Engineering (DCSELab), Ho Chi Minh City University of Technology (HCMUT), 268 Ly Thuong Kiet Street, District 10, Ho Chi Minh City, Viet Nam

<sup>2</sup> Viet Nam National University Ho Chi Minh City, Linh Trung Ward, Thu Duc City, Ho Chi Minh City, Viet Nam

<sup>3</sup> Faculty of Electronics and Telecommunication, Sai Gon University

<sup>4</sup> Faculty of Mechanical Engineering, Higher Institute of Materials and Advanced Mechanics of Le Mans, France

<sup>5</sup> Realmaker Inc., R304 B23 Sinseon-ro, Nam-gu, Busan, KS012, Republic of Korea

\*Corresponding author: nttien@hcmut.edu.vn

**Abstract**

In the last few decades, solar panel cleaning robots (SPCR) have been widely used for sanitizing photovoltaic (PV) panels as an effective solution for ensuring PV efficiency. However, the dynamic load generated by the SPCR during operation might have a negative impact on PV panels. To reduce these effects, this paper presents the utilization of ANSYS software to simulate multiple scenarios involving the impact of SPCR on PV panels. The simulation scenarios provided in the paper are derived from the typical movements of SPCR observed during practical operations. The simulation results show the deformation process of PV panels, and a second-order polynomial is established to describe the deformed amplitude along the centerline of PV panels. This second-order polynomial contributes to the design process of a damper system for SPCR aiming to reduce the influence of SPCR on PV panels. Moreover, the experiments are conducted to examine the correlation between the results of the simulation and the experiment.

**Keywords:** Solar energy, Photovoltaic panel, Solar panel cleaning robot, PV deflection

**1. INTRODUCTION**

In the 4.0 industrial revolution period, the human necessity to use energy is higher than ever before, and it is a big challenge for the energy industry in the world. In that context, many countries are conducting a transition from fossil fuels to renewable energy sources. Among the various renewable energy sources, solar energy has emerged as a solution for a sustainable future due to its cost-effectiveness, smaller installation space requirement, lower maintenance costs, and high performance compared to other energy sources [1]. In fact, the total installed solar panels have increased by nearly 650 GW [2] over the past decade, which is expected to increase by 1,100 GW in 2026 [3]. However, maintaining the performance of a photovoltaic (PV) panel system poses significant challenges due to various factors. One of the major issues is the accumulation of dust and debris on the surface of PV panels, which can lead to a decrease in efficiency of up to 30% [4]. Therefore, periodic cleaning of the PV panel system is necessary to ensure its efficiency.

Currently, there are numerous studies on cleaning PV panels that have shown many cleaning methods around the world, such as manual brushing, nanocoatings, chemicals, electrostatic force, ultrasonic waves, and automated approaches such as an automatic water spraying system or a robot with cleaning tools [5], [6]. Each method of cleaning PV panels has its advantages and disadvantages, which depends on factors such as the installation structure of the panels and the characteristics of dust in a particular area. Among these methods, the utilization of mobile robots is considered a popular solution, to date, due to its high level of automation, fast cleaning speed, and overall efficiency [7]. Nevertheless, the dynamic load generated by the cleaning robot when moving on the surface of the PV panel can experience deformation and induce microcracks in the silicon cells, which directly impact the panels' lifespan and performance [8]. Consequently, the panels degrade at a rate of approximately 0.8% to 1.1% per year [9], resulting in a decrease in photovoltaic efficiency of around 20% [10]. To solve the above problem, the application of damping mechanisms has become widely adopted in order to minimize the effects of robots on the PV panel during the cleaning process [11]. Besides the fact that there is limited research on the surface of PV panels, the design of the shock absorber assembly depends on the particular terrain where the robot operates. Thus, there are restricted studies on the design of damper systems for solar panel cleaning robots (SPCR).

This paper examines the deformation of PV panels caused by the weight of the SPCR and presents a polynomial describing the profile of the PV panel at maximum deformation. This polynomial describes the coordinates of the deformation points at the most dangerous cross-section, which are exerted by the wheel of the SPCR. The equation contributes to the design process for shock absorbers. The procedure to obtain the objective of this research is as follows:

- The deformation of the PV panel is investigated by computational simulation through ANSYS based on the panel structure and parameters of SPCR.
- The polynomial describing the deformation of the PV panel at the cross-section exhibiting the highest amplitude is determined.
- The correlation between simulation studies and experimental results is achieved.

## 2. OVERALL SYSTEM DESCRIPTION

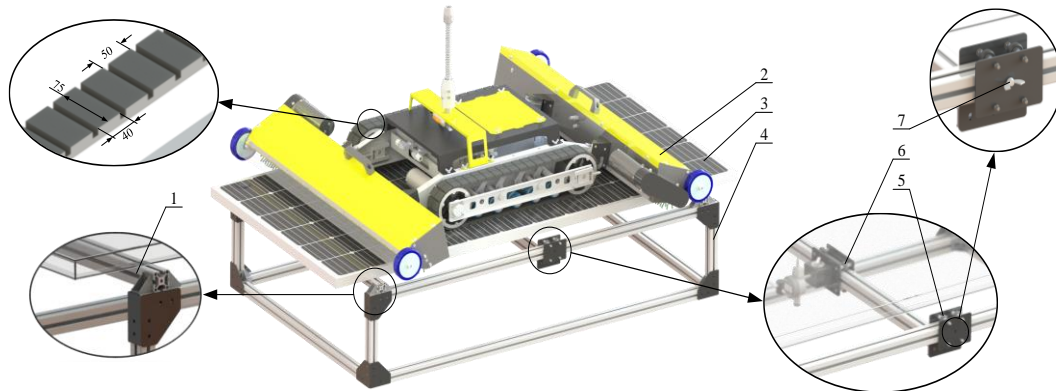


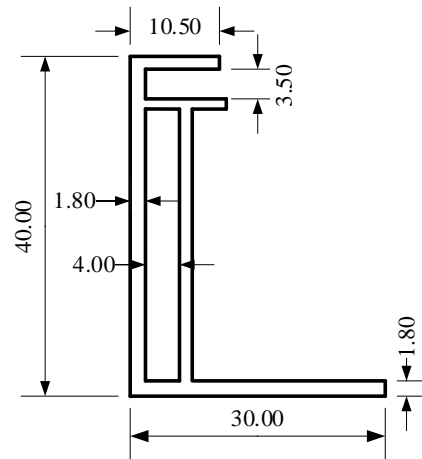
Figure 1. 3D CAD of test bed

Figure 1 depicts the test bed to examine the deformation of the PV module under the load of the SPCR. The experimental system consists of five components: SPCR (2), PV panel (3), support frame (4), 2-axis sliding examine (5), and Mitutoyo 543-400B round-type dial gauge (6). SPCR functions as a load on the PV panel (3), with two-wheel assemblies being contact areas. The PV panel (3) is attached to the support frame (4) using two support bars (1), similar to the actual installation at PV power plants. Because the slippage is not considered in this research, the installation of PV panels is parallel to the ground without loss of generality. To measure the deformation, the round-type dial gauge is traversed across the PV panel thanks to a 2-axis sliding mechanism (5). To measure the deformation of PV panels, the locking nuts (7) are utilized to block the sliders at the location of measured deformation.

## 3. MATERIAL AND METHOD

### 3.1. Physical model

In this simulation, the support bars are assumed to be perfectly rigid, with negligible deformation. Additionally, a PV panel has five adjacent layers in the sequence of protective cover (tempered glass), encapsulant (EVA), semiconductor (Silic), encapsulant (EVA), and back sheet (Tedlar or Polypropylene) [12]. Besides, these layers together form a compact and robust unit, firmly held within an aluminum frame. In these layers, the protective cover, made of tempered glass, serves as the main bearing component and protects the PV panel from external payloads. The EVA and Tedlar layers are thin film materials and do not greatly affect the bearing capabilities of the PV panel. The PV cell layer is the most sensitive and requires protection as it is prone to the formation of microcracks under vibrations, as discussed in Section 1. Therefore, to reduce computational time and simplify the physical model, only the tempered glass layer is investigated. For monocrystalline or polycrystalline PV panels, the standard thickness of the tempered glass layer ranges from 3-4mm [13], [14] and 3.5mm tempered glass was used for this simulation. Additionally, the aluminum frame is also another bearing element in a PV panel. According to Smartclima [15], there are various cross-section profiles available for aluminum frames, with up to 60 different profiles, but the TNY038 one was chosen for modeling the aluminum frame because it is compatible with the parameter of PV panel type RD320TU-36MD. Moreover, insignificant factors like fillets and tiny grooves in PV panels were ignored to avoid errors when meshing and calculating. Hence, based on the combination of some pre-processing conditions, the cross-sectional profile of the frame is shown in Figure 2.



**Figure 2.** The profile of aluminum frame cross-section

To simulate the deformation of a PV panel, three important parameters of the tempered glass layer need to be considered, including mass density, Young's modulus, and Poisson ratio [16]. Referring to previous studies [17], [18], the mechanical properties of aluminum frames and tempered glass are summarized in Table 1.

**Table 1.** Material properties for simulation

Materials	Young's modulus, GPa	Poisson ratio	Mass density, kg.m <sup>-3</sup>
6063-T5 Aluminium	70	0.3	2700
Tempered Glass	73	0.23	2500

According to [19], [20], the PV panels recommended for the installation are located approximately 200 to 400mm from the short edges of the aluminum frame. In addition, areas outside of this zone are considered hazardous where the PV panel might be subjected to wind loads, potentially causing damage. In some cases, the PV panel installation does not adhere to standards, so the PV panels can become highly susceptible to an external load. To assess the worst-case scenario, the clamps, which are the pads to fix between the PV panel and support frame, were positioned at a distance of 200mm from the short edge of the aluminum frame. Specifically, this is done to account for the potential risks and ensure a comprehensive evaluation of the system under adverse conditions. The investigation also revealed that the robot barely slips when operating on PV frames with an incline of 10° [21]. Therefore, in the static state, the SPCR with a mass of 83kg exerts a force of approximately 81.5kg on the PV panel surface. Besides, the boundary conditions for the simulation process are described in Table 2.

**Table 2.** Boundary conditions for the simulation process

Parameters	Value
Overall dimensions, mm	1956×992×40
Width of clamping area, mm	40
External load, kg	81.5
Length of contact area, mm	590
Distance between two belts, mm	673

### 3.2. Simulation method

The finite element method (FEM) is used for strain analysis of PV panels, with the simulation process described in Figure 3. Initially, the mechanical properties shown in Table 1 were defined. Subsequently, a physical

model of the PV panel was created using Ansys SpaceClaim. The contact areas between the belt and the surface of the PV panel, as well as between the support bars and the aluminum truss, were also generated. The physical model of the PV panel was then discretized into smaller elements by Ansys Meshing. The tempered glass sheet, with its simple structure, was meshed using 10 mm-hexahedral elements, while the aluminum frame was meshed using 5 mm-tetrahedral ones. This approach facilitates convergence and enhances result accuracy, considering the complexity of the aluminum frame compared to the tempered glass. Next, the boundary conditions for fixed support and external load were set according to the parameters mentioned in Table 2. Finally, the solution for directional deformation was defined, and the necessary data was extracted for determining the curvature deformation of the PV panel.



**Figure 3.** Steps for a FEM simulation using Ansys software

The PV panel was investigated in two different trajectories of SPCR, as shown in Figure 4. These trajectories represent the typical SPCR motions across consecutive PV panels in practice. Hence, in the scope of this paper, the robot moves along the length of the PV panel chosen to be considered (Figure 4). The magnitude and position of the force applied to the PV panel vary depending on the position of the SPCR. Assuming the force created by SPCR's mass is evenly distributed on the belts, the force acting on the PV panel in any situation is proportional to the belt contact area.

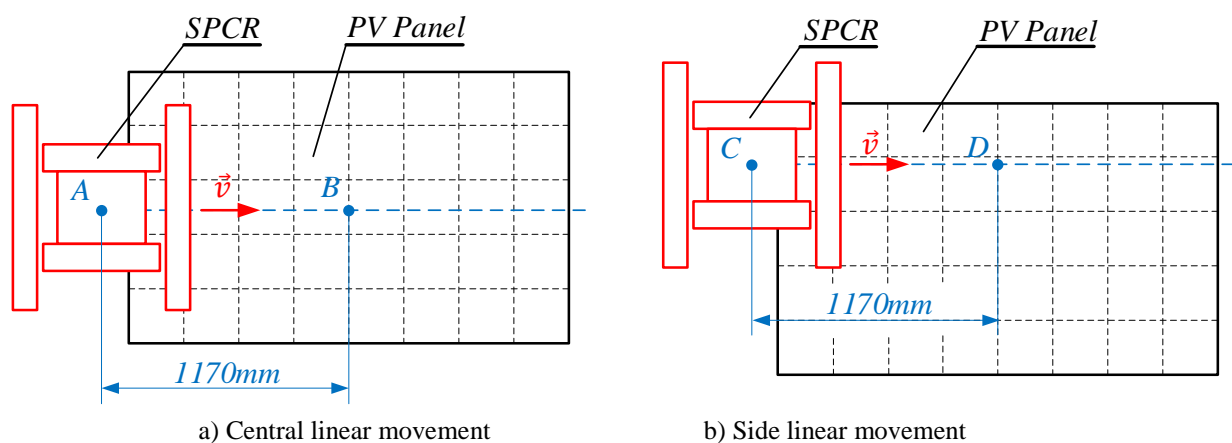


**Figure 4.** Simulation cases for robot movement on the surface of PV panels

Since the system is symmetric, only one-quarter of the panel dimensions were considered. The scenarios are described in detail in Table 3.

**Table 3.** Scenarios descriptions

Scenarios	Descriptions
Central linear movement	The SPCR was moved from point A to point B along the centerline of PV panels, as shown in Figure 4. The simulation was conducted at 10 positions, each spaced 120 mm apart.
Side linear movement	The SPCR's position was moved from point C to point D along to the sides of PV panels.

## 4. RESULTS AND DISCUSSION

### 4.1. Simulation result

Figure 5 shows the deformation contour of the PV panel in the two scenarios. In the first case as shown in Figure 5a), the SPCR moves closer to the center of the PV panel, and the deformation becomes increasingly pronounced due to the growing pressure exerted on the PV panel. The region of significant deformation is primarily focused beneath the center of gravity of the SPCR. The PV panel experiences a maximum displacement of 10.4 mm in this area, which afterward gradually diminishes towards the edges of the support frame. In the second as shown in Figure 5b), the contour shows the same trends as in the first case. However, there is a slight difference in the maximum displacement, that is, the region located near the contact area between the inner belt-based track of the SPCR and the PV panel surface shows the deformation of 11.03 mm.

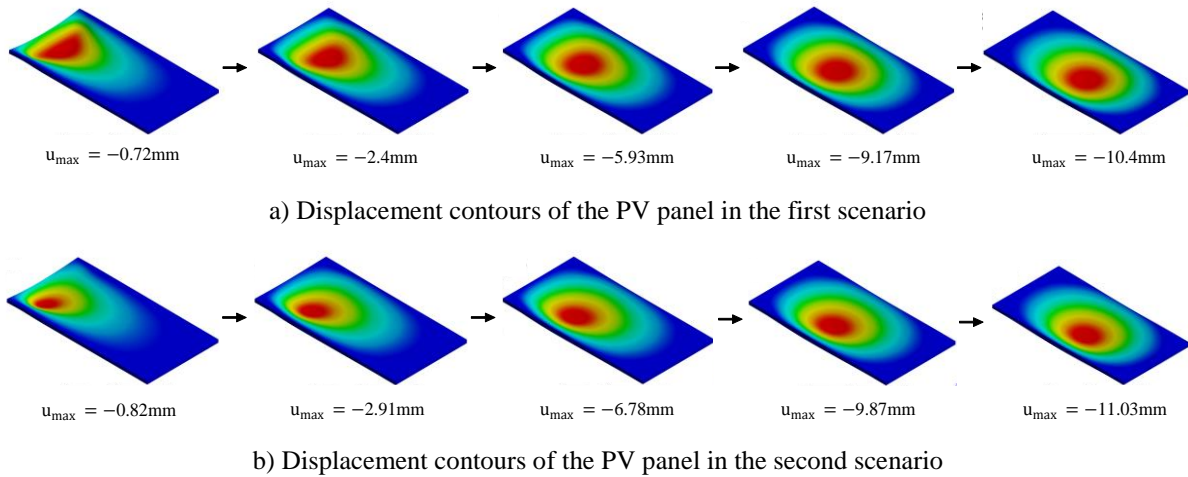


**Figure 5.** Simulation results of the central and slide linear movement cases

Based on the above results, the simulation of deformation at the center of the PV panel in the second case is further considered. Place the origin at the point lying on the short edge of the panel; the x-axis is parallel to the long side of the PV panel under non-deformed; the x-axis is perpendicular to the surface of the PV panel, in Figure 6. Equation (1), derived from the simulation results, characterizes the relationship between the deformation of the PV panel and its length.

$$y = 2.032 \times 10^{-5} x^2 + 0.039x + 8.414 \quad (1)$$

where x represents the horizontal coordinate and y represents the deformation at that specific point.

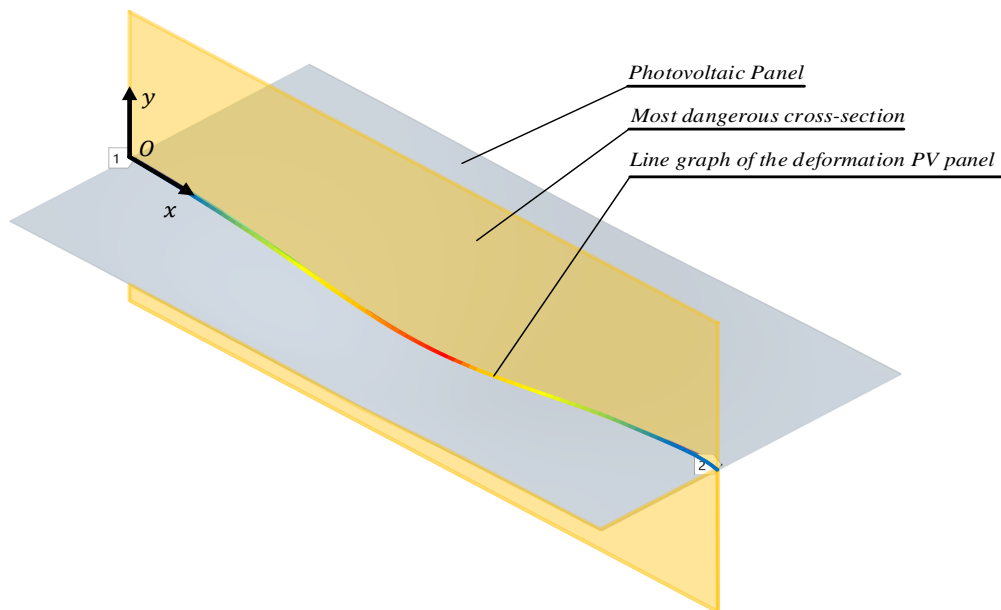


**Figure 6.** Hazardous zone cross-sections of PV panels following the result of the simulation

#### 4.2. Experiment result

Figure 7 shows the experimental setup that examines the most dangerous position of the PV panel as concluded in subsection 4.1. In this study, the Mitutoyo 543-400B round-type dial gauge was employed, offering a precision of 0.01mm. Furthermore, considering the extensive data collection required for the PV panel in experiments, a systematic approach is adopted to maintain the consistency of the measurements. This approach consists of four sequential steps outlined in Table 4.

**Table 4.** Experimental steps to measure the deformation of the panel in the most dangerous case

Step	Descriptions
1	Zero-return the Mitutoyo 543-400B measuring device corresponding to the flat surface of the PV panel without the SPCR.
2	Place the SPCR at the position where the maximum deformation occurs according to the simulation.
3	Mount the measurement tool along the line graph of the deformation PV panel.
4	Proceed by systematically moving the measurement tool linearly along two designated points on the PV panel. Maintain a consistent increment of 10mm between each measurement, recording the deformation observed at each point.

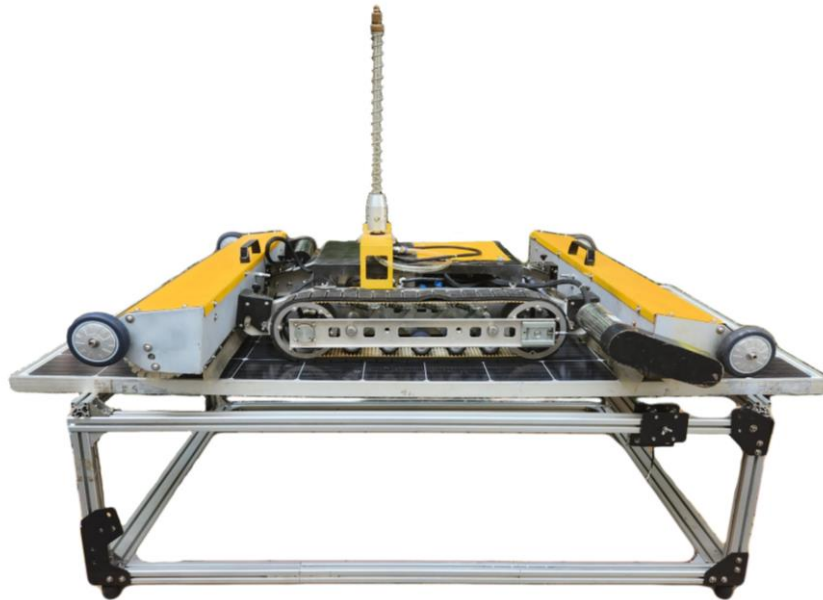


**Figure 7.** Experimental system to measure the deformation of the PV panel in the most dangerous case

Figure 8 describes the line graph of the PV panel at the most dangerous cross-section in both simulation and experimental cases. The horizontal axis is the position where the round-type dial gauge is located, and the vertical axis is the deformation at that specific point. The experimental graph reveals that the deformation pattern of the PV panel, with the SPCR positioned at the middle of the right/left edge, follows a parabolic trend. The point of minimum deformation (-10.88mm), belonging to the parabolic trend, represents the location of the most pronounced deflection.

Figure 8 illustrates two-line graphs derived from simulation data and experimental data. To evaluate the accuracy of the simulation, the correlation coefficient between the deformation line graphs of the simulation data and the experimental data is calculated. According to [22], the correlation coefficient ( $r$ ) between two-line graphs is determined as follows:

$$r = \frac{\sum_{i=1}^n (x_i - \bar{x})(y_i - \bar{y})}{(n-1)\sqrt{s_x^2 s_y^2}} \quad (2)$$

where  $x_i$  and  $y_i$  are the individual data points of the simulation and experimental data sets.  $\bar{x}$  and  $\bar{y}$  are the means of two datasets.  $n = 126$  is the number of samples.  $s_x^2$  and  $s_y^2$  are the variances of two datasets,  $a =$

$\{x, y\}$ , calculated as follows:

$$s_a^2 = \frac{\sum_{i=1}^n (a_i - \bar{a})^2}{n - 1} \quad (3)$$

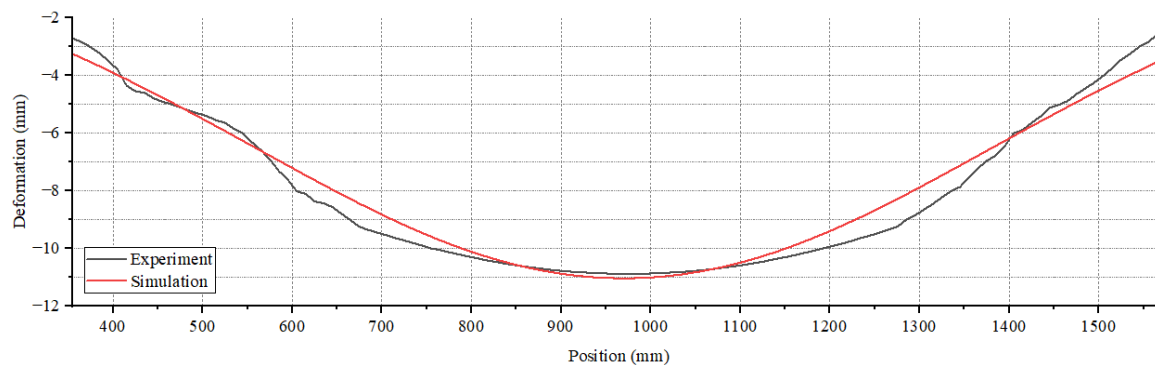


**Figure 8.** Graph of PV panel at the most dangerous cross-section by experiment and simulation

Besides, the correlation coefficient calculated as  $r = 0.988$  (close to +1), which shows experimental result data and simulation result data are positive strong linear relationships according to [22]. The experiment results show minimal deformation at position 975 mm, closely aligning with the simulation result (with an error of approximately 1.31%). In the line graph, the lowest point of deflection is important as it is the basis for designing the range of the working area of the damper system which aims to diminish the negative impact of the SPCR on PV panels. Notably, the experimental result (10.88mm) at the lowest point of deflection is lower than that of the simulation result (11.03 mm), so these conditions are completely valid for the calculations involved. Particularly considering that this study explores the most critical scenario for PV panel mountings (section 3), variations that result in lesser deformation of the panels do not diminish the significance of equation (1). It still remains relevant and valuable in informing the design of damper systems. With the given results, the initial simulation conditions and physical model in Section 3 are suitable. Moreover, the correlation serves as a confirmation of the underlying assumption that tempered glass and aluminum frames are primary load-bearing components of PV panels.

## 5. CONCLUSION

This paper studies the impact of the SPCR on PV panel deflection. A simulation model with appropriate boundary conditions was established to investigate the different deformations of the PV panel in two different scenarios. The results indicated that as the SPCR approached the center of the PV panel, the deformation of the PV panel increased gradually in both cases of central linear movement and side linear movement. Moreover, for maximum deformation of the PV panel, the research provided an equation that was assessed through experimental results with a reasonable difference. The experimental results also demonstrated the reliability of this estimated equation and provided a theoretical basis for the calculation of damper system designs in the future.

However, the paper has some limitations when ignoring the periodic vibrations caused by the rotating brush assembly of the SPCR. These vibrations can contribute to the degradation of the support frame, and the PV panel and induce microcracks. Hence, the impact of the brush assembly on the SPCR will be investigated through experimentation and simulation in the future. Additionally, the PV panel deformation in different mounting configurations will be studied to provide a more comprehensive understanding of the addressed issues.

## Acknowledgments

This research is funded by Viet Nam National University Ho Chi Minh City (VNUHCM) under grant number TX2023-20b-01. We acknowledge the support of time and facilities from National Key Laboratory of Digital Control and System Engineering (DCSELab), Ho Chi Minh City University of Technology (HCMUT), VNUHCM for this study.

## References

- [1] O. Sahu, “Alternative Sources of Energy in Sustainable Development Goals: A Study on Solar Energy,” *International Journal of Management, Public Policy and Research*, vol. 2, no. SpecialIssue, pp. 45–53, Mar. 2023, doi: 10.55829/ijmpr.v2ispecialissue.136.
- [2] A. O. M. Maka and J. M. Alabid, “Solar energy technology and its roles in sustainable development,” *Clean Energy*, vol. 6, no. 3, pp. 476–483, 2022, doi: 10.1093/ce/zkac023.
- [3] International Energy Agency, “Renewables 2021 - Analysis and forecast to 2026,” 2021.
- [4] Karunya University. Department of Electronics and Communication Engineering, Karunya University, Institute of Electrical and Electronics Engineers, and IEEE Electron Devices Society, “ICDCS’16: proceedings of the 3rd International Conference on Circuits and Systems (ICDCS) - 2016: 3rd to 5th - March 2016, Department of Electronics and Communication Engineering, School of Electrical Sciences,”
- [5] Saravanan V.S and Darvekar S.K, “Solar Photovoltaic Panels Cleaning Methods A Review,” *International Journal of Pure and Applied Mathematics*, vol. 118, no. 24, pp. 1-17, 2018.
- [6] B. Kobrin, “Self-cleaning Technologies for Solar Panels,” *n-tech Research*, no. May, pp. 1–15, 2018.
- [7] T. T. N. Nhut Thang Le, Hoang Long Phan, “Survey on the Cleaning Method for Solar Photovoltaic Panel [6].pdf.”
- [8] R. M. Gul, M. A. Kamran, F. U. Zafar, and M. Noman, “The impact of static wind load on the mechanical integrity of different commercially available mono-crystalline photovoltaic modules,” *Engineering Reports*, vol. 2, no. 12, pp. 1–13, 2020, doi: 10.1002/eng2.12276.
- [9] R. L. Achey, “Life Expectancy,” *J Palliat Med*, vol. 19, no. 4, p. 468, 2016, doi: 10.1089/jpm.2015.0452.
- [10] M. Dhimish, V. Holmes, M. Dales, and B. Mehrdadi, “Effect of micro cracks on photovoltaic output power: Case study based on real time long term data measurements,” *Micro Nano Lett*, vol. 12, no. 10, pp. 803–807, 2017, doi: 10.1049/mnl.2017.0205.
- [11] G. Xu, D. Xue, and Y. Wang, “Development and main research status of tracked vehicle suspension system,” 2017.
- [12] P. C. Saibabu, H. Sai, S. Yadav, and C. R. Srinivasan, “Synthesis of model predictive controller for an identified model of MIMO process,” *Indonesian Journal of Electrical Engineering and Computer Science*, vol. 17, no. 2, pp. 941–949, 2019, doi: 10.11591/ijeecs.
- [13] T. Jing, “ECN2017003: Glass Thickness Change from 4.0mm to 3.2mm for Trina Solar 72-cell TALLMAX M PLUS Modules,” 2017. [https://www.trinasolar.com/sites/default/files/Trina\\_EC2017003\\_72\\_TALLMAX M PLUS Glass Thickness Change.pdf](https://www.trinasolar.com/sites/default/files/Trina_EC2017003_72_TALLMAX_M_PLUS_Glass_Thickness_Change.pdf) (accessed May 30, 2023).
- [14] J. Svarc, “Solar Panel Construction,” 2020. <https://www.cleanenergyreviews.info/blog/solar-panel-components-construction> (accessed May 30, 2023).
- [15] Smartclima, “Solar Panel Aluminium Frame.” <https://www.smartclima.com/solar-panel-aluminium-frame.htm> (accessed May 30, 2023).
- [16] J. Dong, H. Yang, X. Lu, H. Zhang, and J. Peng, “Comparative Study on Static and Dynamic Analyses of an Ultra-thin Double-Glazing PV Module Based on FEM,” in *Energy Procedia*, Elsevier Ltd, 2015, pp. 343–348. doi: 10.1016/j.egypro.2015.07.382.
- [17] U. Gunasekaran, P. Emani, and A. M. T.P, “Facades of Tall Buildings - State of the Art,” *Mod Appl Sci*, vol. 4, no. 12, 2010, doi: 10.5539/mas.v4n12p116.
- [18] A. Singh and A. Agrawal, “Experimental investigation on elastic spring back in deformation machining bending mode,” in *International Manufacturing Science and Engineering Conference, MSEC 2015*, 2015. doi: 10.1115/MSEC20159283.
- [19] Winaico, “Recommended Clamping Zones for Solar Panel Installations.” <https://winaico.com/guides/clamping-zones/> (accessed May 30, 2023).
- [20] JA Solar, “JA Solar PV Modules Installation Manual,” 2019. <https://www.jasolar.com/uploadfile/2019/0129/20190129030921131.pdf> (accessed May 30, 2023).
- [21] M. T. Nguyen, C. T. Truong, V. T. Nguyen, V. T. Duong, H. H. Nguyen, and T. T. Nguyen, “Research on Adhesive Coefficient of Rubber Wheel Crawler on Wet Tilted Photovoltaic Panel,” *Applied Sciences (Switzerland)*, vol. 12, no. 13, Jul. 2022, doi: 10.3390/app12136605.
- [22] R. S. Kenett and P. Newbold, “Statistics for Business and Economics,” *Journal of the Royal Statistical Society Series D: The Statistician*, vol. 37, no. 1., pp. 93-94, 1988. doi: 10.2307/2348399.



**[S3-4] Hyperbolic Tangent Reaching Law-Based Sliding Mode Controller for Position Control of Rajiform Biomimetic Underwater Robot**

Van Hien Nguyen<sup>2</sup>, Phuc Long Duong<sup>1,2</sup>, Vu Nguyen Phung<sup>1,2</sup>, Vuong Quang Huy Trinh<sup>2</sup>, Van Tu Duong<sup>1,2</sup>, Huy Hung Nguyen<sup>3</sup>, Tan Tien Nguyen<sup>1,2</sup>

<sup>1</sup> National Key Laboratory of Digital Control and System Engineering (DCSELab), Ho Chi Minh City University of Technology (HCMUT), 268 Ly Thuong Kiet Street, District 10, Ho Chi Minh City, Viet Nam

<sup>2</sup> Viet Nam National University Ho Chi Minh City, Linh Trung Ward, Thu Duc City, Ho Chi Minh City, Viet Nam

<sup>3</sup> Faculty of Electronics and Telecommunication, Sai Gon University, Viet Nam

\*Corresponding author: nttien@hcmut.edu.vn

**Abstract**

This study focuses on the development of a biomimetic underwater robot that mimics the swimming behavior of Rajiform fishes. The proposed robot utilizes two undulating fins for locomotion control, aiming to provide an alternative to conventional propulsion systems in autonomous underwater vehicles. To achieve effective locomotion control, a sliding mode control algorithm with a hyperbolic tangent reaching law is employed. First, the study begins by modeling the robot system, describing the relationship between the vehicle's membrane and the dynamic forces generated, considering its position on a two-dimensional surface is obtained. Subsequently, a hyperbolic tangent-based sliding mode controller is implemented to ensure the proposed robot follows a desired path while minimizing tracking errors, in contrast to the traditional signum function. To evaluate the efficacy of the proposed solution, simulations are conducted as a means of proof-of-concept. These simulations demonstrate the feasibility of the suggested approach and its potential to provide an effective solution for controlling the locomotion of the biomimetic underwater robot.

**Keywords:** *Rajiform, Underwater biomimetic robot, Autonomous underwater vehicle, Position control, Sliding mode control*

**1. INTRODUCTION**

Recent research studies [1]–[3] have demonstrated that the Rajiform swimming type, which involves an undulatory fin motion employed by fish for efficient and rapid movement in water, exhibits smooth and flexible propulsion, surpassing the performance of conventional underwater vehicles propelled by screw propellers. Robotic fish that utilize Rajiform locomotion offer advantages in terms of propulsive efficiency, maneuverability, and stealth, while mitigating the drawbacks associated with large-scale systems, low energy efficiency, and environmental disturbance [4], [5]. Various approaches utilizing different control methods have been explored to enable effective locomotion control for this swimming type.

Chunlin Zhou and K. H. Low [6] introduced a CPG-Based motion control structure of the flapping motion for RoMan II – A fish-like AUV inspired by a manta ray, a kind of fish using the Rajiform swimming type. This research shows the results in contributing the swimming locomotion through controller design and experimental results. The proposed control method in this paper presents a versatile framework that can address locomotion control challenges in various systems. Specifically, it can be applied to tackle the locomotion control problems of fish robots equipped with multiple fins or even more broadly to robots exhibiting rhythmic movement patterns. The model formulation adopted in this study is of a generic nature, allowing for its potential application in a wide range of robotic systems. However, the research did not mention the relationship between the created fin pattern with the robot's motion, which did not clarify the efficiency of the calculated system.

On the other hand, Tiandong Zhang, etc. [7] gained the design and implementation of an innovative biomimetic underwater vehicle (BUV) and its locomotion controller using the CPGs Model and Fuzzy Adaptive PID. A bio-inspired BUV named RoboDact with high maneuverability and good low-speed locomotion stability has been developed. Physical experiments verify the feasibility and effectiveness of the mechanism design and locomotion control system. However, the presented controller is formed in a PID based, which is a linear controller. Thus, the results contained the linear controller problems, in which responses were proved to be more disadvantaged than that of nonlinear controllers.

As a result, Rajiform undulating movement has gained significant interest and research worldwide, with many approaches aiming to control its locomotion in six degrees of freedom (6-DOF) space. This paper presents a different approach to the input-output relationship and 2D locomotion control using a nonlinear controller. Thus, the system's locomotion modeling process is formed, and the sliding mode controller with hyperbolic tangent-based reaching law is designed, followed by the simulation and experiment results in this paper.

## 2. UNDERWATER BIOMIMETIC ROBOT LOCOMOTION SYSTEM MODELING

A typical Rajiform underwater biomimetic simulation robot is described in Figure 1. The force analysis is applied to show the interacting relationship between the robot itself and the outer environment.

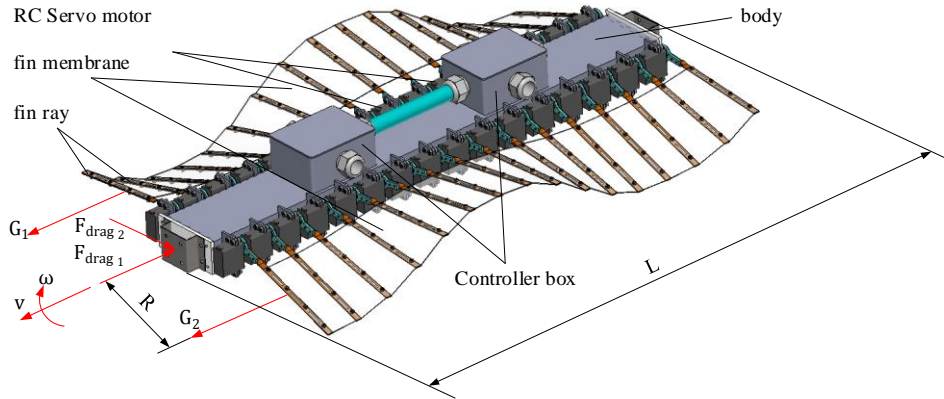


Figure 1. Rajiform robot model

Where  $G_1$  and  $G_2$  are the generated forces of the fin membrane through the pattern produced by the movement of the fin rays ( $N$ );  $F_{drag_1}$  and  $F_{drag_2}$  are the resisting forces that the water affects on the robot's body, in both straight and turn motion of the robot ( $N$ );  $L$  is the length of the proposed robot ( $m$ ); and  $R$  is the distance from the center line of the robot to the midpoint of the fin membrane ( $m$ ) in a straight alignment.

Assume that the force is generated in the center of the fin membrane, the following equation system is formed to describe the dynamic relationship among related forces through 2D motion, including the translational motion equation and turning motion equation following Newton 3<sup>rd</sup> law.

$$\begin{cases} m\dot{v}_r = G_1 + G_2 - F_{drag_1} \\ I\dot{\omega}_r = R(G_1 - G_2) - 2\frac{L}{2}F_{drag_2} \end{cases} \quad (1)$$

Where  $m$  and  $I$  are the proposed robot's mass ( $kg$ ) and inertia momentum ( $Nm$ ). The water drag forces applied on the robot body can be calculated as equations (2) – (3), with the speed of  $v$  on translational motion and angular speed of  $\omega$ .

$$F_{drag_1} = \frac{1}{2}\rho C_D A_1 (v - v_f)^2 \quad (2)$$

$$F_{drag_2} = \frac{1}{2}\rho C_D A_2 \left(\omega \frac{L}{2}\right)^2 \quad (3)$$

where

$\rho$  is the mass density of the environmental fluid,  $kg/m^3$

$C_D$  is the drag co-efficient of model and fluid,  $C_D$

$A_1$  and  $A_2$  are the drag area when the robot on straight and turning motion,  $m^2$

$v_f$  is the velocity of the environmental fluid, when the AUV operates in the static fluid condition, which results in  $v_f = 0$ .

For simplicity's sake, these terms are defined as follows:

$$G_{w_1} \triangleq \frac{1}{2}\rho C_D A_1 \text{ is the translational drag force coefficient.}$$

$$G_{w_2} \triangleq \frac{L^3}{8}\rho C_D A_2 \text{ is the turning drag force coefficient.}$$

Equation (1) can be described in the typical state-space form  $\dot{\mathbf{x}} = \mathbf{Ax} + \mathbf{Bu} + \mathbf{d}$ . Since the real scenario is very different from the calculation itself with only physical equations, disturbances are taken into consideration in the locomotion modeling equation.

$$\begin{bmatrix} \dot{v}_r \\ \dot{\omega}_r \end{bmatrix} = \begin{bmatrix} -\frac{1}{m} G_{w_1} v_r & 0 \\ 0 & -\frac{1}{I} G_{w_2} \omega_r \end{bmatrix} \begin{bmatrix} v_r \\ \omega_r \end{bmatrix} + \begin{bmatrix} \frac{1}{m} & \frac{1}{m} \\ \frac{1}{r} & -\frac{1}{r} \end{bmatrix} \begin{bmatrix} G_1 \\ G_2 \end{bmatrix} + \begin{bmatrix} dv \\ d\omega \end{bmatrix} \quad (4)$$

In the system of Equation (4), the fin-generated forces  $G_1$  and  $G_2$  act as the control input for the locomotion control system, where the output is the robot's location in 3-DOF dimension take place including  $x$ ,  $y$ , and  $\theta$ , wherein  $x$  and  $y$  are the robot's coordinates in 2D plane,  $\theta$  is the turning angle;  $dv$  and  $d\omega$  are the estimated disturbance which impact on the robot in the real environment.

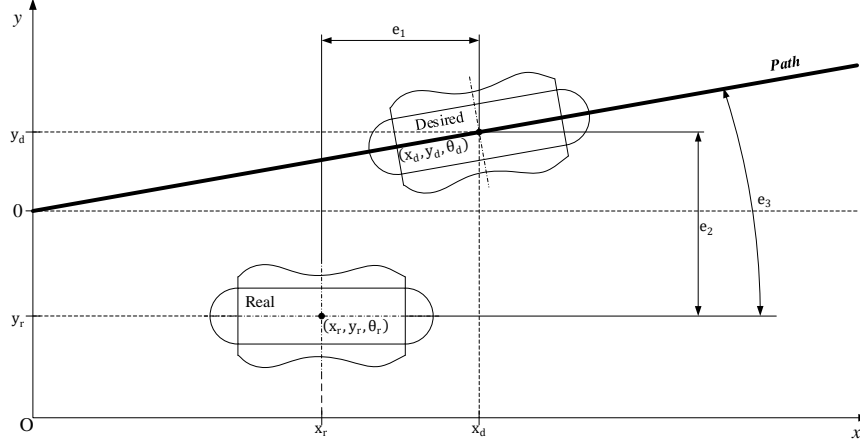


**Figure 2.** Robot's relative location in  $Oxy$  plane in 3-DOF dimension

**Fig. 2** shows the relative coordinates between the real and desired AUV. The relation between  $v$ ,  $\omega$  and its coordinates can be described.

$$\begin{bmatrix} \dot{x} \\ \dot{y} \\ \dot{\theta} \end{bmatrix} = \begin{bmatrix} \cos \theta_r & 0 \\ \sin \theta_r & 0 \\ 0 & 1 \end{bmatrix} \begin{bmatrix} v \\ \omega \end{bmatrix} \rightarrow \begin{cases} e_1 = (x_r - x_d) \cos \theta_d + (y_r - y_d) \sin \theta_d \\ e_2 = -(x_r - x_d) \sin \theta_d + (y_r - y_d) \cos \theta_d \\ e_3 = \theta_r - \theta_d \end{cases} \quad (5)$$

### 3. LOCOMOTION CONTROLLER DESIGN

The sliding mode controller is applied for the robot to track the desired path. The sliding surface and its derivative form are chosen as follows:

$$\begin{cases} s_1 = \dot{e}_1 + \lambda_1 e_1 \\ s_2 = \dot{e}_2 + \lambda_2 e_2 + \lambda_3 e_2 \sin(e_3) \end{cases} \quad (6)$$

By taking the first time derivative of equation (6), it yields:

$$\begin{cases} \dot{s}_1 = \ddot{e}_1 + \lambda_1 \dot{e}_1 \\ \dot{s}_2 = \ddot{e}_2 + \lambda_2 \dot{e}_2 + \lambda_3 \dot{e}_3 \sin(e_2) \end{cases} \quad (7)$$

On the other hand, Gao et al. [8] introduced a new approach to calculate the first derivative sliding variable for the  $n$ -inputs and  $m$ -output dynamics system, which in this case include 2 inputs of the 2-undulating fin force and 3-DOF outputs.

$$\begin{cases} \dot{s}_1 = -Q_1 s_1 - P_1 \text{sign}(s_1) \\ \dot{s}_2 = -Q_2 s_2 - P_2 \text{sign}(s_2) \end{cases} \quad (8)$$

The control input  $G_1$  and  $G_2$  are chosen as follows:

$$\begin{cases} G_1 = \frac{1}{2} (m \dot{v}_c + F_{drag1}) + \frac{1}{2} (I \dot{\omega}_c + 2 \frac{L}{2} F_{drag2}) \\ G_2 = \frac{1}{2} (m \dot{v}_c + F_{drag1}) - \frac{1}{2} (I \dot{\omega}_c + 2 \frac{L}{2} F_{drag2}) \end{cases} \quad (9)$$

where

$$\begin{cases} \dot{v}_c = \frac{1}{\cos e_3} (-\lambda_1 \dot{e}_1 - Q_1 s_1 - P_1 \text{sign}(s_1) - \dot{\omega}_d e_2 - \dot{e}_2 \omega_d - v_r \dot{e}_3 \sin e_3 + \dot{v}_d) \\ \dot{\omega}_c = \dot{\omega}_d + \frac{(-\lambda_2 \dot{e}_2 - Q_2 s_2 - P_2 \text{sign}(s_2) + \dot{\omega}_d e_1 + \dot{\omega}_d \dot{e}_1 - \dot{v}_r \sin e_3)}{\lambda_3 \text{sign}(e_2) + v_r \cos e_3} \end{cases} \quad (10)$$

A candidate Lyapunov function is chosen to analyze the stability of the system of Eq. (7) as:

$$V = \frac{1}{2} s_1^2 + \frac{1}{2} s_2^2 \geq 0 \quad (11)$$

Using the chosen control input, the derivative form for the Lyapunov function can be described along with equations (5), (6), (7), and (9).

$$\dot{V} = s_1 \dot{s}_1 + s_2 \dot{s}_2 = s_1(-Q_1 s_1 - P_1 \text{sign}(s_1)) + s_2(-Q_2 s_2 - P_2 \text{sign}(s_2)) \quad (12)$$

$$\dot{V} = -Q_1 s_1^2 - Q_2 s_2^2 - P_1 |s_1| - P_2 |s_2| \leq 0$$

where  $Q_1, Q_2, P_1, P_2, \lambda_1, \lambda_2, \lambda_3 \geq 0$  are the control parameters, which are designed according to Routh-Hurwitz.

As equation (11) shows, following the Lyapunov stability (the Lyapunov function  $V \geq 0$  and its derivative form  $\dot{V} < 0$ ), the chosen control inputs are proved to be stable. However, the signum-reaching law used in the control input signal is assumed to cause the chattering phenomenon. To resolve this problem, the hyperbolic tangent is taken into consideration.

$$\begin{cases} \dot{v}_c = \frac{1}{\cos e_3} (-\lambda_1 \dot{e}_1 - Q_1 s_1 - P_1 \tanh(s_1) - \dot{\omega}_d e_2 - \dot{e}_2 \omega_d - v_r \dot{e}_3 \sin e_3 + \dot{v}_d \\ \dot{\omega}_c = \dot{\omega}_d + \frac{(-\lambda_2 \dot{e}_2 - Q_2 s_2 - P_2 \tanh(s_2) + \dot{\omega}_d e_1 + \omega_d \dot{e}_1 - \dot{v}_r \sin e_3)}{\lambda_3 \text{sign}(e_2) + v_r \cos e_3} \end{cases} \quad (13)$$

#### 4. SIMULATION RESULTS

The simulation is conducted based on computational modeling to evaluate the performance of the proposed AUV locomotion system. Two distinct patterns, namely curve and straight, are utilized to assess the transient locomotion response of the AUV under the influence of the proposed controller. By employing these trajectories, the simulation aims to examine the AUV's capability to achieve both translational and turning motions.

Random functions are employed to introduce disturbances in the implemented system. These disturbances are incorporated during the simulation to emulate real-world conditions and evaluate the robustness of the AUV locomotion system. By utilizing random functions, the disturbances exhibit unpredictable characteristics, allowing for a comprehensive analysis of the system's response and its ability to handle unexpected environmental influences.

**Table 1.** The controller simulation parameters

Parameters	Value	Parameters	Value
$m, kg$	5	$\lambda_1$	25
$2R, m$	0.52	$\lambda_2$	25
$L, m$	0.8	$\lambda_3$	10
$I, Nm$	0.075	$Q_1$	10
$\rho, kg/m^3$	981.8	$Q_2$	10
$C_D$	0.1	$P_1$	1
$A_1, m^2$	0.031	$P_2$	1
$A_2, m^2$	0.208	$dv$	30%
$g, m/s^2$	9.81	$d\omega$	30%

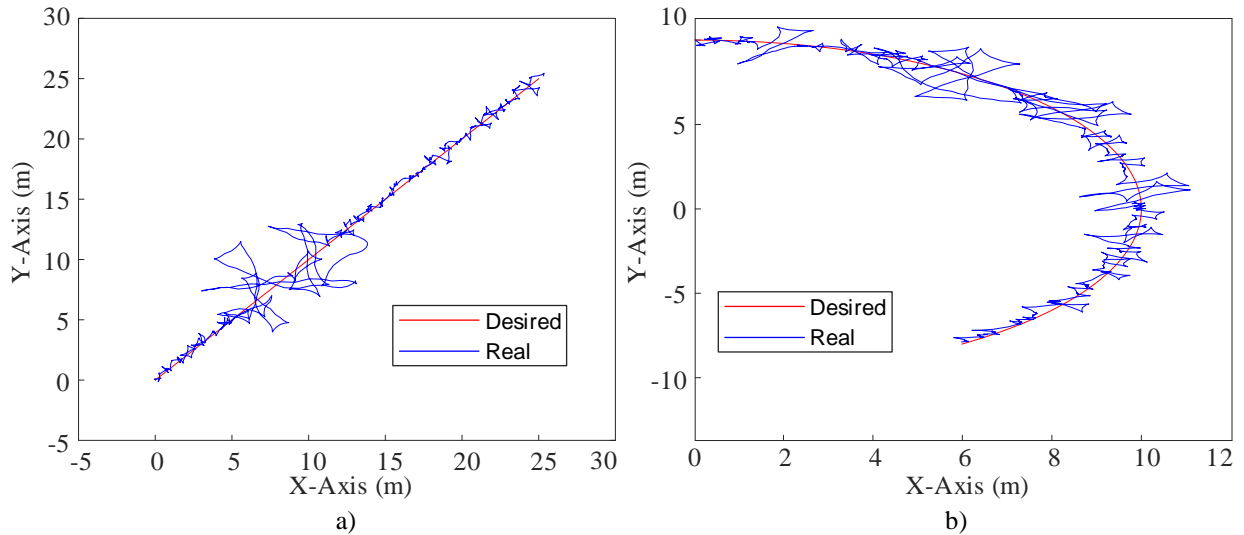


**Figure 3.** AUV locomotion orbit on  $Oxy$  plane using signum reaching law with 30% disturbance

a) Straight movement; b) Curve movement

As shown in the simulation in **Fig. 3**, the signum reaching law is assumed to track the desired path. However, due to the chattering phenomenon, the tracking error severely fluctuates surrounding the desired path under the impact of random disturbance in both straight and curve motion.

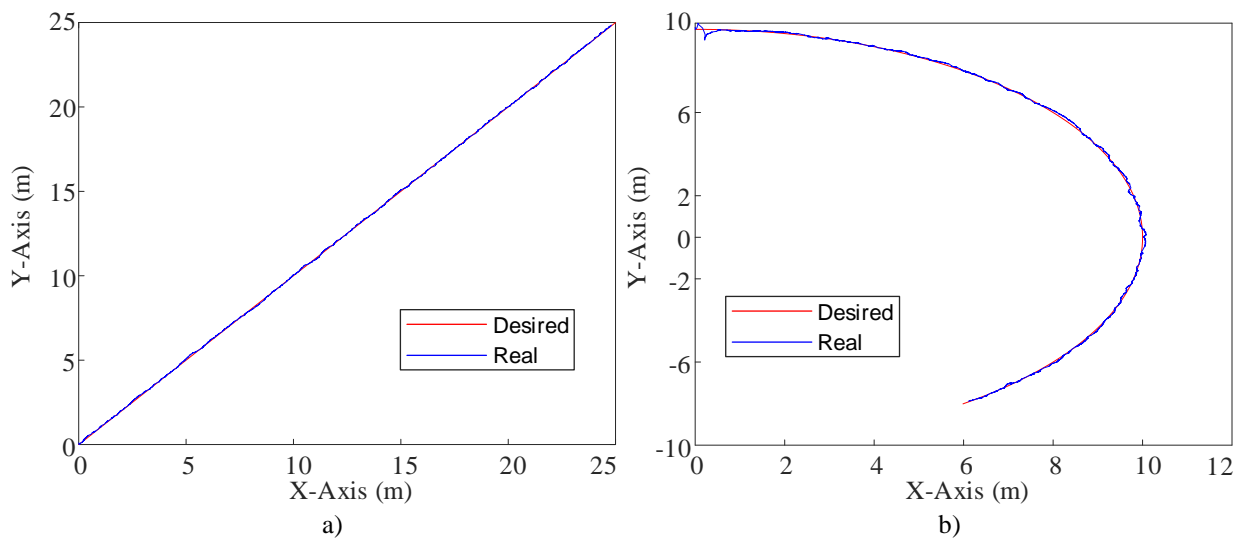


**Figure 4.** AUV locomotion orbit on  $Oxy$  plane using hyperbolic tangent reaching law with 30% disturbance

a) Straight movement; b) Curve movement

On the other hand, with the application of the hyperbolic tangent reaching law, the smoothness of the orbit tracking graph thoroughly increases by getting rid of the unwanted chattering phenomenon. However, the disturbance still slightly affects the simulated tracking path.

## 5. CONCLUSION

This research paper introduces the modeling equations for a Rajiform fish-inspired biomimetic autonomous underwater vehicle (AUV). To control the locomotion tracking of the AUV, a sliding mode controller with a hyperbolic tangent reaching law is implemented. The simulation results demonstrate the tracking performance of the proposed controller and provide a comparison between using the traditional signum function and the hyperbolic tangent function, which proves a much better efficiency of the hyperbolic tangent in tracking the desired path.

Moreover, the study plans to further validate the controller's effectiveness through experimental implementation. An experimental AUV model will be utilized to assess the realistic tracking capabilities of the

suggested controller under real-world conditions. This experimental validation will help ascertain the practical feasibility and performance of the proposed controller in a practical setting.

### Acknowledgments

This research is funded by Viet Nam National University Ho Chi Minh City (VNUHCM) under grant number TX2023-20b-01. We acknowledge the support of time and facilities from National Key Laboratory of Digital Control and System Engineering (DCSELab), Ho Chi Minh City University of Technology (HCMUT), VNUHCM for this study.

### References

- [1] E. L. Blevins and G. V. Lauder, "Rajiform locomotion: Three-dimensional kinematics of the pectoral fin surface during swimming in the freshwater stingray *Potamotrygon orbignyi*," *Journal of Experimental Biology*, vol. 215, no. 18, pp. 3231–3241, Sep. 2012, doi: 10.1242/jeb.068981.
- [2] M. Sfakiotakis, J. Fasoulas, M. Arapis, and N. Spyridakis, "Development and Experimental Evaluation of an Undulatory Fin Prototype Grasping and Manipulation View project OCTOPUS View project Development and Experimental Evaluation of an Undulatory Fin Prototype," in *22nd International Workshop on Robotics in Alpe-Adria-Danube Region, Slovenia, 2013*. [Online]. Available:
- [3] Y. Wang, J. Tan, B. Gu, and D. Zhao, "Design of the undulating fin propulsor with rajiform swimming mode," *Key Eng Mater*, vol. 579–580, pp. 451–459, 2014, doi: 10.4028/www.scientific.net/KEM.579-580.451.
- [4] Y. Li et al., "A comprehensive review on fish-inspired robots," *International Journal of Advanced Robotic Systems*, vol. 19, no. 3. SAGE Publications Inc., May 01, 2022. doi: 10.1177/17298806221103707.
- [5] G. V. Lauder, "Fish locomotion: Recent advances and new directions," *Ann Rev Mar Sci*, vol. 7, pp. 521–545, Jan. 2015, doi: 10.1146/annurev-marine-010814-015614.
- [6] C. Zhou and K. H. Low, "Design and locomotion control of a biomimetic underwater vehicle with fin propulsion," *IEEE/ASME Transactions on Mechatronics*, vol. 17, no. 1, pp. 25–35, Feb. 2012, doi: 10.1109/TMECH.2011.2175004.
- [7] T. Zhang, R. Wang, Y. Wang, L. Cheng, S. Wang, and M. Tan, "Design and Locomotion Control of a Dactylopteridae-Inspired Biomimetic Underwater Vehicle with Hybrid Propulsion," *IEEE Transactions on Automation Science and Engineering*, vol. 19, no. 3, pp. 2054–2066, Jul. 2022, doi: 10.1109/TASE.2021.3070117.
- [8] W. Gao and J. C. Hung, "Variable Structure Control of Nonlinear Systems: A New Approach," 1993.

**[S3-5] Nonlinear Regression of Thrust Force Produced by Rajiform Undulating Fin**

Van Hien Nguyen<sup>1,2</sup>, Phuc Long Duong<sup>1,2</sup>, Vu Nguyen Phung<sup>1,2</sup>, Vuong Quang Huy Trinh<sup>1,2</sup>, Van Tu Duong<sup>1,2</sup>, Huy Hung Nguyen<sup>3</sup>, and Tan Tien Nguyen<sup>1,2,\*</sup>

<sup>1</sup> National Key Laboratory of Digital Control and System Engineering (DCSELab), Ho Chi Minh City University of Technology (HCMUT), 268 Ly Thuong Kiet Street, District 10, Ho Chi Minh City, Viet Nam

<sup>2</sup> Viet Nam National University Ho Chi Minh City, Linh Trung Ward, Thu Duc City, Ho Chi Minh City, Viet Nam

<sup>3</sup> Faculty of Electronics and Telecommunication, Sai Gon University, Viet Nam

\*Corresponding author: nttien@hcmut.edu.vn

**Abstract**

This paper presents a novel undulating discrete fin model inspired by the Rajiform locomotion of underwater species. The Rajiform biomimetic underwater model features sixteen consecutive fin rays interconnected by a flexible membrane that water-exerted force is analyzed in this study. The findings reveal a non-linear relationship between the force and the frequency of the fin movement, which is regressed by a fifth-order Polynomial equation through a surface fitting algorithm. This enables the model's controller to regulate the force by adjusting the frequency values. The results suggest that the undulating discrete fin model has the potential to be used in various underwater applications, such as underwater robotics and propulsion systems.

**Keywords:** Rajiform, Discrete undulating fins, Biomimetic underwater robot, Fish robot, Thrust force, Nonlinear regression

**1. INTRODUCTION**

Advancements in the fields of biology, smart materials, and robotics have played a pivotal role in the progress of biomimetic propulsion and the development of fish-like swimming robots [1]. These robots, known as biologically inspired underwater vehicles (BIUVs), are specifically designed to imitate fish locomotion behaviors to achieve efficient propulsion [1]–[3]. Unlike conventional autonomous underwater vehicles (AUVs), BIUV systems find diverse applications in marine exploration, seabed mapping, military surveillance, environmental assessments, mine detection, and scientific research. What sets BIUVs apart from traditional AUVs are their unique characteristics. Through millions of years of evolution and natural selection, fish have developed highly efficient body mechanisms and swimming modes for underwater locomotion, making them exemplary models for energy-efficient propulsion in man-made underwater vehicles. Unlike screw propellers, the movement of fish fins or bodies offers superior maneuverability and allows for precise posture adjustments in underwater robots [1], [2], [4]. This flexibility proves particularly advantageous for operations conducted at low speeds in confined areas or corners. Additionally, BIUVs exhibit a reduced environmental impact due to their quieter and less polluting nature, largely attributed to the undulating fin movements, which addresses the challenges associated with traditional propellers. These inherent advantages serve as inspiration for researchers and engineers to explore innovative designs that enhance the performance of man-made systems when interacting with the marine environment [5].

Rajiform locomotion is a type of undulatory fin motion utilized by fish to achieve efficient and rapid movement in water. Recent research studies [6]–[8] demonstrated that Rajiform locomotion generates a smooth and flexible movement that outperforms conventional underwater vehicles propelled by screw propellers. Robotic fish that employ Rajiform locomotion have the advantage of superior propulsive efficiency, maneuverability, and stealth while avoiding the drawbacks associated with large scale, low energy efficiency, and environmental disturbance [2], [3]. On the other hand, Nguyen et al. [9] introduced an analysis of the generated force using Gymnotiform on both continuous and discrete fin types. However, this force analysis model came up with only the experimental results on X – Axis created force, as well as the lack of presenting the generated force response over time.

Consequently, Rajiform swimming type for biomimetic underwater robots has become an area of great interest and research worldwide, with many approaches aiming to evaluate the generated force. This paper would mainly focus on re-modeling the thrust generation system on the fin membrane, with additional consideration given to the discretization of the continuous fin. Furthermore, a comparison between the computational calculation and experimental results regarding the generated forces will be taken into consideration as proof of the availability of the suggested model.

## 2. THEORETICAL BACKGROUND

The generated thrust force in the fins of underwater biomimetic robots is the driving factor behind their locomotion. Both continuous and discontinuous dynamic models have been utilized to investigate the undulatory movement of fins in underwater biomimetic robots in the literature. However, given the limitations in robotic manufacturing and the scope of this paper, the continuous fin modeling approach is not considered. Instead, Sfakiotakis et al. [6] proposed a fin discretization model, which consists of fin rays connected by a soft membrane. Undulating motion is generated by controlling the fin ray in a sine wave pattern at  $n$ -th fin ray of  $N$  fin rays with  $L$  fin length.

$$\theta(n, t) = \theta_{max} \sin\left(2\pi ft + \phi_0 - \frac{2\pi n L}{N-1\lambda}\right) \quad (1)$$

where  $\theta(n, t)$  is the angle of  $n$ -th ray.  
 $\phi_0 = 0$  is the initial phase.  
 $\theta_{max}$  is the maximum oscillating amplitude of the sine wave.  
 $\lambda$  is the wavelength, calculated using the number of fin rays.

The thrust generated by the Rajiform biomimetic underwater vehicle is affected by several factors [9]. This research, however, fixes a variety of parameters to inspect the impact of oscillating amplitude and frequency. A computational method based on infinitesimal analysis to model the thrust force in fin discretization is presented in Fig. 1.

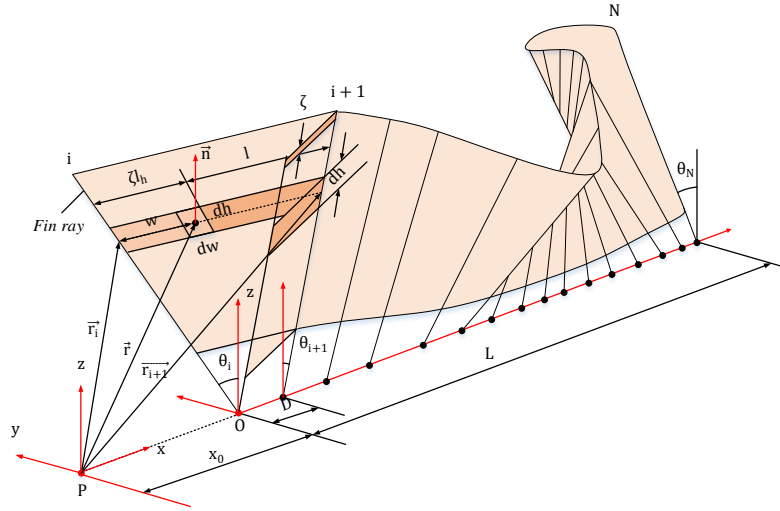


Figure 1. Modeling of discrete fin membrane

From Fig. 1, the inertial coordinate system {P} and the body coordinate system of the fin {O} are shown in Fig. 1. The position  $r$  of any surface element  $ds$  in the inertial coordinate system {P} is expressed by vector  $r_i$  and  $r_{i+1}$ .

$$r = r_{i+1} + w \frac{r_i - r_{i+1}}{\|r_i - r_{i+1}\|} = \begin{bmatrix} x_0 + Di \\ h \sin \theta_{i+1}(t) \\ h \cos \theta_{i+1}(t) \end{bmatrix} + \frac{w}{W_{max}} \begin{bmatrix} -D \\ h[\sin \theta_i(t) - \sin \theta_{i+1}(t)] \\ h[\cos \theta_i(t) - \cos \theta_{i+1}(t)] \end{bmatrix} \quad (2)$$

Nguyen, et al. [9] revealed the forces generated by the discrete undulating Gymnotiform fin at a certain  $q$  point on the fin coordinates, followed by the equation of total force generated by the whole membrane, which is the combination of  $dS$  areas with  $dh$  height and  $dw$  width. The total produced force of the membrane with  $i \in [0, N-1]$ ,  $h \in [h_{min}, h_{max}]$ ,  $w \in [w_{min}, w_{max}]$  is shown in Equation (4).

$$\vec{f} = -\frac{1}{2} \rho C_n \|\vec{V}_n\| \vec{V}_n = -\frac{1}{2} \rho C_n \|\vec{V}_n\|^2 \text{sign}(\vec{V}_n) \quad (3)$$

$$\vec{F}_{fin} = - \iint \frac{1}{2} \rho C_n \|\vec{V}_n\| \vec{V}_n dS = \sum_{i=0}^{N-1} \int_{h_{min}}^{h_{max}} \int_{w_{min}}^{w_{max}} \vec{F}_q dw dh \quad (4)$$



where  $\vec{V}_n$  is the nominal velocity vector of point P, calculated from the normal unit vector of  $dS \vec{n}_0$  and  $D$  denotes the distance between two consecutive fin rays. The nominal velocity vector is calculated by:

$$\vec{V}_n = (\vec{n}_0 \vec{r}_q) \vec{n}_0 \quad (5)$$

where

$$\vec{n}_0 = \frac{\frac{\partial \vec{r}_q}{\partial h} \frac{\partial \vec{r}_q}{\partial w}}{\left\| \frac{\partial \vec{r}_q}{\partial h} \frac{\partial \vec{r}_q}{\partial w} \right\|} = \frac{D \begin{bmatrix} -\frac{h}{D} \sin(\theta_{i+1} - \theta_i) \\ \cos(\theta_i) + \bar{w}(\cos(\theta_{i+1}) - \cos(\theta_i)) \\ -\sin(\theta_i) - \bar{w}(\sin(\theta_{i+1}) - \sin(\theta_i)) \end{bmatrix}}{\sqrt{2D^2 \bar{w}(\bar{w} - 1)(1 - \cos(\theta_{i+1} - \theta_i)) + h^2 \sin^2(\theta_{i+1} - \theta_i) + D^2}} \quad (6)$$

As a result, the force produced by a Rajiform undulating fin model is come up as Equation (8), followed by the analysis on a 3D sketch base in **Fig. 2a**).

$$\vec{F}_{fish} = \vec{F}_{fin1} + \vec{F}_{fin2} = \begin{bmatrix} F_{x1}(f, A, t) + F_{x2}(f, A, t) \\ F_{y1}(f, A, t) - F_{y2}(f, A, t) \\ F_{z1}(f, A, t) + F_{z2}(f, A, t) \end{bmatrix} \quad (7)$$

Nguyen et al. [10] also stated that the optimized number of fin rays per wavelength is 16; the design of Rajiform type robot is come up.

### 3. COMPUTATIONAL AND EXPERIMENTAL RESULTS

In order to introduce the swinging motion of the membrane through adjustment of the oscillating amplitude and frequency parameters, a Central Pattern Generator (CPG) with Hopf oscillator is utilized to generate oscillatory patterns for the purpose of producing rhythmic movements and behaviors in a biomimetic underwater robot implemented in the fin ray [11]. The characteristics of the model are displayed in Table 1.

Fig. 2 shows the experimental model configurations, which are used to test the produced thrust force with comparison to the computational values. A biomimetic autonomous underwater vehicle model with two 16-fin-ray fins of Rajiform type is constructed, in which force generation is measured. This consists of a polyester membrane and 32 FT5330M Feetech RC Servo Motors, which transmits torque to the fin ray via a bent metal sheet bar. To confirm any discrepancies between computational and experimental results, measurements need to be taken in all three directions (x, y, and z).

The experiment is taken to not only measure the generated thrust over time at a certain frequency but also assess that of the thrust over different frequency values at a certain oscillating amplitude.

From the experimental values, a regression using the surface fitting algorithm is taken in order to show an approximate and simple relationship between the frequency and generated thrust.

**Table 1.** Undulating fin model parameters

Parameters	Value
$\theta_{max}, rad$	$\pi/12$
$[h_{min}, h_{max}], m$	$[0, 0.76]$
$[w_{min}, w_{max}], m$	$[0, 0.14]$
$L, m$	0.195
$D, m$	0.013
$\rho, kg/m^3$	981.8
$C_d$	2.8
$m, kg$	5

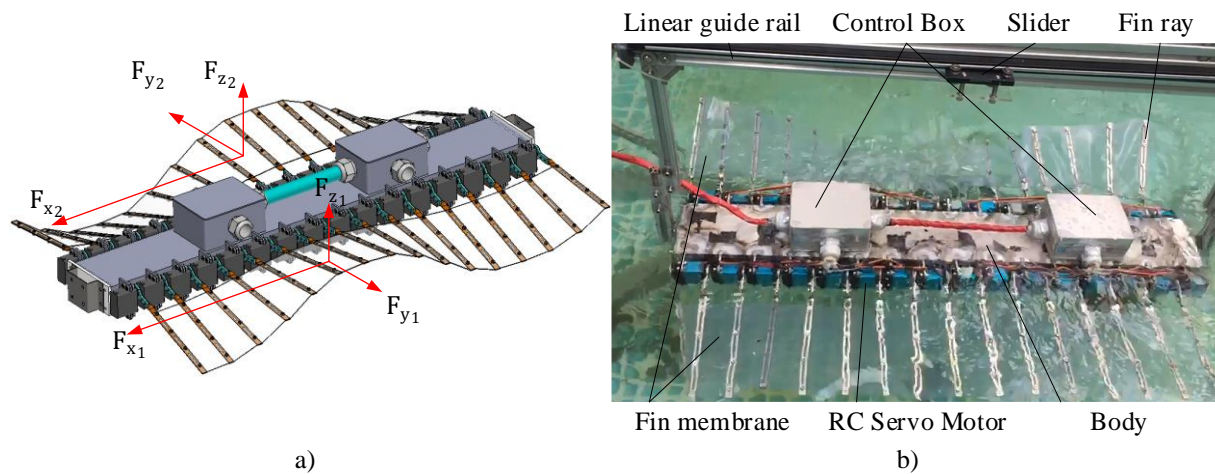


**Figure 2.** a) 3D Rajiform Biomimetic Underwater Robot Model with generated force analysis and b) the experimental model

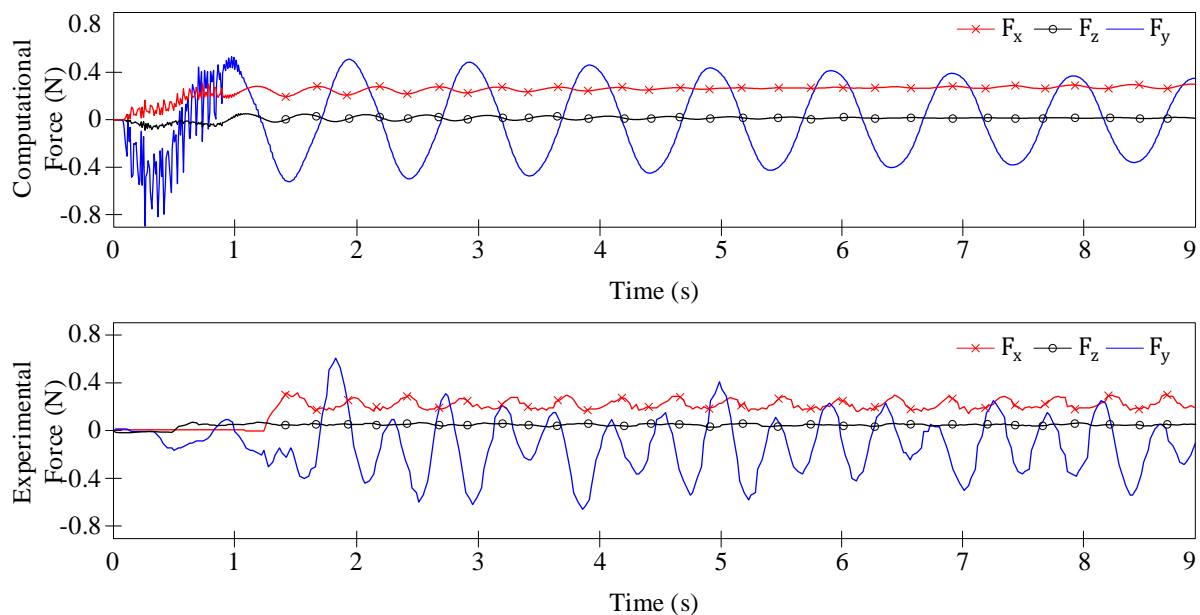


**Figure 3.** Comparison between computational and experimental generated force at 1Hz frequency and 30° amplitude

The comparison between numerical calculations and experimental tests is depicted in Fig. 3. It is evident from both graphs that the generated force, for both methods, exhibits a similar shape and magnitude, with an initial buildup stage that lasts until the first second. Subsequently, the generated force undergoes slight and consistent fluctuations around a particular value. However, there are considerable differences between the two approaches. The numerical calculation demonstrates a smoother response across all three axes of generated force, whereas the experimental data shows a more unstable fluctuation. This disparity can be attributed to realistic factors such as variations in water density, windy weather conditions, and the water drag coefficient, which introduce as disturbances during the experimental trials.

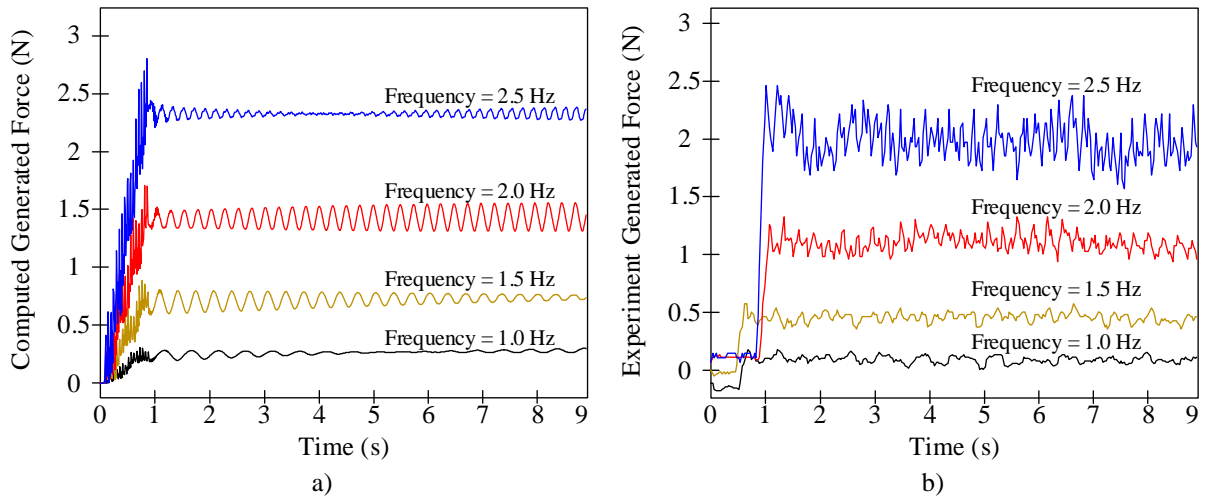


**Figure 4.** Force generated on X-Axis when adjusting the oscillating frequency of the fin, from 1Hz to 2.5Hz at 30° amplitude, in both a) calculated cases and b) experimented cases

The comparison of force created along the X-Axis at different frequency values reveals variations in thrust and its relationship with frequency adjustments. The X-Axis thrust is crucial for the forward movement of the AUV, making it important to consider the impact of frequency on the X-Axis. Moreover, the experimental data presented in Fig. 4 confirms the influence of frequency adjustments on the generated force, as calculated through the computational method. The maximum force is achieved at a frequency of 2.5 Hz. Furthermore, this study has derived two equations using a surface-fitting algorithm for polynomial curves to express the estimated relationship between these variables. These equations are presented below, along with their 95% confidence bounds. The estimated forces are obtained at the mean value.

$$F(f) = 3.481f^5 - 25.32f^4 + 72.02f^3 - 100.1f^2 + 68.36f - 18.16 \quad (8)$$

$$f(F) = 7673F^5 - 10,215F^4 + 7592F^3 - 2352F^2 + 366.3F - 22.24 \quad (9)$$

From the estimated equation (8) and (9), the graph is taken to simplify the calculating process regarding the transformation between the necessary parameters. In this scenario, equation (8) is taken to calculate the estimated generated force from a given frequency value. On the other hand, equation (9) is used to show the reverse interaction to simplify the calculating method of the necessary frequency for reaching a certain value of thrust.

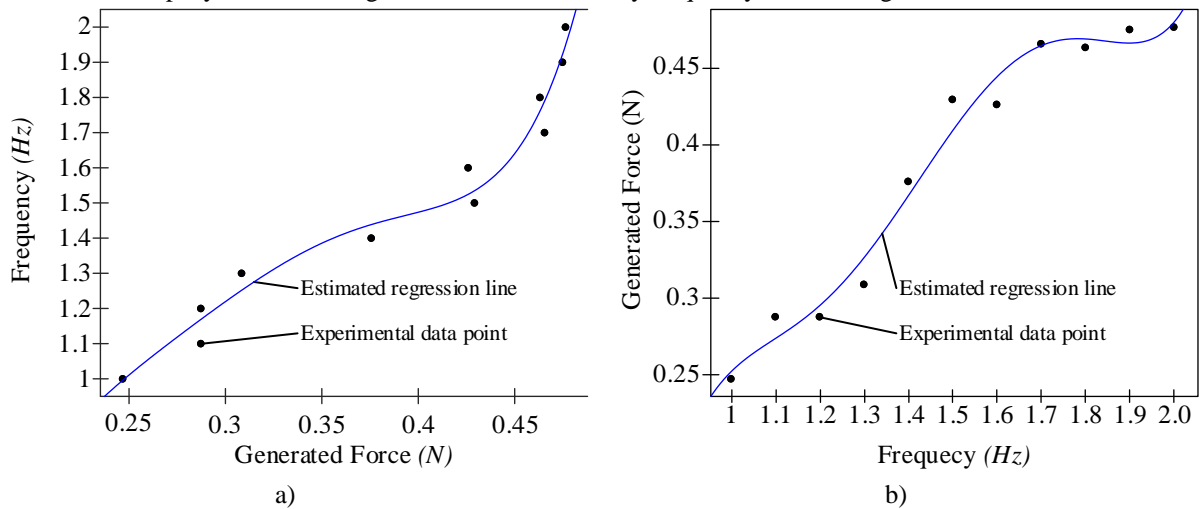


**Figure 5.** Estimated regression model for a) the relationship between generated force and oscillating frequency; b) the relationship between the oscillating frequency and created force

The introduced estimating equations show their approximating specifications. The estimated regression lines show the sum of square errors consecutively at 0.002 and 0.03, along with the R-Square value of 0.98.

#### 4. CONCLUSION

This paper presents the findings regarding the impact of frequency on the force generated by the undulating fin of the Rajiform biomimetic autonomous underwater vehicle. The study establishes regression that describes

the generated force through the discretization of a sine wave, and these equations are compared to experimental results to provide a better understanding of the thrust force produced by the undulating. Furthermore, the paper lays a foundational framework for the locomotion of the Rajiform biomimetic underwater robot by introducing a simple equation that allows control of the produced thrust through adjustment of the frequency parameter.

In future applications, these introduced equations can be utilized to generate thrust and control the locomotion of the AUV on a two-dimensional plane, as they serve as a control input for determining the AUV's position.

### Acknowledgments

This research is funded by Viet Nam National University Ho Chi Minh City (VNUHCM) under grant number TX2023-20b-01. We acknowledge the support of time and facilities from National Key Laboratory of Digital Control and System Engineering (DCSELab), Ho Chi Minh City University of Technology (HCMUT), VNUHCM for this study.

### References

- [1] G. V. Lauder, E. J. Anderson, J. Tangorra, and P. G. A. Madden, "Fish biorobotics: Kinematics and hydrodynamics of self-propulsion," *Journal of Experimental Biology*, vol. 210, no. 16. pp. 2767–2780, Aug. 2007. doi: 10.1242/jeb.000265.
- [2] Y. Li et al., "A comprehensive review on fish-inspired robots," *International Journal of Advanced Robotic Systems*, vol. 19, no. 3. SAGE Publications Inc., May 01, 2022. doi: 10.1177/17298806221103707.
- [3] G. V. Lauder, "Fish locomotion: Recent advances and new directions," *Ann Rev Mar Sci*, vol. 7, pp. 521–545, Jan. 2015, doi: 10.1146/annurev-marine-010814-015614.
- [4] J. K. Jang, S. H. Abbas, and J. R. Lee, "Investigation of underwater environmental effects in rotating propeller blade tracking laser vibrometric measurement," *Opt Laser Technol*, vol. 132, Dec. 2020, doi: 10.1016/j.optlastec.2020.106460.
- [5] P. R. Bandyopadhyay, "Trends in biorobotic autonomous undersea vehicles," *IEEE Journal of Oceanic Engineering*, vol. 30, no. 1. pp. 109–139, Jan. 2005. doi: 10.1109/JOE.2005.843748.
- [6] M. Sfakiotakis, J. Fasoulas, M. Arapis, and N. Spyridakis, "Development and Experimental Evaluation of an Undulatory Fin Prototype Grasping and Manipulation View project OCTOPUS View project Development and Experimental Evaluation of an Undulatory Fin Prototype," in *22nd International Workshop on Robotics in Alpe-Adria-Danube Region, Slovenia, 2013*. [Online]. Available: <https://www.researchgate.net/publication/262246187>
- [7] Y. Wang, J. Tan, B. Gu, and D. Zhao, "Design of the undulating fin propulsor with rajiform swimming mode," *Key Eng Mater*, vol. 579–580, pp. 451–459, 2014, doi: 10.4028/www.scientific.net/KEM.579-580.451.
- [8] E. L. Blevins and G. V. Lauder, "Rajiform locomotion: Three-dimensional kinematics of the pectoral fin surface during swimming in the freshwater stingray *Potamotrygon orbignyi*," *Journal of Experimental Biology*, vol. 215, no. 18, pp. 3231–3241, Sep. 2012, doi: 10.1242/jeb.068981.
- [9] Van Hien Nguyen, Canh An Tien Pham, Van Dong Nguyen, Dae Hwan Kim, and Tan Tien Nguyen, "A Study on Force Generated by Gymnotiform Undulating Fin," in *15th International Conference on Ubiquitous Robots, Hawai'i, USA, 2018*.
- [10] V. D. Nguyen, D. K. Phan, C. A. T. Pham, D. H. Kim, V. T. Dinh, and T. T. Nguyen, "Study on Determining the Number of Fin-Rays of a Gymnotiform Undulating Fin Robot," in *Lecture Notes in Electrical Engineering*, Springer Verlag, 2018, pp. 745–752. doi: 10.1007/978-3-319-69814-4\_72.
- [11] V. D. Nguyen, D. Q. Vo, V. T. Duong, H. H. Nguyen, and T. T. Nguyen, "Reinforcement learning-based optimization of locomotion controller using multiple coupled CPG oscillators for elongated undulating fin propulsion," *Mathematical Biosciences and Engineering*, vol. 19, no. 1, pp. 738–758, 2022, doi: 10.3934/mbe.2022033.

**[S3-24] 5-Axis Robotic Arm Gripper Following a Human Arm**

Geunho Do, HoYeong Kim, Jaewon Choi, Taegang Kim, Seokhyun Jeon, Seongmin Lee,  
Hyeonjong Kim, Junghyuk Ko\*

*National Korea Maritime and Ocean University, Busan, Republic of Korea*

\*Corresponding author: jko@kmou.ac.kr

**Abstract**

Recently, the importance of chemical experiments is increasing and the frequency of experiments is also increasing. As the frequency of experiments increases, the number of accidents related to experiments also increases proportionally. In Korea, more than 50 chemical accidents occur every year, and human casualties are also increasing. If the experimenter can conduct the experiment in a space separated from the experiment object, it will be possible to reduce the loss of life due to an experiment accident. A remote robot arm was designed for safe experimentation by the experimenter. However, the existing robot arm is designed opposite to the shape of the arm, making it difficult to see the movement intuitively. However, unlike existing designs, our robot arm is made in the same shape as a human arm, making it easy to control movements. The composition of the robot arm consists of a stand that supports the motor and a barrel that serves as a shoulder, arm, and hand with three joints in the motor. The outline of the arm was created using a 3D printer. The tongs consisted of two fingers, with rubber marks between them to prevent slipping. When conducting experiments remotely, manipulating the robotic arm will be more inconvenient than conducting experiments by hand. To compensate for this shortcoming, an IMU sensor was used. The IMU sensor detects instantaneous changes in acceleration according to changes in motion when dynamic forces such as acceleration, vibration, and shock acting on an object occur. Obtain the position data of the object through the angular acceleration and angular velocity values detected by the sensor. Four IMU sensors are attached to the experimenter's arm, and angular acceleration and angular velocity values are received as the arm passes through the sensors. Using this data, the moving distance of the arm is calculated, and this value is converted into a signal and transmitted to the motor through the wireless network communication module through the commercial control module. The data transmitted in this way is used to move the robot arm. Since the claw is located at the end of the robot arm, a servo motor was used to reduce the load. A wireless network communication module was used in this servo motor to control the tongs to operate when the user presses a button. When the user moved the arm, the robot arm did the same. However, as a result of analyzing the sensor conversion value and the actual distance during operation, there was a difference of 2 to 3 cm from the target point. It is presumed that the error in the position data due to the vibration of the motor and the noise of the IMU sensor is the cause. However, this degree of difference is judged not to affect the experiment. In the case of the currently manufactured robot arm, there is a limit to the controllable object load due to the lack of motor torque, but more stable operation is expected to be possible if a more powerful motor is used in the actual experiment. Accordingly, it is expected that the allowable load of the motor used in the tongs will increase, and the load of the controllable object will also increase. Analyzing the types of chemical experiment robots that currently exist in the market, there are automated robots for faster repeat experiments and 'Lab Boy' that conducts experiments with C language and coding. Although these robots are focused on a specific experiment, our robotic arm is a robot suitable for a fast-paced future because it can act in an instant that reflects the behavior desired by the experimenter.

**Keywords:** *IMU Sensor, Remote control, Angle acceleration, Wireless network communication, Commercial control module*

**References**

- [1] Ahmad, N., Ghazilla, R. A. R., Khairi, N. M., & Kasi, V. (2013). Reviews on various inertial measurement unit (IMU) sensor applications. *International Journal of Signal Processing Systems*, 1(2), 256-262.
- [2] Steven Eyobu, Odongo, and Dong Seog Han. "Feature representation and data augmentation for human activity classification based on wearable IMU sensor data using a deep LSTM neural network." *Sensors* 18.9 (2018): 2892.
- [3] Bakhshi, Saba, Mohammad H. Mahoor, and Bradley S. Davidson. "Development of a body joint angle measurement system using IMU sensors." 2011 Annual International Conference of the IEEE Engineering in Medicine and Biology Society. IEEE, 2011.
- [4] Kim, Minwoo, et al. "IMU sensor-based hand gesture recognition for human-machine interfaces." *Sensors* 19.18 (2019): 3827.

**[S3-37] A Novel Development of the Decentralized Scheme to Avoid Collision for the Large-Scale System**

The Cuong Le, Minh Tuan Nguyen\*

*Faculty of Mechanical Engineering, Ho Chi Minh City University of Technology (HCMUT), 268 Ly Thuong Kiet, District 10, HCMC, Viet Nam**Viet Nam National University Ho Chi Minh City (VNUHCM), Linh Trung Ward, Thu Duc City, HCMC, Viet Nam*

\*Corresponding author: thinhpfienv2003@yahoo.com

**Abstract**

The development of industries makes the demand for intelligent AGV (Automated Guided Vehicle) systems increase rapidly. Therefore, AGV systems need to be continuously improved to optimize performance, improve scalability, and completely tackle collision and deadlock problems. This study aims to resolve collisions that occur due to the difference between the planning time and the actual travel time of the AGV, which makes these collisions unpredictable. Thus, an algorithm that enhances part planning accuracy by considering the acceleration of AGV has been studied, based on the Dijkstra algorithm. This paper describes the algorithm in detail and shows its effectiveness through a simulation with a chessboard map.

**Keywords:** *Large-scale system, Automated Guided Vehicle, Motion Planning algorithm*

**1. INTRODUCTION**

In the modern era, warehouses [1] have undergone a significant transformation with the advent of advanced technologies, particularly in the fields of automation, inventory management or optimization. One of the key advancements is the implementation of multi-AGV (Automated Guided Vehicle) systems, which offer a highly efficient and flexible approach to material handling [2] and logistics [3] operations within a warehouse. These systems consist of multiple AGVs working collaboratively to deliver goods and navigate through the warehouse environment. Reversely, the simultaneous movement of multiple AGVs in a narrowed space poses a challenge in terms of collision avoidance. Without an effective algorithm to manage and control the movements, the risk of collisions and disruptions to the warehouse operations increases substantially among AGVs. Consequently, the development of collision-free algorithms has become crucial for the successful deployment and operation of multi-AGV systems in modern warehouses [4].

For these purposes, the collision-free algorithm for multi-AGV systems aims to optimize the routes and schedules, ensuring efficient and safe transportation of goods while avoiding any potential collisions. These algorithms consider various factors [5-8], comprising the current positions of AGV, their destination points, the layout of the warehouse, and any existing obstacles or dynamic changes in the environment. One of the fundamental principles of the collision-free algorithm is the concept of decentralized decision-making [9-11]. Rather than relying on a central control unit to dictate the movements of all agents, each AGV is equipped with its own decision-making capabilities. This decentralized approach allows AGVs to communicate and coordinate with each other, exchanging information about their positions, routes, and intentions. By sharing this data, AGVs can collaboratively determine the most optimal paths, avoid potential collisions, and dynamically adjust their trajectories in real-time.

In detail, path planning algorithms, such as the A\* algorithm and potential field methods, calculate optimal paths while considering the presence of other AGVs and obstacles. Motion control algorithms ensure smooth and coordinated movements, minimizing sudden changes in speed or direction. The collision-free planning approach enhances productivity, reduces downtime, and mitigates the risk of accidents and damages. As technology advances, further improvements and optimizations in collision-free planning are anticipated, leading to more sophisticated and reliable multi-AGV systems in modern warehouses. Recently, The Dijkstra algorithm for collision-free planning in the multi-AGV system is a notable approach that addresses the complex task of coordinating multiple AGVs' movements while avoiding collisions in a warehouse environment. One of the key strengths of the Dijkstra algorithm is its ability to consider the entire warehouse layout and create a graph representation that captures the connectivity between different areas and the paths that AGVs can traverse. By incorporating this graph representation, the algorithm can calculate the optimal path for each AGV, taking into

account factors such as the AGV's current position, destination point, and any potential obstacles or AGV congestion along the way.

## 2. DESCRIPTION OF PROPOSED SYSTEM

### 2.1. Working environment

A cross-docking warehouse is a specialized facility designed to optimize the flow of goods through the supply chain. It serves as a distribution hub where products are received from suppliers, sorted, and quickly transferred to outbound vehicles for immediate delivery to customers or other distribution centers. The working layout of a cross-docking warehouse is carefully organized to facilitate the efficient movement of goods and minimize handling and storage time. Normally, this layout as Fig. 1 consists of the following key areas [12]:

**Parking space:** This is where incoming shipments from suppliers are received. The area is equipped with loading docks and often includes a staging area for temporary storage of inbound products. Efficient unloading processes, such as forklifts or conveyor systems, are employed to quickly transfer items from incoming vehicles to the staging area.

**Manual sorting space:** After the products are unloaded and checked for accuracy, they move to the sorting area. Here, the goods are organized based on their destination or specific criteria, such as product type, size, or customer order. This area may utilize conveyor belts, automated sorting systems, or manual sorting stations, depending on the volume and complexity of the operations.

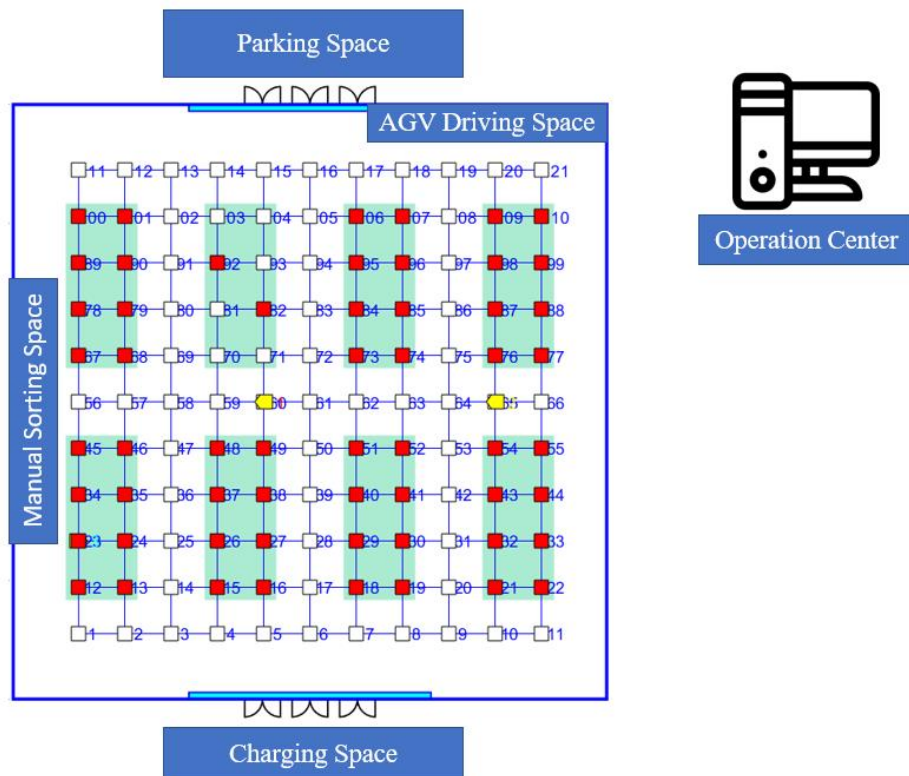


**Figure 1.** Layout of workspace for our system

**AGV driving space:** The working layout of a cross-docking warehouse also includes support areas for various functions. These may include administrative offices, quality control stations, maintenance areas, break rooms, restrooms, and employee facilities. The support areas are strategically positioned to provide easy access and oversight of the entire warehouse operations.

In addition, the heart of the cross-docking warehouse is the cross-docking zone. In this section, products from incoming shipments are matched with outgoing orders or consolidated for further distribution. It involves merging shipments from multiple suppliers, breaking down large shipments into smaller ones, or combining smaller shipments into larger ones. The objective is to optimize delivery routes and minimize transportation costs. Furthermore, for long-term operation, charging space is useful to supply energy when battery of AGV is low. Overall system is managed and controlled by operation center.

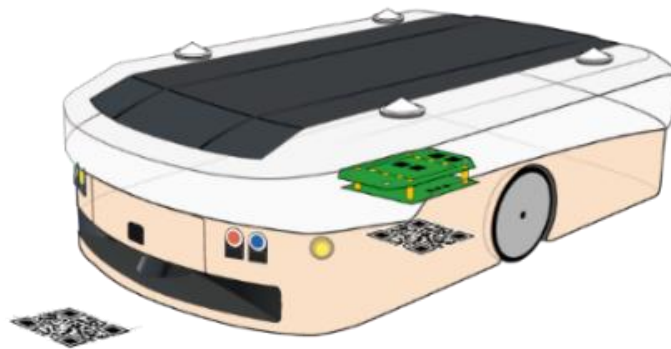


**Figure 2.** AGV navigation by QR code

In this system, our model includes two active wheels, two passive wheels, vision module and lifting platform. Two driving motors are directly attached to active wheels while passive wheels are free. Whenever AGV changes direction, active wheels adjust their velocities according to forward kinematics as well as a number of pulses. In the AGV driving space area, the space is coded in the form of a grid, each mesh is called a workstation (node), located by a QR code as shown in Fig. 2. Based on that, the AGV can determine the location, position and direction of movement, and send information about your position to the central system. The packages are placed in the cargo area and the rest are aisles.

## 2.2. Mathematical model

The AGV has the structure as shown in Figure 3. Some parameters of this vehicle include that  $Ox_Iy_I$  is the coordinate system attached to the ground,  $Ox_r y_r$  is the coordinate system attached to the AGV,  $\theta$  represents the deviation angle between these two coordinate systems, A is the center of the road connecting the two drive wheels, C is the center of mass AGV, R is the radius of each wheel, and L is the distance between the centers of the two wheels.

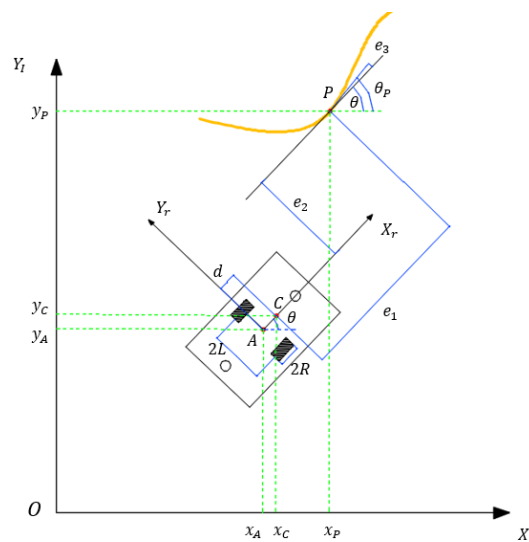


**Figure 3.** Modeling of our AGV to track the reference trajectory

The equation of velocity for the center of mass C of AGV in the coordinate system attached to the ground is as below:



$$\begin{cases} \dot{x}_c^I = R \frac{(\dot{\varphi}_R + \dot{\varphi}_L)}{2} \cos\theta - dR \frac{(\dot{\varphi}_R - \dot{\varphi}_L)}{2L} \sin\theta \\ \dot{y}_c^I = R \frac{(\dot{\varphi}_R + \dot{\varphi}_L)}{2} \sin\theta + dR \frac{(\dot{\varphi}_R - \dot{\varphi}_L)}{2L} \cos\theta \\ \dot{\theta}_c = R \frac{(\dot{\varphi}_R - \dot{\varphi}_L)}{2L} \end{cases} \quad (1)$$

As Fig. 3, three error parameters of AGV and the reference point P need to be identified. It is considered that  $e_1, e_2, e_3$  are the errors in X, Y and Z axis respectively, and  $\theta_p$  is an angle between directional movement and reference point. In the relative coordinate attached to the tracking point C, we have

$$\begin{bmatrix} e_1 \\ e_2 \\ e_3 \end{bmatrix} = \begin{bmatrix} \cos\varphi & \sin\varphi & 0 \\ -\sin\varphi & \cos\varphi & 0 \\ 0 & 0 & 1 \end{bmatrix} \begin{bmatrix} x_R - x_C \\ y_R - y_C \\ \varphi_R - \varphi_C \end{bmatrix} \quad (2)$$

Or,

$$\begin{bmatrix} \dot{e}_1 \\ \dot{e}_2 \\ \dot{e}_3 \end{bmatrix} = \begin{bmatrix} v_R \cos e_3 \\ v_R \sin e_3 \\ w_R \end{bmatrix} = \begin{bmatrix} -1 & e_2 \\ 0 & -d - e_1 \\ 0 & -1 \end{bmatrix} \begin{bmatrix} v \\ w \end{bmatrix} \quad (3)$$

### 3. DESIGN OF MOTION PLANNER

The result of motion planning is the timing that the AGV needs to follow when moving to the workstations, in order to eliminate collisions and deadlocks. Therefore, it depends a lot on the accuracy of this algorithm. It should be recognized that for cross-docking, AGVs move on routes that are combinations of straight  $path_i$  segments. There, the AGV accelerates from 0 m/s and decelerates to 0 m/s when reaching the turn, for example Figure 5. The improved motion planning algorithm for the AGV is divided into four parts.

- (1). Identify the travel time  $\Delta_{time}$  between two nodes in the same route.
- (2). Then, link these travel times  $\Delta_{time}$  between two nodes into the complete schedule.
- (3). After determining this schedule, our system can be aware the potential collision of this AGV with the others according to the type of collisions.
- (4). The previously outlined handling options are applied on a case-by-case basis.

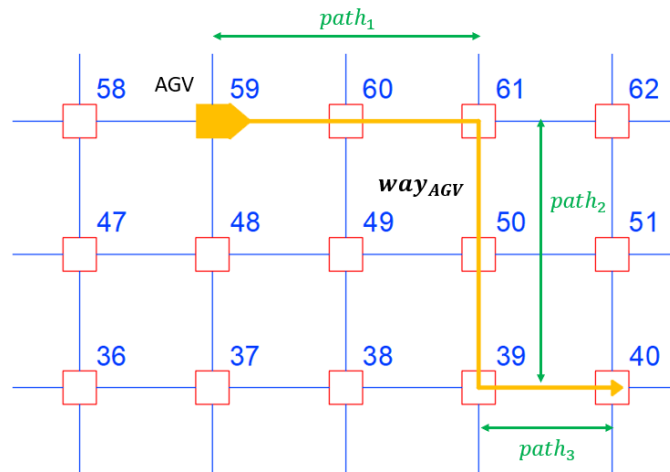


**Figure 4.** Description of traveling route for AGV ( $way_{AGV}$ ) from many straight trajectory  $path_i$

#### 4. RESULTS OF RESEARCH

In this section, our system is simulated in the personal computer with technical specifications such i7 core, 3300Hz, 8G RAM and Win10 OS. The simulation environment is done in MATLAB software, cross docking as shown in Figure 1 with the following main parameters: The distance between two workstations is  $d_{node} = 3.9 \text{ m}$ . The target velocity of the AGV is  $v_{TH} = 1 \text{ (m/s}^2\text{)}$ . Acceleration of AGV depends on load, divided into four levels: large ( $0.18 \text{ m/s}^2$ ), medium ( $0.36 \text{ m/s}^2$ ), light ( $0.72 \text{ m/s}^2$ ), no load ( $1 \text{ m/s}^2$ ). The time the AGV rotates in place is  $t_{90} = 4 \text{ (s)}$  when rotated  $90^\circ$  and  $t_{180} = 6 \text{ (s)}$  when rotated  $180^\circ$ . The safe threshold of the system is  $\mu_1 = 11.9 \text{ (s)}$ ,  $\mu_2 = 8 \text{ (s)}$ .

In these experiments, it is aware that the previous planner [12] exists some limitations in the estimation of travel time for AGV to move to target nodes. For the complicated routes or carry larger cargo, these limitations could cause some fails in collision avoidance or leading to unfortunate crash. However, in this study, the proposed method overcomes these drawbacks. In detail, we consider that AGV<sub>2</sub> is moving from workstation 54 as Fig. 5. After 3.4s from this movement of AGV<sub>2</sub>, another vehicle such AGV<sub>1</sub> start receiving its task to move from workstation 60 to workstation 38. In this stage, our system is responsible to schedule the movement of AGV<sub>1</sub>. Our experiment selects the time point as the time when AGV<sub>1</sub> starts moving, the schedule of these 02 AGVs is made and described in Table 1.

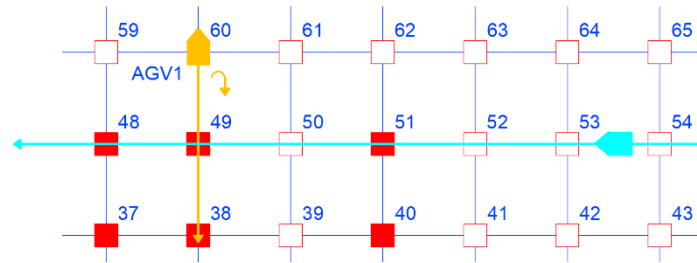


Figure 5. Example of layout in the collision at one intersection

Table 1. Competitive schedule between AGV<sub>1</sub> and AGV<sub>2</sub> in this example using our method and Z. Z. [12]

AGV <sub>1</sub>	Workstation	60	49	88
	Z.Z [12] (s)	0	7.9	11.8
	Our method (s)	0	10.4	14.8

AGV <sub>2</sub>	Workstation	54	53	52	51	50	49	...
	Z.Z [12] (s)	-3.4	0.5	4.4	8.3	12.2	16.1	...
	Our method(s)	-3.4	1	4.9	8.8	12.7	16.6	...

Due to the tracking data, our system chooses the time point when AGV<sub>1</sub> locates at workstation 60 and AGV<sub>2</sub> is on the way to the workstation 53. Then, AGV<sub>1</sub> has to turn around and moves toward to the workstation 49 while AGV<sub>2</sub> is forwarding to workstation 49. By using previous method, the estimated time of AGV<sub>1</sub> is 7.9 seconds which is faster than our approach. It could be explained evidently that the turning time is not counted in previous method, hence it is not proper in practice. For AGV<sub>2</sub>, method of Z. Z. [12] computes the less time for each route because it prescribes all routes are similar and the same. However, in each intersection, AGVs have to decelerate to avoid possible collisions. In that case, it takes more time to travel if using our approach. Since there is no potential collision, in a short time AGV<sub>2</sub> straightly moves without any stop. AGV<sub>1</sub> takes a lot of time to change direction and moves later. At the workstation 49, it is clearly seen that the probable collision is detected. In this

stage, with  $\mu_2 = 8$ , some descriptions to compare between our method and the other method [12] are denoted as Table 2.

**Table 2.** Illustrative comparison between our method and the other method [12]

Workstation 49	Z. Z. [12]	Our approach
$ \frac{1}{49}t_{come} - \frac{2}{49}t_{come} $	$ 16.1-7.9  = 8.2 > \mu_2$	$ 16.6-10.4  = 6.2 < \mu_2$
Statement	No collision	Possible collision
Action	Agree with the scheduled trajectory of AGV <sub>1</sub>	Need to re-generate the motion plan to avoid collision at workstation 49

## 5. CONCLUSION

In our study, a method to detect the potential collision in the large-scale system including various AGVs was proposed. The working layout consists of many vertical lines and horizontal ones which vehicle tracks as reference trajectory. Besides, in our design, a digital camera is attached to the bottom of AGV to identify the lane and acknowledge to main microprocessor. Our method suggested a mechanism comprising four steps to detect the probable collision as well as proposed the novel plan to avoid. To demonstrate the effectiveness and feasibility of our approach, an example to compare between the proposed method and the previous method was analyzed and explained. In future, the hardware platform of multi-vehicle system should be created to realize our algorithm. Also, the improved scheme by integrating with intelligent algorithm such machine learning or reinforce learning could be applied to enhance the behavior of this system.

## References

- [1] Zhen, L., & Li, H. (2022). A literature review of smart warehouse operations management. *Frontiers of Engineering Management*, 9(1), 31-55.
- [2] Hu, Y., Yang, H., & Huang, Y. (2022). Conflict-free scheduling of large-scale multi-load AGVs in material transportation network. *Transportation Research Part E: Logistics and Transportation Review*, 158, 102623.
- [3] Li, Y. (2023, February). Research on Multi-AGVs Cooperative Transportation Strategy in Warehouse Logistics Environment Based on HCA Algorithm. In *2023 IEEE 2nd International Conference on Electrical Engineering, Big Data and Algorithms (EEBDA)* (pp. 1753-1758). IEEE.
- [4] Boysen, N., De Koster, R., & Weidinger, F. (2019). Warehousing in the e-commerce era: A survey. *European Journal of Operational Research*, 277(2), 396-411.
- [5] Shin, H., & Chae, J. (2020). A performance review of collision-free path planning algorithms. *Electronics*, 9(2), 316.
- [6] Vivaldini, K. C., Rocha, L. F., Becker, M., & Moreira, A. P. (2015). Comprehensive review of the dispatching, scheduling and routing of AGVs. In *CONTROLO'2014-proceedings of the 11th Portuguese conference on automatic control* (pp. 505-514). Springer International Publishing.
- [7] Li, B., Liu, H., Xiao, D., Yu, G., & Zhang, Y. (2017). Centralized and optimal motion planning for large-scale AGV systems: A generic approach. *Advances in Engineering Software*, 106, 33-46.
- [8] Fazlollahtabar, H., & Hassanli, S. (2018). Hybrid cost and time path planning for multiple autonomous guided vehicles. *Applied Intelligence*, 48, 482-498.
- [9] Draganjac, I., Miklić, D., Kovačić, Z., Vasiljević, G., & Bogdan, S. (2016). Decentralized control of multi-AGV systems in autonomous warehousing applications. *IEEE Transactions on Automation Science and Engineering*, 13(4), 1433-1447.
- [10] Maoudj, A., Kouider, A., & Christensen, A. L. (2023). The capacitated multi-AGV scheduling problem with conflicting products: Model and a decentralized multi-agent approach. *Robotics and Computer-Integrated Manufacturing*, 81, 102514.
- [11] De Ryck, M., Versteyshe, M., & Shariatmadar, K. (2020). Resource management in decentralized industrial Automated Guided Vehicle systems. *Journal of Manufacturing Systems*, 54, 204-214.
- [12] Zheng Zhang, Qing Guo, Juan Chen, and Peijiang Yuan, "Collision-Free Route Planning for Multiple AGVs in Automated Warehouse Based on Collision Classification," *IEEE Access*, vol. 6, pp. 26022-26035, 2018.

**[S3-46] Prediction of Aerodynamic Coefficient Using Deep Learning**Bo Ra Kim<sup>1,2</sup>, Seung Hun Lee<sup>1</sup>, Seung Hyun Jang<sup>1,2</sup>, Min Yoon<sup>1,2,\*</sup><sup>1</sup>Department of Mechanical Eng., Korea Maritime & Ocean Univ., Busan, South Korea<sup>2</sup>Interdisciplinary Major of Ocean Renewable Energy Eng., Korea Maritime & Ocean Univ., Busan, South Korea

\*Corresponding author: minyoon@kmou.ac.kr

**Abstract**

In this study, three asymmetrical airfoils (S809, S822 and SD7062) are selected, and the flow data is constructed through numerical analysis results of the pressure fields and aerodynamic coefficients. A convolutional neural network model combining U-Net and VGG16 is used to predict the airfoil performance. As a result, it is confirmed that lift and drag coefficients have error of 0.3% and 0.2%, respectively, between the trained data and predicted result.

**Keywords:** Airfoil, Aerodynamics characteristics, CFD, Deep Learning, CNN

**1. INTRODUCTION**

Although many studies on airfoil have been conducted and a large amount of data has been accumulated. However, even when performing CFD analysis, it still requires a lot of time and iterative analysis. To solve this problem, recent research has integrated artificial intelligence into the airfoils. Sekar et al. [1] used deep learning for inverse design of airfoils. Chen et al. [2] used CNN to predict aerodynamic properties such as lift and drag coefficients of airfoils. Thuerey et al. [3] predicted pressure and velocity fields using CNN for various airfoil shapes and angles of attack. We proposed a combination of VGG16 and U-Net artificial intelligence models to predict the aerodynamic characteristics and pressure fields of airfoils using input data obtained from CFD simulations.

**2. NUMERICAL ANALYSIS**

We conducted the  $k$ - $kl$ - $\omega$  transition model [4] and steady state. For each airfoil, the angle of attack was divided into 133 angles with increments of 0.25° from -13.5° to +19.5°. The freestream velocity was divided into increments of 1 m/s from 6 m/s to 19 m/s. As a result, 5,187 sets of pressure field and aerodynamic values were constructed. The neural network model for prediction was composed of the U-Net model with an encoder–decoder type neural network structure and the VGG16 model with 16 layers. The airfoil shape data and Reynolds number were selected as input data. The study aimed to predict the airfoil's pressure fields and lift characteristics as output data.

**3. RESULTS**

Figure 1 shows pressure contours for CFD, prediction and error. Figure 1 (a) shows the result of applying banded contour data as the training data, and Figure 1 (b) has the result values with continuous contour data applied as the training data. Results indicate that the prediction of pressure field learned with continuous contour (b) is improved compared to one learned with banded contour (a). Table 1 represents the predicted fluid properties of the conditions applied in Figure 1. The prediction results of learning banded data are similar to those of learning continuous data in terms of lift coefficient ( $C_L$ ), but the drag coefficient ( $C_D$ ) has improved.

**Table 1.** Prediction of trained airfoil aerodynamics of the conditions applied in Figure 1

Parameter	Banded		Continuous	
	$C_L$	$C_D$	$C_L$	$C_D$
CFD	1.332	0.0218	1.332	0.0218
Prediction	1.328	0.0222	1.328	0.0215
Error	0.30%	1.83%	0.30%	1.16%

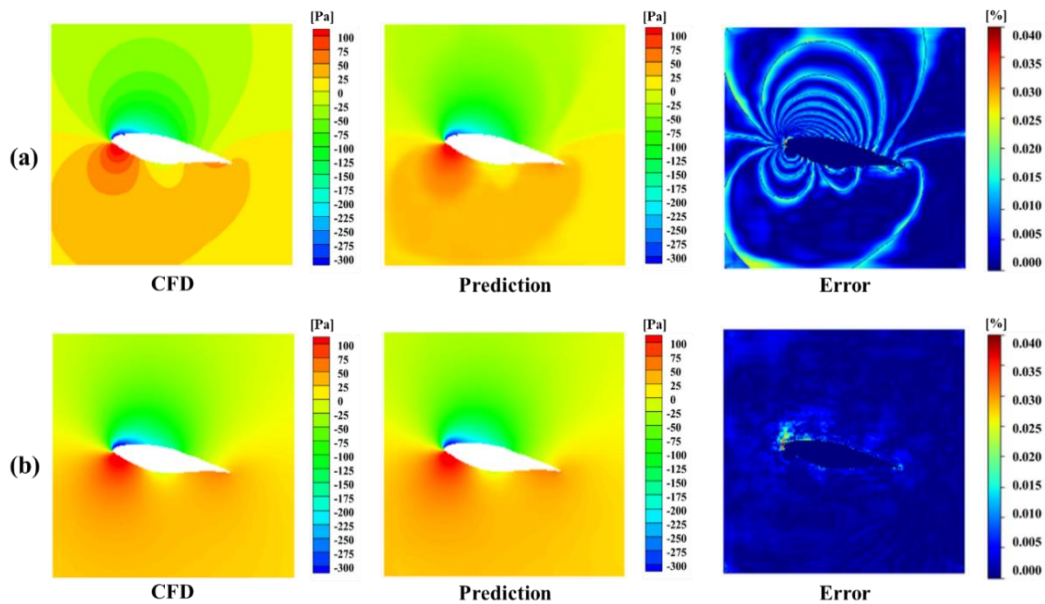


**Figure 1.** 2D contours of the pressure of S809 at  $Re = 1.03 \times 10^6$  and  $\alpha = +11^\circ$  with (a) banded and (b) continuous levels

#### 4. CONCLUSION

An artificial intelligence model combining VGG16 and U-Net models was proposed to predict aerodynamic coefficients for three airfoil shapes. Using the existing training data, the total prediction error of the banded contour has a mean absolute error of 0.37% for  $C_L$  and 0.22% for  $C_D$ . When using the improved training data with continuous contour, the total prediction error improved to 0.3% for  $C_L$  and 0.2% for  $C_D$ . The time required for one CFD analysis was 30 minutes per case and 108 days were required to generate 5187 data, while the artificial intelligence method took 40 seconds per epoch and 11.25 hours for 1000 epochs in total.

#### Acknowledgments

This work was supported by the National Research Foundation of Korea (NRF) grant funded by the Korea government (MSIT) (No. 2021R1F1A1053438) and Center for Women in Science, Engineering and Technology (WISSET) grant funded by the Ministry of Science and ICT (MSIT) under the team research program for female engineering students.

#### References

- [1] V. Sekar, M. Zhang, C. Shu and B.C. Khoo “Inverse design of airfoil using a deep convolutional neural network” *AIAA Journal*, 57(3) (2019), pp. 993-1003.
- [2] H. Chen, L. He, W. Qian and S. Wang “Multiple aerodynamic coefficient prediction of airfoils using a convolutional neural network” *Symmetry*, 12(4) (2020), pp. 544.
- [3] N. Thuerey, K. Weißenow, L. Prantl and X. Hu “Deep learning methods for Reynolds-averaged Navier–Stokes simulations of airfoil flows”, *AIAA Journal*, 58(1) (2020), pp. 25-36.
- [4] D.K. Walters and D. Cokljat “A three-equation eddy-viscosity model for Reynolds-averaged Navier–Stokes simulations of transitional flow”, *Journal of fluids engineering*, 130(12) (2008).

**[S4-7] Multi-Scale Approach for Low Concentration CO<sub>2</sub> Selective Adsorption**

Tuan Huy Lo, Il Seouk Park\*

*Department of Mechanical Engineering, Kyungpook National University, Daegu, Republic of Korea, 41566*

\*Corresponding author: einstein@knu.ac.kr

**Abstract**

Physical adsorption is an up-and-coming technology for separating CO<sub>2</sub>, which can lead to efficient CO<sub>2</sub> capture with minimal energy costs. Additionally, the adsorption behaviour of CO<sub>2</sub> can be influenced by various structural properties. This study employed a multi-scale simulation approach to investigate the behaviour of CO<sub>2</sub> adsorption processes on carbon-based materials, namely graphene and activated carbon, to gain a deep understanding of the CO<sub>2</sub> adsorption behaviour at various length scales to optimize the performance of CO<sub>2</sub> capture processes for different materials. The methodology involved utilizing density functional theory (DFT) to calculate the interaction between CO<sub>2</sub> and adsorbent, then analysing carbon-based materials' adsorption mechanism through structural parameters, adsorption energy, and surface electronic properties. Grand canonical Monte Carlo (GCMC) was utilized to determine adsorption isotherms, selectivity, and isosteric heats, while molecular dynamics (MD) was utilized to calculate radial distribution (RDF) and diffusion. Finally, a computational model was developed using the Ansys Fluent program, linked by a user-defined function, for accurately predicting the distribution of concentration and temperature field in the adsorption system. The results showed that the density of states (DOS) of graphene matched well with the previous DFT simulation, indicating the accuracy of the multi-scale simulation approach. Furthermore, the adsorption isotherms and breakthrough curves were in good agreement with the experimental data, providing further validation for the approach's reliability. Overall, this study provided valuable insights into the behaviour of CO<sub>2</sub> adsorption processes on carbon-based materials, which could potentially develop more efficient CO<sub>2</sub> capture processes. The novelty and importance of this research lie in the multi-scale simulation approach, which accurately captures the intricate details of CO<sub>2</sub> adsorption behaviour at various length scales. Future research could utilize these findings for machine learning to further optimize CO<sub>2</sub>-capturing systems' performance.

**Keywords:** CO<sub>2</sub> capture, CFD, Molecular simulations, Density functional theory

**[S4-30] The Intelligent Waste Management System Using IoT for Smart Cities**Thai Le<sup>1</sup>, Linh Do<sup>2</sup>, Duy Thanh Tran<sup>3,4,\*</sup><sup>1,2</sup> Ho Chi Minh City University of Banking, Ho Chi Minh City, Viet Nam, 700000<sup>3</sup> University of Economics and Law, Ho Chi Minh City, Viet Nam, 700000<sup>4</sup> Viet Nam National University, Ho Chi Minh City, Viet Nam, 700000

\*Corresponding author: thanhtd@uel.edu.vn

**Abstract**

Given the rapid growth of urban populations and the increasing challenges of waste management, there is an urgent need for innovative solutions to effectively address these issues. This abstract introduces a comprehensive study on the creation of an Intelligent Waste Management System (IWMS) that utilizes Internet of Things (IoT) technology specifically designed for smart cities.

The objective of this research is to develop a smart and efficient waste management system that utilizes IoT devices, data analytics, and intelligent decision-making algorithms. The proposed IWMS aims to optimize waste collection, reduce operational costs, minimize environmental impact, and improve overall waste management practices in smart cities. By implementing this system, the advantages include increased efficiency in waste collection, optimized use of resources, improved environmental sustainability, and overall enhancement of waste management practices.

The proposed approach integrates IoT sensors and connected devices into waste bins, collection vehicles, and waste processing facilities. These sensors enable real-time monitoring of waste levels, temperature, humidity, and other relevant parameters. The collected data is transmitted to a central IoT platform, where it is analyzed and processed using advanced data analytics and machine learning algorithms. The system employs intelligent decision-making algorithms to optimize waste collection routes, predict fill levels, and schedule timely collection. This approach ensures that collection resources are dynamically allocated based on real-time data, reducing unnecessary trips, minimizing fuel consumption, and optimizing operational efficiency. Additionally, the system can identify anomalies such as fires, leaks, or odors in waste bins, enabling prompt actions and ensuring public health and safety.

The research aims to evaluate the performance and effectiveness of the proposed IWMS through extensive field trials and data analysis. The outcomes of the study will showcase the significant improvements achieved in waste collection efficiency, resource utilization, environmental sustainability, and overall waste management practices. The findings will provide valuable insights for policymakers, waste management authorities, and urban planners in the adoption and implementation of intelligent waste management systems in smart cities.

The uniqueness and innovation of this research lie in combining IoT technologies with data analytics and smart decision-making algorithms to create an intelligent waste management system. The scientific contributions of this idea include:

1. **Integrated IoT Solution:** Our proposed IWMS integrates IoT sensors and devices to gather real-time data on waste parameters, allowing for proactive waste management decisions. This integration ensures that waste collection is optimized, leading to cost and environmental impact reduction.
2. **Advanced Data Analytics:** By utilizing advanced data analytics and machine learning algorithms, the system can analyze and process the collected data, providing valuable insights into waste collection patterns, fill levels, and anomalies. This enables data-driven decision-making and enhances operational efficiency.
3. **Intelligent Decision-Making:** Our system employs intelligent algorithms to optimize waste collection routes, predict fill levels, and schedule timely collections. This intelligent decision-making approach minimizes unnecessary trips, reduces fuel consumption, and improves overall waste collection efficiency.
4. **Environmental Sustainability:** Through optimized waste collection routes and reduced operational costs, our proposed IWMS contributes to environmental sustainability. The system minimizes carbon emissions, promotes recycling and waste reduction initiatives, and enhances overall waste management practices.

**Keywords:** *Internet of Things, IoT, waste management, smart cities, intelligent decision-making, data analytics, sustainability*

### Acknowledgments

We would like to extend our sincere appreciation and gratitude to Mr. Thanh Tran for his invaluable support and guidance throughout the completion of this study. His unwavering commitment and assistance have been instrumental in the successful execution of our research project.

### References

- [1] Chiarello, F., Rinaldi, S., Scarpiniti, M., Castorina, G., & Tinnirello, I. (2020). An IoT-based waste management system for smart cities. *IEEE Internet of Things Journal*, 7(9), 7840-7849.
- [2] Deka, G. C., & Hazarika, S. M. (2020). IoT-based intelligent waste management system for smart cities. In *2020 7<sup>th</sup> International Conference on Smart Computing and Communications (ICSCC)* (pp. 1-6). IEEE.
- [3] Albert, A., Das, P., & Janakiraman, R. (2019). Intelligent waste management using IoT. In *2019 International Conference on Smart Systems and Inventive Technology (ICSSIT)* (pp. 579-583). IEEE.
- [4] Gope, P., & Dey, N. (2020). IoT-based smart waste management system: A review. *Environmental Science and Pollution Research*, 27(10), 10237-10253.
- [5] Kumar, V., & Bhattacharya, A. (2019). IoT-based solid waste management system for smart cities. In *2019 International Conference on Computer, Communication, and Signal Processing (ICCCSP)* (pp. 1-6). IEEE.
- [6] Miraz, M. H., Saha, H., & Ullah, K. M. M. (2020). An IoT-based intelligent waste management system for smart cities. In *2020 International Conference on Electrical, Computer, and Communication Engineering (ECCE)* (pp. 1-4). IEEE.
- [7] Priya, S. G., & Geetha, V. (2019). An intelligent waste management system for smart cities using IoT. *International Journal of Recent Technology and Engineering*, 8(1), 1362-1366.
- [8] Raju, P., Pandey, A., & Sharma, R. (2018). An intelligent IoT based waste management system for smart cities. In *2018 International Conference on Communication and Signal Processing (ICCSP)* (pp. 0738-0742). IEEE.
- [9] Saini, M., Sharma, M., Kaur, G., & Kaur, M. (2021). Intelligent waste management system using IoT in smart cities. In *Proceedings of the 12<sup>th</sup> International Conference on Computing, Communication and Networking Technologies (ICCCNT)* (pp. 1-5). IEEE.
- [10] Zhang, J., Jin, Y., Wang, H., & Zhao, Y. (2019). Intelligent waste management system based on the internet of things. In *2019 18<sup>th</sup> International Symposium on Distributed Computing and Applications for Business Engineering and Science (DCABES)* (pp. 156-159). IEEE.



## [S4-47] A Study of the Synthesis of Zeolite Using Residual By-Products of Indirect Carbonation

Seonmi Shin<sup>1,2</sup>, Myoung-Jin Kim<sup>1,2,\*</sup>

<sup>1</sup>Department of Civil and Environmental Engineering, Korea Maritime and Ocean University, Busan, Republic of Korea,

<sup>2</sup>Interdisciplinary Major of Ocean Renewable Energy Engineering, Korea Maritime and Ocean University, Busan, Republic of Korea

\*Corresponding author: kimmj@kmou.ac.kr

### Abstract

Active research is focused on the synthesis of zeolites using industrial by-products rich in Si and Al. Since the synthesis of zeolites using pure chemical reagents is expensive, many researchers strive to develop methods that utilize industrial by-products containing a great deal of Si and Al. These methods include fusion, hydrothermal, and fusion-hydrothermal reactions.

While active research focuses on the synthesis of zeolites using industrial by-products rich in Si and Al, limited studies have been conducted on synthesizing zeolites with the residual by-products of indirect carbonation. Indirect carbonation is a CCUS technology that involves extracting Ca and Mg from raw materials, Ca- or Mg-rich industrial by-products and natural minerals, using solvents. The extracted Ca and Mg are then reacted with CO<sub>2</sub>, converting them into stable CaCO<sub>3</sub> and MgCO<sub>3</sub>. However, valuable components such as Si and Al remain in these residues after the Ca or Mg has been eluted from industrial by-products using solvents, and the amount of these residual by-products is substantial.

In this study, we aim to assess the feasibility of synthesizing zeolites from residual by-products of indirect carbonation through two ways: fusion hydrothermal reaction and hydrothermal reaction. To generate the residual by-products, coal fly ash was mixed with three solvents (0.3M HCl, 0.3M NH<sub>4</sub>Cl, seawater) and then filtered. The fusion-hydrothermal reaction and hydrothermal reaction were performed on both the three residual by-products and the parent coal fly ash to synthesize zeolite. XRD and FE-SEM analyses confirmed that zeolite P was successfully synthesized in both the residual by-products of indirect carbonation as well as the parent coal fly ash. It was observed that the zeolites synthesized from the residual by-products exhibited similar characteristics to those synthesized from coal fly ash.

Thus, this study validated the possibility of synthesizing and recycling zeolites using the residual by-products of indirect carbonation, which are regarded as landfill waste.

**Keywords:** *Indirect carbonation, Industrial by-products, Residual by-products, Zeolite*

### Acknowledgments

This work was supported by the National Research Foundation of Korea (NRF) grant funded by the Korea government (MSIT) (No. 2021R1A2C2009914). This research was supported by Korea Institute of Marine Science & Technology Promotion (KIMST) funded by the Ministry of Oceans and Fisheries (20220149).

### References

- [1] Hong, Jaime Li Xin, et al. "Conversion of coal fly ash into zeolite materials: synthesis and characterizations, process design, and its cost-benefit analysis." *Industrial & Engineering Chemistry Research* 56.40 (2017): 11565-11574.
- [2] Querol, Xavier, et al. "Synthesis of zeolites from coal fly ash: an overview." *International Journal of coal geology* 50.1-4 (2002): 413-423.
- [3] Wee, Jung-Ho. "A review on carbon dioxide capture and storage technology using coal fly ash." *Applied Energy* 106 (2013): 143-151.
- [4] Yoldi, M., et al. "Zeolite synthesis from industrial wastes." *Microporous and Mesoporous materials* 287 (2019): 183-191.

## [S4-48] An Experimental Study on the Fracture Energy of Seawater Mortar Reinforced with Recycled PET Fibers

Meeju Lee<sup>1,2</sup>, Kyeongjin Kim<sup>3</sup>, Jeongho Kim<sup>3</sup>, Seungbok Lee<sup>3</sup>, Jaeha Lee<sup>1,3,\*</sup>

<sup>1</sup>*Interdisciplinary Major of Ocean Renewable Energy Engineering, Korea Maritime & Ocean University, Busan, 49112, Republic of Korea*

<sup>2</sup>*Department of Civil and Environmental Engineering, Korea Maritime & Ocean University, Busan, 49112, Republic of Korea*

<sup>3</sup>*Department of Civil Engineering, Korea Maritime & Ocean University, Busan, 49112, Republic of Korea*

\*Corresponding author: jeaha@kmou.ac.kr

### Abstract

In this study, we conducted an experiment to evaluate the fracture energy of fiber-reinforced mortar using recycled PET (Polyethylene Terephthalate) fiber. We considered two types of recycled PET fiber. One type of fiber consists of shredded rPET bottles, with a length of 20 mm and a width of 2 mm, while the other type resembles textiles used for clothing, with a length of 51 mm. To make the mortar applicable to marine concrete structures, we used seawater as the mixing water. Additionally, the incorporation of nano-particles improved the bond strength in the Interfacial Transfer Zone (ITZ) and improved the bond strength of surface-treatment (NaOH, Silane coated) PET fibers. We confirmed the performance improvement through tests on compressive strength, tensile strength, and fracture energy. The results showed that the fracture energy of the specimens incorporating surface-treated PET fibers improved by 802% compared to that of plain mortar. Microstructure analyses such as XRD and SEM confirmed the presence of hydration products and the improvement in bond strength. XRD analysis included a hydration analysis of each specimen, which revealed the presence of Friedel's salt when seawater was used. SEM analysis confirmed that bond strength was enhanced by nano-silica and dimples were formed on the surface of PET fibers hydrolyzed with a NaOH solution. The observed increase in fracture energy of recycled PET fiber-reinforced mortar suggests that it can be used to enhance the impact resistance of marine concrete structures.

**Keywords:** Recycled PET, Nano-particle, Mortar, Fracture energy, SEM, XRD, Bond strength

### Acknowledgments

This work was supported by the National Research Foundation of Korea (NRF) grant funded by the Korea government (MSIT) (No. 2021R1I1A3044831)

### References

- [1] Lin, Xiuyi, et al. "Recycling polyethylene terephthalate wastes as short fibers in Strain-Hardening Cementitious Composites (SHCC)." *Journal of hazardous materials*, 357 (2018): 40-52.
- [2] Xiao, Jianzhuang, et al. "Use of sea-sand and seawater in concrete construction: Current status and future opportunities." *Construction and Building Materials*, 155 (2017): 1101-1111.
- [3] Yu, Jing, et al. "Using nano-silica to improve mechanical and fracture properties of fiber-reinforced high-volume fly ash cement mortar." *Construction and Building Materials* 239 (2020): 117853.

## [S4-54] Direct Carbonation for Zero By-Product in Mineral Carbonation Process using Oyster Shells and Seawater

Eunbit Koh<sup>1,2</sup>, Myoung-Jin Kim<sup>1,2,\*</sup>

<sup>1</sup> Department of Civil and Environmental Engineering, Korea Maritime and Ocean University, Busan, Republic of Korea

<sup>2</sup> Interdisciplinary Major of Ocean Renewable Energy Engineering, Korea Maritime and Ocean University, Busan, Republic of Korea

\*Corresponding author: kimmj@kmou.ac.kr

### Abstract

In mineral carbonation, direct carbonation is a technology that involves direct reaction of calcium and magnesium sources with carbon dioxide to store and utilize them as carbonate minerals. Previous studies in our lab have shown that indirect carbonation using oyster shells and seawater is economically and environmentally advantageous for producing high-purity calcium carbonate. However, it requires an excessive number of calcined shells in the calcium elution process, resulting in a significant quantity of residual by-products. Therefore, the objective of this study is to directly carbonize the residual by-products of indirect carbonation in order to achieve a mineral carbonation process with zero by-products, using shells and seawater.

XRF and XRD analysis of the residual by-products obtained through indirect carbonation indicated that calcium and magnesium were present at concentrations of 75% and 15%, respectively. The analysis also confirmed that the main components were  $\text{Ca}(\text{OH})_2$ ,  $\text{Mg}(\text{OH})_2$ , and  $\text{CaCO}_3$ . In the direct carbonation process, the residual by-product and distilled water were mixed 1:10 (g:mL) and reacted with carbon dioxide. The carbonation reaction was terminated at pH 7, and the resulting precipitate was filtered to separate the solids. When the filtrate was stirred at room temperature and 60°C for a period of time, a white solid was produced. The two types of solids produced in the experiment were analyzed as follows. Firstly, the solid produced by direct carbonation was analyzed by XRD, which confirmed the formation of calcium carbonate and nesquehonite, a type of magnesium carbonate. TGA analysis showed that the weight of magnesium carbonate and calcium carbonate decreased by 18.1% and 21.4%, respectively, between 300~500°C and 500~820°C. In addition, XRD analysis confirmed that when the filtrate obtained after direct carbonation was stirred, nesquehonite was produced at room temperature and hydromagnesite at 60°C. More than 90% of the dissolved magnesium in the filtrate was precipitated, and the crystallinity of the synthesized magnesium compounds increased when the stirring time was increased from 1 hour up to 24 hours.

In this study, residual by-products produced from the indirect carbonation process using calcined shells and seawater were directly carbonated and recycled into calcium carbonate and magnesium carbonate. The manufactured calcium carbonate and magnesium carbonate can be used for paint, rubber, paper filler, materials for construction products, food additives, flame retardants, and more.

**Keywords:** Direct carbonation, Calcium carbonate, Magnesium carbonate, Zero By-Product

### Acknowledgments

This work was supported by the National Research Foundation of Korea (NRF) grant funded by the Korea government (MSIT) (No. 2021R1A2C2009914). This research was supported by Korea Institute of Marine Science & Technology Promotion (KIMST) funded by the Ministry of Oceans and Fisheries (20220149).

### References

- [1] Trushina, Daria B., et al. "CaCO<sub>3</sub> vaterite microparticles for biomedical and personal care applications." *Materials Science and Engineering, C* 45 (2014): 644-658.
- [2] Wang, Yulian, et al. "Synthesis, characterization and mechanism of porous spherical nesquehonite by CO<sub>2</sub> biomimetic mineralization." *Advanced Powder Technology*, 33.12 (2022): 103856.

**[S4-55] Carbon Dioxide Conversion to Bioplastic (Poly 3-Hydroxybutyrate) through Microbial Electrosynthesis System**

Giang T. H. Le<sup>1,2</sup>, Dipak A. Jadhav<sup>1</sup>, Jung-Min Lee<sup>1,2</sup>, Miri Jae<sup>1,2</sup>,  
Ju-Hyeong Kim<sup>1,2</sup>, Kyu-Jung Chae<sup>1,2,\*</sup>

<sup>1</sup> Department of Environmental Engineering, College of Ocean Science and Engineering, Korea Maritime and Ocean University, 727 Taejong-ro, Yeongdo-gu, Busan 49112, Republic of Korea

<sup>2</sup> Interdisciplinary Major of Ocean Renewable Energy Engineering, Korea Maritime and Ocean University, 727 Taejong-ro, Yeongdo-gu, Busan 49112, Republic of Korea

\*Corresponding author: ckjdream@kmou.ac.kr

**Abstract**

Among diverse bioelectrochemical technologies, microbial electrosynthesis (MES) has been known as a potential system for carbon capture and biological conversion of carbon dioxide into value-added chemicals and biofuels. This study aims to conduct an in-situ conversion from CO<sub>2</sub> to a bioplastic material such as Poly (3-hydroxybutyrate) (PHB), a biodegradable and biocompatible biopolymer that exists as intracellular granules. The symbiotic interactions between electroactive acetogen and PHB-accumulating bacteria have been employed, resulting in the reduction of CO<sub>2</sub> into volatile fatty acid (VFA), then serving as the essential carbon source for the PHB accumulation in MES reactor. The investigation has been conducted with different factors, including imposed cell voltage, modified cathode material, carbon and inoculum sources. As a result of the optimization process, the highest VFA production in the system was 356.01 (mg/L) at 2.5 V with PEDOT: PSS as the modified cathode material. The result indicates that at lower than 2.5 V, almost no VFA was detected in the system. In comparison, the food-waste as inoculum has a higher capability in PHB production than the anaerobic sludge. Meanwhile, PHB is accumulated in the system with a maximum concentration was 22.79 (mg PHB/g VSS) at 1.82 V and inoculum as food-waste. The optimized operation factor chosen for further investigation in PHB production was PEDOT: PSS as cathode material, CO<sub>2</sub> as carbon source and cell potential should be provided at 2.5 V, inoculum as a mixture from anaerobic sludge and food-waste. This research approaches the development of sustainable technologies, which generate valued bioplastic from the bio-electrochemical system while removing the major component of greenhouse gas. However, further long-term optimization operation is required to enhance the conversion of CO<sub>2</sub> to PHB.

**Keywords:** *Bioplastic, Poly (3-hydroxybutyrate), In-situ, Carbon capture and Utilization, Microbial electrosynthesis*

**Acknowledgments**

This work was supported by the National Research Foundation of Korea (NRF) grant funded by the Korea government (MSIT) (No. RS-2023-00209009), in part by “Cooperative Research Program for Agriculture Science and Technology Development (Project No. PJ016259022023)” funded by Rural Development Administration in Republic of Korea, and in part from the National Research Foundation of Korea (NRF) grant funded by the Korea government (MSIT) (No. RS-2023- 00219497).

**[S4-56] Improvement of Hydrogen Production through Methanogen Suppression in Microbial Electrolysis Cells for Swine Manure Treatment**

Trang T. Q. Le<sup>1,2</sup>, Dipak A. Jadhav<sup>1</sup>, Mohammed Hussien<sup>1,2</sup>, Jung-Min Lee<sup>1,2</sup>, Sumin Jo<sup>1,2</sup>,  
Miri Jae<sup>1,2</sup>, Kyung-Jung Chae<sup>1,2,\*</sup>

<sup>1</sup> Department of Environmental Engineering, College of Ocean Science and Engineering, Korea Maritime and Ocean University, 727 Taejong-ro, Yeongdo-gu, Busan 49112, Republic of Korea

<sup>2</sup> Interdisciplinary Major of Ocean Renewable Energy Engineering, Korea Maritime and Ocean University, 727 Taejong-ro, Yeongdo-gu, Busan 49112, Republic of Korea

\*Corresponding author: ckjdream@kmou.ac.kr

**Abstract**

Microbial electrolysis cells (MECs) are potential candidates for hydrogen production based on their high performance and effectiveness in treating complex organic compounds. However, the competition between electrogenic bacteria and methanogens in the system significantly limits the increase in biohydrogen production. Until now, many studies have focused on inhibiting methanogens in fermentation systems. Nevertheless, MECs have still lacked a cost-effective method to control non-electrogenic bacteria. Some chemicals used for controlling methane production are continuously employed, but they are not the optimal choice due to their harmful nature and high cost. Therefore, this study aims to identify economical and highly profitable approaches to suppress methane and non-hydrogen-producing bacteria, while simultaneously enhancing hydrogen production in MECs. In this work, anaerobic digestion sludge was used as the inoculum, and the substrate was obtained from a swine manure fermented plant, known for its rich VFAs and nutrient content. Three pretreatment methods, including physical, chemical, and combined treatments, were selected for both the substrate and inoculum. The results pertaining to methane suppression, the activity of electrogenic bacteria, and the microbial community were analyzed. The preliminary findings highlight the effectiveness of the pretreatment methods in suppressing methane production in a complex substrate and inoculum. This study identifies practical and efficient pretreatment method to mitigate methane production, supporting the implementation of MEC systems on the larger scale.

**Keywords:** Wastewater treatment, Hydrogen production, Methane suppression, Microbial electrolysis cell (MEC), Swine manure

**Acknowledgments**

This work was supported by the National Research Foundation of Korea (NRF) grant funded by the Korea government (MSIT) (No. RS-2023-00209009), in part by “Cooperative Research Program for Agriculture Science and Technology Development (Project No. PJ016259022023)” funded by Rural Development Administration in Republic of Korea, and in part of the National Research Foundation of Korea (NRF) grant funded by the Korea government (MSIT) (No. RS-2023- 00219497).

## [S5-18] Capacitated Drone Routing Problem with Time Windows and Scheduled Lines: Mathematical Formulation

Dang Le To Uyen, Phan Nguyen Ky Phuc\*, Pham Ngoc Xuan Mai

*International University, Ho Chi Minh City, Viet Nam, 700000*

\*Corresponding author: pnkphuc@hcmiu.edu.vn

### Abstract

The use of drones has emerged as a promising solution for last-mile delivery challenges faced by last-mile delivery services and e-commerce companies. In the recent decade, many leading companies have tried to implement drone last-mile delivery in urban areas and drone delivery is considered to be beneficial in both environmental and economic perspectives. This paper considers a last-mile delivery system in which a set of drones operate cooperatively with a public transportation system to deliver parcels from a center depot to customer locations. Public transport stations, or transfer nodes, are considered as battery swapping spots for drones. The proposed system is studied with the aim to address the limitation of drone battery capacity, thus increasing the flight range of drones. A mathematical model is presented to solve the problem. The result shows that the energy consumption and flight range of drones are highly impacted by the integration of the public transport station.

**Keywords:** *Drone delivery, Capacitated vehicle routing problem, Time window, Scheduled line*

### 1. INTRODUCTION

Together with urbanization, the rapid growth of e-commerce in recent years has brought many considerable challenges for last mile delivery systems [1]. The increase in the number of online orders per person has led to a high volume of parcels to be delivered in a concentrated geographic area. This also resulted in more delivery vans and trucks entering the city, putting a burden on existing infrastructure and the environment. Increasing customer demand for fast and cheap delivery is another challenge for the last-mile delivery service. Additionally, the fluctuation in online shopping activities and seasonal sales requires a last-mile delivery service that is easily scalable on short notice [1]. Lastly, the aging workforce in many countries highlights the manpower problem for low-paid jobs such as parcel delivery [1].

To stay competitive in the market with new challenges mentioned about, in the recent decade, several firms have started to invest more in the application of drones in delivery. Amazon was one of the first players when it deployed the Prime Air delivery system in 2013. In the same year, Deutsch Post DHL launched the Parcelcopter project that uses aerial vehicles to transport medicine to the island of Juist in the North Sea. One year later, Project Wing of Alphabet, the parent company of Google was presented.

In terms of operations, there are practical constraints and challenges that limit the use of drones in last-mile delivery. Delivery drones have limited battery capacity, which leads to limited flight time and flight range. Since current delivery drones can only handle medium package weights, each drone can only serve a small number of customers per delivery trip. Furthermore, deployment of drone delivery systems requires significant capital investment for new infrastructure such as charging stations or drone ports, and weather conditions can cause delays or damage to drones while performing delivery.

This paper is dedicated to studying the capacitated vehicle routing problem with time window and scheduled line (CDRPTW-SL) in a novel proposed system that helps to increase the flight range of drones by integrating them with public transport systems. Inspired by the works of [5] and [3], the proposed problem is to extend the classical Vehicle Routing Problem with Time Windows (VRPTW) by integrating drones with the public transport system. The problem is formulated as a Mixed Integer Linear Programming (MILP) model.

Public transport for package delivery has gained interest from both researchers and logistics companies. In the Netherlands, a project named City Cargo Amsterdam ran a pilot experiment using cargo trams in 2007, where two cargo trams were utilized to transport cargo in the city center of Amsterdam [3]. [3] studied the use of predetermined transportation routes for freight transport, considering synchronization constraints. The integration of drones into public transport systems has also been considered recently. A low-level drone round trip routing

in a stochastic time-dependent network when drones are integrated into a transportation network is studied in [4]. [2] investigated integrating drones into existing public transport infrastructure where drones can either directly serve customers if capable or move along with public vehicles to extend the flight range. [5] proposed a mathematical model based on VRP to study the integration of multiple drones into a single public transport route, where drones use public transport vehicles as moving charging stations.

## 2. MATHEMATICAL FORMULATION

### 2.1. Problem description

The problem is formally defined on a graph  $G = (V, A)$  where  $V$  is the set of nodes (depot, transfer nodes, and customers) and  $A$  represents the set of arcs where  $A = \{(i, j) | i, j \in V\}$ . Each arc  $(i, j) \in A$  is associated with a travel time  $t_{ij}$ . Each customer  $i \in C$  is associated with a parcel weight  $w_i$  and a service time  $s_i$ . As the deliveries will require the presence of customer, each customer is associated with a time window  $[l_i, u_i]$ . It is assumed that travel time and service time are known in advance.

A set of homogeneous drones  $D$  is equipped at the depot with the same maximum weight capacity  $Q^D$  and battery capacity  $\theta$ . Each drone can carry multiple parcels as long as the total weight of the parcels does not exceed  $Q^D$ . The battery consumption of a drone while traversing an arc  $(i, j)$  is assumed to be  $t_{ij} \times \phi$ , with  $\phi_{ij}$  is the battery consumption rate.

A public transport system is considered in the network, which includes a set of transfer nodes given as  $B$  and a set of scheduled lines given as  $E$  ( $E \in A$ ). Each scheduled line is defined by the directed arc between two transfer nodes, i.e.,  $E = \{(i, j) | i, j \in B\}$ . For each schedule line  $(i, j) \in E$ , there is a set of indices for the associated schedule departures times from transfer node  $i$  to  $j$ ,  $K^{ij}$ . The departure time  $i, j$ s then denoted as  $p^w, \forall (i, j) \in E, \forall w \in K^{ij}$ . Furthermore, a departure from a transfer node is assumed to be able to simultaneously carry a limited number of drones, thus implying a carrying capacity  $\mu^D$ .

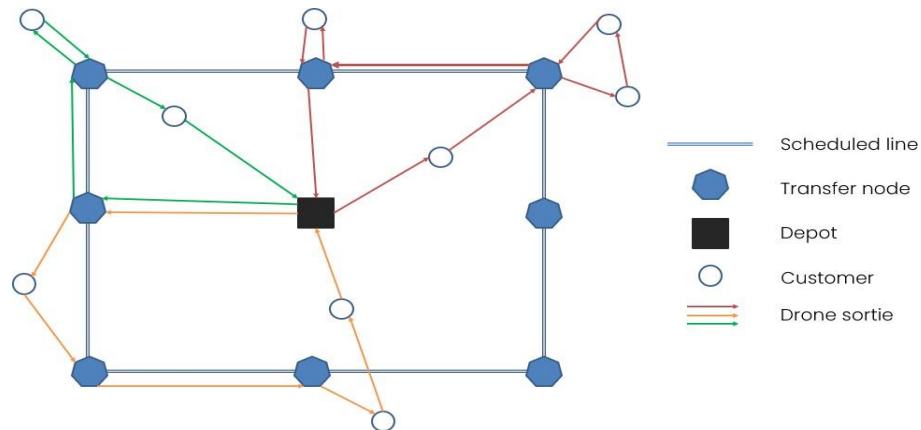


Figure 1. An example network of the CDRPTW-SL

### 2.2. Nomenclature

The notations of sets and parameters used in the formulation of the problem are explained in Tables 1 – 3.

Table 1. Sets

Set	Definition
$V$	Set of all nodes, including depot, customer, transfer node $i, j = 1 \dots  V $
$C$	Set of customers
$D$	Set of drones
$A$	Set of arcs in the graph defined by $V \times V$
$B$	Set of transfer nodes
$E$	Set of scheduled lines $(i, j)$
$\mathcal{K}^{ij}$	Set of indices for the departure times from transfer node $i$ to transfer node $j$

**Table 2.** Parameters

Parameter	Definition
$t_{ij}$	Flying time from node $i$ to node $j$ , $\forall i, j \in V$
$s_i$	The service time at node $i$ , $\forall i \in C$
$p_{ij}^w$	The departure time from transfer node $i$ on scheduled line $(i, j)$ , indexed by $w$
$Q$	Carrying capacity of the drone
$\mu^D$	The maximum number of drones that can be simultaneously carried on each scheduled line
$d_i$	A package of weight associated with customer $i$ , $i \in C$
$\theta$	The maximum energy can be stored in the drone's battery
$\phi_{ij}$	The battery consumption rate of a drone while traversing arc $(i, j)$ ,
$[l_i, u_i]$	Time window of node $i$ , $i \in C$
$C^D$	Fixed unit cost of using drone
$c_{ij}$	Cost of using the scheduled line $(i, j)$ for transferring one drone
$M$	A very large number

**Table 3.** Decision variable

Decision variable	Definition
$x_{ij}^d$	Binary variable equal to 1 if arc $(i, j)$ is traversed by the drone $d$ ; 0 otherwise, $\forall i, j \in V$ , $d \in D$ .
$y^d$	Binary variable equal to 1 if drone $d$ is used; 0 otherwise, $\forall d \in D$ .
$q_{ij}^{dw}$	A binary variable equal to 1 if a scheduled line $(i, j)$ is used to carry drone $d$ at the departure time indexed $w$ ; 0 otherwise, $\forall (i, j) \in E$ , $d \in D$ , $w \in \mathcal{K}^{ij}$
$r_{id}$	A continuous variable representing the departure time of the drone $d$ from node $i$ , $\forall i \in V$ , $d \in D$ .
$w_i^d$	An integer variable representing the cumulative weight of drone $d$ after unloading at node $i$ , $\forall i \in C$ , $d \in D$ .
$v^d$	An integer variable representing the total weight that drone $d$ picks up at the depot for operation, $\forall d \in D$
$h_{id}$	A continuous variable representing the battery level of drone $d$ when it departs from node $i$ , $\forall i \in V$ , $d \in D$

### 2.3. Mathematical model

#### Objective

#### function

$$\text{Minimize } Z = \sum_{d=1}^{\mu^D} C^D y^d + \sum_{i,j \in E} \sum_{d \in D} \sum_{w \in \mathcal{K}^{ij}} q_{ij}^{dw} c_{ij} \quad (1)$$

#### Routing and flow constraints

$$\sum_{i \in V, i \neq j} x_{ij}^d - \sum_{k \in V, k \neq j} x_{jk}^d = 0, \quad \forall j \in B \cup C, d \in D \quad (2)$$

$$x_{ij}^d = 1 \Rightarrow \sum_{k \in B, k \neq j} x_{ki}^d = 1 \quad \forall d \in D, i \in V \setminus \{C, 0^+, 0^-\}, j \in V \setminus \{B, 0^+\}, i \neq j \quad (3)$$

$$x_{ij}^d = 1 \Rightarrow \sum_{k \in B, k \neq j} x_{jk}^d = 1, \quad \forall d \in D, i \in V \setminus \{B, 0^-\}, j \in V \setminus \{C, 0^+, 0^-\}, i \neq j \quad (4)$$

$$x_{ij}^d = 1 \Rightarrow \sum_{k \in V, k \neq j} x_{ki}^d = 1 \quad \forall d \in D, i, j \in V \setminus \{C, 0^+, 0^-\}, i \neq j \quad (5)$$

$$\sum_{j \in V \setminus \{0^+, 0^-\}} x_{0^+j}^d = y^d, \quad \forall d \in D \quad (6)$$

$$\sum_{i \in V \setminus \{0^+, 0^-\}} x_{i0^+}^d = y^d, \quad \forall d \in D \quad (7)$$

$$\sum_{i \in V, i \neq j} \sum_{d \in D} x_{ij}^d = 1, \quad \forall j \in C \quad (8)$$

$$\sum_{i \in V} \sum_{j \in V, j \neq i} x_{ij}^d = 0 \Rightarrow y^d = 0, \quad \forall d \in D \quad (9)$$



$$\sum_{i \in V} \sum_{j \in C, j \neq i} x^d \geq 1 \Rightarrow y^d = 1, \forall d \in D \quad (10)$$

$$x_{ij}^d = 1 \Rightarrow r_{id} + t_{ij} + s_j \leq r_{jd}, \forall d \in D, \forall i, j \in V, i \neq j \quad (11)$$

$$x_{ij}^d = 1 \Rightarrow r_{jd} \leq u_j, \forall d \in D, i, j \in V, i \neq j \quad (12)$$

$$x_{ij}^d = 1 \Rightarrow r_{jd} - s_j \geq l_j, \forall d \in D, i, j \in V, i \neq j \quad (13)$$

#### Weight capacity constraints

$$\sum_{i \in V} \sum_{j \in C, j \neq i} a_j x_{ij}^d = v^d, \forall d \in D \quad (14)$$

$$v^d \leq Q, \forall d \in D \quad (15)$$

#### Synchronization constraints

$$\sum_{w \in \mathcal{K}^{ij}} q^{dw} \geq x^d, \forall d \in D, (i, j) \in E \quad (16)$$

$$x_{ij}^d \geq q^{dw}, \forall d \in D, (i, j) \in E, w \in \mathcal{K}^{ij} \quad (17)$$

$$q_{ij}^{dw} = 1 \Rightarrow r_{id} = p^w, \forall d \in D, (i, j) \in E, w \in \mathcal{K}^{ij} \quad (18)$$

$$\sum_{d \in D} q^{dw} \leq \mu^D, \forall (i, j) \in E, w \in \mathcal{K}^{ij} \quad (19)$$

#### Drone's battery consumption

$$x_{ij}^d = 1 \Rightarrow h_{jd} = \theta, \forall d \in D, i \in V, j \in B, i \neq j \quad (20)$$

$$x_{0^+j}^d = 1 \Rightarrow h_{0^+j} = \theta, \forall d \in D, i, j \in V, i \neq j \quad (21)$$

$$x_{ij}^d = 1 \Rightarrow h_{jd} = h_{id} - \phi_{ij} * t_{ij}, \forall d \in D, i \in V, j \in V \setminus \{B\}, i \neq j \quad (22)$$

$$x_{ij}^d = 1 \Rightarrow h_{id} - \phi_{ij} * t_{ij} \geq 0, \forall d \in D, i \in V, j \in B, i \neq j \quad (23)$$

#### Decision variable domains

$$x_{ij}^d \in \{0, 1\}, \forall i, j \in V, \forall d \in D \quad (24)$$

$$x_{0^+0}^d - x_{0^-0}^d = 0, \forall d \in D \quad (25)$$

$$y^d \in \{0, 1\}, \forall d \in D \quad (26)$$

$$q_{ij}^{dw} \in \{0, 1\}, \forall d \in D, \forall (i, j) \in E, \forall w \in \mathcal{K}^{ij} \quad (27)$$

$$r_{id} \in R^+, \forall i \in V, \forall d \in D \quad (28)$$

$$h_{id} \in R^+, \forall i \in V, \forall d \in D \quad (29)$$

$$p^d \in R^+, \forall i \in V, \forall d \in D \quad (30)$$

$$v^d \in R^+, \forall i \in V, \forall d \in D \quad (31)$$

The objective function (1) aims to minimize the total cost of using drones for delivering and using scheduled lines for transferring drones. Eq. (2) incorporates the flow conservation between nodes. Eqs. (3) – (5) are set to prevent drones from using transfer nodes as hubs or a simple middle node. Constraints (6) and (7) guarantee that if a drone is used, it will depart from and return to the depot exactly once. Constraint (8) ensures that each customer is visited exactly once. Eqs. (9) – (10) make sure that if a drone is selected for delivery, it will visit at least one customer. Subtour elimination is handled by Eq. (11). Eqs. (12) and (13) ensure that time windows are respected. Eq. (14) indicates the total load that each drone is supposed to deliver, while Eq. (15) incorporates the limited weight capacity of each drone. Eqs. (16) – (17) handle the synchronization between drone's route and the scheduled line. Eq. (16) makes sure that if a drone is selected to traverse over the scheduled line  $(i, j)$ , it will take a departure at the transfer node  $i$  while Eq. (17) indicates that if a drone does not traverse the schedule line  $(i, j)$ , it does not take any departure from the transfer node  $i$ . Eq. (18) forces the departure time of a drone from a transfer node  $i$  to be equal to one of the departure schedules of that node if the drone is to travel over the scheduled line  $(i, j)$ . The maximum number of drones carried simultaneously on each scheduled line is considered by Eq. (19). Eq. (20) indicates the battery level of a drone when it departs from a transfer node, while Eq. (21) shows the battery level of a drone at the depot. The battery level of a drone after it traverses an arc is evaluated by Eq. (22). Eq. (23) ensures that a drone has enough energy to fly to a transfer node for charging. Eqs. (24) – (31) specify

the value of each variable used in the model.

### 3. NUMERICAL EXAMPLE

The proposed mathematical model is examined using a small size example problem. In the considered problem, a set of 5 drones is equipped at a single center depot to serve 5 customers. A public transportation system with 4 transfer nodes is integrated in the system. Detailed parameters and network information are presented in Tables 4 – 6 in the Appendix section.

The mathematical model is verified and implemented in CPLEX Solver. The initial result has proved that the model is effective for solving the small size problem containing 5 customers and 4 transfer nodes. The network and solution are illustrated by Figure 2.

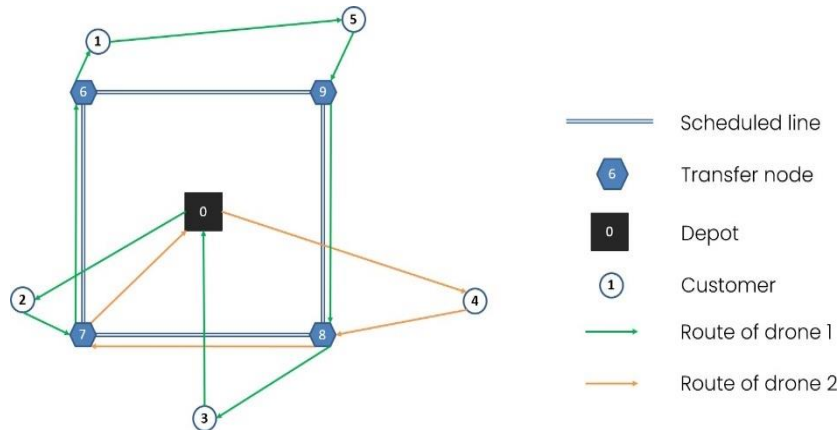


**Figure 2.** Solution illustration for the problem

The route (sortie) of done is as follows:

Drone 1	0	2	7	6	1	5	9	8	3	0
Drone 2	0	4	8	7	0					

Drone 1 goes from the depot to customer 2, then flies to transfer node 7 to change the battery. The drone then boards a public vehicle from transfer node 7 to transfer node 6. After leaving transfer node 6, the drone serves customers 1, 5 before flying to transfer node 9 to change the battery. The drone then boards a public vehicle from transfer node 9 to transfer node 8 on a scheduled line before serving customer 3 and finally returning to the depot. Similarly, drone 2 is responsible for serving customer 4 and uses scheduled line (8, 7) to return to the depot. With the optimal route presented above, the solution results in the minimum cost of \$160.

It can be seen that the synchronization constraint is followed, ensuring that the drone follows predetermined route and departure time of scheduled lines. Additionally, the energy constraint provides motivation for the drones to find transfer nodes for battery swapping when their energy level falls below a certain threshold. The optimal result is achieved within reasonable computational time. It is noteworthy that this result is preliminary and was obtained using a small size test instance and the model is to be tested with larger instances to fully evaluate its effectiveness.

### 4. CONCLUSION

Overall, the integration of drones into a public transportation system has the potential to revolutionize the last-mile delivery service, improving efficiency and reducing the impact on the environment. Future research regarding the integration of drones and public transport could consider applying heuristic or metaheuristic approaches to solve the problem more effectively. Other settings, such as multiple depots or two-echelon systems are also promising extensions for this study.

## Appendix: Data for numerical example

Table 4. Network information

	Node $i$	x-coordinate	y-coordinate	$d_i$	$l_i$	$u_i$	$s_i$
Start depot	0	40	50	0	0	300	0
Customer	1	22	75	30	10	190	10
	2	10	35	20	20	220	10
	3	40	15	40	50	230	10
	4	85	35	30	20	200	10
	5	65	82	10	30	220	10
Transfer node	6	20	70	0	0	300	0
	7	20	30	0	0	300	0
	8	60	30	0	0	300	0
	9	60	70	0	0	300	0

Table 5. Sets and parameters

$Depot$	{0}
$C$	{1, 2, 3, 4, 5}
$B$	{6, 7, 8, 9}
$\mathcal{K}^{ij}$	{50, 100, 150, 200, 250, 300}
$Q$	130
$\mu^D$	3
$C^D$	\$50

Table 6. Scheduled line route

Departure node	Destination node
7	8
8	7
8	9
9	8
9	10
10	9
10	7
7	10

## References

- [1] Boysen, N., Fedtke, S., & Schwerdfeger, S. (2020). Last-mile delivery concepts: a survey from an operational research perspective. *OR Spectrum*. Doi:10.1007/s00291-020-00607-8
- [2] Choudhury, S., Solovey, K., Kochenderfer, M. J., & Pavone, M. (2021). Efficient Large-Scale Multi- Drone Delivery using Transit Networks. *Journal of Artificial Intelligence Research*, 70, 757-788. <https://doi.org/10.1613/jair.1.12450>
- [3] Ghilas, V., Demir, E., & Van Woensel, T. (2016). An adaptive large neighborhood search heuristic for the Pickup and Delivery Problem with Time Windows and Scheduled Lines. *Computers & Operations Research*, 72, 12–30. Doi:10.1016/j.cor.2016.01.018
- [4] Huang, H., Savkin, A. V., & Huang, C. C. (2020). Round Trip Routing for Energy-Efficient Drone Delivery Based on a Public Transportation Network. *IEEE Transactions on Transportation Electrification*, 6(3), 1368-1376. <https://doi.org/10.1109/tte.2020.3011682>
- [5] Moadab, A., Farajzadeh, F., & Valilai, O. F. (2022). Drone routing problem model for last-mile delivery using the public transportation capacity as moving charging stations. *Scientific Reports*, 12(1). <https://doi.org/10.1038/s41598-022-10408-4>

## [S5-23] Predictive Maintenance for Machine Breakdown - An Application in Manufacturing

Nguyen Thi Thanh Xuan\*, Tran Duc Vi

*School of Industrial Engineering and Management, International University  
Viet Nam National University Ho Chi Minh City, Thu Duc City, Ho Chi Minh City, Viet Nam*

\*Corresponding author: xuannghuyen80294@gmail.com

### Abstract

In recent years, several researchers and practitioners have focused on Predictive Maintenance (PdM) in manufacturing using Machine Learning (ML) methodologies, particularly in capital-intensive industries such as semiconductor manufacturing. Building a decision tool that detects problems in semiconductor industry equipment or processes as soon as feasible to maintain high process efficiencies is vital to cost reduction and process control. One of the Semiconductor Manufacturers recently requested the best option for improving their capacity without increasing capital expenditure for the installation of new equipment, which is to reduce downtime (as their annual downtime percentage is around 1%, a significant effect on their productivity). The dataset used in the study is an actual collection of data from a Semiconductor Backend Manufacturing. The data in the analyzed dataset was significantly imbalanced, with missing values, constant data, and meaningless attributes. However, the imbalanced properties of the dataset make implementing a predictive model difficult. In this study, the Synthetic Minority Over-sampling Technique (SMOTE) and Cost-Sensitive Learning (CS) are used techniques alongside the best model found with the best performance within three distinct machine learning algorithms: Logistic Regression (LR), Random Forest (RF), and Gradient Boosting (GB), which are used to analyze the procedure to make imbalanced data perform remarkable results once the data has been balanced. The recall score, as well as the highest TPR and lowest FPR, will be utilized to evaluate. Our experimental results reveal that RF in combination with cost-sensitive learning is the optimal model for optimal performance, with the largest area under the ROC curve (AUC).

**Keywords:** Imbalance dataset, Predictive maintenance, SMOTE, Cost-Sensitive learning.

### 1. INTRODUCTION

The research factory in the Semiconductor field has a complex and multi-step manufacturing process with hundreds of steps [1]. Figure 1 describes the manufacturing overall flow of the Semiconductor Backend process. Maintenance planning for fault prediction prior to an actual defect by developing a forecasting model can assist in decreasing downtime, enhancing labor efficiency and productivity, optimizing maintenance costs, and reducing failure rates.

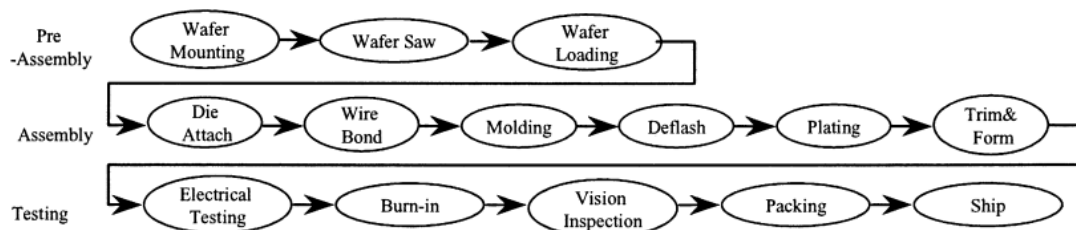


**Figure 1.** Semiconductor back-end manufacturing flow

Following the multi-product demand prediction, the volume is predicted to expand quickly, and the forecast demand can be spiked up to 100 million products (from the 2<sup>nd</sup> quarter in 2022 to the 4<sup>th</sup> quarter in 2023), necessitating all plant performance in peak efficiency and productivity. Meanwhile, the Capacity Planning Team proposes having some improvement possibilities to expand the capacity of specific sub-processes to achieve high volume forecasts and avoid capital spending for just the short term to save the high cost. As a result, we need a better maintenance approach that can forecast exactly when machines break down [2] [3] so that we can pay attention to them quickly and avoid hard breakdowns during production time to reach the goal of “zero defect”

manufacturing [4]. The topic of reliable detection of equipment failure states in the backend process of semiconductor manufacturing is studied in this paper using real data. The dataset's distribution is inherently highly imbalanced. As a result, we focus on establishing a good predictive model for spotting errors that can forecast and avoid future recurrence.

The rest of the paper is organized as follows: Section 2 briefly overviews relevant acknowledgment. Section 3 presents a general framework for fault detection. Section 4 presents experiments and results with an emphasis on the implementation of many ML methods with applied SMOTE as data balancing technique for classification and prediction, as well as several metrics for evaluation. Section 5 presents the conclusion.

## 2. RELEVANT OF WORK

### 2.1. Predictive maintenance overview

Three types of maintenance strategies and terminology are defined [5]: (1) Run-to-Failure (R2F) - the simplest maintenance plan for repairing broken parts, (2) Preventive Maintenance (PM) - time-based maintenance or scheduled maintenance that is carried out on a regular basis based on a predetermined schedule in time to predict breakdowns, and (3) Predictive Maintenance PdM - which is the main concern on this study. PdM is a novel approach to maintenance, but the dearth of research has made implementation difficult. ML has the potential for predictive maintenance. Unexpected faults in industrial equipment may result in severe accidents and losses for manufacturers due to interactive behavior [6].

### 2.2. Predictive maintenance applications

Semiconductor manufacturing is a sophisticated industry, where several ML and Deep Learning approaches have been documented and applied to defect detection. K-Nearest Neighbor (KNN) [7] based approach was proposed and Supervised Aggregative Feature Extraction (SAFE) outperformed other techniques. The confidence matrix was evaluated with Generalized Linear models, Random Forest, Gradient Boosting, and Deep Learning. MLP was ranked with the highest score (91.95% accuracy) and PCA was the optimal method in the data pre-processing phase [8].

The original Baseline Predictive Maintenance used the exponential model to predict the remaining useful life, but this approach has several problems, a data-driven method was proposed [9] with two phases: the learning process & training model, which contains 3 sub-processes: (1) data acquisition and preprocessing, which can be single sensory or multi-sensory, (2) feature engineering, which contains feature extraction, concatenation, and selection; and (3) model training and predicting, in which well-trained. Sampling Methods for Imbalanced Learning (SMOTE) [10] and Handling Imbalanced Datasets [11] were introduced in 2006. SMOTE is a powerful method that has been successful in various applications while Evaluation Metrics [12] are used to evaluate the quantity of accurate and misclassified models. Figure 2 presents the Evaluation Metric formula.

$$\begin{aligned} \text{Accuracy} &= (\text{TP} + \text{TN}) / (\text{TP} + \text{FN} + \text{FP} + \text{TN}) \quad (1) \\ \text{FP rate} &= \text{FP} / (\text{TN} + \text{FP}) \quad (2) \\ \text{TP rate} = \text{Recall} &= \text{TP} / (\text{TP} + \text{FN}) \quad (3) \\ \text{Precision} &= \text{TP} / (\text{TP} + \text{FP}) \quad (4) \\ F\text{value} &= \frac{(1 + \beta^2) \text{Recall} * \text{Precision}}{\beta^2 \text{Recall} + \text{Precision}} \quad (5) \end{aligned}$$

**Figure 2.** Evaluation Metric formula

With:

TP: True Positive - number of fail cases that are correctly identified as fail.

TN: True Negative - number of pass cases that are correctly identified as pass.

FP: False Positive - number of pass cases that are incorrectly identified as fail, also known as Type I error.

FN: False Negative - number of fail cases that are misclassified as pass, also known as Type II error.

### 3. METHODOLOGY

#### 3.1. Dataset overview

The dataset used in this study is real-time collected data from a linked machine in Burn-in. Process & Equipment Engineers analyze the data and report results following MTBF (Mean Time Between Failure). Three issues of the dataset were identified: missing values, irrelevant features, and imbalanced class distribution. The following introduces a table of summary:

**Table 1.** Overview of the studied dataset

Number of attributes (sensors and measurement points of a machine in the process)	14
Number of instances	504605
Labels	-1: PASS, 1: FAIL
Number of "PASS"	461971
Number of "FAIL"	42634

#### 3.2. Proposed framework

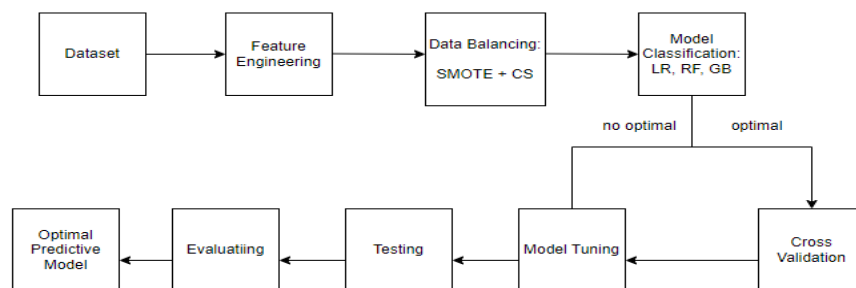


**Figure 3.** Research Framework

Figure 3 presented a structure for the investigation. The dataset needs to be cleaned by checking missing and unique data values, then filled with data imputation. Approaches used to address unbalanced data are divided into two groups: SMOTE (data-driven) and CS (algorithmic-based). The details of this research framework are presented below steps:

1. Feature Engineering: The dataset is checked for 50% of missing data and 4 features are removed. KNN Imputation is used to replace missing values with genuine ones that maximize the data point's expected value.
2. Data Balancing: This is the most focused part of this study; predictive models need SMOTE as data balancing methods to solve the issue, while CS uses unbalanced data.
3. Model Classification: The most effective model is achieved by implementing three ML algorithms based on different data-balancing techniques.
4. Model Tuning: Parameter tuning is used to select the best parameters for ML algorithms, which are tested in loops and applied to the test set for result evaluation. The tuning's outcome is applied to the test set for result evaluation. The following is a summary of parameter values after the tuning process:

**Table 2.** Optimal parameters' value of each algorithm after the tuning process

Classifier	Parameter	Not-Balance	SMOTE	CS
LR	C	1000	1000	1000
RF	# of trees	100	450	150
GB	# of trees	500	500	500

5. Cross Validation: The dataset is divided into ten sections, with one section chosen as the test set and the other nine designated as training. This ensures that all cases in the dataset have been tested and the data has been thoroughly examined. This study will use 10-fold cross-validation.
6. Model Evaluation: Precision, Recall, F1-Score, and ROC-AUC are used to evaluate a predictive model, while Accuracy often does not express the actual effect for an imbalanced dataset.

#### 4. RESULT AND ANALYSIS

The implementation procedure is divided into different scenarios: Scenario 1: Not Balanced (NB). Scenario 2: SMOTE, and Scenario 3: CS. Three different ML algorithms are then studied for each scenario. This study uses AUC, Recall, and TNR as metrics of evaluation. AUC is used to categorize an unbalanced dataset, Recall measures how many errors were found, and TNR measures how few false alarms were generated. The improved classification was reflected by higher AUC, Recall, and TNR.

##### 4.1. Performance of algorithms on the raw dataset

The results on the raw dataset in Table 3 are not good due to a highly imbalanced characteristic. GB gets 91.3% accuracy, but the false negative rate is equal to 0.96. This means that the model predicts all labels are "PASS" and does not correct any points.

**Table 3.** Classification results of Raw Dataset

Algorithm	Accuracy	Precision	Recall	F1-score	AUC	FPR	FNR
LR	93.40%	0.77	0.31	0.44	0.65	0.01	0.68
RF	90.50%	0.27	0.06	0.10	0.52	0.02	0.94
GB	91.30%	0.40	0.04	0.08	0.52	0.01	0.96

##### 4.2. Data balancing result analysis

Performance measures are shown based on the trials' achieved precision, recall (TPR), AUC, and F1-score. Accuracy is not a useful metric to evaluate overall performance in a sample that is very uneven. The target outcomes listed in the table are used as the main metrics for classifier evaluation. Precision is a useful metric for assessing the performance of the classification model, along with metrics like TNR. The efficiency of each combination within each phase of the analysis process is evaluated objectively, with the highest TPR, F1-score, lowest FPR, and TNR used to compare the best results for each method. The detailed results on all algorithms are shown in Figure 5, Figure 6, and Figure 7 by AUC, TPR, and F1-Score:

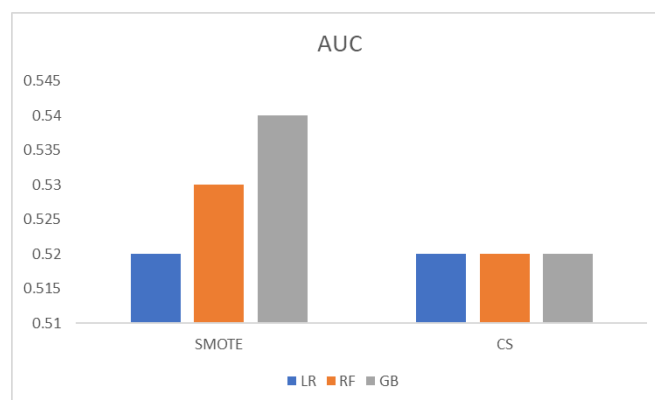


**Figure 4.** AUC result of each classifier on data balancing techniques

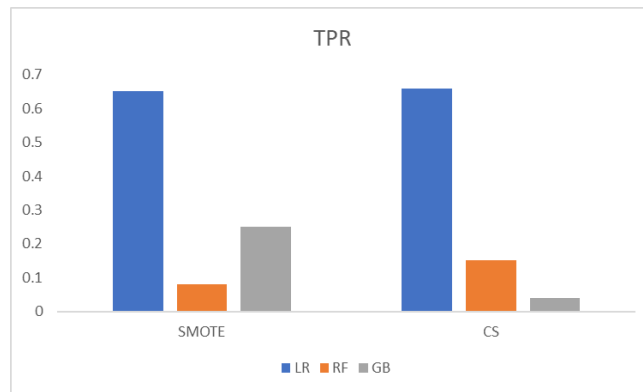


**Figure 5.** TPR result of each classifier on data balancing techniques

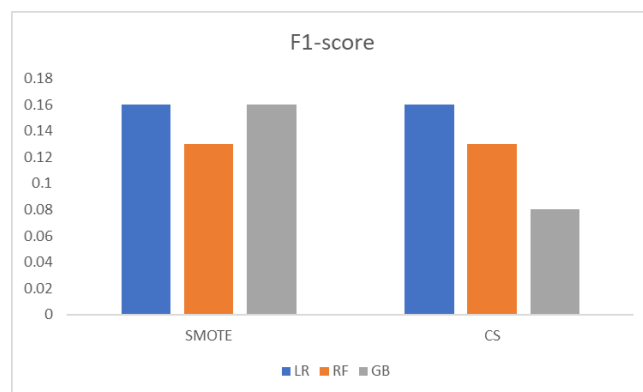


**Figure 6.** F1 result of each classifier on data balancing techniques

Table 4 presents the results in detail of ML algorithms on each data balancing technique. The table shows that training the LR model on the data may produce optimal results in terms of AUC and Recall with the scenario of CS. The number of true positive labels LR predicted is also 32, which is the highest value.

**Table 4.** Classification results with Data Balancing

Algorithm	Data Balancing	AUC	TN	FP	FN	TP	TNR	Precision	Recall	FPR	F1-score
LR	SMOTE	0.52	198	314	17	31	0.39	0.09	0.65	0.61	0.16
RF	SMOTE	0.53	462	50	41	7	0.90	0.33	0.08	0.02	0.13
GB	SMOTE	0.54	424	88	36	12	0.83	0.12	0.25	0.17	0.16
LR	CS	0.52	187	325	16	32	0.37	0.09	0.66	0.63	0.16
RF	CS	0.52	504	8	44	4	0.98	0.12	0.15	0.10	0.13
GB	CS	0.52	509	3	46	2	0.99	0.40	0.04	0.01	0.01

## 5. CONCLUSION

This study investigated the application of ML for fault prediction on real data. Results showed that predictive models using all data balancing techniques outperformed models using unbalanced data. LR combined with cost-sensitive learning was the best model providing optimal performance with the highest AUC. This finding could help decision-makers choose the best model for predicting failures in semiconductor manufacturing and provide tools for cost reduction. For future work, a deeper analysis of ML algorithms [13] [14] (xgBoost or Generative Adversarial Networks...) may be considered in future works, where the optimization of loss function or



maximization of accuracy is discussed. Moreover, dealing with highly imbalanced datasets is a potential topic for further investigation.

### References

- [1] Butte, S. P., et al. (2018). Machine learning based predictive maintenance strategy: a super learning approach with deep neural networks. 2018 IEEE Workshop on Microelectronics and Electron Devices (WMED), pp. 1-5, doi: 10.1109/WMED.2018.8360836.
- [2] Carvalho, T. P., et al. (2019). A systematic literature review of machine learning methods applied to predictive maintenance. *Computers & Industrial Engineering*, vol. 137.
- [3] Gian Antonio Susto. (2012). A Predictive Maintenance System for Epitaxy Processes Based on Filtering and Prediction Techniques. *IEEE Transactions on Semiconductor Manufacturing*, vol. 25, no. 4, pp. 638-649 .
- [4] Haibo He, M. I. (2009). Learning from Imbalanced Data.
- [5] He, Q. P. (2007). Fault detection using the k-nearest neighbor rule for semiconductor manufacturing processes.
- [6] Henriquez, P. A. (2013). Review of automatic fault diagnosis systems using audio and vibration signals.
- [7] Hung, Y.-H. e. (2021). Improved Ensemble-Learning Algorithm for Predictive Maintenance in the Manufacturing Process. *Applied Sciences*.
- [8] Psarommatis, F., May, G., Dreyfus, P.-A., & Kiritsis, D. (2019). Zero defect manufacturing: state-of-the-art review, shortcomings and future directions in research. *International Journal of Production Research*, vol. 58, no. 1, pp. 1-17.
- [9] Salem, M. T. (2018). An experimental evaluation of fault diagnosis from imbalanced and incomplete data for smart semiconductor manufacturing.
- [10] Sivakumar, A. I., & Chong, C. S. (2001). A simulation-based analysis of cycle time distribution, and throughput in semiconductor backend manufacturing.
- [11] Sotiris Kotsiantis, D. K. (2006). Handling imbalanced datasets: A review. *GESTS International Transactions on Computer Science and Engineering*, vol. 30, no. 1, pp. 25-36.
- [12] Weiting Zhang, D. Y. (2018). Data-Driven Methods for Predictive Maintenance of.
- [13] Zhongzhen Yan, H. C. (2022). Research on prediction of multi-class theft crimes by an optimized decomposition and fusion method based on XGBoost.
- [14] Ziqiang Pu, et al. (2023). Sliced Wasserstein cycle consistency generative adversarial networks for fault data augmentation of an industrial robot. *Expert Systems with Applications*, vol. 222.

**[S5-25] Overview in IT-based Power Plants and Electric Users**

Thi-Ngot Pham<sup>1,2</sup>, Jun-Ho Huh<sup>1,3,\*</sup>

<sup>1</sup> *Interdisciplinary Major of Ocean Renewable Energy Engineering, (National) Korea Maritime and Ocean University, Busan, 49112, Republic of Korea*

<sup>2</sup> *Department of Data Informatics of (National) Korea Maritime and Ocean University, Busan, 49112, Republic of Korea*

<sup>3</sup> *Associate Professor (Tenured) of Department of Data Sciences, National Korea Maritime and Ocean University, 49112, Republic of Korea*

\*Corresponding author: 72network@kmou.ac.kr

**Abstract**

Recently, new renewable energy power plants such as Solar Power Plants, Small-Scale Solar Power Plants for residential use (such as solar power plants linked with parking lot monitoring systems; Safety Monitoring Systems for Energy Power Plants), wind power plants, and Small Modular Reactor (SMR) have been established. In addition, new IT services are emerging with the appearance of various devices. These services range from those that focus on the needs of producers (power plants) to those that cater to the needs of users. In this topical collection, we aim to solicit papers on these diverse services. From a user perspective, services such as virtualizing electric energy in conjunction with big data studies, similar to the energy-gauge User Interface (UI) of electric vehicles, have been commercialized. These services aim not only to monitor real-time power usage but also to predict future applications. Meanwhile, the papers for this Topical collection will include some original developments, such as monitoring the power usage of old Plants with digital meters through Multimedia Technology. Therefore, in this proceeding, we will discuss the Overview in IT-based Power Plants and Electric Users and the future.

**Keywords:** *Renewable energy, Small modular reactor, User interface, Multimedia technology*

**[S5-31] Multi-Criteria Decision-Making with Preference Scale**Sanghyuk Lee<sup>1,\*</sup>, Youpeng Yang<sup>2</sup>, Kyeong Soo Kim<sup>3</sup>, Fei Ma<sup>4</sup><sup>1</sup> School of Engineering, New Uzbekistan University, Tashkent, Uzbekistan 100007<sup>2</sup> Department of Mechatronics and Robotics, School of Advanced and Technology, Xi'an Jiaotong-Liverpool University, Suzhou, Jiangsu, China 215123<sup>3</sup> Department of Communications and Networking, School of Advanced and Technology, Xi'an Jiaotong-Liverpool University, Suzhou, Jiangsu, China 215123<sup>4</sup> Department of Statistics and Actuarial Science, School of Science, Xi'an Jiaotong-Liverpool University, Suzhou, Jiangsu, China 215123

\*Corresponding author: sanghyuk@newuzbekistanuniversity.uz

**Abstract**

Multi-criteria recommendation system design needs to be concrete preference definition between criteria. Based on the preference, related utility function should be verified through criteria. Criteria ordering and inside of criterion priority have been investigated by binary relation and rearranged by multiplying permutation matrices. The obtained results extend to the lexicographic ordering on each attribute, and it helps multi-criteria decision-making. In order to realize utility function, fundamental knowledge became its justification. Finally, it provides the preference among criteria, and ordering is also illustrated. Multiplying the permutation matrix on left and right side helps to rearrange criterion with the preference order; it finalizes the lexicographic order on the attributes. By the rearrange criterion, relation with lexicographic ordering is also shown.

**Keywords:** *Intuitionistic Fuzzy Sets, Multi-criteria, Preference, Lexicographic order*

**1. INTRODUCTION**

Researches on multi-criteria decision-making has provided the useful background to constitute recommendation system, pattern recognition and other decision related studies [1]. Being different from the single criterion decision-making problem, it needs to evaluate the preference between criterion and successive total ordering in multi-criteria. Without the priority knowledge on between criteria, it could lead to the disorder representation. First of all, it needs to arrange criteria ordering whether it is based on the preference or any other evaluation [2]. The preference needs to be assigned or defined in advance, and it should be related with the utility function based on the preference [3]. Without criterion preference, multi-criteria decision-making becomes simple averaging or criterion disorder.

In order to get the criteria ordering, utility function should be readied based on the preference with binary relation as mentioned. For the finite  $X$  with preference  $\succeq$ , preference relation guarantees utility function  $u: X \rightarrow R$ [2]. With the explicit utility function, the results lead to the lexicographic order on attributes. Explicit utility function structure is also challenge. With simple way, preference  $\succeq$  is useful to consider it as utility function. For the finite consumption, it is rather easy to find a utility function for any given preferences.

In this paper, binary relation and its rearrangement has been carried out. First, criterion rearrangement is done by studying preference and utility function over the criterion for multi-criteria problem. Preference can be decided by objective and subjective viewpoints. Binary relation – preference – applies utility function which set the order of criterion. Next, order insider each criterion should be followed to arrange order with lexicographically. It helps to arrange the attribute order with sequentially. In order to set each attribute priority in criterion, similarity measure is considered. Assume the criterion value includes like, dislike and hesitation, similarity measure, the proposed similarity measure is calculated the closedness between attribute and criterion. Here, intuitionistic fuzzy sets (IFSs) analysis including similarity measure on IFSs is needed in advance. General fuzzy sets (FSs) similarity measure has been studied in before by numerous researchers [4-7]. We provide the similarity in this research with simple structure using distance measure. After similarity measure on IFSs design, attribute order inside each criterion constitutes the lexicographic order together with criterion preference. The total order doe each attribute help to multi-criteria decision-making because attribute order is expressed via lexicographic order. Furthermore, we arrange criteria and attribute by multiplying permutation matrix on left and right side.

The paper is composed as follows. In the next section, fundamental knowledge on the preference and utility functions are introduced to justify the well ordering on each criterion and attribute. In section 3, similarity measure for each attribute to calculate the properness to the specific criterion is derived. In this regards, each criterion properness needs to be set as FSs or IFSs structure. Similarity measure on the fuzzy sets (FSs) and IFSs are introduced in the same section. In section 4, ordering is carried by multiplying the permutation matrix to arrange criterion. Derivation and illustrative example are also explained in section 4. Finally, conclusions are presented in section 5.

## 2. PRELIMINARIES

Organizing lexicographical order on the multi-criteria decision problem, knowledge on criterion preference and well ordering in each criterion is necessary. First utility function related with preference is introduced, and brief surveying on the well-ordered set is also illustrated.

### 2.1. Preference and utility function

With the existing research on the preference  $\succeq$ , utility function between two items represent;

$$x \succeq y \rightarrow u(x) \geq u(y)$$

Preference can provide the lexicographic ordering justification; however, it heavily depends on the subjective viewpoints [2]. For the criteria ordering, it is inevitable to assign preference between criteria as much as close to the objectively. As mentioned in the existing research [3], preference has the following properties;

- If  $X$  is finite/continuous and  $\succeq$  is a preference then there exists  $u: X \rightarrow R$  that represent  $\succeq$ .

The proof is illustrated in the existing research [2]. In the assumption, finite  $X$  indicate the limited number of criteria, and it can be discrete and extended to continuous further.

Simply, utility function can be considered as its cardinality such as;

$$u(x) = |\succeq(x)|$$

where  $\succeq(x) = \{y \in X, y \succeq x\}$ , and  $|\cdot|$  indicate the cardinal number.

In multi-criteria problem, it can be assumed that the number of criteria is finite and the reference is also defined together with utility function.

### 2.2. Binary relation

Brief description on binary relation  $R$  is summarized with the existing knowledge, and it is noted that the rational binary relation is called as a preference [2]. And the Rationality is satisfied if the binary relation satisfies completeness and transitivity together.

- $R$  is complete on  $X$  if  $xRy$  or  $yRx$  are satisfied  $\forall x, y \in X$ , and the transitivity is denoted for all  $x, y, z \in X$ , if  $xRy$  and  $yRx$ , then  $xRz$ .

- $R$  is antisymmetric is  $xRy$  and  $yRx$  then  $x = y$ .

- Linear relation is defined as the following;

- Relation is rational if  $R$  is complete and transitive; sometimes it called preference. And linear relation if  $R$  is rational and antisymmetric.

The finite ordinals, which are identified with the nonnegative integers, are defined recursively: begin with the empty set (identified with 0), set  $n$  to equal  $\{0, 1, \dots, n-1\}$ , and let  $\in$  supply the ordering. An infinite ordinal  $S$  also equals the set of all ordinals less than  $S$ , for example, the set of all finite ordinals which is denoted by  $\omega$ . The well-ordering theorem states that for any set  $X$  there is a binary relation  $\leq$  on  $X$  such that  $(X, \leq)$  is well-ordered.

The mentioned binary relation can be applied to the criteria preference and the attribute belongingness in the specific criterion. The well-ordered binary relation guarantees the lexicographic ordering. Hence, it is the fundamental knowledge to solve the multi-criteria decision making. In the next chapter, we provide the similarity measure design with the attribute belongingness; that is expressed with FSs and IFSs.

## 3. SIMILARITY MEASURE FOR THE PREFERENCE

Similarity measure with respect to the referred criterion provides the closedness to the criterion preference. In this section, we provide the similarity measure on the IFSs which are considered as the attribute value for each criterion.

### 3.1. Intuitionistic fuzzy sets

As the extension of fuzzy sets (FSs), IFSs include hesitation of information and data uncertainty. From the definition, it is noticed that the information is categorized more detail [8-10]. Together with membership degree  $\mu_I(x)$ , non-membership degree  $\nu_I(x)$  is expressed in the following definition, respectively.

**Definition 3.1** [8,9]. IFSs  $I$  for the universe of discourse  $X = \{x_1, x_2, \dots, x_n\}$  is defined as follows:

$$V = \{(x, \mu_I(x), \nu_I(x)) | x \in X, \mu_I(x) \in [0,1], \nu_I(x) \in [0,1], 0 \leq \mu_I(x) + \nu_I(x) \leq 1\}$$

where,  $\mu_I(x)$  and  $\nu_I(x)$  denote a membership function and non-membership function of  $x$  in  $I$ , respectively.

From the Definition 3.1, it is clear that membership degree of IFS  $V$  should be restricted in  $(\mu_I(x), \nu_I(x))$ . Degree of uncertainty can be defined by  $1 - \mu_I(x) - \nu_I(x) = \pi_I(x)$ . Furthermore, if  $\mu_I(x) + \nu_I(x) = 1$ , then IFSs  $V$  is considered as a standard fuzzy set. To evaluate the uncertainty or entropy on IFSs, hesitance information, membership and non-membership degree have to be considered. By considering hesitance, fuzzy set property is defined.

**Definition 3.2** For IFSs  $V$  in the universe of discourse, if  $\mu_I(x) + \nu_I(x) = 1$  and  $\mu_I(x) + \nu_I(x) = 0$ , then  $I$  is considered as a FS and null set, respectively.

All degree points represent the all values of  $0 \leq \mu(x) \leq 1$  and  $0 \leq \nu(x) \leq 1$ . And all points are defined as FSs, IFSs and PFSs by their definition. We illustrated the relation of membership and non-membership value with figure in later. In the reference, null set was modeled by having no any other information about data themselves. It represents the coordination of  $\mu_I(x) - \nu_I(x)$  plane. Even the hesitance is illustrated by the area under the fuzzy line. Inside of the area, it is clear to obtain the relation of  $\mu_I(x) + \nu_I(x) + \text{hesitancy} = 1$ . By the graphical representation, it is clear that hesitance satisfies one as  $\mu_I(x) + \nu_I(x) \rightarrow 0$ , that is, *hesitancy* approaches to origin. From Fig. 1, sets on the fuzzy line means that it has no hesitance. Under the fuzzy line, relations between membership degree and non-membership degree are defined by  $0 \leq \mu_I(x) + \nu_I(x) \leq 1$ .

### 3.2. Similarity measure

Many researches on similarity measure have been carried out by the numerous researchers; it was designed based on distance measure and fuzzy number [4-7]. Similarity measure represents the similar degree between different information and data, and many similarity measure design has been proposed based on the definition [5, 6].

**Definition 3.3** [11] A real function  $s: F^2 \rightarrow R^+$  is called a similarity measure, if  $s$  has the following properties:

(S1)  $s(A, B) = s(B, A)$ ,  $A, B \in F(X)$

(S2)  $s(D, D^c) = 0$ ,  $D \in P(X)$

(S3)  $s(C, C) = \max_{A, B \in F} s(A, B)$ ,  $C \in F(X)$

(S4)  $A, B, C \in F(X)$ , if  $A \subset B \subset C$ , then  $s(A, B) \geq s(A, C)$  and  $s(B, C) \geq s(A, C)$ .

where  $R^+ = [0, \infty)$ ,  $X$  is the universal set,  $F(X)$  is the class of all fuzzy sets of  $X$ ,  $P(X)$  is the class of all crisp sets of  $X$ , and  $D^c$  is the complement of  $D$ .

The proposed similarity measure needs to be satisfied the Definition 3.3, and numerous similarity measures could be derived.

#### 3.2.1. Similarity measure design on FSs with distance measure

In this subsection, the similarity measure for FSs is introduced with the distance measure. In order to illustrate with explicitly, distance measure is needed and the definition is introduced by Liu [11].

One of distance measure, *Hamming distance* is commonly used as distance measure between fuzzy sets  $A$  and  $B$  in the following equation:

$$d(A, B) = \frac{1}{n} \sum_{i=1}^n |\mu_A(x_i) - \mu_B(x_i)|$$

where  $X = \{x_1, x_2, \dots, x_n\}$ ,  $|k|$  was the absolute value of  $k$ .  $\mu_A(x)$  is the membership function of  $A \in F(X)$ .

With the Definition 3.3 similarity measure is proposed. It can be represented as explicit structure, and the proposed similarity measures were illustrated in previous research [4, 5].

**Theorem 3.1** [4]. For any set  $A, B \in F(X)$ , if  $d$  satisfies Hamming distance measure, then

$$s(A, B) = d((A \cap B), [0]_X) + d((A \cup B), [1]_X) \tag{1}$$

is the similarity measure between set  $A$  and  $B$ .

Numerous other similarity measures are also possible to design. Other similarity measure shows the relevant structures satisfying Definition 3.3, and its proof is also found in previous result [4,5].

Similarity measures (1) is illustrated by the combination of common and uncommon information between two fuzzy sets  $A$  and set  $B$ . The results on similarity measures are derived with the distance measure which are based computation of the degree of similarity. Liu has also proposed an axiomatic definition of the similarity measure for  $\forall A, B \in F(X)$  and  $\forall D$  in crisp set [11].

### 3.2.2. Similarity measure on IFSs

There is some research on the analysis of IFSs entropy has been considered [12, 13]. They allow us to measure the degree of hesitation for the IFSs, and non-probabilistic type entropy measure with a geometric interpretation of IFSs. It was proposed an axiomatic definition of IFSs, which was considered by taking into account fuzzy set consideration.

**Definition 3.4** [12] A real function  $I: IFS(X) \rightarrow R^+$  is called an entropy on IFS(X) if  $I$  has the following properties:

- (IP1)  $I(A) = 0$ , if and only if  $A$  is a fuzzy set,
- (IP2)  $I(A) = Cardinal(X) = N$  if and only if  $\mu_A(x) = \nu_A(x) = 0$  for all  $x \in X$ ,
- (IP3)  $I(A) = I(A^c)$  for  $A \in IFSs(X)$ ,
- (IP4) If  $A < B$ , then  $I(A) \geq I(B)$ .

Where  $A < B$  denotes that  $\mu_A(x) \leq \mu_B(x)$  and  $\nu_A(x) \leq \nu_B(x)$  for all  $x \in X$ , which means that IFS  $B$  has less hesitancy than IFS  $A$ .  $\mu_A(x)$ ,  $\nu_A(x)$ , and  $\pi_A(x)$  are the degree of membership, non-membership, and hesitation of  $x$  in  $A$ , that is expressed by  $\pi_A(x) = 1 - \mu_A(x) - \nu_A(x)$ .

**Theorem 3.2** [14] Following equation satisfies a similarity measure on IFS(X).

$$S_L(A, B) = 1 - D_L(A, B)$$

Where  $D_L(A, B)$  is expressed by the hesitancy distance between two IFSs, that is,

$$D_L(A, B) = \frac{1}{N} \sum_{i=1}^N d(\pi_A(x_i), \pi_B(x_i)).$$

Then, similarity measure has the following explicit formulation [34].

$$S_L(A, B) = 1 - \frac{1}{N} \sum_{i=1}^N d(\pi_A(x_i), \pi_B(x_i)) \tag{2}$$

Proof is delivered in [14]. The theorem derived by the consideration of hesitation distance.

## 4. LEXICOGRAPHIC ORDERING AND EXAMPLE

After completing each criterion belonging for attributes, criterion ordering will be carried out through with preference. Preference ordering is followed by multiplying relevant matrix. Afterward, attributes order will be followed by left multiplying again.

By organizing the matrix form on each attribute and criterion;

$$B = \begin{bmatrix} b_{11} & \dots & b_{1M} \\ \vdots & \ddots & \vdots \\ b_{N1} & \dots & b_{NM} \end{bmatrix} = [c_1 \quad \dots \quad c_M]$$

where  $b_{ij}$  is the belongingness of attribute  $i$  for the criterion  $j$ . And  $i = 1, 2, \dots, N$  and  $j = 1, 2, \dots, M$ ,  $N$  and  $M$  denote the number of attributes and criteria.

For example, preference is assigned as  $c_k > c_l > c_p > \dots > c_1$ , arbitrary criterion  $k, l, p = 1, 2, \dots, M$ , then we can rearrange preference order by right multiplying matrix  $P$ ;

$$P = [p_k \quad p_l \quad \dots \quad p_1]$$

$P = M \times M$  matrix,  $p_k = [0 \dots 1 \dots 0]^T$ ,  $p_l = [0 \dots 1 \dots 0]^T$  and  $p_1 = [1 \quad 0 \dots 0]^T$ , where one in each column vector  $p_k$ ,  $p_l$  and  $p_1$  correspond  $k$ -th,  $l$ -th and first element in each column vector. By multiplication, we can get the following.

$$BP = [c_k \quad c_l \quad \dots \quad c_1]$$

Next, attribute ordering is needed by left multiplying matrix successively. Matrix multiplication rearrange the highest belonging inside of criterion with lexicographic order. Matrix  $A_1, A_2, \dots$ , and  $A_N$  indicate the attribute ordering with descending row vectors for the defined preference order of criterion. It is cleared by introducing matrix components; the first matrix  $A_1$  constitutes row vectors  $a_i, i = 1, 2, \dots, N$ .  $a_i = [0 \dots 1 \dots 0]$ , one in  $a_i$  indicates  $i - th$  element from  $N$  attributes; it is also the highest value from the most preference criterion.  $A_2$  also constitutes with row vectors with  $a_j = [0 \dots 1 \dots 0]$ , one in  $a_j$  indicates  $j - th$  element from  $N$  attributes; it is the highest value from the next preference criterion.  $A_3$  to the  $A_N$  organized as accordingly.

$$A_1 = \begin{bmatrix} a_k \\ a_l \\ \dots \\ a_1 \end{bmatrix}$$

$A_1 = N \times N$  matrix,  $a_k = [0 \dots 1 \dots 0]$ ,  $a_1 = [1 \ 0 \dots 0]$ , where one in each vector  $a_k$ , and  $a_1$  correspond  $k - th$ , and the first element in each row vector.

By completing the matrix multiplication,  $A_1 A_2 \dots A_N BP$ , we can get the lexicographic order with the following structure; criterion preference and attributes are assumed after matrix multiplication.

**Table 1.** Belonging matrix for attribute with multi criteria (Criterion preference  $c_2 - c_1 - c_3$ )

	$c_1(0.4, 0.2)$	$c_2(0.5, 0.2)$	$c_3(0.6, 0.2)$
$a_1$	(1.0, 0.0)	(0.8, 0.0)	(0.7, 0.1)
$a_2$	(0.8, 0.1)	(1.0, 0.0)	(0.9, 0.1)
$a_3$	(0.6, 0.2)	(0.8, 0.0)	(1.0, 0.0)

With the simple IFSs similarity measure

$$s(a_i, c_j) = 1 - \frac{1}{n} \sum_{i=1}^n |\mu_a(x_i) - \mu_c(x_i)|, \forall x_i \in X \tag{3}$$

Following calculation is obtained.

**Table 2.** Similarity measure calculation with (3)

	$c_1$	$c_2$	$c_3$
$a_1$	0.6	0.3	0.1
$a_2$	0.4	0.5	0.3
$a_3$	0.2	0.3	0.4

**Table 3.** After multiplying permutation matrix (attribute rearrange  $a_2 - a_1 - a_3$ )

	$c_2$	$c_1$	$c_3$
$a_2$	0.5	0.4	0.3
$a_1$	0.3	0.6	0.1
$a_3$	0.3	0.2	0.4

From the Table 3, as  $a_2 > a_1 > a_3$  is obtained. The result says that the most preference attribute is  $a_2$  from all attributes.

### 5. CONCLUSION

Multi-criteria decision-making problem has been resolved with the preference and lexicographical order. To make order on the attribute in the multi-criteria decision-making, utility function with reference is needed. It could be surjective or objective. After setting criteria, it needs to formulate the order inside of each criterion. For the fitness to the criterion, similarity measure is proposed. Criterion can be described with FSs or IFSs to express the like or dislike together. In the paper, we suggest simple similarity measure without proof. Finally, multiplying permutation matrix makes the belongingness matrix with order. In the illustrative example, lexicographic order is shown with the procedure mentioned.

### Acknowledgments

I am grateful to the faculty and staff of the Software Engineering department at New Uzbekistan University, Tashkent, for their guidance and support throughout this project.

### References

- [1] Yager, R. R., Pythagorean membership grades in multicriteria decision making, *IEEE Transactions on Fuzzy Systems* vol. 22, no. 4, pp. 958–965, 2014.
- [2] M. Mandler, The lexicographical method in preference theory, *Economic Theory*, 71, pp. 553–577, 2021
- [3] J. Chipman, The foundations of utility, *Econometrica*, 28, pp. 193–224, 1960.
- [4] N.R. Pal and S.K. Pal, Object-background segmentation using new definitions of entropy, *IEEE Proc.*, Vol. 36, 284–295, 1989.
- [5] S.H. Lee, Y.T. Kim, S.P. Cheon, and S.S. Kim, Reliable data selection with fuzzy entropy, *LNAI*, Vol. 3613, pp. 203–212, 2005.
- [6] S.H Lee, W. Pedrycz, and Gyoyong Sohn. Design of Similarity and Dissimilarity Measures for Fuzzy Sets on the Basis of Distance Measure, *International Journal of Fuzzy Systems*, 2009, 11: 67-72.
- [7] Y. Rébillé, Decision making over necessity measures through the Choquet integral criterion, *Fuzzy Sets and Systems*, Vol. 157, no. 23, pp. 3025–3039, 2006.
- [8] K. T. Atanassov, Intuitionistic fuzzy sets, *Fuzzy Sets Syst.*, vol. 20, pp. 87–96, 1986.
- [9] K. T. Atanassov and G. Gargov, Interval valued intuitionistic fuzzy sets, *Fuzzy Sets Syst.*, vol. 31, pp. 343–349, 1989.
- [10] K. T. Atanassov, *On Intuitionistic Fuzzy Sets Theory*. Heidelberg, Germany: Springer, 2012.
- [11] Liu, X., Entropy, distance measure and similarity measure of fuzzy sets and their relations, *Fuzzy sets and systems*, vol. 52, no. 3, pp. 305–318, 1992.
- [12] Li, D. and Cheng, C., New similarity measures of intuitionistic fuzzy sets and application to pattern recognitions, *Pattern Recognition Letters*, vol. 23, pp. 221–225, 2002
- [13] Li, Y., Olson, D. L. and Zheng, Q., Similarity measures between intuitionistic fuzzy (vague) sets: A comparative analysis, *Pattern Recognition Letters*, 28, no. 2, pp. 278–285, 2007.
- [14] Jean-Ho Park, Jai-Hyuk Hwang, Wook-Je Park, He Wei, Sang-Hyuk Lee, Similarity measure on intuitionistic fuzzy sets, *Journal of Central South University of Technology*. 20, pp. 2233-2238, 2013.



**[S5-51] Deep Learning Model Combined with CNN and LSTM used for Fault Diagnosis of Sensors in the Monitoring of Anaerobic Digestion**Hyein Jung<sup>1,2</sup>, YoungChae Song<sup>1,2</sup>, Junghui Woo<sup>3</sup>, Keugtae Kim<sup>4</sup>, Seong-Wook Oa<sup>5</sup><sup>1</sup>*Department of Civil and Environmental Engineering, Korea Maritime and Ocean University*<sup>2</sup>*Interdisciplinary Major of Ocean Renewable Energy Engineering, Korea Maritime and Ocean University*<sup>3</sup>*Nuclear Power Equipment Research Center, Korea Maritime and Ocean University*<sup>4</sup>*Division of Construction, Environmental and Energy, The University of Suwon*<sup>5</sup>*School of Railroad Civil System Engineering, Woosong University*

\*Corresponding author: soyc@kmou.ac.kr

**Abstract**

In anaerobic digestion, organic matter undergoes a series of biochemical reaction steps to produce methane while stabilizing: hydrolysis, acid production, acetic acid production, and methanogenesis. Anaerobic microorganisms, such as acidogenic bacteria and methanogenic archaea, involved in the biochemical reaction steps have unique physiological characteristics. So, the response of each step to operational conditions in anaerobic digesters or environmental changes can vary. In the anaerobic digestion of organic waste, where its composition and quantity frequently change, imbalances can occur in the rates of the biochemical reaction steps. If the imbalances are not addressed promptly, the stability of the anaerobic process gradually deteriorates, ultimately leading to process failure. However, by continuously monitoring the process state, the imbalances can be detected early and mitigated with simple measures before they become severe. Physicochemical data, such as pH, alkalinity, COD, SCOD, VFA, MPR, and CH<sub>4</sub> (%), serve as the state variables for diagnosing imbalances in the biochemical reaction steps. These variables can be predicted using soft sensors that utilize real-time data from electrochemical sensors. However, electrochemical sensors often fail in the harsh environment of anaerobic digesters. It indicates that ensuring the normal functioning of electrochemical sensors in real time is crucial for effective process monitoring. In this study, we collected extended periods of output data from electrochemical sensors such as pH, EC, and ORP, which are used to infer the state variables of anaerobic digesters. We developed a combined deep-learning model consisting of a CNN and LSTM to diagnose the functioning of these sensors. The raw sensor data was normalized using the StandardScaler function from the Sci-kit learn package in Python. The issue of imbalanced data resulting from a lack of failure data was addressed by augmenting drift values that may occur due to sensor failures in the collected output data. The sensor output data 2108 were prepared and labeled as normal, pH failure, EC failure, and ORP failure (each 527 data points). One-hot encoding was performed using the get\_dummies function from the Pandas package in Python. These prepared data were divided into training (49%), validation (21%), and test sets (30%) using the train\_test\_split function from the Sci-kit learn package. Using the Keras module in the Tensorflow package, a deep sequential classification model was constructed by stacking a CNN layer and an LSTM layer for feature extraction from the sensor data, and an FC layer was added as an output layer. The activation function used for the CNN and LSTM layers was ReLU, while softmax was used for the output FC layer. RMSprop was employed as the optimizer with a learning rate of 0.001. After training, the model achieved an accuracy of 99.56% in diagnosing normal and faulty conditions when evaluated on the test data. The f1-score, representing the harmonic mean of precision and recall, was approximately 0.99. The combined CNN and LSTM model proved a powerful tool based on a deep-learning for fault diagnosis of pH, EC, and ORP sensors.

**Keywords:** *Deep learning, Anaerobic digestion, Sensor fault detection*

**Acknowledgments**

This work was supported by Korea Environment Industry & Technology Institute (KEITI) through R&D demonstration project of non-CO<sub>2</sub> mitigation technology Program, funded by Korea Ministry of Environment. (MOE) (202200330002) and the National Research Foundation of Korea (NRF) grant funded by the Korea government (MIST) (NRF- 2022R1A2C1009440).

**[S5-57] Building a New Machine Learning Model to Detect the Insurance Fraud**Ai Vu<sup>1</sup>, Anh Tran<sup>2,3</sup>, Duy Thanh Tran<sup>2,3,\*</sup><sup>1</sup> HCM City University of Foreign Languages - Information Technology, Ho Chi Minh City, Viet Nam, 700000<sup>2</sup> University of Economics and Law, Ho Chi Minh City, Viet Nam, 700000<sup>3</sup> Viet Nam National University, Ho Chi Minh City, Viet Nam, 700000

\*Corresponding author: thanhtd@uel.edu.vn

**Abstract**

In today's modern world, everyone is trying to protect what they own in one way or another. The Covid-19 pandemic has posed challenges to many countries in the early stages of the vaccine revolution, as each country strives to protect its people. Many individuals rushed to get vaccinated as a means of insuring themselves. This is the fundamental concept behind insurance businesses. People are willing to pay money as a safeguard against unforeseen losses they may face. In the United States alone, the insurance industry is valued at \$1.28 trillion, while the US consumer market loses at least \$80 billion to insurance fraud every year. Alongside the success and profitability that the insurance industry brings, insurance companies are also confronted with money laundering and fraud, which are significant concerns. One prevalent fraud topic in this context is insurance fraud, as it causes harm to both insurance companies and the healthcare system of the nation.

Applying data analytics and machine learning is one of the effective methods used to detect fraud-related issues. This paper aims to propose the most accurate and simplest solution based on machine learning to detect fraudulent insurance claims. The primary challenge in detecting fraudulent activities lies in the massive number of claims that pass through the companies' systems. However, this challenge can also be turned into an advantage if officials recognize that they possess a substantial database by combining the claims data. This database can be utilized to develop improved models for flagging suspicious claims.

This paper will explore various methods that have been used to address similar problems, aiming to test the best methods that have been previously employed. It will search and study these methods, aiming to enhance and construct a predictive model capable of flagging suspicious claims. The research will involve testing different models and comparing their performance to develop a simple, time-efficient, and accurate model that can identify suspicious claims without burdening the system it operates on.

The main purpose of this paper is to create a model used to determine whether a specific insurance claim is fraudulent or not. The model will be designed after testing multiple algorithms to find the best model that can accurately detect suspicious claims. This aims to propose a more customized model for insurance companies that aligns with their systems. The algorithms mentioned in this paper, including RandomForestClassifier, LogisticRegression, KNeighborsClassifier, and XGBClassifier, are used to conduct detection based on a dataset published by Kaggle, and the accuracy of the algorithms is evaluated. The experimental results show that the Random Forest Classifier algorithm achieves the highest accuracy in detecting fraud. This forms the basis for the proposed development of an application that supports the detection and flagging of suspicious fraudulent claims, helping insurance companies save money and time, and improving their efficiency in responding to such claims.

**Keywords:** *Data visualization, Data analysis, Fraudulent detection, Machine learning, Supervised learning*

**Acknowledgments**

We would like to extend our sincere appreciation and gratitude to Professor Jun-Ho Huh and Dr. Thanh Tran for his invaluable support and guidance throughout the completion of this study. His unwavering commitment and assistance have been instrumental in the successful execution of our research project.

**References**

- [1] Aisha Abdallah, M. A, "Fraud detection system: A survey.", *Journal of Network and Computer Applications*, (2016), pp. 90-113
- [2] Alejandro Correa Bahnsen, D.A, "Feature engineering strategies for credit card fraud detection", *Expert Systems with Applications*, (2016), pp. 134-142.

- [3] Bart Baesens, S. H, “Data engineering for fraud detection”, Decision Support Systems (2021)
- [4] Eunji Kim, J. L.-k.-a.-i, “Champion-challenger analysis for credit card fraud detection: Hybrid”, Expert Systems with Applications, (2019), pp. 214-224.
- [5] Fabrizio Carcillo, Y.-A. L. “Combining unsupervised and supervised learning in credit card fraud detection”, Information Sciences, (2021), pp. 317-331.
- [6] Jarrod West, M. B, “Intelligent financial fraud detection: A comprehensive review”, ScienceDirect, (2016), pp. 47-66.
- [7] Javad Forough, S. M, “Ensemble of deep sequential models for credit card fraud detection”, Applied Soft Computing Journal, (2021).
- [8] X. Liu, J. W, “Exploratory undersampling for class-imbalance learning”, Systems, Man, and Cybernetics, Part B: Cybernetics, (39) (2009), pp. 539-550.
- [9] Callahan, Alison, and Nigam H. Shah, "Machine learning in healthcare.", Key Advances in Clinical Informatics. Academic Press, (2017), pp. 279-291.

**[S5-68] Experiment and Numerical Simulation of Microchannel Pulsating Heat Pipes**

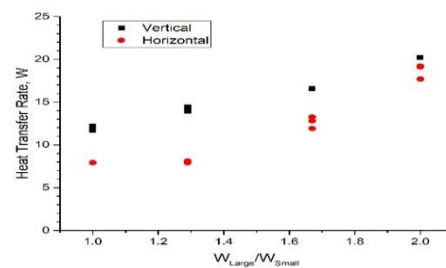
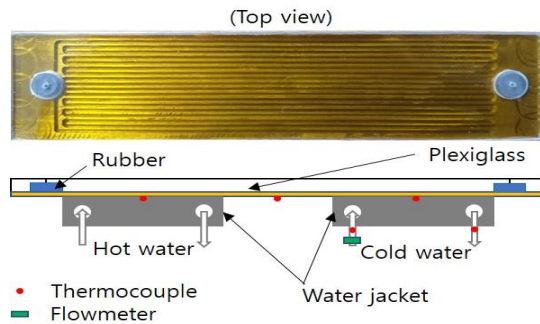
Hye-Seong Hwang, Duy-Tan Vo, Kwang-Hyun Bang\*

*Korea Maritime and Ocean University, Busan, South Korea*

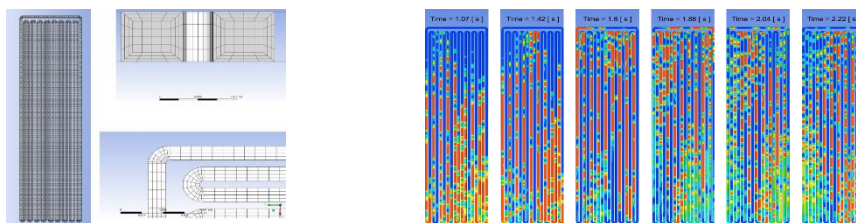
\*Corresponding author: khsang@kmou.ac.kr

**Abstract**

The thermal performance of micro pulsating heat pipes (MPHP) has been investigated experimentally. The MPHP was engraved on a 1 mm thick copper plate of 25x100 mm. The upper cover was made with Plexiglas plate so that the flow motions were visualized with a high-speed video camera. The working fluid was FC-72, degassed. The experimental condition was a temperature-boundary, i.e., the heating part was maintained at 75°C and the cooling part at 23°C in general using water jackets and constant temperature circulation baths. The experimental parameters were channel size (0.8x0.8 mm, 0.6x0.6 mm), number of turns (5,7,9), and dual patterns of channel size (1.0-0.5 mm) primarily for investigating optimum design for horizontal installation of heat pipe. In single channel-size, the better thermal performance was found in the 0.8x0.8 mm than 0.6x0.6 mm, but it failed to operate when laid horizontally. A dual channel-size MPHP was found to work in horizontal installation and the heat transfer rate was comparably good to that of vertical installation. The optimum value of the ratio of the larger channel size to the smaller channel size was found to be 2.0 in the present experimental conditions.



A three-dimensional numerical simulation of closed-type pulsating heat pipes (PHPs) has been carried out using Ansys Fluent. The Volume of Fluid (VOF) was chosen for two-phase flow model and the continuum surface force model was added to the momentum equation. The implementation of variable density and vapor pressure relations for the working fluid was crucial for successful simulation. For simulations, the pulsating heat pipes were composed of microchannels engraved on a 1 mm thick copper plate. The channel width was between 0.5 and 1.0 mm of uniform or dual size and the number of turns were 7 or 9. The working fluid was degassed FC-72. The comparison of the calculated heat transfer rate to experimental data were reasonable for vertical installation of PHP. However, pulsating quickly stopped for horizontal installation. For dual-size channel PHPs, which works for horizontal orientation, implementation of capillary pressure difference on the model is under development.



**Keywords:** Pulsating heat pipe, Heat dissipation, Evaporation and condensation, Fluent

## [S6-9] Application of GATS, a Hybrid Mega Heuristic Model, to Solve Flow Shop Scheduling Problems with Changeover Times in Operations. A Case Study

Nguyen Nhu Phong\*, Nguyen Thi Kim Ngan

*HCMC University of Technology, Viet Nam*

\*Corresponding author: nnphong@hcmut.edu.vn

### Abstract

Flow Shop Scheduling (FSS) Problems are NP-hard combinatorial optimization problems. It is quite difficult to achieve an optimal solution for real size problems with mathematical modelling approaches because of its NP-hard structure. Mega-heuristics algorithms, like Genetic Algorithm (GA) and Tabu Search (TS) play a major role in searching for near-optimal solutions for NP-hard optimization problems. This paper develops the GATS model by combining GA and TS for solving FSS problems. In the model, GA is used as the platform for global search, and TS is used to support GA in local search. The performance of the model is compared with traditional heuristics, being used. The result indicates that the model is a good approach for FSS problems.

*Keywords:* Flow shop scheduling problems, Changeover times, Genetic algorithm, Tabu search

### 1. INTRODUCTION

Scheduling is the allocation of resources to perform a collection of tasks over a period of time. Scheduling problems determine the order or sequence for processing a set of jobs through several machines in an optimal manner. FSS problems consider  $m$  different machines and  $n$  jobs; each job consists of  $m$  operations and each operation requires a different machine and all the jobs are processed in the same processing order. For FSS problems, Chen et al, applied GA to FSS problems with make-span as the criterion. The convergence speed of simple GAs is relatively slow (Gen and Cheng 2000). For improving the convergence speed to the global optimum is the use of local search in GAs (Krasnogor and Smith 2000). Within the hybrid approach, GAs are used to perform global exploration among populations, while heuristic methods are used to perform local exploitation around chromosomes. Because of the complementary properties of GAs and conventional heuristics, the hybrid approach often outperforms either method operating alone (Gao, Gen, and Sun, 2006).

The problem to be solved is a FSS problem with assumption that the orders are ready at the start of the scheduling process. The objective of the problem is to minimize the total weighted tardiness of orders. The constraints are on the sequence of orders, on the sequence of operations in the orders, and on machine changeover time. The model of the problem is built based on the above assumptions, objective and constraints. The GATS is built based on the combination of GA and TS with the foundation of GA. Based on the model of the problem, the GATS will find a good solution for the problem, this solution will be compared with the solution of the currently used heuristic model to evaluate the effectiveness of the algorithm.

### 2. LITERATURE REVIEW

#### 2.1. Genetic algorithm

Genetic algorithm (GA), first introduced by Holland in 1975, is an artificial intelligence search method that uses the process of evolution and natural selection of individuals called chromosomes. In order to apply GA to a problem, generally the solution space of the problem is represented by a population of chromosomes where each chromosome is a possible solution to the problem. A method of coding is the selection of a string format for the chromosomes. A fitness value is associated with each chromosome. The fitness function is a measure of the extent to which the objective of the problem is achieved. A certain number of chromosomes are chosen to form the initial generation. The chromosomes of the next generation are generated by applying genetic operators, including selection, crossover, mutation and replacement, to the chromosomes of the existing generation.

Starting from an initial population, the algorithm produces a new population of individuals, which are presumably more fit than their ancestors. The process is repeated until a pre-specified termination rule becomes true. At each generation, every new chromosome corresponds to a solution.

## 2.2. Tabu search

Tabu search (TS) was suggested by Glover and Laguna in 1997. In order to apply TS to a problem, generally the solution space of the problem is represented by a population of codes. An evaluation value is associated with each code. The evaluation function is a measure of the extent to which the objective of the problem is achieved. The Fbest value is the best evaluation value, found during the search. TS guides a local search procedure to explore the solution space beyond local optimality. In order to avoid cycling and becoming trapped in local optima, certain moves that lead to previously explored regions are forbidden. Attributes of recently visited solutions are set to be tabu for a certain number of iterations, and these moves are stored in the *tabu list*.

A typical TS implementation starts from an initial solution and moves from the current solution to the best one among its neighbourhoods at each iteration, even if this new solution is worse than the one available, until a pre-specified termination rule becomes true.

## 3. THE FLOW SHOP SCHEDULING PROBLEM

The problem to be solved is a FSS problem with 10 orders,  $O_i$ ,  $i=1\div 10$ , scheduling on 4 machines,  $M_1$ ,  $M_2$ ,  $M_3$ ,  $M_4$ . Each order has 3 parts, P1, P2, P3, processed in 8 operations,  $O_j$ ,  $j=1\div 8$ , distributed on the 4 machines.

	M1	M2	M3	M4
P1	O1	O4	-	O8
P2	O2	O5	O7	
P3	O3	O6	-	

The weight  $W_i$ ,  $i=1\div 10$ , and the due date  $D_i$ ,  $i=1\div 10$ , of order  $i$  are estimated in Table 1. The processing time  $P_{ij}$  of order  $i$ ,  $i=1\div 10$ , on operation  $j$ ,  $j=1\div 8$ , are estimated in Table 2.

**Table 1.** The weight  $W_i$ ,  $i=1\div 10$ , and the due date  $D_i$ ,  $i=1\div 10$ , of order  $i$

<b>i</b>	1	2	3	4	5	6	7	8	9	10
<b>W<sub>i</sub></b>	3.70	3.40	3.30	4.65	3.90	2.35	2.70	4.55	4.65	4.30
<b>D<sub>i</sub> (h)</b>	24	36	40	60	68	80	88	88	96	96

**Table 2.** The processing time  $P_{ij}$  of order  $i$ ,  $i=1\div 10$ , on operation  $j$

<b>j</b>	<b>P<sub>1j</sub></b>	<b>P<sub>2j</sub></b>	<b>P<sub>3j</sub></b>	<b>P<sub>4j</sub></b>	<b>P<sub>5j</sub></b>	<b>P<sub>6j</sub></b>	<b>P<sub>7j</sub></b>	<b>P<sub>8j</sub></b>	<b>P<sub>9j</sub></b>	<b>P<sub>10j</sub></b>
1	2.34	6.17	6.20	7.09	2.47	9.56	3.44	14.74	5.26	1.39
2	2.25	0.94	7.05	3.22	1.07	5.26	1.81	7.49	5.26	0.66
3	0.00	3.99	4.34	4.38	2.60	9.52	0.00	16.75	14.74	0.44
4	2.63	1.33	1.08	9.00	2.60	12.56	1.32	17.54	16.52	1.29
5	1.06	1.00	6.58	9.00	4.21	12.64	0.65	17.54	16.52	1.29
6	0.00	8.33	6.58	3.60	3.95	12.64	0.00	13.33	15.79	0.40
7	2.67	3.29	1.13	2.21	0.68	4.00	1.11	5.26	1.60	0.44
8	4.08	3.31	3.42	12.00	3.95	6.12	2.21	8.22	5.26	1.32

The changeover times in hours on operation  $j$ ,  $j=4\div 8$  are equal to 0,  $S_j = 0$ ,  $j=4\div 8$ . The changeover times in hours on operation  $j$ ,  $j=1\div 3$  are the same and depend on the current order  $i=1\div 10$ , and the next order,  $i'=1\div 10$ .

**Table 3.** Changeover time (h)  $S_j, j=1\div 3$ 

	1	2	3	4	5	6	7	8	9	10
1	0.0	0.5	2.0	0.0	0.0	2.0	2.0	2.0	2.0	2.0
2	0.5	0.0	0.0	0.0	2.0	2.0	2.0	2.0	2.0	2.0
3	2.0	0.0	0.0	2.0	0.5	2.0	0.5	0.5	2.0	0.5
4	0.0	0.0	2.0	0.0	0.0	0.0	2.0	2.0	2.0	2.0
5	0.0	2.0	0.5	0.0	0.0	2.0	0.5	2.0	0.5	0.5
6	2.0	2.0	2.0	0.0	2.0	0.0	0.5	2.0	0.0	0.0
7	2.0	2.0	0.5	2.0	0.5	0.5	0.0	0.5	2.0	0.0
8	2.0	2.0	0.5	2.0	2.0	2.0	0.5	0.0	0.0	0.0
9	2.0	2.0	2.0	2.0	0.5	0.0	2.0	0.0	0.0	2.0
10	2.0	2.0	0.5	2.0	0.5	0.0	0.0	0.0	2.0	0.0

The model is set up with variables  $TS_{ij}$  being the start time,  $TE_{ij}$  being the completion time of order  $i$  at operation  $j$ ,  $T_i$  being the tardiness time of order  $i$ . The constraints on the sequence of operation on each order are as follows.

$$TS_{i4} \geq TE_{i1}, TS_{i5} \geq TE_{i2}, TS_{i6} \geq TE_{i3}, TS_{i7} \geq TE_{i5}, TS_{i8} \geq \max(TE_{i4}, TE_{i6}, TE_{i7}).$$

The start time of order  $i$  at operation  $j$ ,  $TS_{ij}$  depends on the end time of the previous order  $i'$ ,  $TE_{ij}$  and the changeover time between the orders on operation  $j$ .

$$TS_{ij} = TC_{ij} + S_j$$

The end time of order  $i$  on operation  $j$ ,  $TE_{ij}$  is determined by the start time and processing time of the order.

$$TC_{ij} = TS_{ij} + P_{ij}$$

The tardiness time of order  $i$ ,  $T_i$  is determined by the end time in the last operation and due time of the order.

$$T_i = \text{Max}(0, TE_{i8} - D_i)$$

The objective function that minimizes the total tardiness is defined as follows.

$$T_{\text{best}} = \text{Min } T, T = \sum(W_i * T_i, i=1\div 11)$$

The company is currently using the EDD dispatching method. The sequence of dispatching  $S$ , the value of the objective function are as follows:

$$S = (1, 2, 3, 4, 5, 6, 7, 8, 9, 10); T = 215.95 \text{ (h)}$$

#### 4. THE GATS MODEL FOR THE FLOW SHOP SCHEDULING PROBLEM

The above FSS problem is a NP hard problem with the solution space size of  $10!$  or 3,628,800. The GATS model is used to solve the problem. In the model, GA is used to perform a global search of the solution space, and TS is used to perform a local search to refine the solution found by GA. The GATS procedure is as follows:

Step 1: Initialize the GATS model.

Step 2: Generate the initial population  $P^{(0)}$ . Set  $k=0$ .

Step 3: Generate elite population  $P_E^{(k)}$ .

Step 4: Generate the genetic population  $P_G^{(k)}$ .

Step 5: Generate the neighbourhood population  $P_N^{(k)}$ .

Step 6: Generate the next population  $P^{(k+1)}$ . Set  $k=k+1$ .

Step 7: Check the termination rule. If No, return to step 3. If Yes, finish the loop.

Step 8: Run the algorithm a number of times to choose the best scheduling result.

##### 4.1. Step 1: Initialize the GATS model.

This step setups factors of GATS models, including the method of coding, the GA parameters, the TS parameters, and the termination rule.

**The method of coding:** each chromosome is a string of 10 genes. Each gene is corresponding to an order. The orders are numbered from 1 to 10. The sequence of genes represents the sequence of order scheduled:

$$C = [G1, G2, G3, G4, G5, G6, G7, G8, G9, G10]$$

The *GA parameters* include fitness function, the population size, and the parameters of GA operators. The fitness function  $F$  is defined as  $F_i = T_{\max} - T_i$ . Where  $F_i$ ,  $T_i$  are the fitness and objective values of chromosome  $i$ ,  $T_{\max}$  is the maximum objective value in the population. The crossover method is *POX*, the mutation method is *SWAP*, and the replacement method is acceptance threshold. The population size  $P$ , the crossover probability  $P_c$ , the mutation probability  $P_m$ , and threshold  $K$  are chosen as follows:  $P = 10$ ,  $P_c = 0.8$ ;  $P_m = 0.2$ ,  $K=2$ .

The *TS parameters* include the *neighbourhood operator*, and the *tabu list*. The neighbourhood operator uses the method of permutation of adjacent genes in the string to find the neighbourhood. *Tabu list* will contain the strings found in the previous steps.

The *termination rule*: The best objective value  $T_{best}$  of the population does not improve, or decrease, after 10 consecutive iterations.

#### 4.2. Step 2: Generate the initial population $P^{(0)}$ , set $k=0$ .

$P^{(0)}$  consists of 10 chromosomes. There are 3 chromosomes generated from 3 heuristic rules, EDD, SPT and LPT. The remaining chromosomes  $R1, \dots, R7$  are randomly generated as shown in the following table.

**Table 4.** The initial population  $P^{(0)} = \{ EDD, SPT, LPT, R1, R2, R3, R4, R5, R6, R7 \}$

$P^{(0)}$	G1	G2	G3	G4	G5	G6	G7	G8	G9	G10	$F_i$	$P_i$
EDD	1	2	3	4	5	6	7	8	9	10	1217.6710	0.1754
SPT	5	3	2	1	4	10	7	8	9	6	1210.7427	0.1744
LPT	10	7	1	5	2	3	4	6	9	8	1120.0530	0.1613
R1	1	5	4	3	2	6	10	9	8	7	1094.8691	0.1577
R2	5	3	4	1	2	10	8	9	6	7	986.0005	0.1420
R3	6	8	7	9	10	1	3	2	4	5	455.6409	0.0656
R4	10	6	9	7	8	5	1	4	2	3	315.4120	0.0454
R5	8	10	7	9	6	3	5	2	4	1	283.1211	0.0408
R6	7	8	10	9	6	2	3	5	4	1	260.3407	0.0375
R7	8	9	6	4	3	2	5	1	7	10	0.0000	0.0000

#### 4.3. Step 3: Generate elite population $P_E^{(k)}$ .

The step uses the selection operator to generate  $P_E^{(k)}$  from  $P^{(k)}$ . Each chromosome in the current population has a corresponding fitness value  $F_i$ , and is selected for inclusion in  $P_E^{(k)}$  with selection probability  $P_i$  determined as follows:

$$P_i = F_i / \sum_{i=1}^{10}(F_i)$$

With population  $P^{(0)}$ , the values of  $F_i$  and  $P_i$  are calculated as shown in the table above. Based on  $P_i$ , 10 random numbers are generated, the chromosomes, selected into the population  $P_E^{(0)}$  are as follows.

$$P_E^{(0)} = \{R3, R2, LPT, SPT, EDD, SPT, SPT, EDD, R2, R5\}$$

#### 4.4. Step 4: Generate the genetic population $P_G^{(k)}$ .

This step uses the crossover and mutation operators to generate genetic population  $P_G^{(k)}$  from the elite population  $P_E^{(k)}$ . The genetic population  $P_G^{(k)}$  includes the new chromosome generated from the crossover and mutation operators. The chromosomes of  $P_E^{(0)}$  are selected to be included in the crossover list  $P_c$  with the crossover probability of 0.6. After generating random numbers, the set  $P_c$  is determined as follows:

$$P_c = \{R3, LPT, SPT, EDD\}$$

Each pair of chromosomes in  $P_c$  is selected to cross over by the *POX* method, resulting in 12 new chromosomes in population  $P^C$  as shown in the following table.



**Table 5.** Population  $P^C$ 

$P^C$	G1	G2	G3	G4	G5	G6	G7	G8	G9	G10	Fi
C1	2	1	3	4	5	10	7	8	9	6	1245.02
C2	5	3	1	2	4	6	7	8	9	10	1156.34
C3	10	1	5	2	3	6	7	4	9	8	1083.70
C4	1	7	2	3	4	5	8	6	9	10	1080.84
C5	7	9	10	1	3	6	2	8	4	5	603.65
C6	6	8	1	2	3	4	5	7	9	10	553.08
C7	10	7	1	5	4	2	3	9	8	6	1104.16
C8	5	3	2	1	10	7	4	6	8	9	1069.54
C9	8	7	10	1	3	2	4	5	9	6	806.04
C10	6	5	3	9	2	1	4	10	7	8	611.50
C11	6	8	7	5	10	1	3	2	9	4	617.67
C12	10	7	1	9	2	3	4	6	8	5	941.70

The chromosomes of  $P_E^{(0)}$  are also selected to be included in the mutation list  $P_m$  with the mutation probability of 0.2. After generating random numbers,  $P_m$  is determined as follows:

$$P_m = \{EDD\}$$

Each chromosome in  $P_m$  is selected to mutate by the SWAP method, resulting in 1 new chromosome in population  $P^M$  as shown in the following table.

**Table 6.** Population  $P^M$ 

$P^M$	G1	G2	G3	G4	G5	G6	G7	G8	G9	G10	Fi
M1	1	10	3	4	5	6	7	8	9	2	1030.69

After crossover and mutation, 13 new chromosomes are created in the population  $P_G^{(0)}$ :

$$P_G^{(0)} = \{C1, C2, C3, C4, C5, C6, C7, C8, C9, C10, C11, C12, M1\}$$

#### 4.5. Step 5: Generate the neighbourhood population $P_N^{(k)}$ .

This step uses the neighbourhood operator to generate the neighbourhood population  $P_N^{(k)}$  from genetic population  $P_G^{(k)}$ . Each chromosome in  $P_G^{(k)}$  will have a neighbourhood defined by the neighbourhood operator. In this neighbourhood, the best chromosome will be selected to go forward. For example, with C1 there are 9 neighbouring chromosomes, in which C11 is the best and is chosen, as shown in the following table.

**Table 7.** The neighbouring chromosomes of C1

	G1	G2	G3	G4	G5	G6	G7	G8	G9	G10	Fi
C1	2	1	3	4	5	10	7	8	9	6	1245.02
<b>C11</b>	<b>1</b>	<b>2</b>	<b>3</b>	<b>4</b>	<b>5</b>	<b>10</b>	<b>7</b>	<b>8</b>	<b>9</b>	<b>6</b>	<b>1285.22</b>
C12	2	3	1	4	5	10	7	8	9	6	1282.16
C13	2	1	4	3	5	10	7	8	9	6	1259.76
C14	2	1	3	5	4	10	7	8	9	6	1268.09
C15	2	1	3	4	10	5	7	8	9	6	1212.12

C16	2	1	3	4	5	7	10	8	9	6	1248.52
C17	2	1	3	4	5	10	8	7	9	6	1265.44
C18	2	1	3	4	5	10	7	9	8	6	1228.27
C19	2	1	3	4	5	10	7	8	6	9	1205.94

Same for the remaining chromosomes of  $\mathbf{P}_G^{(k)}$ . The neighbourhood population  $\mathbf{P}_N^{(k)}$  consists of the best neighbour chromosomes:  $\mathbf{P}_N^{(k)} = \{N1, N2, N3, N4, N5, N6, N7, N8, N9, N10, N11, N12, N13\}$

**Table 8.** The neighbourhood population  $\mathbf{P}_N^{(k)}$

$\mathbf{P}_N^{(k)}$	G1	G2	G3	G4	G5	G6	G7	G8	G9	G10	Fi
N1	1	2	3	4	5	10	7	8	9	6	1285.22
N2	5	3	1	2	4	6	7	8	10	9	1196.64
N3	10	1	5	3	2	6	7	4	9	8	1085.44
N4	1	7	3	2	4	5	8	6	9	10	1158.11
N5	7	9	10	1	3	6	2	4	8	5	707.71
N6	6	8	1	2	3	5	4	7	9	10	652.32
N7	10	7	1	5	2	4	3	9	8	6	1118.06
N8	5	3	2	1	10	7	4	8	6	9	1088.80
N9	8	7	10	1	3	2	5	4	9	6	879.98
N10	6	5	3	2	9	1	4	10	7	8	659.86
N11	6	7	8	5	10	1	3	2	9	4	657.54
N12	10	7	1	2	9	3	4	6	8	5	996.89
N13	1	10	3	4	5	6	7	8	2	9	1070.62

#### 4.6. Step 6: Generate the next population $\mathbf{P}^{(k+1)}$ .

This step uses the replacement operator to generate the next population  $\mathbf{P}^{(k+1)}$  from the populations  $\mathbf{P}_G^{(k)}$  &  $\mathbf{P}_N^{(k)}$ . The chromosomes from  $\mathbf{P}_G^{(k)}$  &  $\mathbf{P}_N^{(k)}$  will be added to the current population  $\mathbf{P}^{(k)}$  to make the next population  $\mathbf{P}^{(k+1)}$ , if their fitness values exceed the acceptable threshold, here is selected as the value of the fifth chromosome of  $\mathbf{P}^{(k)}$  in the ranking. In order to keep the next population size constant, the chromosomes with the lowest value are removed from the next population. After applying the replacement operator, the next population  $\mathbf{P}^{(1)}$  is determined from  $\mathbf{P}_N^{(0)}$  as follows.

**Table 9.** The next population  $\mathbf{P}^{(1)} = \{N1, C1, EDD, SPT, N2, N4, C2, LPT, N7, C7\}$

	G1	G2	G3	G4	G5	G6	G7	G8	G9	G10	Fi
N1	1	2	3	4	5	10	7	8	9	6	1285.22
C1	2	1	3	4	5	10	7	8	9	6	1245.02
EDD	1	2	3	4	5	6	7	8	9	10	1217.67
SPT	5	3	2	1	4	10	7	8	9	6	1210.74
N2	5	3	1	2	4	6	7	8	10	9	1196.63
N4	1	7	3	2	4	5	8	6	9	10	1158.11

C2	5	3	1	2	4	6	7	8	9	10	1156.34
LPT	10	7	1	5	2	3	4	6	9	8	1120.05
N7	10	7	1	5	2	4	3	9	8	6	1118.06
C7	10	7	1	5	4	2	3	9	8	6	1104.16

#### 4.7. Step 7: Check the termination rule.

After iteration 1, N1 is the best chromosome with the best objective value of 148.40, appearing only once. The termination rule is not satisfied, so iteration 2 is executed. The result after 14 iterations is as follows.

**Table 10.** The result after 14 iterations

Iteration	G1	G2	G3	G4	G5	G6	G7	G8	G9	G10	Tbest
0	1	2	3	4	5	6	7	8	9	10	215.95
1	1	2	3	4	5	10	7	8	9	6	148.40
2	1	2	3	4	5	7	8	9	10	6	141.62
3	1	2	3	4	5	7	8	9	10	6	141.62
4	1	3	2	4	5	8	7	10	9	6	126.43
5	1	3	2	4	5	10	8	7	9	6	123.07
...	1	3	2	4	5	10	8	7	9	6	123.07
14	1	3	2	4	5	10	8	7	9	6	123.07

Seeing that from the 5th iteration to the 14th iteration, the best objective value remains the same, the termination rule is satisfied, the algorithm ends. The scheduling result in this run is as follows:

$$S = (1, 3, 2, 4, 5, 7, 8, 9, 10, 6), L = 123.07 \text{ (h)}$$

#### 4.8. Step 8: Run the algorithm a number of times to choose the best scheduling result.

The algorithm is run 5 times with the results as shown in the following table.

**Table 11.** The result after 4 runs

Run	G1	G2	G3	G4	G5	G6	G7	G8	G9	G10	Lbest	n
1	1	3	2	4	5	10	8	7	9	6	123.07	14
2	1	3	2	4	5	8	7	10	9	6	126.43	17
3	1	3	2	4	5	10	8	7	9	6	123.07	14
4	1	3	2	4	5	10	8	7	9	6	123.07	16
5	1	3	2	4	5	10	8	7	9	6	123.07	19

The best scheduling result is found on the 3rd run, with a number of iterations n of 14. The sequence of dispatching S, the value of the objective function are as follows:  $S = (1, 3, 2, 4, 5, 7, 8, 9, 10, 6)$ ;  $L = 123.07$

## 5. CONCLUSION

The GATS model has been used to solve the Flow Shop Scheduling Problem with 10 orders on 4 machines. In the model, GA is used as the platform to perform a global search of the solution space, and TS is used to perform a local search to refine the solution found by GA. The results show that the GATS model gives better objective value of tardiness time than the heuristic EDD method, being used. However, the factors of the model, including the population size, the crossover probability  $P_c$ , the mutation probability  $P_m$ , the method of finding the

neighbourhood chromosomes, the method and parameter of the termination rule, are only selected empirically, so the results are not very good. The future research is to use experimental design DOE to determine the model parameters to get suboptimal results.

### References

- [1] Etiler, B Toklu, M Atak, Jwilson. A genetic algorithm for flow shop scheduling problems, *Journal of the Operational Research Society*, (2004) 55, 830–835.
- [2] Moch Saiful Umam, Mustafid Mustafid, Suryono Suryono. A hybrid genetic algorithm and tabu search for minimizing makespan in flow shop scheduling problem. *Computer and Information Sciences*, 34 (2022), 7459–7467.
- [3] Justin Schrack, Roy Ortega, Kevin Dabu, Daniel Truong, Michal Aibin, Ania Aibin. *Combining Tabu Search and Genetic Algorithm to Determine Optimal Nurse Schedules*, 2021.
- [4] Yunus Demira, Selçuk Kürşat İşleyen. An effective genetic algorithm for flexible job-shop scheduling with overlapping in operations, *International Journal of Production Research*, 2014.
- [5] Kevin Boston, Pete Bettinger. *Combining Tabu Search and Genetic Algorithm Heuristic Techniques to Solve Spatial Harvest Scheduling Problems*, *Forest Science*, 48(1), 2002.
- [6] Burduk A., Musiał K., Kocharńska J., Górnicka D., Stetsenko A., 2019. Tabu Search and genetic algorithm for production process scheduling problem, *LogForum*, 15 (2), 181-189.

## [S6-16] Addressing the Housing Shortage for Harbor Workers during High-Risk Respiratory Seasons: A Step-by-Step Logistics Design Process for Providing Safe Accommodation

Le Duc Dao\*, Huynh Nguyen Khang Thinh, Trinh Minh Khoa, Lam Hien Dang Khoa,  
Truong Quoc Khoi, Phan Van Bach

*Faculty of Mechanical Engineering, Ho Chi Minh City University of Technology (HCMUT), 268 Ly Thuong  
Kiet Street, District 10, Ho Chi Minh City, Viet Nam*

*Viet Nam National University Ho Chi Minh City, Linh Trung Ward, Thu Duc City, Ho Chi Minh City, Viet Nam*

\*Corresponding author: lddao@hcmut.edu.vn

### Abstract

This article presents a project management plan for the implementation of a sleep box system to address the challenges faced by Vietnam's global economy due to respiratory health issues, particularly the lack of loading and unloading personnel at major harbors. The proposed solution aims to offer at least 120 slots to cater to a workforce of equal size, ensuring that the demands of the commodities industry are met. The article employs various techniques like the Analytic Hierarchy Process (AHP), Weighted Scoring Method (WSM), and Program Evaluation Review Technique (PERT) to determine the most suitable building type, optimal suppliers for each category of raw materials, and schedule, organize, and coordinate tasks within the project. The proposed sleep box system is found to be the most suitable option due to its capacity for providing privacy space, a critical feature in reducing the spread of respiratory viruses. The project management plan includes a linear organizational structure, a multifaceted project consisting of six constituent components, a Work Breakdown Structure (WBS), and a comprehensive feasibility analysis. After distributing responsible human resources, several issues emerged, leading to four proposed solutions, each evaluated based on key performance indicators (KPIs) like time and cost. Option 4, with a 4.7% increase in time and a 4.8% increase in cost, is found to be the most balanced approach, given both time and capital constraints. The article's original contribution lies in the comprehensive project management plan that ensures the feasibility, efficiency, and cost-effectiveness of the sleep box system implementation.

**Keywords:** *Project management, Sleep box system, Harbor workers, Respiratory health issues*

### 1. INTRODUCTION

In the face of various widespread respiratory health issues, including the COVID-19 pandemic, the global economy of Viet Nam has faced considerable challenges, one critical aspect being the lack of loading and unloading personnel at major harbors. This shortage has led to a staggering 70-80% decrease in productivity [1], severely impacting the supply chain and international trade. While a proposition was put forth to alleviate the issue by deploying workers from alternative regions, it was ultimately scrapped, leaving the quandary unresolved. As Viet Nam faces yet another resurgence of the COVID-19 epidemic, the exigency for a viable solution becomes even more paramount. In this article, we endeavor to proffer an innovative approach to address this pressing challenge and bolster the resilience of our harbors against future disruptions. Notably, our perspective in this article is that of a harbor owner, rather than a third-party investor, which allows for a more holistic understanding of the harbor's operations and the unique challenges faced.

In order to tackle this conundrum, we propose the implementation of a sleep box system designed to accommodate the needs of these crucial harbor workers. Our solution aims to offer at least 120 slots to cater to a workforce of equal size, ensuring that the demands of the commodities industry are met. The decision to adopt the sleep box system was reached using the Analytic Hierarchy Process (AHP) method, which we will present in detail further in the article. While optimizing setup and operational costs is a key consideration, the present article will predominantly concentrate on the deployment of this solution through effective project management.

To guarantee the successful execution of our sleep box system, we will undertake a methodical approach to deployment. This process will commence with a comprehensive feasibility analysis, followed by the establishment of a Work Breakdown Structure (WBS), which defines all the elements of the project in a hierarchical framework and establishes their relationships to the project end item(s) [2]; and Responsibility Assignment Matrix (RAM). Utilizing Microsoft Project (MS project), we will monitor the project's progress and address any issues that arise, particularly those concerning the allocation of human resources. By adhering to this well-organized plan, we anticipate providing a robust and sustainable solution to the harbor workforce crisis while improving overall

productivity amidst ongoing respiratory health challenges, such as COVID-19, the flu, and other airborne illnesses.

## 2. FEASIBILITY ANALYSIS

### 2.1. Types of building feasibility

The selection of a building type constitutes a crucial juncture, given its substantial implications on both the workers' way of life and the financial capacity of the port manager. Three prospective building types warrant consideration, namely Sleepbox, Dormitory, and Beehouse. Our research employs the AHP, which allows consideration of both objective and subjective factors in selecting the best alternative [3], to determine the most fitting building type. The AHP methodology considers four essential facets, namely building price, convenience, space, and respiratory problem (RP) precautions. As our study primarily focuses on providing amenities for loading and unloading harbor workers during respiratory problems like the COVID-19 pandemic, we accord the highest priority to RP precaution.

Table 1 shows the pairwise comparison matrix, calculated using the AHP method, for building price, convenience, space, and RP precaution. These criteria were used to evaluate the suitability of each building type. The data was collected using the Delphi method, wherein a group of real estate experts engage in discussions, leading to these obtained results.

**Table 1.** Pairwise comparison matrix of types of living (CR = 4.3%)

	Building price	Convenience	Space	RP precaution	Total
Building price	1	1/5	1/3	1/7	5.5%
Convenience	5	1	3	1/3	26.2%
Space	3	1/3	1	1/5	11.8%
RP precaution	7	3	5	1	56.5%

\*CR: Consistency ratio with a value of less than 10% is considered acceptable, while a value greater than 10% indicates that the pairwise comparisons may be inconsistent.

**Table 2.** Final score for the most suitable types of living

	Building price	Convenience	Space	RP precaution	Total
Dormitory	0.003465	0.194666	0.087674	0.035595	0.3214
Beehouse	0.01067	0.050828	0.022892	0.10961	0.194
Sleepbox	0.040865	0.016506	0.007434	0.419795	<b>0.4846</b>

Having compared and computed the AHP between the Sleepbox, Dormitory, and Bee house types, we have found that Sleepbox is the most suitable option. This is largely due to its capacity for providing the utmost privacy space, a critical feature in reducing the spread of the respiratory virus.

### 2.2. Raw materials feasibility analysis

The present article emphasizes the significance of selecting appropriate raw materials and furniture for ensuring long-term success and worker comfort. Furthermore, securing the right suppliers can lead to cost savings

and enhanced project operations. Our study centers on three categories of materials for the Sleepbox: Building material, Internal furniture, and Electric and water network.

Each material type necessitates distinct supplier criteria, such as price, reliability, and quality for building materials, whereas Internal furniture may prioritize varying factors. To identify the optimal suppliers for each category, we employ the Weighted Scoring Method (WSM). Following the WSM assessment, we recommend Greentech Company for building materials, Navier Company for toilets and sinks, and An Hoang Phat Company for electrical and water systems.

### 2.3. Technique and technology feasibility analysis

The technical and technological feasibility of Sleepbox construction refers to the practicality of building Sleepboxes, considering factors like construction methods, materials, and available technology, to ensure an efficient and cost-effective implementation. Fortunately, the construction of Sleepbox models is not entirely unfamiliar to the Vietnamese people, with several construction companies having standardized models and procedures for building such structures. Before the actual construction process, six stages must be carried out to ensure feasibility and smooth implementation.

Firstly, funds must be prepared either by self-financing or through external fundraising, which often involves borrowing from a bank. Next, the construction site must be prepared by cleaning and leveling the ground to create a suitable platform for construction. Subsequently, the sleepbox architecture model must be designed, either by hiring an architecture company or selecting from an available model.

In the fourth stage, the necessary materials and equipment for construction must be determined, such as wood, steel, and wires. To ensure the best quality at an optimal cost, a suitable third-party construction company must be selected. Finally, the construction process commences, with a Work Breakdown Structure (WBS) established to facilitate its smooth and efficient execution.

### 2.4. Financial and Economic feasibility analysis

In the financial feasibility analysis of the Sleepbox project, the perspective considered is that of a harbor owner, meaning that there is no need to purchase land. The total cost to build 120 Sleepboxes, estimated based on the quantity required and the model used, is around 2.4 billion VND. Each Sleepbox is estimated to cost around 20 million VND to build, assuming a standard size of 1.2m width and 2.2m length.

From an economic perspective, the Sleepbox project is intended to contribute to the overall benefits of the harbor by providing essential commodities for loading and unloading workers. As such, it is not expected to generate any profit in itself. However, over a period of ten years, the investment can be recovered to some extent through the salvage value of the Sleepboxes. Therefore, the Sleepbox project can be considered economically feasible, with the long-term benefits outweighing the initial investment costs.

## 3. PROJECT PLANNING

### 3.1. Project organizational structure

The project shall adhere to a linear organizational structure, in which functions, plans, and daily tasks are distributed along functional lines, fostering employee expertise development. However, in the event of irregularities, such as potential isolation directives, the organization will adopt an online structure. A comprehensive depiction of the organizational hierarchy is provided in Figure 1.

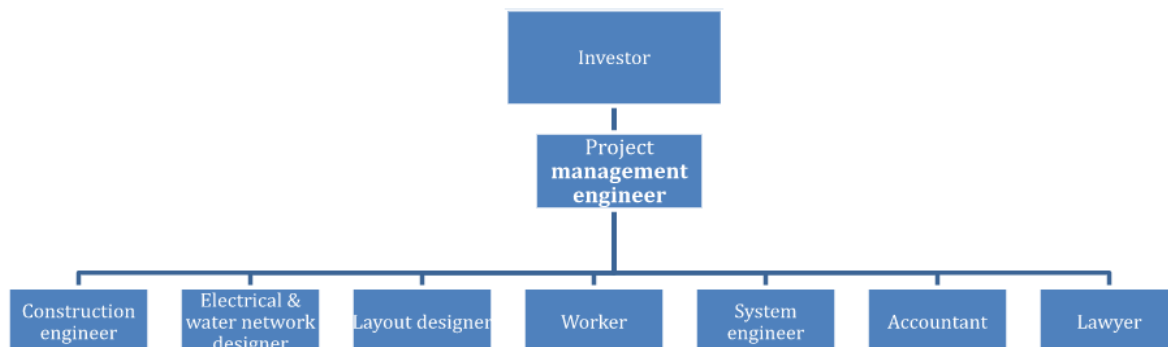


Figure 1. Organizational structure diagram

The interfacing of the project management team, comprised of the investor and project management engineer, with the functional departments is crucial for the successful execution of the project. The project management engineer assumes the responsibility of overseeing all activities and subsequently communicating progress to the investor. Without a well-developed organizational structure, the project timeline and financial outlay may deviate from initial projections, leading to potential conflicts and even abandonment of the project.

### 3.2. Project task

The present study delineates a multifaceted project consisting of six constituent components, designated alphabetically. In practice, these components will be broken down into smaller, more detailed tasks depending on the characteristics of the project.

**Table 3.** The main activities for the project

No.	Name of task	Symbol
1	Preparation	A
2	Design	B
3	Construction and installation	C
4	Acceptance test	D
5	Recruitment	E
6	Completing the project	F

After establishing the 6 main activities for the project, we build the Work Breakdown Structure (WBS). Each work package has its optimistic completed time, pessimistic completed time, most likely completed time and average completed time.

## 4. RESOURCE ALLOCATION

### 4.1. Scheduling

Program Evaluation Review Technique (PERT) method is applied to ascertain the likelihood of punctual project completion. It is a project management tool used to schedule, organize, and coordinate tasks within a project. The technique was developed in the late 1950s by the United States Department of Defense as a way to manage the development of large defense projects. There are 4 main steps in the method. The method encompasses four primary stages, delineated herein:

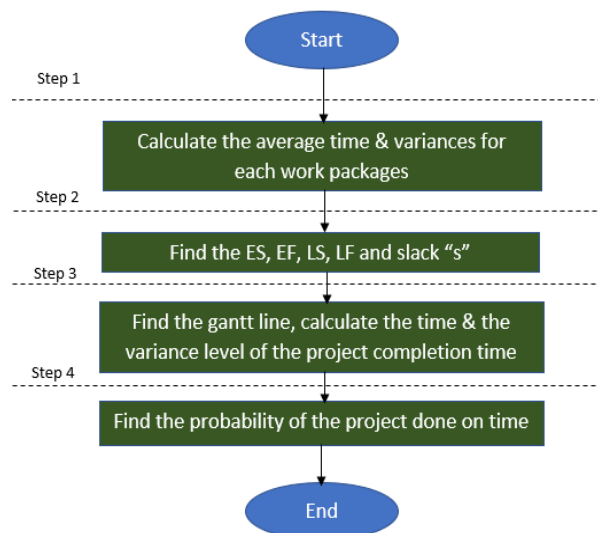


**Figure 2.** PERT process

Upon completion of Steps 1 and 2, the activity-on-node (AON) network and Gantt chart can be constructed. The Gantt chart encompasses 44 tasks, spanning from initial tasks, such as establishing and assigning tasks to the project management team and researching legal proceedings, to concluding tasks, which include reporting to investors, summarizing, and handing over to the project owner. This visual representation assists managers in monitoring the project schedule, discerning the critical path, and tracking progress.



Following the execution of Steps 3 and 4, the probability of timely project completion is determined. Thus, the project's target duration is set at 218 days.

#### 4.2. Resource allocation

After determining the Gantt line and distributing responsible human resources to each task using the earliest start time (EST), it could be noticed that there are some problems:

- System engineering's work is overloaded at 2 tasks: Customer analysis and Potential analysis.
- Lawyer and System engineer's work is overloaded at 2 tasks: Bidding construction and installation.
- Inside Plastering, Equipment Installation and Equipment inspection are the overloaded tasks that need more human resources.

There are 4 proposed solutions to the problems, each solution and its results would be described as follows:

**Table 4.** The solutions and results for human allocation problem

Solution	Description	Result
1	Delay all the overloaded tasks	Problem solved; however, the delay is <b>226.4 days</b> .
2	Adding more System and Construction engineer workforces and delaying Bidding infrastructure tasks	Problem solved, max day to complete the project is <b>218 days</b> , which means that the method is viable.  Total cost is: <b>599,304,000 VND</b>
3	Adding more System Engineer workforce then delaying Construction engineer's and Lawyer's task.	Problem solved; however, the delay is <b>223.4 days</b> .  Total cost is: <b>572,424,000 VND</b>
4	Adding more Construction Engineer workforce then delaying System engineer's and Lawyer's task.	Problem solved, max day to complete the project is <b>217.4 days</b> , which means that the method is viable.  Total cost is: <b>594,504,000 VND</b>

To choose the best result, we can evaluate the outcomes based on the key performance indicators (KPIs). We will set the KPI is no more than 5%, which means that no more than 5% increase in cost and time.

**Table 5.** The key performance indicators (KPIs) for each approach's result

Method	Time (Base: no more than 5% increase)	Cost (Base: no more than 5% increase)
1	9% increase	0% increase
2	5.3% increase	5.58% increase
3	0.8% increase	7.9% increase
4	4.7% increase	4.8% increase

Through the implementation of this assessment, investors are afforded the opportunity to select a suitable approach in alignment with their strategic objectives. Expedited investment timelines with minimal cost concerns may favor Option 1, while financially-driven investors might opt for Option 3. A balanced approach, considering both time and capital constraints, may be best represented by Option 4, as it demonstrates superiority over Option 2. The ultimate decision lies within the context of real-world scenarios, requiring a trade-off between capital allocation and completion timelines.

## 5. CONCLUSION

Based on the comprehensive analysis and findings presented in this scientific research paper, it can be concluded that the implementation of a sleep box system for harbor workers is a promising solution to address the challenges faced by the global economy of Viet Nam, particularly in the context of respiratory health issues such

as the COVID-19 pandemic. By providing suitable accommodation and amenities for loading and unloading personnel, the sleep box system aims to enhance productivity and bolster the resilience of harbors against future disruptions.

The feasibility analysis conducted in this study evaluated various aspects such as building types, raw materials, and technology, ensuring a well-rounded understanding of the project. The selection of sleep boxes as the most suitable building type, based on the Analytic Hierarchy Process (AHP) methodology, highlights the emphasis on respiratory problem precautions and the need for privacy space. Additionally, the identification of optimal suppliers for raw materials and furniture further contributes to the long-term success and worker comfort.

The project planning phase outlines a systematic approach to deployment, including the organizational structure, project tasks, scheduling using the Program Evaluation Review Technique (PERT), and resource allocation. The proposed solutions to address human resource allocation issues provide flexibility and cost-effectiveness while ensuring timely project completion.

From a financial and economic perspective, the sleep box project demonstrates feasibility, with the initial investment costs outweighed by the long-term benefits to the harbor and its workers. The project contributes to the overall well-being of the harbor by providing essential amenities, although it may not generate direct profits.

In conclusion, this scientific research paper offers a comprehensive and innovative approach to tackle the challenges faced by harbors in Viet Nam. The proposed sleep box system, supported by rigorous analysis and planning, presents a viable solution to enhance productivity, address respiratory health concerns, and improve the overall resilience of the harbor workforce. It is anticipated that the successful implementation of this project will have a positive impact on the supply chain, international trade, and the economy as a whole, while ensuring the well-being and safety of harbor workers in the face of ongoing health challenges.

## References

- [1] Khánh, N. (2021). Thiếu công nhân, cảng biển phải từ chối đơn hàng, Mt.gov.vn. Cổng Thông tin điện tử Bộ Giao thông vận tải. Available at: <https://mt.gov.vn/vn/tin-tuc/75674/thieu-cong-nhan--cang-bien-phai-tu-choi-don-hang.aspx> (Accessed: May 6, 2023).
- [2] Larson, E.W. (2021). "Project Management: The managerial process". New York, NY: McGraw Hill.
- [3] Jadhav, A. and Sonar, R. (2009). "Analytic Hierarchy Process (AHP), weighted scoring method (WSM), and hybrid knowledge based system (HKBS) for software selection: A comparative study", 2009 Second International Conference on Emerging Trends in Engineering & Technology [Preprint]. doi:10.1109/icetet.2009.33).
- [4] S. Bushuyev and A. Puzichuk, "Development organizational structure for value-oriented reengineering project of construction enterprises," 2021 IEEE 16th International Conference on Computer Sciences and Information Technologies (CSIT), LVIV, Ukraine, 2021, pp. 367-370, doi: 10.1109/CSIT52700.2021.9648758.
- [5] Yang Minghai, Ding Ronggui and Wang Yangwei, "Organizational structure design of overseas branches of electric power construction enterprises based on project management —Taking the case of international engineering branch of Shandong Electric Power Construction Company," 2009 International Conference on Computers & Industrial Engineering, Troyes, France, 2009, pp. 1131-1136, doi: 10.1109/ICCIE.2009.5223929.
- [6] Zoghi, S. (2015). "Engineering Economics and its role in the engineering curricula," 2015 ASEE Annual Conference and Exposition Proceedings [Preprint]. Available at: <https://doi.org/10.18260/p.23958>.
- [7] Markow, M. J. (2012). Engineering economic analysis practices for highway investment: A synthesis of highway practice. Washington: Transportation Research Board.
- [8] Meredith, J. R. and Mantel, S. J. (2010). Project Management: A managerial approach. Hoboken, NJ: John Wiley & Sons.
- [9] Rose, K. H. and Davidson, J. (2009). Book review: Project management: A managerial approach, 7<sup>th</sup> Edition, Project Management Journal.

## [S6-27] Rearrangement of Finished Product Warehouse of Tran Hiep Thanh Textile Joint Stock Company

Nguyen Viet Hai Duy, Dinh Ba Hung Anh\*

Department of Industrial System Eng., Faculty of Mechanical Engineering, Ho Chi Minh City University of Technology (HCMUT), 268 Ly Thuong Kiet Street, District 10, Ho Chi Minh City, Viet Nam

\*Corresponding author: anhdbh@gmail.com

### Abstract

Warehouses are an integral part of a logistics system as well as a supply chain, especially for the way businesses conduct production in the apparel industry. This study deals with improving the performance of finished goods warehouse of Tran Hiep Thanh Textile Joint Stock Company by using algorithms to improve space, re-plan storage devices and allocate product locations. The study uses tools to support CRAFT, CORLAP, collect and analyze statistical data, AHP, linear model, ABC classification method and Excel, Visio, AutoCAD software.

**Keywords:** CRAFT, CORELAP, REL relationship diagram, Storage device planning

### 1. INTRODUCTION

Warehouse operations are one of the most important activities that directly affect the revenue of a business. Thanks to the warehouse operation, it is easier for businesses to trade and distribute goods with import, export and storage activities, helping to optimize the average cost per unit to the maximum (Janka et al. [2]; Mai Ha Phan et al. [5]).

Tran Hiep Thanh Textile Joint Stock Company is a company specializing in manufacturing and supplying all kinds of products for the industrial fashion industry. To be a reliable supplier and partner for garment companies in domestic and foreign markets. The average order delay rate from June 2022 to August 2022 of the warehouse is 0.4, which is quite a large number for any company. Therefore, this situation needs to be rectified as soon as possible. First, we will find the cause of the above situation, then find effective remedies. Through data analysis and consultation with finished product warehouse staff, the author has found a number of causes for the delay in orders.

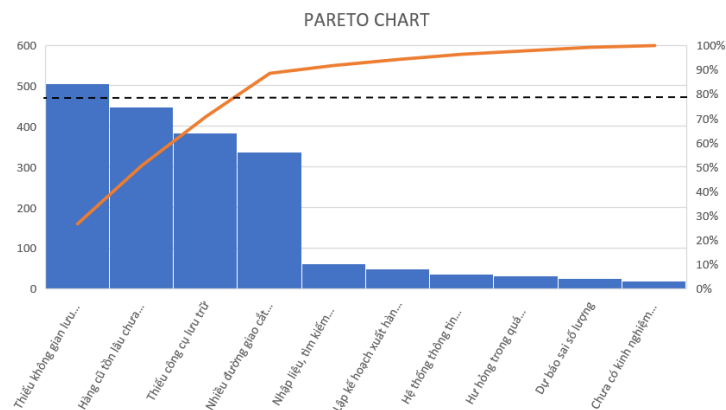


**Figure 1.** Order delay rate of warehouse, Tran Hiep Thanh Textile Joint Stock Company

From the chart of Figure 1, it can be seen that 80% of the problems that the warehouse is facing come from 4 main causes including: (1) Lack of storage space. Due to the lack of storage space, goods at the warehouse often have to be left in places other than the warehouse. (2) Lack of storage engine. Limited storage capacity, not taking advantage of the maximum storage space of the warehouse. (3) Old goods that have been around for a long time have not been properly arranged. This affects work productivity when employees only arrange products according to experience, not according to company policy. (4) Many intersections and bottlenecks in the warehouse. Parts in the warehouse have not been arranged properly, so when performing import/export tasks, interruptions often occur, reducing work productivity.

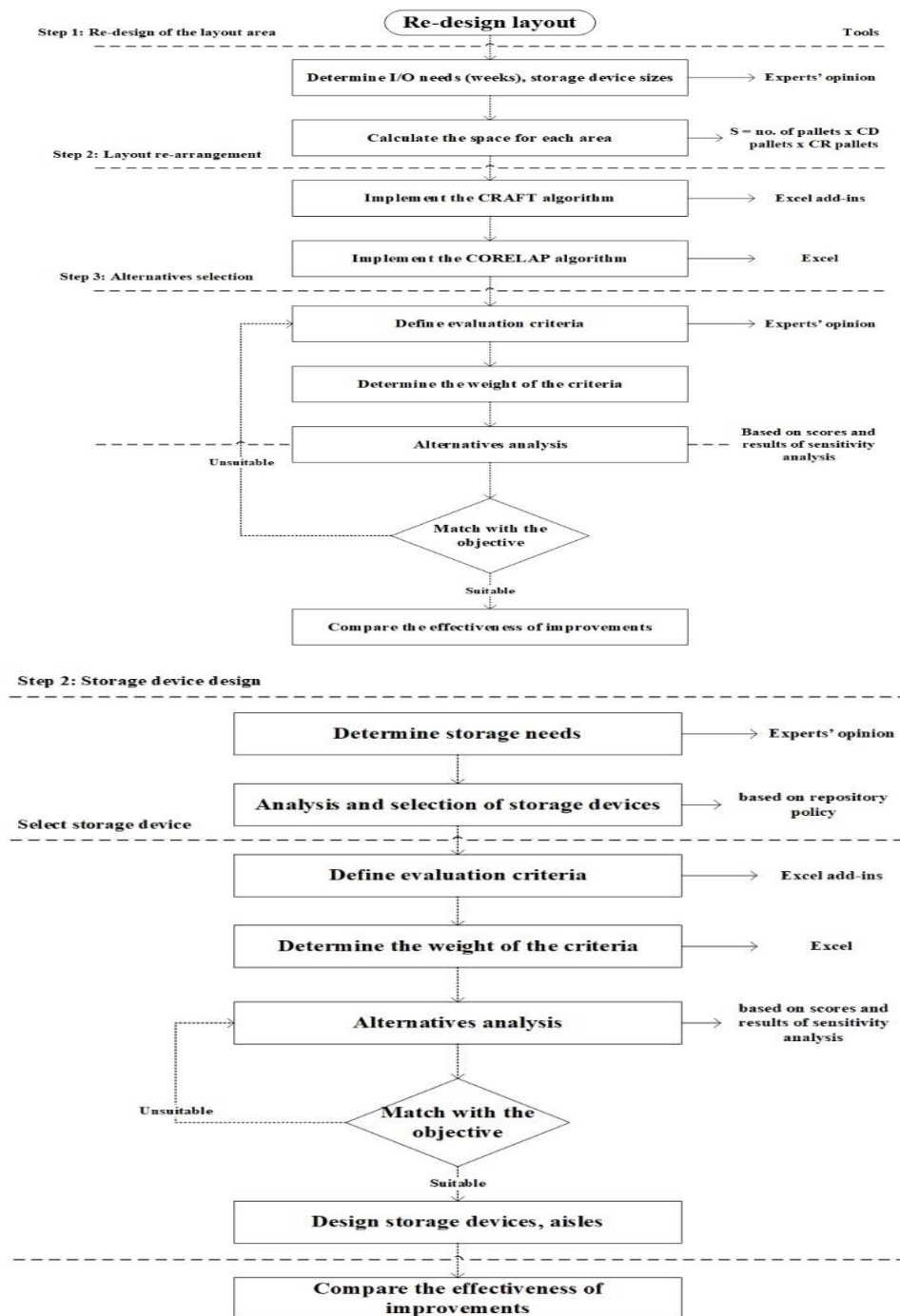


**Figure 2.** Research process

There are a few studies that have mentioned the application of the above algorithms to solve the problem of ground. Author K.Y. Typpayawong [3] conducted a study on a chicken slaughterhouse to solve the problem of insufficient storage space for goods produced during the day by redesigning the storage device incorporating the product grouping method and use a linear programming model to allocate goods. Thereby improving storage space utilization by 45%, reducing travel distance by 45%, and shortening picking time by 40%. Author Kerem [4] has applied ground improvement algorithms such as CORELAP, CRAFT to design the premises of the production area at the fabric company; thereby proposing an improved ground with improved efficiency of 36.82%. The details of the research process are shown in Figure 2.

After collecting data on the area of each area in the warehouse, the quantity of goods, the level of storage, the first step will be to redesign the area of each area in the warehouse. After that, the rearrangement of areas in the warehouse will be performed using CRAFT and CORELAP algorithms. Next, using the AHP method by determining a set of evaluation criteria for each alternative, then determining the weights of the criteria, and finally

calculating the weights for each alternative based on the composite pairwise comparison matrix. The next step will be to improve and select storage equipment among the popular types of shelves today such as Selective shelves, Double - deep racks, VNA shelves,... Finally, a linear model is used to reallocate finished goods locations, and the ABC classification method is used to group the main products in the warehouse.

## 2. RESEARCH CONDUCTING

### 2.1. Re-design of some functional parts

Storage area: With the statistics of the order situation and the number of orders put down from June 15, 2022 to June 29, 2022, the area of the following areas can be calculated:

Sample cutting area: The largest number of orders given is equivalent to 17 pallets.  $S = 17 \text{ pallets} \times 1.4\text{m} \times 1\text{m} = 20 \text{ (m}^2\text{)}$

Shipping area: The maximum number of frames that can be handled at one time is 21 pallets.  $S = 21 \times 1.4\text{m} \times 1\text{m} = 30 \text{ (m}^2\text{)}$

Import area: The maximum number of frames that can be handled at one time is 25 pallets.  $S = 25 \times 1.4\text{m} \times 1\text{m} = 35 \text{ (m}^2\text{)}$

Waiting area for import and export queue: Required storage space.  $= 70 \times 1.4 \times 1 = 100 \text{ (m}^2\text{)}$

### 2.2. Warehouse layout

#### Layout improvement according to CRAFT algorithm

The algorithm is performed on a warehouse with an area of 810 m<sup>2</sup> (30m x 27m) equivalent to 206 cells; each cell is about 4m<sup>2</sup> with the support of Excel software with the function Excel adds - in CRAFT layout. Areas are designated A1- A11. Building the initial plan as input data of the CRAFT algorithm, the parts will be arranged based on the layout order of the current plan with the previously defined space requirements. Make improvements, since the from - to matrix and the coordinates of the parts are updated after each swap of pairs 8 - 3, 6 - 7, 4 - 5, 3 - 6 and stops at pairs 4-7; due to increased migration costs compared to the previous swap.

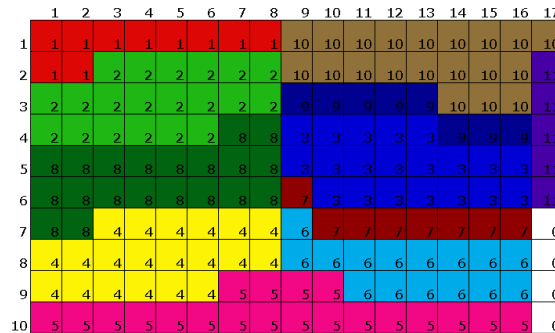


Figure 3. Layout improved by CRAFT

#### Layout improvement according to CORELAP algorithm

The algorithm is built based on the REL relation graph. Then proceed to arrange the parts on the REL diagram according to the law of priority in the west corner. Make a spreadsheet of TCR values to determine the layout order of the parts. The part with the highest TCR value will be placed first in the center of the floor. Component A3 is placed in the middle of the floor and unit A10 is placed adjacent. In order to arrange the A4 part, it is necessary to calculate the PR values at the possible locations. The position for the largest PR coefficient will place A4 in it. Do the same with the remaining parts until the final ground is found.

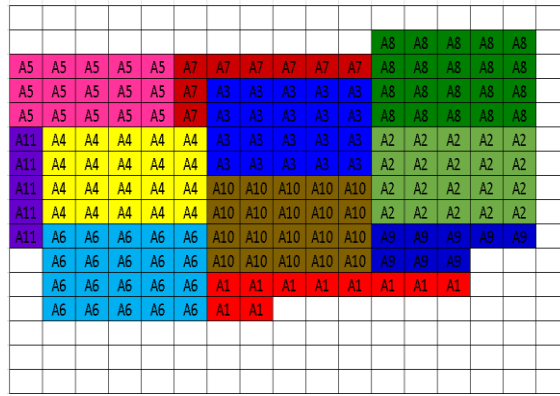


Figure 4. The layout improved by COREL

**Apply AHP to select the layout plan:**

Choose from the following options:

- Alternatives 1 (PA 1) is the current site.
- Alternatives 2 (PA 2) is an improved ground using the CRAFT algorithm.
- Alternatives 3 (PA 3) is an improved ground using the COREL algorithm.

Table 1. The pairwise comparison matrix sums up the alternatives

Alternatives	Distance (0.54)	Adjacency (0.15)	Operation management (0.15)	Implementation costs (0.16)	Weights
PA1	0.35	0.24	0.18	0.2	0.284
PA2	0.32	0.56	0.48	0.58	0.422
PA3	0.33	0.2	0.34	0.22	0.294

Based on the above results, it is found that Alternatives 2 - applying the CRAFT algorithm is the one with the highest score. Therefore, Alternatives 2 was selected as the new site layout plan.

**Improving storage devices**

With the current storage policy of the warehouse is FIFO (First in first out); and prioritize equipment with storage density, low investment costs and because the warehouse needs high accessibility to create favorable conditions for employees when picking up goods. Based on those criteria, select Selective shelves with parameters that can be met. Regarding the aisle configuration, in order to have an aisle suitable for moving equipment and convenient for employees to move, choose the width of the aisle to pick up goods as 3.2m, and the width of the horizontal aisle is 4m. Based on parameters such as the height of the warehouse ceiling is 5.5m, the height of a shelf is 1.62m and the safe distance from the warehouse ceiling, the number of available storage floors is 3 floors. Layout of shelves horizontally of the warehouse: The shelf area is limited by the aisle at the end of the row and the width of the horizontal aisle.

- With the length of a Selective shelf of 2.5m, the number of shelves in a row can be divided by  $= \frac{30-4-0.5}{2.5} = 5$  shelves = 10 frame.
- On the left side of the warehouse diagram with 4 paths between areas. From there, it can be calculated that X number of shelves is:  $1.3X + 3.2 \times 4 = 27 - 3 \Rightarrow X \approx 8(\text{arrays})$
- The calculation is similar to the right side of the warehouse diagram.
- Calculating storage space utilization  $= \frac{12.5 \times 1.3 \times 13}{12.5 \times 24 + 12.5 \times 20} \times 100\% = 38.41\%$
- The total amount of frames is: 390 frames.

**Allocate storage locations for finished goods in the warehouse**

**Objective function:** Minimizing the transportation distance between locations in the warehouse to the doors.

$$Min \sum_{j=1}^n \sum_{k=1}^q \frac{T_j}{S_j} \sum_{i=1}^m p_i d_{ik} \times x_{jk} \quad (1)$$

**Constraint:**

$$\sum_{j=1}^n x_{jk} = 1, k = 1, \dots, q \quad (2)$$

$$\sum_{k=1}^q x_{jk} = S_j, j = 1, \dots, n \quad (3)$$

$$x_{jk} = \{0,1\} \text{ with all } j \text{ and } k \quad (4)$$

Constraint (2): Each storage location can only store 1 product

Constraint (3): The total storage location for product  $j$  is equal to the number of storage units needed for product  $j$

Constraint (4): Is product  $j$  assigned to the warehouse location  $k$

**Symbol:**

$i$ : Warehouse door number

$j$ : Sequence number product

$k$ : Sequence number of storage location

$q$ : number of storage units

$n$ : number of product types

$m$ : number of doors

$S_j$ : Number of inventory units needed for product  $j$

$T_j$ : Number of moves in/out of the warehouse of product  $j$

$p_i$ : Percentage of moving in/out from warehouse to warehouse doors

$d_{ik}$ : Distance required to move from the entrance/exit to the storage locations

**Decisive variable:**

$x_{jk} = 1$  if product  $j$  is placed in warehouse  $k$  and vice versa = 0

Step 1: Calculate the ratio  $T_j/S_j$ , sorted in descending order and sorted by ABC

Step 2: Calculate  $f_k$  values for all storage locations.  $f_k = \sum_{i=1}^m p_i d_{ik}$

Step 3: Start placing products in storage locations.

The product with the lowest  $f_k$  value and the highest  $T_j/S_j$  ratio means that this product has a high in-and-out frequency and requires few storage locations; so place this product in the position closest to the door. Same goes for other Class A products. With the remaining B and C products, they will be placed in the remaining positions after the A products are arranged.

**3. RESULT AND CONCLUSION**

Make improvements to research objects such as warehouse usefulness, time to find and pick up goods, and finally, travel time. After redesigning the area of the functional areas and planning the storage equipment, the warehouse usefulness increased to 38.41% (20.61% increase compared to the unimproved period). Pick-up time and travel time were reduced by 30% and 40% respectively after rearranging parts in the warehouse and allocating locations for finished goods. With the new premises and location of finished goods, employees can be proactive in their work and ensure the work is completed on time. In addition, employees feel more comfortable with the help of multiple transportation tools.

With the presented results, this study is said to have succeeded in applying CRAFT, CORELAP floor layout algorithms, designing and selecting storage devices, reallocating finished goods position, with the goal of improving the utilization of warehouse storage space, reducing the time to find and retrieve goods and thereby improve the operational efficiency of the warehouse. However, due to time and resource constraints, the research is only done for some main product lines of the warehouse and the research paper has not mentioned the inventory liquidation options to increase storage space.

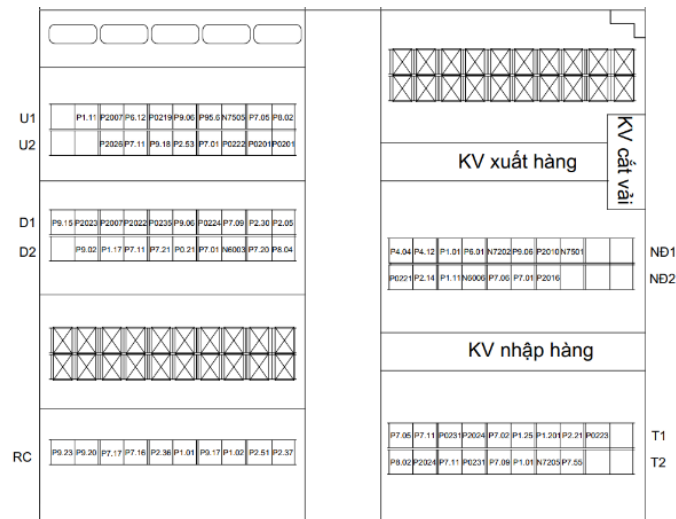


Figure 5. Final product layout

### Acknowledgement

We acknowledge Ho Chi Minh City University of Technology (HCMUT), VNUHCM for supporting this study.

### References

- [1] Armin Klausnitzer R. L. 2018 "Optimal facility layout and material handling network design". Computers and Operations Research.
- [2] Janka Saderova, Andrea Rosova, Marian Sofranko and Peter Kacmary (2016), "Example of Warehouse System Design Based on the Principle of Logistics", Faculty of Mining, Ecology, Process Control and Geotechnologies, Technical University of Kosice, Letna 9.
- [3] K.Y. Tipayawong, and Apichat Sopadang (2013). "Improving Warehouse Layout Design of a Chicken Slaughterhouse using Combined ABC Class Based and Optimized Allocation Techniques". Proceedings of the World Congress on Engineering 2013 Vol. I, WCE 2013, July 3 - 5, 2013, London, U.K.
- [4] Kerem Toker (2012), "Application of Combined SWOT and AHP: A Case Study for a Manufacturing Firm", Beykent University, Istanbul, Turkey.
- [5] Mai Ha Phan, Ha Quang Thinh Ngo, Tien Trung Kieu and Linh Y Thai (2018), "Redesigning Finished Product Warehouse Layout - A Case Study", Ho Chi Minh City University of Technology (HCMUT), Ho Chi Minh City, Vietnam.
- [6] R. Stern et al., "Multi-agent pathfinding: Definitions variants and benchmarks", Proc. Int. Symp. Combinatorial Search, pp. 151-159, 2019.
- [7] Talbi El-Ghazali 2009 Metaheuristics: "From Design to Implementation" (NJ, US: John Wiley & Sons).



## [S6-29] Multi-Objective Model in Aggregate Production Planning: A Case Study of ScanCom Vietnam Plant

Nguyen Truong Xuan Thinh\* Duong Vo Nhi Anh, Do Vinh Truc

*International University – Viet Nam National University Ho Chi Minh City, Ho Chi Minh City, Viet Nam*

\*Corresponding author: ielsiu19273@student.hcmiu.edu.vn

### Abstract

This study develops an effective aggregate production planning (APP) model for ScanCom, a wooden furniture manufacturing company, to address challenges in demand and supply volatility. The objective is to create a flexible and adaptive production plan that efficiently utilizes resources while meeting customer needs and maximizing profit. A multi-objective APP model is proposed, considering production costs, workforce change costs, and overtime utilization. The research covers six products manufactured at ScanCom's plant, based on forecasted demand for 2023. This research aims to provide decision-makers at ScanCom with an effective production strategy and implementation suggestions. The proposed model can be further enhanced and applied to future scenarios, contributing to the improvement of production systems.

**Keywords:** *Aggregate production planning, Multi-objective, Goal programming, Optimization*

### 1. INTRODUCTION

In the current era of industrialization, production planning has become a crucial part of every manufacturing company and it serves as the backbone of the entire manufacturing process. Effective production, both in the short and long term, requires planners/decision-makers to determine optimal quantities of products to be produced, inventory level, materials, workforce, and other elements required for production while considering various factors such as forecasted demand, available resources, labor requirements, and coordination of all relevant activities to achieve the company goals.

However, production planning is not without its challenges. The production plan is mostly employed under a variety of uncertainties ranging from internal factors to external factors. Consequently, one of the most significant challenges faced by planners is how to achieve the ideal utilization of on-hand resources while minimizing different types of costs and maximizing business revenue. Therefore, production planning has never been an easy task and it has become increasingly difficult due to rising competition brought on by production expansion and economic growth.

Thus, effective production planning has a direct impact on the manufacturing system and overall business performance. The outcomes of this decision-making have a substantial effect on purchasing decisions, labor decisions, and sales performance. Therefore, the key to winning for production planners is to efficiently utilize resources and successfully manage uncertainties that arise – this problem also is as known as Aggregate Production Planning.

### 2. PROBLEM STATEMENT

Effective production planning is essential for any manufacturing organization to meet the demands of its customers. Nevertheless, the current production planning approach of ScanCom may not be suitable in dealing with the volatility of demand and supply. Consequently, the factory often encounters the risk of material shortage, which can lead to stockouts resulting in lost sales and dissatisfied customers. Alternatively, the factory is exposed to overproduction which can result in excess inventory, tying up valuable resources, causing financial strain and space constraints. Hence, those could lead to severe consequences if the management does not have proper planning with current on-hand materials.

To cope with the issue in the short term, the logistics team has made several temporary adjustments in production planning which cause unintended costs. For instance, switching the production line from one product to another because of not having available materials on hand will increase machine/personnel idle time as well as setup time leading to considerably raised labour cost and setup cost. In the worst situation, lacking materials would bring a halt to the whole production in the plant, and then an immense expense will come from this for ScanCom.

Furthermore, those temporary actions induce costs incurred not only during production but also throughout

the supply chain such as extra freights when changing the mode of transportation from sea to air to expedite shipments, penalty costs for delayed fulfilment for distributors mentioned in the contract as well as a decrease in customer satisfaction. On the other hand, the Domino effect of this problem could bring chaos to the operation of other departments as well; and the production planning team would take a significant number of hours to replan the workforce, machines, and resources for normal production.

Thus, one of the improvements for this current persistent problem of the ScanCom plant is to have a robust production plan in place which can adapt to unforeseen changes in demand and supply. To achieve this, production planners need to adopt a flexible and adaptive approach to production planning.

### 3. LITERATURE REVIEW

Many investigations related to the APP problem have been studied with a vast number of methods and expansions from small-scale to medium-large-scale problems, from conventional to contemporary algorithms, from single-objective to multi-objective, and so forth. A combined method between TOPSIS and compromise programming was developed for multi-objective APP model by Yu et al. (2022). The research aimed to deal with an APP problem for a manufacturing company producing a single product to satisfy the uncertain demand while adapting to changing the rate of production, labor level, inventory, back orders, overtime, and other variables. The model considered three main objectives related to sales profit maximization, repairing cost, and production costs minimization and it could be converted into bi-objective function by applying the advanced TOPSIS method. Thanks to the extended TOPSIS method, the authors made significant improvements in helping decision makers to determine the optimal workforce (hiring/laying off) in each period, suitable total overtime, and inventory levels. Another interesting approach was presented by Hafezalkotob et al. (2019), in which the authors suggested a reformed linear model applied for integrated production planning with multi factories using numerous methods of cooperative game theory. The findings analyzed the potential cost savings through the collaboration among plants thanks to the exchange of workforce and inventory, which results in decreasing inventory and labor costs. Moreover, one of the challenging and infrequent approaches to solve the APP in a highly intuitive manner is through simulation and this was implemented in the study conducted by Jamalnia & Feili (2013). Particularly, the research employed a hybrid methodology of discrete event simulation (DES) and system dynamics (SD) to construct a practical APP model by using the Arena simulation software. The model incorporated operational-level and shop-floor activities, as well as aggregate-level strategic decisions to evaluate the effectiveness of APP strategies (i.e., chase/level/mixed strategy), with profitability as the primary criterion. The highlighted point of this solving approach is that the simulation could provide the interdependent interactions of different APP components visually and provide valuable insights for the management regarding strategic decision-making.

Considering uncertainty in formulating mathematical models, the frequently used methodology is fuzzy programming. Djordjevic & Stojic (2019) introduced a new approach in dealing with APP in automotive industry under uncertainty, specifically, the authors developed a fuzzy linear programming model that considers the time needed involved in the manufacturing process, the inventory management, and the customer delivery. The uncertainties in the paper include the deviation of customer demand from forecasted values and production output, the production time, the timing of safety stock storage in the warehouse, and the required preparation time for customer delivery, which were modelled by using fuzzy sets that were created using historical data recorded in the database or based on experience. Throughout real-world data experiments, the results demonstrated that the proposed model was effective in reducing the time required for production and warehouse operation, while also improving the overall performance of the supplier. In the same year, Tirkolae et al. (2019) also implemented fuzzy combined with Mixed-Integer Linear Programming (MILP) methodology but with an advanced approach that involved developing a multi-objective and multi-period model to accommodate the uncertainty of seasonal demand. Specifically, the developed model took the outsourcing and workforce overtime factors into account, the objectives are to minimize different types of cost and maximize customer gratification, and the triangular fuzzy numbers were employed to handle uncertain demand (seasonal). After conducting a sample experiment, the paper indicated that different results may be obtained when uncertain conditions and real-world assumptions are considered in developing a practical APP.

### 4. MODEL FORMULATION

In this paper, a pre-emptive goal programming is developed to solve the multi-objective aggregate production planning problem and the assumptions involved in the proposed APP problem are as follows:

- Workers possess identical skills meaning that they have the same level of productivity.
- Workers engage in a standard work schedule of eight hours per day.

- The initial level of the workforce is determined for each product.
- There is no backorder due to the policy of ScanCom.
- Labor cost, production cost, and holding cost are deterministic and fixed.

## Notations

### Sets:

$I$ : set of the products

$T$ : set of the planning periods

### Indices:

$i$ : index of the product

$t$ : index of the planning period

### Model parameters:

$rev_i$ : the unit revenue of the product  $i$  (\$/unit)

$c_{1i}$ : the unit production cost for product  $i$  at regular time (\$/unit)

$c_{2i}$ : the unit production cost for product  $i$  at overtime (\$/unit)

$c_{3i}$ : the unit inventory cost for holding product  $i$  at the end of each period (\$/unit)

$LT_i$ : the labor production time for manufacturing product  $i$  (hours/unit)

$LC$ : the labor cost for manufacturing product at regular time (\$/hour)

$LCOT$ : the labor cost for manufacturing product at overtime (\$/hour)

$I_{i,0}$ : the initial inventory of product  $i$  at the start of planning horizon (units)

$W_0$ : the number of initial workers (man-period)

$Q_{i,t}^{min}$ : the minimum required demand of product  $i$  in period  $t$  (units)

$Q_{i,t}^{max}$ : the forecast demand of product  $i$  in period  $t$  (units)

$WCap^{min}$ : the minimum workforce level of the plant (mans)

$WCap^{max}$ : the maximum workforce level of the plant (mans)

$SCap^{max}$ : the storage capacity of the plant (units)

$c_4$ : the cost for hiring one worker (\$/man)

$c_5$ : the cost for laying off one worker (\$/man)

$Z_1$ : the aspiration level of profits to be achieved

$Z_2$ : the aspiration level of cost of hiring or laying-off workers

$Z_3$ : the aspiration level of overtime

### Decision variables:

$Q_{i,t}$ : the quantity of product  $i$  sold in period  $t$  (units)

$x_{i,t}$ : the quantity of product  $i$  manufactured in period  $t$  at regular time (units)

$y_{i,t}$ : the quantity of product  $i$  manufactured in period  $t$  at overtime (units)

$H_t$ : the number of hiring workers in period  $t$  (man-period)

$L_t$ : the number of laying off workers in period  $t$  (man-period)

$W_t$ : the number of workers required in period  $t$  (man-period)

$OT_t$ : the total hours of overtime in period  $t$  (hours)

$I_{i,t}$ : the inventory of product  $i$  at the end of period  $t$  (units)

### Auxiliary variables:

$d_p^-$ : the deviation variable of underachievement of the goal  $Z_1$

$d_p^+$ : the deviation variable of overachievement of the goal  $Z_1$

$d_{wf}^-$ : the deviation variable of underachievement of the goal  $Z_2$

$d_{wf}^+$ : the deviation variable of overachievement of the goal  $Z_2$

$d_{ot}^-$ : the deviation variable of underachievement of the goal  $Z_3$

$d_{ot}^+$ : the deviation variable of overachievement of the goal  $Z_3$

### Goal Constraints and Objective Functions

$$Z = \text{Min } P_1(d_p^-) + \text{Min } P_2(d_{wf}^+) + \text{Min } P_3(d_{ot}^+) \quad (1)$$

subject to:

**Goal 1: Profit goal**

$$\sum_{i \in I} \sum_{t \in T} (rev_i \cdot Q_{i,t}) - \sum_{i \in I} \sum_{t \in T} [c_{1i} \cdot x_{i,t} + c_{2i} \cdot y_{i,t}] - \sum_{t \in T} (LC \cdot W_t) - \sum_{t \in T} (LCOT \cdot OT_t) - \sum_{i \in I} \sum_{t \in T} (c_{3i} \cdot I_{i,t}) - d_p^+ + d_p^- = Z_1 \quad (2)$$

**Goal 2: Hiring and layoff goal**

$$\sum_{t \in T} (c_4 \cdot H_t + c_5 \cdot L_t) - d_{wf}^+ + d_{wf}^- = Z_2 \quad (3)$$

**Goal 3: Labor overtime goal**

$$\sum_{i \in I} \sum_{t \in T} (LT_i \cdot y_{i,t}) - d_{ot}^+ + d_{ot}^- = Z_3 \quad (4)$$

❖ **Constraints:**

**The inventory level/balance constraints:**

$$I_{i,t-1} + x_{i,t} + y_{i,t} - I_{i,t} = Q_{i,t}, \forall i \in I, t \in T \quad (5)$$

$$Q_{i,t}^{\min} \leq Q_{i,t} \leq Q_{i,t}^{\max}, \forall i \in I, t \in T \quad (6)$$

$$\sum_{i \in I} I_{i,t} \leq SCap^{\max}, \forall t \in T \quad (7)$$

**Relationship among the number of workers:**

$$W_{t-1} + H_t - L_t = W_t, \forall t \in T \quad (8)$$

$$WCap^{\min} \leq W_t \leq WCap^{\max}, \forall t \in T \quad (9)$$

$$\sum_{i \in I} LT_i \cdot x_{i,t} \leq 8 \cdot W_t, \forall t \in T \quad (10)$$

$$\sum_{i \in I} LT_i \cdot y_{i,t} = OT_t, \forall t \in T \quad (11)$$

$$OT_t \leq 40 \cdot W_t, \forall t \in T \quad (12)$$

**Non-negative constraints:**

$$Q_{i,t}, x_{i,t}, y_{i,t}, W_t, OT_t, H_t, L_t, I_{i,t}, d_p^+, d_p^-, d_{wf}^+, d_{wf}^-, d_{ot}^+, d_{ot}^- \geq 0, \forall i \in I, t \in T \quad (13)$$

## 5. COMPUTATIONAL RESULTS

To illustrate how flexible the presented model is, a dataset was gathered from ScanCom manufacturing company located at Song Than Industrial Park, Binh Duong Province. This dataset serves as the input for the mathematical model being proposed.

**Table 5.1.** The unit sales revenue

Product, <i>i</i>	Product name	Unit sales revenue (\$/unit), <i>rev<sub>i</sub></i>
1	Italica Carver Easy Chair	9.71
2	Royan Stacking Chair	18.25
3	Montmartre Side Chair	6.32
4	Ibis Rectangle Table 150x90cm	19.63
5	Sjalland Square Table	11.20
6	Lynx Rectangle Table 180-240x100cm	40.57

**Table 5.2.** The cost of unit production at regular, at OT, and holding cost

Product, <i>i</i>	Production cost at normal time (\$/unit), $c_{1i}$	Production cost at OT (\$/unit), $c_{2i}$	Holding cost (\$/unit), $c_{3i}$
1	8.36	12.54	0.08
2	15.72	23.58	0.08
3	5.44	8.17	0.08
4	16.91	25.37	0.08
5	9.65	14.47	0.08
6	34.95	52.43	0.08

**Table 5.3.** The labor production time needed for producing each product

Product, <i>i</i>	Labor time for each product (hours/unit), $LT_i$
1	1.9
2	3.2
3	1.2
4	3.8
5	2.3
6	7.8

**Table 5.4.** The cost labor at regular, at OT, and hiring/lay-off cost

Labor cost (regular time) (\$/hour), $LC$	Labor cost (OT) (\$/hour), $LCOT$	Hiring cost (\$/man), $c_4$	Lay-off cost (\$/man), $c_5$
1.22	1.83	87	950

**Table 5.5.** The capacity of the plant and workforce

Initial workforce (man), $W_0$	Minimum workforce (man), $WCap^{min}$	Maximum workforce (man), $WCap^{max}$	Storage capacity (unit), $SCap^{max}$
100	100	1,800	200,000

**Table 5.6.** The initial inventory of each product at the start of planning horizon

Product, <i>i</i>	Initial inventory (units), $I_{i,0}$
1	8,382
2	5,809
3	268
4	0
5	1,369
6	1,865

**Table 5.7.** The minimum required product quantities in each planning period

Product, <i>i</i>	Quantity (units), $Q_{i,t}^{min}$											
	Period, <i>t</i>											
	1	2	3	4	5	6	7	8	9	10	11	12
1	563	499	483	461	414	411	496	584	737	698	724	734
2	247	279	246	229	246	267	290	306	331	361	385	421
3	201	175	168	188	183	166	198	207	192	224	251	262
4	443	392	344	336	354	335	358	393	505	543	608	709
5	134	101	98	136	105	101	99	123	175	176	177	189
6	235	201	193	196	187	192	210	284	306	253	273	292

**Table 5.8.** The forecast product quantities in each planning period

Product, <i>i</i>	Quantity (units), $Q_{i,t}^{max}$											
	Period, <i>t</i>											
	1	2	3	4	5	6	7	8	9	10	11	12
1	5,628	4,985	4,825	4,611	4,144	4,113	4,963	5,841	7,371	6,979	7,238	7,344
2	1,235	1,394	1,228	1,143	1,229	1,336	1,452	1,528	1,653	1,803	1,924	2,104
3	1,007	875	842	942	914	832	992	1,035	959	1,121	1,253	1,311
4	3,104	2,744	2,408	2,351	2,476	2,342	2,506	2,753	3,535	3,804	4,256	4,966
5	537	404	392	542	421	404	395	492	699	702	706	754
6	1,176	1,004	963	982	935	958	1,052	1,420	1,529	1,267	1,364	1,462

**Table 5.9.** The target values for goal programming model

Goal (target)	Value
$Z_1$ (Profit)	440,323 (\$)
$Z_2$ (Hiring and Layoff)	150,253 (\$)
$Z_3$ (Labor Overtime)	203,152 (hours)

## 6. CONCLUSION

This paper focuses on addressing the challenges of demand and supply volatility faced by a wooden furniture manufacturing company through the examination of aggregate production planning problems. A multi-objective programming model is introduced to solve the aggregate production planning problem, with a hierarchical optimization approach targeting three main objectives. These objectives include minimizing production costs, minimizing costs related to hiring and laying off workers, and minimizing the overall use of overtime shifts. The findings of this study demonstrate the model's adaptability and resilience, allowing management to assess numerous scenarios by altering priority rankings based on various strategic assumptions. Hence, incorporating computerized production planning into the company's management system is crucial, and it is anticipated that the proposed model will contribute significantly to enhancing the company's global supply chain management in the future.

## References

- [1] Yu, V. F., Kao, H.-C., Chiang, F.-Y., & Lin, S.-W. (2022). Solving aggregate production planning problems: An extended TOPSIS approach. *Applied Sciences*, 12(14), 6945.
- [2] Hafezalkotob, A., Chaharbaghi, S., & Lakeh, T. M. (2019). Cooperative Aggregate Production Planning: A Game Theory Approach. *Journal of Industrial Engineering International*, 15(S1), 19–37.
- [3] Jamalnia, Abouzar, & Feili, A. (2013). A simulation testing and analysis of Aggregate Production Planning Strategies. *Production Planning & Control*, 24(6), 423–448. <https://doi.org/10.1080/09537287.2011.631595>
- [4] Djordjevic, I., Petrovic, D., & Stojic, G. (2019). A fuzzy linear programming model for Aggregated Production Planning (APP) in the automotive industry. *Computers in Industry*, 110, 48–63. <https://doi.org/10.1016/j.compind.2019.05.004>
- [5] Tirkolae, E. B., Goli, A., & Weber, G.-W. (2019). Multi-objective aggregate production planning model considering overtime and outsourcing options under fuzzy seasonal demand. *Lecture Notes in Mechanical Engineering*, 81–96. [https://doi.org/10.1007/978-3-030-18789-7\\_8](https://doi.org/10.1007/978-3-030-18789-7_8)
- [6] Mehdizadeh, E., Niaki, S. T., & Hemati, M. (2018). A bi-objective aggregate production planning problem with learning effect and machine deterioration: Modeling and solution. *Computers & Operations Research*, 91, 21–36. <https://doi.org/10.1016/j.cor.2017.11.001>
- [7] Ramezani, R., Rahmani, D., & Barzinpour, F. (2012). An aggregate production planning model for two phase production systems: Solving with genetic algorithm and Tabu Search. *Expert Systems with Applications*, 39(1), 1256–1263. <https://doi.org/10.1016/j.eswa.2011.07.134>
- [8] Leung, S. C. H., & Chan, S. S. W. (2009). A goal programming model for aggregate production planning with Resource Utilization Constraint. *Computers & Industrial Engineering*, 56(3), 1053–1064. <https://doi.org/10.1016/j.cie.2008.09.017>
- [9] Leung, S. C., Wu, Y., & Lai, K. K. (2003). Multi-site aggregate production planning with multiple objectives: A goal programming approach. *Production Planning & Control*, 14(5), 425–436. <https://doi.org/10.1080/0953728031000154264>

## [S6-41] Application of Multi-Criteria Classification and Inventory Management Model for Spare Parts: A Vietnamese Case Study

Tai Duc Nguyen, Mai-Ha Phan\*

*Department of Industrial System Engineering, Faculty of Mechanical Engineering, Ho Chi Minh City University of Technology (HCMUT), 268 Ly Thuong Kiet Street, District 10, Ho Chi Minh City, Viet Nam  
Viet Nam National University Ho Chi Minh City, Linh Trung Ward, Thu Duc City, HCMC, Viet Nam*

\*Corresponding author: ptmaiha@hcmut.edu.vn

### Abstract

In the manufacturing sector, especially for lines manufacturing with a variety of machinery and equipment, spare parts inventory management plays a very important role. Determining the inventory to reduce the probability of missing spare parts when needed, while ensuring the economic problem of ordering costs and holding costs is a very important activity for businesses. This study applies a multi-criteria classification method, to determine the importance of different inventories, thereby analyzing and evaluating the appropriate inventory model for each different classification group. The scope of the study will be applied to a carton packaging factory.

**Keywords:** *Multi-criteria classification, Inventory system, Spare parts, Safety stock*

### 1. INTRODUCTION

Each manufacturing enterprise now has a variety of large and small machines to serve the operation. Coupled with this factor is the regular repair and replacement of spare parts to ensure the production circuit is smooth and not stalled. The problem is that if there are too many spare parts in stock, it will increase inventory costs, on the contrary, if there is a shortage of spare parts, it will affect the production process and reduce the service level of the business. Therefore, providing spare parts of the right type, in the right quantity, at the right time to ensure a smooth production process, satisfy customer needs, and create quality products at low cost is an important task of the enterprise.

Another issue to consider is that in an organization, even of moderate size, thousands of units may hold inventory. To effectively control this huge inventory, the traditional approach is to classify inventory into different groups. Then, different inventory control policies can be applied to different groups. ABC analysis is a well-known and practical classification based on the Pareto principle. However, traditional ABC analysis is based on a single measurement, such as the use of the cash value of annual inventory. Recent studies have recognized that other criteria, such as inventory cost, material importance, delivery time, popularity, obsolescence, replaceability, quantity required each year, and scarcity are also important in classifying inventory.

This study applies a multi-criteria classification method, to determine the importance of different inventories, thereby analyzing and evaluating the appropriate inventory management model for each different classification group.

### 2. LITERATURE REVIEW

#### 2.1. Inventory classification

The literature on inventory classification is extensive. This section briefly overviews some related research on multi-criteria classification models.

A study by author Ramanathan (2006) [1] developed a weighted linear optimization model for this problem. The basic concept of the model in this paper is similar to the concept of data envelope analysis (DEA). First, the model converts all criterion measurements into a scalar score, which is the weighted sum of the measurements against the individual criteria. To avoid subjectivity in weight assignment, the weights are generated by linear optimization just like the DEA. The classification is then done by grouping the items based on the generated score. However, linear optimization is required for each item. Processing time can be very long when the number of items in stock is large with thousands of items in stock.

Some extensions to classical ABC analysis were discussed by Flores (1987) [2]. The study proposed a cross-tabulation matrix method to classify inventory according to two criteria. Criteria matrices have applications provided which are rated on some practical scale. The number of matching categories must be determined by the

user. (In this study three categories of categories were identified.) In other situations, more or less categories may be appropriate. Combining criteria may require different analytical methods. The use of this matrix can provide a clear method for taking into account a wide range of criteria in developing inventory policies. However, the methodology becomes complex as it expands to more criteria.

An artificial neural network (ANN) has been applied by the author group F.Y. Partovi and M. Anandarajan (2002) [3]. This paper presents a new approach to ABC classification of different SKUs using AI-based techniques by ANN for SKU classification in the pharmaceutical industry, namely two learning methods that have been used in the pharmaceutical industry, that is BP and GA. The classification results of these methods are compared with statistical techniques of MDA, which are proposed as an alternative technique for inventory classification. The development of these models is based on the actual decisions of inventory managers. The reliability of the models was tested by comparing their classifier ability with two datasets (retained data and extrinsic data set). The results indicate that the ANN classification models have higher prediction accuracy than the MDA technique. In addition, the results indicate that the ANN (GA) network is a superior classifier to the ANN (BP) network. However, although these classification models have some advantages, they also have limitations. First, the number of variables that can be included in these models is limited. Second, modelling cannot and should not completely replace professional judgment. This metaphysics is too complex to apply and confusing for inventory managers.

### 1.2. Inventory model

To take advantage of the inventory management models, it is important to choose the appropriate model with the type of material through an appropriate review of the existing literature.

Rinaldi et al. (2023) have proposed a simulation model for spare parts inventory management of an ETO company [4]. First, the items have been classified according to their criticality and demand pattern. Later, a simulation model has been developed to reproduce the inventory policy used to currently manage the relevant items. Finally, a new procedure integrating the simulation model has been developed to define the optimal setting of each relevant item; each set has been identified with the aim of minimizing the total cost of inventory management by defining a proper combination of operating leverages (EOQ and OP).

A heuristic method was presented by Karin et al. (2009) to find a cost-effective balance between maintenance frequencies, spare parts inventories and repair capacity in order to achieve a target availability level [5]. We considered a single k-out-of-N system under condition-based maintenance. They showed that 'simply' extending the METRIC approach yields inferior results since the relationship between the decision parameters and the operational availability is not a monotonous one. It is relatively easy to modify this optimisation algorithm for several model variants, such as the inclusion of component wear-out and the extension to an installed base of k-out-of-N systems under block replacement. For the latter model, they found that our optimisation heuristic yields costs that are on average 0:8% more than the costs found by enumeration. At the same time, the computation times were a lot smaller, minutes compared to hours or even days.

### Proposed model

This proposed method will include two stages:

- Stage 1: Apply a multi-criteria classification model to determine the importance of each type of spare part.
- Stage 2: Analyze and evaluate inventory management models to choose the most suitable model.

### 1.3. Inventory classification

This study will apply the classification method referenced in the article "A simple classifier for multiple criteria ABC analysis" [6] by author Wan Lung Ng. This method will propose a weighted linear optimization model to help solve the multi-criteria classification problem.

In this paper, they proposed a simple model for multiple criteria inventory classification. The model converted all criteria measures of an inventory item into a scalar score. The classification based on the calculated scores using ABC principle is then applied. With proper transformation, the study can obtain the scores of inventory items without a linear optimizer.

For illustration purpose, we apply our solution scheme on a case study at a Vietnam carton packaging factory. Let us consider three criteria: annual usage value, average unit cost and lead time for inventory classification. All the criteria are positive related to the score of the inventory items. Currently, the plant has nearly 3000 spare parts. Usage demand data of these items from July 2017 to June 2022 will be considered in this study.



Consider an inventory with  $I$  items and these items are to be classified based on  $J$  criteria. The measurement of the  $i$ th item under the  $j$ th criteria is denoted as  $y_{ij}$ . All criteria measures were assumed are positively related to the score of an item. If there is a negatively related criterion, transformation such as taking negativity or taking reciprocals can be applied for conversions. The treatment in [7] using transformation formula (1) can be adopted to convert all measurement in a 0–1 scale for all items.

$$\frac{y_{ij} - \min_{i=1,2,\dots,I} \{y_{ij}\}}{\max_{i=1,2,\dots,I} \{y_{ij}\} - \min_{i=1,2,\dots,I} \{y_{ij}\}} \tag{1}$$

Table 1 shows the measures under each criterion as well as transformed measures of spare parts in a scale of 0–1.

**Table 1.** Measures of inventory items and transformed measures

Item no.	Annual usage value	Average unit cost	Lead time	Annual usage value (transformed)	Average unit cost (transformed)	Lead time (transformed)
1	5840.64	49.92	2	1.00	0.22	0.17
2	5670	210	5	0.97	1.00	0.67
3	5037.12	23.76	4	0.86	0.09	0.50
...	...	...	...	...	...	...

Another pre-processing procedure we needed is the decision-maker has to rank the importance of criteria. Although this involves certain degree of subjectivity, this is a far weaker requirement than that in AHP. Pair-wise comparisons in the AHP require a decision-maker to specify not only the direction of preference (e.g. criterion 1 is more preferable than criterion 2) but also degree of preference (e.g. equal importance, weak preference, essential preference, demonstrable preference, absolute preference, etc). This study requires only ranking rather than specifying a precise degree or magnitude.

To facilitate the inventory classification under multiple criteria, we define a non-negative weight  $w_{ij}$  which is the weight of contribution of performance of the  $i$ th item under the  $j$ th criteria to the score of the item. The score of the  $i$ th item (denoted as  $S_i$ ) is expressed as a weighted sum of performance measures under multiple criteria. A weighted linear optimization model is shown as the following for each item  $i$ :

$$(P1) \max S_i = \sum_{j=1}^J w_{ij} y_{ij} \tag{2}$$

$$\sum_{j=1}^J w_{ij} = 1 \tag{3}$$

$$w_{ij} - w_{i(j+1)} \geq 0, j = 1, 2, \dots, (J - 1) \tag{4}$$

$$w_{ij} \geq 0, j = 1, 2, \dots, J \tag{5}$$

The model (P1) is a linear optimization model. Certainly, one can solve a series of linear optimization for all inventory items. However, this requires a linear optimizer available for decision-maker. In addition, the processing time can be very long especially when number of inventory items is large. Therefore, we adopt a transformation to simplify our model. The simplified model can be easily solved without a linear optimizer.

Denote

$$u_{ij} = w_{ij} - w_{i(j+1)}, i = 1, 2, \dots, I \text{ and } j = 1, 2, \dots, (J - 1) \tag{6}$$

$$u_{iJ} = w_{iJ}, i = 1, 2, \dots, I \tag{7}$$

After some transformations, we can convert the model (P1) to the following (P2) for all inventory items:

$$(P2) \max S_i = \sum_{j=1}^J u_{ij} x_{ij} \tag{8}$$

$$u_{ij} \geq 0, j = 1, 2, \dots, J \tag{9}$$

The formulation (P2) is a linear program in the Canonical form with only one equality constraint. This implies there is only one optimal solution  $u_{ij}$  being non-zero and all others are zero. Furthermore, the only non-zero decision variable ( $u_{ij} > 0$ ) must be equal to  $\frac{1}{j}$ . Hence, the score  $S_i$  of the  $i$ th inventory item can be easily

obtained as  $\max_{j=1,2,\dots,J} (\frac{1}{j} \sum_{k=1}^j y_{jk})$ . Alternatively, one can obtain the maximal score  $S_i$  by the dual of (P2). The

dual formulation of (P2) is as the following with dual variable  $z_i$  :

$$(P2 \text{ dual}) \min z_i \quad (10)$$

$$\text{s.t. } z_i \geq \frac{1}{j} x_{ij}, j = 1, 2, \dots, J \quad (11)$$

The  $\min z_i$  for item  $i$  can straightforwardly be obtained as  $\max_{j=1,2,\dots,J} \frac{1}{j} x_{ij}$ .

After the transformation, the multiple criteria inventory classification procedure is simple and efficient. With each inventory item, we perform the following steps on a spreadsheet package.

- Step 1. Calculate all partial averages.
- Step 2. Compare and locate the maximum among these partial averages. The corresponding value is the score  $S_i$  of the  $i$ th item.
- Step 3. Sort the scores  $S_i$ 's in the descending order.
- Step 4. Group the inventory items by principle of ABC analysis.

The whole process requires no linear optimizer and is easy-to-implement on a common spreadsheet package which can be handled by decision makers without special training.

Table 2 shows the calculated partial averages and the located maximal scores.

**Table 2.** Partial averages and scores of inventory items

Item no.	Annual usage value (transformed)	Average unit cost (transformed)	Lead time (transformed)	Partial average		
				1	2	3
1	1.00	0.22	0.17	1.00	0.61	0.46
2	0.97	1.00	0.67	0.97	0.99	0.88
3	0.86	0.09	0.50	0.86	0.48	0.48
...	...	...	...	...	...	...

Table 3 shows the classification based on our proposed model.

**Table 3.** Classification based on our proposed model of each item

Item no.	Annual usage value (transformed)	Average unit cost (transformed)	Lead time (transformed)	$S_i$ value	Class
1	5840.64	49.92	2	1.00	A
2	5670	210	5	0.99	A
3	5037.12	23.76	4	0.86	A
...	...	...	...	...	...

Within the scope of the study, the next part would only plan inventory for class A. Class B and C spare parts will do weekly or monthly tracking depending on the policy of the enterprise.

#### 1.4. Inventory management model

After classifying the spare parts being used at the factory, the study will conduct inventory planning for class A parts using 3 standard and effective inventory methods: EOQ; EOIs; Min-Max, then use the actual past demand

of spare parts to evaluate the effectiveness of 3 models, thereby choosing the most suitable model for the business. This study will use the Microsoft Excel platform to build these models.

This research chooses EOQ and EOI because these are models suitable for independent, repeatable, and continuous demand supplies. The model shows the optimal order level based on the minimum ordering and inventory costs for a given demand. The EOQ model requires continuous updating of input, output, and inventory data (which can be done manually or by machine) to determine if inventory levels have been reduced to reorder levels. While the EOI model only requires periodic updates at predetermined intervals. EOI model with relatively high holding costs due to large inventory, but in return for the advantages will reduce ordering costs, reduce procedures and increase purchasing volume to enjoy large volume discounts. It should be noted that the major drawback of these two models is that they are based on too many assumptions that are difficult to achieve in practice. Therefore, it should be practical to gradually remove assumptions, accepting actual conditions by adding uncertain factors to the model. For this study, the safety inventory factor (calculated by the service level model) will be added to match the actual material needs.

For Min-Max, this classic stochastic inventory system is suitable for independent, repeatable demand, which helps reduce the risk of lost orders without holding excess inventory at the warehouse, in line with the nature of the spare parts at the enterprise.

In this study, the service level will be chosen with a value of 97.5%.

Table 4 shows the parameter values of the three proposed models.

**Table 4.** Parameter values of the three proposed models

Item no.	EOQ		EOI		Min - Max		
	Q	B	T	E	SS	Min	Max
1	47	26	7	73	6	26	73
2	56	35	6	93	6	35	91
...	...	...	...	...	...	...	...

The study provides four criteria for model selection, which are calculated in turn as follows:

Out-of-stock rate = 6-year total shortage / 6-year total demand

Annual ordering cost ratio = Average annual ordering cost / Maximum average annual ordering cost of the three models.

Annual holding cost ratio = Average annual holding cost / Maximum average annual holding cost of the three models.

Maximum number of missing parts at a time = Maximum number of missing parts for 6 years / Maximum number of missing parts for 6 years of three models.

Table 5 shows the score value of three inventory management system (IMS) and weight of each criterion. These weights were obtained based on opinions from expert's enterprises.

**Table 5.** Weight of each criterion and score of three inventory management system

	Out-of-stock rate	Annual Ordering Cost Ratio	Annual holding cost ratio	Maximum number of missing parts	Score
	30%	25%	25%	20%	
EOQ	0.013	0.887	0.076	1.000	0.4446
EOI	0.011	1.000	0.997	0.818	0.6659
Min-Max	0.007	0.572	1.000	0.909	0.5769

Since all the criteria are negative related to the score of the inventory management systems, the EOQ model with smallest score would be the most alternative and be chosen.

Table 6 compares the proposed model with the company's policy for class A parts.

**Table 6.** Compares the proposed model with enterprise's policy

	Enterprise's Policy	Proposed Model	Improvement
Out-of-stock rate	5.2120%	1.3110%	3.90%
Annual average ordering cost ratio	132,832,029	108,651,863	18.20%
Annual average holding cost ratio	201,128,129	151,307,024	24.77%

According to the proposal of the study, the results can be significantly improved if the company applies this model to manage spare parts inventory at the factory.

### 3. CONCLUSION

This study applies a multi-criteria classification method of spare parts referenced from a previous study, then analyzes and evaluates inventory management models to choose the most suitable model based on enterprise criteria.

According to the results obtained, businesses can reduce the probability of out-of-stock up to only 1.3%. Also reduced by 18.2% and 24.17% for ordering and holding costs respectively. Enterprises can apply this model to reduce the probability of shortage of spare parts and reduce the company's ordering and holding costs.

For future research, it is necessary to expand the application of appropriate inventory management policy to class B and C spare parts. Furthermore, analyze and evaluate to find another inventory management model which is more efficient than this proposed model.

### Acknowledgements

We acknowledge Ho Chi Minh City University of Technology (HCMUT), VNUHCM for supporting this study.

### References

- [1] R. Ramanathan, ABC inventory classification with multiple-criteria using weight linear optimization, *Computers and Operations Research*, 33 (2006), pp. 695–700.
- [2] B. E. Flores, D. C. Whybark, Implementing multiple criteria ABC analysis, *Journal of Operations Management*, 7 (1) (1987), 79–84.
- [3] F. Y. Partovi, M. Anandarajan, "Classifying inventory using an artificial neural network approach," *Computers and Industrial Engineering*, 41 (2002), pp. 389–404.
- [4] Rinaldi, Marta, et al. "A new procedure for spare parts inventory management in ETO production: a case study." *Procedia Computer Science*, 217 (2023), pp. 376–385.
- [5] de Smidt-Destombes, Karin S., Matthieu C. van der Heijden, and Aart van Harten. "Joint optimisation of spare part inventory, maintenance frequency and repair capacity for k-out-of-N systems." *International Journal of Production Economics*, 118.1 (2009), pp. 260–268.
- [6] Ng, Wan Lung. "A simple classifier for multiple criteria ABC analysis." *European Journal of Operational Research*, 177.1 (2007), pp. 344–353.
- [7] F. Y. Partovi, W. E. Hopton, "The analytic hierarchy process as applied to two types of inventory problems," *Production and Inventory Management Journal*, 35 (1) (1993), pp. 13–19.

**[S6-42] Building Model Supporting Maintenance Schedule at a Technology Solution Company**

Tuan-Phat Ngo, Mai-Ha Phan\*

*Department of Industrial Systems Engineering, Faculty of Mechanical Engineering, Ho Chi Minh City University of Technology (HCMUT), 268 Ly Thuong Kiet Street, District 10, Ho Chi Minh City, Viet Nam  
Viet Nam National University Ho Chi Minh City, Linh Trung Ward, Ho Chi Minh City, Viet Nam*

\*Corresponding author: ptmaiha@hcmut.edu.vn

**Abstract**

Currently, many companies are not only incorporating technology into their products and services, but also aligning their missions with the goal of conserving electrical energy to uphold environmental responsibility. Consequently, these companies prioritize the maintenance of their machinery and equipment to achieve optimal performance. To optimize costs, these companies often seek professional maintenance services. These service providers employ efficient resource allocation strategies when responding to orders. Implementing optimal scheduling and resource allocation methods proves to be an effective approach for reducing operational costs, increasing resource utilization, and minimizing waste, thus creating a competitive edge in the market. This research aims to establish suitable models for real-world air conditioning maintenance orders in company X and apply appropriate algorithms to efficiently allocate resources while ensuring service quality. The study employs two models, namely the clustering model and manpower allocation model, along with the K-means algorithm and Tabu-embedded simulated annealing algorithm to solve the resource allocation problem and identify corresponding solutions. Actual data from company X in July 2022 is used to evaluate the effectiveness of the proposed model. The results demonstrate a significant reduction in resources (with an average decrease of 34% compared to previous resource allocation methods). The proposed solution model is expected to be implemented in company X to further enhance efficiency and significantly reduce operating costs.

**Keywords:** *Clustering, Manpower allocation, K-means, Tabu-embedded simulated annealing, air conditioning optimization and management technology solutions*

**1. INTRODUCTION**

Vietnam has witnessed a deceleration in its previously rapid GDP growth rate. According to statistical data from The World Bank, the country's GDP growth rate stood at 2.9% in 2020 and 2.6% in 2021, primarily attributed to the adverse effects of the Covid-19 pandemic. Nonetheless, the positive growth rate signifies an ongoing process of economic recovery. Energy demand remains indispensable for fulfilling various infrastructure and activities within the country. In response to the need for energy efficiency, numerous technology companies have emerged, focusing on resolving energy-saving challenges. However, these startups encounter hurdles in establishing viable business models, with particular emphasis on resource efficiency in a complex economic environment.

Within the realm of resource optimization, several research studies have been undertaken. Valls et al. (2009) investigated workforce scheduling, incorporating skill factors in service companies, resulting in feasible plans that meet temporal and resource constraints [1]. Dennis (2011) devised a spreadsheet-based scheduling method for optimal resource allocation in an internal call center, leading to significant reductions in staffing requirements and operating costs [2]. Li et al. (2018) conducted research on scheduling optimization for maintenance and repair activities, offering decision-making support to mitigate subjective errors [3]. These studies underscore the substantial impact of human resource dispatching on a company's operating costs.

In recent years, technology solution companies have shown particular interest in addressing the service model moderation issue. They are progressively embracing proposed solutions to streamline their operations. The present study concentrates on personnel allocation within a company, specifically focusing on the management and optimization of air conditioning operations. The objective is to curtail operating costs while ensuring the provision of high-quality air conditioning maintenance and repair services.

## 2. LITERATURE REVIEW

Moderation within the service environment plays a crucial role in strategically selecting and organizing appropriate resources to meet requirements while ensuring operational quality and cost-effectiveness. Previous research has extensively investigated the application of optimization models to minimize costs. For example, Lim et al. (2004) conducted a study on personnel allocation to address the spatial demands within a port in Singapore [4]. Their study proposed a personnel allocation model that incorporated time-frame constraints, which are commonly encountered in practical scenarios. Busato et al. (2019) conducted a study on resource optimization within the domain of food production [5]. The aim of this research is to create a decision support system that can determine the optimal configuration of transport units in each field of a silage production system. The objective is to minimize the total operational cost of the production system while adhering to time constraints for completing the operation. The decision support system will provide valuable insights into the optimal number of transport units required in each field, allowing for efficient and cost-effective management of the silage production process. In their study, Hasan et al. (2019) implemented the fuzzy target planning model with the aim of optimizing resource utilization within a company [6]. The proposed model is particularly effective in situations where there is a requirement to minimize capacity shortages for multiple tasks, as well as reduce overtime costs while adhering to a prioritized hierarchy. By applying the fuzzy target planning model, Hasan et al. sought to enhance resource allocation strategies, leading to improved efficiency and cost-effectiveness in the company's operations.

## 3. PROBLEM STATEMENT AND FORMULATION

### 3.1. Problem statement

Company X offers solutions for the management and digitalization of air conditioning systems. Their approach involves the installation of monitoring devices that enable users to measure energy consumption, monitor air conditioner operation, and integrate environmental parameters to develop suitable control algorithms. Alongside intelligent monitoring capabilities, these devices also possess smart control functions facilitated by an integrated control application, Bluetooth connectivity, compatibility with various air conditioner brands, and automatic scene settings. Leveraging customer usage behavior data and artificial intelligence, the company assists customers in assessing air conditioner conditions and devising appropriate maintenance and cleaning plans.

During the process of data collection and observation in the company's maintenance operations, it was observed that maintenance requests made on the same day in remote areas require a considerable amount of travel time. Recognizing that travel time represents an inefficiency, it becomes crucial to conduct a comprehensive study and gather the required data to evaluate the extent of time wastage associated with the utilization of workforce resources. The calculation formula for quantifying the amount of time wasted aligns with formula (1) as below:

$$\text{Level of waste} = \frac{\text{working time} - \text{maintenance time}}{\text{working time}} (\%) \quad (1)$$

Using a dataset comprising 40 observations encompassing variables such as timekeeping and maintenance duration, the study applies Minitab software to compute descriptive statistics (Figure 1). Subsequently, the waste level is determined by applying formula (1), which takes into account the average maintenance time of 46.12 minutes (Figure 1), an 8-hour workday allocation for technicians, and the utilization data of the maintenance team in July 2022, as illustrated in Figure 2.

Statistics										
Variable	N	N*	Mean	SE Mean	StDev	Minimum	Q1	Median	Q3	Maximum
Maintenance time	40	0	46.115	0.580	3.671	35.700	43.300	46.450	49.025	52.600

**Figure 1.** Statistical values describing air conditioner maintenance time

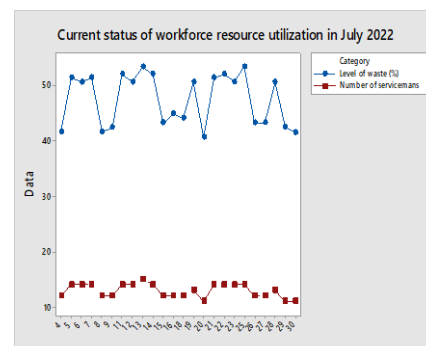


**Figure 2.** Current status of workforce resource utilization in July 2022

Based on the data presented in Figure 2, the analysis reveals a wasted time level of 47.37% when utilizing servicemans (corresponding to a resource efficiency of 52.63%). A higher wasted time level indicates excessive workforce utilization without effectively utilizing the entire working time of the employees to generate value for the company. This results in elevated operating costs. Consequently, the study proposes a solution to mitigate operating costs by reducing resource waste. To achieve this, a combined approach is suggested, integrating air conditioning maintenance scheduling and maintenance serviceman routing. This solution aims to minimize wasted time within the team, enhance work efficiency, and improve customer service, particularly by addressing travel-related time wastage. In this study, a clustering model is employed to schedule maintenance activities, while a team resource allocation model is utilized to efficiently allocate resources to meet the maintenance requirements.

Model for scheduling maintenance activities

In this study, the clustering model is employed to group air conditioners based on their proximity in terms of location and capacity of air conditioners. The clustering model utilized in this study is constructed based on the clustering model proposed in the study conducted by Al-Sultana et al. (1996) [7]:

Notations:

$i$ : air conditioner  $i = 1, \dots, m$

$j$ : working day  $j = 1, \dots, c$

Variables:

$$w_{ij} = \begin{cases} 1, & \text{if air conditioner } i \text{ is serviced on } j \\ 0, & \text{otherwise} \end{cases}$$

$z_j$ : central value that represents a working day  $j$

Parameters:

$p_{ij}$ : capacity of air conditioner  $j$  during a working day  $j$   $0 \leq p_{ij} \leq 1$

$p_e$ : minimum capacity requirement is necessary to ensure optimal air conditioner operation and maintenance efficiency.

$p_u$ : maximum capacity requirement is necessary to ensure optimal air conditioner operation and maintenance efficiency.

$a_i$ : latitude of air conditioner  $i$

$b_i$ : longitude of air conditioner  $i$

$x_i$ : location of air conditioner  $i$  in the clustering model, with  $x_i = (a_i, b_i, p_{ij})$

**Objective:**

$$\text{Minimize } \sum_{i=1}^m \sum_{j=1}^c w_{ij} \|x_i - z_j\|^2 \quad (2)$$

**Constraints:**

$$\sum_{j=1}^c w_{ij} = 1, \forall i = 1, 2, \dots, m \quad (3)$$

$$p_e \leq p_{ij} \leq p_u, \forall i = 1, 2, \dots, m, \forall j = 1, 2, \dots, c \quad (4)$$

The objective function (2) of the maintenance scheduling division model aims to minimize the overall Euclidean distance between air conditioners and the center of workdays. Constraint (3) ensures that each air conditioner is serviced exclusively on a single working day. Constraint (4) is implemented to ensure that maintenance is conducted prior to any potential air conditioner failure.

Following the completion of the grouping process, the study proceeded to group the air conditioners on maintenance days, taking into account the average capacity of each group. Air conditioners with higher average capacity will be given priority for servicing.

Based on the research by Aloise et al. (2009), the clustering problem involving Euclidean distance is classified as an NP-hard problem, falling within the realm of the Halting problem, a problem category described by Jack Copeland [8]. While it is possible to efficiently verify any solution to an NP-hard problem, there is currently no efficient method to find such solutions. Therefore, this study suggests the utilization of the K-means algorithm to identify optimal clusters for the air conditioning maintenance scheduling model, leveraging the proposed clustering and clustering model.

### 3.2. Model for allocating maintenance servicemans

Research on constructing a model for allocating workforce based on the study conducted by Lim et al. (2006) [4]:

Notations:

$i, j$  : air conditioner  $i, j = 1, 2, \dots, N$

$k$ : serviceman  $k = 1, 2, \dots, M$

Variables:

$$x_{ijk} = \begin{cases} 1, & \text{if serviceman } k \text{ travels from air conditioner } i \text{ to air conditioner } j, i \neq j \\ 0, & \text{otherwise} \end{cases}$$

$t_i$ : arrival time at air conditioner  $i$

$w_i$ : waiting time at air conditioner  $i$

$M$ : total number of serviceman

Parameters:

$N$ : total number of demand nodes (air conditioners) in a day

$c_{ij}$ : distance cost between node  $i$  and  $j$

$t_{ij}$ : travel time cost between nodes  $i$  and  $j$

$d_i$ : demand in numbers of servicemen at node  $i$

$e_i$ : earliest arrival time at node  $i$

$l_i$ : latest arrival time at node  $i$

$s_i$ : service time at node  $i$

$m_k$ : total shift time of serviceman  $k$

**Objectives:**

$$\text{Minimize } M \tag{5}$$

$$\text{Minimize } \sum_{i=0}^N \sum_{j=0}^N \sum_{k=1}^M c_{ij} x_{ijk}, \text{ v\o{r}i } i \neq j \tag{6}$$

$$\text{Minimize } \sum_{i=0}^N \sum_{j=0}^N \sum_{k=1}^M t_{ij} x_{ijk}, \text{ v\o{r}i } i \neq j \tag{7}$$

$$\text{Minimize } \sum_{i=0}^N \sum_{j=0}^N \sum_{k=1}^M w_j x_{ijk}, \text{ v\o{r}i } i \neq j \tag{8}$$

**Constraints:**

$$\sum_{k=1}^M \sum_{i=0}^N x_{ijk} = d_j, \forall j \tag{9}$$

$$x_{ijk} (t_i + t_{ij} + s_i + w_i) \leq t_j, \forall i, j, k \tag{10}$$

$$t_0 = w_0 = s_0 = 0 \tag{11}$$

$$e_i \leq t_i + w_i \leq l_i, \forall i \tag{12}$$

$$\sum_{i=0}^N \sum_{j=0}^N x_{ijk} (t_{ij} + s_i + w_i) \leq m_k, \forall k \tag{13}$$

$$\sum_{i=1}^N x_{0jk} = 1, \sum_{i=1}^N x_{i0k} = 1, \forall k \tag{14}$$

The objective function (5) of the model aims to minimize the number of servicemen required. The objective function (6) of the model seeks to minimize the travel distance of workforce resources. The objective function (7) of the model focuses on minimizing the execution time of maintenance tasks. Lastly, the objective function (8) of the model aims to minimize the waiting time for maintenance operations to be performed. Constraint (9) represents the maintenance requirement of air conditioner  $j$ , indicating that it necessitates  $d_j$  maintenance personnel. Constraint (10) ensures that serviceman  $k$ , upon completing the maintenance task for air conditioner  $i$ , promptly transitions to air conditioner  $j$ . Constraint (12) guarantees that the maintenance for air conditioner  $i$  commences within the scheduled timeframe. Constraint (13) imposes a limitation on the working time of serviceman  $k$ , ensuring it does not exceed shift  $m_k$ . In constraint (14), the first equation guarantees that serviceman  $k$  departs from the company, while the second equation ensures that serviceman  $k$  returns to the company upon fulfilling the assigned maintenance obligations.

Similar to the maintenance scheduling model, the maintenance crew dispatching model also falls under the category of NP-hard problems. Additionally, the maintenance crew dispatching model is a multi-objective model. When dealing with multi-objective optimization models, there are two approaches to model solving: sequential optimization and global optimization. To effectively find a solution for the dispatching model, appropriate algorithms and solutions are required. Previous studies have demonstrated various algorithmic approaches to address the human resource allocation problem. For instance, Abboud et al. (1998) explored the application of mobile algorithms to solve personnel allocation problems [9]. Dohn et al. (2009) employed a branch-and-bound approach to solve the human resource allocation problem by incorporating constraints on work groups [10]. Furthermore, Lim et al. (2004) proposed a combination of two heuristic algorithms (Tabu-search and Simulated annealing) to address the second model [4].



## 4. RESULTS AND DISCUSSIONS

### 4.1. Computation results

The study gathers data from the historical records of company X's system to identify air conditioners requiring maintenance during the first week of July 2022. The extracted information comprises the air conditioner's ID, address, and capacity. The longitude and latitude of each air conditioner's location are determined using the customer's address and the assistance of the Google Maps tool. Table 1 provides a comprehensive overview of the collected data for the week commencing July 1, 2022.

**Table 1.** Information of air conditioners that need to be serviced in the week of July 1, 2022

Air conditioner ID	Longitude	Latitude	Capacity
1	106.6854	10.77522	86
2	106.6962	10.77662	87
...	...	...	...
416	106.678	10.74409	96
417	106.6995	10.77623	88

The problem model is solved using the Python programming language, and the program is executed to obtain the maintenance scheduling and team dispatching results. After running the program for 15 minutes, the outcomes are obtained. Figure 3 illustrates a comparison between the resource wastage and the number of air conditioners that have been maintained, both in the actual usage scenario and when the proposed plan is implemented.

Based on the maintenance scheduling and crew dispatching results for the week of July 1, 2022, the average resource utilization rate was calculated as 75.58%, indicating a waste level of 24.42% (a decrease of 22.01% compared to the initial scheduling and dispatching results). The maximum required workforce during the week was determined to be 7-10 individuals (a reduction of 2-7 individuals).

### 4.2. Sensitivity analysis

The input parameter data of air conditioning maintenance time and serviceman movement speed can greatly influence objective functions such as the number of servicemen. This is especially important because in practice managers need to estimate the number of maintenance servicemen in advance to make decisions regarding the preparation of crew resources. Therefore, the study conducted a sensitivity analysis by running a simulation of the air conditioning maintenance time parameter and the serviceman's movement speed was random. The research involves utilizing the random number generator from the random library in Python programming language to simulate the maintenance scheduling and crew dispatching process. The simulation is performed 30 times, where each run considers random values for maintenance time distributed according to the normal distribution  $N(46.12, 3.67)$ , and the serviceman's movement speed is generated based on the Uniform distribution  $U(15, 40)$ .

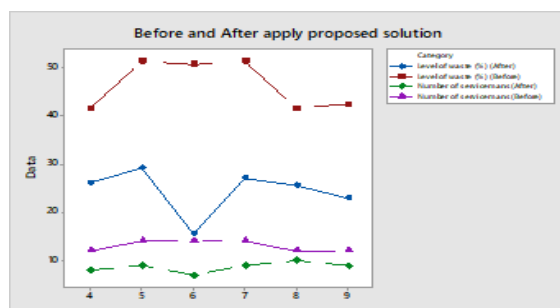


**Figure 3.** Actual results before (actual) and after when applying the proposed solution

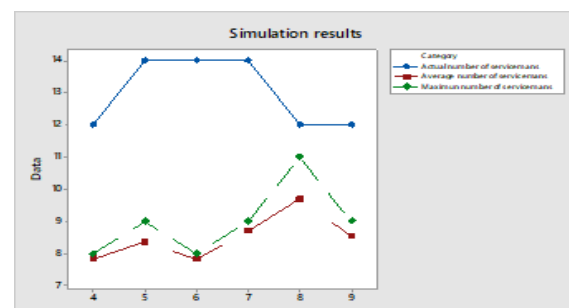


**Figure 4.** Results of Sensitivity Analysis Objective Function Number of Serviceman

Based on the findings presented in Figure 4, it can be observed that the maximum number of servicemen consistently remains lower than the number of servicemen recorded in the historical data. This provides

confirmation that the proposed models and algorithms, as outlined in the solution section of the study, lead to improvements in the maintenance scheduling and serviceman dispatching processes at company X. More specifically, by conducting the simulation 30 times, the study reveals a substantial reduction in the waste of servicemans' resources, resulting from a decrease in the required workforce (with an average reduction of 34% in the number of servicemans needed per working day).

## 5. CONCLUSION

In conclusion, the study has utilized existing research accomplishments to address the resource management challenge at company X. Specifically, the Tabu-embedded simulated annealing algorithm has been applied, along with programming language expertise, to devise solutions for the maintenance scheduling and serviceman dispatching problem. This contribution aids decision-makers in generating suitable moderation outcomes, providing support for effective decision-making.

In addition, the study conducts research, proposes a feasibility assessment, and develops an information system aimed at facilitating the collection of air conditioner data within the company's system. This system enables automated data processing and integration with scheduling and control algorithms at the team level, with the ultimate goal of optimizing resources within the company.

## Acknowledgments

We acknowledge Ho Chi Minh City University of Technology (HCMUT), VNUHCM for supporting this study.

## References

- [1] Valls, V., Pérez, Á., & Quintanilla, S. (2009). Skilled workforce scheduling in service centres. *European Journal of Operational Research*, 193(3), 791-804.
- [2] Dietz, D. C. (2011). Practical scheduling for call center operations. *Omega*, 39(5), 550-557.
- [3] Li, H., Mi, S., Li, Q., Wen, X., Qiao, D., & Luo, G. (2020). A scheduling optimization method for maintenance, repair and operations service resources of complex products. *Journal of Intelligent Manufacturing*, 31(7), 1673-1691.
- [4] Lim, A., Rodrigues, B., & Song, L. (2004). Manpower allocation with time windows. *Journal of the Operational Research Society*, 55(11), 1178-1186.
- [5] Busato, P., Sopegno, A., Pampuro, N., Sartori, L., & Berruto, R. (2019). Optimisation tool for logistics operations in silage production. *Biosystems Engineering*, 180, 146-160.
- [6] Hasan, M. G., Qayyum, Z., & Hasan, S. S. (2019). Multi-objective annualized hours manpower planning model: a modified fuzzy goal programming approach. *Ind. Eng. Manag. Syst*, 18(1), 52-66.
- [7] Al-Sultana, K. S., & Khan, M. M. (1996). Computational experience on four algorithms for the hard clustering problem. *Pattern recognition letters*, 17(3), 295-308.
- [8] Aloise, D., Deshpande, A., Hansen, P., & Popat, P. (2009). NP-hardness of Euclidean sum-of-squares clustering. *Machine learning*, 75(2), 245-248.
- [9] Abboud, N., Inuiguchi, M., Sakawa, M., & Uemura, Y. (1998). Manpower allocation using genetic annealing. *European Journal of Operational Research*, 111(2), 405-420.
- [10] Dohn, A., Kolind, E., & Clausen, J. (2009). The manpower allocation problem with time windows and job-teaming constraints: A branch-and-price approach. *Computers & Operations Research*, 36(4), 1145-115.

## [S6-62] Dynamical Analysis and Optimal Management of Chaotic Multi-Echelon Supply Chain System with Temporary Disruptions

Seung-Pil Lee<sup>1</sup>, Hwan-Seong Kim<sup>1,\*</sup>, Dae-Hyeun Kim<sup>1</sup>, Sam-Sang You<sup>2</sup>

<sup>1</sup> Department of Logistics, Korea Maritime and Ocean University, Busan, Republic of Korea

<sup>2</sup> Division of Mechanical Engineering, Korea Maritime and Ocean University, Busan, Republic of Korea

\*Corresponding author: kimhs@kmou.ac.kr

### Abstract

As industrialization progresses rapidly, production volume increases, and consumer consumption patterns change rapidly. Because consumer patterns change rapidly and non-linearly, it can be difficult for consumers to make decisions. This unpredictability of consumer behavior leads to an increase in processes such as refunds and exchanges. In addition, due to recent pandemics or logistics disruptions, disruption has occurred in each chain of the supply chain, adversely affecting the entire supply chain system. We model these nonlinear, unpredictable, and disruptive occurrences and analyze system stability through dynamic analysis. And in the face of disruption, efficient control algorithms can optimize management systems while reducing potential risks by applying control theory to decision support systems. In light of market volatility, new decision-making strategies can be used to optimize digital supply chain networks. Adjustments can provide valuable insights for effective administrative readiness.

**Keywords:** Multi-echelon supply chain, Disruptions, Dynamical analysis, Control theory, Optimal management

### 1. INTRODUCTION

As industrialization is rapidly progressing, production volume is increasing, and consumers' consumption patterns are also changing rapidly. As consumer patterns change rapidly and non-linearly, it can be difficult for consumers to make decisions. This unpredictability in consumer behavior leads to increased processes such as refunds and exchanges. Additionally, companies cannot keep large amounts of inventory for extended periods of time, especially for products with short shelf lives or those that are sensitive to trends. Managing inventory of perishable items is more complex and delicate compared to other types of products

### 2. METHODOLOGY

The actual business market is composed of numerous stakeholders and is intricately interconnected, making it highly challenging to comprehend in its entirety. It exhibits complex and nonlinear relationships, characterized by chaotic dynamics and unpredictability. Lorenz introduced the concept of chaotic systems in weather prediction, describing them as highly random and sensitive. Even small changes in the system input can lead to unpredictable outcomes or drastically different results as the system evolves through chaotic processes.

#### 2.1. Multi-echelon supply chain modeling

In a typical supply chain, the product flow starts with the manufacturers who produce the desired products and send them to distributors. The distributors then maintain safety stocks and ensure the smooth flow of products to the retailers. Based on customer orders, the products are finally delivered to the end customers. In the reverse direction, customers can place orders or provide feedback to the retailers to access the inventory stock. However, if there is a mismatch between orders and demands, waste can be generated, leading to significant economic losses across the entire supply chain system. Moreover, wastes can be detrimental to the environment, especially for short lead-time items such as perishable products or cold chains of fresh food.

$$\begin{aligned}\dot{x} &= qy - (m+1)x \\ \dot{y} &= wx - xz - y \\ \dot{z} &= xy - (e+1)z \\ \dot{w} &= rz - (m+1)w\end{aligned}$$

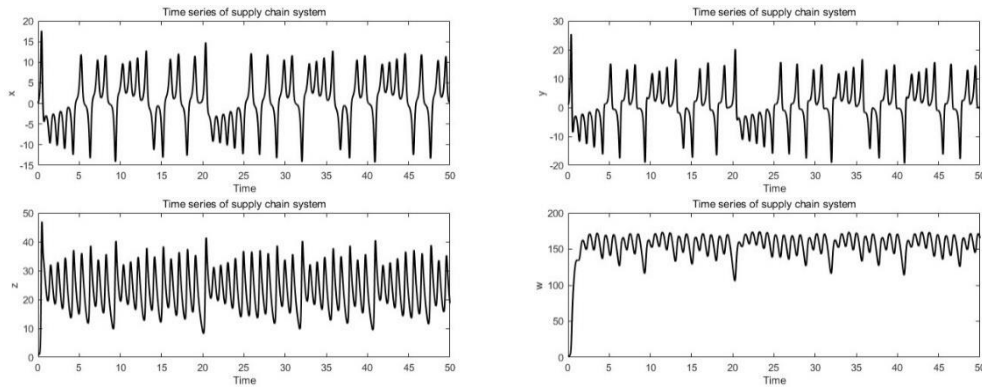


Figure 1. Times series of state variables

### 2.2. Multi-echelon Supply chain modeling document

This is a typical *phenomenon* of bullwhip effect (BWE) or *Forrester effect* that was first described by Forrester (1961) who explained the demand and variance amplification in an industrial system.

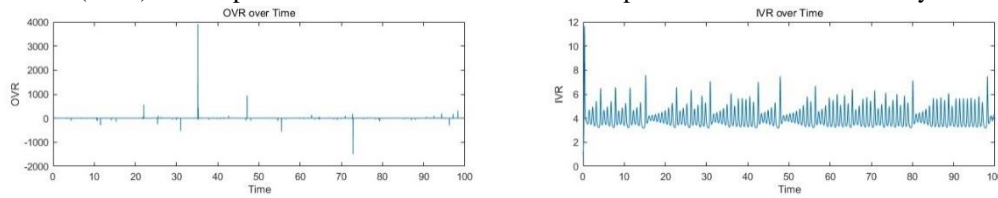


Figure 2. Bullwhip effect index for evaluating supply chain model

### 3. NUMERICAL SIMULATION

In this numerical analysis, market conditions constantly change with volatility, becoming more unstable or chaotic.

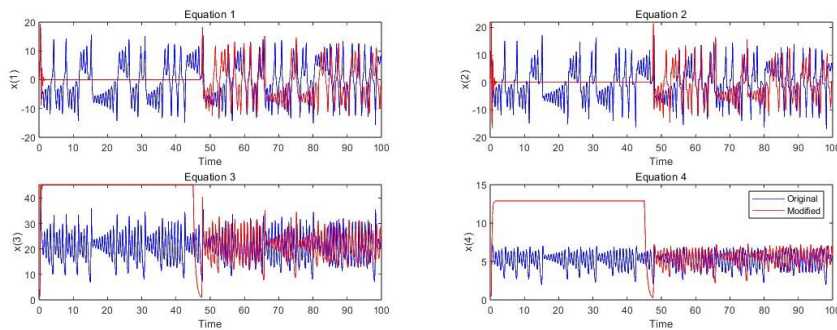


Figure 3. Times series of disruptions supply chain model

#### 4. CONCLUSION

A company or organization's stability is jeopardized during a business crisis, which can be triggered by internal or external factors. In the midst of a volatile market, businesses strive to navigate their vulnerable supply chains while grappling with uncertainty. Conventional logistics management software may not offer effective solutions to address supply chain disruptions caused by an unpredictable market. To tackle this challenge, a novel four-dimensional supply chain model has been introduced to study intricate and dynamic interactions among participants. The model extensively examines the nonlinear properties through stability analysis of equilibrium points, bifurcation diagram analysis, phase portrait analysis, and analysis of time-series responses.

#### References

- [1] Beamon, B. M. Supply chain design and analysis: Models and methods. *International Journal of Production Economics*, 55(3) (1998), pp. 281–294.

**Proceedings of The 4th International Conference  
on Advanced Convergence Engineering (ICACE2023)**

**Many Authors, Ho Chi Minh City University of Technology, VNU-HCM, Shanghai  
University of Engineering Science, Korea Maritime & Ocean University, BK 21 Four,  
Global R&E Program for Interdisciplinary Technologies of Ocean Renewable Energy,  
Ho Chi Minh City Department of Science and Technology**

**NHÀ XUẤT BẢN ĐẠI HỌC QUỐC GIA THÀNH PHỐ HỒ CHÍ MINH**

**Trụ sở:**

Phòng 501, Nhà Điều hành ĐHQG-HCM, P. Linh Trung, TP Thủ Đức, TP.HCM.

ĐT: 028 62726361

E-mail: [vnuhp@vnuhcm.edu.vn](mailto:vnuhp@vnuhcm.edu.vn)

Website: [www.vnuhcmexpress.edu.vn](http://www.vnuhcmexpress.edu.vn)

**Chịu trách nhiệm xuất bản và nội dung**

**TS ĐỖ VĂN BIÊN**

**Biên tập**

**SIN KẾ DUYÊN**

**Sửa bản in**

**NHƯ NGỌC**

**Trình bày bìa**

**LÊ THANH LONG**

**Đôi tác liên kết**

**PHÒNG THÍ NGHIỆM TRỌNG ĐIỂM ĐIỀU KHIỂN SỐ VÀ KỸ THUẬT HỆ THỐNG  
TRƯỜNG ĐẠI HỌC BÁCH KHOA, ĐHQG-HCM**

Xuất bản lần thứ 1. Số lượng in: 160 cuốn, khổ 20 x 29 cm. Số XNĐKXB: 2861-2023/CXBIPH/1-49/ĐHQGTPHCM. QĐXB số: 214/QĐ-NXB cấp ngày 12/9/2023. In tại: Công ty TNHH Dịch vụ - Kỹ thuật Đức Cảnh. Địa chỉ: 42/6/2 đường Đồng Xoài, Phường 13, Quận Tân Bình, TP.HCM. Nộp lưu chiểu: Năm 2023. ISBN: **978-604-479-148-7**.

Bản quyền tác phẩm đã được bảo hộ bởi Luật Xuất bản và Luật Sở hữu trí tuệ Việt Nam.  
Nghiêm cấm mọi hình thức xuất bản, sao chụp, phát tán nội dung khi chưa có sự đồng ý  
của tác giả và Nhà xuất bản.

**ĐỂ CÓ SÁCH HAY, CẦN CHUNG TAY BẢO VỆ TÁC QUYỀN!**

# SPONSORS

